frontiers | Research Topics

# Factors that impact the survival of non-small cell lung cancer

**Edited by**
Kristin Higgins, Jessy Deshane and Fiona Hegi-Johnson

**Published in**
Frontiers in Oncology

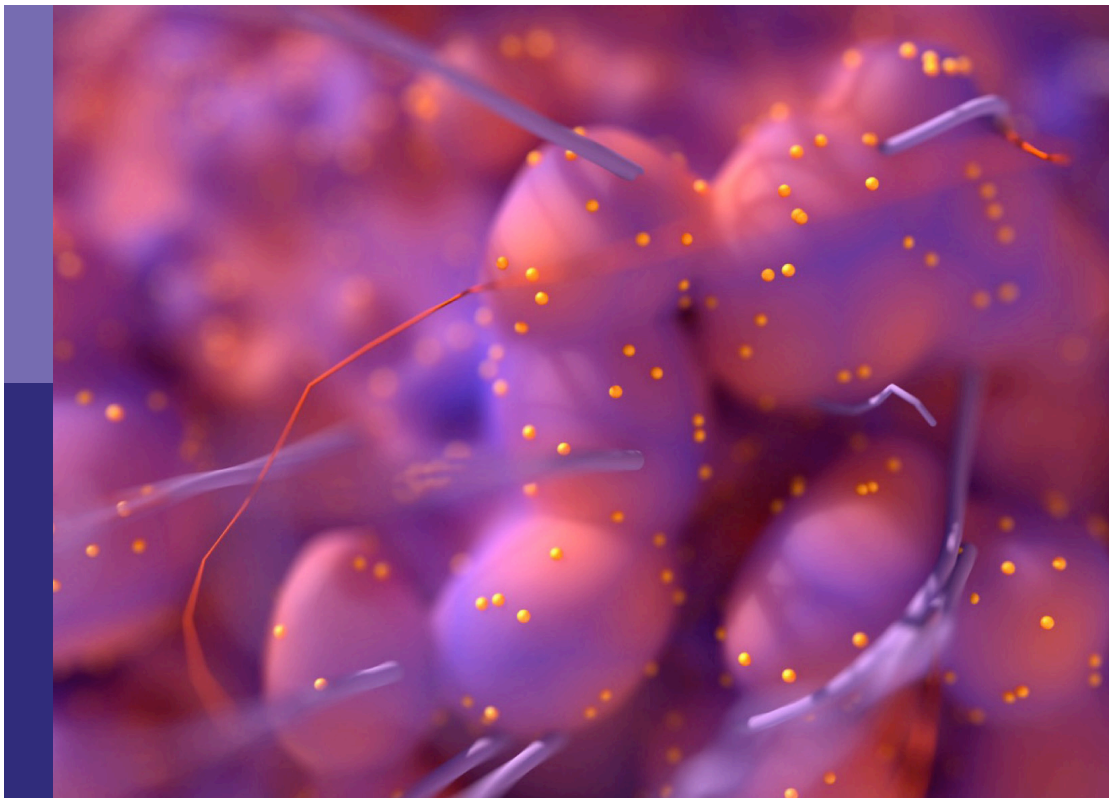

ISSN 1664-8714
ISBN 978-2-83251-015-5
DOI 10.3389/978-2-83251-015-5

## About Frontiers

Frontiers is more than just an open access publisher of scholarly articles: it is a pioneering approach to the world of academia, radically improving the way scholarly research is managed. The grand vision of Frontiers is a world where all people have an equal opportunity to seek, share and generate knowledge. Frontiers provides immediate and permanent online open access to all its publications, but this alone is not enough to realize our grand goals.

## Frontiers journal series

The Frontiers journal series is a multi-tier and interdisciplinary set of open-access, online journals, promising a paradigm shift from the current review, selection and dissemination processes in academic publishing. All Frontiers journals are driven by researchers for researchers; therefore, they constitute a service to the scholarly community. At the same time, the *Frontiers journal series* operates on a revolutionary invention, the tiered publishing system, initially addressing specific communities of scholars, and gradually climbing up to broader public understanding, thus serving the interests of the lay society, too.

## Dedication to quality

Each Frontiers article is a landmark of the highest quality, thanks to genuinely collaborative interactions between authors and review editors, who include some of the world's best academicians. Research must be certified by peers before entering a stream of knowledge that may eventually reach the public - and shape society; therefore, Frontiers only applies the most rigorous and unbiased reviews. Frontiers revolutionizes research publishing by freely delivering the most outstanding research, evaluated with no bias from both the academic and social point of view. By applying the most advanced information technologies, Frontiers is catapulting scholarly publishing into a new generation.

## What are Frontiers Research Topics?

Frontiers Research Topics are very popular trademarks of the *Frontiers journals series*: they are collections of at least ten articles, all centered on a particular subject. With their unique mix of varied contributions from Original Research to Review Articles, Frontiers Research Topics unify the most influential researchers, the latest key findings and historical advances in a hot research area.

Find out more on how to host your own Frontiers Research Topic or contribute to one as an author by contacting the Frontiers editorial office: frontiersin.org/about/contact

# Factors that impact the survival of non-small cell lung cancer

**Topic editors**

Kristin Higgins — Emory University, United States

Jessy Deshane — University of Alabama at Birmingham, United States

Fiona Hegi-Johnson — University of Melbourne, Australia

**Citation**

Higgins, K., Deshane, J., Hegi-Johnson, F., eds. (2023). *Factors that impact the survival of non-small cell lung cancer*. Lausanne: Frontiers Media SA.

doi: 10.3389/978-2-83251-015-5

# Table of contents

frontiers | Frontiers in Oncology

TYPE Editorial
PUBLISHED 09 February 2023
DOI 10.3389/fonc.2023.1148340



OPEN ACCESS

EDITED AND REVIEWED BY
Lizza E.L. Hendriks,
Maastricht University Medical Centre,
Netherlands

*CORRESPONDENCE
Fiona Hegi-Johnson
Fiona.Hegi-Johnson@petermac.org

SPECIALTY SECTION
This article was submitted to
Thoracic Oncology,
a section of the journal
Frontiers in Oncology

RECEIVED 20 January 2023
ACCEPTED 23 January 2023
PUBLISHED 09 February 2023

CITATION
Hegi-Johnson F and Higgins KA (2023)
Editorial: Factors that impact the survival of
non-small cell lung cancer.
*Front. Oncol.* 13:1148340.
doi: 10.3389/fonc.2023.1148340



# Editorial: Factors that impact the survival of non-small cell lung cancer

Fiona Hegi-Johnson[1,2]* and Kristin A. Higgins[3]

[1]Department of Radiation Oncology, Peter MacCallum Cancer Centre, Melbourne, VIC, Australia,
[2]Sir Peter MacCallum Department of Oncology, The University of Melbourne, VIC, Australia,
[3]Department of Radiation Oncology, Winship Cancer Institute, Emory University, Atlanta, GA, United States

KEYWORDS

**non-small cell lung cancer (NSCLC), surgery, radiotherapy, immunotherapy, epidemiology**

Editorial on the Research Topic
Factors that impact the survival of non-small cell lung cancer

There has never been a more exciting time to be a thoracic oncologist.

The last decades of biological discovery have led to meaningful gains in survival through the development of EGFR tyrosine kinase inhibitors (TKIs) and immunotherapy, and as this collection demonstrates, an increasing understanding of the factors that influence survival.

This collection, of the most highly cited and popular articles published within Frontiers in Oncology in Non-Small Cell Lung cancer over the last 5 years, illustrates the great depth and breadth of this field and focuses in particular on the biology and treatment outcomes of lung cancer patients with adenocarcinomas.

As Baak et al. show, NSCLC patients are diverse, and it is increasingly clear that the paradigms to predict outcomes which are based largely upon stage, histology and treatment can no longer effectively predict survival. Their intriguing finding that biological factors, such as clonality, proliferation and intra-tumour heterogeneity may differentiate between subpopulations of patients with different survival is to some extent justified by the other articles in this collection.

Despite the startling gains in survival seen in recent immunotherapy trials in both early stage NSCLC (1, 2) and metastatic NSCLC (3) the biology of the immune response remains poorly defined, and the intricacies of this response, and the mechanisms of resistance, which develop in the majority of patients treated with immunotherapy will require a sustained commitment to overcome. To this end, it is heartening to see so much emerging preclinical data exploring the mechanisms underpinning immunotherapy response and resistance. The predictive power of novel tumour biomarker signatures are explored by Yang et al. who demonstrate that RNA sequencing of long-coding RNA may help to predict survival in adenocarcinoma patients.

Our understanding of oncogenic pathways in lung adenocarcinoma also continues to deepen, and the evaluation of CDCA4, a gene that encodes transcription factors involved in cell proliferation and DNA synthesis in a small surgical cohort of patients provides yet another pathway to be interrogated in larger datasets and preclinical models (Tan et al.). A further two papers in this collection interrogate large patient databases to assess whether genomic signatures associated with macrophage switching(Chen et al.) and TGF-beta expression in radiotherapy patients are associated with overall survival (Zhang et al.). Using genomic analysis from a database and CRISPR silencing of acetyl-CoA acyltransferase (ACAA1) Feng and Shen also investigated causes of immunotherapy response and resistance in KRAS driven NSCLC

demonstrating and appears to drive the development of an immunosuppressive tumour microenvironment dominated by CD4+. T-Helper(TH)1, TH2 and TREG cells.

Imaging biomarkers continue to evolve, and offer the promise of non-invasive, multiple time-point assessments of tumour biology. Although, as pointed out by O'Connor et al. (4) CT-based radiomics still requires refinement and the use of large scale training datasets before a validated methodology is established it is encouraging to see work that employs large cohorts of patients with uniform biology to develop tools that are specific to the East Asian adenocarcinoma population (Wang et al.). Similarly, Jiang et al. review the correlations between EGFR mutation status and 18-F-FDG avidity, which also has useful real world applications for disease monitoring in patients being treated with tyrosine kinase inhibitors (TKIs).

The collection also captures the truly multidisciplinary nature of NSCLC management, and deals not only with improving survival but also with treatment and prognostication in patients with pleural effusions(Li et al., Qiao et al.) and with the ability of non-medication based approaches to improve analgesia and quality of life (Tang et al.).

In early stage disease, useful data is explored that looks at disease and treatment characteristics influencing survival in both surgical (Huang et al.) and radiotherapy(Yang et al., Li et al.) patients with both adenocarcinoma and squamous histologies. Given the paucity of clinical trial data that is specific to the histological subtypes of adenocarcinoma and squamous cell carcinomas, these retrospective analyses provide some useful guidance to support changes that are occurring in clinical practice to de-intensify local treatment approaches, such as the movement towards segmentectomy rather than lobectomy.

The efficient and rapid evaluation of emerging treatment strategies in clinical trials is handled in a different way by a paper exploring the value of early-stage endpoints as surrogate markers for later endpoints of durable response such as long-term progression free and overall survival (Shameer et al.). As the authors point out the sue of early end-point surrogates, permitting the assessment of survival outcomes at 4 or 6 months holds great promise to reduce the cost of clinical trials but needs significant future work in this area before these strategies can be validated for wider clinical use.

Finally, to underscore the importance of prevention, an increasing body of data underscores the importance of smoking cessation on both cancer causation and mortality after diagnosis. As Koshiaris (5) and Jha (6) have pointed out smoking accounts continues to account for an enormous proportion of cancer deaths, with an increasing burden falling on low- and middle-income countries. However, there is relatively little data on the interplay between smoking and response to therapies. Given the high levels of both EGFR expression and the high incidence of smoking in the East Asian population it is encouraging to see the exploration of this relationship, although the finding that smoking is a less powerful driver of response to TKI's than gender raises further intriguing biological questions to be explored in future work (Xiao et al.).

In summary, the future is bright for non-small lung cancer, as the thoracic oncology community continues to work together to advance the science for our patients.

## Author contributions

FH-J and KH have drafted and reviewed this manuscript prior to submission. All authors contributed to the article and approved the submitted version

## Conflict of interest

The authors declare that the research was conducted in the absence of any commercial or financial relationships that could be construed as a potential conflict of interest.

## Publisher's note



## References

1. Antonia SJ, Villegas A, Daniel D, Vicente D, Murakami S, Hui R, et al. Overall survival with durvalumab after chemoradiotherapy in stage III NSCLC. *N Engl J Med* (2018) 379(24):2342–50. doi: 10.1056/NEJMoa1809697

2. Herbst RS, Majem M, Barlesi F, Carcereny E, Chu Q, Monnet I, et al. COAST: An open-label, phase II, multidrug platform study of durvalumab alone or in combination with oleclumab or monalizumab in patients with unresectable, stage III non-small-cell lung cancer. *J Clin Oncol* (2022) 40(29):3383–93. doi: 10.1200/jco.22.00227

3. Herbst RS, Baas P, Kim DW, Felip E, Pérez-Gracia JL, Han JY, et al. Pembrolizumab versus docetaxel for previously treated, PD-L1-positive, advanced non-small-cell lung cancer (KEYNOTE-010): A randomised controlled trial. *Lancet* (2016) 387(10027):1540–50. doi: 10.1016/S0140-6736(15)01281-7

4. O'Connor JP, Aboagye EO, Adams JE, Aerts HJ, Barrington SF, Beer AJ, et al. Imaging biomarker roadmap for cancer studies. *Nat Rev Clin Oncol* (2017) 14(3):169–86. doi: 10.1038/nrclinonc.2016.162

5. Koshiaris C, Aveyard P, Oke J, Ryan R, Szatkowski L, Stevens R, et al. Smoking cessation and survival in lung, upper aero-digestive tract and bladder cancer: Cohort study. *Br J Cancer* (2017) 117(8):1224–32. doi: 10.1038/bjc.2017.179

6. Jha P. Avoidable global cancer deaths and total deaths from smoking. *Nat Rev Cancer* (2009) 9:655–64. doi: 10.1038/nrc2703

frontiers in Oncology

SYSTEMATIC REVIEW
published: 25 August 2020
doi: 10.3389/fonc.2020.01531

# Impact of Sex and Smoking on the Efficacy of EGFR-TKIs in Terms of Overall Survival in Non-small-Cell Lung Cancer: A Meta-Analysis

*Jian Xiao*[1,2], *Liang Zhou*[3,4,5], *Bixiu He*[1,2]* *and Qiong Chen*[1,2]*

[1] Department of Geriatrics, Respiratory Medicine, Xiangya Hospital of Central South University, Changsha, China, [2] National Clinical Research Center for Geriatric Disorders, Xiangya Hospital of Central South University, Changsha, China, [3] Department of Critical Care Medicine, People's Hospital of Ningxia Hui Autonomous Region, Yinchuan, China, [4] Department of Geriatrics, People's Hospital of Ningxia Hui Autonomous Region, Yinchuan, China, [5] Ningxia Geriatrics Center, Yinchuan, China

**Background:** To comprehensively understand the impact of sex and smoking on the efficacy of epidermal growth factor receptor-tyrosine kinase inhibitor (EGFR-TKI) therapy in terms of overall survival (OS) in non-small-cell lung cancer (NSCLC).

**Methods:** PubMed, Cochrane Library, Embase, and Scopus were searched from inception to March 17, 2019. OS was analyzed based on hazard ratios (HRs) and 95% confidence intervals (CIs) and estimated using the random effects model.

**Results:** Our meta-analysis included 22 studies involving 11,874 patients. In the primary analysis, we found no statistically significant efficacy difference for EGFR-TKI intervention between females and males (pooled HR 0.95, 95% CI 0.87–1.04, $P = 0.30$) and no obvious efficacy difference between never smokers and ever smokers (pooled HR 0.91, 95% CI 0.76–1.09, $P = 0.31$). In the subgroup analysis of placebo control treatment, we found that female NSCLC patients who received EGFR-TKI therapy had a longer OS than male patients (pooled HR 0.86, 95% CI 0.75–1.00, $P = 0.04$), while smoking status showed no significant effect on the efficacy of EGFR-TKI treatment in terms of the OS of NSCLC patients in all subgroup analyses.

**Conclusion:** The efficacy of EGFR-TKI therapy for NSCLC patients is independent of smoking status but dependent on sex, and females have a longer OS than males.

**Keywords: meta-analysis, epidermal growth factor receptor-tyrosine kinase inhibitor, overall survival, non-small-cell lung cancer, sex**

OPEN ACCESS

***Edited by:***
*Jorge J. Nieva, University of Southern California, United States*

***Reviewed by:***
*Jai Narendra Patel, Levine Cancer Institute, United States*
*Tao Dong, University of Oxford, United Kingdom*

***Correspondence:**
*Bixiu He*
*hebixiu000@tom.com*
*Qiong Chen*
*xyqiongchen@163.com*

***Specialty section:***
*This article was submitted to Thoracic Oncology, a section of the journal Frontiers in Oncology*

***Received:*** *17 November 2019*
***Accepted:*** *16 July 2020*
***Published:*** *25 August 2020*

***Citation:***
*Xiao J, Zhou L, He B and Chen Q (2020) Impact of Sex and Smoking on the Efficacy of EGFR-TKIs in Terms of Overall Survival in Non-small-Cell Lung Cancer: A Meta-Analysis. Front. Oncol. 10:1531. doi: 10.3389/fonc.2020.01531*

## INTRODUCTION

Lung cancer is one of the most common cancers in men and women, and there is no doubt that lung cancer poses the greatest threat to human life, as it results in one-quarter of all cancer deaths (1). However, non-small-cell lung cancer (NSCLC) accounts for more than 85% of lung cancer, (2) and it is well-known that there is a significant difference in the development of NSCLC between male and female patients and between patients of different smoking statuses (3, 4).

Overactivation of epidermal growth factor receptor (EGFR) tyrosine kinases is a key mechanism leading to the development of NSCLC (5). In recent years, epidermal growth factor receptor-tyrosine kinase inhibitors (EGFR-TKIs) have achieved good clinical efficacy in the treatment of NSCLC. At present, three generations of EGFR-TKIs have been widely used in the clinical treatment of NSCLC, such as gefitinib, afatinib, and osimertinib, which represent first-, second-, and third-generation EGFR-TKIs, respectively (6). Of course, other new EGFR-TKIs are also on the way to development and being promoted (7). There is no doubt that EGFR-TKI therapy plays a pivotal and irreplaceable role in the treatment of patients with NSCLC.

Previous meta-analyses focused on EGFR-mutated NSCLC patients and the progression-free survival (PFS) have concluded that female and non-smoking NSCLC patients have better efficacy with EGFR-TKIs than male patients and smokers (8–10). However, as we know that EGFR-TKIs treatment also shows some kind of treatment effects for NSCLC patients with unknown or wild-type EGFR status, and the association of overall survival (OS) with EGFR-TKIs treatment in NSCLC patients. Those previous studies could be expanded.

In the meantime, we found two meta-analyses that comprehensively and thoroughly studied the effect of sex on the efficacy in terms of OS of immune checkpoint inhibitors in cancer treatment (11, 12). We were very interested in these two studies, which prompted us to re-examine the impact of sex and smoking status, the two most common and important clinical features in NSCLC, on the efficacy of EGFR-TKIs. Thus, we have done and now report a meta-analysis of the association of sex and smoking with the efficacy of EGFR-TKIs in terms of OS in NSCLC.

# METHODS

## Search Strategy and Selection Criteria

We performed this meta-analysis according to the PRISMA guidelines (13). PubMed, Cochrane Library, Embase, and Scopus were searched from inception to March 17, 2019. Two authors independently searched the databases. The main search terms were "lung cancer," "survival," "hazard ratio," "EGFR" and "randomized controlled trials." Full details of our search strategies for the databases are shown in the **Supplementary Material** (**Supplementary Content 1**). Titles, abstracts and full-text articles were reviewed independently by two authors. Inconsistencies were discussed by all authors to reach consensus. Reference lists were also reviewed to identify additional relevant studies.

The literature inclusion criteria were as follows: randomized controlled clinical trials for NSCLC that contained any single EGFR-TKI treatment; the treatment plans in the corresponding control group did not contain any other EGFR-TKIs; the prognosis endpoint was OS, and the corresponding hazard ratios (HRs) and 95% confidence intervals (CIs) were reported according to sex and/or smoking status; and the full-text manuscripts were published in English. The exclusion criteria were as follows: retrospective studies of clinical cases; abstracts, reports, and papers from conferences; literature reviews and meta-analyses.

**Abbreviations:** EGFR, epidermal growth factor receptor; EGFR-TKIs, epidermal growth factor receptor-tyrosine kinase inhibitors; NSCLC, non-small-cell lung cancer; OS, overall survival; HR, hazard ratio; CI, confidence interval; PFS, progression-free survival.

## Data Extraction and Study Quality Assessment

Two authors independently extracted data from the included studies. Discrepancies were resolved by all authors through discussion to reach consensus. The following variables were extracted from each study: first author, publication year, EGFR mutation status, trial name, lines of therapy, EGFR-TKI intervention drug, control treatment plan, total number of patients, median age (years), median follow-up time (months), overall HR with 95% CI, HR with 95% CI according to patient sex, and HR with 95% CI according to smoking status. When duplicate publications were identified from one trial, we included only the most complete report.

The methodological quality of the included studies was assessed using the five-point Jadad score (14), which judges manuscripts according to the descriptions of randomization, blinding and withdrawals and dropouts. The details are as follows: whether randomized or not; whether randomization was described or not; whether double-blinded or not; whether blinding was described or not; and whether withdrawals and dropouts were described or not. For each of the above questions, if the answer is yes, the study gets 1 point; if the answer is no, the study gets 0 points. The quality scale ranges from 0 to 5 points for each controlled trial. A score of 2 or less indicates a low-quality study, while a score of 3–5 indicates a high-quality study.

## Data Analysis

The HRs and 95% CIs were extracted from each study according to the classification of overall HR, HR in male patients, HR in female patients, HR in never smokers and HR in ever (former and/or current) smokers. For the overall HRs, we used the random effects model to calculate the pooled HR directly. For the HRs classified by sex and smoking status, we first calculated the interaction HRs and 95% CIs for each study and thereafter obtained the pooled HR using the random effects model. The heterogeneity between studies was identified using the Q-test and quantified using $I^2$-values (11, 12). Potential publication bias was evaluated using the Egger and Begg test. To assess the differences between males and females or never smokers and ever smokers, we performed calculations using log HR to evaluate whether the variations differed from the null hypothesis by using the $\chi^2$-test (11, 12).

We performed subgroup analyses to further explore the variation of the effect of sex and smoking status on EGFR-TKI therapy efficacy. We only considered subgroups that included no less than two studies. The subgroups were EGFR status (unknown, wild-type, and mutation), lines of therapy (>1 and 1), EGFR-TKI intervention (gefitinib, erlotinib, and others), and control treatment (placebo, chemotherapy and others).

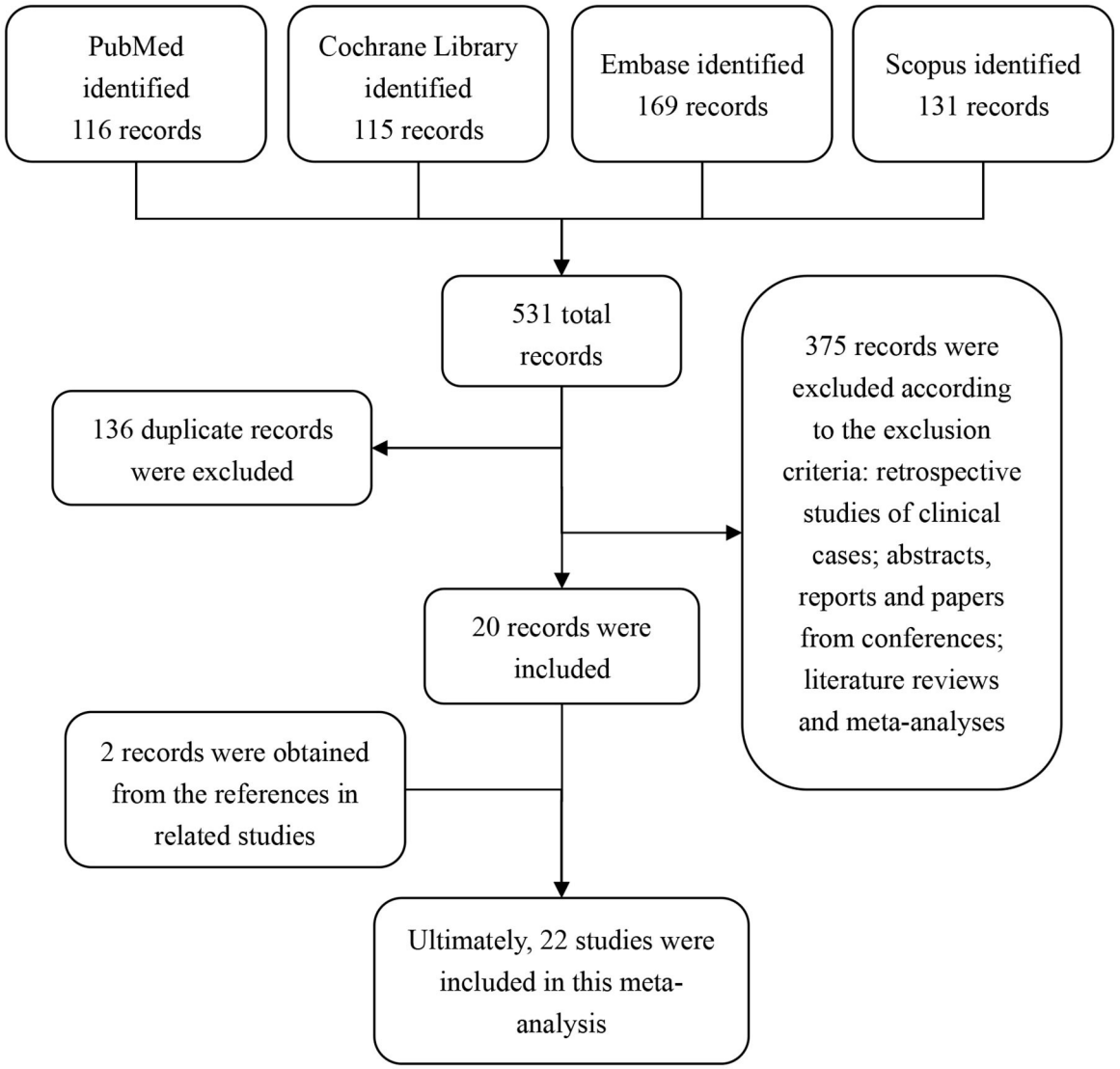


**FIGURE 1 |** Flow diagram of the study selection.

We performed all data analyses using Stata 14.0 (StataCorp LP, USA). All reported *P*-values are 2-sided, and a *P*-value of 0.05 indicated statistical significance. An HR < 1 indicated that EGFR-TKI efficacy was better than non-EGFR-TKI efficacy, EGFR-TKI efficacy in females was better than in males, and EGFR-TKI efficacy in never smokers was better than in ever smokers.

# RESULTS

## Literature Search

By searching our search terms in the database, we obtained 531 potential publications. A total of 136 records were excluded because of duplicated titles. By reviewing the abstract and full text, 375 records were further excluded according to our inclusion and exclusion criteria. Therefore, 20 publications were selected. In addition, by reviewing the references from these 20 selected studies, we found an additional 2 studies that were also in line with our inclusion criteria. Ultimately, 22 studies (15–36) were included in this meta-analysis (**Figure 1**).

## Characteristics of the Identified Studies

We assessed the quality of the 22 studies by the Jadad score. The mean score was 3.64 (ranging from 3 to 5), and no study received a low-quality score (scored 2 or less), indicating that these included studies possessed high methodological quality. The Jadad scores for each study are listed in the **Supplementary Table S1** in the **Supplementary Material**).

As shown in **Table 1**, for the 22 included studies, 3 involved patients with wild-type EGFR, and 5 involved patients with EGFR mutations, and the other 14 studies did not consider EGFR mutations in patients, which we defined as EGFR unknown.

**TABLE 1 |** Main characteristics and results of the 22 studies included in the meta-analysis.

| Article source | EGFR situation | Trial name | Lines of therapy | EGFR-TKI intervention | Control treatment | Total patients | Median age (years) | Median follow-up (months) | Overall HR (95% CI) | Sex of HR (95% CI) | | Smoking of HR (95% CI) | |
|---|---|---|---|---|---|---|---|---|---|---|---|---|---|
| | | | | | | | | | | Male | Female | Never | Ever |
| Thatcher et al. (15) | Unknown | ISEL | >1 | Gefitinib | Placebo | 1,692 | 62/61 | 7.2 | 0.89 (0.77–1.02) | 0.91 (0.78-1.06) | 0.77 (0.60-0.97) | 0.67 (0.49-0.91) | 0.92 (0.80-1.05) |
| Tsao et al. (16) | Unknown | BR.21 | >1 | Erlotinib | Placebo | 731 | 62/59 | NR | 0.70 (0.58–0.85) | 0.76 (0.62–0.94) | 0.80 (0.59–1.07) | 0.42 (0.28–0.64) | 0.87 (0.71–1.05) |
| Kim et al. (17) | Unknown | INTEREST | >1 | Gefitinib | Docetaxel | 1,433 | 61/60 | 7.6 | 1.02 (0.91–1.15) | 1.08 (0.95–1.24) | 0.95 (0.78–1.17) | 0.93 (0.70–1.23) | 1.05 (0.92–1.19) |
| Maruyama et al. (18) | Unknown | V-15-32 | >1 | Gefitinib | Docetaxel | 489 | NR | 21 | 1.12 (0.89–1.40) | 1.10 (0.83–1.43) | 1.23 (0.81–1.84) | 0.93 (0.58–1.48) | 1.13 (0.87–1.45) |
| Cappuzzo et al. (19) | Unknown | SATURN | >1 | Erlotinib | Placebo | 889 | 60/60 | 11.4/11.5 | 0.81 (0.70–0.95) | 0.88 (0.74–1.05) | 0.64 (0.46–0.91) | 0.69 (0.45–1.05) | 0.84 (0.71–0.99) |
| Fukuoka et al. (20) | Unknown | IPASS | 1 | Gefitinib | Carboplatin plus paclitaxel | 1,217 | 57/57 | 17 | 0.90 (0.79–1.02) | 0.77 (0.59–1.02) | 0.93 (0.81–1.08) | 0.90 (0.78–1.03) | 0.99 (0.62–1.60) |
| Lee et al. (21) | Unknown | TOPICAL | 1 | Erlotinib | Placebo | 670 | 77/77 | NR | 0.94 (0.81–1.10) | Female vs. male 0.81 (0.59–1.01) | | Never vs. ever 0.64 (0.36–1.14) | |
| Pérol et al. (22) | Unknown | IFCT-GFPC 0502 | >1 | Erlotinib | Observation | 310 | 56.4/59.8 | 25.6 | 0.87 (0.68–1.13) | 0.88 (0.66–1.18) | 0.89 (0.52–1.53) | 0.83 (0.34–2.01) | 0.88 (0.68–1.15) |
| Kelly et al. (23) | Wild-type | PDX-012 | >1 | Erlotinib | Pralatrexate | 201 | 62/63 | NR | 1.19 (0.88–1.64) | 1.08 (0.75–1.56) | 1.64 (0.92–2.94) | NR | NR |
| Miller et al. (24) | Unknown | LUX-Lung 1 | >1 | Afatinib | Placebo | 585 | 58/59 | NR | 1.08 (0.86–1.35) | 1.17 (0.83–1.65) | 1.02 (0.76–1.37) | 1.20 (0.90–1.61) | 0.43 (0.31–0.61) |
| Ciuleanu et al. (25) | Unknown | TITAN | >1 | Erlotinib | Docetaxel or pemetrexed | 424 | 59/59 | 27.9/24.8 | 0.96 (0.78–1.19) | 0.86 (0.67–1.10) | 1.23 (0.78–1.94) | 0.86 (0.49–1.51) | 0.93 (0.78–1.11) |
| Garassino et al. (26) | Wild-type | TAILOR | >1 | Erlotinib | Docetaxel | 219 | 66/67 | 33 | 1.27 (0.95–1.69) | 1.18 (0.84–1.67) | 1.47 (0.84–2.56) | 1.69 (0.89–3.23) | 1.12 (0.81–1.54) |
| Inoue et al. (27) | Mutation | NEJ002 | 1 | Gefitinib | Carboplatin plus paclitaxel | 228 | NR | 23 | 0.89 (0.63–1.24) | 0.92 (0.53–1.61) | 0.88 (0.57–1.35) | 0.88 (0.57–1.37) | 0.98 (0.58–1.65) |
| Ellis et al. (28) | Unknown | NCIC CTG BR.26 | >1 | Dacomitinib | Placebo | 720 | 63.5/65.5 | 23.4/24.4 | 1.00 (0.83–1.21) | NR | NR | 0.74 (0.56–0.98) | 1.13 (0.91–1.40) |
| Gregorc et al. (29) | Unknown | PROSE | >1 | Erlotinib | Pemetrexed or docetaxel | 263 | 66/64 | 32.4 | 1.15 (0.83–1.59) | Female vs. male 0.90 (0.64–1.27) | | Never vs. ever 0.80 (0.51–1.27) | |
| Li et al. (30) | Wild-type | NR | >1 | Erlotinib | Pemetrexed | 123 | 54.3/55.1 | 14.7 | 1.01 (0.66–1.54) | 1.24 (0.73–2.11) | 0.64 (0.31–1.33) | 0.81 (0.34–1.90) | 1.10 (0.68–1.80) |
| Karachaliou et al. (31) | Unknown | EURTAC | 1 | Erlotinib | Cisplatin plus docetaxel or gemcitabine | 97 | NR | 49.4 | 0.71 (0.45–1.12) | Female vs. male 0.96 (0.59–1.56) | | NR | NR |
| Zhou et al. (32) | Mutation | OPTIMAL | 1 | Erlotinib | Gemcitabine plus carboplatin | 154 | 57/59 | 25.9 | 1.19 (0.83–1.71) | 1.31 (0.75–2.31) | 1.20 (0.74–1.93) | 1.44 (0.93–2.24) | 0.85 (0.44–1.64) |
| Wu et al. (33) | Mutation | ENSURE | 1 | Erlotinib | Gemcitabine plus cisplatin | 217 | 57.5/56 | 28.9/27.1 | 0.91 (0.63–1.31) | 0.86 (0.45–1.64) | 0.92 (0.59–1.44) | 0.99 (0.65–1.52) | 0.68 (0.32–1.43) |
| Yang et al. (34) | Mutation | LUX-Lung 3 and LUX-Lung 6 | 1 | Afatinib | Pemetrexed-cisplatin or gemcitabine-cisplatin | 631 | 60/59 | 41/33 | 0.81 (0.66–0.99) | 0.71 (0.51–0.99) | 0.84 (0.65–1.09) | 0.72 (0.57–0.92) | 1.02 (0.69–1.50) |
| Zhao et al. (35) | Unknown | INFORM | >1 | Gefitinib | Placebo | 296 | 55/55 | 17.8 | 0.88 (0.68–1.14) | 0.89 (0.64–1.24) | 0.93 (0.61–1.41) | 0.94 (0.65–1.35) | 0.82 (0.57–1.19) |
| Shi et al. (36) | Mutation | CONVINCE | 1 | Icotinib | Cisplatin plus pemetrexed | 285 | 56 | 39.6 | 1.03 (0.76–1.39) | 1.19 (0.69–2.04) | 0.96 (0.67–1.39) | 1.02 (0.72–1.45) | 1.20 (0.64–2.27) |

*EGFR, epidermal growth factor receptor; TKI, tyrosine kinase inhibitor; HR, hazard ratio; CI, confidence interval; NR, none reported.*

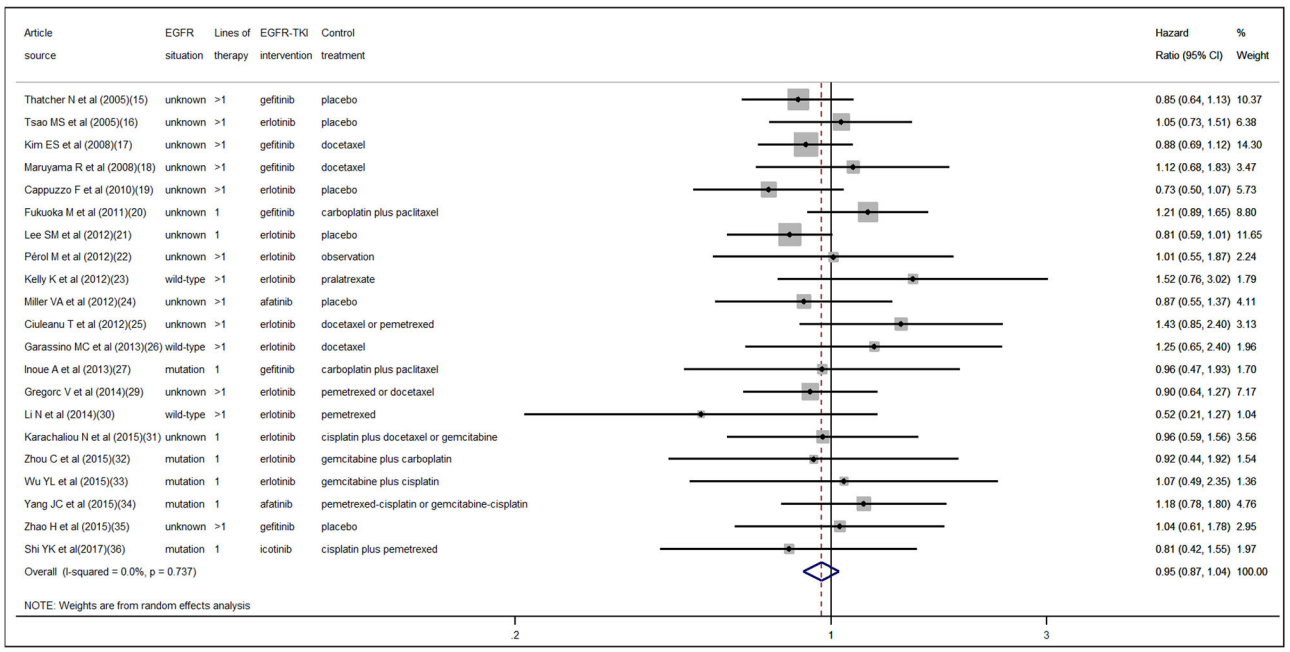


**FIGURE 2 |** Forest plot of the pooled analysis of the interaction hazard ratios of sex.

Eight of 22 studies were for first-line treatment, and 14 of 22 studies were for second-line or beyond treatments. Compared with placebo or standard chemotherapy, the EGFR-TKI interventions included gefitinib, erlotinib, dacomitinib, afatinib, and icotinib. In total, 11,874 patients were involved in these included trials.

In particular, Ellis et al. (28) did not report the HR for sex, and Kelly et al. (23) and Karachaliou et al. (31) did not report the HRs for smoking status that we needed. Lee et al. (21) Gregorc et al. (29) and Karachaliou et al. (31) reported the interaction HR of sex (female vs. male) in their subgroup analysis. Additionally, Lee et al. (21) and Gregorc et al. (29) reported the interaction HR of smoking status (never vs. ever smokers) in their subgroup analysis. For these interaction HRs with 95% CIs, we extracted and applied them in our meta-analysis directly (**Table 1**).

## Primary Analysis

According to the pooled result of overall HRs, we found that the therapeutic effect of EGFR-TKI intervention was better than that of the control treatment (pooled HR 0.94, 95% CI 0.89–1.00, $P = 0.05$) in NSCLC (**Figure S1** in the **Supplementary Material**). When pooling the interaction HRs of sex, the results showed no statistically significant efficacy difference in EGFR-TKI intervention between females and males (pooled HR 0.95, 95% CI 0.87–1.04, $P = 0.30$) (**Figure 2**). Similarly, based on the pooled interaction HR of smoking status, there was also no statistically significant efficacy difference in EGFR-TKI intervention between never smokers and ever smokers (pooled HR 0.91, 95% CI 0.76–1.09, $P = 0.31$) (**Figure 3**).

## Heterogeneity and Publication Bias

Statistically significant interstudy heterogeneity was identified among both overall HRs (I-squared = 38.4%, $P = 0.04$) and smoking status interaction HRs (I-squared = 58.6%, $P < 0.01$) but not in sex interaction HRs (I-squared = 0.00%, $P = 0.74$) (**Figure S1** in the **Supplementary Material**, **Figures 2**, **3**). Both Egger and Begg tests indicated no evidence of publication bias.

## Subgroup Analysis

We further performed subgroup analyses according to EGFR status (unknown, wild-type, and mutation), lines of therapy (>1 and 1), EGFR-TKI intervention (gefitinib, erlotinib, and others), and control treatment (placebo, chemotherapy, and others). According to the pooled interaction HRs of sex, we found a statistically significant OS advantage for females compared with males only for the EGFR-TKI intervention compared with the control placebo treatment (pooled HR 0.86, 95% CI 0.75–1.00, $P = 0.04$), while the other groups showed no statistically significant difference (**Table 2**). Furthermore, as shown in **Table 3**, no statistically significant difference was determined in any of the subgroups according to the pooled interaction HRs of smoking status.

# DISCUSSION

OS and PFS are the main endpoints in clinical trials of cancer. It is well-known that PFS is not in line with OS in many cases, (37) and in such cases, cancer patients may not obtain benefit from OS even though they have an improved PFS. To reduce time, save costs, and improve drug development efficiency, an increasing number of cancer clinical trials have set the research

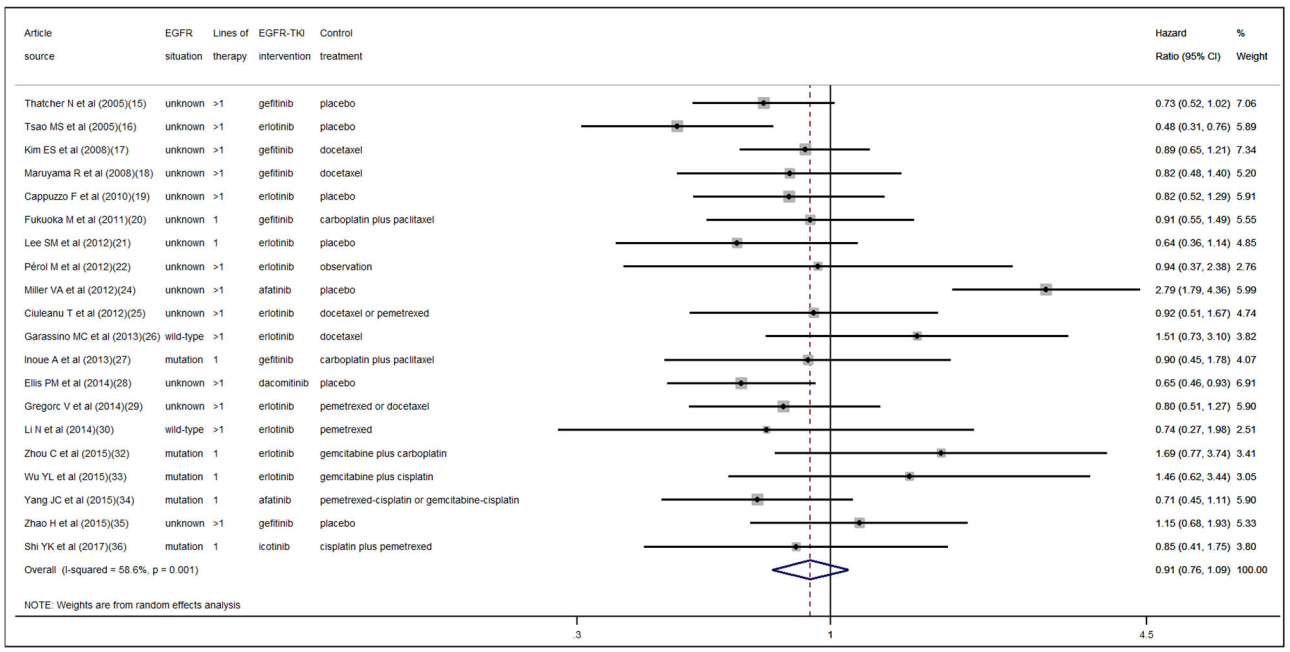


**FIGURE 3 |** Forest plot of the pooled analysis of the interaction hazard ratios of smoking status.

**TABLE 2 |** Differences in efficacy of EGFR-TKI therapy in females and males by subgroup.

| Subgroups | | Number of trials | Pooled interaction HR | P-interaction |
|---|---|---|---|---|
| Overall | | 21 | 0.95 (0.87–1.04) | 0.30 |
| EGFR situation | Unknown | 13 | 0.94 (0.85–1.03) | 0.19 |
| | Wild-type | 3 | 1.06 (0.60–1.89) | 0.83 |
| | Mutation | 5 | 1.02 (0.78–1.34) | 0.86 |
| Lines of therapy | >1 | 13 | 0.94 (0.84–1.05) | 0.26 |
| | 1 | 8 | 0.98 (0.84–1.15) | 0.82 |
| EGFR-TKI intervention | Gefitinib | 6 | 0.97 (0.84–1.11) | 0.64 |
| | Erlotinib | 12 | 0.93 (0.82–1.07) | 0.31 |
| | Others | 3 | 0.98 (0.74–1.30) | 0.91 |
| Control treatment | Placebo | 6 | 0.86 (0.75–1.00) | 0.04 |
| | Chemotherapy | 13 | 1.01 (0.89–1.14) | 0.89 |
| | Others | 2 | 1.21 (0.77–1.91) | 0.42 |

**TABLE 3 |** Differences in efficacy of EGFR-TKI therapy according to smoking status by subgroup.

| Subgroups | | Number of trials | Pooled interaction HR | P-interaction |
|---|---|---|---|---|
| Overall | | 20 | 0.91 (0.76–1.09) | 0.31 |
| EGFR situation | Unknown | 13 | 0.87 (0.69–1.10) | 0.24 |
| | Wild-type | 2 | 1.15 (0.58–2.27) | 0.68 |
| | Mutation | 5 | 0.95 (0.69–1.32) | 0.77 |
| Lines of therapy | >1 | 13 | 0.91 (0.71–1.17) | 0.46 |
| | 1 | 7 | 0.87 (0.69–1.10) | 0.25 |
| EGFR-TKI intervention | Gefitinib | 6 | 0.86 (0.73–1.03) | 0.10 |
| | Erlotinib | 10 | 0.86 (0.67–1.10) | 0.23 |
| | Others | 4 | 1.03 (0.50–2.11) | 0.95 |
| Control treatment | Placebo | 8 | 0.88 (0.59–1.29) | 0.50 |
| | Chemotherapy | 12 | 0.91 (0.77–1.06) | 0.22 |

endpoint to PFS. However, compared with PFS, OS is simple, reliable, straightforward, clear, and accurate in the evaluation of the endpoint of cancer patients. Therefore, more attention should be paid to OS. In our current study, we studied the impact of sex and smoking status on the efficacy of EGFR-TKI therapy in terms of OS in NSCLC patients and obtained meaningful findings.

We first demonstrated the advantage in OS for NSCLC patients who received EGFR-TKI intervention compared with other systemic therapies. Thereafter, we found no significant OS differences for EGFR-TKI intervention between the sexes and smoking status compared with other systemic therapies. Finally, in the subgroup analyses, when compared with placebo, we demonstrated that female NSCLC patients who received EGFR-TKI therapy had a longer OS than males. However, smoking status showed no significant effect on the efficacy of EGFR-TKI treatment in terms of the OS of NSCLC patients in all of our subgroup analyses.

In recent years, significant sex-based differences in biology, epidemiology and treatment responses have become evident (38). There are sex-related differences in the clinicopathological characteristics of NSCLC patients, and female sex is a separate advantage survival prognostic factor (4). Consistently, after adjustments for other prognostic factors, males with NSCLC have

a poorer prognosis than females (39). As NSCLC is considered a sex-related disease, further investigation is warranted to advance the treatment of NSCLC patients.

In a previous meta-analysis conducted by Lee et al. (40), EGFR-TKI treatment significantly prolonged PFS for female compared with male NSCLC patients with EGFR mutations. Afterwards, another meta-analysis also performed by Lee et al. (41) further concluded that, there was no difference in OS between EGFR-TKI and chemotherapy, as well as no difference in OS between female and male EGFR mutation-positive NSCLC patients. However, in our current study, we found that NSCLC patients who received EGFR-TKI intervention had longer OS than those who received other systemic therapies, although no significant OS differences for EGFR-TKI intervention were found between the sexes. In the subgroup analysis of the placebo control group, we demonstrated that female NSCLC patients who received EGFR-TKI therapy had a longer OS than males.

For the studies on chemotherapy in patients with NSCLC, Wakelee et al. (42) reported that women had a 1.9-month statistically significant improvement in OS compared with men. Wheatley-Price et al. (43) also concluded that females had a higher response rate to chemotherapy and a longer OS than males. For our current study, when the control group was treated with chemotherapy, it significantly biased our judgment of the difference in efficacy of EGFR-TKI between the sexes. When we removed the interference of chemotherapy and other factors in the subgroup analysis and compared EGFR-TKIs with the standard placebo, we found that the efficacy of EGFR-TKIs in female patients was significantly better than that in male patients. These results indicate that there is indeed a sex difference in the efficacy of EGFR-TKIs in patients with NSCLC.

It is well-known that tobacco smoking is an important cause of the development and progression of NSCLC. The incidence of EGFR mutations in NSCLC differs according to smoking history (44). EGFR mutations are highly prevalent in never smokers with NSCLC (45). Current smoking is an independent poor prognostic factor for survival for advanced non-squamous NSCLC patients without EGFR mutations who undergo pemetrexed continuation maintenance therapy (46). In addition, according to a recently reported large population-based study, NSCLC in never smokers was found to be clinically different from smoking-associated NSCLC, and the study also concluded that the OS in never-smokers was longer than that in smokers (47).

The impact of smoking status on the efficacy of EGFR-TKIs in terms of PFS in NSCLC is contradictory according to previous meta-analyses (9, 10, 40). For the meta-analyses that studied OS, Sohn et al. (48) reported that, compared with chemotherapy or placebo, receiving EGFR-TKI therapy appeared to show longer OS among patients with NSCLC for never smokers than that seen in ever smokers. In contrast, Lee et al. (41) found no difference in OS according to smoking status for NSCLC patients who underwent EGFR-TKI treatment compared with chemotherapy. We consider this contradictory phenomenon to be due to the different inclusion criteria and the different number of included studies. However, in our current study, we found no significant OS differences for EGFR-TKI intervention compared with other systemic therapies between different smoking statuses in NSCLC patients, and further subgroup analyses also showed that smoking status had no significant effect on the efficacy of EGFR-TKI treatment.

In summary, since sex and smoking status are the two main clinical features of lung cancer, our current research has important guiding significance for the clinical treatment of lung cancer. Our results suggest that we do not need to worry that smoking status will affect the efficacy of EGFR-TKIs and that EGFR-TKIs will have better efficacy in female patients than in male patients. However, on the other hand, the efficacy of EGFR-TKIs in male patients is not so ideal, indicating that more treatment options for male lung cancer patients need to be further developed in the future.

Our current study has several limitations. First, as a meta-analysis, it relies on published results rather than the individual data of patients. Second, those excluded studies that lack published sex and smoking status subgroup analysis data may also contain potential differences. Finally, aside from sex and smoking status, differences in OS outcomes may be influenced by other non-pharmacological factors.

## CONCLUSIONS

Two main conclusions can be drawn from our current meta-analysis. The first is that the efficacy of EGFR-TKI therapy for NSCLC patients is sex-dependent, and females have a longer OS advantage than males. The second point is that smoking status has no effect on the efficacy of EGFR-TKI therapy in terms of the OS of NSCLC patients.

## DATA AVAILABILITY STATEMENT

All datasets generated for this study are included in the article/**Supplementary Material**.

## AUTHOR CONTRIBUTIONS

JX and QC: concept and design. JX and LZ: acquisition, analysis or interpretation of data, and statistical analysis. JX and BH: drafting of the manuscript. JX, BH, and QC: critical revision of the manuscript for important intellectual content. BH and QC: administrative, technical or material support, and study supervision. All authors contributed to the article and approved the submitted version.

## FUNDING

This work was supported by the National Natural Science Foundation of China (Nos. 81572284 and 81770045).

## SUPPLEMENTARY MATERIAL

The Supplementary Material for this article can be found online at: https://www.frontiersin.org/articles/10.3389/fonc.2020.01531/full#supplementary-material

## REFERENCES


1. Siegel RL, Miller KD, Jemal A. Cancer statistics, 2019. *CA Cancer J Clin*. (2019) 69:7–34. doi: 10.3322/caac.21551
2. Reck M, Popat S, Reinmuth N, De Ruysscher D, Kerr KM, Peters S. Metastatic non-small-cell lung cancer (NSCLC): ESMO clinical practice guidelines for diagnosis, treatment and follow-up. *Ann Oncol*. (2014) 25(Suppl. 3):iii27–39. doi: 10.1093/annonc/mdu199
3. Ferketich AK, Niland JC, Mamet R, Zornosa C, D'Amico TA, Ettinger DS, et al. Smoking status and survival in the national comprehensive cancer network non-small cell lung cancer cohort. *Cancer*. (2013) 119:847–53. doi: 10.1002/cncr.27824
4. Hsu LH, Chu NM, Liu CC, Tsai SY, You DL, Ko JS, et al. Sex-associated differences in non-small cell lung cancer in the new era: is gender an independent prognostic factor? *Lung Cancer*. (2009) 66:262–7. doi: 10.1016/j.lungcan.2009.01.020
5. Liu TC, Jin X, Wang Y, Wang K. Role of epidermal growth factor receptor in lung cancer and targeted therapies. *Am J Cancer Res*. (2017) 7:187–202.
6. Tan CS, Kumarakulasinghe NB, Huang YQ, Ang YLE, Choo JR, Goh BC, et al. Third generation EGFR TKIs: current data and future directions. *Mol Cancer*. (2018) 17:29. doi: 10.1186/s12943-018-0778-0
7. Wang S, Song Y, Liu D. EAI045: The fourth-generation EGFR inhibitor overcoming T790M and C797S resistance. *Cancer Lett*. (2017) 385:51–4. doi: 10.1016/j.canlet.2016.11.008
8. Pinto JA, Vallejos CS, Raez LE, Mas LA, Ruiz R, Torres-Roman JS, et al. Gender and outcomes in non-small cell lung cancer: an old prognostic variable comes back for targeted therapy and immunotherapy? *ESMO Open*. (2018) 3:e000344. doi: 10.1136/esmoopen-2018-000344
9. Hasegawa Y, Ando M, Maemondo M, Yamamoto S, Isa SI, Saka H, et al. The role of smoking status on the progression-free survival of non-small cell lung cancer patients harboring activating epidermal growth factor receptor (EGFR) mutations receiving first-line EGFR tyrosine kinase inhibitor vs. platinum doublet chemotherapy: a meta-analysis of prospective randomized trials. *Oncologist*. (2015) 20:307–15. doi: 10.1634/theoncologist.2014-0285
10. Zhang Y, Kang S, Fang W, Hong S, Liang W, Yan Y, et al. Impact of smoking status on EGFR-TKI efficacy for advanced non–small-cell lung cancer in EGFR mutants: a meta-analysis. *Clin Lung Cancer*. (2015) 16:144–51.e1. doi: 10.1016/j.cllc.2014.09.008
11. Wallis CJD, Butaney M, Satkunasivam R, Freedland SJ, Patel SP, Hamid O, et al. Association of patient sex with efficacy of immune checkpoint inhibitors and overall survival in advanced cancers: a systematic review and meta-analysis. *JAMA Oncol*. (2019) 5:529–36. doi: 10.1001/jamaoncol.2018.5904
12. Conforti F, Pala L, Bagnardi V, De Pas T, Martinetti M, Viale G, et al. Cancer immunotherapy efficacy and patients' sex: a systematic review and meta-analysis. *Lancet Oncol*. (2018) 19:737–46. doi: 10.1016/S1470-2045(18)30261-4
13. Moher D, Liberati A, Tetzlaff J, Altman DG. Preferred reporting items for systematic reviews and meta-analyses: the PRISMA statement. *J Clin Epidemiol*. (2009) 62:1006–12. doi: 10.1016/j.jclinepi.2009.06.005
14. Jadad AR, Moore RA, Carroll D, Jenkinson C, Reynolds DJ, Gavaghan DJ, et al. Assessing the quality of reports of randomized clinical trials: is blinding necessary? *Control Clin Trials*. (1996) 17:1–12. doi: 10.1016/0197-2456(95)00134-4
15. Thatcher N, Chang A, Parikh P, Rodrigues Pereira J, Ciuleanu T, von Pawel J, et al. Gefitinib plus best supportive care in previously treated patients with refractory advanced non-small-cell lung cancer: results from a randomised, placebo-controlled, multicentre study (Iressa Survival Evaluation in Lung Cancer). *Lancet*. (2005) 366:1527–37. doi: 10.1016/S0140-6736(05)67625-8
16. Tsao MS, Sakurada A, Cutz JC, Zhu CQ, Kamel-Reid S, Squire J, et al. Erlotinib in lung cancer - molecular and clinical predictors of outcome. *N Engl J Med*. (2005) 353:133–44. doi: 10.1056/NEJMoa050736
17. Kim ES, Hirsh V, Mok T, Socinski MA, Gervais R, Wu YL, et al. Gefitinib vs. docetaxel in previously treated non-small-cell lung cancer (INTEREST): a randomised phase III trial. *Lancet*. (2008) 372:1809–18. doi: 10.1016/S0140-6736(08)61758-4
18. Maruyama R, Nishiwaki Y, Tamura T, Yamamoto N, Tsuboi M, Nakagawa K, et al. Phase III study, V-15–32, of gefitinib vs. docetaxel in previously treated Japanese patients with non-small-cell lung cancer. *J Clin Oncol*. (2008) 26:4244–52. doi: 10.1200/JCO.2007.15.0185
19. Cappuzzo F, Ciuleanu T, Stelmakh L, Cicenas S, Szczesna A, Juhasz E, et al. Erlotinib as maintenance treatment in advanced non-small-cell lung cancer: a multicentre, randomised, placebo-controlled phase 3 study. *Lancet Oncol*. (2010) 11:521–9. doi: 10.1016/S1470-2045(10)70112-1
20. Fukuoka M, Wu YL, Thongprasert S, Sunpaweravong P, Leong SS, Sriuranpong V, et al. Biomarker analyses and final overall survival results from a phase III, randomized, open-label, first-line study of gefitinib vs. carboplatin/paclitaxel in clinically selected patients with advanced non-small-cell lung cancer in Asia (IPASS). *J Clin Oncol*. (2011) 29:2866–74. doi: 10.1200/JCO.2010.33.4235
21. Lee SM, Khan I, Upadhyay S, Lewanski C, Falk S, Skailes G, et al. First-line erlotinib in patients with advanced non-small-cell lung cancer unsuitable for chemotherapy (TOPICAL): a double-blind, placebo-controlled, phase 3 trial. *Lancet Oncol*. (2012) 13:1161–70. doi: 10.1016/S1470-2045(12)70412-6
22. Perol M, Chouaid C, Perol D, Barlesi F, Gervais R, Westeel V, et al. Randomized, phase III study of gemcitabine or erlotinib maintenance therapy vs. observation, with predefined second-line treatment, after cisplatin-gemcitabine induction chemotherapy in advanced non-small-cell lung cancer. *J Clin Oncol*. (2012) 30:3516–24. doi: 10.1200/JCO.2011.39.9782
23. Kelly K, Azzoli CG, Zatloukal P, Albert I, Jiang PY, Bodkin D, et al. Randomized phase 2b study of pralatrexate vs. erlotinib in patients with stage IIIB/IV non-small-cell lung cancer (NSCLC) after failure of prior platinum-based therapy. *J Thorac Oncol*. (2012) 7:1041–8. doi: 10.1097/JTO.0b013e31824cc66c
24. Miller VA, Hirsh V, Cadranel J, Chen YM, Park K, Kim SW, et al. Afatinib vs. placebo for patients with advanced, metastatic non-small-cell lung cancer after failure of erlotinib, gefitinib, or both, and one or two lines of chemotherapy (LUX-Lung 1): a phase 2b/3 randomised trial. *Lancet Oncol*. (2012) 13:528–38. doi: 10.1016/S1470-2045(12)70087-6
25. Ciuleanu T, Stelmakh L, Cicenas S, Miliauskas S, Grigorescu AC, Hillenbach C, et al. Efficacy and safety of erlotinib vs. chemotherapy in second-line treatment of patients with advanced, non-small-cell lung cancer with poor prognosis (TITAN): a randomised multicentre, open-label, phase 3 study. *Lancet Oncol*. (2012) 13:300–8. doi: 10.1016/S1470-2045(11)70385-0
26. Garassino MC, Martelli O, Broggini M, Farina G, Veronese S, Rulli E, et al. Erlotinib vs. docetaxel as second-line treatment of patients with advanced non-small-cell lung cancer and wild-type EGFR tumours (TAILOR): a randomised controlled trial. *Lancet Oncol*. (2013) 14:981–8. doi: 10.1016/S1470-2045(13)70310-3
27. Inoue A, Kobayashi K, Maemondo M, Sugawara S, Oizumi S, Isobe H, et al. Updated overall survival results from a randomized phase III trial comparing gefitinib with carboplatin-paclitaxel for chemo-naive non-small cell lung cancer with sensitive EGFR gene mutations (NEJ002). *Ann Oncol*. (2013) 24:54–9. doi: 10.1093/annonc/mds214
28. Ellis PM, Shepherd FA, Millward M, Perrone F, Seymour L, Liu G, et al. Dacomitinib compared with placebo in pretreated patients with advanced or metastatic non-small-cell lung cancer (NCIC CTG BR.26): a double-blind, randomised, phase 3 trial. *Lancet Oncol*. (2014) 15:1379–88. doi: 10.1016/S1470-2045(14)70472-3
29. Gregorc V, Novello S, Lazzari C, Barni S, Aieta M, Mencoboni M, et al. Predictive value of a proteomic signature in patients with non-small-cell lung cancer treated with second-line erlotinib or chemotherapy (PROSE): a biomarker-stratified, randomised phase 3 trial. *Lancet Oncol*. (2014) 15:713–21. doi: 10.1016/S1470-2045(14)70162-7
30. Li N, Ou W, Yang H, Liu QW, Zhang SL, Wang BX, et al. A randomized phase 2 trial of erlotinib vs. pemetrexed as second-line therapy in the treatment of patients with advanced EGFR wild-type and EGFR FISH-positive lung adenocarcinoma. *Cancer*. (2014) 120:1379–86. doi: 10.1002/cncr.28591
31. Karachaliou N, Mayo-de las Casas C, Queralt C, de Aguirre I, Melloni B, Cardenal F, et al. Association of EGFR L858R mutation in circulating free DNA with survival in the EURTAC Trial. *JAMA Oncol*. (2015) 1:149–57. doi: 10.1001/jamaoncol.2014.257
32. Zhou C, Wu YL, Chen G, Feng J, Liu XQ, Wang C, et al. Final overall survival results from a randomised, phase III study of erlotinib vs. chemotherapy as first-line treatment of EGFR mutation-positive advanced non-small-cell

lung cancer (OPTIMAL, CTONG-0802). *Ann Oncol*. (2015) 26:1877–83. doi: 10.1093/annonc/mdv276
33. Wu YL, Zhou C, Liam CK, Wu G, Liu X, Zhong Z, et al. First-line erlotinib vs. gemcitabine/cisplatin in patients with advanced EGFR mutation-positive non-small-cell lung cancer: analyses from the phase III, randomized, open-label, ENSURE study. *Ann Oncol*. (2015) 26:1883–9. doi: 10.1093/annonc/mdv270
34. Yang JC, Wu YL, Schuler M, Sebastian M, Popat S, Yamamoto N, et al. Afatinib vs. cisplatin-based chemotherapy for EGFR mutation-positive lung adenocarcinoma (LUX-Lung 3 and LUX-Lung 6): analysis of overall survival data from two randomised, phase 3 trials. *Lancet Oncol*. (2015) 16:141–51. doi: 10.1016/S1470-2045(14)71173-8
35. Zhao H, Fan Y, Ma S, Song X, Han B, Cheng Y, et al. Final overall survival results from a phase III, randomized, placebo-controlled, parallel-group study of gefitinib vs. placebo as maintenance therapy in patients with locally advanced or metastatic non-small-cell lung cancer (INFORM; C-TONG 0804). *J Thorac Oncol*. (2015) 10:655–64. doi: 10.1097/JTO.0000000000000445
36. Shi YK, Wang L, Han BH, Li W, Yu P, Liu YP, et al. First-line icotinib vs. cisplatin/pemetrexed plus pemetrexed maintenance therapy for patients with advanced EGFR mutation-positive lung adenocarcinoma (CONVINCE): a phase 3, open-label, randomized study. *Ann Oncol*. (2017) 28:2443–50. doi: 10.1093/annonc/mdx359
37. Amir E, Seruga B, Kwong R, Tannock IF, Ocana A. Poor correlation between progression-free and overall survival in modern clinical trials: are composite endpoints the answer? *Eur J Cancer*. (2012) 48:385–8. doi: 10.1016/j.ejca.2011.10.028
38. Donington JS, Colson YL. Sex and gender differences in non-small cell lung cancer. *Semin Thorac Cardiovasc Surg*. (2011) 23:137–45. doi: 10.1053/j.semtcvs.2011.07.001
39. Radkiewicz C, Dickman PW, Johansson ALV, Wagenius G, Edgren G, Lambe M. Sex and survival in non-small cell lung cancer: A nationwide cohort study. *PLoS ONE*. (2019) 14:e0219206. doi: 10.1371/journal.pone.0219206
40. Lee CK, Wu YL, Ding PN, Lord SJ, Inoue A, Zhou C, et al. Impact of specific epidermal growth factor receptor (EGFR) mutations and clinical characteristics on outcomes after treatment with EGFR tyrosine kinase inhibitors vs. chemotherapy in EGFR-mutant lung cancer: a meta-analysis. *J Clin Oncol*. (2015) 33:1958–65. doi: 10.1200/JCO.2014.58.1736
41. Lee CK, Davies L, Wu YL, Mitsudomi T, Inoue A, Rosell R, et al. Gefitinib or Erlotinib vs chemotherapy for EGFR mutation-positive lung cancer: individual patient data meta-analysis of overall survival. *J Natl Cancer Inst*. (2017) 109:djw279. doi: 10.1093/jnci/djw279
42. Wakelee HA, Wang W, Schiller JH, Langer CJ, Sandler AB, Belani CP, et al. Survival differences by sex for patients with advanced non-small cell lung cancer on Eastern cooperative oncology group trial 1594. *J Thorac Oncol*. (2006) 1:441–6. doi: 10.1097/01243894-200606000-00011
43. Wheatley-Price P, Blackhall F, Lee SM, Ma C, Ashcroft L, Jitlal M, et al. The influence of sex and histology on outcomes in non-small-cell lung cancer: a pooled analysis of five randomized trials. *Ann Oncol*. (2010) 21:2023–8. doi: 10.1093/annonc/mdq067
44. Ren JH, He WS, Yan GL, Jin M, Yang KY, Wu G. EGFR mutations in non-small-cell lung cancer among smokers and non-smokers: a meta-analysis. *Environ Mol Mutagen*. (2012) 53:78–82. doi: 10.1002/em.20680
45. Chapman AM, Sun KY, Ruestow P, Cowan DM, Madl AK. Lung cancer mutation profile of EGFR, ALK, and KRAS: meta-analysis and comparison of never and ever smokers. *Lung Cancer*. (2016) 102:122–34. doi: 10.1016/j.lungcan.2016.10.010
46. Lin L, Zhao J, Hu J, Zou G, Huang F, Han J, et al. Current smoking has a detrimental effect on survival for epidermal growth factor receptor (EGFR) and anaplastic lymphoma kinase (ALK) negative advanced non-squamous non-small cell lung cancer (NSCLC) patients treated with pemetrexed continuation maintenance. *J Cancer*. (2018) 9:2140–6. doi: 10.7150/jca.24872
47. Lofling L, Karimi A, Sandin F, Bahmanyar S, Kieler H, Lambe M, et al. Clinical characteristics and survival in non-small cell lung cancer patients by smoking history: a population-based cohort study. *Acta Oncol*. (2019) 58:1618–27. doi: 10.1080/0284186X.2019.1638521
48. Sohn HS, Kwon JW, Shin S, Kim HS, Kim H. Effect of smoking status on progression-free and overall survival in non-small cell lung cancer patients receiving erlotinib or gefitinib: a meta-analysis. *J Clin Pharm Ther*. (2015) 40:661–71. doi: 10.1111/jcpt.12332

**Conflict of Interest:** The authors declare that the research was conducted in the absence of any commercial or financial relationships that could be construed as a potential conflict of interest.

frontiers in Oncology

ORIGINAL RESEARCH
published: 22 October 2020
doi: 10.3389/fonc.2020.564796

# ACAA1 Is a Predictive Factor of Survival and Is Correlated With T Cell Infiltration in Non-Small Cell Lung Cancer

*Huiyi Feng and Weixi Shen* *

*Department of Oncology, Shenzhen Hospital of Southern Medical University, Shenzhen, China*

Non-small cell lung cancer (NSCLC) is the predominant subtype of lung cancers. KRAS mutation is the second most prevalent mutation in NSCLC. KRAS mutant cancer cells suppress the anti-tumor T cell response. However, the underlying mechanism is still unknown. Here, we analyzed the differential expression of acetyl-CoA acyltransferase 1 (ACAA1) in various types of cancers using the TIMER database and validated the results in the NSCLC cell line H1944. We silenced oncogenic KRAS by siRNA targeting $KRAS^{G13D}$, and employed an MAPK signaling pathway inhibitor to clarify the possible regulatory pathway. Moreover, we analyzed the correlation of ACAA1 expression level with B cells, $CD4^+$ T cells, $CD8^+$ T cells, neutrophils, macrophages, and dendritic cells. Correlations between expression of ACAA1 and several biomarkers of mutation burden were also tested. Finally, we evaluated the prognostic value of ACAA1 in a wide range of cancers using the Kaplan-Meier Plotter Database. We found lower expression of ACAA1 in tumor tissue than in adjacent normal tissue in various cancers. This result was confirmed using a GEO dataset. Knock-down of mutant KRAS resulted in increased ACAA1 mRNA level in H1944 cells. ACAA1 mRNA level was significantly upregulated in H1944 after treatment with MAPK pathway inhibitor sorafenib, indicating that oncogenic KRAS may downregulate ACAA1 through MAPK signaling. ACAA1 was negatively correlated with biomarkers of tumor mutation burden, including BRCA1, ATM, ATR, CDK1, PMS2, MSH2, and MDH6. Conversely, ACAA1 expression was positively correlated with infiltrating $CD4^+$ cells and with Th1, Th2, Treg cells in the lung tumor microenvironment. Finally, we showed that ACAA1 is a predictive factor for survival in several cancer types. In summary, decreased ACAA1 expression is correlated with poor prognosis and decreases immune infiltration of $CD4^+$ T cells in LUAD and LUSC. ACAA1 also predicts T cell exhaustion in LUSC. The mechanism underlying KRAS/ACAA1 axis-mediated regulation of immune cell infiltration requires further investigation.

**Keywords: non-small cell lung cancer, KRAS mutation, immune cell infiltration, immune checkpoint blockade, tumor metabolites**

OPEN ACCESS

***Edited by:***
*Jessy Deshane, University of Alabama at Birmingham, United States*

***Reviewed by:***
*Manuel Cobo Dols, Junta de Andalucía, Spain*
*Alessandro Russo, A.O. Papardo, Italy*

***Correspondence:**
*Weixi Shen*
*13600436895@126.com*

***Specialty section:***
*This article was submitted to Thoracic Oncology, a section of the journal Frontiers in Oncology*

***Received:*** *05 June 2020*
***Accepted:*** *28 September 2020*
***Published:*** *22 October 2020*

***Citation:***
*Feng H and Shen W (2020) ACAA1 Is a Predictive Factor of Survival and Is Correlated With T Cell Infiltration in Non-Small Cell Lung Cancer. Front. Oncol. 10:564796. doi: 10.3389/fonc.2020.564796*

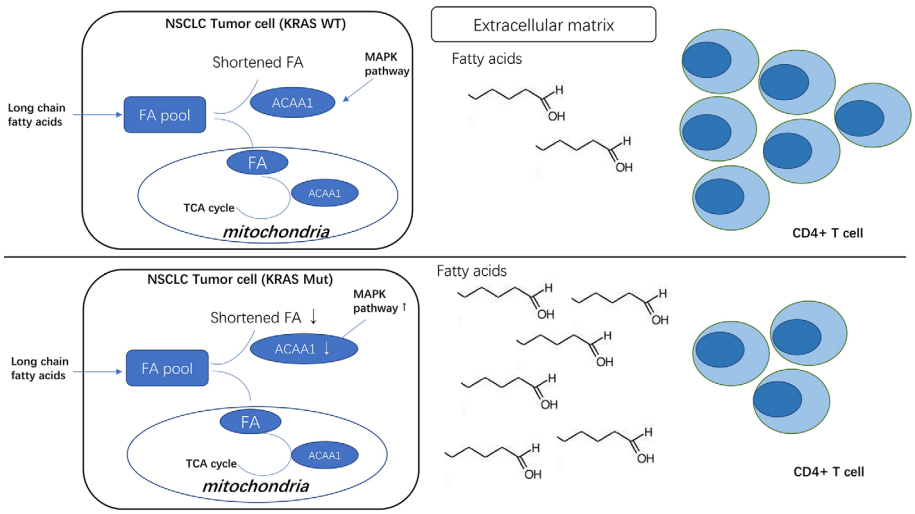


**GRAPHICAL ABSTRACT** |

## INTRODUCTION

Lung cancer is the second leading malignancy for new cases and the first for mortality among all types of malignancies (1). Non-small cell lung cancer (NSCLC), which included lung adenocarcinoma (LUAD) and lung squamous cancer (LUSC), is the predominant subtype of lung cancer. KRAS mutation is the second prevalent mutation in NSCLC (2). Cancer cells with KRAS mutations can avoid being attacked by the immune system, facilitating immune evasion or immunosuppression phenotypes of the tumor. Immunosuppression is a basic requirement for transforming cell survival and cancer development. There are several potential mechanisms by which KRAS mutant cancer cells may suppress the anti-tumor T cell response. Among these, the ability of KRAS mutant cells to convert $CD4^+$ Th cells into functional Tregs is crucial to inhibit T cell activation and promote a tolerogenic microenvironment (3). Another mechanism includes secretion of suppressive cytokines IL10 and TGFβ1 through MAPK signaling pathway (4), leading to T cell dysfunction. However, the precise mechanisms by which oncogenic KRAS induces immunosuppressive tumor microenvironment remain elusive.

By increasing the mutation burden of tumor cells, oncogenic KRAS also induces the production of a large number of neoantigens that may be recognized by $CD8^+$ and $CD4^+$ T cells. Specific anti-tumor T lymphocyte response can be induced after transferring KRAS mutant epitopes to adaptive T cells previously attacked (5). Tumor mutation burden is a prognostic factor for survival in a wide range of cancers (6), as well as a predictive factor for efficacy of PD-1/PD-L1 blockade immunotherapy (7).

MAPK signaling pathway is a key regulator of PD-L1 expression in lung adenocarcinoma (8). Activation of the MAPK pathway increases the expression of PD-L1 at both the mRNA and protein level, while repression of this pathway down-regulates PD-L1. Similar results were also observed in breast cancer. A preclinical study showed that combination of MAPK and PD-1 inhibitors leads to better efficacy in various types of cancers (9). Tumor cell and immune cell interaction is also regulated by MAPK pathway. In fact, MEK inhibition increases $CD8^+$ T cell infiltration within the tumor, while combination of MEK and PD-1 inhibitors synergistically promotes tumor regression (10).

We noted that oncogenic KRAS suppresses the expression of acetyl-CoA acyltransferase 1 (ACAA1) *via* the MAPK signaling pathway. ACAA1 is an enzyme involved in lipid β-oxidation and provides substrates to the tricarboxylic acid (TCA) cycle, a critical step in cellular metabolism. ACAA1 is also a biomarker in type 2 diabetes (T2D), predicting the pre-diabetic metabolic signature in mouse models (11). Nwosu et al. observed that up-regulated activity of MAPK/RAS/NFκB signaling in liver cancer was associated with poor survival and identified 148 down-regulated metabolic genes regulated by the MAPK signaling pathway. These differential genes, including ACAA1, were enriched in fatty acid β-oxidation. Metabolomic studies also showed a high dependence of the tumor cells on glutamine to promote the TCA cycle (12).

Based on these scientific findings, we were motivated to analyze the potential role of ACAA1 in KRAS-mutant NSCLC and elucidate the correlation of ACAA1 with the immunosuppressive phenotype in the tumor microenvironment.

## MATERIALS AND METHODS

### TIMER Database Analysis

TIMER is a comprehensive resource for systematic analysis of immune infiltrates across diverse cancer types (https://cistrome.shinyapps.io/timer/) (13). TIMER applies a deconvolution with a previously published statistical method to infer the abundance of

tumor-infiltrating immune cells (TIICs) from gene expression profiles. The TIMER database includes 10,897 samples across 32 cancer types from The Cancer Genome Atlas (TCGA) to estimate the abundance of immune infiltrates. First, we analyzed differential expression of ACAA1 in pan cancer. We aimed to exclude confounding factors, such as ACAA1 expression in tumor stromal cells or immune cells. We excluded the cancer types that had no statistical significance and employed those showing statistical significance for downstream analysis. Second, we analyzed the correlation of ACAA1 expression with the abundance of immune infiltrating cells, including B cells, $CD4^+$ T cells, $CD8^+$ T cells, neutrophils, macrophages, and dendritic cells. Third, correlations between ACAA1 expression and markers of different T cell subsets, including Th1 cells (TBX21, STAT4, STAT1, IFN-γ, TNF-α), Th2 cells (GATA3, STAT6, STAT5A, IL13), Th17 cells (STAT3, IL17A), and Treg cells (FOXP3, CCR8, STST5B, TGFB1). T cell exhaustion markers, including PDCD1, CTLA4, LAG3, TIM-3, GZMB, were also analyzed (14). The correlation module generated the expression scatter plots between a pair of user-defined genes in given cancer types, together with the estimated statistical significance. ACAA1 was used for the x-axis with gene symbols; related marker genes are represented on the y-axis as gene symbols. The gene expression level was displayed with $\log_2$ RSEM. P value Spearman's correlation coefficient was calculated automatically by the server.

## GEPIA Database Analysis

To verify the relationship between KRAS and ACAA1, we searched the expression correlation in GEPIA (15), an interactive web that includes 9,736 tumors and 8,587 normal samples from TCGA and the GTEx projects, which analyzes RNA expression. Gene expression correlation analysis was performed for given sets of TCGA expression data. We analyzed the expression pattern of ACAA1 and KRAS to identify the co-expression of several biomarkers indicating tumor mutation burden, including BRCA1, ATM, ATR, CDK1, PMS2, MLH1, MSH2, and MDH6. The Spearman method was used to determine the correlation coefficient.

## Cell Line and siRNA Transfection

Lung adenocarcinoma cell line H1944 was used to determine the regulation of ACAA1 expression. H1944 cells harbor KRAS mutation G13D. SiRNAs targeting $KRAS^{G13D}$ (5' GGAGG GCUUUCUUUGUGUA 3', 5' UCAAAGACAAAGU GUGUAA 3'), were transfected into H1944 cells using Lipofectamine 3000. One day before transfection, 25,000 cells were seeded in 24-well plates. On the day of transfection, 40 nM siRNA was diluted into 25 μl of Opti-mem, while 0.75 μl of lipofectamine was diluted in a final volume of 25 μl of Opti-mem. SiRNA and lipofectamine were mixed and allowed to react at room temperature for 10 min. After replacing complete medium with Opti-mem in each well, the total 50 μl siRNA-lipo complex was added to the wells. Twelve hours after transfection, Opti-mem medium was replaced with complete medium. Forty-eight hours after transfection, the cells were harvested, and total RNA and total proteins were extracted and used for the relevant experiments.

## MAPK Pathway Inhibition

To identify upstream regulatory pathways of ACAA1, H1944 cells were treated with the MAPK-ERK pathway inhibitor sorafenib. One day before treatment, 500,000 cells were seeded in 6-well plates. On the day of treatment, 5 μM or 10 μM of pathway inhibitor were added to the wells. The cells were collected at different timepoints (6, 12, 24, and 48 h) after treatment, and total RNA and protein were extracted using Trizol or NP40 cell lysis buffer. Subsequently, the RNA was used for q-PCR analysis.

## Kaplan-Meier Plotter Database Analysis

Kaplan-Meier plotter analyzes the correlation of RNA-seq data in over 20 cancer types with overall survival (OS) and progression-free survival (PFS) in 7,489 patients (https://kmplot.com/analysis/index.php?p=service&cancer=pancancer_rnaseq). The database is an online server indicating prognostic biomarkers in pan cancer. We searched the target gene ACAA1 in the server to identify in which types of cancer ACAA1 potentially shows prognostic value. The gene expression level cutoff was defined as 50% of RFKM, above which the expression was defined high, and conversely low. P value was calculated automatically by the server.

## Statistical Analysis

Survival curves were generated by the Kaplan-Meier plots displayed with HR and P or Cox P-values from a log-rank test. The correlation of gene expression was evaluated by Spearman's correlation and statistical significance. P-values <0.05 were considered statistically significant.

# RESULTS

## Expression of ACAA1 Is Lower in Tumor Tissues Than in Adjacent Normal Tissue in Various Types of Cancer

First, we aimed at elucidating whether ACAA1 had different expression patterns in tumor tissue and paired adjacent normal tissue. We included all cancer types and performed the analysis in the TIMER database (**Figure 1A**). ACAA1 expression was significantly down-regulated in 15 types of cancers (CHOL, COAD, ESCA, HNSC, KICH, KIRC, KIRP, LIHC, LUAD, LUSC, READ, SKCM, STAD, THCA, UCEC), and up-regulated in only one type of cancer, PRAD. As our research interest is focused on lung cancer, we re-analyzed ACAA1 expression in tumor tissue and adjacent normal tissue using a GEO dataset (GSD 3837) (16). ACAA1 showed lower mRNA levels in tumor tissues than in paired adjacent normal tissues (**Figure 1B**). Thus, the expression pattern indicated that ACAA1 acts as a tumor suppressor in most types of cancers. (abbreviations: CHOL: Cholangiocarcinoma; COAD: colon adenocarcinoma ESCA: Esophageal Squamous Cell Carcinoma

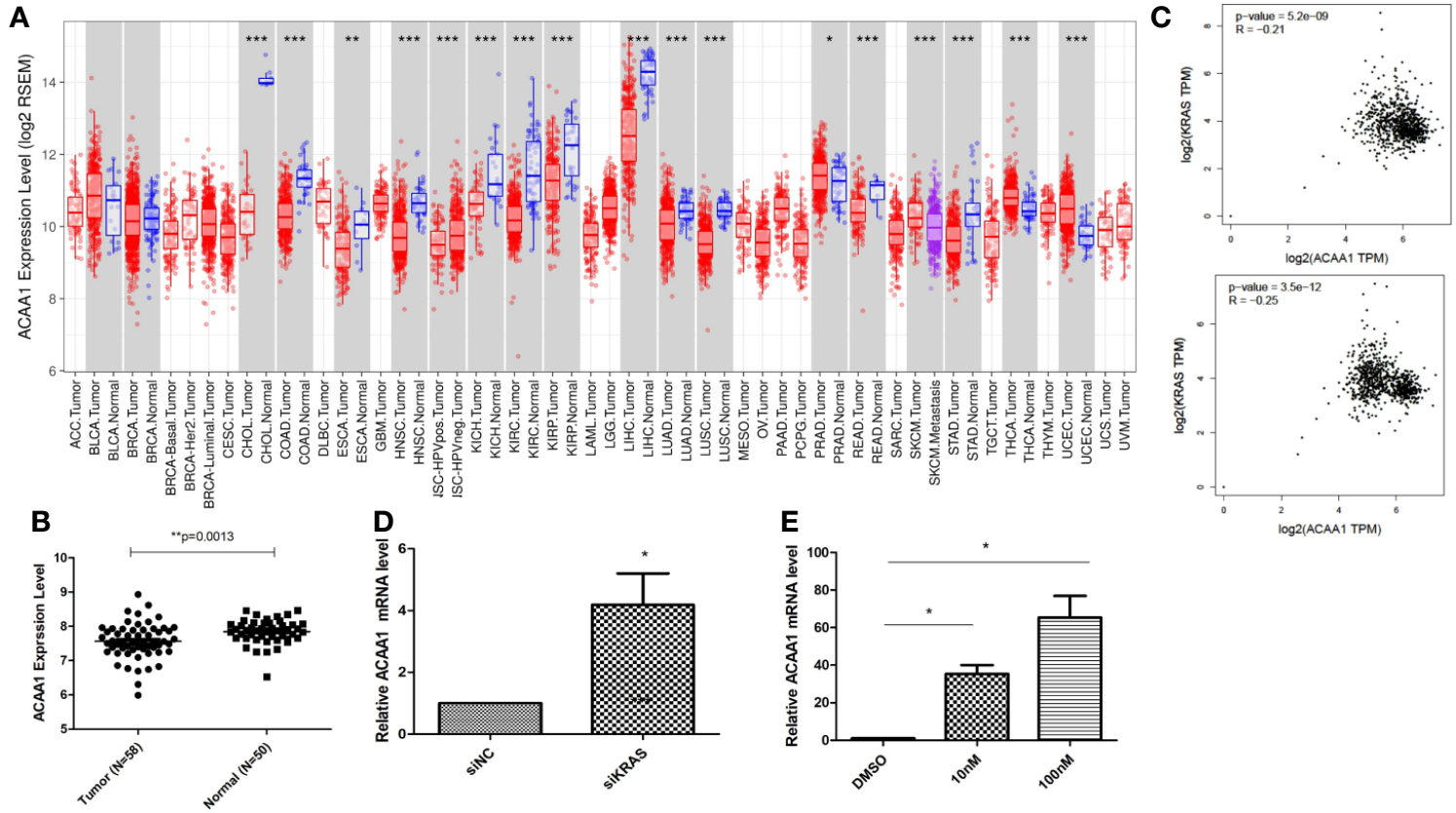


**FIGURE 1** | **(A)** ACAA1 expression is down-regulated in 15 types of cancer (CHOL, COAD, ESCA, HNSC, KICH, KIRC, KIRP, LIHC, LUAD, LUSC, READ, SKCM, STAD, THCA, UCEC). **(B)** The mRNA levels of ACAA1 are lower in tumor tissues than paired adjacent normal tissues (GSD 3837). **(C)** ACAA1 expression is negatively correlated with oncogenic KRAS. **(D)** Knock-down of mutant KRAS in H1944 cells results in increased ACAA1 mRNA level. **(E)** ACAA1 mRNA level is significantly upregulated in H1944 after sorafenib treatment. *p < 0.05.

HNSC: Head-neck squamous cell carcinoma KICH: Kidney chromophobe KIRC: Kidney renal clear cell carcinoma KIRP: Kidney renal papillary cell carcinoma LIHC: Liver hepatocellular carcinoma LUAD: Lung adenocarcinoma LUSC: Lung squamous cell carcinoma READ: Rectum adenocarcinoma SKCM: skin cutaneous melanoma STAD: Stomach adenocarcinoma THCA: Thyroid carcinoma)

To analyze how oncogenic KRAS regulates ACAA1 expression and the related upstream signaling pathway, we used lung adenocarcinoma cell line H1944, which harbors $KRAS^{G13D}$ mutation. We knocked down $KRAS^{G13D}$ by siRNA and tested knockdown efficiency using q-PCR (**supplementary Figure 1A**). Knock-down of mutant KRAS resulted in increased ACAA1 mRNA levels (**Figure 1D**). Next, we inhibited downstream pathways of KRAS. After treatment with MAPK inhibitor, ACAA1 mRNA was significantly upregulated (**Figure 1E**). Based on these findings, we propose that ACAA1 is downregulated by oncogenic KRAS through the MAPK signaling pathway. We also confirmed the expression correlation of ACAA1 and KRAS using the GEPIA database. In LUAD and LUSC, ACAA1 expression was negatively correlated with oncogenic KRAS (**Figure 1C**).

## ACAA1 Is Negatively Correlated With Tumor Mutation Burden in Lung Cancer

KRAS mutation is the second most prevalent mutation in lung cancer, and we observed that KRAS regulated the mRNA of ACAA1. We focused on these LUAD and LUSC in the downstream analysis. Tumor mutation burden is widely used as a biomarker for predicting efficacy of immune checkpoint blockade (17). We therefore analyzed the correlation of ACAA1 expression and biomarkers of tumor burden mutation (**Figure 2**). We found that ACAA1 was negatively correlated to BRCA1, ATM, ATR, CDK1, PMS2, MSH2, and MDH6, with statistically significant differences. BRCA1, ATM, ATR, and CDK1 are involved in DNA damage response (DDR) pathway. BRCA1 and CDK1 are the key signaling components of ATM and ATR protein kinases. Four mismatch-excision repair (MMR)-related genes, PMS2, MLH1, MSH2, and MDH6 were also tested. Except for MLH1, the other three biomarkers were negatively correlated to ACAA1. Together, these findings indicate that ACAA1 might function in maintaining DNA stability and DDR. As lung cancers harboring KRAS mutation have high response rate to PD-1/PD-L1 blockade, KRAS mutation might be a potential driver of DNA instability and DNA damage repair defects, thereby leading to the production of more neoantigens. ACAA1 might be a mediator in this process, through altering intracellular nutrients and metabolic signature.

## ACAA1 Expression Is Positively Correlated With $CD4^+$ Cell Infiltration

Next, we investigated whether ACAA1 expression was correlated to infiltration of immune cell in the tumor microenvironment, including B cells, $CD8^+$ and $CD4^+$ T cells, macrophages, neutrophils, and dendritic cells (**Figure 3A**). We found that $CD4^+$ T cells were positively correlated to ACAA1 expression in LUAD and LUSC, a correlation which showed statistical significance (r=0.2, p=9.44e-06, and r=0.318, p=1.36e-12 in LUAD and LUSC, respectively). Based on this, we propose that LUAD and LUSC harboring KRAS mutation probably recruit less $CD4^+$ T cells by suppressing ACAA1 expression, providing tumors with an immunosuppressive microenvironment. The insufficient number of $CD4^+$ T cells in the tumor microenvironment might be due to the decrease of either T cell infiltration or polarization of $CD4^+$ cells.

The TIMER database also provides a comparison of tumor infiltration levels among tumors with different somatic copy number alterations for a given gene. We confirmed that ACAA1 functionally recruited the immune cells using this feature of the database. As shown in **Figure 3B**, copy number variation of ACAA1 was negatively correlated to $CD4^+$ cells both in LUAD and in LUSC. Although we do not know whether copy number alternation of ACAA1 leads to its gain or loss of function, this result partially demonstrates that ACAA1 influences immune cells infiltration in a direct or indirect manner. Taken together, the two above results show that ACAA1 was positively correlated to T cell polarization. Reduced expression of ACAA1 in the tumor cells also indicates lower level of mature T cells in tumor stroma.

## ACAA1 Is Positively Correlated With Th1, Th2, and Treg Cells in the Tumor Microenvironment of Lung Cancer

Further, we analyzed whether ACAA1 expression was closely related to Th1, Th2, Th17, and Treg cells by examining the expression of biomarkers from these cells. Functionally, Th1 cells facilitate differentiation of $CD8^+$ cells to toxic T cells. Th2 and Th17 cells are instead negative regulators of Th1 cells. Treg cells have dual function in cancer immunology (18). These cells enable immunosuppressive cancer phenotypes by inhibiting T cell proliferation (19). $FOXP3^+$ Treg is thought to promote tumor growth and metastasis by inhibiting anti-tumor immunity, and Treg accumulation in cancer is usually related to poor prognosis (20). We found that ACAA1 expression was positively correlated with TBX2, STAT4, and TNF-α, but negatively correlated with STAT1 and IFNG in LUAD, with similar expression correlation in LUSC (**Figure 4A**). As TBX2 is the main marker of Th1 cells, these results indicate a positive relationship between ACAA1 and Th1 cell infiltration in the tumor stroma. Among the Th2 cell markers (**Figure 4B**), in LUAD, ACAA1 was positively correlated to STAT6, while in LUSC, it was correlated with all Th2 cell markers, including GATA3, STAT6, STAT5A, and IL-13. STAT6 promotes naïve T cell differentiation to Th2 cells. Thus, a decrease in STAT6 in the tumor stroma results in decreased Th2 cells. ACAA1 expression levels also positively correlated with Treg cell markers (**Figure 4C**), with the best correlation in TGFB1, the major cytokine promoting T cell differentiation to Treg cells. Reduction of TGFB1 inhibits Treg cells in the tumor microenvironment. However, we found no significant correlation of ACAA1 to Th17 cells (**Supplementary Figure 1B**).

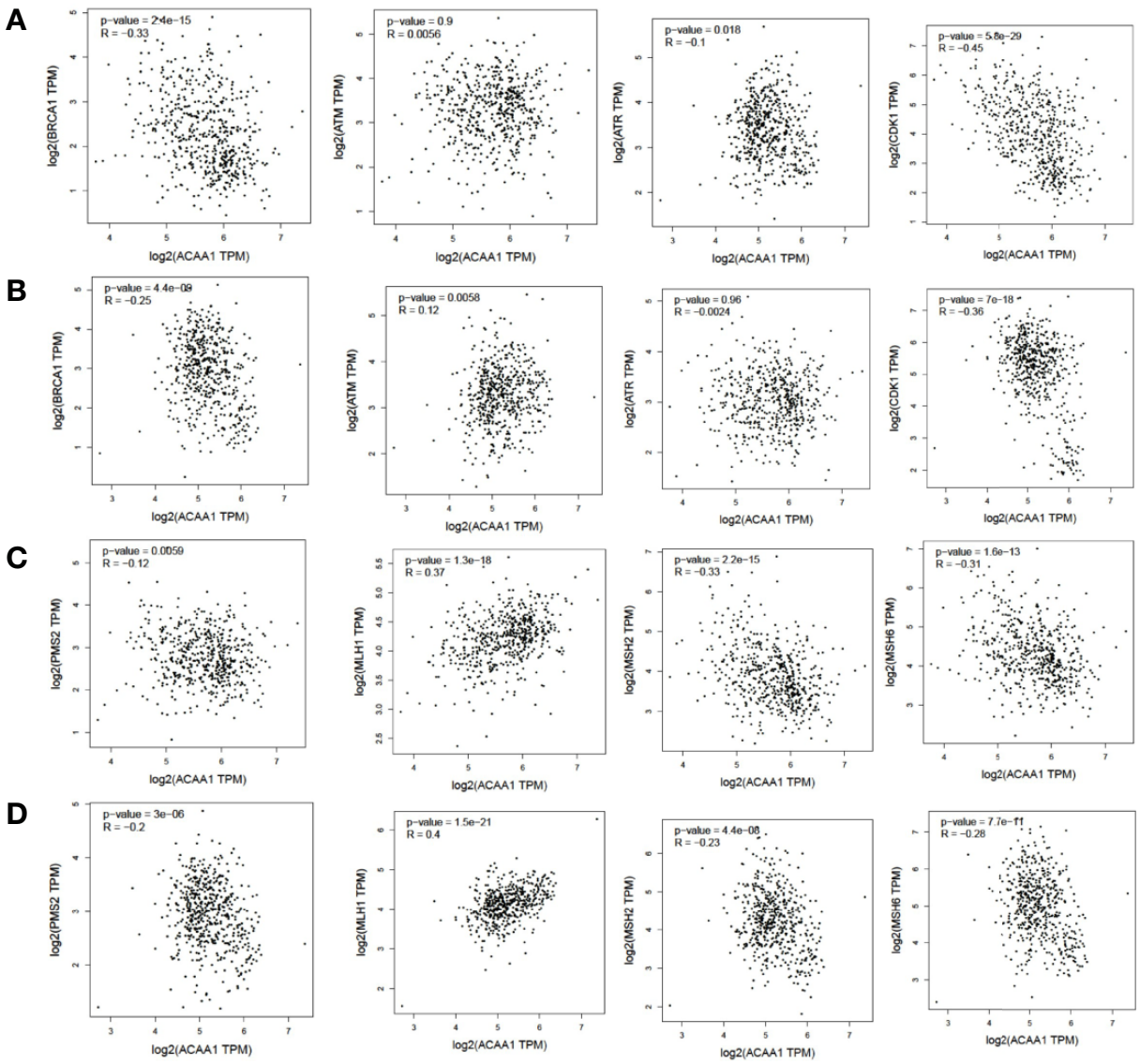


**FIGURE 2** | **(A, C)** In lung adenocarcinoma (LUAD), ACAA1 is correlated with BRCA1 (r= -0.33, p=2.4e-15), ATM (r= -0.0056, p=0.9), ATR (r= -0.1, p=0.015), CDK1 (r= -0.45, p=5.5e-29), PMS2 (r= -0.12, p=0.0059), MLH1 (r= 0.37, p=1.3e-18), MSH2 (r= -0.33, p=2.2e-15), and MDH6 (r= -0.31, p=1.6e-13). **(B, D)** In lung squamous carcinoma (LUSC), ACAA1 is correlated with BRCA1 (r= -0.25 p=4.4e-9), ATM(r= 0.12, p=0.0058), ATR (r= -0.0024, p=0.96), CDK1 (r= -0.36, p=7e-18), PMS2 (r= -0.2, p=3e-6), MLH1 (r= 0.4, p=1.5e-21), MSH2 (r= -0.23, p=4.4e-8), and MDH6 (r= -0.26, p=7.7e-11).

## ACAA1 Is a Biomarker of T Cell Exhaustion in LUSC

The results presented above indicate that $CD4^+$ T cell infiltration correlated with ACAA1, and most subsets of $CD4^+$ cells were reduced in the tumor stroma. Subsequently, we analyzed the biomarkers indicating T cell exhaustion, to clarify the relationship between ACAA1 and this dysfunction state. We plotted the correlation of ACAA1 expression and stromal biomarkers of T cell exhaustion, including PD-1 (PDCD1), CTLA4, LAG3, HAVCR2, and GZMB. Expression of ACAA1 correlated positively with HAVCR2 and GZMB, and negatively with LAG3, showing statistical significance in LUAD (**Figure 4D**). In LUSC, ACAA1 expression was positively correlated to that of PD-1(PDCD1), CTLA4, LAG3, HAVCR2, and GZMB, with statistical significance. PDCD1 is an important biomarker of T cell exhaustion (21). Up-regulated PD-1 on T cells inhibits T cell differentiation to effector T cells and promotes T cell apoptosis. A previous study showed that oncogenic KRAS increases tumor PD-L1 expression and promotes $CD8^+$ cells infiltration to the tumor stroma (22). In our study, we did not observe that KRAS mutation increased PD-L1 expression (**Supplementary Figure 1C**), nor a solid correlation of ACAA1 with PD-L1 expression in cancer cells using GEPIA (TCGA datasets) (**Supplementary Figure 1D**). More studies are needed

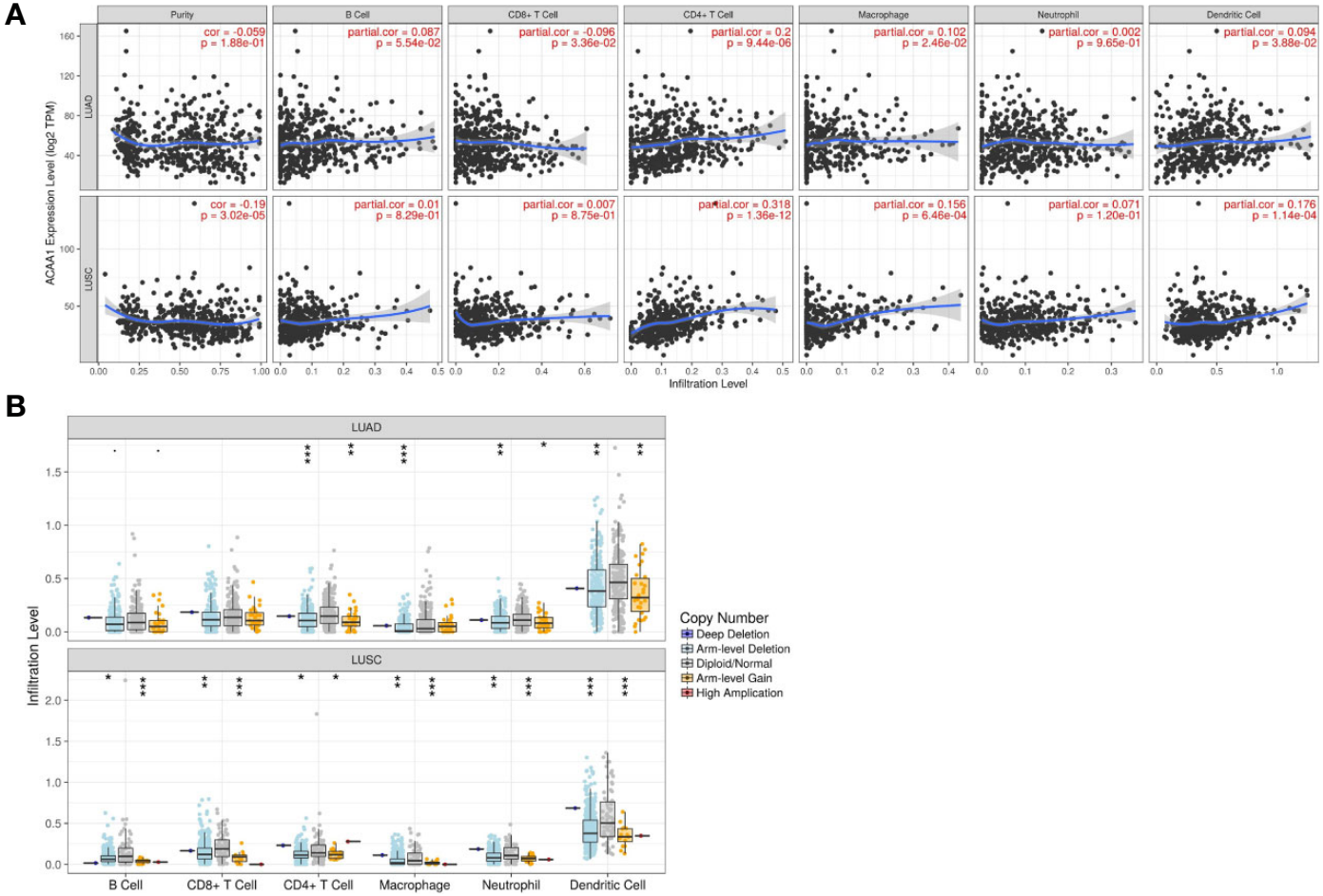


**FIGURE 3** | **(A)** ACAA1 is positively correlated with CD4$^+$ T cell in lung adenocarcinoma (LUAD) and lung squamous cancer (LUSC) with statistical significance (r=0.2, p=9.44e-06 in LUAD; and r=0.318, p=1.36e-12 in LUSC). **(B)**. Copy number variation of ACAA1 negatively correlates with CD4$^+$ cells both in LUAD and in LUSC. *p < 0.05, **p < 0.01, ***p < 0.001.

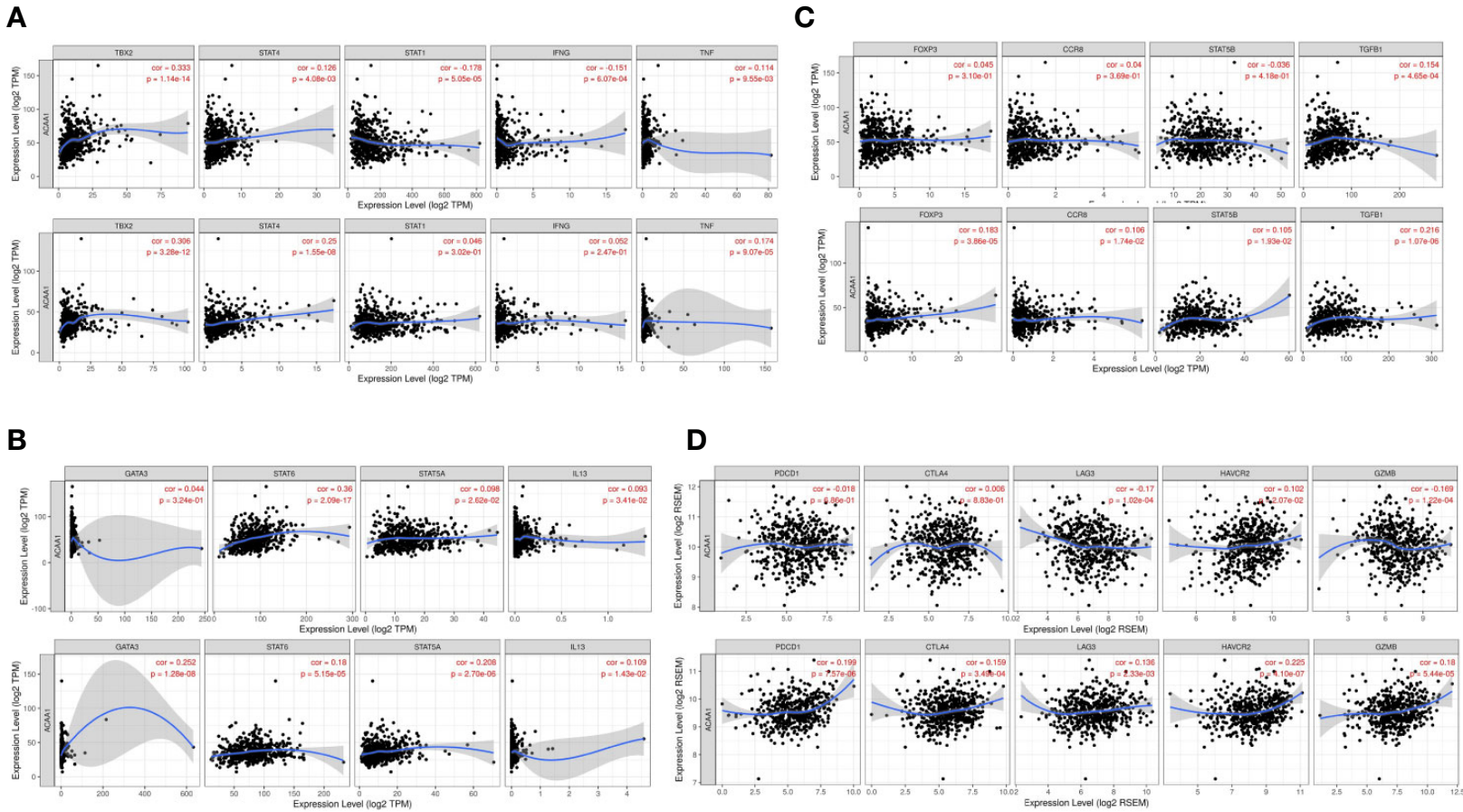


**FIGURE 4** | ACAA1 expression levels also positively correlate with **(A)** Th1 cell markers **(B)** Th2 cell markers **(C)** Treg cell markers **(D)**. ACAA1 is a biomarker of T cell exhaustion in lung squamous cancer (LUSC).

to confirm their co-expression pattern. Nevertheless, ACAA1 seems to have different roles in LUSC and LUAD. In fact, in LUAD, ACAA1 did not show a consistent co-expression pattern with T cell exhaustion markers.

## ACAA1 Is a Predictive Factor of Survival in a Wide Range of Cancer Types

ACAA1 was associated with immune cells infiltration and T cell polarization. Lastly, we investigated whether ACAA1 was a predictive factor of OS (**Figure 5A–M**) and PFS (**Supplementary Figures 2** and **3**). To this aim, we searched the survival data on Kaplan-Meier Plotter Database, which automatically generated the survival plots. ACAA1 significantly correlated with 13 out of 20 types of cancer, including bladder cancer, breast cancer, head-neck cancer, kidney renal cancer, kidney papillary cancer, liver cancer (hepatocyte carcinoma), lung cancer (lung adenocarcinoma), pheochromocytoma and paraganglioma, sarcoma, thymoma, thyroid carcinoma, uterine corpus endometrial carcinoma, and rectum adenocarcinoma. Cancers with higher ACAA1 expression level displayed higher overall survival, while those with reduced ACAA1 expression had worst outcomes. Collectively, these findings suggest that ACAA1 acts as a tumor suppressor in many types of cancers, possibly by altering the nutrient configuration and immune suppression.

# DISCUSSION

Recent studies indicated that NSCLC harboring KRAS mutation show higher clinical response rate to and efficacy of PD-1/PD-L1 blockade (22, 23). However, the potential underlying mechanisms are still obscure. Our study suggests that oncogenic KRAS suppresses ACAA1 expression through MAPK signaling pathway. We found that ACAA1 positively correlates with $CD4^+$ cell infiltration and T cell exhaustion. Moreover, reduced ACAA1 expression is associated with lower overall survival in various types of cancer, indicating that ACAA1 acts as a tumor suppressor in a wide range of malignancies. Oncogenic KRAS enhances immune checkpoint inhibitor efficacy by providing an inflammatory tumor microenvironment (24). Additionally, oncogenic KRAS also increases tumor PD-L1 expression and promotes $CD8^+$ cells infiltration into the tumor stroma (22). Moreover, NSCLC harboring KRAS mutation present a higher tumor mutation burden, leading to tumor immunogenicity. Here, we found that ACAA1 was positively correlated with $CD4^+$ cell infiltration. Copy number variation of ACAA1 also pointed to lower abundance of $CD4^+$ in the tumor microenvironment. Although the impact of ACAA1 mutation on cancer has not been thoroughly investigated yet, these results partially demonstrate that ACAA1 functionally recruits immune cells to the tumor microenvironment.

The mean TMB and the proportion of patients with a TMB >10 or >20 mut/Mb is significantly higher for KRAS-mutated patients (10.3 mut/Mb) than for EGFR, ALK, ROS1 or MET exon 14-mutated patients (3.1 to 6.2 mut/Mb) (25). The higher mutation burden of KRAS mutant lung cancer may be due to the higher proportion of smokers among the patients presenting this type of cancer (26). However, whether the occurring KRAS mutation simply coincides with other genetic mutations or is the direct cause of the downstream DNA instability remains unknown. One potential mechanism by which oncogenic KRAS could regulate tumor mutation burden is *via* promoting fatty acid accumulation in tumor cells (27). A former study showed that oncogenic KRAS induces fatty acid synthase (FASN) to enhance lipogenesis with a specific lipid signature in lung adenocarcinoma (28). KRAS also activates ERK2 protein by upregulating ERK1. Consistently, FASN inhibition blocks cellular proliferation of KRAS-driven lung cancer cells. Importantly, saturated fatty acids play a negative role in DDR by compromising the induction of p21 and Bax expression in response to double-strand breaks and ssDNA. Moreover, saturated fatty acids appear to regulate p21 and Bax expression *via* Atr-p53-dependent and -independent pathways (28). ACAA1 transfers acetyl-CoA to fatty acids and provides substrates to the TCA cycle. Therefore, downregulated ACAA1 expression may result in accumulation of fatty acids in cancer cells, consequently leading to DNA instability.

Nonetheless, how ACAA1 mediates immune cell infiltration, as well as whether this phenomenon is causally related to ACAA1 expression or just coincidental, was still unknown. If there were a causal relationship, an appropriate explanation to it would be that metabolic shifts in tumor cells might alter the nutrient configuration in tumor stroma. Tumor cells and immune cells interact with each other through microenvironmental nutrient competition (29–31). Cancer cells utilize glycolysis as their predominant energy source, a biological phenomenon called "Warburg effect". Nutrient competition between cancer cells and immune cells extends the function of Warburg effect to a cell-extrinsic advantage. Warburg effect promotes depletion of extracellular glucose in the tumor microenvironment, which renders tumor-infiltrating T cells dysfunctional. Glucose in the tumor stroma is reduced due to the increased glycolysis within tumor cells, which restricts glucose availability to T cells and leads to their dysfunction (32). Tumor cells produce and secrete lactic acid into the tumor microenvironment. In addition to glucose metabolism, amino acid and fatty acid metabolism also change in tumor cells. Importantly, all these metabolites affect T cell polarization. Oxidative phosphorylation (OXPHOS) and fatty acid oxidation (FAO) fuel Treg cells. Memory T cells rely on FAO, while activated Tregs primarily depend on glycolysis and fatty acid synthesis. Nutrient availability in the tumor microenvironment favors different subtypes of T cells (33). ACAA1 was recently also implicated in regulating infiltration of T cell subtypes in the tumor stroma. Yang and colleagues reported that the anti-tumor response of mouse $CD8^+$ T cells can be potentiated by modulating cholesterol metabolism. They found that, in mice, inhibition of acetyl-CoA acetyltransferase 1 (Acat1) in $CD8^+$ T cells restores their antitumor effect and reduces cancer progression and metastasis (34). Following $CD8^+$ T cell activation, the mRNA levels of a subset of genes involved in cholesterol biosynthesis and

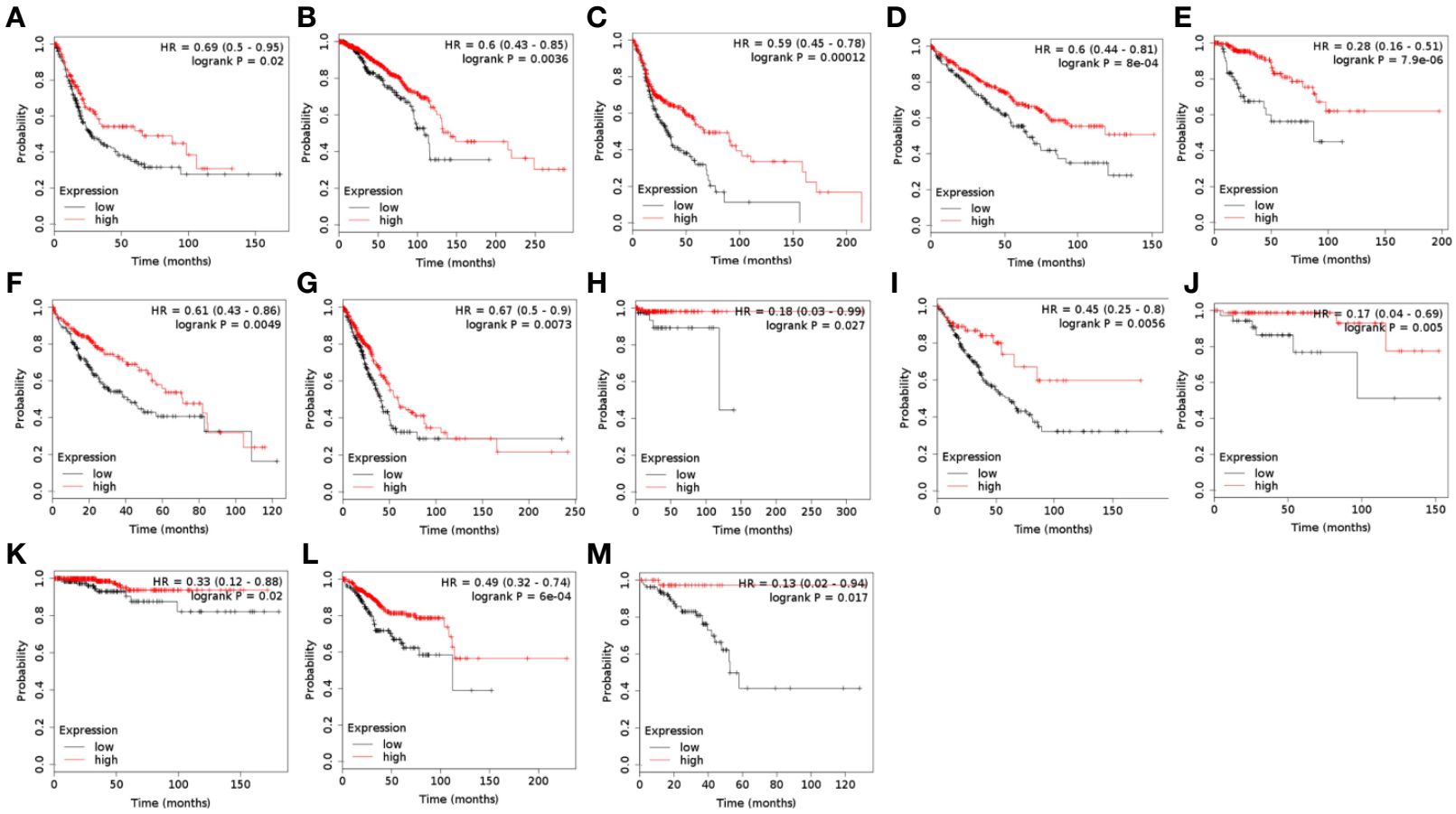


**FIGURE 5** | ACAA1 is a predictive factor for survival in a wide range of cancer types. **(A)** Bladder cancer. **(B)** Breast cancer. **(C)** Head-neck cancer. **(D)** Kidney renal cancer. **(E)** Kidney papillary cancer. **(F)** Liver cancer. **(G)** Lung cancer. **(H)** Pheochromocytoma and Paraganglioma. **(I)** Sarcoma **(J)** Thymoma. **(K)**Thyroid carcinoma. **(L)** Uterine corpus endometrial carcinoma. **(M)** Rectum adenocarcinoma.

transport pathways are upregulated, while genes implicated in the cholesterol efflux pathway are downregulated. Acat1 (ACAA1 in our study) mRNA levels are significantly upregulated at early time points, when $CD8^+$ cells are activated. Moreover, inhibitors targeting Acat1 could restore $CD8^+$ cell function, and a combination of PD-1/PD-L1 antibody and Acat1 inhibitor demonstrated greater efficacy than the single agents. Interestingly, Patsoukis and colleagues showed that PD-1 preserves effector T-cell function by inhibiting glycolysis and promoting fatty acid oxidation in $CD4^+$ T cells through carnitine palmitoyltransferase I (CPT1A) (35). Besides predicting the efficacy of PD-1/PD-L1 inhibition, Zhang et al. reported that the ACAA1 expression level was negatively correlated to several inhibitors, including Scr inhibitor (AZD0530), MEK1/2 inhibitor (AZD6244), EGFR inhibitor (Erlotinib), HER inhibitor (Lapatinib), and VEGFR2/3 inhibitor (ZD-6474) (36). Their findings reaffirmed the important role of ACAA1in predicting therapeutic efficacy.

More studies are needed to demonstrate nutrient competition between tumor cells and immune cells. *In vitro* metabolic analysis can improve our understanding of the metabolic phenotypes specific of tumor cells and immune cells, and how they interact with each other. However, the information provided by *in vitro* studies may not be generalizable *in vivo*. The metabolic phenotype of nutrient competition relies on the supply of related fuels, such as glucose, amino acids, and fatty acids, which are certainly present at lower concentrations *in vivo* than in laboratory culture conditions. The consequence of the limited supply of these fuels in a discrete immune microenvironment in the body is likely a change in metabolic as well as nutrition-sensitive signaling pathways that affect the fate and function of immune cells. The lack of research tools for measuring nutrient distribution at the single-cell level also severely hinders our understanding of when and where nutrients are available in the body. Therefore, elucidating how nutrient supply affects immune cell metabolism and tumor-stroma interactions remains a major challenge in the field of immune metabolism.

The function of ACAA1 is to provide substrates entering the TCA cycle to fuel the cell. Suppression of ACAA1 might therefore lead to reduced activity of this cycle. The TCA cycle is a series of critical reaction used by all aerobic organisms. The main metabolic shift in solid tumors known as Warburg effect refers to the preferable use of glycolysis in cancer cells to gain fuel, instead of the more effective pathway of oxidative phosphorylation (37). By generating and secreting lactate into the tumor microenvironment, tumor cells provide acidic and hypoxic conditions to the tumor stroma and increase the nutritional pressure on effector T cells (38). Consequently, metabolites from tumor cells accumulate in the tumor microenvironment and lead to T cell metabolic switch, resulting in T cell dysfunction and exhaustion (39).

## CONCLUSION

Here, we showed that decreased ACAA1 expression correlates with poor prognosis and decreased immune infiltration of $CD4^+$ T cells in LUAD and LUSC, and predicts T cell exhaustion in LUSC. As ACAA1 catalyzes fatty acid entry into the TCA cycle, we speculate that this phenotype could be due to nutrient competition between cancer cells and immune infiltrates. Nevertheless, clinical cohort is inevitable in validation the predictive power of this marker and the exact mechanism warrants further investigation.

## DATA AVAILABILITY STATEMENT

The datasets presented in this study can be found in online repositories. The names of the repository/repositories and accession number(s) can be found in the article/ **Supplementary Material**.

## AUTHOR CONTRIBUTIONS

WS provided the general idea. HF did the analysis and wrote the manuscript. All authors contributed to the article and approved the submitted version.

## FUNDING

The study was kindly granted by Sanming Project of Medicine in Shenzhen (No. SZSM201612023).

## ACKNOWLEDGMENTS

We would like to thank Dr. Chihan Li from the Chinese University of Hong Kong for his helpful suggestions.

## SUPPLEMENTARY MATERIAL

The Supplementary Material for this article can be found online at: https://www.frontiersin.org/articles/10.3389/fonc.2020.564796/full#supplementary-material

**SUPPLEMENTARY FIGURE 1 | (A)** $KRAS^{G13D}$ by knockdown efficiency by siRNA using q-PCR. **(B)** No significant correlation of ACAA1 to Th17 cells in LUAD and LUSC. **(C)** KRAS mutation did not increase PD-L1 expression. **(D)** No solid correlation of ACAA1 with PD-L1 expression in cancer cells using GEPIA database analysis.

**SUPPLEMENTARY FIGURE 2 |** ACAA1 was not a predictive factor of PFS. **(A)** Bladder Carcinoma **(B)** Breast cancer **(C)** Cervical squamous cell carcinoma **(D)** Esophageal Adenocarcinoma **(E)** Esophageal Squamous Cell Carcinoma **(F).** Head-neck squamous cell carcinoma **(G)** Kidney renal clear cell carcinoma **(H)**. Kidney renal papillary cell carcinoma **(I).** Liver hepatocellular carcinoma **(J)** Lung adenocarcinoma.

**SUPPLEMENTARY FIGURE 3 |** ACAA1 was not a predictive factor of PFS. **(A)** Lung squamous cell carcinoma **(B)**. Ovarian cancer **(C)** Pancreatic ductal adenocarcinoma. **(D)** Pheochromocytoma and Paraganglioma. **(E)** Rectum adenocarcinoma **(F).** Sarcoma **(G)** Stomach adenocarcinoma **(H)**Testicular Germ Cell Tumor **(I).**Thyroid carcinoma **(J)** Uterine corpus endometrial carcinoma.

**SUPPLEMENTARY FIGURE 4 |** ACAA1 was not a predictive factor of OS in the following types of cancers. **(A)** Cervical squamous cell carcinoma **(B)** Esophageal Adenocarcinoma **(C)** Esophageal Squamous Cell Carcinoma **(D)** Ovarian cancer **(E).** Pancreatic ductal adenocarcinoma **(F)** Stomach adenocarcinoma **(G)** Testicular Germ Cell Tumor.

## REFERENCES


1. Siegel RL, Miller KD, Jemal A. Cancer statistics, 2019. *CA: Cancer J Clin* (2019) 69(1):7–34. doi: 10.3322/caac.21551
2. Ding L, Getz G, Wheeler DA, Mardis ER, McLellan MD, Cibulskis K, et al. Somatic mutations affect key pathways in lung adenocarcinoma. *Nature* (2008) 455(7216):1069–75. doi: 10.1038/nature07423
3. Dias Carvalho P, Guimaraes CF, Cardoso AP, Mendonca S, Costa AM, Oliveira MJ, et al. KRAS Oncogenic Signaling Extends beyond Cancer Cells to Orchestrate the Microenvironment. *Cancer Res* (2018) 78(1):7–14. doi: 10.1158/0008-5472.can-17-2084
4. Zdanov S, Mandapathil M, Abu Eid R, Adamson-Fadeyi S, Wilson W, Qian J, et al. Mutant KRAS Conversion of Conventional T Cells into Regulatory T Cells. *Cancer Immunol Res* (2016) 4(4):354–65. doi: 10.1158/2326-6066.cir-15-0241
5. Tran E, Robbins PF, Lu Y-C, Prickett TD, Gartner JJ, Jia L, et al. T-Cell Transfer Therapy Targeting Mutant KRAS in Cancer. *New Engl J Med* (2016) 375(23):2255–62. doi: 10.1056/NEJMoa1609279
6. Hieronymus H, Murali R, Tin A, Yadav K, Abida W, Moller H, et al. Tumor copy number alteration burden is a pan-cancer prognostic factor associated with recurrence and death. *eLife* (2018) 7:e37294. doi: 10.7554/eLife.37294
7. Cao D, Xu H, Xu X, Guo T, Ge W. High tumor mutation burden predicts better efficacy of immunotherapy: a pooled analysis of 103078 cancer patients. *Oncoimmunology* (2019) 8(9):e1629258. doi: 10.1080/2162402x.2019.1629258
8. Stutvoet TS, Kol A, de Vries EG, de Bruyn M, Fehrmann RS, Terwisscha van Scheltinga AG, et al. MAPK pathway activity plays a key role in PD-L1 expression of lung adenocarcinoma cells. *J Pathol* (2019) 249(1):52–64. doi: 10.1002/path.5280
9. Bedognetti D, Roelands J, Decock J, Wang E, Hendrickx W. The MAPK hypothesis: immune-regulatory effects of MAPK-pathway genetic dysregulations and implications for breast cancer immunotherapy. *Emerg Topics Life Sci* (2017) 1(5):429–45. doi: 10.1042/etls20170142
10. Ebert PJR, Cheung J, Yang Y, McNamara E, Hong R, Moskalenko M, et al. MAP Kinase Inhibition Promotes T Cell and Anti-tumor Activity in Combination with PD-L1 Checkpoint Blockade. *Immunity* (2016) 44 (3):609–21. doi: 10.1016/j.immuni.2016.01.024
11. Kumar A, Shiloach J, Betenbaugh MJ, Gallagher EJ. The beta-3 adrenergic agonist (CL-316,243) restores the expression of down-regulated fatty acid oxidation genes in type 2 diabetic mice. *Nutr Metab (Lond)* (2015) 12:8–. doi: 10.1186/s12986-015-0003-8
12. Nwosu ZC, Battello N, Rothley M, Pioronska W, Sitek B, Ebert MP, et al. Liver cancer cell lines distinctly mimic the metabolic gene expression pattern of the corresponding human tumours. *J Exp Clin Cancer Res CR* (2018) 37(1):211. doi: 10.1186/s13046-018-0872-6
13. Li T, Fan J, Wang B, Traugh N, Chen Q, Liu JS, et al. TIMER: A Web Server for Comprehensive Analysis of Tumor-Infiltrating Immune Cells. *Cancer Res* (2017) 77(21):e108–e10. doi: 10.1158/0008-5472.can-17-0307
14. Pan JH, Zhou H, Cooper L, Huang JL, Zhu SB, Zhao XX, et al. LAYN Is a Prognostic Biomarker and Correlated With Immune Infiltrates in Gastric and Colon Cancers. *Front Immunol* (2019) 10:6:6. doi: 10.3389/fimmu.2019.00006
15. Tang Z, Li C, Kang B, Gao G, Zhang Z. GEPIA: a web server for cancer and normal gene expression profiling and interactive analyses. *Nucleic Acids Res* (2017) 45(W1):W98–W102. doi: 10.1093/nar/gkx247
16. Saito S, Espinoza-Mercado F, Liu H, Sata N, Cui X, Soukiasian HJ. Current status of research and treatment for non-small cell lung cancer in never-smoking females. *Cancer Biol Ther* (2017) 18(6):359–68. doi: 10.1080/15384047.2017.1323580
17. Goodman AM, Kato S, Bazhenova L, Patel SP, Frampton GM, Miller V, et al. Tumor Mutational Burden as an Independent Predictor of Response to Immunotherapy in Diverse Cancers. *Mol Cancer Ther* (2017) 16(11):2598–608. doi: 10.1158/1535-7163.mct-17-0386
18. Dobrzanski M. Expanding Roles for CD4 T Cells and Their Subpopulations in Tumor Immunity and Therapy. *Front Oncol* (2013) 3(63):26–63. doi: 10.3389/fonc.2013.00063
19. Woo EY, Yeh H, Chu CS, Schlienger K, Carroll RG, Riley JL, et al. Cutting edge: Regulatory T cells from lung cancer patients directly inhibit autologous T cell proliferation. *J Immunol (Baltimore Md 1950)* (2002) 168(9):4272–6. doi: 10.4049/jimmunol.168.9.4272
20. Akimova T, Zhang T, Negorev D, Singhal S, Stadanlick J, Rao A, et al. Human lung tumor FOXP3+ Tregs upregulate four "Treg-locking" transcription factors. *JCI Insight* (2017) 2(16):e94075. doi: 10.1172/jci.insight.94075
21. Wherry EJ, Kurachi M. Molecular and cellular insights into T cell exhaustion. *Nat Rev Immunol* (2015) 15(8):486–99. doi: 10.1038/nri3862
22. Liu C, Zheng S, Jin R, Wang X, Wang F, Zang R, et al. The superior efficacy of anti-PD-1/PD-L1 immunotherapy in KRAS-mutant non-small cell lung cancer that correlates with an inflammatory phenotype and increased immunogenicity. *Cancer Lett* (2020) 470:95–105. doi: 10.1016/j.canlet.2019.10.027
23. Passiglia F, Cappuzzo F, Alabiso O, Bettini AC, Bidoli P, Chiari R, et al. Efficacy of nivolumab in pre-treated non-small-cell lung cancer patients harbouring KRAS mutations. *Br J Cancer* (2019) 120(1):57–62. doi: 10.1038/s41416-018-0234-3
24. Dias Carvalho P, Machado AL, Martins F, Seruca R, Velho S. Targeting the Tumor Microenvironment: An Unexplored Strategy for Mutant KRAS Tumors. *Cancers* (2019) 11(12). doi: 10.3390/cancers11122010
25. Berland L, Heeke S, Humbert O, Macocco A, Long-Mira E, Lassalle S, et al. Current views on tumor mutational burden in patients with non-small cell lung cancer treated by immune checkpoint inhibitors. *J Thorac Dis* (2019) 11 (Suppl 1):S71–80. doi: 10.21037/jtd.2018.11.102
26. Galuppini F, Dal Pozzo CA, Deckert J, Loupakis F, Fassan M, Baffa R. Tumor mutation burden: from comprehensive mutational screening to the clinic. *Cancer Cell Int* (2019) 19(1):209. doi: 10.1186/s12935-019-0929-4
27. Zeng L, Wu G-Z, Goh KJ, Lee YM, Ng CC, You AB, et al. Saturated fatty acids modulate cell response to DNA damage: implication for their role in tumorigenesis. *PloS One* (2008) 3(6):e2329–e. doi: 10.1371/journal.pone.0002329
28. Gouw AM, Eberlin LS, Margulis K, Sullivan DK, Toal GG, Tong L, et al. Oncogene KRAS activates fatty acid synthase, resulting in specific ERK and lipid signatures associated with lung adenocarcinoma. *Proc Natl Acad Sci U States America* (2017) 114(17):4300–5. doi: 10.1073/pnas.1617709114
29. Gupta S, Roy A, Dwarakanath BS. Metabolic Cooperation and Competition in the Tumor Microenvironment: Implications for Therapy. *Front Oncol* (2017) 7:68. doi: 10.3389/fonc.2017.00068
30. Chang C-H, Qiu J, O'Sullivan D, Michael D B, Noguchi T, Curtis Jonathan D, et al. Metabolic Competition in the Tumor Microenvironment Is a Driver of Cancer Progression. *Cell* (2015) 162(6):1229–41. doi: 10.1016/j.cell.2015.08.016
31. Lyssiotis CA, Kimmelman AC. Metabolic Interactions in the Tumor Microenvironment. *Trends Cell Biol* (2017) 27(11):863–75. doi: 10.1016/j.tcb.2017.06.003
32. Sukumar M, Roychoudhuri R, Restifo Nicholas P. Nutrient Competition: A New Axis of Tumor Immunosuppression. *Cell* (2015) 162(6):1206–8. doi: 10.1016/j.cell.2015.08.064
33. Yin Z, Bai L, Li W, Zeng T, Tian H, Cui J. Targeting T cell metabolism in the tumor microenvironment: an anti-cancer therapeutic strategy. *J Exp Clin Cancer Res* (2019) 38(1):403. doi: 10.1186/s13046-019-1409-3
34. Yang W, Bai Y, Xiong Y, Zhang J, Chen S, Zheng X, et al. Potentiating the antitumour response of CD8(+) T cells by modulating cholesterol metabolism. *Nature* (2016) 531(7596):651–5. doi: 10.1038/nature17412
35. Patsoukis N, Bardhan K, Chatterjee P, Sari D, Liu B, Bell LN, et al. PD-1 alters T-cell metabolic reprogramming by inhibiting glycolysis and promoting

lipolysis and fatty acid oxidation. *Nat Commun* (2015) 6:6692–. doi: 10.1038/ncomms7692
36. Zhang X, Yang H, Zhang J, Gao F, Dai L. HSD17B4, ACAA1, and PXMP4 in Peroxisome Pathway Are Down-Regulated and Have Clinical Significance in Non-small Cell Lung Cancer. *Front Genet* (2020) 11:273. doi: 10.3389/fgene.2020.00273
37. Alfarouk KO, Verduzco D, Rauch C, Muddathir AK, Adil HHB, Elhassan GO, et al. Glycolysis, tumor metabolism, cancer growth and dissemination. A new pH-based etiopathogenic perspective and therapeutic approach to an old cancer question. *Oncoscience* (2014) 1(12):777–802. doi: 10.18632/oncoscience.109
38. Kouidhi S, Elgaaied AB, Chouaib S. Impact of Metabolism on T-Cell Differentiation and Function and Cross Talk with Tumor Microenvironment. *Front Immunol* (2017) 8:270. doi: 10.3389/fimmu.2017.00270
39. Kouidhi S, Ben Ayed F, Benammar Elgaaied A. Targeting Tumor Metabolism: A New Challenge to Improve Immunotherapy. *Front Immunol* (2018) 9:353. doi: 10.3389/fimmu.2018.00353

**Conflict of Interest:** The authors declare that the research was conducted in the absence of any commercial or financial relationships that could be construed as a potential conflict of interest.

frontiers in Oncology

ORIGINAL RESEARCH
published: 07 July 2021
doi: 10.3389/fonc.2021.599719

# Genetic Variations in the Transforming Growth Factor-β1 Pathway May Improve Predictive Power for Overall Survival in Non-small Cell Lung Cancer

*Hong Zhang[1], Weili Wang[2], Wenhu Pi[3], Nan Bi[4], Colleen DesRosiers[5], Fengchong Kong[6], Monica Cheng[5], Li Yang[7], Tim Lautenschlaeger[5], Shruti Jolly[6], Jianyue Jin[2] and Feng-Ming (Spring) Kong[2,7]**

[1] Department of Radiation Oncology, School of Medicine, University of Maryland Baltimore, Baltimore, MD, United States, [2] Department of Radiation Oncology, Case Western Reserve University Comprehensive Cancer Center, Cleveland, OH, United States, [3] Laboratory of Cellular and Molecular Radiation Oncology, Department of Radiation Oncology, Radiation Oncology Institue of Enze Medical Health Academy, Affiliated Taizhou Hospital of Wenzhou Medical University, Taizhou, China, [4] Department of Radiation Oncology, National Cancer Center/National Clinical Research Center for Cancer/Cancer Hospital, Chinese Academy of Medical Sciences and Peking Union Medical College, Beijing, China, [5] Departments of Radiation Oncology, IU Simon Cancer Center, Indiana University School of Medicine, Indianapolis, IN, United States, [6] Michigan Medicine Radiation Oncology, University Hospital, Ann Arbor, MI, United States, [7] Department of Clinical Oncology, The University of Hong Kong-Shenzhen Hospital, Li Ka SHing Medical School, Shenzhen, China

OPEN ACCESS

**Edited by:**
Kristin Higgins,
Emory University, United States

**Reviewed by:**
Sibo Tian,
Emory University, United States
Aparna Kesarwala,
Emory University, United States

***Correspondence:**
Feng-Ming (Spring) Kong
kong0001@hku.hk;
fxk132@case.edu

**Specialty section:**
This article was submitted to Thoracic Oncology, a section of the journal Frontiers in Oncology

**Received:** 28 August 2020
**Accepted:** 12 February 2021
**Published:** 07 July 2021

**Citation:**
Zhang H, Wang W, Pi W, Bi N, DesRosiers C, Kong F, Cheng M, Yang L, Lautenschlaeger T, Jolly S, Jin J and Kong F-M (2021) Genetic Variations in the Transforming Growth Factor-β1 Pathway May Improve Predictive Power for Overall Survival in Non-small Cell Lung Cancer. Front. Oncol. 11:599719. doi: 10.3389/fonc.2021.599719

**Purpose:** Transforming growth factor-β1 (TGF-β1), a known immune suppressor, plays an important role in tumor progression and overall survival (OS) in many types of cancers. We hypothesized that genetic variations of single nucleotide polymorphisms (SNPs) in the TGF-β1 pathway can predict survival in patients with non-small cell lung cancer (NSCLC) after radiation therapy.

**Materials and Methods:** Fourteen functional SNPs in the TGF-β1 pathway were measured in 166 patients with NSCLC enrolled in a multi-center clinical trial. Clinical factors, including age, gender, ethnicity, smoking status, stage group, histology, Karnofsky Performance Status, equivalent dose at 2 Gy fractions (EQD2), and the use of chemotherapy, were first tested under the univariate Cox's proportional hazards model. All significant clinical predictors were combined as a group of predictors named "Clinical." The significant SNPs under the Cox proportional hazards model were combined as a group of predictors named "SNP." The predictive powers of models using Clinical and Clinical + SNP were compared with the cross-validation concordance index (C-index) of random forest models.

**Results:** Age, gender, stage group, smoking, histology, and EQD2 were identified as significant clinical predictors: Clinical. Among 14 SNPs, BMP2:rs235756 (HR = 0.63; 95% CI:0.42–0.93; $p = 0.022$), SMAD9:rs7333607 (HR = 2.79; 95% CI 1.22–6.41; $p = 0.015$), SMAD3:rs12102171 (HR = 0.68; 95% CI: 0.46–1.00; $p = 0.050$), and SMAD4: rs12456284 (HR = 0.63; 95% CI: 0.43–0.92; $p = 0.016$) were identified as powerful predictors of SNP. After adding SNP, the C-index

of the model increased from 84.1 to 87.6% at 24 months and from 79.4 to 84.4% at 36 months.

**Conclusion:** Genetic variations in the TGF-β1 pathway have the potential to improve the prediction accuracy for OS in patients with NSCLC.

**Keywords: machine learning, single nuclear polymorphism, overall survival, non-small cell lung cancer, TGF-β1**

## INTRODUCTION

Lung cancer is the leading cause of cancer death and the second most commonly diagnosed type of cancer in the USA. It was estimated that 235,760 new cases would be diagnosed in 2020, accounting for about 12.5% of all cancers diagnosed, and only 23% of cases are diagnosed at an early stage (1, 2). The 5-year survival rate is only about 22.6% in the USA, though there is already a 13% improvement over the last 5 years for all lung cancers (2, 3). Approximately, 83% of patients with lung cancer are identified with non-small cell cancer (NSCLC) (4), and radiation therapy (RT) is a mainstay local treatment used for all stages of the disease (5). However, the survival benefit of RT to an individual patient varies with the baseline clinical and genetic factors of each patient. Some clinical factors, such as age, stage group, and histology, have a strong correlation with the overall survival (OS) of patients with NSCLC after RT (6). There is a need for an integrated clinical and genetic model for survival prediction.

Recent studies have shown a strong correlation between transforming growth factor- β1 (TGF-β1) and OS in various types of cancer (7). TGF-β1 is a prototype of a multifunctional cytokine and plays an important role in tumor angiogenesis, stroma formation, immune suppression, carcinogenesis, tumor metastasis progression, and prognosis for patients with cancer. Single nucleotide polymorphisms (SNPs) of TGF-β1 have been significant factors for prognosis in colon and pancreatic cancers (8, 9). We hypothesized that functional SNPs of the TGF-β1 pathway genes can regulate the TGF-β1 expression level and function of the downstream pathway genes for tumor progression and the immune system of the host, thus contributing to OS in patients with NSCLC.

## MATERIALS AND METHODS

### Study Population

This study included 166 patients with inoperable stages I–III NSCLC, enrolled through prospective studies approved by the institutional review board (IRB) of participating centers. All patients signed written informed consent. Patients received definitive thoracic radiotherapy (≥55 Gy EQD2) with or without chemotherapy. All patients were treated with three-dimensional conformal RT techniques as described in previous studies (10, 11). Clinical factors, including total equivalent dose at 2 Gy fractions (EQD2), age, gender, ethnicity, smoking history, histology, stage group, Karnofsky performance score (KPS), and the use of chemotherapy, were collected prospectively.

### Selection of SNPs

We selected 14 functional SNPs present in the 11 genes responsible for the TGF-β1 pathways based on the following criteria: (1) tag SNPs in the candidate genes; (2) a minor allele frequency greater than 10%; and (3) previously reported significant findings with correlation with the outcome of RT or chemotherapy or cancer risk.

### Sample Collection and Genotyping

The buffy coat was collected from each patient before the commencement of treatment and stored at −80°C. Genomic DNA was extracted from the buffy coat using the Blood Mini Kit of Gentra® Puregene® (Qiagen, Valencia, CA) according to the protocol of the manufacturer. The concentrations of genomic DNA were measured by a Nano Drop 2000c Spectrophotometer (Nano Drop Technologies, Inc., Wilmington, DE). Quantified DNA samples were placed on a matrix-assisted laser desorption/ionization time-of-flight mass spectrometer (Sequenom, Inc., San Diego, CA) according to the protocol of the manufacturer. For pre-genotyping quality control, randomly selected samples were blindly run in duplicate or triplicate. For post-genotyping quality control, low call-rate SNPs that had a call rate of <90% in all samples or the samples that had a call rate of <90% in all SNPs were excluded from further analysis.

### Statistical Analysis

The analysis was performed with R (12), and the missing data were imputed with the most frequent values. A power analysis was performed based on the data. The Cox proportional hazards model (13) was used to carry out univariate analysis, and the random survival forest tree (14) was used to carry out multivariate analysis. For discrete clinical factors, the median survival time (MST) with 95% CIs and the 24-month survival time with 95% CIs were calculated. At first, the Cox proportional hazards model was used to estimate the hazard ratio (HR) and 95% confidence interval (CI) of each predictor. The OS and event indicator, used as the output variables, were calculated from the beginning of treatment to the last visit or death. All significant predictors ($p < 0.05$) selected from clinical factors with the univariate Cox proportional hazards model were combined as a group of predictors named "Clinical." The independence between SNPs was tested before running a multivariate model. To show the results of the independence test, the linkage disequilibrium (LD) (15) was calculated and plotted. Then, each SNP was tested with the Cox proportional hazards model. The significant SNPs were combined as a group of predictors named "SNP." Two models, *RModel1* and *RModel2*, were built as random survival forest trees on Clinical and Clinical + SNP, respectively. The

justification for using the random survival forest tree instead of the Cox proportional hazards model as the multivariate model was given that: (1) the ensemble structure of the random survival forest tree could avoid the overfitting issue, given the limited number of patients and numerous predictors used in the study; (2) the random survival forest tree could handle both categorical and continuous predictors smoothly; (3) the Cox model assumes that continuous predictor variables have linear relationships with the risk of the event occurring, which is usually not true (16).

The predictive power of *RModel1* and *RModel2* were estimated and compared in terms of the concordance index (C-index) (17) with a 3-fold cross-validation (18). The 3-fold cross-validation randomly and evenly divided the whole data set into three groups. Then, the random survival forest classifier was trained by using two groups as training data. The trained classifier was tested using the remaining group to get the evaluation metrics. In this way, three evaluation metrics could be achieved using three disparate groups as testing data, and the mean evaluation metrics were used in the evaluation.

# RESULTS

## Patient Clinical Factors

A total of 166 patients were included in this study. The death probability was 0.51 for the data. The postulated HR was set as 2. The postulated proportions of the sample size allotted to one group were 0.5. Type I error was 0.05, as stated above. The power of 166 patients was 0.7, which is less than the traditional 0.8, but it is still reasonable (19). The median age was 65.7 (64.1, 67.8) years. About 75.3% (68.7, 81.9%) patients received concurrent and adjuvant chemotherapy. The overall MST was 24.5 (19.3, 30.6) months, and the median follow-up time was 22.8 (9.2, 36.3) months. The clinical factors of the patients shown in **Table 1**, including gender ($p = 0.0084$), stage group ($p = 0.016$ for stage group 2 and $p = 0.19$ for stage group 3), smoking ($p = 0.061$ for former smokers and $p = 0.041$ for smokers), histology ($p = 0.024$ for squamous, $p = 0.022$ for large cell, and $p = 0.0018$ for other), age ($p = 0.011$), and EQD2 ($p = 0.00024$), were significant. This group of significant clinical factors was defined as Clinical. The favorable factors were female, early-stage group, no smoking, adenocarcinoma, young, and high EQD2, consistent with published studies (20). Ethnicity, the use of chemotherapy, and KPS did not show a significant correlation with survival and were not included in the multivariate analysis.

The effect of clinical factors in patients with stage III NSCLC was also tested similarly, and the results were similar to that discussed above. Detailed findings were shown in the **Supplementary File**.

## Individual SNPs and OS

The correlation of all SNPs with OS was summarized in **Table 2**. The genetic model for each SNP followed the previous publication (21). Among them, four SNPs, including BMP2:rs235756 ($p = 0.022$), SMAD9:rs7333607 ($p = 0.015$), SMAD3:rs12102171 ($p = 0.050$), and SMAD4: rs12456284 ($p = 0.016$), were significant predictors for OS. The Kaplan-Meier (KM) plots of these four SNPs are shown in **Figure 1** with *p*-values for the log-rank test listed. All *p*-values for the log-rank test were significant with the cut-off value of 0.05.

BMP2:rs235756 (HR = 0.63; 95% CI:0.42–0.93) in a recessive model showed lower risk for patients with minor allele (T). The MST increased from 22 months for patients with the wild-type (C) to 37.9 months for patients carrying the minor allele (T) (Log-rank $p = 0.020$, **Figure 1A**).

SMAD9:rs7333607 (HR = 2.79; 95% CI 1.22–6.41) in a recessive model was correlated with an increased risk of death among patients carrying the minor allele (G). Patients with minor allele (G) of this SNP had a significantly shorter MST of 7.1 months compared with 25.1 months for patients with the wild type (A) (Log-rank $p = 0.011$, **Figure 1B**).

SMAD3:rs12102171 (HR = 0.68; 95% CI: 0.46–1.00) was in a dominant model. Patients carrying the minor allele (T) had a significantly decreased risk of death. This decrease in risk resulted in an increased MST by nearly 11.8 months: from 18.8 months for those with the wild-type genotype (C) to 30.6 months for patients carrying the minor allele (T) (Log-rank $p = 0.050$, **Figure 1C**).

SMAD4: rs12456284 (HR = 0.63; 95% CI: 0.43–0.92) in a dominant model which correlated with a decreased risk of death among patients carrying the minor allele (G). These patients with the minor allele (G) of this SNP had a significantly longer MST of 32 months compared with 22 months for patients with the wild type (A) (Log-rank $p = 0.011$, **Figure 1D**).

The effect of SNPs in patients with stage III NSCLC was also tested similarly, and the results were similar to that discussed above. Detailed findings were shown in the **Supplementary File**.

## A Combined Model of Integrating *Clinical and SNP* Factors for Survival

The LD plot of 14 SNPs is shown in **Figure 2**. Most SNPs showed strong independence ($R^2 < 0.2$). The significant SNPs were independent of each other, and the multivariate analysis of each SNP was valid.

After a long-term follow-up of 18–100 months, the random forest classifier of *RModel2* with 1,000 trees trained with Clinical+SNP significantly increased the C-index compared to that of *RModel1* as shown in **Figure 3A**. For example, the C-index of *RModel1* at 24 months was 84.1%. After adding SNP as predictors, the C-index of *RModel2* increased to 87.6%. At 36 months, the C-index increased from 79.4 to 84.4%. A *t*-test was applied on the C-index of the two models, and the *p*-value was 0.003 for both models, which indicated that *RModel2* performed better than *RModel1* in terms of the C-index.

# DISCUSSION

This study analyzed the correlation with clinical outcomes in patients with several adverse genotypes, and the results suggest that the cumulative influence by multiple genetic variants within the TGF-β signaling pathways could improve the prediction accuracy for survival among patients with NSCLC after RT.

**TABLE 1 |** Selected clinical factors of NSCLC patient population.

| Factors | Cases # *n* (%) | MST, 95% CI (month) | 2 years survival, 95%CI (%) | HR (95% CI) | *P*-value |
|---|---|---|---|---|---|
| **Gender** | | | | | |
| Male | 127 (76.5) | 22.0 | 45.1 (37.2, 54.7) | | |
| Female | 39 (23.5) | 38.2 | 65.8 (53.2, 82.7) | 0.52 (0.32,0.85) | **0.0084** |
| **Ethnicity** | | | | | |
| Caucasian | 158 (95.2) | 24.5 | 50.2 (42.9, 58.7) | | |
| No Caucasian | 8 (4.8) | 25.6 | 50.0 (25.0, 100) | 0.85 (0.34,2.09) | **0.73** |
| **Stage** | | | | | |
| 1 | 32 (19.3) | 39.4 | 71.7 (57.7, 89.2) | | |
| 2 | 19 (11.4) | 14.3 | 26.3 (12.4,55.8) | 2.26 (1.16,4.38) | **0.016** |
| 3 | 115 (69.3) | 23.0 | 47.6 (39.2,57.9) | 1.39 (0.85,2.27) | **0.19** |
| **Smoking** | | | | | |
| No smoking | 6 (3.6) | NA | 83.3 (58.3,100) | | |
| Former smoker | 79 (47.6) | 23.1 | 48.1 (38.3,60.5) | 6.64 (0.92,48.03) | **0.061** |
| Smoker | 81 (48.8) | 22.0 | 47.0 (36.6,60.4) | 7.93 (1.09,57.55) | **0.041** |
| **Chemotherapy** | | | | | |
| No | 41 (24.7) | 22.0 | 48.7 (35.5,66.7) | | |
| Yes | 125 (75.3) | 25.1 | 50.3 (41.7,60.6) | 0.84 (0.55,1.28) | **0.43** |
| **Histology** | | | | | |
| Adenocarcinoma (1) | 35 (21.1) | 37.2 | 65.7 (51.7,83.5) | | |
| Squamous (2) | 56 (33.7) | 22.2 | 47.5 (35.9,62.7) | 1.91 (1.09, 3.34) | **0.024** |
| Other (3) | 75 (45.2) | 18.6 | 38.5 (27.3,54.2) | 2.42 (1.41,4.17) | **0.0014** |
| Age | | | | 1.02 (1.005,1.04) | **0.011** |
| KPS | | | | 1.00 (0.98,1.008) | **0.51** |
| EQD2 | | | | 0.97 (0.96,0.993) | **0.00024** |

*MST, median survival time; HR, hazard ratio. Bold indicate statistical significance at P value of 0.05.*

**TABLE 2 |** Genetic correlation with OS, univariate analysis (*N = 166*).

| Gene | SNP | Wild genotype# | Model* | HR for the minor allele (95%CI) | Effect of minor on survival | *P*-value |
|---|---|---|---|---|---|---|
| BMP2 | rs235756 | C (63.2%) | rec | 0.63 (0.42,0.93) | **Favorable** | **0.022** |
| ACVR2A | rs1424954 | A (34.6%) | rec | 1.72 (0.92,3.18) | Unfavorable | **0.088** |
| BMP1 | rs3857979 | C (75.9%) | rec | 1.17 (0.76,1.81) | Unfavorable | **0.47** |
| INHBC | rs4760259 | C (90.7%) | rec | 1.07 (0.58,2.01) | Unfavorable | **0.82** |
| SMAD3 | rs4776342 | A (58.8%) | add | 0.76 (0.52,1.12) | Favorable | **0.17** |
| TGFB1 | rs4803455 | A (25.9%) | dom | 1.38 (0.88,2.18) | Unfavorable | **0.16** |
| SMAD3 | rs6494633 | C (76.9%) | rec | 1.06 (0.68,1.63) | Unfavorable | **0.81** |
| SMAD7 | rs7227023 | A (0.6%) | dom | 1.11 (0.15,7.95) | Unfavorable | **0.92** |
| SMAD9 | rs7333607 | A (95.8%) | rec | 2.79 (1.22,6.41) | **Unfavorable** | **0.015** |
| SMAD1 | rs11724777 | A (69.0%) | rec | 0.76 (0.49,1.16) | Favorable | **0.20** |
| SMAD1 | rs11939979 | A (19.0%) | dom | 1.02 (0.64,1.64) | Unfavorable | **0.93** |
| SMAD3 | rs12102171 | C (62.0%) | dom | 0.68 (0.46,1.00) | **Favorable** | **0.050** |
| SMAD4 | rs12456284 | A (55.4%) | dom | 0.63 (0.43,0.92) | **Favorable** | **0.016** |
| SMAD6 | rs12913975 | A (6.8%) | dom | 1.23 (0.57,2.64) | Unfavorable | **0.60** |

*#The percentage was based on our data *Genetic model of inheritance: dom, dominant model; rec, recessive model; add, additive model. SNP, single nucleotide polymorphism. Bold indicate statistical significance at P value of 0.05.*

The survival significance of TGF-β1 pathway genomics has a biologic rationale. The TGF-β is a prototype of a multifunctional cytokine and is the ligand for the TGF-β type I and II receptors. TGF-β composes of TGF-β1, 2, 3, and other about 30 family members, including the activin/inhibin subfamily, such as BMP subfamily (Bone Morphogenetic Proteins BMPs) and the mullerian inhibitory substance (22, 23). BMPs are the intracellular signaling

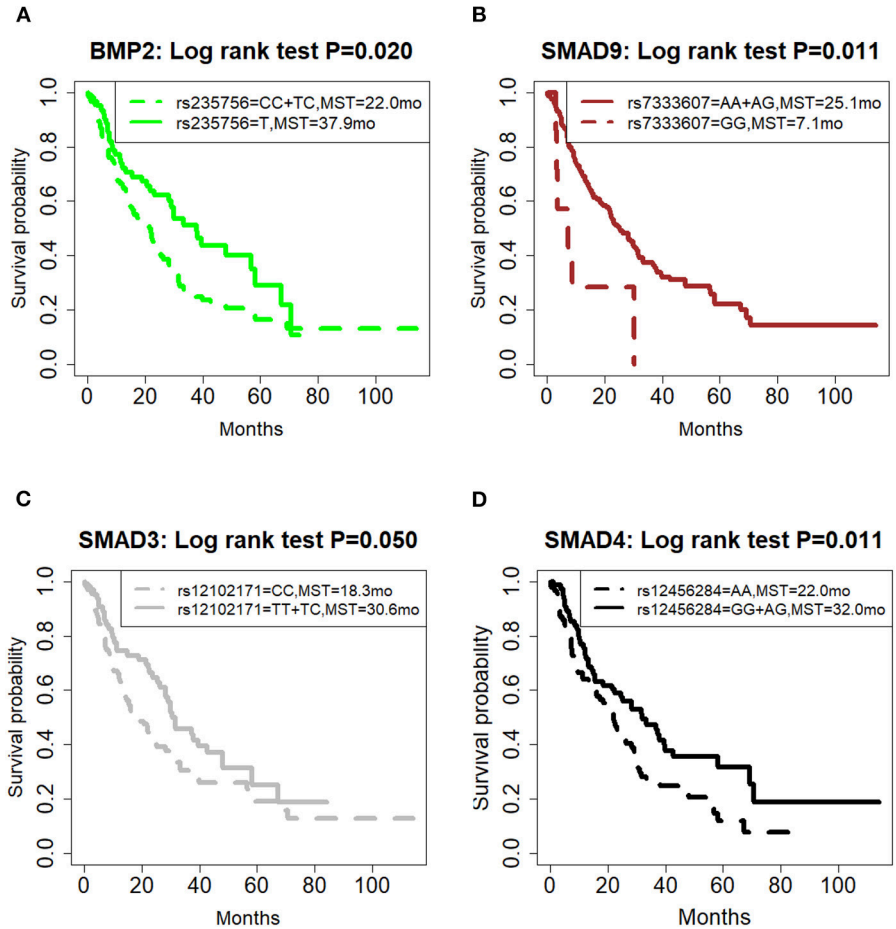


**FIGURE 1 |** Effect of genetic variation on Kaplan-Meier overall survival curve. **(A)** BMP2:rs235756; **(B)** SMAD9:rs7333607; **(C)** SMAD3:rs12102171; **(D)** SMAD4: rs12456284; MST in months. MST, median survival time.

members which can activate downstream signaling genes in TGF-β signaling pathways (24, 25). Smad proteins (Smad 1 through 9) are transcriptional regulators which are important for intracellular TGF-β signaling (26). In TGF-β signaling pathways, those subfamily genes have a similar effect on cell growth, cell proliferation and differentiation, and cell death and plays a key role in embryonic development, immune system regulation, and the duo roles of diseases, such as skeletal diseases, fibrosis, and cancer (23, 27–30). TGF-β signaling is very important in lung health and disease, regulating lung organogenesis and homeostasis, including alveolar cells and epithelial cells differentiation, fibroblast activation, and extracellular matrix organization. Whereas, TGF-β is the most potent epithelial-mesenchymal transition (EMT) inducer in NSCLC formation (31). DNA variants like SNPs can affect gene expressions and the functions of core disease-related genes (32).

The findings that SNPs in the TGF-β1 pathway genes can predict survival are clinically meaningful SNPs and consistent with the previous reports. Signature of TGF-β predicts metastasis-free survival in NSCLC (33, 34). SNPs of TGF-β1 gene have been reported to associate with OS in patients with NSCLC treated with definitive radio (chemo) therapy (35–37). The signature of a single SNP may only provide a modest or undetectable effect, whereas the amplified effects of combined SNPs in the same pathway may enhance predictive power (7, 38). In radiation, TGF-β1 may help in predicting radiation-induced lung toxicity (RILT) (39–41).

The SNPs identified in the study with prognostic values are consistent with reports from other investigators on their significance in other cancers (42–44). BMP2:rs235756 is in the downstream region of the BMP2 gene and has already been shown to alter normal BMP function. Several studies suggested that BMP2:rs235756 increased the production of the BMP protein and the concentration of serum ferritin levels, which promoted BMP signaling in cancer progression (42–44). BMP2 is highly expressed in lung cancer and is involved in regulating lung cancer angiogenesis and metastasis (45, 46). Silencing the expression of BMP-2 inhibits lung cancer cell proliferation and migration (47). BMP2:rs235756 has previously been reported as a significant biomarker for OS in patients with lung cancer (21). For patients who underwent RT, BMP2:rs235756 was shown

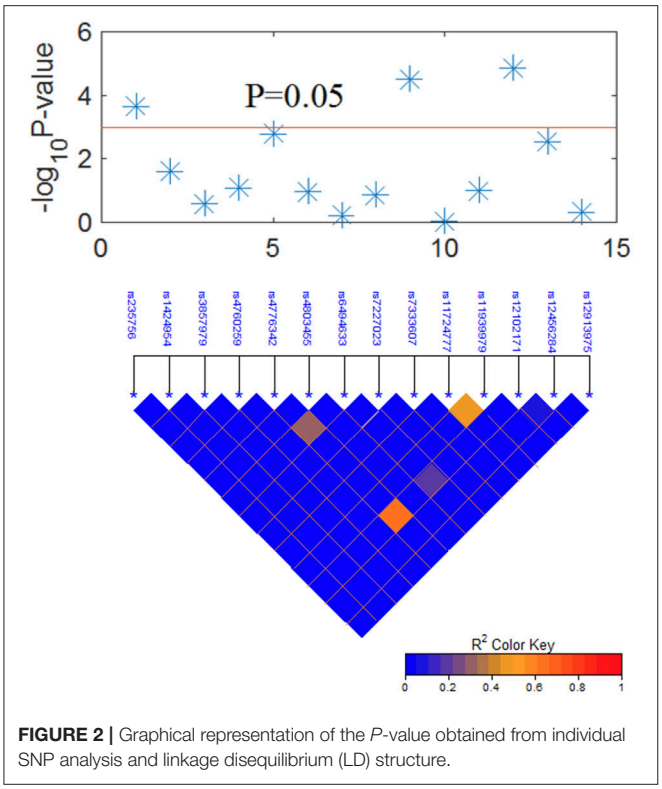


**FIGURE 2 |** Graphical representation of the *P*-value obtained from individual SNP analysis and linkage disequilibrium (LD) structure.

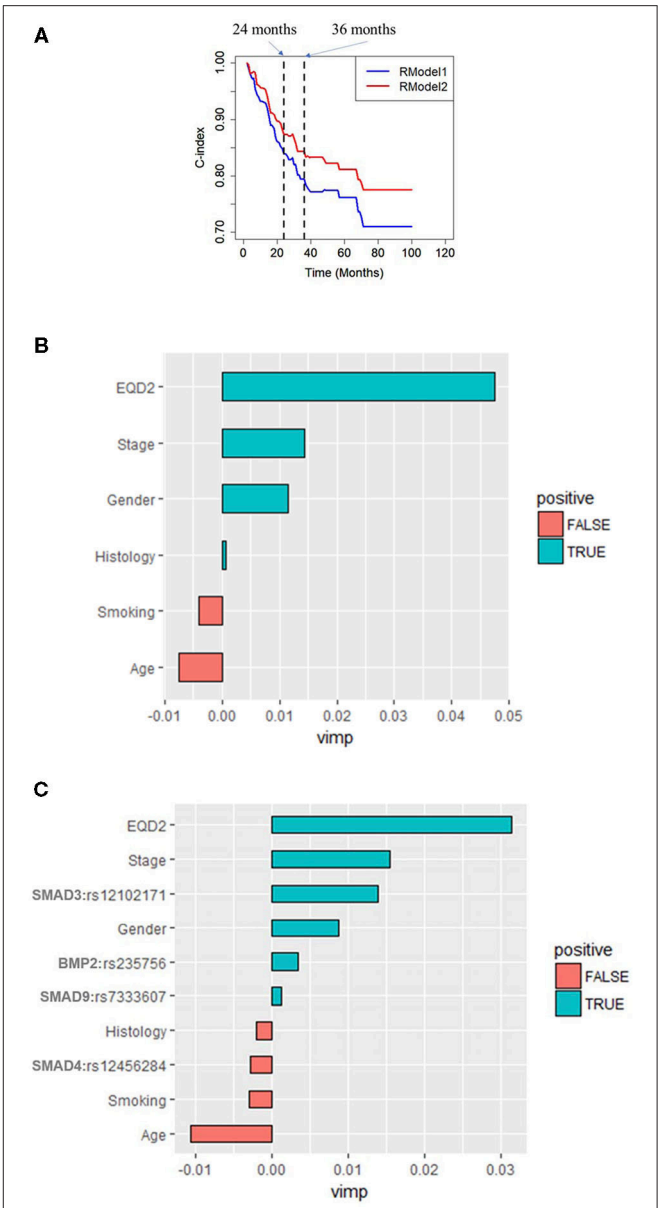


**FIGURE 3 | (A)** Time-dependent C-index of *RModel1* and *RModel2*. *RModel2* increased the C-index from 0.73 to 0.78 compared with *RModel1* at 24 months. Importance of predictors (VIMP) in the random forest for **(B)** *RModel1* and **(C)** *RModel2*. *RModel1*: a model of combining only clinical predictors. *RModel2*: a model of combining significant clinical and genetic factors.

to predict radiation pneumonitis (48), which is an important clinical outcome.

Furthermore, this study also suggested that SMAD3:rs12102171 correlated with OS in NSCLC. SMAD3:rs12102171, located in the intron region between exon3 and 4 of the SMAD3 gene, is known for its function as a mediator of TGF-β pro-fibrotic activities. Inflammatory cells and fibroblasts without smad3 do not auto-induce TGF-β, but Smad3 null mice are resistant to radiation-induced fibrosis (49). TGF-β/Smad3 signaling plays critical roles in biological processes, such as epithelial-mesenchymal transition (EMT) lung cancer cell progression and lung cancer patient survival (21, 50). That report showed a significant correlation with osteoarthritis (51). SMAD9:rs7333607 is located in the intron region of the SMAD9 gene and only correlated with lung cancer survival (21).

Smad4 belongs to the Smad gene family, acts as a mediator of TGF-β signaling pathways (26), and was classified as a tumor suppressor gene which plays important roles in maintaining tissue homeostasis and suppressing tumorigenesis (1). The loss of SMAD4 expression significantly correlated with poor OS in patients with cancers, such as pancreatic cancer, colorectal cancer, and prostate cancer (52, 53). The SNP rs12456284 locates 3′ UTR region of the Smad4 gene, was predicted to influence the potential miRNA binding, and downregulate the gene expression with Smad4 associated with gastric cancer (54). Genetic variants in the BMP/Smad4/Hamp hepcidin-regulating pathway, such as Hamp rs1882694, BMP2 rs1979855, rs3178250, and rs1980499, were associated with OS, local-regional progression-free survival, progression-free survival, and distant metastasis-free survival in patients receiving definitive RT for NSCLC but not rs12456284 (55).

In a tree analysis of the study, the variable importance (VIMP) measures the increase (or decrease) in prediction error for the forest classifier when a variable is randomly "noised-up." A large positive VIMP shows that the prediction accuracy of the forest classifier is significantly degraded when a variable is noised-up. Thus, a large VIMP shows a more predictive variable. The

VIMP of each variable in the *RModel1* and *RModel2* are listed in **Figures 3B,C**. It is shown that EQD2 and stage group were always two important predictors in the two models. SMAD3:rs12102171 was more important than other predictors, except for EQD2 and stage group, which was not reported before. BMP2:rs235756 and SMAD4: rs12456284 have a similar importance as smoking, which has been consistently shown as an important predictor in the clinical OS of patients with NSCLC. SMAD9:rs7333607 was less important and it may be overlooked should the results be validated by independent studies.

The present study has several limitations. First, this study has limited statistical power because of the small sample size in each stage group and the analysis of the limited number of SNPs. Second, the selection of the SNPs was rather arbitrary, which was limited by the published data at the start of this study. Additional SNPs candidates may be further identified; future studies can use the methodology of the study to develop better models with the inclusion of more candidates and more external validations. Although it showed the promise of genetic variation in guiding personalized medicine, the study shall be considered exploratory. The findings should be validated by an independent study population.

## CONCLUSIONS

In this study, we systematically evaluated genetic variations in the TGF-β1 pathway as predictors of the outcomes for patients with NSCLC treated with RT. Four SNPs (SMAD3:rs12102171, BMP2:rs235756, SMAD9:rs7333607, and SMAD4: rs12456284) showed strong correlations with OS in patients with NSCLC after RT. The current model improves prediction accuracy by adding genetic variations in the TGF-β1 pathway.

## DATA AVAILABILITY STATEMENT

The datasets presented in this study can be found in online repositories. The names of the repository/repositories and accession number(s) can be found below: NCBI (accession numbers are: SCV001478478–SCV001478481).

## ETHICS STATEMENT

The studies involving human participants were reviewed and approved by IRB. The patients/participants provided their written informed consent to participate in this study. Written informed consent was obtained from the individual(s) for the publication of any potentially identifiable images or data included in this article.

## AUTHOR CONTRIBUTIONS

Concept and design: JJ, HZ, and F-MK. Acquisition, analysis, or interpretation of data: HZ, WW, WP, NB, JJ, and F-MK. Drafting of the manuscript: HZ, JJ, and F-MK. Critical revision of the manuscript for important intellectual content: WW, NB, WP, FK, MC, LY, TL, and SJ. Statistical analysis: HZ, CD, and JJ. Obtained funding: F-MK. Administrative, technical, or material support: WW, WP, and NB. Study supervision: JJ and F-MK.

## FUNDING

This study was supported in parts by the National Institutes of Health (grant number R01CA142840, PI: F-MK) and Shenzhen Science and Technology grant KQTD20180411185028798 (PI: F-MK).

## SUPPLEMENTARY MATERIAL

The Supplementary Material for this article can be found online at: https://www.frontiersin.org/articles/10.3389/fonc.2021.599719/full#supplementary-material

## REFERENCES

1. Siegel RL, Miller KD, Jemal AJC. Cancer statistics, 2019 (2019) 69:7–34. doi: 10.3322/caac.21551
2. Siegel RL, Miller KD, Fuchs HE, Jemal A. Cancer statistics, 2021. *CA Cancer J Clin.* (2021) 71:7–33. doi: 10.3322/caac.21654
3. Staff A. *Cancer Facts and Figures*. Atlanta: American Cancer Society, Cancer (2018).
4. Miller KD, Siegel RL, Lin CC, Mariotto AB, Kramer JL, Rowland JH, et al. Cancer treatment and survivorship statistics, 2016. *CA Cancer J Clin.* (2016) 66:271–89. doi: 10.3322/caac.21349
5. Cheng M, Jolly S, Quarshie WO, Kapadia N, Vigneau FD, Spring Kong FM. Modern radiation further improves survival in non-small cell lung cancer: an analysis of 288,670 Patients. *J Cancer*. (2019) 10:168. doi: 10.7150/jca.26600
6. Wang W, Huang L, Jin JY, Jolly S, Zang Y, Wu H, et al. IDO immune status after chemoradiation may predict survival in lung cancer patients. *Cancer Res.* (2018) 78:809–16. doi: 10.1158/0008-5472.CAN-17-2995
7. Lin M, Stewart DJ, Spitz MR, Hildebrandt MA, Lu C, Lin J, et al. Genetic variations in the transforming growth factor-beta pathway as predictors of survival in advanced non-small cell lung cancer. *Carcinogenesis.* (2011) 32:1050–6. doi: 10.1093/carcin/bgr067
8. Bellam N, Pasche B. TGF-β signaling alterations and colon cancer. *Cancer Genetics*. (2010) 85–103.
9. Javle M, Li Y, Tan D, Dong X, Chang P, Kar S, et al. Biomarkers of TGF-β signaling pathway and prognosis of pancreatic cancer. *PloS ONE.* (2014) 9:e85942. doi: 10.1371/journal.pone.0085942
10. Chapet O, Kong FM, Quint LE, Chang AC, Ten Haken RK, Eisbruch A, et al. CT-based definition of thoracic lymph node stations: an atlas from the University of Michigan. *Int J Radiat Oncol Biol Phys.* (2005) 63:170–8. doi: 10.1016/j.ijrobp.2004.12.060
11. Kong FM, Hayman JA, Griffith KA, Kalemkerian GP, Arenberg D, Lyons S, et al. Ten Haken, Final toxicity results of a radiation-dose escalation study in patients with non-small-cell lung cancer (NSCLC): predictors for radiation pneumonitis and fibrosis. *Int J Radiat Oncol Biol Phys.* (2006) 65:1075–86. doi: 10.1016/j.ijrobp.2006.01.051
12. Team RC. *R Language Definition*. Vienna: R foundation for statistical computing (2000).

13. Lin DY, Wei L-J. The robust inference for the Cox proportional hazards model. *J Am Stat Assoc.* (1989) 84:1074–8. doi: 10.1080/01621459.1989.10478874
14. Ishwaran H, Kogalur UB, Blackstone EH, Lauer MS. Random survival forests. *Ann Appl Stat.* (2008) 2:841–60. doi: 10.1214/08-AOAS169
15. Hill W, Robertson A. Linkage disequilibrium in finite populations. *Theoret Appl Genet.* (1968) 38:226–31. doi: 10.1007/BF01245622
16. Kattan MW, Hess KR, Beck JR. Experiments to determine whether recursive partitioning (CART) or an artificial neural network overcomes theoretical limitations of Cox proportional hazards regression. *Comput Biomed Res.* (1998) 31:363–73. doi: 10.1006/cbmr.1998.1488
17. Gerds TA, Kattan MW, Schumacher M, Yu C. Estimating a time-dependent concordance index for survival prediction models with covariate dependent censoring. *Stat Med.* (2013) 32:2173–84. doi: 10.1002/sim.5681
18. Kohavi R. A study of cross-validation and bootstrap for accuracy estimation and model selection. *IJCAI.* (1995) 14:1137–45.
19. Mann M, Crouse D, Prentice E. Appropriate animal numbers in biomedical research in light of animal welfare considerations. *Lab Anim Sci.* (1991) 41:6–14.
20. Kawaguchi T, Takada M, Kubo A, Matsumura A, Fukai S, Tamura A, et al. Performance status and smoking status are independent favorable prognostic factors for survival in non-small cell lung cancer: a comprehensive analysis of 26,957 patients with NSCLC. *J Thorac Oncol.* (2010) 5:620–30. doi: 10.1097/JTO.0b013e3181d2dcd9
21. Lin M, Stewart DJ, Spitz MR, Hildebrandt MA, Lu C, Lin J, et al. Genetic variations in the transforming growth factor beta pathway as predictors of survival in advanced non-small cell lung cancer. *Carcinogenesis.* (2011) 32:1050–6. doi: 10.1158/1538-7445.AM10-1675
22. Miyazawa K, Shinozaki M, Hara T, Furuya T, Miyazono K. Two major Smad pathways in TGF-β superfamily signalling. *Genes Cells.* (2002) 7:1191–204. doi: 10.1046/j.1365-2443.2002.00599.x
23. Weiss A, Attisano L. The TGFbeta superfamily signaling pathway. *Wiley Interdiscip Rev Dev Biol.* (2013) 2:47–63. doi: 10.1002/wdev.86
24. Mueller TD, Nickel J. Promiscuity and specificity in BMP receptor activation. *FEBS Lett.* (2012) 586:1846–59. doi: 10.1016/j.febslet.2012.02.043
25. Nickel J, Mueller TD. Specification of BMP Signaling. *Cells.* (2019) 8:1579. doi: 10.3390/cells8121579
26. Massagué J. TGFβ signalling in context. *Nat Rev Mol Cell Biol.* (2012) 13:616–30. doi: 10.1038/nrm3434
27. de Caestecker MP, Piek E, Roberts AB. Role of transforming growth factor-β signaling in cancer. *J Natl Cancer Inst.* (2000) 92:1388–402. doi: 10.1093/jnci/92.17.1388
28. Zinski J, Tajer B, Mullins MC. TGF-beta family signaling in early vertebrate development. *Cold Spring Harb Perspect Biol.* (2018) 10:a033274. doi: 10.1101/cshperspect.a033274
29. Batlle E, Massague J. Transforming growth factor-beta signaling in immunity and cancer. *Immunity.* (2019) 50:924–40. doi: 10.1016/j.immuni.2019.03.024
30. MacFarlane EG, Haupt J, Dietz HC, Shore EM. TGF-beta family signaling in connective tissue and skeletal diseases. *Cold Spring Harb Perspect Biol.* (2017) 9:a038331. doi: 10.1101/cshperspect.a022269
31. Saito A, Horie M, Nagase T. TGF-beta signaling in lung health and disease. *Int J Mol Sci.* (2018) 19:2460. doi: 10.3390/ijms19082460
32. Boyle EA, Li YI, Pritchard JK. An expanded view of complex traits: from polygenic to omnigenic. *Cell.* (2017) 169:1177–86. doi: 10.1016/j.cell.2017.05.038
33. Gordian E, Welsh EA, Gimbrone N, Siegel EM, Shibata D, Creelan BC, et al. Transforming growth factor beta-induced epithelial-to-mesenchymal signature predicts metastasis-free survival in non-small cell lung cancer. *Oncotarget.* (2019) 10:810–24. doi: 10.18632/oncotarget.26574
34. Chen Y, Zou L, Zhang Y, Chen Y, Xing P, Yang W, et al. Transforming growth factor-beta1 and alpha-smooth muscle actin in stromal fibroblasts are associated with a poor prognosis in patients with clinical stage I-IIIA nonsmall cell lung cancer after curative resection. *Tumour Biol.* (2014) 35:6707–13. doi: 10.1007/s13277-014-1908-y
35. Jurisic V, Vukovic V, Obradovic J, Gulyaeva LF, Kushlinskii NE, Djordjevic N. EGFR polymorphism and survival of NSCLC patients treated with Tkis: a systematic review and meta-analysis. *J Oncol.* (2020) 2020:1973241. doi: 10.1155/2020/1973241
36. Xue SL, Zheng YH, Su HF, Deng X, Zhang XB, Zou CL, et al. Association between single nucleotide polymorphisms of the transforming growth factor-beta1 gene and overall survival in unresectable locally advanced non-small-cell lung cancer patients treated with radio (chemo) therapy in a Chinese population. *Med Oncol.* (2013) 30:512. doi: 10.1007/s12032-013-0512-0
37. Yuan ST, Ellingrod VL, Schipper M, Stringer KA, Cai X, Hayman JA, et al. Genetic variations in TGFbeta1, tPA, and ACE and radiation-induced thoracic toxicities in patients with non-small-cell lung cancer. *J Thorac Oncol.* (2013) 8:208–13. doi: 10.1097/JTO.0b013e318274592e
38. Li Q, Yang J, Yu Q, Wu H, Liu B, Xiong H, et al. Associations between single-nucleotide polymorphisms in the PI3K-PTEN-AKT-mTOR pathway and increased risk of brain metastasis in patients with non-small cell lung cancer. *Clin Cancer Res.* (2013) 19:6252–60. doi: 10.1158/1078-0432.CCR-13-1093
39. Wang S, Campbell J, Stenmark MH, Zhao J, Stanton P, Matuszak MM, et al. Plasma levels of IL-8 and TGF-beta1 predict radiation-induced lung toxicity in non-small cell lung cancer: a validation study. *Int J Radiat Oncol Biol Phys.* (2017) 98:615–21. doi: 10.1016/j.ijrobp.2017.03.011
40. Kong FM, Washington MK, Jirtle RL, Anscher MS. Plasma transforming growth factor-beta 1 reflects disease status in patients with lung cancer after radiotherapy: a possible tumor marker. *Lung Cancer.* (1996) 16:47–59. doi: 10.1016/S0169-5002(96)00611-3
41. Zhao L, Sheldon K, Chen M, Yin MS, Hayman JA, Kalemkerian GP, et al. The predictive role of plasma TGF-beta1 during radiation therapy for radiation-induced lung toxicity deserves further study in patients with non-small cell lung cancer. *Lung Cancer.* (2008) 59:232–9. doi: 10.1016/j.lungcan.2007.08.010
42. Milet J, Déhais V, Bourgain C, Jouanolle AM, Mosser A, Perrin M, et al. Common variants in the BMP2, BMP4, and HJV genes of the hepcidin regulation pathway modulate HFE hemochromatosis penetrance. *Am J Hum Genet.* (2007) 81:799–807. doi: 10.1086/520001
43. An P, Wu Q, Wang H, Guan Y, Mu M, Liao Y, et al. TMPRSS6, but not TF, TFR2 or BMP2 variants are associated with increased risk of iron-deficiency anemia. *Hum Mol Genet.* (2012) 21:2124–31. doi: 10.1093/hmg/dds028
44. Ji Y, Flower R, Hyland C, Saiepour N, Faddy H. Genetic factors associated with iron storage in Australian blood donors. *Blood Transfus.* (2016) 16:123–9. doi: 10.2450/2016.0138-16
45. Langenfeld EM, Langenfeld J. Bone morphogenetic protein-2 stimulates angiogenesis in developing tumors. *Mol Cancer Res.* (2004) 2:141–9.
46. Langenfeld E, Kong Y, Langenfeld J. Bone morphogenetic protein 2 stimulation of tumor growth involves the activation of Smad-1/5. *Oncogene.* (2006) 25:685. doi: 10.1038/sj.onc.1209110
47. Chu H, Luo H, Wang H, Chen X, Li P, Bai Y, et al. Silencing BMP-2 expression inhibits A549 and H460 cell proliferation and migration. *Diagn Pathol.* (2014) 9:123. doi: 10.1186/1746-1596-9-123
48. Yang J, Xu T, Gomez DR, Yuan X, Nguyen Q-N, Jeter M, et al. Polymorphisms in BMP2/BMP4, with estimates of mean lung dose, predict radiation pneumonitis among patients receiving definitive radiotherapy for non-small cell lung cancer. *Oncotarget.* (2017) 8:43080. doi: 10.18632/oncotarget.17904
49. Flanders KC. Smad3 as a mediator of the fibrotic response. *Int J Exp Pathol.* (2004) 85:47–64. doi: 10.1111/j.0959-9673.2004.00377.x
50. Ooshima A, Park J, Kim SJ. Phosphorylation status at Smad3 linker region modulates transforming growth factor-beta-induced epithelial-mesenchymal transition and cancer progression. *Cancer Sci.* (2019) 110:481–8. doi: 10.1111/cas.13922
51. Kang B, Zhao F, Zhang X, Deng X, He X. Association between the interaction of SMAD3 polymorphisms with body mass index and osteoarthritis susceptibility. *Int J Clin Exp Pathol.* (2015) 8:7364. doi: 10.7860/JCDR/2017/22371.10073
52. Shugang X, Hongfa Y, Jianpeng L, Xu Z, Jingqi F, Xiangxiang L, et al. Prognostic value of SMAD4 in pancreatic cancer: a meta-analysis. *Transl Oncol.* (2016) 9:1–7. doi: 10.1016/j.tranon.2015.11.007

53. Ma Y, Yan F, Li L, Liu L, Sun J. Deletion and down-regulation of SMAD4 gene in colorectal cancers in a Chinese population. *Chin J Cancer Res.* (2014) 26:525–31. doi: 10.3978/j.issn.1000-9604.2014.09.02
54. Wu D-M, Zhu H-X, Zhao Q-H, Zhang Z-Z, Wang S-Z, Wang M-L, et al. Genetic variations in the SMAD4 gene and gastric cancer susceptibility. *World J Gastroenterol.* (2010) 16:5635. doi: 10.3748/wjg.v16.i44.5635
55. Yang J, Xu T, Gomez DR, Yuan X, Nguyen QN, Jeter M, et al. Nomograms incorporating genetic variants in BMP/Smad4/Hamp pathway to predict disease outcomes after definitive radiotherapy for non-small cell lung cancer. *Cancer Med*. (2018) 7:2247–55. doi: 10.1002/cam4.1349

**Conflict of Interest:** The authors declare that the research was conducted in the absence of any commercial or financial relationships that could be construed as a potential conflict of interest.

frontiers in Oncology

ORIGINAL RESEARCH
published: 26 July 2021
doi: 10.3389/fonc.2021.672916

# Correlation Between Early Endpoints and Overall Survival in Non-Small-Cell Lung Cancer: A Trial-Level Meta-Analysis

*Khader Shameer[1]*, Youyi Zhang[1], Dan Jackson[2], Kirsty Rhodes[2], Imran Khan A. Neelufer[3], Sreenath Nampally[1], Andrzej Prokop[4], Emmette Hutchison[5], Jiabu Ye[6], Vladislav A. Malkov[1], Feng Liu[6], Antony Sabin[2], Jim Weatherall[3], Cristina Duran[5], Renee Bailey Iacona[6], Faisal M. Khan[1] and Pralay Mukhopadhyay[6]*

[1] Data Science and Artificial Intelligence, BioPharmaceuticals Research and Development (R&D), AstraZeneca, Gaithersburg, MD, United States, [2] Oncology Biometrics, Oncology Research and Development, AstraZeneca, Cambridge, United Kingdom, [3] Data Science and Artificial Intelligence, BioPharmaceuticals Research and Development, AstraZeneca, Macclesfield, United Kingdom, [4] Oncology Biometrics, Oncology Research and Development, AstraZeneca, Warsaw, Poland, [5] Digital Health, Oncology Research and Development, AstraZeneca, Cambridge, United Kingdom, [6] Oncology Biometrics, Oncology R&D, AstraZeneca, Gaithersburg, MD, United States

Early endpoints, such as progression-free survival (PFS), are increasingly used as surrogates for overall survival (OS) to accelerate approval of novel oncology agents. Compiling trial-level data from randomized controlled trials (RCTs) could help to develop a predictive framework to ascertain correlation trends between treatment effects for early and late endpoints. Through trial-level correlation and random-effects meta-regression analysis, we assessed the relationship between hazard ratio (HR) OS and (1) HR PFS and (2) odds ratio (OR) PFS at 4 and 6 months, stratified according to the mechanism of action of the investigational product. Using multiple source databases, we compiled a data set including 81 phase II–IV RCTs (35 drugs and 156 observations) of patients with non-small-cell lung cancer. Low-to-moderate correlations were generally observed between treatment effects for early endpoints (based on PFS) and HR OS across trials of agents with different mechanisms of action. Moderate correlations were seen between treatment effects for HR PFS and HR OS across all trials, and in the programmed cell death-1/programmed cell death ligand-1 and epidermal growth factor receptor trial subsets. Although these results constitute an important step, caution is advised, as there are some limitations to our evaluation, and an additional patient-level analysis would be needed to establish true surrogacy.

**Keywords: surrogate endpoints, progression-free survival, correlation analysis, trial-level analysis, meta-regression analysis**

OPEN ACCESS

***Edited by:***
*Fiona Hegi-Johnson, University of Melbourne, Australia*

***Reviewed by:***
*Yu Yang Soon, National University Hospital, Singapore*
*Xabier Mielgo Rubio, Hospital Universitario Fundación Alcorcón, Spain*

****Correspondence:***
*Khader Shameer*
*shameer.khader@astrazeneca.com*

***Specialty section:***
*This article was submitted to Thoracic Oncology, a section of the journal Frontiers in Oncology*

***Received:*** *26 February 2021*
***Accepted:*** *06 July 2021*
***Published:*** *26 July 2021*

***Citation:***
*Shameer K, Zhang Y, Jackson D, Rhodes K, Neelufer IKA, Nampally S, Prokop A, Hutchison E, Ye J, Malkov VA, Liu F, Sabin A, Weatherall J, Duran C, Iacona RB, Khan FM and Mukhopadhyay P (2021) Correlation Between Early Endpoints and Overall Survival in Non-Small-Cell Lung Cancer: A Trial-Level Meta-Analysis. Front. Oncol. 11:672916. doi: 10.3389/fonc.2021.672916*

# INTRODUCTION

In clinical trials that assess novel therapeutic agents in patients with non-small-cell lung cancer (NSCLC), overall survival (OS) is considered the gold-standard endpoint for establishing clinical benefit (1–3). 'Early' endpoints, such as progression-free survival (PFS) and objective response rate (ORR), are evaluated in oncology trials as indicators of biological drug activity. For example, PFS rate at 6 months (PFS6) is often used as the key endpoint in phase II trials to accelerate approval of novel therapies (3–5). Approximately two-thirds of all regulatory approvals for cancer drugs in the US are based on these surrogate endpoints, which also form the basis of early go/no go decisions in the drug development pipeline (for instance, the decision to initiate phase III trials) (1–3, 6). This is because they permit shorter trial durations and the use of smaller patient cohorts, thereby allowing for faster, more cost-effective trials (3, 6). The use of early endpoints can overcome certain limitations associated with using OS, including the impact of subsequent therapy and patient crossover between trial arms (7). Analyses to support the use of these early endpoints in oncology trials has also been extended to evaluating PFS as a surrogate endpoint for health-related quality of life (8–10).

Surrogate endpoints are a measure of the treatment effect that correlates with OS, the long-term, established clinical endpoint (11). To be a reliable substitute for OS, regulatory agencies require that these early endpoints follow the pattern of the late endpoint both as an epidemiological marker and as a therapeutic responder (11–13).

Using early endpoints as surrogates for OS has the potential to be misleading in terms of treatment benefit (14, 15). Previous analyses have not always demonstrated a clear relationship between these endpoints, and the correlation of early endpoints with OS across clinical trials of anti-cancer drugs with different mechanisms of action (MoA) is not well established (2, 16–18). This is important when considering the high failure rate of oncology trials in general, and phase III trials in particular, which is largely due to a failure to meet the primary efficacy endpoint and is associated with high human and financial costs (19–21).

Compiling trial-level data from randomized controlled trials (RCTs) could help to develop a predictive framework to ascertain the correlation trends between treatment effects for early (e.g., odds ratio [OR] for PFS at 4 or 6 months [PFS4 or PFS6]) and late (e.g., hazard ratio [HR] OS) endpoints in clinical trials. In turn, this could improve early go/no go decision making in the drug development pipeline, optimize the selection of early endpoints, constitute a first step towards establishing surrogacy of early endpoints for OS, and support payer recognition of PFS for reimbursement. Here, we compile trial-level data from RCTs of NSCLC and use the data set to evaluate correlations between treatment effects for early endpoints (based on PFS) and HR OS for all trials and stratified according to the MoA of the investigational product.

# METHODS

## Systematic Literature Review

A trial-level data set was compiled, which included phase II–IV RCTs of Stages I–IV NSCLC (**Supplementary Figure 1**). The data set was collected from multiple source databases, namely Citeline's Trial Trove, clinicaltrials.gov, PubMed, and an internal AstraZeneca database (constrained search). First, an initial list of trials was compiled based on Trialtrove and clinicaltrials.gov, with search restricted to between January 2000 and January 2019, using the following search terms: non-small-cell lung cancer/NSCLC (disease); phase II to phase IV (to identify randomized controlled trials). Additional evidence was extracted from PubMed for external publications (using PubMed ID numbers), and from the internal AstraZeneca database for clinical study reports on AstraZeneca trials. The search strategy for compiling the data set included considerations of whether PFS (assessed by blinded independent central review or by the investigator per Response Evaluation Criteria in Solid Tumors [RECIST]) and OS data were available, the trial was interventional/multi-arm, and the data were analysis-ready. Trials that did not have a full data set (i.e., HR OS and HR PFS data) were excluded. Between-trial biases (e.g., crossover, differences in length of follow-up, etc.) and attrition rates were not considered as part of the inclusion/exclusion criteria.

## Meta-Analysis: Data Extraction

The following treatment effect estimates were extracted from the identified trial reports, where available (reported HRs per Cox regression): HR OS, HR PFS, OR PFS4, and OR PFS6. ORs for PFS4 and PFS6 were calculated by extracting information from the curated data on how many patients had/did not have progression at 4 or 6 months, respectively, in the investigational arm and the control arm (attained by data mining of the reported Kaplan–Meier curves using the 'WebPlotDigitizer' tool (22) and establishing a contingency table based on these data (using actual count values). Fisher's exact tests were then used to calculate ORs in a manner similar to computing ORs based on the proportion of PFS directly but using conditional maximum likelihood estimator (MLE) rather than unconditional MLE.

## Meta-Analysis: Correlation and Meta-Regression Analysis

Correlation and random-effects meta-regression analyses were carried out to assess relationships between HR OS and HR PFS, OR PFS4, and OR PFS6 across all trials and stratified according to the MoA of the investigational product. Spearman's rank correlation coefficients (Rho) were derived for all comparisons between trial-level treatment effects; an absolute value of a correlation (Spearman's rho) close to 1 (for HR vs HR comparisons) or −1 (for HR vs OR comparisons) indicated a strong monotonic association. Associations were categorized as very high (0.9 – 1.0); high (0.7 – <0.9); moderate (0.5 – <0.7); low (0.3 – <0.5); and negligible (0 – <0.3), as used previously (23). Trial-level associations were quantified through random-effects meta-regression. $R^2$ was used to quantify the proportion of heterogeneity accounted for by the regression (restricted maximum likelihood method) using the "metafor" R package (24); log HR was used to decrease the effect of outliers and support the normality assumptions made by meta-regression models. Meta-regression analyses were performed across different data-strata, stratified by the MoA of the investigational product.

# RESULTS

## Literature Search Results and Data Selection for Downstream Analysis

In total, the data set included 81 industry-wide RCTs with 35 drugs and 156 observations, as shown in the PRISMA flow diagram (**Figure 1**, **Supplementary Table 1**). Among the 15 different MoA groups identified in these trials, epidermal growth factor receptor (EGFR) inhibition constituted the largest group, with 25 trials included, followed by programmed cell death-1/programmed cell death ligand-1 (PD-1/PD-L1) inhibition (18 trials), vascular endothelial growth factor receptor (VEGFR) inhibition (13 trials), and DNA damage response (DDR) inhibition (six trials). These four major trial subsets were used for downstream analysis by MoA. Other MoAs included in the data set were as follows: tubulin inhibition (four trials); anaplastic lymphoma kinase (ALK) inhibition (four trials); mitogen-activated protein kinase (MEK) inhibition (three trials); and one trial each for inhibition of Toll-like receptor-9 (TLR-9), poly ADP ribose polymerase (PARP), thymidylate synthase (TYMS), insulin-like growth factor-1 receptor (IGF-1R), cytotoxic T-lymphocyte-associated protein-4 (CTLA-4), matrix metalloproteinase (MMP), and mucin-1 (MUC-1). The MoA was not available for one of the trials. Approximately 16% of trials allowed crossover, mostly in trials of PD-1/PD-L1 inhibitors.

## Trial-Level Correlation and Random-Effects Meta-Regression Analysis

### HR OS *vs* HR PFS

Based on 69 trials, a moderate correlation was observed between HR OS and HR PFS for all trials (i.e. irrespective of MoA) (random-effects meta-regression $R^2$, 51.6%; $P < 0.001$) (**Figure 2A** and **Table 1**); the random-effect meta-regression $Tau^2$ for between-trial variance was 0.034 (standard error, 0.008). Moderate correlations were also observed between HR OS and HR PFS for PD-1/PD-L1 inhibitors (random-effects meta-regression $R^2$, 76.1%; $P < 0.001$) and EGFR inhibitors trials (random-effects meta-regression $R^2$, 28.3%; $P < 0.001$) (**Figure 2B** and **Table 1**). The slopes were similar for PD-1/PD-L1 and EGFR inhibitors trials, but with different intercepts. The random-effects meta-regression $R^2$ for EGFR inhibitors trials was small, suggesting that the regression fit was not reliable for this MoA. Negligible and high correlations were observed for VEGFR and DDR inhibitors, respectively, although these were based on very few observations (14 and 9, respectively) (**Figure 2B** and **Table 1**).

### HR OS *vs* OR PFS 4/6 Months

Based on 64 trials, low correlations were observed between both HR OS and OR PFS4 (random-effects meta-regression $R^2$, 10.9%; $P < 0.001$) and HR OS and OR PFS6 (random-effects meta-regression $R^2$, 23.1%; $P < 0.001$) for all trials. The meta-regression $R^2$ was small, suggesting that the regression fit was not reliable (**Supplementary Figures 2** and **3** and **Supplementary Tables 2** and **3**).

Moderate correlations were observed between HR OS and OR PFS4 for PD-1/PD-L1 inhibitors (random-effects meta-regression $R^2$, 72.5%; $P < 0.001$) and EGFR inhibitors trials (random-effects meta-regression $R^2$, 35.6%; $P < 0.001$) (**Figure 3** and **Table 2**). Similar correlations to those observed between HR OS and OR PFS4 were observed between HR OS and OR PFS6 for PD-1/PD-L1 inhibitors (random-effects meta-regression $R^2$, 86.1%; $P < 0.001$) and EGFR inhibitors trials (random-effects meta-regression $R^2$, 36.2%; $P < 0.001$) (**Figure 3** and **Table 2**). The slopes were similar for PD-1/PD-L1 and EGFR inhibitors trials, but with different intercepts. The random-effects meta-regression $R^2$ for EGFR inhibitors trials was small, suggesting that the regression fit was not reliable for this MoA. For VEGFR and DDR inhibitors trials, negligible to low correlations were observed between both HR OS and OR PFS4 and HR OS and OR

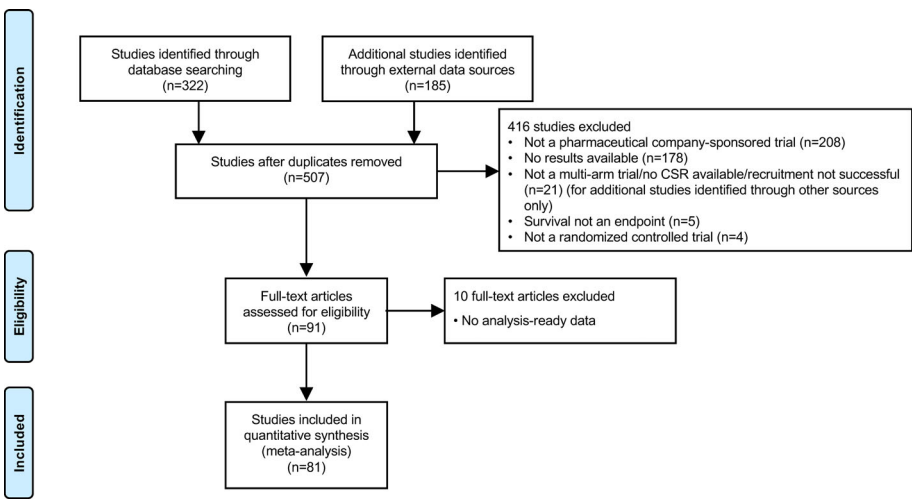


**FIGURE 1** | PRISMA flow diagram. CSR, clinical study report.

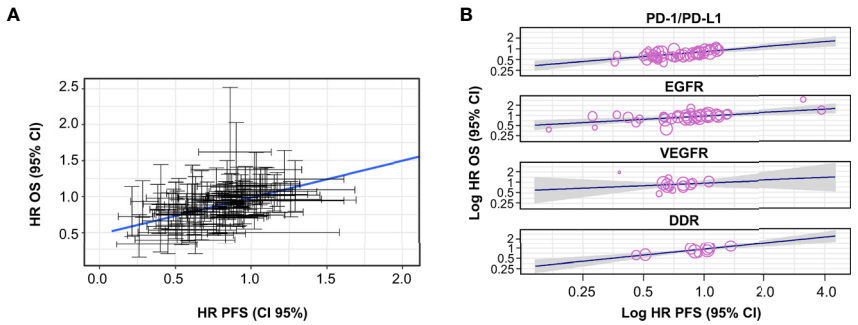


**FIGURE 2** | Correlation between HR OS and HR PFS, **(A)** across all trials and **(B)** by MoA. The gray-shaded area in panel **(B)** represents the pointwise 95% CI for the mean of the Y given X. CI, confidence interval; DDR, DNA damage response; EGFR, epidermal growth factor receptor; HR, hazard ratio; MoA, mechanism of action; OS, overall survival; PD-1/PD-L1, programmed cell death-1/programmed cell death ligand-1; PFS, progression-free survival; VEGFR, vascular endothelial growth factor receptor.

**TABLE 1** | Correlation between HR OS and HR PFS across all trials and by MoA.

| Label | All trials | 4 major MoAs combined | PD-1/PD-L1 inhibitors | EGFR inhibitors | VEGFR inhibitors | DDR inhibitors |
|---|---|---|---|---|---|---|
| Spearman's Rho* | 0.548 | 0.575 | 0.608 | 0.641 | 0.066 | 0.812 |
| Spearman's Rho 95% CI, bootstrap | (0.381; 0.689) | (0.404; 0.717) | (0.345; 0.801) | (0.368; 0.822) | (–0.557; 0.725) | (0.205; 1.000) |
| Number of drugs | 32 | 20 | 5 | 6 | 5 | 4 |
| Number of trials | 69 | 54 | 17 | 21 | 10 | 6 |
| Number of observations† | 121 | 99 | 41 | 35 | 14 | 9 |
| Slope, meta-regression | 0.410 (0.303; 0.516) | 0.423 (0.304; 0.541) | 0.465 (0.291; 0.640) | 0.322 (0.150; 0.495) | 0.239 (–0.270; 0.749) | 0.593 (0.367; 0.819) |
| Random-effects, meta-regression $R^2$ | 51.59% | 48.89% | 76.06% | 28.27% | 0% | 100% |
| P-value | <0.001 | <0.001 | <0.001 | <0.001 | 0.357 | <0.001 |

**The reported Rho values are negative as an HR <1, and an OR >1, indicate benefit with the investigational product. †Cohort level.*
*CI, confidence interval; DDR, DNA damage response; EGFR, epidermal growth factor receptor; HR, hazard ratio; MoA, mechanism of action; OS, overall survival; PD-1/PD-L1, programmed cell death-1/programmed cell death ligand-1; PFS, progression-free survival; VEGFR, vascular endothelial growth factor receptor.*

PFS6, although these were based on very few observations (11 and 6, respectively) (**Figure 3** and **Table 2**).

Changes in random-effects meta-regression $R^2$, random-effects meta-regression $I^2$, Spearman's rho, and Spearman's rho upper/lower bound 95% CI for HR OS versus the different PFS-based treatment effects are summarized in **Figure 4**.

## DISCUSSION

Compiling trial-level data from oncology RCTs to ascertain correlation trends between treatment effects for early and late endpoints have the potential to improve early go/no go decision making in the drug development pipeline, optimize the selection of early endpoints, and support payer recognition of PFS for reimbursement, allowing for faster and more cost-effective oncology trials.

Using a comprehensive, trial-level summary data set of 35 drugs, 81 trials, and 156 observations in the NSCLC setting, we evaluated correlations between treatment effects for early endpoints (based on PFS) and HR OS. Low-to-moderate correlations were observed between HR PFS and HR OS across RCTs of agents with different MoAs. Trends were similar for PD-1/PD-L1 checkpoint inhibitors and EGFR inhibitors, although, in the latter case, the random-effects meta-regression $R^2$ was small, suggesting that the regression fit was not reliable for this MoA. Moderate and low-to-moderate correlations, respectively, were also observed between treatment effects for OR PFS4/6 and HR OS in trials of PD-1/PD-L1 checkpoint inhibitors and EGFR inhibitors. These results suggest that, for these classes of agents, an improvement in OR PFS4/6 can be associated with OS benefit, and that PFS4 could potentially be used instead of PFS6 in early phase clinical trials, thereby speeding up the completion of these trials while providing support for initiating phase III trials.

The trial-level correlations also constitute a first step toward establishing the surrogacy of PFS for OS, although patient-level analyses would also be required for this purpose (25). Nevertheless, the results for PD-1/PD-L1 checkpoint inhibitor trials in the current analysis are broadly consistent with the results of another recent meta-analysis that assessed the surrogacy of PFS for OS with PD-1/PD-L1 checkpoint inhibitors at both the trial and patient level; in the trial-level analysis, based on 40 RCTs across various solid tumors, high correlation was observed between HR PFS and HR OS, with modest or limited benefit in PFS associated with meaningful improvement in OS (23). In the patient-level analysis, a positive

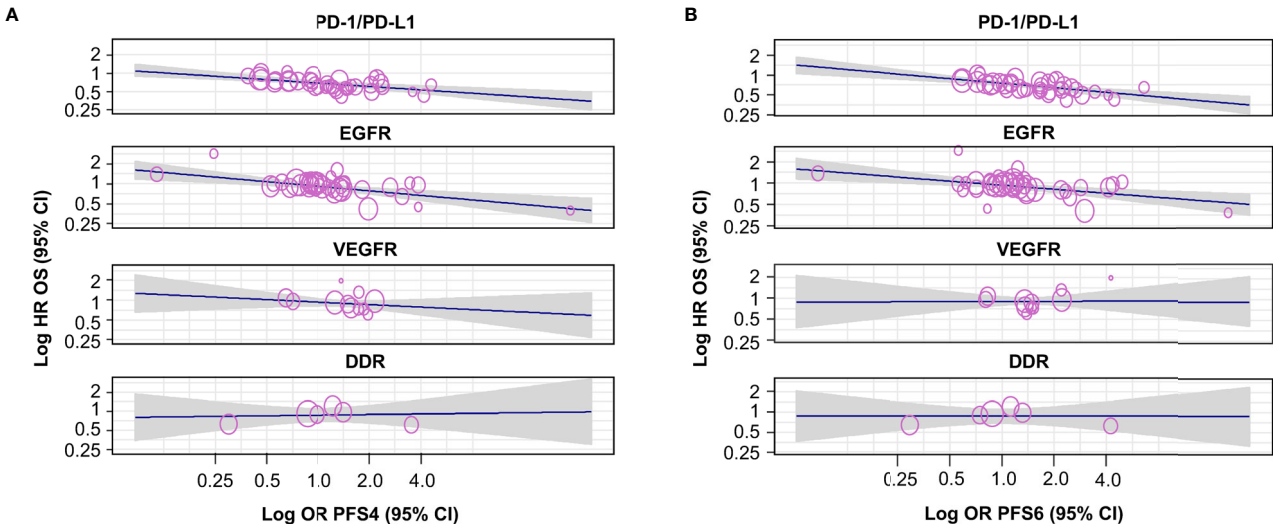


**FIGURE 3** | Correlation by MoA between HR OS and **(A)** OR PFS4 and **(B)** OR PFS6. The gray-shaded area in panels **(A, B)** represents the pointwise 95% CI for the mean of the Y given X. The reported Rho values are negative as an HR <1, and an OR >1, indicating benefit with the investigational agent. CI, confidence interval; DDR, DNA damage response; EGFR, epidermal growth factor receptor; HR, hazard ratio; MoA, mechanism of action; OR, odds ratio; OS, overall survival; PD-1/PD-L1, programmed cell death-1/programmed cell death ligand-1; PFS4/6, progression-free survival rate at 4/6 months; VEGFR, vascular endothelial growth factor receptor.

**TABLE 2** | Correlation by MoA between HR OS and OR PFS4/OR PFS6.

| | Correlations with HR OS | | | | | | | |
|---|---|---|---|---|---|---|---|---|
| | PD-1/PD-L1 inhibitors | | EGFR inhibitors | | VEGFR inhibitors | | DDR inhibitors | |
| | OR PFS4 | OR PFS6 | OR PFS4 | OR PFS6 | OR PFS4 | OR PFS6 | OR PFS4 | OR PFS6 |
| Spearman's Rho* | –0.579 | –0.633 | –0.535 | –0.427 | –0.443 | 0.224 | 0.029 | 0.086 |
| Spearman's Rho 95% CI, bootstrap | (–0.800;–0.274) | (–0.802;–0.383) | (–0.760;–0.230) | (–0.705;–0.085) | (–0.993; 0.146) | (–0.638; 0.795) | (–1.000; 1.000) | (–0.920; 1.000) |
| Number of drugs | 5 | 5 | 6 | 6 | 5 | 5 | 4 | 4 |
| Number of trials | 16 | 16 | 21 | 21 | 8 | 8 | 5 | 5 |
| Number of observations† | 38 | 38 | 37 | 37 | 11 | 11 | 6 | 6 |
| Slope, meta-regression | –0.192 (–0.280; –0.104) | –0.229 (–0.321; –0.136) | –0.230 (–0.344; –0.116) | –0.191 (–0.297; –0.086) | –0.125 (–0.356; 0.106) | 0.007 (–0.269; 0.283) | 0.033 (–0.285; 0.352) | 0 (–0.299; 0.299) |
| Random-effects, meta-regression $R^2$ | 72.48% | 86.13% | 35.63% | 36.17% | 0% | 0% | 0% | 0% |
| P-value | < 0.001 | < 0.001 | < 0.001 | < 0.001 | 0.289 | 0.959 | 0.838 | 0.999 |

**The reported Rho values are negative as an HR <1, and an OR >1, indicate benefit with the investigational product. †Cohort level.*
*CI, confidence interval; DDR, DNA damage response; EGFR, epidermal growth factor receptor; HR, hazard ratio; MoA, mechanism of action; OR, odds ratio; OS, overall survival; PD-1/PD-L1, programmed cell death-1/programmed cell death ligand-1; PFS4/6, progression-free survival rate at 4/6 months; VEGFR, vascular endothelial growth factor receptor.*

association was observed between PFS and OS in NSCLC (Kendall's Tau, 0.793; 95% CI, 0.789–0.797), as well as in other solid tumors, such as head and neck squamous cell carcinoma and bladder cancer. However, modest or limited improvement in RECIST-based endpoints did not rule out meaningful OS benefit, suggesting that they are imperfect surrogates that do not fully capture the clinical benefit of PD-1/PD-L1 checkpoint inhibitors (23). This warrants caution when basing early discontinuation of novel agents in this class on these surrogate endpoints.

Another meta-regression analysis of trials in patients with NSCLC provided no evidence of trial-level correlations (meta-regression $R^2$, 0.08; 95% CI, 0–0.31) between treatment effects for PFS and OS for targeted therapies, such as EGFR inhibitors (16). In the current analysis, a moderate correlation was observed between treatment effects for HR OS and HR PFS for EGFR inhibitor trials, although the random-effects meta-regression $R^2$ was small, suggesting that the regression fit was not reliable for this MoA. Taken together, these results suggest that PFS is an imperfect surrogate for OS in trials of EGFR inhibitors.

An analysis of 60 RCTs in patients with lung cancer assessed in six meta-analyses showed that PFS was a valid surrogate endpoint for OS in trials of chemotherapy and radiotherapy for patients with locally advanced lung cancers at trial level ($R^2$ range, 0.89–0.97) (18).

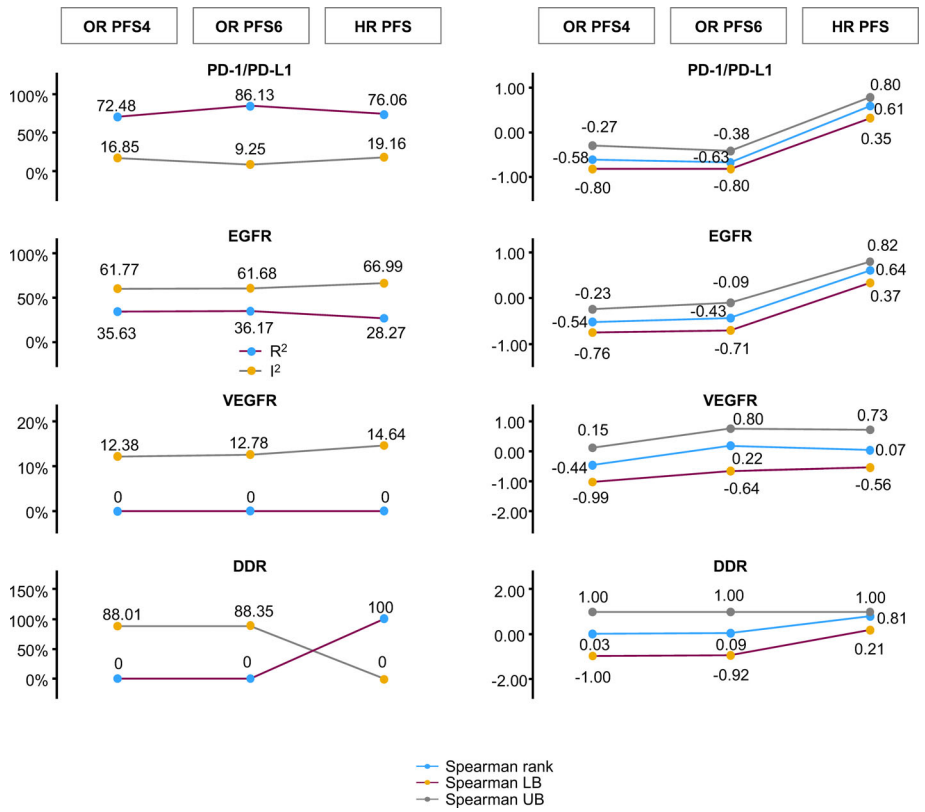


**FIGURE 4** | Changes in random-effects meta-regression $R^2$ and $I^2$, Spearman's rho, and Spearman's rho upper/lower bound 95% CI for HR OS versus PFS-based treatment effects. The statistics for random-effects meta-regression for OR PFS at 4 months, OR PFS at 6 months, and HR PFS are compared with HR OS in a single plot. This represents the comparison of random-effects meta-regression $R^2$ and $I^2$ on the left, and Spearman's rank correlation at 95% CI bootstrap with its upper bound and lower bound on the right. CI, confidence interval; DDR, DNA damage response; EGFR, epidermal growth factor receptor; HR, hazard ratio; LB, lower bound; OR, odds ratio; OS, overall survival; PD-1/PD-L1, programmed cell death-1/programmed cell death ligand-1; PFS, progression-free survival; PFS4/6, progression-free survival rate at 4/6 months; UB, upper bound; VEGFR, vascular endothelial growth factor receptor.

Analyses of trials assessing anti-angiogenic agents and EGFR inhibitors in first-line metastatic colorectal cancer showed modest correlations between PFS and OS ($R^2$ range, 0.45–0.69) (26). A trial-level meta-analysis of the correlation between PFS and OS in trials assessing chemotherapy or targeted therapy in metastatic breast cancer showed that HR PFS was a significant predictor of HR OS; however, when assessing by line of therapy, the association was significant in second-line and beyond trials, but not in the first-line trials (27). In the current analysis, no evaluation was conducted by line of therapy (first-line versus second-line and beyond), and it is therefore not possible to conclude whether there were any differences by line of therapy. The current analysis is also limited by the fact that the studies included were in the NSCLC setting only; it cannot be assumed that similar results would be observed with other cancers.

Moreover, the analysis was not stratified by the stage of disease under study, the nature of the control arm, the length of follow-up, or the line of therapy, potentially confounding the results. Regarding the different stages of disease included in the analysis, it is worth noting that all studies were in the locally advanced/advanced setting (stage III/IV), with no studies in patients with stage I/II disease and a majority of studies (62/81) in patients with stage IIIB/IV disease (with an additional 14 studies in patients with stage IV disease, two in patients with stage III/IV disease, one in patients with stage IIIA/B disease, and two in patients with stage III disease). Therefore, the results of this analysis largely reflect the locally advanced/advanced setting. An analysis by stage of disease would be of interest in follow-up investigations to assess any potential differences between early-stage and late-stage disease. Inclusion of different lines of therapy in the analysis is also a limitation, with inclusion of 46 trials in the first-line setting, and 31 in the second-line and above setting (four not available). Because the treatment intent is different for first-line versus further lines of therapy, an analysis by line of therapy would be of interest in follow-up investigations. Finally, the inclusion of studies with different lengths of follow-up is a common challenge in meta-analyses (28); a limitation of this analysis is the method commonly used for pooling of data when follow-up duration variables were not used.

Although the approach used to extract the data is reproducible, the specific extracted data points for PFS at 4 and 6 months may deviate in value, as these data were obtained

through data mining of Kaplan-Meier curves. Additional limitations include cross-mechanism grouping; trial outcomes being closer to one for HR OS; and the studies included in the analysis being a heterogeneous mix of MoAs and study designs, with some studies pre-dating 2010 [i.e., before the first trials of PD-1/PD-L1 checkpoint inhibitors in NSCLC (29)]. As a result of these additional limitations, the correlation might have been more or less pronounced in analyses stratified by MoA, compared with combined analyses. Phase II or crossover studies were also considered in the modeling, with approximately 16% of trials allowing crossover; based on a separate analysis of crossover, it is thought, however, that this should not have affected the results significantly. In addition, inclusion of phase II studies could have also impacted the results. However, only 13 of 81 trials included in the analysis were phase II trials (plus 1 phase II/III trial and 1 phase IV trial), and 66 of 81 studies were phase III trials; therefore, the results largely reflect phase III trials. Conclusions cannot be drawn for the VEGFR and DDR inhibitors trial subsets because of the low number of observations; this is because when estimation methods are based on asymptotical assumptions, they can easily be biased when the sample size is small, and a recommendation is that meta-regression should generally not be considered when there are fewer than 10 studies available (30).

For this analysis, we also decided to only assess trial-level correlations and use a systematic approach largely based on the clinicaltrials.gov database, with searches carried out over 18 months. In this approach, not all studies are reported, and some studies only provide partial information or are ongoing. However, even when the treatment has a positive impact on the early endpoint and the early endpoint and OS are positively correlated, it is still possible that the treatment has no impact or a negative impact on OS, which challenges the use of surrogate endpoints. Therefore, because of the nature of a trial-level analysis, when assessing the validity of a surrogate, it is important to consider potential confounding factors and whether it is possible for the treatment to affect the early endpoint for different patients than those for whom the early endpoint affects OS.

Following this trial-level analysis, other trial-level parameters could be built into a digital health aid, including different tumor types, additional early endpoints, such as ORR, and other non-RECIST-based endpoints, to continue building a predictive framework that may help to ascertain the correlation trends across early-to-late endpoints in clinical trials and reduce the failure rate of pivotal phase III trials (20, 21). The challenges of early-phase study design of immunotherapies require new approaches that include incorporating additional endpoints, for instance, in the dose selection process, to improve efficacy and reduce toxicity (31). In recent years, there have been calls for more widespread use of data-driven tools to augment shared decision making, to incorporate the patient perspective and increase trial participation (32), and to address issues associated with the conduct of randomized clinical trials during pandemics (33).

Furthermore, high-quality real-world evidence (RWE) could be leveraged to enable drug approvals in oncology (34, 35), linking it to the value proposition of drugs (36–38). Regulatory bodies, such as the US Food and Drug Administration, have recently shown a willingness to expedite access to new cancer medicines by using RWE (39).

## CONCLUSIONS

Using a comprehensive, trial-level, summary data set in the NSCLC setting, we generally observed low-to-moderate correlations between treatment effects for early endpoints (based on PFS) and HR OS across trials of agents with different MoAs. Moderate correlations were observed among trials of PD-1/PD-L1 checkpoint inhibitors and EGFR inhibitors. Caution is advised when drawing on the surrogacy of early endpoints for OS based on the current analysis, as an additional patient-level analysis would be needed to establish true surrogacy, and there are several limitations to the analysis. Exploration of additional endpoints, beyond RECIST, is needed to identify other early indicators of efficacy that might better predict HR OS. Moreover, compiling trial-level data for other solid tumors is required to optimize the selection of early endpoints across different cancer indications. By incorporating additional trial-level parameters and building composite biomarkers using machine intelligence methods, in collaboration with innovative trial design efforts, we envisage improving the prediction of HR OS from early endpoints.

## DATA AVAILABILITY STATEMENT

The original contributions presented in the study are included in the article/**Supplementary Material**. Further inquiries can be directed to the corresponding author.

## AUTHOR CONTRIBUTIONS

KS developed the project and analytics strategy with critical inputs from RI, CD, FMK, PM, and JW. YZ, VAM, SN, and EH led data compilation. AS, DJ, KR, IKAN, JY, FL, and KS contributed to the statistical analyses. IKAN conducted analyses. The original manuscript was written by KS, with additions to the manuscript and edits provided by YZ, DJ, KR, SN, AP, EH, JY, VM, FL, AS, JW, CD, RI, FMK, and PM. All authors contributed to the article and approved the submitted version.

## FUNDING

This study was funded by AstraZeneca.

## ACKNOWLEDGMENTS

The authors would like to thank the patients, their families and caregivers, and all investigators involved in this study. Medical writing support, which was in accordance with Good Publication Practice (GPP3) guidelines, was provided by Carole Mongin-

Bulewski, PhD, and Aaron Korpal, PhD, of Cirrus Communications (Manchester, UK), Ashfield MedComms, an Ashfield Health company, and was funded by AstraZeneca.

## SUPPLEMENTARY MATERIAL

The Supplementary Material for this article can be found online at: https://www.frontiersin.org/articles/10.3389/fonc.2021.672916/full#supplementary-material

**Supplementary Figure 1 |** Clinical trial search strategy. An initial list of trials was extracted from clinicaltrials.gov (left column) and Trialtrove (right column). The category 'additional evidence from publications (external)' indicates additional evidence extracted through PubMed; 'additional evidence from CSRs (AZ)' indicates additional evidence extracted through the internal AstraZeneca database. AZ, AstraZeneca; CSR, clinical study report; NSCLC, non-small-cell lung cancer; OS, overall survival; PFS, progression-free survival; Ph, phase; RCT, randomized controlled trial.

**Supplementary Figure 2 |** Correlation across all trials and by MoA between HR OS and OR PFS4. The gray-shaded area in the figure represents the pointwise 95% CI for the mean of the Y given X. The reported Rho values are negative as an HR <1, and an OR >1, indicate benefit with the investigational agent. CI, confidence interval; DDR, DNA damage response; EGFR, epidermal growth factor receptor; HR, hazard ratio; MoA, mechanism of action; OR, odds ratio; OS, overall survival; PD-1/PD-L1, programmed cell death-1/programmed cell death ligand-1; PFS4, progression-free survival rate at 4 months; VEGFR, vascular endothelial growth factor receptor.

**Supplementary Figure 3 |** Correlation across all trials and by MoA between HR OS and OR PFS6. The gray-shaded area in the figure represents the pointwise 95% CI for the mean of the Y given X. The reported Rho values are negative as an HR <1, and an OR >1, indicate benefit with the investigational agent. CI, confidence interval; DDR, DNA damage response; EGFR, epidermal growth factor receptor; HR, hazard ratio; MoA, mechanism of action; OR, odds ratio; OS, overall survival; PD-1/PD-L1, programmed cell death-1/programmed cell death ligand-1; PFS6, progression-free survival rate at 6 months; VEGFR, vascular endothelial growth factor receptor.

## REFERENCES


1. Pilz LR, Manegold C, Schmid-Bindert G. Statistical Considerations and Endpoints for Clinical Lung Cancer Studies: Can Progression-Free Survival (PFS) Substitute Overall Survival (OS) as a Valid Endpoint in Clinical Trials for Advanced Non-Small-Cell Lung Cancer? *Transl Lung Cancer Res* (2012) 1:26–35. doi: 10.3978/j.issn.2218-6751.2011.12.08
2. US Department of Health and Human Services, Food and Drug Administration, and Oncology Center of Excellence. *Clinical Trial Endpoints for the Approval of Cancer Drugs and Biologics: Guidance for Industry* (2018). Available at: https://www.fda.gov/media/71195/download (Accessed December 16, 2020).
3. Hamada T, Kosumi K, Nakai Y, Koike K. Surrogate Study Endpoints in the Era of Cancer Immunotherapy. *Ann Transl Med* (2018) 6(Suppl 1):S27. doi: 10.21037/atm.2018.09.31
4. Dy GK, Mandrekar SJ, Nelson GD, Meyers JP, Adjei AA, Ross HJ, et al. A Randomized Phase II Study of Gemcitabine and Carboplatin With or Without Cediranib as First-Line Therapy in Advanced non-Small-Cell Lung Cancer. *J Thorac Oncol* (2013) 8:79–88. doi: 10.1097/JTO.0b013e318274a85d
5. Strzebonska K, Waligora M. Umbrella and Basket Trials in Oncology: Ethical Challenges. *BNC Med Ethics* (2019) 20:58. doi: 10.1186/s12910-019-0395-5
6. Kim C, Prasad V. Cancer Drugs Approved on the Basis of a Surrogate End Point and Subsequent Overall Survival: An Analysis of 5 Years of US Food and Drug Administration Approvals. *JAMA Intern Med* (2015) 175:1992e4. doi: 10.1001/jamainternmed.2015.5868
7. Wilson MK, Karakasis K, Oza AM. Outcomes and Endpoints in Trials of Cancer Treatment: The Past, Present, and Future. *Lancet Oncol* (2015) 16: e32–42. doi: 10.1016/S1470-2045(14)70375-4
8. Gutman SI, Piper M, Grant MD, Basch E, Olianksy DM, Aronson N. Progression-Free Survival: What Does it Mean for Psychological Well-Being or Quality of Life? *AHRQ Methods Effective Health Care* (2013). AHRQ Publication No. 13-EHC074-EF. Rockville, MD: Agency for Healthcare Research and Quality. Available at: www.effectivehealthcare.ahrq.gov/reports/final.cfm.
9. Kovic B, Guyatt G, Brundage M, Thabane L, Bhatnagar N, Xie F. Association Between Progression-Free Survival and Health-Related Quality of Life in Oncology: A Systematic Review Protocol. *BMJ Open* (2016) 6(9):e012909. doi: 10.1136/bmjopen-2016-012909
10. Kovic B, Jin X, Kennedy SA, Hylands M, Pedziwiatr M, Kuriyama A, et al. Evaluating Progression-Free Survival as a Surrogate Outcome for Health-Related Quality of Life in Oncology. A Systematic Review and Quantitative Analysis. *JAMA Intern Med* (2018) 178:1586–96. doi: 10.1001/jamainternmed.2018.4710
11. US Department of Health and Human Services, Food and Drug Administration. *Surrogate Endpoint Resources for Drug and Biologic Development* (2018). Available at: https://www.fda.gov/drugs/development-resources/surrogate-endpoint-resources-drug-and-biologic-development (Accessed December 16, 2020).
12. Davidson MH. Introduction: Utilization of Surrogate Markers of Atherosclerosis for the Clinical Development of Pharmaceutical Agents. *Am J Cardiol* (2011) 87:1A–7A. doi: 10.1016/s0002-9149(01)01418-7
13. Cohn JN. Introduction to Surrogate Markers. *Circulation* (2004) 109(Suppl IV):IV-20–1. doi: 10.1161/01.CIR.0000133441.05780.1d
14. Haslam A, Hey SP, Gill J, Prasad V. A Systematic Review of Trial-Level Meta-Analyses Measuring the Strength of Association Between Surrogate End-Points and Overall Survival in Oncology. *Eur J Cancer* (2019) 106:196–221. doi: 10.1016/j.ejca.2018.11.012
15. Kim C, Prasad V. Strength of Validation for Surrogate End Points Used in the US Food and Drug Administration's Approval of Oncology Drugs. *Mayo Clinic Proc* (2016). doi: 10.1016/j.mayocp.2016.02.012
16. Blumenthal GM, Karuri SW, Zhang H, Zhang L, Khozin S, Kazandjian D, et al. Overall Response Rate, Progression-Free Survival, and Overall Survival With Targeted and Standard Therapies in Advanced non-Small-Cell Lung Cancer: US Food and Drug Administration Trial-Level and Patient-Level Analyses. *J Clin Oncol* (2015) 33:1008–14. doi: 10.1200/JCO.2014.59.0489
17. Prasad V, Lim C, Burotto M, Vandross A. The Strength of Association Between Surrogate End Points and Survival in Oncology. *JAMA Intern Med* (2015) 115:1389–98. doi: 10.1001/jamainternmed.2015.2829
18. Maugen A, Pignon JP, Burdett S, Domerg C, Fisher D, Paulus R, et al. On Behalf of the Surrogate Lung Project Collaborative Group. Surrogate Endpoints for Overall Survival in Chemotherapy and Radiotherapy Trials in Operable and Locally Advanced Lung Cancer: A Re-Analysis of Meta-Analyses of Individual Patients' Data. *Lancet Oncol* (2013) 14:619–26. doi: 10.1016/S1470-2045(13)70158-X
19. Pretorius S, Grignolo A. Phase III Trial Failures: Costly, But Preventable. *Appl Clin Trials* (2016) 25(8):36–42.
20. DiMasi JA, Feldman L, Seckler A, Wilson A. Trends in Risks Associated With New Drug Development: Success Rates for Investigational Drugs. *Clin Pharmacol Ther* (2010) 87:272–7. doi: 10.1038/clpt.2009.295
21. Wiklund SJ. A Modelling Framework for Improved Design and Decision-Making in Drug Development. *PloS One* (2019) 14:e0220812. doi: 10.1371/journal.pone.0220812
22. Rohatgi A. *Webplotdigitizer* (2020). Available at: https://automeris.io/WebPlotDigitizer/citation.html (Accessed December 8, 2020).
23. Ye J, Ji X, Dennis P, Abdullah H, Mukhopadhyay P. Relationship Between Progression-Free Survival, Objective Response Rate, and Overall Survival in Clinical Trials of PD-1/PD-L1 Immune Checkpoint Blockade: A Meta-Analysis. *Clin Pharmacol Ther* (2020) 108:1274–88. doi: 10.1002/cpt.1956

24. Viechtbauer W, Viechtbauer MW. *Package 'Metafor', The Comprehensive R Archive Network* (2015). Available at: https://cran.r-project.org/web/packages/metafor/metafor.pdf (Accessed December 16, 2020).
25. Buyse M, Molenberghs G, Burzykowski T, Renard D, Geys H. The Validation of Surrogate Endpoints in Meta-Analyses of Randomized Experiments. *Biostatistics* (2000) 1:49–67. doi: 10.1093/biostatistics/1.1.49
26. Shi Q, de Gramont A, Grothey A, Zalcberg J, Chibaudel B, Schmoll H-J, et al. Individual Patient Data Analysis of Progression-Free Survival Versus Overall Survival as a First-Line End Point for Metastatic Colorectal Cancer in Modern Randomized Trials: Findings From the Analysis and Research in Cancers of the Digestive System Database. *J Clin Oncol* (2015) 33:22–8. doi: 10.1200/JCO.2014.56.5887
27. Adulin G, Cyrus JWW, Dranitsaris G. Correlation Between Progression-Free Survival and Overall Survival in Metastatic Breast Cancer Patients Receiving Anthracyclines, Taxanes, or Targeted Therapies: A Trial-Level Meta-Analysis. *Breast Cancer Rest Treat* (2015) 154:591–608. doi: 10.1007/s10549-015-3643-5
28. Deeks JJ, Higgins JPT, Altman DG, on behalf of the Cochrane Statistical Methods Groups. *Analysing Data and Undertaking Meta-Analyses. Cochrane Handbook for Systematic Reviews of Interventions. Chapter 10* (2020). Available at: https://training.cochrane.org/handbook/current/chapter-10 (Accessed May 11, 2021). Version 6.1.
29. Santini FC, Helmann MD. PD-1/PD-L1 Axis in Lung Cancer. *Cancer J* (2019) 24:15–9. doi: 10.1097/PPO.0000000000000300
30. Higgins JPT, Thomas J, Chandler J, Cumpston M, Li T, Page MJ, et al. *Cochrane Handbook for Systematic Reviews of Interventions, Version 6.1* (2020). Available at: www.training.cochrane.org/handbook (Accessed December 16, 2020). Cochrane.
31. Wages NA, Chiuzan C, Panageas KS. Design Considerations for Early-Phase Clinical Trials of Immune-Oncology Agents. *J Immunother Cancer* (2018) 22:81. doi: 10.1186/s40425-018-0389-8
32. Unger JM, Cook E, Tai E, Bleyer A. The Role of Clinical Trial Participation in Cancer Research: Barriers, Evidence, and Strategies. *Am Soc Clin Oncol Educ Book* (2016) 35:186–98. doi: 10.1200/EDBK_156686
33. Ogburn EL. More Efficient and Effective Clinical Decision-Making. *Harvard Data Sci Rev* (2021) 3:1. doi: 10.1162/99608f92.46ee6c04
34. Banerjee R, Prasad V. Are Observational, Real-World Studies Suitable to Make Cancer Treatment Recommendations? *JAMA Netw Open* (2020) 3: e2012119. doi: 10.1001/jamanetworkopen.2020.12119
35. Greschock J, Lewi M, Hartog B, Tendler C. Harnessing Real-World Evidence for the Development of Novel Cancer Therapies. *Trends Cancer* (2020) 6:907–9. doi: 10.1016/j.trecan.2020.08.006
36. Deverka PA, Douglas MP, Phillips KA. Use of Real-World Evidence in US Payer Coverage Decision-Making for Next-Generation Sequencing-Based Tests: Challenges, Opportunities, and Potential Solutions. *Value Health* (2020) 23:540–50. doi: 10.1016/j.jval.2020.02.001
37. Seymour EL, de Souza JA, Mark FA. Incorporating Value-Based Care Into Oncology. *Cancer J* (2020) 26:311–22. doi: 10.1097/PPO.0000000000000459
38. Swift B, Jain K, White C, Chandrasekeran V, Bhandari A, Hughes DA, et al. Innovation at the Intersection of Clinical Trials and Real-World Data Science to Advance Patient Care. *Clin Transl Sci* (2018) 11:450–60. doi: 10.1111/cts.12559
39. Raphael MJ, Gyawali B, Booth CM. Real-World Evidence and Regulatory Drug Approval. *Nat Rev Clin Oncol* (2020) 17:271–2. doi: 10.1038/s41571-020-0345-7


**Conflict of Interest:** KR, EH, FL, AS, JW, RI, and FK are full-time employees of AstraZeneca and own AstraZeneca stock. SK, YZ, DJ, SN, AP, JY, and CD are full-time employees of AstraZeneca. PM was a full-time employee of AstraZeneca at the time that the study was conducted and owns AstraZeneca stock. IK and VM were full-time employees of AstraZeneca at the time that the study was conducted.

The authors declare that this study received funding from AstraZeneca. The funder had the following involvement with the study: Study design and concept, collection, analysis and interpretation of the data, review and approval of the final draft and approval to submit for publication.

frontiers in Oncology

ORIGINAL RESEARCH
published: 10 January 2022
doi: 10.3389/fonc.2021.777930

# Total Protein–Chloride Ratio in Pleural Fluid Independently Predicts Overall Survival in Malignant Pleural Effusion at the First Diagnosis

*Xin Qiao*[1], *Zhi-Rong Zhang*[2], *Xin-Yu Shi*[1] *and Feng-Shuang Yi*[1]*

[1] Department of Respiratory and Critical Care Medicine, Beijing Institute of Respiratory Medicine and Beijing Chao-Yang Hospital, Clinical Center for Pleural Diseases, Capital Medical University, Beijing, China, [2] Department of Thoracic Surgery, Beijing Chao-Yang Hospital, Capital Medical University, Beijing, China

**Objective:** Pre-treatment biomarkers to estimate overall survival (OS) for malignant pleural effusion (MPE) are unidentified, especially those in pleural fluid. We evaluated the relationship between OS and total protein–chloride ratio in malignant pleural effusion (PE TPCIR).

**Materials and Methods:** A retrospective study was undertaken to identify patients from 2006 to 2018 who had pathologically or cytologically confirmed MPE and received no tumor-targeted therapy. We recorded the pre-treatment clinicopathologic characteristics and follow-up status. OS was estimated by the Kaplan–Meier method, and the association between variables and OS was evaluated by Cox proportional hazards models.

**Results:** We screened 214 patients who met the eligibility criteria. The optimal cutoff value for the PE TPCIR was set at 0.53. The univariate analysis showed that there was a significant correlation between PE TPCIR and OS ($P < 0.001$). The multivariate analysis between OS and the variables selected from the univariate analysis showed that the levels of neutrophil, alkaline phosphatase, neuron-specific enolase, platelets, albumin in peripheral blood, and white blood cells in pleural effusion were also independent predictors of OS.

**Conclusion:** In patients with MPE, pre-treatment PE TPCIR independently predicts OS. Although further research is necessary to generalize our results, this information will help clinicians and patients to determine the most appropriate treatment for MPE patients.

**Keywords: malignant pleural effusion, total protein (TP), chloride ($Cl^-$), overall survival, prognostic factor**

OPEN ACCESS

***Edited by:***
*Fiona Hegi-Johnson,*
*University of Melbourne, Australia*

***Reviewed by:***
*Janaki Deepak,*
*University of Maryland, Baltimore, United States*
*Girindra Raval,*
*Augusta University, United States*
*Sabrina Matosz,*
*Augusta University, United States,*
*in collaboration with reviewer GR*

***Correspondence:**
*Feng-Shuang Yi*
*yifengshuang@ccmu.edu.cn*

***Specialty section:***
*This article was submitted to Thoracic Oncology, a section of the journal Frontiers in Oncology*

***Received:*** *16 September 2021*
***Accepted:*** *10 December 2021*
***Published:*** *10 January 2022*

***Citation:***
*Qiao X, Zhang Z-R, Shi X-Y and Yi F-S (2022) Total Protein–Chloride Ratio in Pleural Fluid Independently Predicts Overall Survival in Malignant Pleural Effusion at the First Diagnosis. Front. Oncol. 11:777930. doi: 10.3389/fonc.2021.777930*

## INTRODUCTION

Malignant pleural effusion (MPE) is the second leading cause (only after parapneumonic effusion) of exudative pleural effusion, with more than 125,000 patients hospitalized annually in the United States and with an estimated hospitalization cost of over $5 billion each year (1). At present, the global incidence of MPE is affected by the elevated incidence of malignant tumors and the

improvement of systematic treatment, which leads to high medical expenses (2). Despite improvements in cancer treatment, the therapy of MPE remains palliative (3), and the presence of MPE still implies a reduced survival rate (4). The median survival after the diagnosis of MPE will be affected by the origin, histological type, and stage of the primary tumor and is usually 3 to 12 months. Compared with patients who receive current standard care, advanced cancer patients receiving early palliative treatment had more improvements in the quality of life, longer survival, and less aggressive care at the end of life (5). Obviously, accurate prognosis can help to identify patients with the worst prognosis, determine appropriate treatments, and minimize unnecessary treatments and discomfort in the final stages of life.

Systemic and local inflammatory states have been considered to be associated with outcomes of cancer, and the pattern of inflammatory cell infiltration seems to affect survival (6, 7). Recently, some studies have reported various biomarkers in peripheral blood (4, 8–10) or some clinicopathological factors (11, 12) that may predict the prognosis of MPE patients or have analyzed the correlation of intrapleural immunomodulatory responses (8–10, 13–18), but simple parameters in pleural effusion have been rarely tested as possible predictors for survival in MPE patients.

It is well known that exudate is associated with inflammation or malignant processes resulting in increased capillary permeability. It is formed by active secretions or leakage and contains a high level of protein. As a result, the level of protein in pleural effusion has been studied as a simple marker for local inflammatory response (10, 14). Chloride is a biochemical marker commonly used for pleural fluid. It can be used to distinguish the etiology of pleural effusion which will significantly increase to support the diagnosis of infection, but it has not been paid enough attention in scientific research.

In our study, we comprehensively evaluated the prognostic value of clinical and laboratory characteristics in MPE patients before the tumor targeted therapy was taken, especially the markers in pleural effusion, determined the median survival time, and evaluated the prognostic variables associated with OS in MPE patients.

# MATERIALS AND METHODS

## Participants

A retrospective analysis of a prospectively maintained database was carried out on identifying all patients who were diagnosed according to cancer cells in pleural effusion or pleural biopsy between June 2006 and April 2018 at Beijing Chao-Yang Hospital. In order to avoid the influence of immune-related issues and treatments on various indicators, patients with significant infection, autoimmune disease, or underlying hematological diseases, without pre-treatment complete blood or pleural count values, and who had received anticoagulant or tumor-targeted therapy were excluded. A total of 214 patients met the criteria for admission and were incorporated into our study. The research protocol was approved by the Institutional Review Board of Beijing Chao-Yang Hospital.

## Data Collection and Follow-Up

The demographic data of the patients and their clinicopathological characteristics, including laboratory variables of peripheral blood and pleural effusion, histologic type, and extrapleural metastasis, were retrospectively collected from the database collection of our institution. The patients were routinely followed up every 6 months during the first year after diagnosis. Thereafter, the follow-up should be performed annually and kept for at least 1 year. The follow-up was maintained through personal contact with patients by phone, including asking for information about tumor recurrence and survival status. OS, defined as the interval between the diagnostic date and the date of death or last follow-up, was recorded.

## Statistical Analyses

The PE TPClR values were obtained by dividing the level of total protein by the level of chloride in pleural effusion obtained during diagnostic thoracentesis or thoracoscopy. The optimal cutoff value for age was determined by the median, and those of the other variables were determined by maximally selected rank statistics (8), which were analyzed using R software, version 3.5.1, and the "maxstat" package. The cutoff value for the PE TPClR was 0.53. Continuous data were expressed as mean ± standard deviation. Categorical data were expressed by the frequency and percentage. Continuous data were analyzed by using Student's *t*-test or one-way analysis, and categorical data were analyzed by using $\chi^2$ test. Survival curves were analyzed by the Kaplan–Meier method, and differences were compared using the log-rank test. The relationship between the PE TPClR and survival was assessed by univariable and multivariable Cox regression models. All statistically significant univariates were included in the multivariable model. Univariate and multivariate Cox regression models provided HR and 95% CI, respectively. A Cox proportional hazards model was used to fit all individual prognostic variables to determine their independent factors. SPSS 23.0 software was used for statistical analysis. The sample power of the study was calculated by PASS 11.0.

# RESULTS

## Patient Characteristics

The study cohort was comprised of 214 patients, and the sample power of our study reached up to 86.3%, in accordance with the two-sided log-rank test. The significance level was 0.05. The baseline characteristics of the population in this study are shown in **Table 1**. The median age of the patients was 65 years (range, 56–73 years), and there are 109 (50.9%) male and 105 (49.1%) female. The majority of patients had an ECOG PS of 0–2 (56.1%), were never smokers (61.2%), and exhibited pulmonary adenocarcinoma histology (57.5%). At the time of diagnosis, 55.1% of the patients had extrapleural metastases.

**TABLE 1** | Baseline characteristics of the study population according to PE TPClR.

| Characteristic | All patients (*n* = 214) | PE TPClR | | *P*-value |
|---|---|---|---|---|
| | | ≤0.53 (*n* = 188) | >0.53 (*n* = 26) | |
| OS (months), median (IQR) | 15 (12, 17) | 16 (13, 19) | 8 (5, 11) | <0.001 |
| Age (years), median (IQR) | 65 (56, 73) | 65 (56, 73) | 64 (53, 75) | 0.778 |
| Sex, *N* (%) | | | | 0.348 |
| Male | 109 (50.9) | 98 (52.1) | 11 (42.3) | |
| Female | 105 (49.1) | 90 (47.9) | 15 (57.7) | |
| ECOG PS, *N* (%) | | | | 0.549 |
| 0–2 | 120 (56.1) | 104 (55.3) | 16 (61.5) | |
| 3–4 | 94 (43.9) | 84 (44.7) | 10 (38.5) | |
| Smoking status, *N* (%) | | | | 0.371 |
| Ever/current | 83 (38.8) | 75 (39.9) | 8 (30.8) | |
| Never | 131 (61.2) | 113 (60.1) | 18 (59.2) | |
| Histology, *N* (%) | | | | 0.698 |
| ADC | 123 (57.5) | 106 (56.4) | 17 (65.4) | |
| SQC | 10 (4.7) | 9 (4.8) | 1 (3.8) | |
| SCLC | 10 (4.7) | 9 (4.8) | 1 (3.8) | |
| Mesothelioma | 13 (6.1) | 13 (6.9) | 0 (0) | |
| Others | 58 (27.0) | 51 (27.1) | 7 (27.0) | |
| Extrapleural metastasis, *N* (%) | | | | 0.887 |
| Yes | 118 (55.1) | 104 (55.3) | 14 (53.8) | |
| No | 96 (44.9) | 84 (44.7) | 12 (46.2) | |
| WBC, $\times10^9$/L, median (IQR) | 6.93 (5.76, 8.33) | 6.92 (5.72,8.35) | 7.25 (6.16, 7.98) | 0.604 |
| N, $\times10^9$/L, median (IQR) | 4.69 (3.56, 5.83) | 4.60 (3.59, 5.80) | 5.10 (3.40, 6.00) | 0.685 |
| Hb (g/L, M ± SD) | 129.53 ± 17.30 | 129.64 ± 17.46 | 128.69 ± 16.37 | 0.793 |
| ALB [g/L, median (IQR)] | 34.10 (31.20, 37.13) | 33.90 (30.90, 36.58) | 36.65 (33.40, 38.28) | 0.003 |
| LDH [U/L, median (IQR)] | 195.00 (164.75, 240.25) | 199.00 (165.00, 243.00) | 179.50 (161.00, 206.00) | 0.179 |
| $Ca^{2+}$, [mmol/L, median (IQR)] | 2.14 (2.07, 2.23) | 2.13 (2.06, 2.22) | 2.22 (2.15, 2.29) | 0.001 |
| PE ADA [U/L, median (IQR)] | 13.00 (9.00, 17.00) | 13.00 (9.00, 16.00) | 16.00 (11.75, 26.00) | 0.002 |
| PE LDH [U/L, median (IQR)] | 354.50 (197.50, 577.25) | 339.50 (186.25, 521.50) | 469.50 (263.00, 1,111.75) | 0.024 |
| NLR, median (IQR) | 3.25 (2.11, 4.53) | 3.25 (2.18, 4.52) | 3.42 (1.78, 4.90) | 0.824 |
| PLR, median (IQR) | 183.17 (131.70, 244.82) | 183.39 (134.08, 244.52) | 172.42 (116.98, 246.85) | 0.495 |
| LMR, median (IQR) | 3.04 (2.17, 4.49) | 3.06 (2.19, 4.38) | 2.99 (2.10, 5.67) | 0.495 |
| CAR, median (IQR) | 0.04 (0.15, 0.96) | 0.04 (0.16, 0.95) | 0.04 (0.01, 0.15) | 0.584 |
| PE TPClR, median (IQR) | 0.44 (0.40, 0.48) | 0.43 (0.39, 0.47) | 0.59 (0.55, 0.62) | <0.001 |

*OS, overall survival; ECOG PS, Eastern Cooperative Oncology Group performance status; ADC, adenocarcinoma; SQC, squamous cell carcinoma; SCLC, small cell carcinoma; WBC, white blood cell; N, neutrophil; Hb, hemoglobin; M ± SD, mean ± standard deviation; ALB, albumin; LDH, lactic dehydrogenase; $Ca^{2+}$, calcium ion; PE, pleural effusion; ADA, adenosine deaminase; NLR, neutrophil to lymphocyte ratio; LMR, lymphocyte to monocyte ratio; CAR, C-reactive protein to albumin ratio; TPClR, total protein–chloride ratio.*

## Association of the Pretreatment PE TPClR With Baseline Clinical Factors in MPE

According to the best cutoff value of PE TPClR, all patients were classified into low group or high group. The clinical and laboratory characteristics related to the two groups are shown in **Table 1**. The median and interquartile range of the PE TPClR were 0.43 (0.39, 0.47) and 0.59 (0.55, 0.62), respectively. Age, sex, ECOG PS, smoking status, histology, extrapleural metastasis, white blood cell (WBC), neutrophil (N), hemoglobin, lactic dehydrogenase (LDH), neutrophil to lymphocyte ratio (NLR), platelet to lymphocyte ratio, lymphocyte to monocyte ratio (LMR), and C-reactive protein to albumin ratio (CAR) had no significant difference between the two groups. However, besides the PE TPClR ($P < 0.001$), the levels of albumin (ALB; $P = 0.003$), calcium ($P = 0.001$), PE adenosine deaminase ($P = 0.002$), and PE LDH ($P = 0.024$) exhibited significant differences between the two groups.

## Association of Clinicopathological Factors and OS

The univariate associations between clinicopathologic factors and OS are shown in **Table 2**. Small cell carcinoma-type histology, high levels of WBC, N, alkaline phosphatase (ALP), and C-reactive protein (CRP), erythrocyte sedimentation rate, carcino-embryonic antigen, squamous cell carcinoma antigen, neuron-specific enolase (NSE) in peripheral blood, LDH, total protein (TP), glucose in pleural effusion, NLR, CAR, PE TPClR, low level of lymphocytes, mean platelet volume, and ALB in peripheral blood, $CL^-$ in pleural effusion, and LMR were significantly related to worse outcomes (all $P < 0.05$).

## PE TPClR Predicted OS Independently

Finally, we conducted a multivariate Cox analysis to determine whether PE TPClR independently predicted OS or not (**Table 3**). After adjusting, we found that pre-treatment PE TPClR was

**TABLE 2 |** Univariate analysis of potential associations between patient characteristics and OS.

| Variable | HR | 95%CI | *P*-value |
|---|---|---|---|
| Age, years | | | |
| ≤65 | 1.00 | | |
| >65 | 1.027 | 0.748, 1.410 | 0.868 |
| Sex | | | |
| Female | 1.00 | | |
| Male | 1.270 | 0.924, 1.745 | 0.140 |
| ECOG PS | | | |
| 0–2 | 1.00 | | |
| 3–4 | 1.349 | 0.979, 1.860 | 0.068 |
| Smoking habit | | | |
| Never | 1.00 | | |
| Ever/current | 1.272 | 0.924, 1.752 | 0.141 |
| Histology | | | |
| ADC *vs*. | 1.042 | 0.754, 1.441 | 0.803 |
| SQC *vs*. | 1.170 | 0.547, 2.501 | 0.686 |
| SCLC *vs*. | 2.270 | 1.153, 4.470 | 0.018 |
| Mesothelioma *vs*. | 0.470 | 0.220, 1.004 | 0.051 |
| Extrapleural metastasis | | | |
| No | 1.00 | | |
| Yes | 1.303 | 0.950, 1.789 | 0.101 |
| WBC, $\times10^9$/L | | | |
| ≤5.03 | 1.00 | | |
| s>5.03 | 2.242 | 1.292, 3.891 | 0.004 |
| N, $\times10^9$/L | | | |
| ≤3.69 | 1.00 | | |
| >3.69 | 2.115 | 1.446, 3.093 | <0.001 |
| L, $\times10^9$/L | | | |
| ≤1.26 | 1.00 | | |
| >1.26 | 0.703 | 0.507, 0.976 | 0.036 |
| Hb, g/L | | | |
| ≤116 | 1.00 | | |
| >116 | 0.754 | 0.525, 1.082 | 0.125 |
| PLT, $\times10^9$/L | | | |
| ≤373 | 1.00 | | |
| >373 | 0.604 | 0.342, 1.066 | 0.082 |
| MPV, fl | | | |
| ≤9.7 | 1.00 | | |
| >9.7 | 0.721 | 0.521, 0.999 | 0.049 |
| ALB, g/L | | | |
| ≤29.6 | 1.00 | | |
| >29.6 | 0.673 | 0.458, 0.990 | 0.045 |
| LDH, U/L | | | |
| ≤176 | 1.00 | | |
| >176 | 1.261 | 0.900, 1.768 | 0.178 |
| ALP, U/L | | | |
| ≤65 | 1.00 | | |
| >65 | 1.871 | 1.156, 3.028 | 0.011 |
| $Ca^{2+}$, mmol/L | | | |
| ≤2.00 | 1.00 | | |
| >2.00 | 0.686 | 0.440, 1.070 | 0.097 |
| FIB, mg/dl | | | |
| ≤321.8 | 1.00 | | |
| >321.8 | 1.504 | 0.998, 2.226 | 0.051 |
| CRP, mg/dl | | | |
| ≤0.86 | 1.00 | | |
| >0.86 | 1.818 | 1.281, 2.579 | 0.001 |
| ESR, mm/h | | | |
| ≤12 | 1.00 | | |
| >12 | 1.651 | 1.157, 2.357 | 0.006 |
| CEA, ng/ml | | | |
| ≤3.49 | 1.00 | | |
| >3.49 | 1.602 | 1.152, 2.229 | 0.005 |

*(Continued)*

**TABLE 2** | Continued

| Variable | HR | 95%CI | *P*-value |
|---|---|---|---|
| SCC, ng/ml | | | |
| ≤1 | 1.00 | | |
| >1 | 1.404 | 1.005, 1.961 | 0.047 |
| NSE, ng/ml | | | |
| ≤28.9 | 1.00 | | |
| >28.9 | 2.484 | 1.555, 3.967 | <0.001 |
| CYFRA, ng/ml | | | |
| ≤2.09 | 1.00 | | |
| >2.09 | 1.600 | 0.966, 2.651 | 0.068 |
| PE TCs/μl | | | |
| ≤2,420 | 1.00 | | |
| >2,420 | 0.739 | 0.469, 1.591 | 0.191 |
| PE WBCs/μl | | | |
| ≤383 | 1.00 | | |
| >383 | 0.647 | 0.411, 1.018 | 0.060 |
| PE LDH, U/L | | | |
| ≤155 | 1.00 | | |
| >155 | 1.960 | 1.182, 3.250 | 0.009 |
| PE ADA, U/L | | | |
| ≤19 | 1.00 | | |
| >19 | 0.776 | 0.502, 1.201 | 0.255 |
| PE TP, g/L | | | |
| ≤54.9 | 1.00 | | |
| >54.9 | 1.891 | 1.216, 2.941 | 0.005 |
| PE $Cl^-$, mmol/L | | | |
| ≤109.6 | 1.00 | | |
| >109.6 | 0.419 | 0.249, 0.704 | 0.001 |
| PE Glu, mmol/L | | | |
| ≤9.28 | 1.00 | | |
| >9.28 | 1.651 | 1.020, 2.674 | 0.041 |
| NLR | | | |
| ≤1.79 | 1.00 | | |
| >1.79 | 1.941 | 1.210, 3.114 | 0.006 |
| LMR | | | |
| ≤5.71 | 1.00 | | |
| >5.71 | 0.489 | 0.270, 0.883 | 0.018 |
| PLR | | | |
| ≤181.63 | 1.00 | | |
| >181.63 | 1.301 | 0.947, 1.790 | 0.105 |
| CAR | | | |
| ≤0.03 | 1.00 | | |
| >0.03 | 1.786 | 1.265, 2.521 | 0.001 |
| PE TPClR | | | |
| ≤0.53 | 1.00 | | |
| >0.53 | 2.302 | 1.498, 3.535 | <0.001 |

*OS, overall survival; ECOG PS, Eastern Cooperative Oncology Group performance status; ADC, adenocarcinoma; SQC, squamous cell carcinoma; SCLC, small cell carcinoma; WBC, white blood cell; N, neutrophil; L, lymphocyte; Hb, hemoglobin; PLT, platelet; MPV, mean palate volume; ALB, albumin; LDH, lactic dehydrogenase; ALP, alkaline phosphatase; $Ca^{2+}$, calcium ion; FIB, fibrinogen; CRP, C-reactive protein; ESR, erythrocyte sedimentation rate; CEA, carcino-embryonic antigen; SCC, squamous cell carcinoma antigen; NSE, neuron-specific enolase; CYFRA, cytokeratin 19 fragment; PE, pleural effusion; TCs, total cells; ADA, adenosine deaminase; TP, total protein; Cl, chloride; Glu, glucose; NLR, neutrophil to lymphocyte ratio; LMR, lymphocyte to monocyte ratio; PLR, platelet to lymphocyte ratio; CAR, C-reactive protein to albumin ratio; TPClR, total protein–chloride ratio.*

associated with OS independently (HR, 3.182; 95% CI, 2.203–5.003; $P < 0.001$). The median survival time was significantly higher for patients with PE TPClR ≤0.53 than for those with TPClR >0.53 (16 *vs*. 8 months; $P < 0.001$), as shown in **Figure 1**. N ($P < 0.001$), platelet ($P = 0.004$), ALB ($P = 0.024$), ALP ($P = 0.005$), NSE ($P < 0.001$), and PE WBC ($P = 0.001$) were also independently correlated with OS. Analyses including pre-treatment WBC, NLR, LMR, and CAR in the multivariate model are shown above, but they were not significantly related to OS ($P = 0.381$, $P = 0.541$, $P = 0.471$, and $P = 0.167$, respectively).

## DISCUSSION

In our study, we have extensively screened out commonly used clinical laboratory indexes, which included MPE from a variety of causes that are not limited to lung cancer, and found that the PE TPClR is an important prognostic factor for OS in MPE patients. The PE TPClR is effective, safety, easy to calculate, inexpensive, and generally applicable in clinical settings from the different indicators in MPE (19). Therefore, the PE TPClR could potentially be an attractive and ideal prognostic variable for predicting the survival of MPE

**TABLE 3 |** Multivariate analysis of potential associations between patient characteristics and OS.

| Variable | HR | 95%CI | *P*-value |
|---|---|---|---|
| N, $\times10^9$/L | | | |
| ≤3.69 | 1.00 | | |
| >3.69 | 2.310 | 1.560, 3.419 | <0.001 |
| PLT, $\times10^9$/L | | | |
| ≤373 | 1.00 | | |
| >373 | 0.422 | 0.234, 0.760 | 0.004 |
| ALB, g/L | | | |
| ≤29.6 | 1.00 | | |
| >29.6 | 0.633 | 0.426, 0.941 | 0.024 |
| ALP, U/L | | | |
| ≤65 | 1.00 | | |
| >65 | 2.047 | 1.244, 3.368 | 0.005 |
| NSE, ng/ml | | | |
| ≤28.9 | 1.00 | | |
| >28.9 | 2.880 | 1.750, 4.739 | <0.001 |
| PE WBCs/μl | | | |
| ≤383 | 1.00 | | |
| >383 | 0.436 | 0.271, 0.703 | 0.001 |
| PE TPClR | | | |
| ≤0.53 | 1.00 | | |
| >0.53 | 3.182 | 2.203, 5.003 | <0.001 |

*OS, overall survival; N, neutrophil; PLT, platelet; ALB, albumin; ALP, alkaline phosphatase; NSE, neuron-specific enolase, PE, pleural effusion; WBCs, white blood cells; TPClR, total protein–chloride ratio.*

patients, and more valuable prognostic information can be provided for clinicians and patients through it. As far as we know, this is the first study on the effect of simultaneous detection of TP and chloride levels in pleural effusions on the prognosis of MPE.

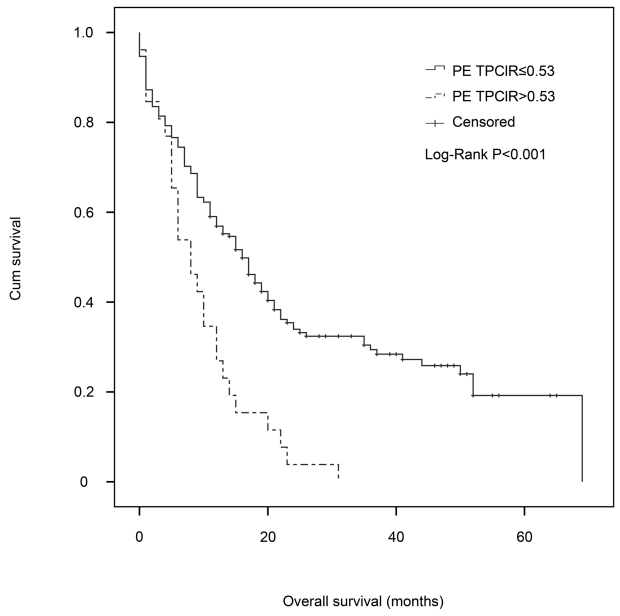


**FIGURE 1** | Kaplan–Meier estimates of overall survival for patients with malignant pleural effusion in the pleural effusion total protein–chloride ratio (PE TPClR) ≤0.53 and PE TPClR >0.53 groups. There was a significant difference in survival between the groups ($P < 0.001$; stratified log-rank test).

Inflammation, which is reported to play a significant role in different stages of oncogenesis, is now considered as a marker of cancer (20). As we have mentioned above, plenty of research have explored the most commonly used indicators of inflammatory response, such as leukocytes, leukocyte subtypes, cytokines, CRP, LDH, ALP, and their potential effects on the prognosis of cancer patients. However, markers in pleural effusions are rarely used as possible predictors for survival in patients with MPE.

In our study, a higher level of total protein in pleural effusion was related to a shorter OS in the univariate analysis. It is different from some previous studies on the relationship between the total protein in pleural fluid and survival time. Abrao et al. showed that, when the pleural fluid total protein value was <3.6 g/dl, the median survival was 74 days, which was statistically significant in the multivariate analysis (14). They believe that, over time, the progress of the disease may affect hypoalbuminemia, but we think that exudative pleural effusion, which contains a high level of protein, is resulting in increased capillary permeability. When inflammation occurs, higher capillary permeability may cause the protein in exudation to increase.

There was no in-depth study of chlorides in pleural effusions except for the identification of drowning types. In our previous study (21), we found that the $Cl^-$ level in pleural fluid was an independent indicator for prognosis in MPE patients. Few studies have found that chloride intracellular channels 3 and 4, controlling the intracellular distribution of $Cl^-$ to provide ionic counterbalance, are over-expressed in human mesothelioma (22), and the concentration of $Cl^-$ in heart-failure-associated pleural effusion is higher than that in serum, indicating that $Cl^-$ may play an important role in the formation and retention of body fluid in the thoracic cavity (23). There are many studies on

the level of chloride in the cerebrospinal fluid, which show that the concentration of chloride decreases when the level of chloride in the blood decreases. The pH of the cerebrospinal fluid decreases, and inflammatory exudation and adhesion are obvious. According to the existing literature, tumor cells produce hydrogen ions by glucose metabolism. Therefore, low pleural fluid pH and low glucose reflect a higher pleural tumor load and are related to poor survival. Heffner et al. confirmed that when pleural pH was less than 7.28, the prognosis of MPE was poor (24). Our results may be corroborated by the correlation between pH and chloride levels in pleural effusions. Therefore, a high level of PE TPClR was associated with a shorter OS.

The main limitation of our study is that it is a retrospective study with a relatively small sample size. Although a high statistical significance has been achieved, it is still necessary to conduct further studies on more patients. Further studies are needed to identify other sensitive biomarkers in pleural effusion to determine the best combination of marker analysis.

## CONCLUSION

PE TPClR can be used to predict the prognosis of MPE patients. It can help clinicians select patients for appropriate palliative care. More research is needed to clarify the underlying mechanisms and to identify new strategies to improve the prognosis of these patients.

## DATA AVAILABILITY STATEMENT

The original contributions presented in the study are included in the article/supplementary material. Further inquiries can be directed to the corresponding author.

## ETHICS STATEMENT

The studies involving human participants were reviewed and approved by the ethics committee at Beijing Chao-Yang Hospital. Written informed consent for participation was not required for this study in accordance with the national legislation and institutional requirements.

## AUTHOR CONTRIBUTIONS

XQ designed the study, did patient recruitment and assessment, collected information, analyzed the relevant data, and drafted the manuscript. Z-RZ and X-YS analyzed the relevant data and drafted the manuscript. F-SY conceived the idea, guided the study, and revised the paper critically to ensure the integrity of this research. All authors contributed to the article and approved the submitted version.

## FUNDING

This work was supported by grants from the National Natural Science Foundation of China (nos. 31700790 and 82000098).

## REFERENCES

1. Taghizadeh N, Fortin M, Tremblay A. US Hospitalizations for Malignant Pleural Effusions: Data From the 2012 National Inpatient Sample. *Chest* (2017) 151:845–54. doi: 10.1016/j.chest.2016.11.010
2. Psallidas I, Kalomenidis I, Porcel JM, Robinson BW, Stathopoulos GT. Malignant Pleural Effusion: From Bench to Bedside. *Eur Respir Rev: an Off J Eur Respir Soc* (2016) 25:189–98. doi: 10.1183/16000617.0019-2016
3. Feller-Kopman DJ, Reddy CB, DeCamp MM, Diekemper RL, Gould MK, Henry T, et al. Management of Malignant Pleural Effusions. An Official ATS/STS/STR Clinical Practice Guideline. *Am J Respir Crit Care Med* (2018) 198:839–49. doi: 10.1164/rccm.201807-1415ST
4. Clive AO, Kahan BC, Hooper CE, Bhatnagar R, Morley AJ, Zahan-Evans N, et al. Predicting Survival in Malignant Pleural Effusion: Development and Validation of the LENT Prognostic Score. *Thorax* (2014) 69:1098–104. doi: 10.1136/thoraxjnl-2014-205285
5. Temel JS, Greer JA, Muzikansky A, Gallagher ER, Admane S, Jackson VA, et al. Early Palliative Care for Patients With Metastatic Non–Small-Cell Lung Cancer. *N Engl J Med* (2010) 363:733–42. doi: 10.1056/NEJMoa1000678
6. Liu D, Jin J, Zhang L, Li L, Song J, Li W. The Neutrophil to Lymphocyte Ratio May Predict Benefit From Chemotherapy in Lung Cancer. *Cell Physiol Biochem: Int J Exp Cell Physiol Biochem Pharmacol* (2018) 46:1595–605. doi: 10.1159/000489207
7. Wang SC, Chou JF, Strong VE, Brennan MF, Capanu M, Coit DG. Pretreatment Neutrophil to Lymphocyte Ratio Independently Predicts Disease-Specific Survival in Resectable Gastroesophageal Junction and Gastric Adenocarcinoma. *Ann Surg* (2016) 263:292–7. doi: 10.1097/SLA.0000000000001189
8. Lee YS, Nam HS, Lim JH, Kim JS, Moon Y, Cho JH, et al. Prognostic Impact of a New Score Using Neutrophil-to-Lymphocyte Ratios in the Serum and Malignant Pleural Effusion in Lung Cancer Patients. *BMC Cancer* (2017) 17:557. doi: 10.1186/s12885-017-3550-8
9. Kasapoglu US, Arinc S, Gungor S, Irmak I, Guney P, Aksoy F, et al. Prognostic Factors Affecting Survival in Non-Small Cell Lung Carcinoma Patients With Malignant Pleural Effusions. *Clin Respir J* (2016) 10:791–9. doi: 10.1111/crj.12292
10. Abrao FC, de Abreu IR, Fogarolli M, Caxeiro G, Bezerra CB, de Cerqueira Cesar FP, et al. Prognostic Factors of 30-Day Mortality After Palliative Procedures in Patients With Malignant Pleural Effusion. *Ann Surg Oncol* (2015) 22:4083–8. doi: 10.1245/s10434-015-4491-6
11. Zamboni MM, da Silva CT Jr, Baretta R, Cunha ET, Cardoso GP. Important Prognostic Factors for Survival in Patients With Malignant Pleural Effusion. *BMC Pulmon Med* (2015) 15:29. doi: 10.1186/s12890-015-0025-z
12. Yoon DW, Cho JH, Choi YS, Kim J, Kim HK, Zo JI, et al. Predictors of Survival in Patients Who Underwent Video-Assisted Thoracic Surgery Talc Pleurodesis for Malignant Pleural Effusion. *Thorac Cancer* (2016) 7:393–8. doi: 10.1111/1759-7714.12354
13. Beije N, Kraan J, den Bakker MA, Maat A, van der Leest C, Cornelissen R, et al. Improved Diagnosis and Prognostication of Patients With Pleural Malignant Mesothelioma Using Biomarkers in Pleural Effusions and Peripheral Blood Samples - a Short Report. *Cell Oncol* (2017) 40:511–9. doi: 10.1007/s13402-017-0327-7
14. Abrao FC, Peixoto RDA, Abreu IRLBD. Prognostic Factors in Patients With Malignant Pleural Effusion Is It Possible to Predict Mortality in Patients With Good Performance Status. *J Surg Oncol* (2016) 113:570–4. doi: 10.1002/jso.24168

15. Terra RM, Antonangelo L, Mariani AW, de Oliveira RL, Teixeira LR, Pego-Fernandes PM. Pleural Fluid Adenosine Deaminase (ADA) Predicts Survival in Patients With Malignant Pleural Effusion. *Lung* (2016) 194:681–6. doi: 10.1007/s00408-016-9891-2
16. Verma A, Phua CK, Sim WY, Algoso RE, Tee KS, Lew SJ, et al. Pleural LDH as a Prognostic Marker in Adenocarcinoma Lung With Malignant Pleural Effusion. *Med (Baltimore)* (2016) 95:e3996. doi: 10.1097/MD.0000000000003996
17. Park D-S, Kim D, Hwang K-E, Hwang Y-R, Park C, Seol C-H, et al. Diagnostic Value and Prognostic Significance of Pleural C-Reactive Protein in Lung Cancer Patients With Malignant Pleural Effusions. *Yonsei Med J* (2013) 54:396. doi: 10.3349/ymj.2013.54.2.396
18. Arellano-Orden E, Romero-Romero B, Sanchez-Lopez V, Martin-Juan J, Rodriguez-Panadero F, Otero-Candelera R. Survivin Is a Negative Prognostic Factor in Malignant Pleural Effusion. *Eur J Clin Invest* (2018) 48:e12895. doi: 10.1111/eci.12895
19. Wang XJ, Yang Y, Wang Z, Xu LL, Wu YB, Zhang J, et al. Efficacy and Safety of Diagnostic Thoracoscopy in Undiagnosed Pleural Effusions. *Respiration* (2015) 90:251–5. doi: 10.1159/000435962
20. Hanahan D, Weinberg RA. Hallmarks of Cancer: The Next Generation. *Cell* (2011) 144:646–74. doi: 10.1016/j.cell.2011.02.013
21. Zhang X, Yi FS, Shi HZ. Predicting Survival for Patients With Malignant Pleural Effusion: Development of the CONCH Prognostic Model. *Cancer Manag Res* (2021) 13:4699–707. doi: 10.2147/CMAR.S305223
22. Tasiopoulou V, Magouliotis D, Solenov EI, Vavougios G, Molyvdas PA, Gourgoulianis KI, et al. Transcriptional Over-Expression of Chloride Intracellular Channels 3 and 4 in Malignant Pleural Mesothelioma. *Comput Biol Chem* (2015) 59 Pt A:111–6. doi: 10.1016/j.compbiolchem.2015.09.012
23. Kataoka H. Effusion-Serum Chloride Gradient in Heart Failure-Associated Pleural Effusion- Pathophysiologic Implications. *Circ Rep* (2020) 2:357–63. doi: 10.1253/circrep.CR-20-0018
24. Heffner JE, Nietert PJ, Barbieri C. Pleural Fluid pH as a Predictor of Survival for Patients With Malignant Pleural Effusions. *Chest* (2000) 117:79–86. doi: 10.1378/chest.117.1.79

**Conflict of Interest:** The authors declare that the research was conducted in the absence of any commercial or financial relationships that could be construed as a potential conflict of interest.

**Publisher's Note:** All claims expressed in this article are solely those of the authors and do not necessarily represent those of their affiliated organizations, or those of the publisher, the editors and the reviewers. Any product that may be evaluated in this article, or claim that may be made by its manufacturer, is not guaranteed or endorsed by the publisher.

frontiers in Oncology

ORIGINAL RESEARCH
published: 17 January 2022
doi: 10.3389/fonc.2021.775583

# Identification and Validation of a Novel Six-lncRNA-Based Prognostic Model for Lung Adenocarcinoma

*Lingge Yang[1†], Yuan Wu[1†], Huan Xu[1], Jingnan Zhang[1], Xinjie Zheng[1], Long Zhang[1], Yongfang Wang[2], Weiyu Chen[1*] and Kai Wang[1*]*

[1] Department of Respiratory Medicine, The Fourth Affiliated Hospital, College of Medicine, Zhejiang University, Yiwu, China,
[2] Department of Respiratory Medicine, The Second Affiliated Hospital, Zhejiang University School of Medicine, Hangzhou, China

OPEN ACCESS

**Edited by:**
Jessy Deshane,
University of Alabama at Birmingham,
United States

**Reviewed by:**
Elisa Roca,
Casa di cura Pederzoli, Italy
Kayla Goliwas,
University of Alabama at Birmingham,
United States

***Correspondence:**
Kai Wang
kaiw@zju.edu.cn
Weiyu Chen
weiyuchen@zju.edu.cn

[†]These authors have contributed equally to this work

**Specialty section:**
This article was submitted to Thoracic Oncology, a section of the journal Frontiers in Oncology

**Received:** 14 September 2021
**Accepted:** 16 December 2021
**Published:** 17 January 2022

**Citation:**
Yang L, Wu Y, Xu H, Zhang J, Zheng X, Zhang L, Wang Y, Chen W and Wang K (2022) Identification and Validation of a Novel Six-lncRNA-Based Prognostic Model for Lung Adenocarcinoma. Front. Oncol. 11:775583. doi: 10.3389/fonc.2021.775583

**Objective:** This study was conducted in order to establish a long non-coding RNA (lncRNA)-based model for predicting overall survival (OS) in patients with lung adenocarcinoma (LUAD).

**Methods:** Original RNA-seq data of LUAD samples were extracted from The Cancer Genome Atlas (TCGA) database. Univariate Cox survival analysis was performed to select lncRNAs associated with OS. The least absolute shrinkage and selection operator (LASSO) regression analysis and multivariate Cox analysis were performed for building an OS-associated lncRNA prognostic model. Moreover, receiver operating characteristic (ROC) curves were generated to assess predictive values of the hub lncRNAs. Consequently, qRT-PCR was conducted to validate its prognostic value. The potential roles of these lncRNAs in immunotherapy and anti-angiogenic therapy were also investigated.

**Results:** The lncRNA-associated risk score of OS (LARSO) was established based on the LASSO coefficient of six individual lncRNAs, including CTD-2124B20.2, CTD-2168K21.1, DEPDC1-AS1, RP1-290I10.3, RP11-454K7.3, and RP11-95M5.1. Kaplan–Meier analysis revealed that LUAD patients with higher LARSO values had a shorter OS. Furthermore, a new risk score (NRS), including LARSO, stage, and N stage, could better predict the prognosis of LUAD patients compared with LARSO alone. Evaluation of the prognostic model in our cohort demonstrated that patients with higher scores had a worse prognosis. In addition, correlation analysis between these six lncRNAs and immune checkpoints or anti-angiogenic targets suggested that LUAD patients with high LARSO might not be sensitive to immunotherapy or anti-angiogenic therapy.

**Conclusions:** This robust six-lncRNA prognostic signature may be used as a novel and powerful prognostic biomarker for lung adenocarcinoma.

**Keywords: lung adenocarcinoma, lncRNA, prognostic model, least absolute shrinkage and selection operator (LASSO), overall survival**

## INTRODUCTION

Lung cancer is the leading cause of cancer-related morbidity and mortality worldwide (1). Lung adenocarcinoma (LUAD), the most common histological type of lung cancer, is highly heterogeneous and accounts for approximately 40% of all lung cancer cases (2). Although advances have been made in improving diagnosis and developing new treatments, the overall survival of (OS) patients has not significantly improved, with 5-year survival rates being <18%. One of the main reasons for poor prognosis is that most patients are diagnosed only when in an advanced stage, thus losing the chance to undergo surgery (3). Therefore, identifying accurate prognostic biomarkers for early lung cancer diagnosis, especially for LUAD, remains of crucial importance.

Long non-coding RNAs (lncRNAs) are widely defined as RNA transcripts lacking protein-coding abilities, with a length longer than 200 nucleotides (4, 5). lncRNAs are essential in the regulation of various cellular and physiologic functions, including gene activation/silencing (6, 7), chromatin dynamic (8), post-translational modification (9), and alternative splicing (10), and have been reported to be involved in tumorigenesis and tumor metastasis (11, 12). For example, lncRNAs named HOTAIR could serve as a modular scaffold to reprogram chromatin state, promoting cancer metastasis (13). Moreover, DLX6AS lncRNA acts as competing endogenous RNAs (ceRNAs) that can sponge target microRNAs or proteins and can promote cancer proliferation and invasion by reducing the endogenous function of miR-181b in pancreatic cancer (14, 15). Human colorectal cancer-specific CCAT1 lncRNA can inhibit long-range chromatin interactions with its enhancers (16).

Increasing evidence suggests that aberrant expression of lncRNAs is associated with various human cancers, such as ovarian (17) and non-small cell lung cancer (NSCLC) (18). Notably, some lncRNAs have been implicated as effective biomarkers for cancer diagnosis and prognostication (19). In this study, we aimed to identify and validate potential lncRNA biomarkers for the diagnosis and prognosis of LUAD. RNA sequencing (RNA-seq) data for LUAD were retrieved from The Cancer Genome Atlas (TCGA). A novel lncRNA-based prognostic signature was discovered for LUAD based on bioinformatics approaches. The six-lncRNA signature illustrated desirable sensitivity and specificity after collecting validation sets and follow-up.

## MATERIAL AND METHODS

### Data Collection and Processing

HTseq-FPKM (fragments per kilobase million), the VarScan2 data of exon group mutation, and clinical information of LUAD patients were downloaded from TCGA (https://portal.gdc.cancer.gov) (20). FPKM was transferred into TPM (transcripts per million). In addition, the expression matrix of lncRNAs was extracted.

### Univariate Cox Survival Analysis

The LUAD patients were grouped based on the median value of lncRNA expression. Based on clinical information of LUAD patients, univariate survival analysis of overall survival (OS) was performed by survival package (21) of R 4.0.2 software. The lncRNAs associated with OS were significantly extracted for further model building.

### OS-Associated Prognostic Model Building

lncRNA expression matrix associated with OS as well as clinical information of related TCGA-LUAD patients was retrieved. The least absolute shrinkage and selection operator (LASSO) regression model was built according to the survival state of patients (i.e., dead or alive) by glmnet package (nfold = 10, $\lambda$ = lambda.min) (22). The lncRNAs whose regression coefficients were not 0 were included for multivariate Cox regression analysis, and forestplot package (23) was used for analyzing and plotting. The risk score equation named lncRNA-associated risk score of OS (LARSO) was obtained depending on the coefficients of lncRNAs associated with prognosis in the regression model. The ggplot2 package (24) and timeROC package (25) were used to generate a scatter map and a heat map of lncRNA expression after calculating the LARSO value of each sample. Time-dependent (1, 3, and 5 years) receiver operating characteristic (ROC) and Kaplan–Meier curves were also generated. The largest Youden index of ROC was selected as the best cutoff value of LARSO, and the patients were divided into high-risk and low-risk groups according to this value. Nomogram and calibrate curves were plotted using an rms package (26). The results of the Cox regression analysis were visualized.

### Correlation Analysis Between LARSO and Clinicopathological Features of TCGA-LUAD

Clinical information and the key gene (EGFR, KRAS, ALK, ROS1, and BRAF) mutation status of LUAD patients in TCGA were extracted for investigating the correlation between LARSO and clinicopathological features. Univariate Cox regression analysis was performed to pick out factors correlated with OS, and further multivariate Cox regression analysis was performed to obtain independent prognosis factors associated with OS. Furthermore, we analyzed the correlation between LARSO and these factors overall and the differences between high- and low-risk groups. In order to obtain a new risk score (NRS), LASSO regression analysis was carried out again according to the method described above. Prognostic values of the novel prognostic model with clinical characteristics were reanalyzed.

### Validation Set Collection and Follow-Up

LUAD tissues and paired normal adjacent tissues were collected from 48 LUAD patients in the Second Affiliated Hospital of Zhejiang University School of Medicine from March 2018 to August 2020 (Approval No. IR2019001101; approval on April 3, 2019). Clinicopathological characteristics and prognostic survival information included age, sex, smoking habit, tumor size, pathogenic site, and clinical TNM stage. The follow-up date ended on June 8 in 2021, and outpatient and telephone follow-up were performed.

This study was approved by the Institutional Review Committee of the Second Affiliated Hospital of Zhejiang University School of Medicine. All the patients and their guardians gave written informed consent before surgery.

## qRT-PCR

Total RNA in the tumor samples was extracted using the RNA-Quick Purification Kit (RN001, ES Science, Beijing, China) according to the instructions of the manufacturer. One microgram of RNA was then reverse-transcribed into cDNAs using the PrimeScript™ RT Reagent Kit (RR037A, TaKaRa, Japan). qRT-PCR analysis was performed using TB Green Premix Ex Taq™ kit (RR420A, TaKaRa, Japan) on a CFX96 Real-Time System (Bio-Rad, UK). β-Actin was used as the housekeeping gene, and the primer information is listed in **Table S1**.

## Validation of Prognostic Value

The CT values of the first LUAD patient sample for qPCR were set as control. $2^{-\triangle\triangle CT}$ was performed for all the samples to obtain the relative expression values of lncRNAs in the prognostic model. Relative LARSO and NRS values of LUAD patients were calculated by the risk score equation. These results were integrated with the prognosis information of patients. Hence, the related scatter plot, heat map, ROC curve, and Kaplan–Meier curve were analyzed and plotted to validate the prognostic value of our model.

## Gene Set Enrichment Analysis

The patients were divided into high-risk and low-risk groups according to the cutoff value of LARSO in the modeling set. KEGG and hallmark pathway enrichment analyses in gene set enrichment analysis (GSEA, https://www.gsea-msigdb.org/gsea) were performed for TCGA transcriptome matrix normalized by TPM. The results (FDR < 0.05) were visualized (27).

## Correlation Analysis Between Immune-Related Genes and lncRNAs in the LARSO Prognostic Model

Immune-related genes (IRGs) were downloaded from the ImmPort database (https://immport.niaid.nih.gov) (28). IRG expression matrix profiles, including antigen processing and presentation, interferons and interferon receptors, TCR signaling pathway, TNF family members and receptors, and TGFb family members and receptors, were extracted from the TCGA transcriptome matrix profile described above. The correlation coefficient between IRGs and lncRNA in the prognostic model was calculated by the psych package (29) and plotted by the ggplot2 package (24).

## Correlation Analysis of Immune Infiltration

Score evaluation of 22 immune cells in the TCGA transcriptome matrix profile described above was performed in the CIBERSORTx database (https://cibersort.stanford.edu/) (30, 31). The correlation between these scores and lncRNA expression was analyzed. Besides, differences in immune cell scores between high- and low-risk groups were analyzed to evaluate the correlation between the prognostic model and immune infiltration.

## Correlation Analysis of Immune Checkpoints and Anti-Angiogenic Targets With lncRNAs in the LARSO Prognostic Model

Expression matrices of immune checkpoints including PDCD1 (PD-1), CD274 (PD-L1), PDCD1LG2 (PD-L2), and CTLA4 were extracted from the transcriptome matrix in TCGA described above. Expression matrices of anti-angiogenic targets including KDR (VEGFR-2), FLT4 (VEGFR-3), FLT1 (VEGFR-1), EGFR, PDGFRB (PDGFR-2), KIT, PDGFRA (PDGFR-1), and FGFR1-4 were also extracted from this matrix in TCGA. The correlation between these immune checkpoints or targets and lncRNA expression was analyzed and plotted. We also compared the differences of these immune checkpoints or targets between the high- and low-risk groups.

## Statistical Analysis

The statistical results were analyzed and plotted by R 4.0.2 and GraphPad 8.0 software. Mean ± standard deviation (SD) displayed the measurement data. Student's *t*-test was used to compare the difference between high- and low-risk groups. A chi-square test was used to compare the difference between high- and low-risk groups for enumeration data. Spearman test was used for correlation analysis, and log-rank tests were used for survival analysis. $P$ <0.05 was considered statistically significant ($^{*}P < 0.05$, $^{**}P < 0.01$, $^{***}P < 0.001$, $^{****}P < 0.0001$).

# RESULTS

## Construction of a Regression Equation Based on the Six-lncRNA Prognostic Risk Scoring Model

Three hundred thirty-six lncRNAs correlated with OS were retrieved from the TCGA database. There were only 20 lncRNAs that exhibited effective co-efficiency in regression *via* LASSO regression analysis (**Figures 1A, B**). Among them, six lncRNAs, i.e., CTD-2124B20.2, CTD-2168K21.1, DEPDC1-AS1, RP1-290I10.3, RP11-454K7.3, and RP11-95M5.1, were finally identified *via* expression profile analysis as well as Cox regression analysis. All six lncRNAs showed correlations with the status of the patients (alive or dead) and significantly affected OS (**Figure 1C**). Based on the results above, we obtained a LARSO regression equation: LARSO = 0.007613542 × CTD-2124B20.2 expression value + 0.003865727 × CTD-2168K21.1 expression value + 0.001419855 × DEPDC1-AS1 expression value + 0.001170444 × RP1-290I10.3 expression value + 0.003746008 × RP11-454K7.3 expression value + 0.0036433 × RP11-95M5.1 expression value. In addition, correlation coefficients of the six lncRNAs were >0 in the regression equation, which implied that these lncRNAs were potential oncogenic factors. Next, hazard

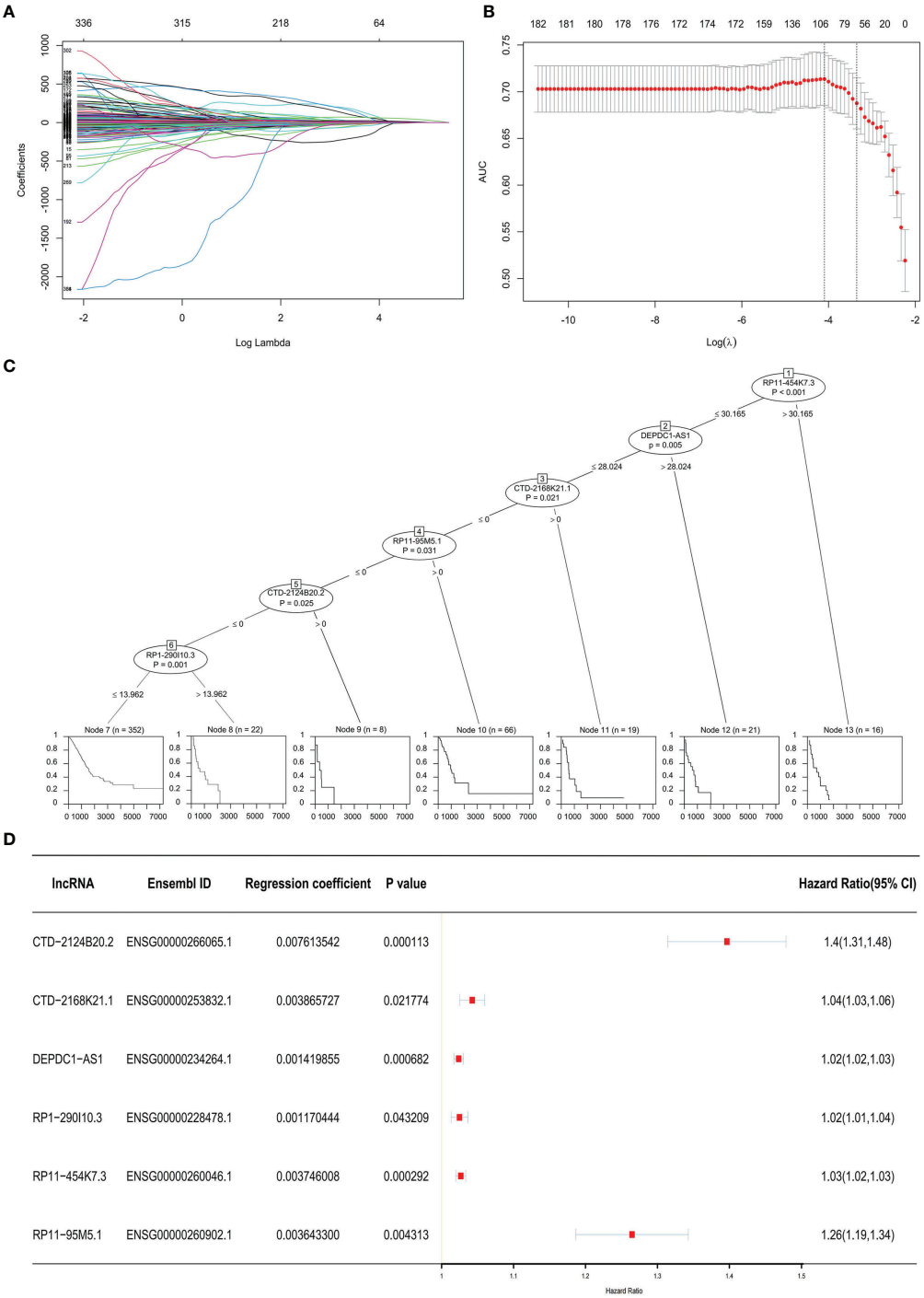


**FIGURE 1** | Prognostic model. **(A)** Least absolute shrinkage and selection operator (LASSO) coefficient distribution diagram of 336 long non-coding RNAs (lncRNAs): *x*-coordinate was log (*λ*) for screening the best tuning parameter (*λ*). **(B)** Tuning parameter (*λ*) in the LASSO regression model was selected according to 10-fold cross-validation. Plotting was performed based on this value as well as the area under the receiver operating characteristic curve. A vertical dashed line was drawn at the best value by using the minimum standard and 1 standard error of the minimum standard (1-SE standard). **(C)** Visualization of the Cox regression analysis: the significant lncRNAs ($P < 0.05$) in the Cox regression were displayed. The impacts of these lncRNAs on the prognosis of lung adenocarcinoma (LUAD) patients are shown below by a single survival curve. **(D)** Forest map with HR: the Ensembl ID of the six lncRNAs, regression coefficient in LASSO regression, and *P*-value in the Cox regression analysis were displayed; a vertical line was drawn at HR = 1.

ratio (HR) values further confirmed that lncRNAs were potential oncogenes (HR > 1). Hence, it was suggested that the selected six lncRNAs were risk factors of LUAD (**Figure 1D**).

## Construction of a Six-lncRNA Signature for Predicting OS

Based on the LARSO regression equation above, LARSO values of each LUAD case in the TCGA database were calculated. Afterwards, all the TCGA-LUAD patients were divided into high-risk ($n$ = 48) and low-risk groups ($n$ = 465) according to the cutoff point (LARSO = 0.110). Next, we analyzed the lncRNA relative expression of every TCGA-LUAD patient, the expression distribution of lncRNAs, and the survival state of patients, both in the high- and low-risk groups (**Figure 2A**). The relative expression of six lncRNAs and the number of deaths were higher in the high-risk group compared with those in a low-risk group. Notably, the six-lncRNA signature reached AUC values of 0.63 in the 1-year ROC curve, 0.6 in the 3-year ROC curve, and 0.59 in the 5-year ROC curve, suggesting an effective performance in OS prediction (**Figure 2B**). Moreover, Kaplan–Meier curves (**Figure 2C**) suggested statistically significant differences between the high- and low-risk groups ($P$ < 0.0001). Similarly, a significant difference was also observed in median survival time between the high-risk group (624 days) and the low-risk group (1,559 days).

By analyzing the prediction accuracy through calibration curves, we demonstrated that the 2-year OS prediction had the highest accuracy *via* the six-lncRNA signature prognostic model (**Figure 2D**). A nomogram was also built to evaluate the prediction abilities of this prognostic model on 1-, 3-, and 5-year survival probability (**Figure 2E**). This result suggested that the expression of these six lncRNAs was negatively correlated with patient survival, i.e., lower expression, higher survival.

## LARSO Was Correlated With Clinicopathologic Features of LUAD Patients

The correlation analysis between LARSO and the clinicopathologic features of TCGA-LUAD was then investigated. As shown in **Table 1**, statistical differences between the high- and low-risk groups were found in T stage ($P$ < 0.0001), N stage ($P$ = 0.0342), survival status ($P$ < 0.0001), and cancer status ($P$ = 0.0002). Moreover, higher LARSO values implied larger tumor size, lymph nodes metastasis, more death of LUAD patients, or more survival of patients with tumor.

Furthermore, we conducted univariate and multivariate Cox regression analysis for the above factors (**Table 2**). Group (HR = 0.3519, $P$ < 0.001), LARSO (HR = 26401, $P$ < 0.001), stage, and TNM stage were all correlated with OS. Above all, LARSO (HR = 1,867.458, $P$ = 0.00642) and T3 stage (HR = 2.644,

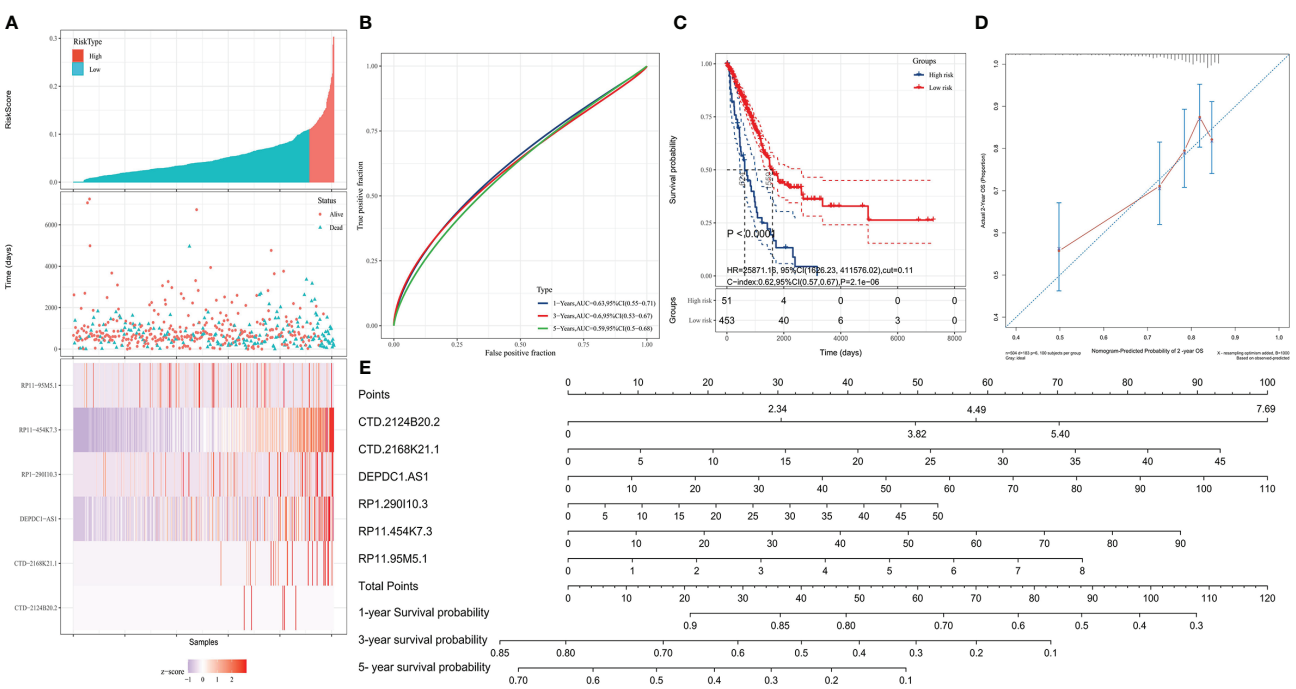


**FIGURE 2** | Validation of the prognostic model. High- and low-risk groups were divided according to the lncRNA-associated risk score of OS (LARSO) value. **(A)** The histogram, scatter plot, and heat map showed the risk grouping, patient survival status, and the expression of the six lncRNAs, respectively. **(B)** Receiver operating characteristic (ROC) curves were shown at 1, 3, and 5 years based on the LARSO scores and prognosis of LUAD patients. **(C)** Kaplan–Meier survival curves were plotted: the overall survival time of patients in the high-risk group was significantly shorter than that in the low-risk group ($P$ < 0.0001). **(D)** Calibration curve: the $x$-coordinate was the probability of 2-year survival predicted by the model, and the $y$-coordinate represented the actual 2-year survival. **(E)** Column map: the 1-, 3-, and 5-year survival rates of patients could be predicted by scoring the expression level of the six lncRNAs. A log-rank test was used for survival analysis.

**TABLE 1 |** Correlation between LARSO and the clinicopathological characteristics of lung adenocarcinoma patients in the TCGA database (*N* = 514).

| Variables | Low risk (*N* = 465) | High risk (*N* = 48) | $\chi^2$ | *t* | *P*-value |
|---|---|---|---|---|---|
| **Gender** | | | | | |
| Female | 252 | 24 | 0.3078 | | 0.5790 |
| Male | 213 | 24 | | | |
| **Age (years)** | 65.22 ± 9.94 | 66.06 ± 11.00 | | 0.5486 | 0.5835 |
| **Histological type** | | | | | |
| Lung acinar adenocarcinoma | 18 | 0 | 7.045 | | 0.7954 |
| Lung adenocarcinoma mixed subtype | 93 | 13 | | | |
| Lung adenocarcinoma—not otherwise specified (NOS) | 289 | 31 | | | |
| Lung bronchioloalveolar carcinoma mucinous | 5 | 0 | | | |
| Lung bronchioloalveolar carcinoma non-mucinous | 19 | 0 | | | |
| Lung clear cell adenocarcinoma | 1 | 0 | | | |
| Lung micropapillary adenocarcinoma | 3 | 0 | | | |
| Lung mucinous adenocarcinoma | 2 | 0 | | | |
| Lung papillary adenocarcinoma | 20 | 3 | | | |
| Lung signet ring adenocarcinoma | 1 | 0 | | | |
| Lung solid pattern predominant adenocarcinoma | 5 | 0 | | | |
| Mucinous (colloid) carcinoma | 9 | 1 | | | |
| **Clinical stage** | | | | | |
| Unknown | 8 | 0 | | | |
| Stage I | 253 | 21 | 5.221 | | 0.1563 |
| Stage II | 110 | 11 | | | |
| Stage III | 73 | 11 | | | |
| Stage IV | 21 | 5 | | | |
| **T classification** | | | | | |
| Tx | 3 | 0 | | | |
| T1 | 156 | 12 | 25.04 | | **<0.0001****** |
| T2 | 252 | 24 | | | |
| T3 | 43 | 4 | | | |
| T4 | 11 | 8 | | | |
| Unknown | 0 | 0 | | | |
| **N classification** | | | | | |
| Nx | 11 | 0 | | | |
| N0 | 305 | 25 | 4.487 | | **0.0342*** |
| N1/N2/N3 | 148 | 23 | | | |
| Unknown | 1 | 0 | | | |
| **M classification** | | | | | |
| Mx | 132 | 8 | | | |
| M0 | 309 | 35 | 1.422 | | 0.2330 |
| M1 | 20 | 5 | | | |
| Unknown | 4 | 0 | | | |
| **Anatomic neoplasm subdivision** | | | | | |
| L-lower | 69 | 8 | 0.9692 | | 0.9144 |
| L-upper | 110 | 12 | | | |
| R-lower | 89 | 7 | | | |
| R-middle | 19 | 2 | | | |
| R-upper | 168 | 14 | | | |
| Discrepancy/unknown | 10 | 5 | | | |
| **ECOG performance status** | | | | | |
| 0 | 93 | 7 | 2.066 | | 0.5588 |
| 1 | 100 | 14 | | | |
| 2 | 21 | 2 | | | |
| 3 | 3 | 0 | | | |
| Unknown | 296 | 25 | | | |
| **Drug therapy** | | | | | |
| No | 304 | 32 | 0.032 | | 0.8579 |
| Yes | 161 | 16 | | | |
| **Drug response (at the last time)** | | | | | |
| Yes (complete response + partial response + stable disease) | 75 | 3 | 1.049 | | 0.3058 |
| No (progressive disease) | 22 | 3 | | | |
| Unknown | 64 | 10 | | | |
| **Radiotherapy** | | | | | |
| No | 379 | 35 | 2.061 | | 0.1511 |
| Yes | 86 | 13 | | | |

*(Continued)*

**TABLE 1** | Continued

| Variables | Low risk (*N* = 465) | High risk (*N* = 48) | $\chi^2$ | *t* | *P*-value |
|---|---|---|---|---|---|
| **Radiotherapy response (at the last time)** | | | | | |
| Yes (complete response + partial response + stable disease) | 24 | 0 | 3.214 | | 0.0730 |
| No (progressive disease) | 21 | 5 | | | |
| Unknown | 41 | 8 | | | |
| **EGFR mutation** | | | | | |
| No | 403 | 45 | 1.385 | | 0.2393 |
| Yes | 62 | 3 | | | |
| **KRAS mutation** | | | | | |
| No | 334 | 40 | 2.362 | | 0.1243 |
| Yes | 131 | 8 | | | |
| **ALK mutation** | | | | | |
| No | 431 | 45 | 0.0005 | | 0.9822 |
| Yes | 34 | 3 | | | |
| **ROS1 mutation** | | | | | |
| No | 444 | 43 | 2.041 | | 0.1531 |
| Yes | 21 | 5 | | | |
| **BRAF mutation** | | | | | |
| No | 427 | 45 | 0.035 | | 0.8509 |
| Yes | 38 | 3 | | | |
| **Follow-up** | | | | | |
| Alive | 313 | 8 | 48.82 | | **<0.0001****** |
| Dead | 144 | 39 | | | |
| Unknown | 8 | 1 | | | |
| **Cancer status** | | | | | |
| Tumor free | 286 | 20 | 14.36 | | **0.0002***** |
| With tumor | 89 | 21 | | | |
| Discrepancy/unknown | 90 | 7 | | | |

*Patients were divided into the high-risk group (n = 48) and low-risk group (n = 465) according to LASSO = 0.110. Bold values indicate P < 0.05 and *P < 0.05, ***P < 0.001, and ****P < 0.0001.*

**TABLE 2** | Univariate and multivariate analyses for factors influencing overall survival (OS) of lung adenocarcinoma patients in the TCGA database.

| Variables | | Overall survival (OS) | | | |
|---|---|---|---|---|---|
| | | Univariate | | Multivariate | |
| | | HR (95% CI) | *P*-value | HR (95% CI) | *P*-value |
| Group (low risk) | | 0.3519 (0.2467–0.5019) | <0.001*** | – | – |
| LARSO | | 26,401 (1,640–424,906) | <0.001*** | 1,867.458 (8.299–42,020) | 0.00642** |
| Stage | Stage II | 2.472 (1.718–3.557) | <0.001*** | – | – |
| | Stage III | 3.494 (2.383–5.124) | <0.001*** | – | – |
| | Stage IV | 3.817 (2.199–6.624) | <0.001*** | – | – |
| T | T2 | 1.452 (1.017~2.073) | 0.0398* | – | – |
| | T3 | 2.958 (1.758–4.979) | <0.001*** | 2.644 (1.266–5.515) | 0.00963** |
| | T4 | 2.914 (1.501–5.659) | 0.00159** | – | – |
| N (N0) | | 0.388 (0.288–0.521) | <0.001*** | – | – |
| M (M1) | | 2.133 (1.245–3.654) | 0.00583** | – | – |

*All results were calculated by the survival package of R 4.0.2 software.*

*TCGA, The Cancer Genome Atlas; CI, confidence interval; LARSO, lncRNA-associated risk score of overall survival. *P < 0.05, **P < 0.01, ***P < 0.001.*

$P$ = 0.00963) were two independent prognostic factors affecting OS. Thus, we analyzed the correlation between LARSO value and stage or TNM stage and investigated whether there was a significant difference in LARSO value between high- and low-risk groups at a different stage or TNM stage. Our data indicated that a higher LARSO value was correlated with worse or severe TNM stage. Moreover, there were significant differences in LARSO value between stage I and stage IV ($P$ = 0.0125, **Figure 3A**), or T1 and T4 ($P$ < 0.0001), or T2 and T4 ($P$ = 0.0005), or T3 and T4 ($P$ = 0.0288, **Figure 3B**). Also, the LARSO value was different in the N0 and N1/N2/N3 groups ($P$ = 0.0070, **Figure 3C**) and in the M0 and M1 groups ($P$ = 0.0262, **Figure 3D**).

Next, we compared LARSO values in the high- and low-risk groups based on stage, T classification, N classification, or M classification. There were significant differences in LARSO value between the two groups on stage ($P$ < 0.0001, **Figure 3E**) or T classification ($P$ < 0.0001, **Figure 3F**). As for the N stage (**Figure 3G**), a significant difference in LARSO value was found between the high- and low-risk groups ($P$ < 0.0001).

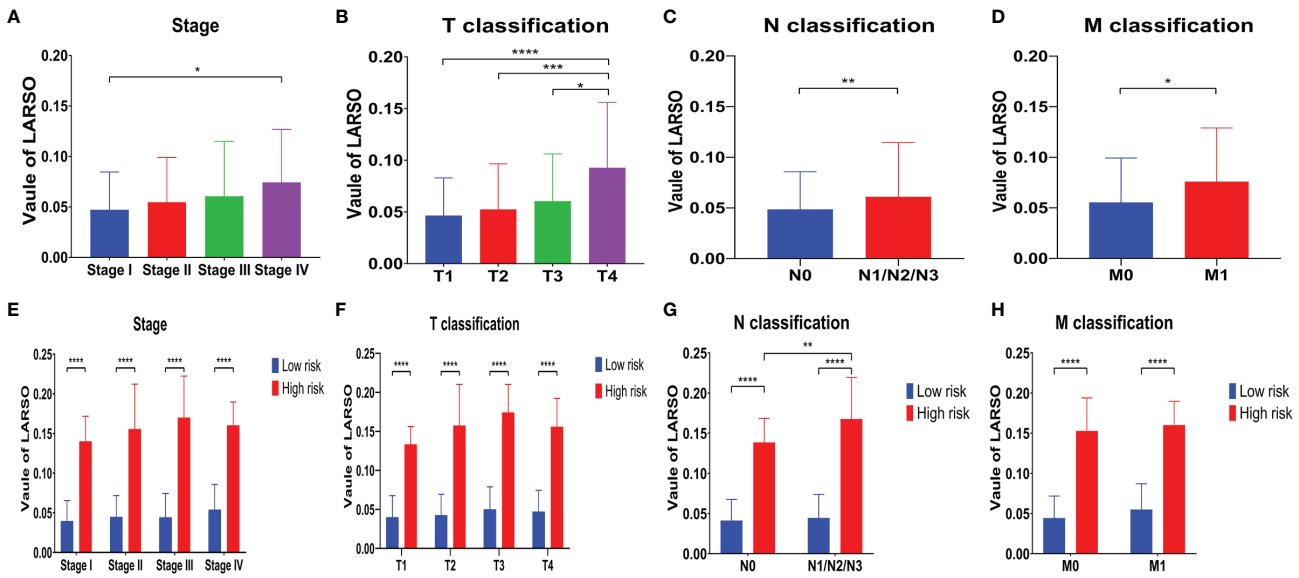


**FIGURE 3** | Correlation analysis between the LARSO value and stage or TNM stage. **(A)** Tumor stage was negatively correlated with LARSO value, i.e., higher stage, lower LARSO value; the difference of LARSO between stage I and stage IV was statistically significant ($P < 0.05$). **(B)** A higher LARSO value was associated with a worse T stage. The LARSO value at T1, T2, or T3 was statistically different from the LARSO value at T4. **(C)** The LARSO value of patients with lymph node metastasis (N1/N2/N3) was significantly higher than patients without lymph node metastasis (N0). **(D)** LARSO value in the M0 group was significantly lower than that in the M1 group ($P < 0.05$). **(E)** The LARSO value between the high- and low-risk groups at different stages was statistically significant, and the LARSO value of the high-risk group was significantly higher than that of the low-risk group ($P < 0.05$). **(F)** The LARSO value in different T stages between the high- and low-risk groups was statistically significant. **(G)** The LARSO value between the high- and low-risk groups was significantly different in various N stages ($P < 0.05$). In addition, the LARSO value in the high-risk group with lymph node metastasis (N1/N2/N3) was significantly higher than that in the non-lymph node metastasis group (N0). **(H)** The difference of LARSO value in different M stages in the high- and low-risk groups was statistically significant. Student's *t*-test was used for testing between groups. *$P < 0.05$; **$P < 0.01$; ***$P < 0.001$; ****$P < 0.0001$.

Besides, there was a significant difference between N0 and N1/N2/N3 in the high-risk group ($P = 0.0033$). Likewise, the difference in LARSO value between the high- and low-risk groups in the M stage was also statistically significant ($P < 0.0001$, **Figure 3H**).

## LARSO Combined With Stages and N Stages Could Better Predict the Prognosis of LUAD Patients

Firstly, clinical factors correlated with OS were obtained *via* univariate Cox regression analysis. Then, these clinical factors were combined with the LARSO data, after which a LASSO regression analysis was performed. Therefore, a new risk score (NRS) was generated: 7.5671594 × LARSO + 0.3127315 × Stage score + 0.2828587 × N score. The scores of stages I, II, III, and IV were graded as 1, 2, 3, and 4, respectively. Similarly, the scores of NX (0), N0 (1), and N1/N2/N3 (2) were also defined.

Based on this NRS regression equation, we calculated the NRS values of each TCGA-LUAD patient. All the patients were divided into a high-risk group ($n = 183$) and a low-risk group ($n = 317$) based on the new cutoff point of the ROC curve (NRS = 1.45). Higher NRS scores and deaths were observed in the high-risk group compared with the low-risk group (**Figure 4A**). Moreover, we found that the AUC value was 0.71 in the 1-year ROC curve, 0.7 in the 3-year ROC curve, and 0.71 in the 5-year ROC curve, indicating NRS with better OS prediction ability compared with LARSO alone (**Figure 4B**), as well as stage (**Figure S1A**) or N stage (**Figure S1B**) alone.

Survival analysis was further performed, suggesting a significant difference in the median survival time, with 3,094 days in the low-risk group, which was about 3.58 times higher than the high-risk group (864 days) ($P < 0.0001$, **Figure 4C**). These results implied that LARSO combined with stage and N stage could support a desirable prediction for LUAD prognosis.

## LARSO and Derived NRS Prognostic Model Validation

To validate our six-lncRNA signature prognostic model, we collected 48 pairs of carcinoma tissues and normal adjacent tissues for investigating the relative expression of six lncRNAs *via* qRT-PCR. Then, the LARSO values of each LUAD patient were calculated through the LARSO regression model. Likewise, we divided all the LUAD patients into high-risk group ($n = 15$) and low-risk group ($n = 33$) according to a cutoff point in a 3-year ROC curve (LARSO = 0.790). The relative expression of these lncRNAs, expression distribution, and survival status of LUAD patients were also examined. As shown in **Figure 4D**, the relative expression of these six lncRNAs and deaths was lower in the low-risk group compared with those in the high-risk group.

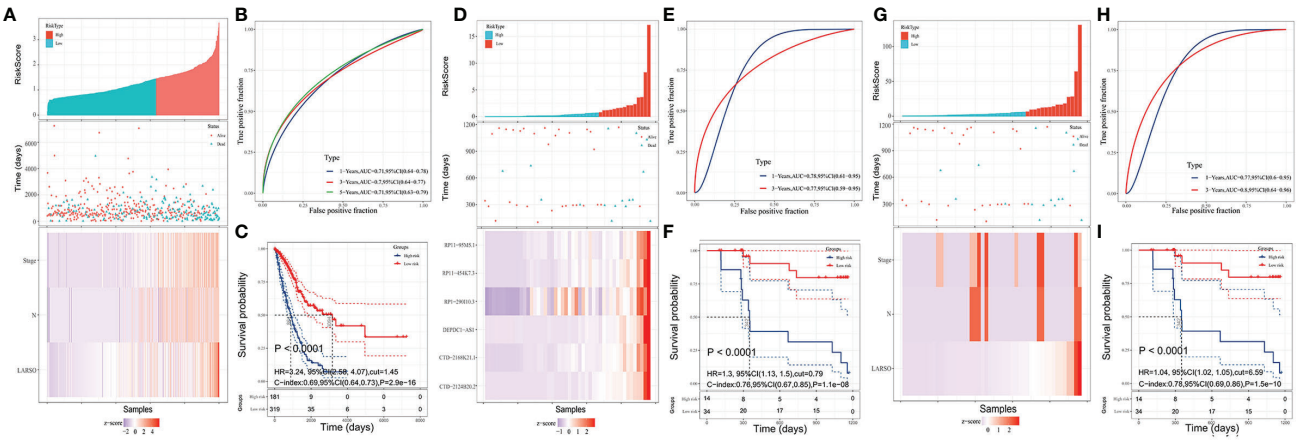

**FIGURE 4** | LARSO combined with stages and N stages for predicting the prognosis of LUAD patients. **(A)** Risk grouping situation, the scatter diagram of patient survival status, and the distribution of LARSO, stage, and N stage in each sample are shown. **(B)** The 1-, 3-, and 5-year ROC curves plotted based on NRS and patient survival. **(C)** Kaplan–Meier analysis: the overall survival time of patients in the high-risk group was significantly shorter than that in the low-risk group ($P < 0.0001$). **(D)** The LARSO values were calculated based on the survival state of 48 patients and the expression of the six lncRNAs. Histogram of the high- and low-risk distribution, scatter plot of patient survival, and the heat map of the expression of the six lncRNAs were displayed. **(E)** The 1- and 3-year ROC curves were drawn based on the LARSO value and the survival state of patients. **(F)** Kaplan–Meier analysis: the overall survival time of patients in the high-risk group was significantly shorter than that in the low-risk group ($P < 0.0001$). **(G)** The risk grouping, the scatter diagram of patient survival status, and the distribution of LARSO, stage, and N stage in each sample were shown after NRS was calculated. **(H)** According to the 1- and 3-year ROC curves drawn based on the NRS value and patient survival time, the AUC value of 1-year ROC was 0.77, while the AUC value of the 3-year ROC was up to 0.8. **(I)** Kaplan–Meier analysis: the overall survival time of patients in the high-risk group was significantly shorter than that in the low-risk group ($P < 0.0001$). A log-rank test was used for survival analysis.

Besides, AUC values of 1-year and 3-year ROC curves were 0.78 and 0.77, which indicated that our LARSO prognostic model has a good prognostic value (**Figure 4E**). However, 5-year ROC curve was not available due to insufficient follow-up time. Survival curves were also performed. A low-risk group demonstrated a prolonged median survival time with 1,162 days follow-up deadline, which was significantly longer than that of the high-risk group (342 days) ($P < 0.0001$, **Figure 4F**).

Furthermore, NRS values in the validation set were calculated, and the cutoff value (NRS = 6.59) was used for dividing patients into high- ($n = 15$) and low-risk ($n = 33$) groups. Similar to previous data, the high-risk group was associated with higher scores and more deaths (**Figure 4G**). Although the AUC value in the 1-year ROC curve (AUC = 0.77) was close to the result in **Figure 4E** (0.78), the AUC value in the 3-year ROC curve (AUC = 0.8) was better than that in **Figure 4E** (0.77) (**Figure 4H**). In addition, Kaplan–Meier curves showed a significant difference between high- and low-risk groups, thus indicating that patients in the low-risk groups had better prognoses ($P < 0.0001$, **Figure 4I**).

## Related Hallmarks and Regulatory Pathways of lncRNAs in the LARSO Prognostic Model

Next, we performed GSEA analysis as well as KEGG pathway analysis, aiming to investigate the related hallmarks and regulatory pathways associated with lncRNAs. GSEA suggested that the six lncRNAs are involved in several pathways, including G2M checkpoint, mTORC1 signaling, E2F targets, MYC targets, DNA repair, glycolysis, oxidative phosphorylation, and reactive oxygen species pathway ($P < 0.05$ and FDR < 0.05, **Figure S2A**). Generally, these hallmark gene sets participate in cell cycle regulation, DNA damage repair, or tumor cell metabolism regulation. Besides, the six lncRNAs might also be involved in various pathways after GSEA analysis in the KEGG pathway, for instance, proteasome, cell cycle, and nucleotide excision repair ($P < 0.05$ and FDR < 0.05, **Figure S2B**). All GSEA results are shown in **Table S2**.

## Correlation Between Immunity and lncRNAs in the LARSO Prognostic Model

In this part, we analyzed the correlation between immunity and lncRNAs in our prognostic model. We found that the correlation between lncRNAs and IRGs was different among six lncRNAs. Firstly, only DEPDC1-AS1 and RP11-454K7.3 had been found in the antigen processing and presentation category (**Figure 5A**). Most IRGs were associated with DEPDC1-AS1 or RP11-454K7.3 ($P < 0.05$), while merely a small part was correlated with RP1-290I10.3 or RP11-95M5.1 ($P < 0.05$). Also, CTD-2168K21.1 had no statistical significance with IRGs in this category. The analysis between these lncRNAs (except for RP11-95M5.1) and other categories, including interleukins and receptors (**Figure 5B**), TCR signaling pathway (**Figure 5C**), and TNF family members and receptors (**Figure 5D**), displayed similar results with antigen processing and presentation category.

RP11-95M5.1 showed no significant correlation with IRGs in these three categories. In addition, in the immune category of TGFb family members and receptors (**Figure 5E**), most IRGs were significantly correlated with DEPDC1-AS1, RP1-290I10.3, and RP11-454K7.3, while a small part was related to RP11-95M5.1.

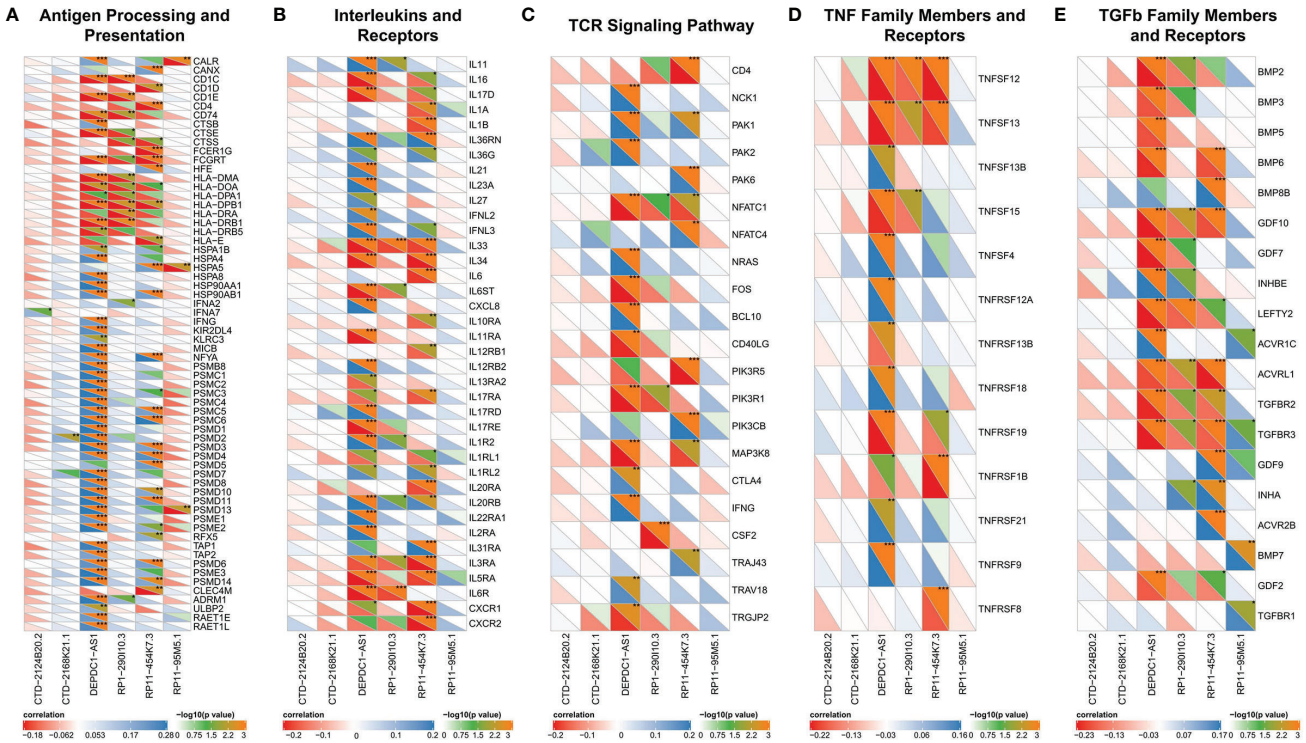


**FIGURE 5** | Correlated immune categories with lncRNAs in the prognostic model. **(A–E)** Correlation analysis between lncRNAs with gene expression in **(A)** antigen processing and presentation category, **(B)** interleukins and receptors category, **(C)** TCR signaling pathway category, **(D)** TNF family members and receptors category, and **(E)** TGFb family members and receptors category. The abscissa represents the lncRNAs, and the genes in the immune categories are on the ordinate. The lower left half triangle represents correlation: red means negative correlation, while blue implies positive correlation. Darker color means stronger correlation. The upper right semi-triangle is the value of –log10 (*P*-value). A larger value implies the darker the color. Spearman test was used for correlation analysis. $^{*}P < 0.05$; $^{**}P < 0.01$; $^{***}P < 0.001$.

Hence, DEPDC1-AS1 and RP11-454K7.3 were more likely to regulate the above five immune categories, while RP1-290I10.3 and RP11-95M5.1 were less likely to be involved. CTD-2124B20.2 and CTD-2168K21.1 might not regulate the immune process of the above five categories.

## Immune Infiltration in the High- and Low-Risk Groups

Through immune infiltration analysis, different proportions of several immune cells were found between the high- and low-risk groups, including plasma cells ($P = 0.0233$), monocytes ($P = 0.0003$), macrophages M1 ($P = 0.0013$), dendritic cells resting ($P = 0.0269$), dendritic cells activated ($P = 0.0294$), eosinophils ($P < 0.0001$), and neutrophils ($P = 0.0256$) (**Figure 6A**). However, similar results were not observed in the correlation analysis between these immune cells and the six lncRNAs (**Figure 6B**). A positive correlation was only found between DEPDC1-AS1 and macrophages M1 (R = 0.276, $P < 0.001$), while a negative correlation was seen between RP11-454K7.3 and neutrophils ($R = -0.118$, $P < 0.001$). Therefore, the immune infiltration might slightly differ between the high- and low-risk groups. Moreover, the small difference of immune cells between the high- and low-risk groups, except for macrophages M1 and neutrophils, was more likely to result from the synergistic effect of all six lncRNAs in the LARSO prognostic model.

## Immunotherapy and Anti-Angiogenic Targeted Therapy Might Be Less Effective in the High-Risk Group

Finally, we investigated the roles of our prognostic model and related lncRNAs in immunotherapy and anti-angiogenic targeted therapy. We first analyzed the expression of four pivotal immune checkpoints (PDCD1, CD274, PDCD1LG2, and CTLA4) in the high- and low-risk groups. There was no significant difference between the two groups (**Figure 6C**). On the other hand, we found that most of the six lncRNAs were not significantly correlated with these immune checkpoints except for DEPDC1-AS1. DEPDC1-AS1 showed positive correlation with PD-1 ($R = 0.162$, $P = 0.00175$), PD-L1 ($R = 0.136$, $P = 0.019$), or CTLA4 ($R = 0.171$, $P < 0.001$) (**Figure 6D**). Therefore, we suggested that the high-risk group might not be sensitive to immunotherapy.

As for the prediction of the efficiency of anti-angiogenic drugs, KDR (VEGFR-2) between the two groups showed a significant difference ($P = 0.0314$), but the VEGFR-2

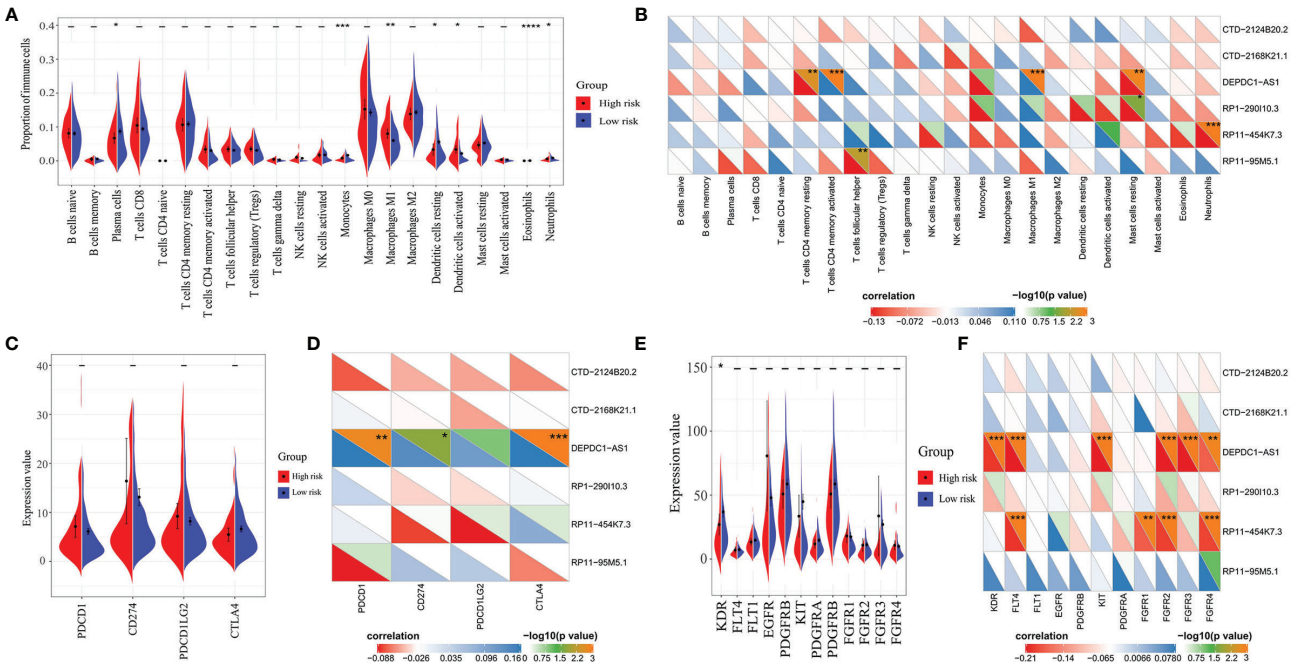


**FIGURE 6** | Correlation analysis of lncRNAs with immune cell infiltration score, immune checkpoint expression, or antivascular target expression between the high- and low-risk groups. **(A)** Significant immune infiltrates between the two groups: plasma cells ($P = 0.0233$), monocytes ($P = 0.0003$), macrophages M1 ($P = 0.0013$), dendritic cells resting ($P = 0.0269$), dendritic cells activated ($P = 0.0294$), eosinophils ($P < 0.0001$), and neutrophils ($P = 0.0256$). **(B)** Correlation analysis between lncRNAs in the prognostic model and immune infiltration score. **(C)** Correlation analysis of four immune checkpoints (PD-1, PD-L1, PD-L2, and CTLA4) between the high- and low-risk groups; no significant difference was found. **(D)** Correlation analysis between immune checkpoints with the six lncRNAs. **(E)** Correlation analysis of common anti-angiogenic targets between the high- and low-risk groups. Only KDR (VEGFR-2) showed a significant difference between the two groups ($P = 0.0314$). **(F)** Correlation analysis between anti-angiogenic targets with the six lncRNAs. Student's *t*-test was used for the different tests between groups. Correlation analysis was performed by the Spearman test. $^{*}P < 0.05$; $^{**}P < 0.01$; $^{***}P < 0.001$; $^{****}P < 0.0001$.

expression in the low-risk group was higher compared with the high-risk group. In contrast, other anti-angiogenic targets showed no significant changes between the two groups (**Figure 6E**). Besides, only DEPDC1-AS1 and RP11-454K7.3 had a limited correlation with several anti-angiogenic targets (**Figure 6F**). Thus, we suggested that targeted therapy focusing on the above anti-angiogenic targets might be less effective for patients in the high-risk group.

## DISCUSSION

Over recent years, increasing numbers of lncRNAs have been discovered and investigated (32). lncRNAs have a vital role in various cellular and physiologic functions and have been strongly associated with the progression of human cancers (11, 12). For example, MALAT1, one of the most common oncogenic lncRNAs in NSCLC, has been reported to modulate miR-124/STAT3 and promote carcinogenesis (33). Moreover, MALAT1 can enhance epithelial–mesenchymal transition (EMT), increasing metastasis *via* the miR-204/SLUG axis in LUAD and promoting brain metastasis (34, 35). In contrast, another lncRNA, LOC285194, acts as a tumor suppressor that targets p53 and is associated with the KRAS/BRAF/SMEK pathway (36). These strongly emphasize the key roles of lncRNA in cancer biology. However, the prognostic values of lncRNAs in lung adenocarcinoma are still not fully understood. Herein, we first reported these six lncRNAs as potential oncogenes and verified their potential for predicting lung adenocarcinoma.

To date, various prognostic gene signatures for lung cancer prognosis have been identified. For example, a six-gene prognostic signature was developed for predicting disease-free survival (DFS) and OS in NSCLC *via* multivariate regression and stratification analyses (37). The AUC values of ROC curves for this six-gene signature predicting DFS were 0.713 in GSE31210, 0.727 in GSE37745, and 0.746 in GSE50081. Another nine-gene signature containing nine glycolysis-related genes was established, and the ROC curve analysis score in this nine-mRNA signature was 0.712 (38). In addition, a 22-gene signature and an 11-gene signature were reported to significantly dichotomize patients with different OS. The two signatures could serve as independent predictors of OS in lung adenocarcinoma and squamous cell carcinoma, respectively, and the AUC values of the risk score were 0.744 for the TCGA-LUAD cohort and 0.684 for the TCGA-LUSC cohorts (39). In our study, we built a LARSO prognostic model for LUAD, which included six novel lncRNAs (DEPDC1-AS1, RP1-290I10.3, RP11-95M5.1, CTD-2124B20.2, CTD-2168K21.1, and RP11-

454K7.3). The best AUC values reached 0.77 for the 1-year ROC curve and 0.8 for the 3-year ROC curve in the validation set. Our prognostic model seemed superior to the above gene signatures on predicting OS of LUAD patients from the AUC values.

TNM is the essential prognostic factor for predicting lung cancer survival time and recurrence rates in the clinic, followed by indexes like sex, age, histological grade, and performance status (40). In our study, the LARSO consisting of six lncRNAs was correlated with performance status and TNM stage. A high LARSO value indicated a more severe stage. The AUC values of this model reached 0.78 in the 1-year ROC curve and 0.77 in the 3-year ROC curve in the validation set, suggesting that LARSO had a more effective performance for OS prediction. Therefore, a comprehensive examination of LUAD patients with high LARSO values should be performed to determine whether they have lymph node metastasis and distant metastasis. Moreover, the AUC value of NRS in the 3-year ROC curve could reach 0.8, further indicating that LARSO combined with stages and N stages could better predict the prognosis of LUAD patients compared with LARSO alone, which suggested to us that in the process of applying our prognostic model, if the clinical staging and N staging of patients cannot be clearly defined, such as the radiological examinations of patients could not determine their stage and they could not be further examined because of their poor basic condition or surgical contraindications, the LARSO could be used for the prediction of prognosis of the patients, while these patients who can obtain a clear stage and N stage could be predicted by the NRS. Due to the small sample size (48 pairs) and potential experimental errors involved in qRT-PCR, the prognostic values of the LARSO and NRS model were similar in the validation set. However, we built the NRS prognostic model by combing LARSO with stage score and N score, which showed a desirable capability for predicting the overall survival of LUAD patients, and the AUC values in NRS were improved compared with the LARSO prognostic model.

Our analysis of the GSEA and KEGG pathway found that these six lncRNAs were most correlated with cell cycle, DNA damage repair, or tumor cell metabolism, which provides hints for the molecular mechanism study about these lncRNAs in the future. As the fundamental requirement for homeostasis, the cell cycle has a vital role in tumor progression, mainly through cell-cycle kinases (cdks) (41), whereas DNA damage-response or DNA-repair genes with germline aberrations induce cancerous tendencies (42). Furthermore, the proliferation and metastasis of tumor cells are strongly influenced by surrounding cells in the tumor microenvironment. The communication between tumor cells and the surrounding cells, such as immune cells, mainly depends on the tumor and correlated cell metabolism (43).

Over the last decade, immunotherapy emerged and greatly changed the landscape of cancer therapy. Immune checkpoint inhibitors for targeted therapy such as anti-PD-1/PD-L1 have shown to be safe and effective against a certain type of cancer (44). In this study, we examined the role of six lncRNAs in tumor immune regulation. However, no significant correlation was observed between these lncRNAs and immune genes or immune-infiltrated cells. Therefore, we concluded that the high-risk group showing high LARSO values might not be sensitive to immunotherapy. In addition, an analysis of immune checkpoint expression between the high- and low-risk groups was also performed. Consistently, there was no significant change of immune checkpoint expression in the two groups, implying that current clinical immunotherapy with immune checkpoint inhibitors might be inefficient for LUAD patients with high LARSO values. Angiogenesis has a critical role in the progression and invasion of cancer cells. Anti-angiogenesis therapy, particularly anti-VEGF therapy, has shown to be effective against several tumors (45). In this study, we found a higher VEGFR-2 expression in the low-risk group than in the high-risk group (**Figure 6E**, $P = 0.0314$). Meanwhile, other anti-angiogenesis targets such as FGFR1, 2, 3, and 4 showed no significant change between the two groups. Thus, we concluded that LUAD patients with high LARSO values might not benefit from anti-angiogenesis targets and that alternative therapies are required.

This study has a few limitations. Firstly, no specific LARSO cutoff value was determined to define the high- and low-risk groups due to calculation variance of RNA-seq data or qRT-PCR. To solve this problem, LARSO cutoff values should be obtained in tests of a small set of samples and verified by large prospective clinical studies. Secondly, although we preliminarily verified the prognostic value of the LARSO model by using qRT-PCR assay, the sample size (48 pairs) was small. So, the value of this model needs to be further verified in large-scale clinical trials. Thirdly, the molecular mechanism, including cell cycle regulation, DNA damage repair, or tumor cell metabolism regulation, of the current model and six lncRNAs was not further investigated in the current study. In the future, we plan to investigate the roles of these lncRNAs based on *in-vivo* and *in-vitro* experiments referring to GSEA results. Finally, the LUAD patients we collected for validation were all diagnosed at stage IA–IIIB and feasible for surgery, so the efficiency of immunotherapy drugs and anti-angiogenic drugs were lacking for further evaluation. Nevertheless, analysis results of immune checkpoints or anti-angiogenesis targets in the LARSO high- and low-risk groups can still provide theoretical support for predicting the efficiency of correlated drugs. Also, further clinical trials need to be performed to verify whether high LARSO can be used as an indicator of drug resistance in immunotherapy as well as anti-angiogenesis therapy.

## CONCLUSION

Six lncRNAs were identified by integrated bioinformatics analysis and further validated using clinical samples. These six lncRNAs have shown to be potential oncogenic and predictive factors of LUAD; a positive correlation was found between the risk of death and lncRNA expression. Furthermore, a prognostic signature was defined based on these six lncRNAs, showing adequate reliability and sensitivity in our study. In addition, we demonstrated that LARSO combined with stages and N stages could better predict the prognosis of LUAD patients compared

with LARSO alone. These findings provide the theoretical basis for effective promotion and exploration of potential biomarkers for predicting LUAD prognosis.

## DATA AVAILABILITY STATEMENT

Publicly available datasets were analyzed in this study. These data can be found here: The Cancer Genome Atlas (TCGA) database (https://portal.gdc.cancer.gov).

## ETHICS STATEMENT

The studies involving human participants were reviewed and approved by the Medical Ethics Committee of the Second Affiliated Hospital of Zhejiang University School of Medicine. The patients/participants provided their written informed consent to participate in this study.

## AUTHOR CONTRIBUTIONS

Conceptualization: KW and WC. Data curation: LY and YW. Formal analysis: LY, YW, and HX. Methodology: LY, YW, and LZ. Software: LY, YW, and HX. Supervision: KW and WC. Validation: LY, YW, JZ, and YFW. Visualization: LY, YW, HX, XZ, and YFW. Writing—original draft: LY and YW. Writing—review and editing: KW and WC. All authors contributed to the article and approved the submitted version.

## FUNDING

This work was supported by the National Natural Science Foundation of China (grants 81902331 and 81871874) and the Zhejiang Provincial Key Research and Development Project (No. 2020C03027).

## ACKNOWLEDGMENTS

We would like to thank the patients who shared their experiences with our physicians. We are grateful to SangerBox (http://sangerbox.com) for providing technical support.

## SUPPLEMENTARY MATERIAL

The Supplementary Material for this article can be found online at: https://www.frontiersin.org/articles/10.3389/fonc.2021.775583/full#supplementary-material

## REFERENCES

1. Bray F, Ferlay J, Soerjomataram I, Siegel RL, Torre LA, Jemal A. Global Cancer Statistics 2018: GLOBOCAN Estimates of Incidence and Mortality Worldwide for 36 Cancers in 185 Countries. *CA Cancer J Clin* (2018) 68 (6):394–424. doi: 10.3322/caac.21492
2. Calvayrac O, Pradines A, Pons E, Mazieres J, Guibert N. Molecular Biomarkers for Lung Adenocarcinoma. *Eur Respir J* (2017) 49(4):1601743. doi: 10.1183/13993003.01734-2016
3. Siegel RL, Miller KD, Jemal A. Cancer Statistics, 2018. *CA Cancer J Clin* (2018) 68(1):7–30. doi: 10.3322/caac.21442
4. Ulitsky I, Bartel DP. lincRNAs: Genomics, Evolution, and Mechanisms. *Cell* (2013) 154(1):26–46. doi: 10.1016/j.cell.2013.06.020
5. Kopp F, Mendell JT. Functional Classification and Experimental Dissection of Long Noncoding RNAs. *Cell* (2018) 172(3):393–407. doi: 10.1016/j.cell.2018.01.011
6. Rinn JL, Chang HY. Genome Regulation by Long Noncoding RNAs. *Annu Rev Biochem* (2012) 81:145–66. doi: 10.1146/annurev-biochem-051410-092902
7. Engreitz JM, Haines JE, Perez EM, Munson G, Chen J, Kane M, et al. Local Regulation of Gene Expression by lncRNA Promoters, Transcription and Splicing. *Nature* (2016) 539(7629):452–5. doi: 10.1038/nature20149
8. Bhan A, Mandal SS. LncRNA HOTAIR: A Master Regulator of Chromatin Dynamics and Cancer. *Biochim Biophys Acta* (2015) 1856(1):151–64. doi: 10.1016/j.bbcan.2015.07.001
9. Lee S, Kopp F, Chang TC, Sataluri A, Chen B, Sivakumar S, et al. Noncoding RNA NORAD Regulates Genomic Stability by Sequestering PUMILIO Proteins. *Cell* (2016) 164(1-2):69–80. doi: 10.1016/j.cell.2015.12.017
10. Tripathi V, Ellis JD, Shen Z, Song DY, Pan Q, Watt AT, et al. The Nuclear-Retained Noncoding RNA MALAT1 Regulates Alternative Splicing by Modulating SR Splicing Factor Phosphorylation. *Mol Cell* (2010) 39(6):925–38. doi: 10.1016/j.molcel.2010.08.011
11. Gibb EA, Brown CJ, Lam WL. The Functional Role of Long Non-Coding RNA in Human Carcinomas. *Mol Cancer* (2011) 10:38. doi: 10.1186/1476-4598-10-38
12. Prensner JR, Chinnaiyan AM. The Emergence of lncRNAs in Cancer Biology. *Cancer Discov* (2011) 1(5):391–407. doi: 10.1158/2159-8290.CD-11-0209
13. Gupta RA, Shah N, Wang KC, Kim J, Horlings HM, Wong DJ, et al. Long non-Coding RNA HOTAIR Reprograms Chromatin State to Promote Cancer Metastasis. *Nature* (2010) 464(7291):1071–6. doi: 10.1038/nature08975
14. Tay Y, Rinn J, Pandolfi PP. The Multilayered Complexity of ceRNA Crosstalk and Competition. *Nature* (2014) 505(7483):344–52. doi: 10.1038/nature12986
15. Ann Y, Chen XM, Yang Y, Mo F, Jiang Y, Sun DL, et al. LncRNA DLX6-AS1 Promoted Cancer Cell Proliferation and Invasion by Attenuating the Endogenous Function of miR-181b in Pancreatic Cancer. *Cancer Cell Int* (2018) 18:143. doi: 10.1186/s12935-018-0643-7
16. Xiang JF, Yin QF, Chen T, Zhang Y, Zhang XO, Wu Z, et al. Human Colorectal Cancer-Specific CCAT1-L lncRNA Regulates Long-Range Chromatin Interactions at the MYC Locus. *Cell Res* (2014) 24(5):513–31. doi: 10.1038/cr.2014.35
17. Huang KC, Rao PH, Lau CC, Heard E, Ng SK, Brown C, et al. Relationship of XIST Expression and Responses of Ovarian Cancer to Chemotherapy. *Mol Cancer Ther* (2002) 1(10):769–76.
18. Wang Z, Jin Y, Ren H, Ma X, Wang B, Wang Y. Downregulation of the Long non-Coding RNA TUSC7 Promotes NSCLC Cell Proliferation and Correlates With Poor Prognosis. *Am J Transl Res* (2016) 8(2):680–7.
19. Qi P, Du X. The Long non-Coding RNAs, a New Cancer Diagnostic and Therapeutic Gold Mine. *Mod Pathol* (2013) 26(2):155–65. doi: 10.1038/modpathol.2012.160
20. Liu J, Lichtenberg T, Hoadley KA, Poisson LM, Lazar AJ, Cherniack AD, et al. An Integrated TCGA Pan-Cancer Clinical Data Resource to Drive High-Quality Survival Outcome Analytics. *Cell* (2018) 173(2):400–16.e411. doi: 10.1016/j.cell.2018.02.052
21. Therneau T. *T T A Package for Survival Analysis in R. R Package Version 3.2-7* (2020).
22. Friedman J, Hastie T, Tibshirani R. Regularization Paths for Generalized Linear Models *via* Coordinate Descent. *J Stat Softw* (2010) 33(1):1–22. doi: 10.18637/jss.v033.i01

23. Gordon M, Lumley T. *Lumley MGaT Forestplot: Advanced Forest Plot Using 'Grid' Graphics* (2020).
24. Villanueva RAM, Chen ZJ. Ggplot2: Elegant Graphics for Data Analysis, 2nd Edition. *Meas-Interdiscip Res* (2019) 17(3):160–7. doi: 10.1080/15366367.2019.1565254
25. Blanche P, Dartigues JF, Jacqmin-Gadda H. Estimating and Comparing Time-Dependent Areas Under Receiver Operating Characteristic Curves for Censored Event Times With Competing Risks. *Stat Med* (2013) 32 (30):5381–97. doi: 10.1002/sim.5958
26. Harrell FE Jr. *Rms: Regression Modeling Strategies. R Package Version 6*. (2021). pp. 2–0.
27. Subramanian A, Tamayo P, Mootha VK, Mukherjee S, Ebert BL, Gillette MA, et al. Gene Set Enrichment Analysis: A Knowledge-Based Approach for Interpreting Genome-Wide Expression Profiles. *P Natl Acad Sci USA* (2005) 102(43):15545–50. doi: 10.1073/pnas.0506580102
28. Bhattacharya S, Dunn P, Thomas CG, Smith B, Schaefer H, Chen J, et al. ImmPort, Toward Repurposing of Open Access Immunological Assay Data for Translational and Clinical Research. *Sci Data* (2018) 5:180015. doi: 10.1038/sdata.2018.15
29. Revelle W. *Psych: Procedures for Psychological, Psychometric, and Personality Research*. Northwestern University, Evanston, Illinois (2020). R package version 2.0.12.
30. Newman AM, Steen CB, Liu CL, Gentles AJ, Chaudhuri AA, Scherer F, et al. Determining Cell Type Abundance and Expression From Bulk Tissues With Digital Cytometry. *Nat Biotechnol* (2019) 37(7):773–82. doi: 10.1038/s41587-019-0114-2
31. Steen CB, Liu CL, Alizadeh AA, Newman AM. Profiling Cell Type Abundance and Expression in Bulk Tissues With CIBERSORTx. *Methods Mol Biol* (2020) 2117:135–57. doi: 10.1007/978-1-0716-0301-7_7
32. Hung T, Chang HY. Long Noncoding RNA in Genome Regulation: Prospects and Mechanisms. *RNA Biol* (2010) 7(5):582–5. doi: 10.4161/rna.7.5.13216
33. Li S, Mei Z, Hu HB, Zhang X. The lncRNA MALAT1 Contributes to Non-Small Cell Lung Cancer Development via Modulating miR-124/STAT3 Axis. *J Cell Physiol* (2018) 233(9):6679-88. doi: 10.1002/jcp.26325
34. Li J, Wang J, Chen Y, Li S, Jin M, Wang H, et al. LncRNA MALAT1 Exerts Oncogenic Functions in Lung Adenocarcinoma by Targeting miR-204. *Am J Cancer Res* (2016) 6(5):1099–107.
35. Shen L, Chen L, Wang Y, Jiang X, Xia H, Zhuang Z. Long Noncoding RNA MALAT1 Promotes Brain Metastasis by Inducing Epithelial-Mesenchymal Transition in Lung Cancer. *J Neurooncol* (2015) 121(1):101–8. doi: 10.1007/s11060-014-1613-0
36. Liu Q, Huang J, Zhou N, Zhang Z, Zhang A, Lu Z, et al. LncRNA Loc285194 Is a P53-Regulated Tumor Suppressor. *Nucleic Acids Res* (2013) 41(9):4976–87. doi: 10.1093/nar/gkt182
37. Shuguang Zuo MW, Zhang H, Chen A, Wu J, Wei J. A Robust Six-Gene Prognostic Signature for Prediction of Both Disease-Free and Overall Survival in Non-Small Cell Lung Cancer. *J Transl Med* (2019) 17(152):152. doi: 10.1186/s12967-019-1899-y
38. Zhang L, Zhang Z, Yu Z. Identification of a Novel Glycolysis-Related Gene Signature for Predicting Metastasis and Survival in Patients With Lung Adenocarcinoma. *J Transl Med* (2019) 17(1):423. doi: 10.1186/s12967-019-02173-2
39. Liu Y, Wu L, Ao H, Zhao M, Leng X, Liu M, et al. Prognostic Implications of Autophagy-Associated Gene Signatures in Non-Small Cell Lung Cancer. *Aging (Albany NY)* (2019) 11(23):11440–62. doi: 10.18632/aging.102544
40. Woodard GA, Jones KD, Jablons DM. Lung Cancer Staging and Prognosis. *Cancer Treat Res* (2016) 170:47–75. doi: 10.1007/978-3-319-40389-2_3
41. Caputi M, Russo G, Esposito V, Mancini A, Giordano A. Role of Cell-Cycle Regulators in Lung Cancer. *J Cell Physiol* (2005) 205(3):319–27. doi: 10.1002/jcp.20424
42. Brown JS, O'Carrigan B, Jackson SP, Yap TA. Targeting DNA Repair in Cancer: Beyond PARP Inhibitors. *Cancer Discov* (2017) 7(1):20–37. doi: 10.1158/2159-8290.CD-16-0860
43. Reina-Campos M, Moscat J, Diaz-Meco M. Metabolism Shapes the Tumor Microenvironment. *Curr Opin Cell Biol* (2017) 48:47–53. doi: 10.1016/j.ceb.2017.05.006
44. Chalela R, Curull V, Enriquez C, Pijuan L, Bellosillo B, Gea J. Lung Adenocarcinoma: From Molecular Basis to Genome-Guided Therapy and Immunotherapy. *J Thorac Dis* (2017) 9(7):2142–58. doi: 10.21037/jtd.2017.06.20
45. Tian W, Cao C, Shu L, Wu F. Anti-Angiogenic Therapy in the Treatment of Non-Small Cell Lung Cancer. *Onco Targets Ther* (2020) 13:12113–29. doi: 10.2147/OTT.S276150


**Conflict of Interest:** The authors declare that the research was conducted in the absence of any commercial or financial relationships that could be construed as a potential conflict of interest.

**Publisher's Note:** All claims expressed in this article are solely those of the authors and do not necessarily represent those of their affiliated organizations, or those of the publisher, the editors and the reviewers. Any product that may be evaluated in this article, or claim that may be made by its manufacturer, is not guaranteed or endorsed by the publisher.

frontiers in Oncology

METHODS
published: 02 February 2022
doi: 10.3389/fonc.2022.837419

# Clinical and Biological Interpretation of Survival Curves of Cancer Patients, Exemplified With Stage IV Non-Small Cell Lung Cancers With Long Follow-up

*Jan P. A. Baak*[1,2*], *Hegen Li*[3*] *and Huiru Guo*[3]

[1] Department of Pathology, Stavanger University Hospital, Stavanger, Norway, [2] Medical Practice Dr. Med Jan Baak AS, Tananger, Norway, [3] Department of Medical Oncology, Longhua University Hospital, Shanghai, China

OPEN ACCESS

**Edited by:**
*Kristin Higgins,*
*Emory University, United States*

**Reviewed by:**
*Min Li,*
*Sun Yat-sen University Cancer Center (SYSUCC), China*
*Stanley J. Robboy,*
*Duke University, United States*

***Correspondence:**
*Jan P. A. Baak*
*jpabaak47@yahoo.com*
*Hegen Li*
*lydia8108@sina.com*

**Specialty section:**
*This article was submitted to Thoracic Oncology, a section of the journal Frontiers in Oncology*

**Received:** *16 December 2021*
**Accepted:** *03 January 2022*
**Published:** *02 February 2022*

**Citation:**
*Baak JPA, Li H and Guo H (2022) Clinical and Biological Interpretation of Survival Curves of Cancer Patients, Exemplified With Stage IV Non-Small Cell Lung Cancers With Long Follow-up. Front. Oncol. 12:837419. doi: 10.3389/fonc.2022.837419*

Worldwide, 18.1 million new invasive cancers and 9.9 million cancer deaths occurred in 2020. Lung cancer is the second most frequent (11.4%) and, with 1.8 million deaths, remains the leading cause of cancer mortality. About 1.7 million of lung cancers are of the non-small cell lung cancer (NSCLC) subtype, and of these, 60%–70% are in advanced stage IV at the time of diagnosis. Thus, the annual worldwide number of new NSCLC stage IV patients is about 1 million, and they have a very poor prognosis. Indeed, 25%–30% die within 3 months of diagnosis. However, the survival duration of the remaining 700,000 new patients per year surviving >3 months varies enormously. Surprisingly, little research has been done to explain these survival differences, but recently it was found that classical patient, tumour and treatment features cannot accurately distinguish short- and very long-term survivors. What then are the causes of these bewildering survival variations amongst "the same cancers"? Clonality, proliferation differences, neovascularization, intra-tumour heterogeneity, genetic inhomogeneity and other cancer hallmarks play important roles. Considering each of these, single or combined, can greatly improve our understanding. Another technique is analysis of the survival curve of a seemingly homogeneous group of cancer patients. This can give valuable information about the existence of subgroups and their biological characteristics. Different basic survival curves and what their shapes tell about the biological properties of these invasive cancers are discussed. Application of this analysis technique to the survival curve of 690 stage IV NSCLC patients with a 3.2–120.0-month survival suggests that this seemingly homogeneously group of patients probably consists of 4–8 subgroups with a very different survival. A subsequent detailed mathematical analysis shows that a model of 8 subgroups gives a very good match with the original survival curve of the whole group.

In conclusion, the survival curve of a seemingly homogeneous group of cancer patients can give valuable information about the existence of subgroups and their biological characteristics. Application of this technique to 690 NSCLC Stage IV patients makes it probable that 8 different subgroups with very different survival rates exist in this group of cancers.

**Keywords: metastatic cancer, non-small cell lung cancer, stage IV, survival curve analysis, detection of different subgroups**

## INTRODUCTION

Worldwide, an estimated 18.1 million new invasive cancer cases and almost 9.9 million cancer deaths occurred in 2020. The average mortality rate of invasive cancers is therefore about 50%. Lung cancer, the second most frequently occurring cancer at 11.4%, with an estimated 1.8 million deaths, remains by far the leading cause of cancer mortality (1). Similar rates for lung cancer are found in the People's Republic of China (2). About 1.7 million of the lung cancers are of the non-small cell lung cancer (NSCLC) subtype, and of these, 60%–70% are in advanced stage IV at the time of diagnosis. Thus, the annual worldwide number of new NSCLC stage IV patients is about 1 million and they are generally regarded as having a very poor prognosis. Indeed, 25%–30% die within 3 months of diagnosis. On the other hand, the survival duration of those remaining approximately 700,000 new patients per year surviving >3 months can vary enormously. In a recent large observational study, median survival was 23.3 months, 1-, 2- and 5-year survival rates are 74%, 49% and 16% respectively and 4%–5% survive 10 years and longer (3). The same surprising enormous survival variation can be found in patients with cancers from other organ sites, even if they have the same histological type, stage and other important prognostic characteristics.

What are the causes of these bewildering survival variations amongst "the same cancers"?

An important aspect is *clonality*. Cancer is an evolutionary process, driven by stepwise, somatic cell mutations with sequential, sub-clonal selection (4). Normal, polyclonal cells have approximately the same proliferation rate. However, sometimes genetic hits occur and change the polyclonal parent cell into neoplastic daughter cells with a new genetic make-up plus growth (proliferation) advantage. As a result, a very small nodule arises, consisting of cells which are genetically somewhat more unstable. Consequently, the risk of the development of another new cell clone with even more genetic instability and higher proliferation, and eventually invasive capacity, increases. These new tumour cells grow in densely packed populations that develop into spheroid or ellipsoid aggregates.

Another important aspect is *neovascularization*. This is an event that separates the development of any solid tumour into two stages: the avascular stage and the vascular stage. Because of this, angiogenesis plays a critical role in the biology of solid neoplasms. The two stages can be dissociated under experimental conditions. When this is accomplished and capillaries are prevented from penetrating the l-mm tumour, the tumour becomes dormant (5, 6).

This led to the concept of dormant cancers (7). Dormant solid tumours were produced *in vivo* by prevention of neovascularization. The beginning of an exponential volume increase was shown to coincide with vascularization of the implant. Although dormant in terms of expansion, these avascular tumours contained a population of viable and mitotically active tumour cells.

The transition from polyclonal to neoplastic cells probably occurs quite often. How long it takes to change from a 1mm diameter dormant tumour (consisting of approximately 1 million cancer cells) to a clinically detectable proliferating invasive cancer, of approximately 10 (7.5–15.0) mm ($10^9$ tumour cells), is less certain. From there to lethal metastases of 1,000 g (rough estimate), or $10^{12}$ cells, depends amongst other factors on *intratumour heterogeneity (ITH)* (8). *Genomic diversity* within single tumours has been recognized as "*genetic inhomogeneity*" (9). Since next-generation sequencing studies have become available, the full extent of genomic ITH is becoming apparent. The degree of ITH can be highly variable, with between 0 and over 8,000 coding mutations found to be heterogeneous within primary tumours or between primary and metastatic or recurrence sites (10). These findings make it more than likely that especially seemingly homogeneous late-stage cancers are, in fact, genetically widely heterogeneous, also in their clinical behaviour. The latter can be observed in the survival curve of these cancers.

It is of obvious clinical and therapeutic significance to understand why patients, with seemingly homogeneous cancers, have such different survival rates. Of course, often, age, gender, performance stage, histologic subtype, no/minimal versus heavy smoking and different treatment modalities are strongly prognostic. In pulmonary adenocarcinoma, the mean number of clonal and sub-clonal non-silent mutations in non-smokers is much smaller than in smokers (8). However, even when these well-established prognostic factors are all considered, also in a multivariate manner, it may not be possible to explain why certain patients die within a rather short time, while others survive for (very) many years, as we recently found. It is important to emphasize that the number of these patients worldwide is very large indeed.

We recently worked on an article on the survival prediction accuracy of prognostic factors in the seemingly homogeneous group of 690 stage IV NSCLC surviving patients between 3.2 and 120.0 months. In the original manuscript, we hypothesized that this group in fact consisted of several hypothetical subgroups with widely varying survival rates. This hypothesis was based on the interpretation of the survival curve of the patients (3).

Survival curves can give valuable information about the clinical behaviour and the biological characteristics of a group

of cancer patients. Such biological interpretation of survival curves was common knowledge in the last 2–3 decades of the 20th century. In fact, the first author of the current manuscript taught this knowledge as a standard part of the curriculum for medical students in Amsterdam. However, the comments of the reviewers of our recent manuscript (3), on our remarks to identify different prognostic subgroups by analysis of the survival curve, made it clear that this survival curve analysis knowledge was not as well-known as we thought. Rather than writing a long new section in that article to explain how we had come to the hypothesis of the existence of 4–8 subgroups with different survival rates, it was advised by the Acting Editor of the revised version of the manuscript that the topic of *Clinico-biologic Interpretation of Survival Curves* would be interesting enough for a separate new manuscript.

This article will first describe different types of survival curves and how to analyse and classify them using essential hallmarks of cancer. Secondly, we will perform quantitative model studies to show that in seemingly homogeneous stage IV NSCLC patients with a 3.2–120.0-month follow-up, about 4–8 subgroups with very different survival rates occur.

## DIFFERENT TYPES OF SURVIVAL CURVES AND THEIR CLINICO-BIOLOGIC INTERPRETATION

We will only consider tumours diagnosed as invasive carcinomas. Please remember that although the examples are hypothetical, many "real-world" examples can be found for each of them.

Basically 2 fundamental types of survival curves exist. The first one is shown in **Figure 1**. The cancer can be detected by the patients when the tumour reaches a certain size, or by radiologic and other screening methods. When the tumours are removed, histopathologic examination will show the invasive nature of the tumour. In the following years, none of the patients develop distant metastases; all survive without evident distant metastases.

The second extreme example of a survival curve type is of patients with cancers, shown in **Figure 2**. One can think of small cell lung cancer. All have died from their metastases at the end of the observation period (which in the current hypothetical example was set at 23 months but can also be set at 6 or 12 months). They seem homogeneous at the start of the follow-up, yet they have considerable differences in survival rates. 60% have died by the 6-month follow-up, 20% between 6 and 12 months and the last 20% between 12 and 23 months.

**Figure 3** shows the third type of survival curve, which occurs quite often. 30% of this group dies within 6 months, 10% between 6 and 12 months and 12% between 12 and 23 months. The remaining 45% of the patients survive until the end of the observation period. Such a curve is found when patients from the 2 different groups A and B are taken together.

It can be concluded from the shape of the survival curves shown in **Figure 3** that a group with a curve with an initial steep decline, followed by a horizontal plateau, consists of one

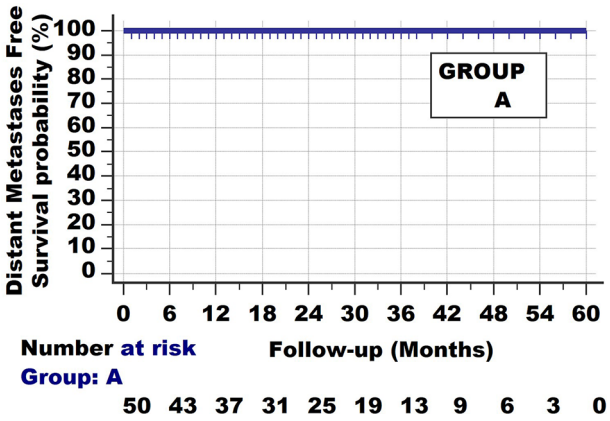


**FIGURE 1** | Invasive cancer group A. Survival curve with long follow-up. None of the patients develop/die from metastatic disease.

subgroup with a long distant metastases survival and 3 other groups with a very poor, poor and less poor survival.

The most basic biologic interpretation of Group A and B is that they both show *Invasion*, as they are pathologically diagnosed as invasive cancers.

They also all have *clonal expansion.* Clonal expansion is not limited to invasive cancers but also occurs in non-invasive neoplasias, such as for endometrial intraepithelial neoplasia (11).

Cancers from Group B patients not only have invasive and clonal expansion properties, just like those from group A, but also all have *distant metastases* at the time of the diagnosis. That the net growth of these metastases differs in these group B cancers is clear from the shape of the survival curve, as most of the patients die from their metastases once these have reached a certain lethal level (which is on average 1–2 kg, although much greater weights can be found in individual patients). (Some patients will die from much smaller

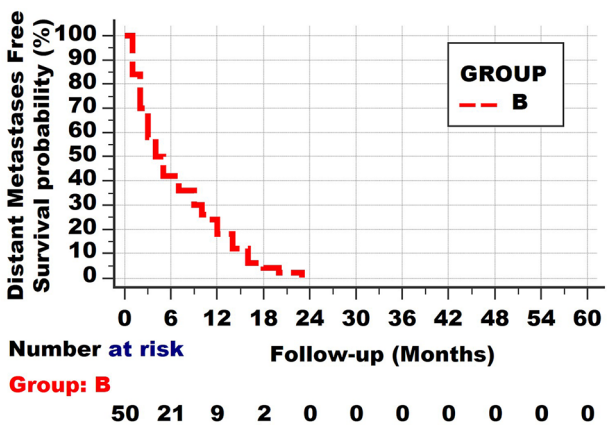


**FIGURE 2** | Invasive cancer group B All patients have died from metastatic disease within 24 months.

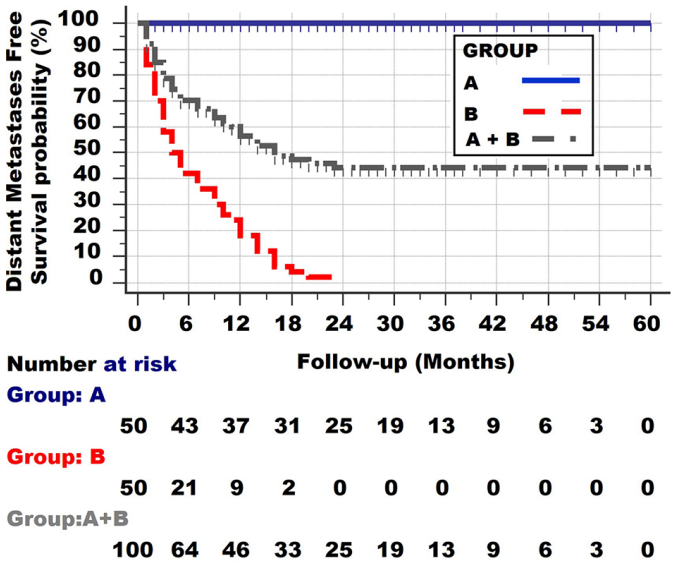


**FIGURE 3** | Survival curve of the two patient groups A and B together. Note the initial rather steep decline, followed by an increasingly more horizontal plateau.

tumours if they are located at vitally essential locations, but these are exceptions). The 60% deaths in the first 6 months have on average reached their lethal metastatic mass within 6 months. Of course, the original volume at diagnosis may have varied, but the most important feature of these 60% of the tumours, compared with the other 20% dying between 6 and 12 months, is their higher net growth (the balance between the proliferation rates and death rates of the tumour cells). Likewise, the patients dying between 12 and 23 months again have a lower net growth rate. One can thus conclude that Group B tumours are both invasive, clonally expanding but also metastatic. One can further conclude from the survival curve of group B that it is not completely homogeneous but still consists of at least 3 subgroups with different proliferation rates (net growth speeds): very fast, fast and less fast.

A fourth type of survival curve is shown in **Figure 4** of a hypothetical group D. At no point is a horizontal plateau found in the survival curve. Instead, at the end of the observation period 50% have died from distant metastases. On the other hand, the slope of the survival curve is much less steep than in the first, second and third subgroups of Group B. The conclusion is that patients of this group D all have distant metastases at the time of diagnosis, but with much lower net growth speeds than those of the subgroups of Group B. Alternatively, one could argue that the metastatic load of patients from Group B was much larger at the time of diagnosis. These 2 features cannot be discerned with the survival curves.

Of course, such a linear curve can be found with different follow-up times, for example 10, 20 and 30 years. Examples are Hodgkin-type lymphomas and certain breast cancers.

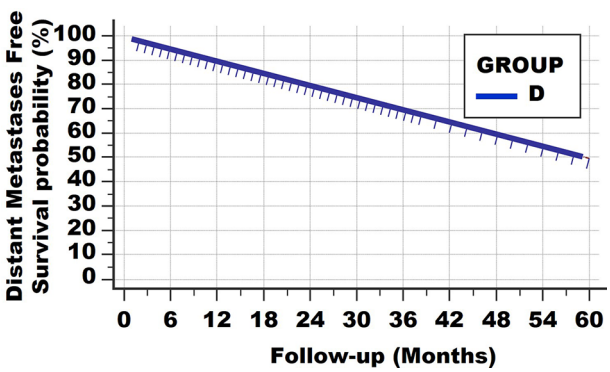


**FIGURE 4** | Survival curve type 4. At no point is a horizontal plateau found. This means that all patients had (occult) metastases at the time of diagnosis. However, the growth speeds vary greatly, resulting in continuous deaths from lethal metastatic load.

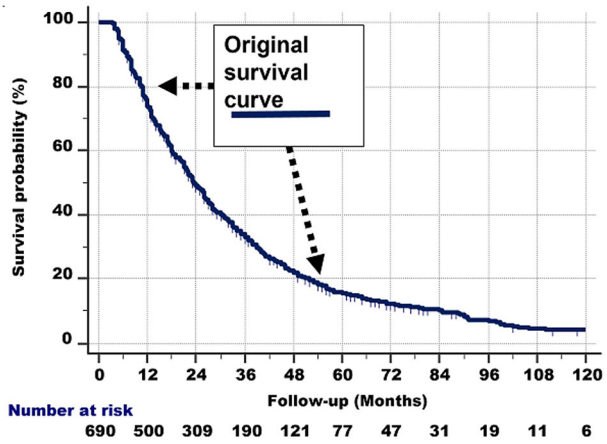


**FIGURE 5** | *Left:* Survival curve of the whole group of 690 stage IV NSCLC patients with a 3.2–120.0-month follow-up, who had received conventional radiotherapy, platinum-based chemotherapy and tyrosine kinase inhibitor-targeted therapy.

## APPLICATION OF SURVIVAL CURVE ANALYSIS IN STAGE IV NSCLC

As described before, about 1.7 million of the lung cancers are NSCLC, and of these, 60%–70% are in advanced stage IV at the time of diagnosis. Thus, the annual worldwide number of new NSCLC stage IV patients is close to 1 million (3). 25%–30% die at <3 months. Yet, of those annually worldwide 700,000 NSCLC stage IV surviving >3 months, 10%–15% (70,000–105,000 new patients worldwide per year) survive >5 years. Surprisingly, little scientific attention has been paid to the question: which factors cause the good prognosis in these NSCLC stage IV-long survivors? In a non-interventional study of 998 consecutive first-onset stage IV NSCLC patients, a large group of 737 stage IV NSCLC patients with very long follow-up (survivals were 3.2–120.0 months), we investigated the accuracies of short- and long-term survival predictive values of baseline factors, radiotherapy (RT), platinum-based chemotherapy (PBT) and tyrosine kinase inhibitors targeted therapy (TKI-TT). Of the 737 patients surviving 3.2–120.0 months, 47 refused radiotherapy, platinum-based therapy and tyrosine kinase inhibitor-targeted therapy (TKI-TT). The median survival (16.1 months) of the 47 patients who refused PBT, RT and TKI-TT was significantly worse than of those with RT, PBT and/or TKI-TT (23.3 months, HR = 1.60, 95% CI = 1.06–2.42, $p$ = 0.04). Of these latter 690 patients, 42% were females, 58% males, median age 63 (range 27–85) years, 1-, 2-, 5- and 10-year survival rates 74%, 49%, 16% and 5%, respectively. 16% were alive with disease (AWD) at the last follow-up. Pathology subtype (adenocarcinoma vs. all others), performance score, TNM

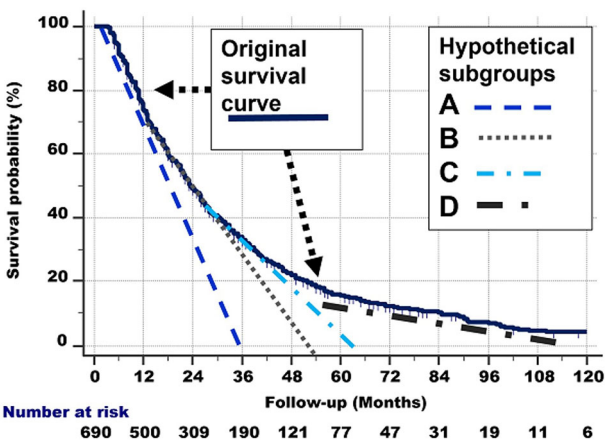


**FIGURE 6** | *Right:* Hypothetical delineation of the curved shape of the survival curve. See the text for details. For the sake of clarity, we have only drawn 4 tangent lines instead of 8.

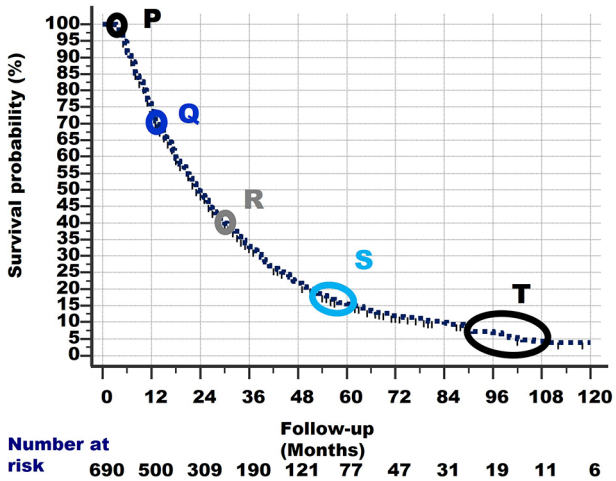


**FIGURE 7** | The survival curve of the 690 patients starts at Point P at 100% survival and 3 months of follow-up, as 261 other patients had already died within 3 months and are excluded from this study. From point P, the survival line shows a curved slope downward to the last point at 4% survival and 120 months of follow-up. At specific points in the survival curve, the slope shows a subtle change (i.e., becomes less steep). These points are denoted as Q, R, S and T. For details of these points, see text.

substage, the number of PBT cycles and TKI-TT had independent predictive value. However, with the multivariate combination of these features, identification results of short-term non-survivors and long-term survivors were poor.

The shape of the survival graph of the 690 patients (**Figure 5**, left part) is curved. As described above, this suggests that the seemingly homogeneous group of 690 patients in fact is heterogeneous, i.e., is comprised of different subgroups with widely different survivals.

A closer inspection of **Figure 5**, left part, shows the following:

1. The survival line is almost straight and decreases steeply from 100% survival probability at the 3-month follow-up, to 70% at 12 months.
2. From that point, the survival curve still goes down, but less steeply. This second nearly straight line is between 70% at 12 months and 45% survival probability at the 30-month follow-up.

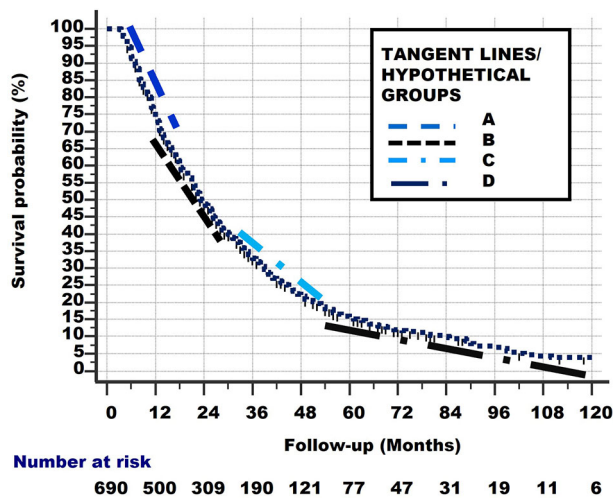


**FIGURE 8** | Linear lines between points P–Q, Q–R, R–S, S–T. These lines are slightly shifted up and down, and to the left and right in the figure, to make them more visible.

**TABLE 1 |** The total number of 690 patients and the characteristics of the 4 hypothetical subgroups, derived from **Figures 7–9**.

| Subgroup | Number | Median Survival Time (Months) | Overall Survival Time (Months) | 3 Months % AWD | 3 Months # AWD | 12 Mo % AWD | 12 Mo # AWD | 24 Mo % AWD | 24 Mo # AWD | 36 Mo % AWD | 36 Mo # AWD | 48 Mo % AWD | 48 Mo ¤ AWD | 60 Mo % AWD | 60 Mo ¤ AWD | 72 Mo % AWD | 72 Mo ¤ AWD | 84 Mo % AWD | 84 Mo ¤ AWD | 96 Mo % AWD | 96 Mo ¤ AWD | 108 Mo % AWD | 108 Mo ¤ AWD | 120 Mo % AWD | 120 Mo ¤ AWD |
|---|---|---|---|---|---|---|---|---|---|---|---|---|---|---|---|---|---|---|---|---|---|---|---|---|---|
| 1 | 173 | 15 | 30 | 173 | 173 | 60% | 104 | 20% | 34.6 | 0% | 0 | 0% | 0 | 0% | 0 | 0% | 0 | 0% | 0 | 0% | 0 | 0% | 0 | 0% | 0 |
| 2 | 173 | 28 | 54 | 173 | 173 | 78% | 135 | 56% | 96.9 | 34% | 58.8 | 12% | 20.8 | 0% | 0 | 0% | 0 | 0% | 0 | 0% | 0 | 0% | 0 | 0% | 0 |
| 3 | 172 | 54 | 108 | 172 | 172 | 89% | 153 | 78% | 134 | 67% | 115 | 55% | 95 | 43% | 74 | 32% | 55 | 21% | 36 | 8% | 14 | 0% | 0 | 0% | 0 |
| 4 | 172 | 72 | 150 | 172 | 172 | 92% | 158 | 84% | 144 | 76% | 131 | 68% | 117 | 60% | 103 | 52% | 89 | 44% | 76 | 36% | 62 | 28% | 48 | 10% | 17 |
| **Total AWD** | 690 | | | 690 | 690 | 80% | 550 | 60% | 410 | 44% | 305 | 34% | 232 | 26% | 177 | 21% | 144 | 16% | 112 | 11% | 76 | 7% | 48 | 3% | 17 |
| **Hypothetical % AWD** | | | | 100% | | 80% | | 60% | | 44% | | 34% | | 26% | | 21% | | 16% | | 11% | | 7% | | 2% | |
| **Observed % AWD in actual total group** | | | | 100% | | 72% | | 50% | | 35% | | 22% | | 16% | | 12% | | 10% | | 7% | | 5% | | 4% | |

**TABLE 2 |** The total 690 stage IV NSCLC patients with 3.2–120.0 months of follow-up, divided into 8 hypothetical subgroups according to the linear tangent method (see text).

| Subgroup | Number | Median Survival Time (Months) | Overall Survival Time (Months) | 3 Mo # AWD | 12 Mo % AWD | 12 Mo # AWD | 24 Mo % AWD | 24 Mo # AWD | 36 Mo % AWD | 36 Mo # AWD | 48 Mo % AWD | 48 Mo ¤ AWD | 60 Mo % AWD | 60 Mo ¤ AWD | 72 Mo % AWD | 72 Mo ¤ AWD | 84 Mo % AWD | 84 Mo ¤ AWD | 96 Mo % AWD | 96 Mo ¤ AWD | 108 Mo % AWD | 108 Mo ¤ AWD | 120 Mo % AWD | 120 Mo ¤ AWD |
|---|---|---|---|---|---|---|---|---|---|---|---|---|---|---|---|---|---|---|---|---|---|---|---|---|
| 1 | 87 | 6 | 12 | 87 | 0% | 0 | 0% | 0 | 0% | 0 | 0% | 0 | 0% | 0 | 0% | 0 | 0% | 0 | 0% | 0 | 0% | 0 | 0% | 0 |
| 2 | 87 | 15 | 30 | 87 | 67% | 58 | 33% | 29 | 0% | 0 | 0% | 0 | 0% | 0 | 0% | 0 | 0% | 0 | 0% | 0 | 0% | 0 | 0% | 0 |
| 3 | 86 | 24 | 48 | 86 | 75% | 65 | 50% | 43 | 25% | 22 | 0% | 0 | 0% | 0 | 0% | 0 | 0% | 0 | 0% | 0 | 0% | 0 | 0% | 0 |
| 4 | 86 | 30 | 60 | 86 | 80% | 69 | 60% | 52 | 40% | 34 | 20% | 17 | 0% | 0 | 0% | 0 | 0% | 0 | 0% | 0 | 0% | 0 | 0% | 0 |
| 5 | 86 | 36 | 72 | 86 | 84% | 84 | 67% | 67 | 50% | 50 | 33% | 33 | 16% | 16 | 0% | 0 | 0% | 0 | 0% | 0 | 0% | 0 | 0% | 0 |
| 6 | 86 | 42 | 84 | 86 | 87% | 86 | 74% | 72 | 61% | 58 | 48% | 43 | 35% | 29 | 17% | 15 | 0% | 0 | 0% | 0 | 0% | 0 | 0% | 0 |
| 7 | 86 | 48 | 96 | 86 | 88% | 88 | 76% | 76 | 64% | 64 | 52% | 50 | 40% | 34 | 28% | 18 | 16% | 9 | 0% | 0 | 0% | 0 | 0% | 0 |
| 8 | 86 | 60 | 150 | 86 | 90% | 77 | 80% | 69 | 70% | 60 | 60% | 52 | 50% | 43 | 40% | 34 | 30% | 26 | 20% | 17 | 10% | 9 | 5% | 4 |
| **TOTAL ALIVE** | 690 | | | 690 | | 527 | | 407 | | 288 | | 195 | | 122 | | 67.4 | | 34.8 | | 17.2 | | 15 | | 4 |
| **Hypothetical % AWD** | | | | 100% | | 70% | | 53% | | 38% | | 26% | | 18% | | 9% | | 5% | | 3% | | 2% | | 1% |
| **Observed % AWD** | | | | 100% | | 72% | | 50% | | 35% | | 22% | | 18% | | 15% | | 12% | | 8% | | 7% | | 5% |

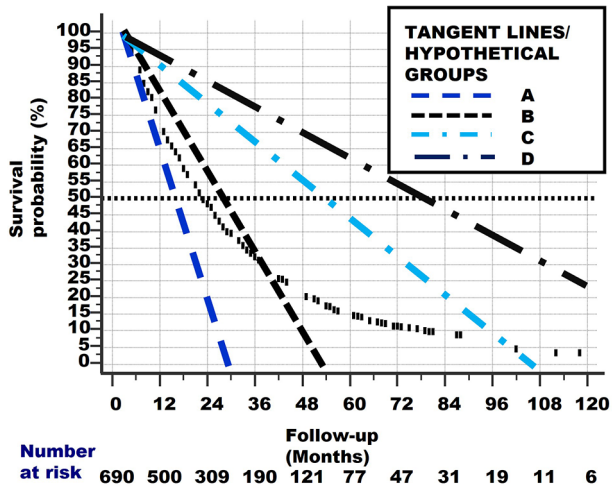


**FIGURE 9** | The original curved survival line is shown as small vertical black lines. The linear tangent lines of the curved survival line from **Figures 7** and **8**, between points P–Q, Q–R, R–S and S–T, are extrapolated from where they originally begun, at point P.

3. Then, after another bend, the curve is nearly straight between 45% and 28% survival probability (the latter is at about 45 months of follow-up). The slope of this third line again is less steep.
4. Between 28% and 18% survival probability (follow-up at 45% and around 55–60 months), another nearly straight line can be discerned.
5. Then, a somewhat less straight line from 18% to 10% can be observed from approximately 60 to 96 months of follow-up, respectively.
6. Beyond the 96-month follow-up, the line is somewhat irregular, but roughly nearly horizontal from 10% to 5% (at the 120-month follow-up).

The right part of **Figure 6** approximates the abovementioned graphically. For the sake of clarity, we have only drawn 4 tangent lines instead of 6.

The quantitative and graphical analyses described in the total group of 690 patients probably consists of different subgroups with different biological behaviour and survival rates.

It is important to note that these 690 individuals had the same histological type (NSCLC) and stage (IV). Thus, all had metastases at the time of diagnosis and also at the entry in this study, at least 3 months after the diagnosis. Yet, some died very

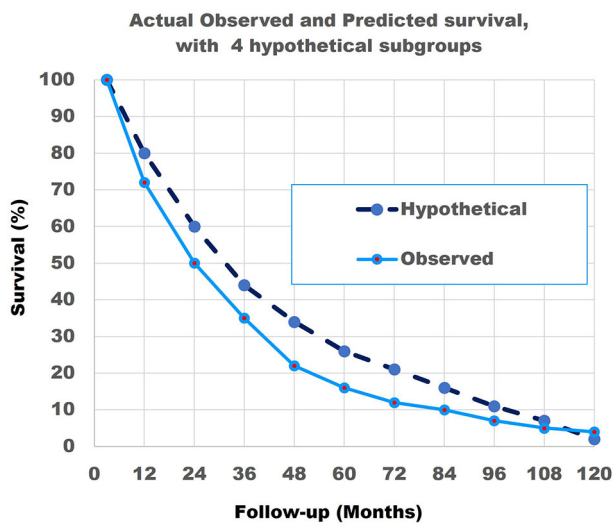


**FIGURE 10** | The actual observed survival curve (light blue continuous line) with the results of the combination of the model with 4 hypothetical straight lines (dark blue broken line). Note that the match is not perfect.

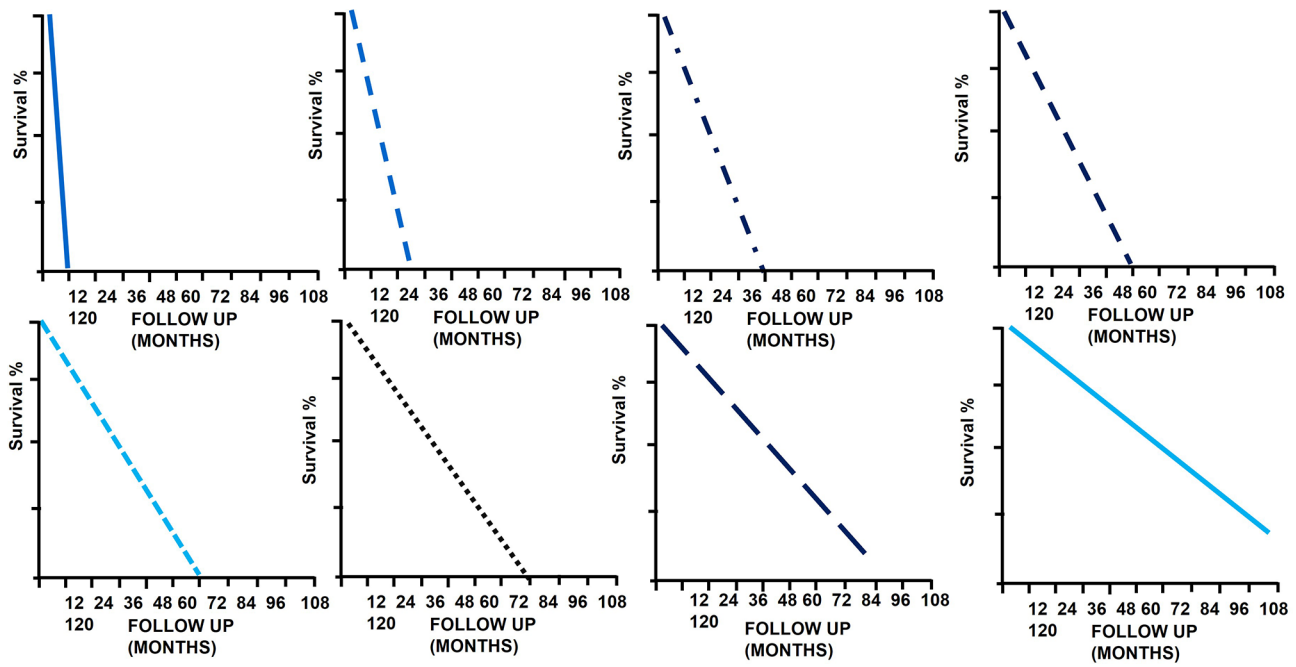


**FIGURE 11** | The survival curves of the 8 hypothetical subgroups.

quickly, (within 12 months), and others survived very long (5–10 years). The 690 "homogeneous" group in retrospect was heterogeneous, i.e., consisted of subgroups with different survival rates.

How many different subgroups exist in the 690 patients?

The Actual Observed survival curve gives important clues. Remember that 261 stage IV NSCLC patients from the same observation period had already died before the 3-month survival and are not considered in the current study. This explains why the survival curve of the 690 patients in **Figure 7** starts at 100%/3-month follow-up. This point is called P.

1. Closer observation shows that there are typical points in the graph, in which the slope of the survival curve shows a subtle

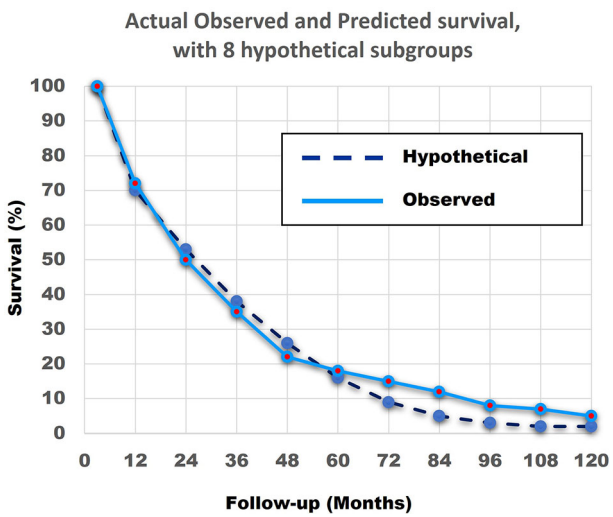


**FIGURE 12** | The actual observed survival curve (light blue continuous line) with the results of the combination of the model with 8 hypothetical straight lines (dark blue broken line). The similarity between the Actual Observed survival curve and the Hypothetical Calculated survival curve from the 8 hypothetical subgroups, with the linear survival curves from **Figure 11**, is remarkable.

change and becomes less steep. These points are shown in **Figure 7** and are located at:

2. Q: 70% survival/14-month follow-up,
3. R: 40%/30 months,
4. S: 18%/54–60 months
5. T: 10%-5%/90–108 months. Note that the number of patients becomes quite low after 90 months of follow-up, which could have caused the less smooth shape of the curve between 90 and 120 months of follow-up.

Linear (straight) lines can be drawn between these points (i.e., P–Q, Q–R, R–S, S–T). These are shown in **Figure 8**. These lines are slightly shifted in the figure, to make them more visible.

Of course, the subgroups which these lines represent did not start to exist at their respective starting points Q, R, S but were all present in the total group at the start of study (i.e., at point P). Consequently, the lines from **Figure 7** can be extrapolated from point P, as lines with the same slope, to the points where they cross the x-axis. These lines are shown in **Figure 8** and represent the hypothetical subgroups.

From **Figure 9**, we can determine the Median Survival Time and Overall Survival Time, and the percentage and total number Alive With Disease for the 4 hypothetical subgroups. **Table 1** and **Figure 10** show these data.

As the match of 4 hypothetical subgroups was not perfect, we then repeated the modelling study for 8 subgroups. **Table 2** shows the total number of 690 patients and their characteristics.

8 hypothetical subgroups are also determined by the linear tangent method used in **Figures 7** and **8**.

**Figure 11** shows the survival curves of these 8 hypothetical subgroups.

**Figure 12** shows that the match of the theoretical line, with the original survival curve of the 690 patients, is close to perfect.

In summary, the abovementioned shows that a combination of patients with linear non-curved survival curves with different survival rates can result in a curved survival line which is very close to the Actual Observed survival curve of the 690 patients. Secondly, it is highly probable that at least 4 and more likely 8 different subgroups with very different survival rates exist in the 690 NSCLC Stage IV patients.

## DATA AVAILABILITY STATEMENT

The original contributions presented in the study are included in the article. Further inquiries can be directed to the corresponding authors.

## AUTHOR CONTRIBUTIONS

JB: concept of study and article, analysis, interpretation of results; drafting of the article and revising it critically for important intellectual content; final approval. HL: revising of the manuscript critically for important intellectual content; final approval. HG: conception and design of the study; analysis and analysis support; interpretation of data; drafting of the article or revising it critically for important intellectual content; final approval. All authors contributed to the article and approved the submitted version.

## FUNDING

This study was funded by a personal grant no. 2021-177 to JB from Medical Practice Dr. Jan Baak Inc., Tananger, Norway, to participate in this study and for the translation correction and publication costs.

## REFERENCES

1. Sung H, Ferlay J, Siegel RL, Laversanne M, Soerjomataram I, Jemal A, et al. Global Cancer Statistics 2020: GLOBOCAN Estimates of Incidence and Mortality Worldwide for 36 Cancers in 185 Countries. *CA Cancer J Clin* (2021) 71(3):209–49. doi: 10.3322/caac.21660
2. Gao S, Li N, Wang S, Zhang F, Wei W, Li N, et al. Lung Cancer in People's Republic of China. *J Thorac Oncol* (2020) 15(10):1567–76. doi: 10.1016/j.jtho.2020.04.028
3. Guo HR, Li HG, Zhu LH, Feng JL, Huang XG, Baak JPA. "How Long Have I Got?" In Stage IV NSCLC Patients With at Least 3 Months Up to 10 Years Survival, Accuracy of Long-, Intermediate and Short-Term Survival Prediction is Not Good Enough to Answer This Question. *Front Oncol* (2021) 11:761042. doi: 10.3389/fonc.2021.761042
4. Nowell PC. The Clonal Evolution of Tumor Cell Populations. *Science* (1976) 194(4260):23–8. doi: 10.1126/science.959840
5. Folkman J. Tumor Angiogenesis: Therapeutic Implications. *N Engl J Med* (1971) 285(21):1182–6. doi: 10.1056/NEJM197111182852108
6. Folkman J. Tumor Angiogenesis. *Adv Cancer Res* (1974) 19(0):331–58. doi: 10.1016/s0065-230x(08)60058-5
7. Gimbrone MAJr, Leapman SB, Cotran RS, Folkman J. Tumor Dormancy *In Vivo* by Prevention of Neovascularization. *J Exp Med* (1972) 136(2):261–76. doi: 10.1084/jem.136.2.261
8. McGranahan N, Swanton C. Clonal Heterogeneity and Tumor Evolution: Past, Present, and the Future. *Cell* (2017) 168(4):613–28. doi: 10.1016/j.cell.2017.01.018
9. Huxley J. *The Biological Aspects of Cancer*. New York: Harcourt, Brace (1958).
10. Johnson BE, Mazor T, Hong C, Barnes M, Aihara K, McLean CY, et al. Mutational Analysis Reveals the Origin and Therapy-Driven Evolution of Recurrent Glioma. *Science* (2014) 343(6167):189–is193. doi: 10.1126/science.1239947
11. Mutter GL, Lin MC, Fitzgerald JT, Kum JB, Baak JP, Lees JA, et al. Altered PTEN Expression as a Diagnostic Marker for the Earliest Endometrial Precancers. *J Natl Cancer Inst* (2000) 92(11):924–30. doi: 10.1093/jnci/92.11.924

**Conflict of Interest:** The authors declare that the research was conducted in the absence of any commercial or financial relationships that could be construed as a potential conflict of interest.

frontiers in Oncology

ORIGINAL RESEARCH
published: 10 February 2022
doi: 10.3389/fonc.2022.793190

# Optimal Initial Time Point of Local Radiotherapy for Unresectable Lung Adenocarcinoma: A Retrospective Analysis on Overall Arrangement of Local Radiotherapy in Advanced Lung Adenocarcinoma

*Xinge Li[1,2], Jie Wang[1], Xu Chang[2], Zhenhua Gao[2,3], Feifei Teng[2], Xue Meng[2]* and Jinming Yu[1,2]**

[1] Department of Radiation Oncology, The First Hospital of China Medical University, Shenyang, China, [2] Department of Radiation Oncology, Shandong Cancer Hospital and Institute, Shandong First Medical University and Shandong Academy of Medical Sciences, Jinan, China, [3] Cheeloo College of Medicine, Shandong University, Jinan, China

Local radiotherapy (LRT) is reported to be of survival benefit for advanced non-small cell lung cancer (NSCLC) in accumulating evidence, but research on the optimal initial time point remains scarce. This IRB-approved retrospective analysis identified patients diagnosed with stage IIIb–IV unresectable lung adenocarcinoma who initiated front-line LRT at our institution between 2017 and 2020. The receiver operating characteristic (ROC) curve analyses were used to cut off the initial time of LRT (before and beyond 53 days). Patients were divided into two groups: one early to initiate radiotherapy group (≤53 days, EAR group) and one deferred radiotherapy group (>53 days, DEF group). The Kaplan–Meier method was used to estimate time-to-event endpoints; the Cox proportional hazard model was used to find out predictors of progression-free survival (PFS) and overall survival (OS). A total of 265 patients with a median age of 57 were enrolled. The median follow-up time was 26.4 months (ranging from 2.2 to 69.7 months). The mOS was 38.6 months and mPFS was 12.7 months. Age >60, bone and brain metastases, multisite metastases, and EGFR 19 mutation were independent predictors associated with OS. Early initiation of local radiotherapy within 53 days after diagnosis resulted in better PFS, but not in OS. A better OS was observed in patients with bone metastasis who underwent local radiotherapy initiated within 53 days.

**Keywords: radiotherapy, local radiotherapy, optimal time point, unresectable lung adenocarcinoma, non-small cell lung cancer**

OPEN ACCESS

***Edited by:***
*Kristin Higgins,*
*Emory University, United States*

***Reviewed by:***
*Xiance Jin,*
*Wenzhou Medical University, China*
*Xiaofei Wang,*
*First Affiliated Hospital of Soochow University, China*

***Correspondence:**
*Xue Meng*
*mengxuesdzl@163.com*
*Jinming Yu*
*sdyujinming@126.com*

***Specialty section:***
*This article was submitted to Thoracic Oncology, a section of the journal Frontiers in Oncology*

***Received:*** *11 October 2021*
***Accepted:*** *17 January 2022*
***Published:*** *10 February 2022*

***Citation:***
*Li X, Wang J, Chang X, Gao Z, Teng F, Meng X and Yu J (2022) Optimal Initial Time Point of Local Radiotherapy for Unresectable Lung Adenocarcinoma: A Retrospective Analysis on Overall Arrangement of Local Radiotherapy in Advanced Lung Adenocarcinoma. Front. Oncol. 12:793190. doi: 10.3389/fonc.2022.793190*

## INTRODUCTION

Lung cancer ranks only second to breast cancer in incidence and the top above any other cancer in mortality around the world, accounting for 18% of cancer deaths, according to GLOBOCAN 2020 data. Traditional surgical resection is the treatment of choice for patients with operable non-small-cell lung cancer (NSCLC) (1, 2). Patients with stage IIIb–IV unresectable NSCLC are seeing a dismal prognosis (2–5). Nevertheless, the springing up of molecular understanding and the development of molecular detection techniques within the last decade have refreshed the management for patients with NSCLC harboring oncogenic mutations (6, 7). Targeted therapeutic strategies, in addition to cytotoxic systemic chemotherapy over the past decade, have fostered a rising shift of survival benefit (8, 9).

Radiotherapy, along with other local ablative strategies, is regarded as efficient means to alleviating symptoms as well as promoting local lesion control in advanced NSCLC (10, 11). The emerging conception of oligometastases brought us more consideration for management of patients with limited number of metastatic lesions (12–14). Several remarkable prospective randomized trials have demonstrated the profit from local consolidative intervention not merely in local control but also in survival outcome for patients with advanced NSCLC. The first multi-institutional randomized trial led by the MD Anderson Cancer Center demonstrated the progression-free survival and overall survival benefit in local consolidative therapy compared with standard maintenance therapy (15, 16). Another randomized trial contemporaneously led by investigators at the University of Texas revealed that stereotactic ablative radiotherapy (SABR) in addition to induction systemic therapy and maintenance therapy prolonged progression-free survival (PFS) from 3.5 to 9.7 months (17). The third randomized trial that showed a considerable improvement in survival with the implementation of SABR for patients with oligometastatic disease was the SABR-COMET trial, of which NSCLC patients took up approximately 18% patients enrolled (18).

Even though reasonable trials indicate the impressive benefit that may be obtained through the implementation of local interventions, debate on its optimal timing remains scarce. Previous studies focused mainly on intervention in the process of consolidation section instead of earlier phases of treatment regimen during which time a little diversification may result in a large discrepancy later on. Thus, we hypothesized that earlier initiation of local radiotherapy for patients with stage IV NSCLC may offer better survival benefit. To address this hypothesis, we investigate the initial timing of radiation therapy and survival outcome of patients with stage IIIb–IV unresectable lung adenocarcinoma, with or without oncogenic mutations.

## MATERIALS AND METHODS

### Patients

We conducted a retrospective study and reviewed the medical records of patients diagnosed with stage IIIb–IV unresectable lung adenocarcinoma at Shandong Cancer Hospital and Institute from January 2017 to March 2020. Patients eligible for this analysis should meet the following criteria: (1) stages IIIb–IV (according to the 7th edition of the American Joint Committee on Cancer staging system) pathologically diagnosed with lung adenocarcinoma; (2) treatment-naïve when at first diagnosis; (3) received local radiation therapy during front-line treatment; (4) aged 18 years or older, with a Karnofsky Performance Status (KPS) of 70 or higher; and (5) has adequate follow-up data. Patients were excluded when (1) with a history of non-standard treatment of immunotherapy; (2) with a history of local interventions other than radiotherapy; and (3) full dose and course of radiotherapy was uncompleted. Patient clinical data, including sex, age at diagnosis, time of diagnosis, Karnofsky Performance Status, status of T, N, M stages, metastasis sites, status of oncogenic mutations, systemic treatment regimen, initial time of radiotherapy, status and time of progression, and status and time of death were collected and collated from medical records (**Figure 1**). Data were cut off by August 22, 2021. This study was approved by the institutional review board of Shandong Cancer Hospital and was conducted in accordance with the Declaration of Helsinki. Informed consent to access the electronic medical record was obtained from each participant.

### Time Division

The initiation time of radiotherapy was calculated as the time interval from diagnosis to the initiation of radiotherapy. Logistic regression analyses were used to assess the initiation time of radiotherapy associated with disease progression. The receiver operating characteristic (ROC) curve analyses were used for the identification of the cutoff values of the time interval. The ROC curve with an area under curve (AUC) of 0.613 was obtained (**Figure 2**). The optimal cutoff values were determined using Youden's index which was calculated as the maximum value of the formula: sensitivity – (1 – specificity). Subsequently, a Youden's index of 0.217 and the cutoff value of 53 days were obtained. Then, the patients were divided into two groups based on this cutoff value: one early to initiate radiotherapy group (≤53 days, EAR group) and one deferred radiotherapy group (>53 days, DEF group).

### Systemic Medication Regimen

Definitive systemic therapy has constantly been the cornerstone of the treatment paradigm for unresectable locally advanced or metastatic NSCLC. In lung adenocarcinoma, patients harboring oncogenic mutations can benefit from tyrosine kinase inhibitor (TKI) therapy. Others received conventional cytotoxic platinum-based chemotherapy. In real-world practice, next-generation sequencing can be time-consuming. Some of these patients thereby received cytotoxic chemotherapy ahead of TKIs in order to get timely treatment during their wait for genomic testing reports. This part of patients was grouped and classified into combination of "chemotherapy and targeted therapy" group in our analysis. All systemic therapy was administered using standard-of-care first-line regimens, with the choice of specific medications at the discretion of the oncologist. Patients who have

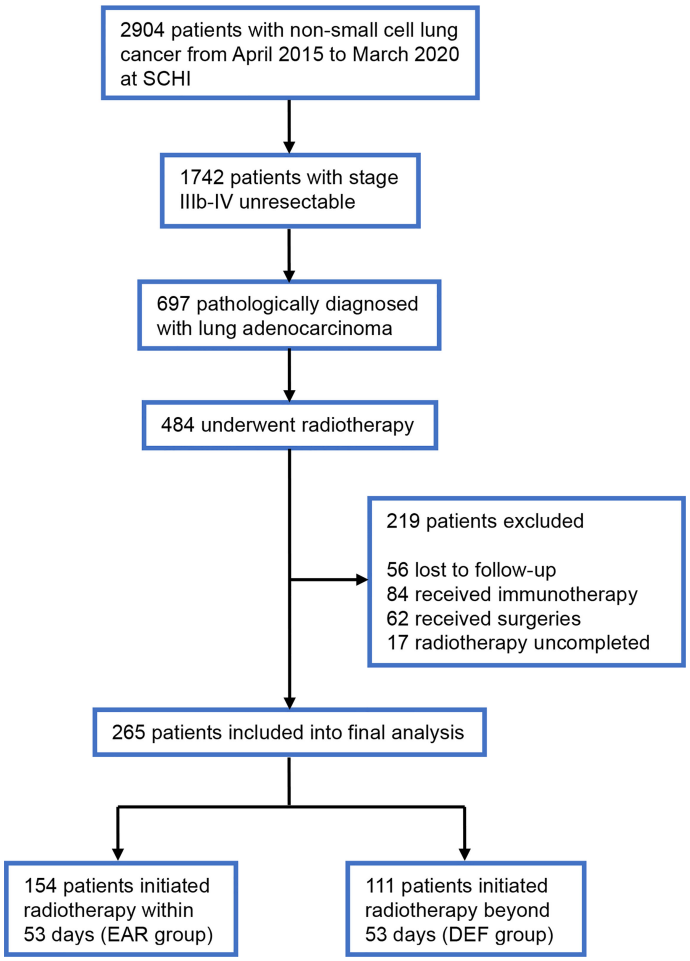


**FIGURE 1** | Flowchart of the patient cohort. SCHI, Shandong Cancer Hospital and Institute; EAR, early to initiate radiotherapy group; DEF, deferred radiotherapy group.

received second-line or above systemic medication were excluded from our analysis. A fraction of patients received immunotherapy was also excluded, to avoid confounding that may be caused by inherent heterogeneities.

## Procedure of Radiotherapy

All radiotherapy patients received was external beams *via* intensity-modulated radiation therapy (IMRT). All patients received standard prescription dose according to their respective stages. Patients enrolled to our analysis were treated using the same treatment planning system, standard procedures, and radiation dose constraints for organs at risk. Each individual gross tumor volume (GTV) was contoured referring to CT, MRI, and FDG-PET reports, then expanded up to 5 mm to clinical target volume (CTV), then another 5 mm to planning target volume (PTV). The prescription dose and fraction mode for different sites were determined by the treating radiologist, ranging from a palliative dose to a definite one based on tumor conditions. If multiple lesions were existing in close proximity, effort was made to treat them with one dose and fractionation. All radiation treatment plans were reviewed by a board consisting of a radiologist, radiographer, and medical physicist based on CB-CHOP standard before implementation. For patients who received more than one course of radiotherapy, only the initiation time of the first course was included into our analysis.

## Follow-Up

Tumor stage was assessed by systemic imaging features: either contrast-enhanced computed tomography (CT) for the brain, chest, abdomen, and bone, or positron emission tomography/computed tomography (PET-CT) with brain magnetic resonance imaging (MRI). Patients' response was measured by imaging technologies mentioned above and characterized by Response Evaluation Criteria in Solid Tumors (RECIST) for both the primary tumor and the metastatic sites of disease. Patients' progression or survival conditions were followed up by telephone number extracted from medical records.

## Statistical Analysis

Progression-free survival (PFS) was calculated as the time period from the date of treatment initiation to the date of disease

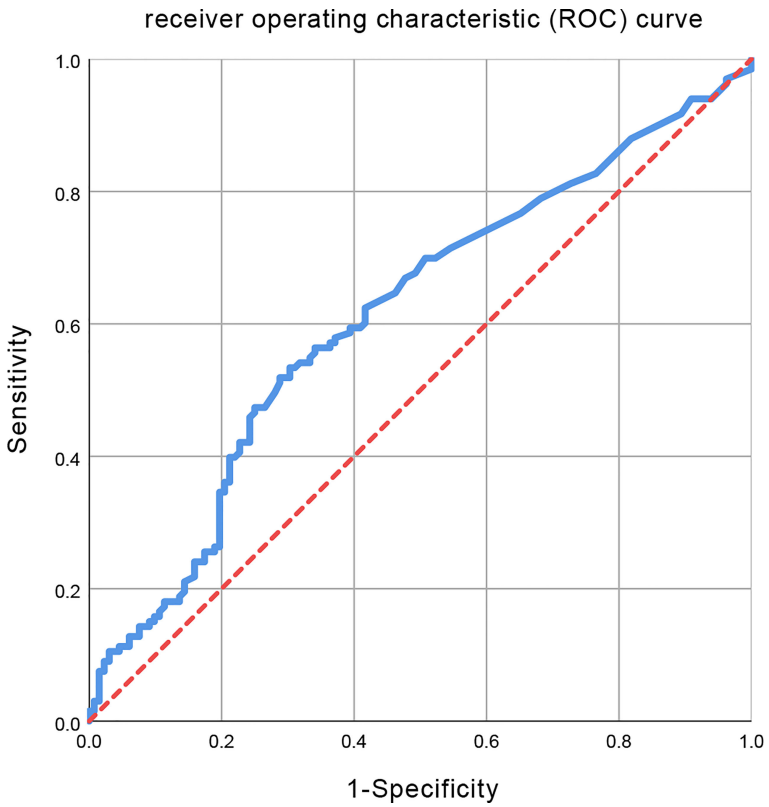


**FIGURE 2** | Receiver operating characteristic (ROC) curve for all initiation time of radiotherapy. The area under the curve (AUC) was 0.613.

progression, including progression *in situ*, in metastasis and new onset of metastatic site. Overall survival (OS) was calculated as the time period from the date of diagnosis to the date of death of any cause or the date of data cutoff. Descriptive statistics were used to summarize baseline characteristics. The chi-square test and Fisher's exact test were used to compare categorical variables. The Kaplan–Meier method and log-rank tests were used for OS and PFS analyses as well as comparison of different groups. $p < 0.05$ was defined as statistically significant. All statistical analyses were performed using SPSS V26.0 (IBM Corporation, Armonk, NY, USA).

# RESULTS

## Patient Characteristics

A total of 265 patients with stage IIIb–IV unresectable lung adenocarcinoma who underwent front-line full-course radiotherapy during the study period were enrolled. The patient characteristics are presented in **Table 1**. The majority of patients (142, 53.6%) were male. The median age was 57 years (range from 24 to 78 years), 165 patients (62.3%) aged under 60 years old and 100 (37.7%) above. Patients with a KPS score above 90 or 80 accounts for 46.8% and 49.1%, respectively, of all patients. Patients with unresectable locally advanced lung adenocarcinoma account for 17.7% of all patients enrolled. The most common site of metastasis was brain (61,23%) of all 265 patients, followed by multisite metastases (57,21.5%), no metastasis, and bone metastasis respectively (50,18.9%). Metastasis sites that were relatively infrequent were classified into other-site group (12,4.5%). Regarding oncogenic mutations, 38.1% patients bore no mutations, 25.7% patients bore EGFR 21, 19.2% EGFR 19, 3.8% ALK, and 13.2% other rare mutations. 154 patients who initiated radiotherapy within 53 days were allocated into the EAR group, and 111 patients that initiated radiotherapy beyond 53 days were allocated into the DEF group. Most of the patients received TKIs combined with chemotherapy in both EAR (56,36.4%) and DEF (36,32.4%) groups, as well as in all patients (92,34.7%). The stages of T and N and types of systemic regimen used are shown in **Table 1**.

## Survival Outcome

The median follow-up time was 26.4 months (ranging from 2.2 to 69.7 months). 205 patients had disease progression (118 in the EAR group, 87 in the DEF group), and 172 patients were alive at the last follow-up (101 in the EAR group, 71 in the DEF group). The median OS (mOS) and median PFS (mPFS) for the cohort was 38.6 months (95% CI, 31.8–45.4) and 12.7 months (95% CI, 11.0–14.4), respectively. As shown in **Figure 3A**, the mOS for the EAR group and DEF group were 37.6 months (95% CI, 27.2–48) and 38.6 months (95% CI, 31.1–46.1), respectively. No significance was observed when comparing these two groups (HR 1.07, 95% CI 0.64–1.79, $p = 0.931$). The mPFS for the EAR group and DEF group

**TABLE 1** | Baseline patient characteristics.

| Characteristics | EAR (≤53 days) N (%) | DEF (>53 days) N (%) | Total N (%) | *p*-value |
|---|---|---|---|---|
| **Sex** | | | | |
| Male | 72 (46.8) | 70 (63.1) | 142 (53.6) | 0.009 |
| Female | 82 (53.2) | 41 (36.9) | 123 (46.4) | |
| **Age** | | | | |
| ≤60 | 94 (61) | 71 (64) | 165 (62.3) | 0.7 |
| >60 | 60 (39) | 40 (36) | 100 (37.7) | |
| **KPS** | | | | |
| ≥90 | 66 (42.9) | 58 (52.3) | 124 (46.8) | 0.117 |
| ≥80 | 78 (50.6) | 52 (46.8) | 130 (49.1) | |
| ≥70 | 10 (6.5) | 1 (0.9) | 11 (4.2) | |
| **T** | | | | |
| 1 | 37 (24) | 18 (16.2) | 55 (20.8) | |
| 2 | 62 (40.3) | 49 (44.1) | 111 (41.9) | 0.411 |
| 3 | 20 (13) | 19 (17.1) | 39 (14.7) | |
| 4 | 35 (22.7) | 25 (22.5) | 60 (22.6) | |
| **N** | | | | |
| 0 | 30 (19.5) | 19 (17.1) | 49 (18.5) | |
| 1 | 6 (3.9) | 5 (4.5) | 11 (4.2) | 0.513 |
| 2 | 62 (40.3) | 37 (33.3) | 99 (37.4) | |
| 3 | 56 (36.4 | 50 (45) | 106 (40) | |
| **M** | | | | |
| 0 | 9 (5.8) | 38 (34.2) | 47 (17.7) | <0.001 |
| 1 | 145 (94.2) | 73 (65.8) | 218 (82.3) | |
| **Metastasis sites** | | | | |
| None | 10 (6.5) | 40 (36) | 50 (18.9) | |
| Brain | 47 (30.5) | 14 (12.6) | 61 (23) | |
| Bone | 33 (21.4) | 17 (15.3) | 50 (18.9) | <0.001 |
| Bilateral pulmonary | 2 (1.3) | 9 (8.1) | 11 (4.2) | |
| Bone and brain | 20 (13) | 4 (3.6) | 24 (9.1) | |
| Other sites | 0 (0) | 12 (10.8) | 12 (4.5) | |
| Multisites | 42 (27.3) | 15 (13.5 | 57 (21.5) | |
| **Oncogenic mutation** | | | | |
| None | 49 (31.8) | 52 (46.8) | 101 (38.1) | |
| EGFR 19 | 30 (19.5) | 21 (18.9) | 51 (19.2) | 0.084 |
| 21 | 46 (29.9) | 22 (19.8) | 68 (25.7) | |
| ALK | 5 (3.2) | 5 (4.5) | 10 (3.8) | |
| Others | 24 (15.5) | 11 (9.9) | 35 (13.2) | |
| **Systemic medication** | | | | |
| Chemo | 28 (18.2) | 36 (32.4) | 64 (24.2) | |
| Bev and chemo | 34 (22.1) | 27 (24.3) | 61 (23) | 0.09 |
| TKIs | 36 (23.4) | 12 (10.8) | 48 (18.1) | |
| TKIs and chemo | 56 (36.4) | 36 (32.4 | 92 (34.7) | |

*EAR, early to initiate radiotherapy group; DEF, deferred radiotherapy group; Bev, bevacizumab; chemo, chemotherapy; TKIs, tyrosine kinase inhibitors.*

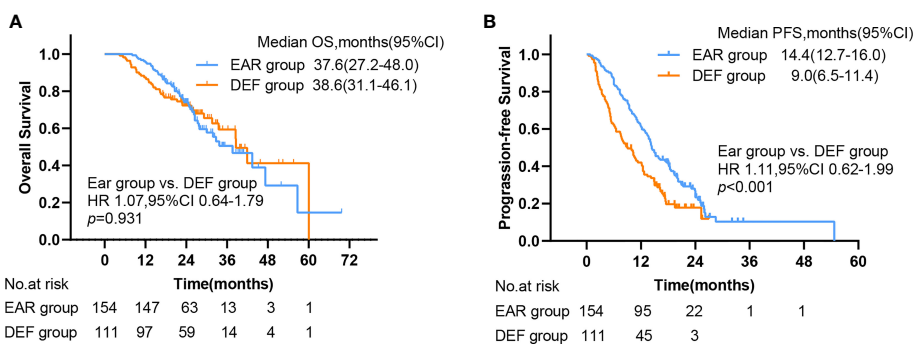


**FIGURE 3** | Kaplan–Meier plots of **(A)** OS and **(B)** PFS in EAR and DEF, with numbers at risk shown below the graph. PFS, progression-free survival; OS, overall survival; CI, confidence interval, EAR, early to initiate radiotherapy group (≤53 days); DEF, deferred radiotherapy group (>53 days).

is shown in **Figure 3B**. The mPFS for the EAR group was 14.4 months (95% CI, 12.7–16.0) and 9 months (95% CI, 6.5–11.4) for the DEF group. A remarkable significance in PFS was observed in the EAR group compared with the DEF group (HR 1.11, 95% CI 0.62–1.99, p < 0.001).

Of note, significant survival differences were noticed in other grouping methods in addition to different initial times of radiotherapy. The mOS for patients aged under 60 was 47.3 (95% CI, 34.3–60.4) and 27.7 (95% CI, 19.0–36.5) for patients aged above 60, with a significant better OS of the former group than the latter (HR 2.14, 95% CI 1.27–3.59, p = 0.005) (**Figure 4A**). The mOS for patients with a KPS score above 90, 80, and 70 was 47.3 (95% CI, 28.9–65.7), 37.6 (95% CI, 29.0–46.2), and 24.9 (95% CI, 23.6–26.3), respectively. The OS for the former group was significantly better than the latter two (**Figure 4B**). The mOS for patients who received chemotherapy, bevacizumab plus chemotherapy, TKIs, and TKIs plus chemotherapy was 41.9 (95% CI, 29.1–54.8), 37.6 (95% CI, 22.9–52.4), 30.0 (95% CI, 22.9–37.2), and 47.3 (95% CI, 31.7–63.0), respectively. The combination of the TKIs and chemotherapy group showed significant better OS compared with other groups (p = 0.008) (**Figure 4C**). The OS for patients who bore no oncogenic mutation, EGFR 19, and EGFR 21 was 32.8 (95% CI, 22.0–43.5), not reached, and 33.5 (95% CI, 23.8–43.2), respectively. The OS for patients with EGFR 19 mutation was significantly better than that of others (**Figure 4D**). The OS for patients with bone and brain metastases (25.2, 95% CI 17.8–32.6) was significantly worse than that of patients with other metastases (**Figure 4E**).

To further investigate the beneficial populations from early initial radiotherapy, we subdivided patients by metastasis sites. Interestingly, the mOS were significantly improved with the use of early initial radiotherapy than deferred radiotherapy for patients with bone metastasis (56.7 versus 17.5 months, HR 4.46, 95% CI 1.28–15.61, p = 0.005) (**Figure 5**). Patients with EGFR mutations occupy nearly half of all patients. Subgroup analysis was added to the EGFR patient cohort. No significance was observed in PFS in the EAR group and DEF group (HR 0.71, 95% CI 0.45–1.14 p = 0.12), or in OS (HR 1.38, 95% CI 0.71–2.70 p = 0.357) (**Figures 6A, B**).

## Univariate and Multivariate Analyses on PFS and OS

On univariable analysis, T2, EGFR 19 mutation, systemic medication, and initial time of radiotherapy were associated with PFS (p < 0.1). On multivariate analysis, KPS ≥ 80 (HR 1.30, 95% CI 0.95–1.76, p = 0.09), T2 (HR 1.46, 95% CI 0.96–2.22, p = 0.07), and initial time of radiotherapy (HR 1.92, 95% CI 1.39–2.66, p < 0.001) were independent predictors associated with decreased PFS. The systemic treatment regimen of combination of TKIs and chemotherapy (HR 0.54, 95% CI 0.32–0.92, p = 0.02) was the independent predictor associated with favorable PFS (**Table 2**).

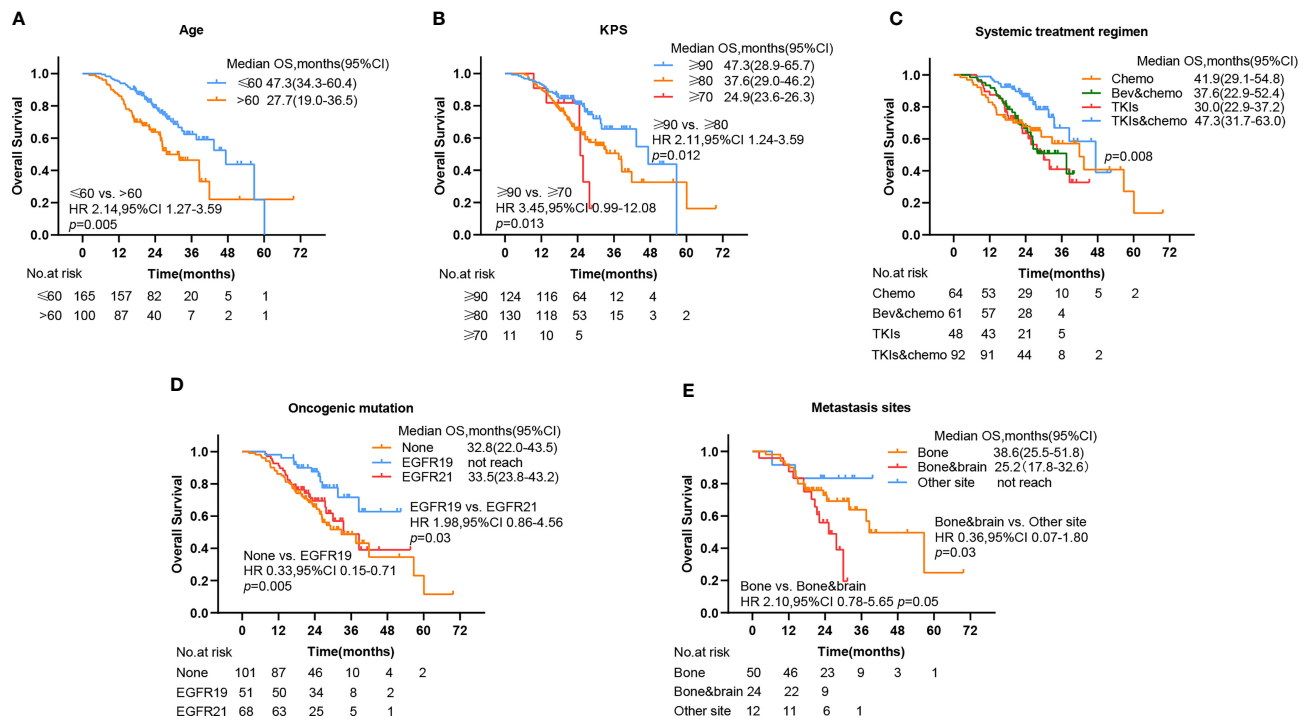


**FIGURE 4** | Kaplan–Meier plots show percent overall survival categorized by **(A)** age, **(B)** KPS, **(C)** systemic treatment regimen, **(D)** oncogenic mutation, and **(E)** metastasis sites, with numbers at risk shown below the graph. PFS, progression-free survival; OS, overall survival, CI, confidence interval, Bev, bevacizumab; chemo, chemotherapy; TKIs, tyrosine kinase inhibitors.

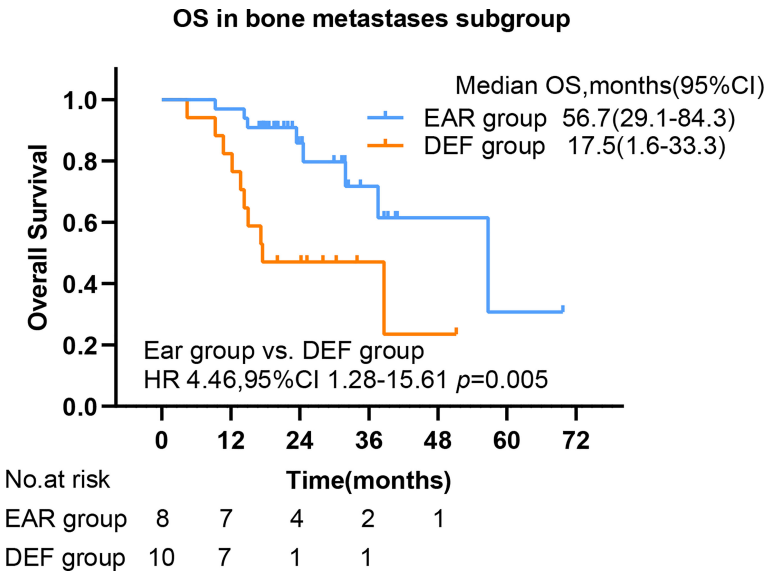


**FIGURE 5** | The OS by bone metastasis. PFS, progression-free survival; OS, overall survival; CI, confidence interval, EAR, early to initiate radiotherapy group (≤53 days); DEF, deferred radiotherapy group (>53 days).

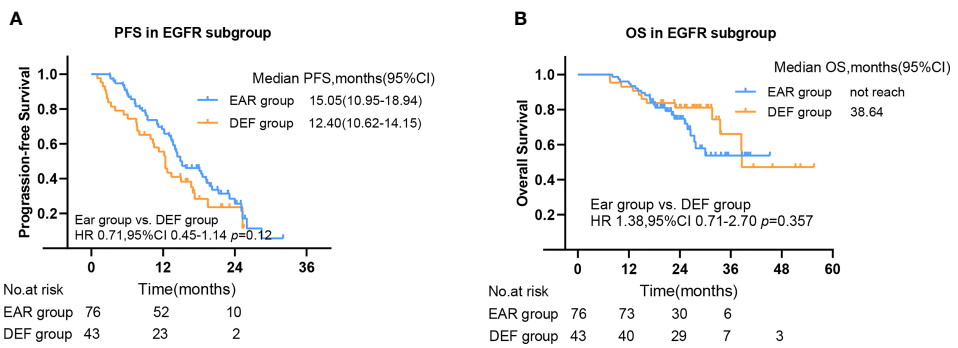


**FIGURE 6** | The PFS **(A)** and OS **(B)** in EGFR mutant subgroup. PFS, progression-free survival; OS, overall survival; CI, confidence interval, EAR, early to initiate radiotherapy group (≤53 days); DEF, deferred radiotherapy group (>53 days).

On univariable analysis, age >60, KPS ≥ 80, KPS ≥ 70, bone and brain metastases, multisite metastases, EGFR 19 mutation, and systemic treatment regimen of combination of TKIs and chemotherapy were associated with OS ($p < 0.1$). On multivariate analysis, age >60 (HR 1.48, 95% CI 0.94–2.31, p = 0.08), bone and brain metastases (HR 2.77, 95% CI 1.16–6.6, p = 0.02), and multisite metastases (HR 2.06, 95% CI 1.01–4.21, p = 0.04) were independent predictors associated with decreased OS. EGFR 19 mutation was an independent predictor associated with favorable OS (**Table 3**).

## Toxicity

The most common toxicity during the treatment course was hematologic toxicity for both EAR (43,27.9%) and DEF (33,29.7%) groups, which was mostly grade 2. The occurrence of gastrointestinal toxicity for two groups was 7.7% and 9.0%. The radiotherapy-related adverse events were mainly pneumonitis, esophagitis, and dermatitis. None of these toxicities mentioned above were statistically significant between two groups. Interestingly, the occurrence of radiation pneumonitis in the DEF group was statistically higher than that in the EAR group in our analysis (p = 0.01) (**Table 4**). All adverse events were tolerable when timely treated.

# DISCUSSION

Lung adenocarcinoma, especially with activating EGFR mutations, has better survival outcome among patients with unresectable NSCLC (19–21). Therefore, exploring an optimal implementation time point of local radiotherapy is meant for this group of patients.

**TABLE 2 |** Univariable and multivariable analyses of covariables associated with PFS.

| Variable | Univariable analysis | | | Multivariable analysis | | |
|---|---|---|---|---|---|---|
| | HR | 95% CI | *p*-value | HR | 95% CI | *p*-value |
| **Sex** | | | | | | |
| Male vs. female | 0.82 | 0.62–1.08 | 0.15 | | | |
| **Age** | | | | | | |
| ≤60 vs. >60 | 0.97 | 0.73–1.29 | 0.85 | 0.79 | 0.58–1.08 | 0.14 |
| **KPS** | | | 0.19 | | | 0.13 |
| ≥90 | | | | | | |
| ≥80 | 1.26 | 0.95–1.67 | 0.11 | 1.30 | 0.95–1.76 | 0.09 |
| ≥70 | 1.48 | 0.77–2.85 | 0.24 | 1.68 | 0.84–3.34 | 0.13 |
| **T** | | | 0.25 | | | 0.30 |
| 1 | | | | | | |
| 2 | 1.42 | 0.96–2.10 | 0.07 | 1.46 | 0.96–2.22 | 0.07 |
| 3 | 1.38 | 0.86–2.23 | 0.17 | 1.37 | 0.83–2.28 | 0.21 |
| 4 | 1.13 | 0.73–1.75 | 0.57 | 1.18 | 0.73–1.90 | 0.49 |
| **N** | | | 0.88 | | | |
| 0 | | | | | | |
| 1 | 1.02 | 0.47–2.19 | 0.95 | | | |
| 2 | 1.00 | 0.68–1.48 | 0.96 | | | |
| 3 | 0.89 | 0.61–1.31 | 0.58 | | | |
| **M** | | | | | | |
| 0 vs. 1 | 0.87 | 0.61–1.26 | 0.48 | | | |
| **Metastasis sites** | | | 0.99 | | | 0.82 |
| None | | | | | | |
| Brain | 0.92 | 0.60–1.42 | 0.72 | 1.23 | 0.75–2.03 | 0.40 |
| Bone | 0.89 | 0.57–1.40 | 0.63 | 1.24 | 0.73–2.08 | 0.41 |
| Bilateral pulmonary | 1.00 | 0.46–2.14 | 1.00 | 0.88 | 0.40–1.96 | 0.76 |
| Bone and brain | 0.91 | 0.53–1.57 | 0.74 | 1.40 | 0.76–2.59 | 0.27 |
| Other sites | 1.11 | 0.53–2.29 | 0.78 | 0.90 | 0.42–1.91 | 0.78 |
| Multi sites | 0.95 | 0.61–1.47 | 0.81 | 1.35 | 0.83–2.21 | 0.22 |
| **Oncogenic mutation** | | | 0.08 | | | 0.44 |
| None | | | | | | |
| EGFR 19 | 0.58 | 0.39–0.86 | 0.007 | 0.67 | 0.38–1.19 | 0.17 |
| 21 | 0.75 | 0.52–1.06 | 0.10 | 1.01 | 0.58–1.75 | 0.96 |
| ALK | 0.68 | 0.33–1.41 | 0.30 | 0.76 | 0.33–1.74 | 0.52 |
| Others | 0.72 | 0.46–1.12 | 0.15 | 0.92 | 0.51–1.64 | 0.78 |
| **Systemic medication** | | | 0.001 | | | 0.05 |
| Chemo | | | | | | |
| Bev and chemo | 0.97 | 0.66–1.43 | 0.90 | 0.90 | 0.59–1.37 | 0.63 |
| TKIs | 0.83 | 0.55–1.24 | 0.37 | 0.88 | 0.49–1.57 | 0.67 |
| TKIs and chemo | 0.51 | 0.35–0.74 | <0.001 | 0.54 | 0.32–0.92 | 0.02 |
| **Time of radiotherapy** | | | | | | |
| EAR vs. DEF | 1.66 | 1.25–2.21 | <0.001 | 1.92 | 1.39–2.66 | <0.001 |

*HR, hazard ratio; CI, confidence interval; Bev, bevacizumab; chemo, chemotherapy; TKIs, tyrosine kinase inhibitors; EAR, early to initiate radiotherapy group; DEF, deferred radiotherapy group.*

This analysis sought to find out the optimal initial timing of radiotherapy in unresectable stage IIIb–IV lung adenocarcinoma. To our knowledge, the present study is the largest one to statistically investigate the optimal initial timing of radiotherapy in unresectable stage IIIb–IV lung adenocarcinoma, and other independent factors associated with survival in the meantime. The results showed that earlier initiation of local radiotherapy did not prolong overall survival compared with deferred consolidative radiotherapy but significantly prolonged progression-free survival than the deferred one.

Several landmark trials have illustrated the benefit of local consolidative therapy. Ruysscher et al. conducted a prospective single-arm phase II trial to investigate the long-term outcome of adding a radical local treatment to systemic therapy in patients with oligometastatic NSCLC. After following up time for over 7 years, they reached the final analysis. The median overall survival was 13.5 months, and the median progression-free survival was 12.1 months (22, 23). Back then, the major systemic treatment was chemotherapy, and 95% of patients received chemotherapy as part of their front-line treatment in this trial. Gomez et al. conducted a prospective phase II clinical trial on patients with oligometastatic NSCLC, trying to assess the effect of the addition of local consolidative therapy to traditional maintenance therapy. The trial was terminated early due to the substantial efficacy improvement in progression-free survival, from 4.4 to 14.2 months, and overall survival from 17.0 to 41.2 months (15, 16). This finding supports for aggressive local therapy. Another phase II randomized clinical trial compared the efficacy of stereotactic ablative radiotherapy (SBRT) plus chemotherapy versus chemotherapy alone in non-driver gene addicted patients with limited metastatic NSCLC. The results showed a triple PFS in the SBRT-plus arm than chemotherapy alone (17).

**TABLE 3 |** Univariable and multivariable analyses of covariables associated with OS.

| Variable | Univariable analysis | | | Multivariable analysis | | |
|---|---|---|---|---|---|---|
| | HR | 95% CI | *p*-value | HR | 95% CI | *p*-value |
| **Sex** | | | | | | |
| Male vs. female | 0.82 | 0.54–1.24 | 0.36 | | | |
| **Age** | | | | | | |
| ≤60 vs. >60 | 1.97 | 1.31–2.96 | 0.001 | 1.48 | 0.94–2.31 | 0.08 |
| **KPS** | | | 0.01 | | | 0.08 |
| ≥90 | | | | | | |
| ≥80 | 1.73 | 1.12–2.69 | 0.01 | 1.46 | 0.92–2.31 | 0.10 |
| ≥70 | 2.76 | 1.14–6.63 | 0.02 | 2.53 | 0.99–6.42 | 0.05 |
| **T** | | | 0.29 | | | |
| 1 | | | | | | |
| 2 | 1.58 | 0.87–2.88 | 0.12 | | | |
| 3 | 1.04 | 0.47–2.29 | 0.92 | | | |
| 4 | 1.14 | 0.57–2.27 | 0.69 | | | |
| **N** | | | 0.95 | | | |
| 0 | | | | | | |
| 1 | 1.22 | 0.41–3.65 | 0.71 | | | |
| 2 | 1.13 | 0.63–2.01 | 0.67 | | | |
| 3 | 1.02 | 0.57–1.82 | 0.94 | | | |
| **M** | | | | | | |
| 0 vs. 1 | 1.62 | 0.89–2.92 | 0.10 | | | |
| **Metastasis sites** | | | 0.06 | | | 0.16 |
| None | | | | | | |
| Brain | 1.56 | 0.76–3.18 | 0.22 | 1.55 | 0.73–3.30 | 0.25 |
| Bone | 1.47 | 0.71–3.00 | 0.29 | 1.28 | 0.59–2.76 | 0.52 |
| Bilateral pulmonary | 1.51 | 0.49–4.67 | 0.47 | 1.49 | 0.46–4.75 | 0.50 |
| Bone and brain | 3.23 | 1.47–7.06 | 0.003 | 2.77 | 1.16–6.60 | 0.02 |
| Other sites | 0.71 | 0.16–3.17 | 0.65 | 0.68 | 0.15–3.16 | 0.63 |
| Multi sites | 2.18 | 1.10–4.33 | 0.02 | 2.06 | 1.01–4.21 | 0.04 |
| **Oncogenic mutation** | | | 0.06 | | | 0.22 |
| None | | | | | | |
| EGFR 19 | 0.39 | 0.20–0.77 | 0.007 | 0.39 | 0.16–0.94 | 0.03 |
| 21 | 0.86 | 0.52–1.42 | 0.57 | 0.78 | 0.34–1.78 | 0.56 |
| ALK | 0.46 | 0.14–1.49 | 0.19 | 0.49 | 0.13–1.89 | 0.30 |
| Others | 0.66 | 0.32–1.37 | 0.27 | 0.80 | 0.32–2.00 | 0.63 |
| **Systemic medication** | | | 0.01 | | | 0.41 |
| Chemo | | | | | | |
| Bev and chemo | 1.19 | 0.68–2.08 | 0.54 | 1.05 | 0.57–1.94 | 0.86 |
| TKIs | 1.31 | 0.73–2.35 | 0.35 | 1.31 | 0.54–3.14 | 0.54 |
| TKIs and chemo | 0.49 | 0.27–0.91 | 0.02 | 0.74 | 0.32–1.70 | 0.46 |
| **Time of radiotherapy** | | | | | | |
| EAR vs. DEF | 0.98 | 0.65–1.48 | 0.93 | | | |

*HR, hazard ratio; CI, confidence interval; Bev, bevacizumab; chemo, chemotherapy; TKIs, tyrosine kinase inhibitors; EAR, early to initiate radiotherapy group; DEF, deferred radiotherapy group.*

The trial was also stopped early after an interim analysis due to a significant improvement in PFS. An observational study conducted by Kwint et al. showed a favorable long-term PFS and OS in stage IV NSCLC treated with radical local treatment. The mPFS was 14 months and mOS was 32 months (24). For local consolidative stereotactic ablative radiotherapy (SABR) specifically to intrapulmonary lesions in stage IV NSCLC, the mPFS reached 34.3 months and mOS was not reached (25). Accumulating evidence from clinical trials, research, and translational investigations regarding the potentially curative roles of radiotherapy in advanced NSCLC is converted from palliative ones (26). For patients with unresectable locally advanced NSCLC, Niho et al. released a feasibility study JCOG0402 evaluating the efficacy of gefitinib plus thoracic radiotherapy after induction chemotherapy in 2012 and failed to meet their criterion for feasibility (27). Radiotherapy techniques have evolved over time. In 2020, Xu et al. conducted a retrospective analysis; the results showed favorable survival in the combination of TKIs and radiotherapy with a 6.7% incidence of grade 3 pneumonitis, which is acceptable (28). Another prospective phase II study LOGIK0902 was conducted to evaluate the efficacy and safety of gefitinib induction followed by chemoradiotherapy in EGFR-mutant locally advanced NSCLC. Results showed that the 2-year OS rate reached 90%, with no radiation pneumonitis or treatment-associated death (6). Herein, our results are basically in line with studies mentioned above. Patients who underwent early radiotherapy had significant longer mPFS compared with deferred consolidative radiotherapy, although no significant OS benefit was observed in our analysis for the entire cohort. In addition, patients aged under 60, with a KPS score over 90, systemically treated with combination of TKIs and chemotherapy or bore EGFR 19

**TABLE 4** | Toxicity profile for the EAR and DEF groups.

| Toxicity Outcomes | EAR group N = 154 (58.1%) | DEF group N = 111 (41.9%) | *p*-value |
|---|---|---|---|
| Hematologic toxicity | | | |
| Grade 1 | 14 (9.1%) | 8 (7.2%) | 0.58 |
| Grade 2 | 22 (14.3%) | 19 (17.1%) | 0.52 |
| Grade 3 | 6 (3.9%) | 5 (4.5%) | 0.80 |
| Grade 4 | 1 (0.6%) | 1 (0.9%) | 0.81 |
| Gastrointestinal toxicity | | | |
| Grade 1 | 8 (5.2%) | 8 (7.2%) | 0.49 |
| Grade 2 | 3 (1.9%) | 2 (1.8%) | 0.93 |
| Grade 3 | 1 (0.6%) | 0 (0) | 0.39 |
| Liver dysfunction | 4 (2.6%) | 5 (4.5%) | 0.40 |
| Skin rash | 2 (1.3%) | 4 (3.6%) | 0.21 |
| Diarrhea | 1 (0.6%) | 0 (0) | 0.39 |
| Radiation pneumonitis | 3 (1.9%) | 9 (8.1%) | 0.01 |
| Radiation esophagitis | 1 (0.6%) | 4 (3.6%) | 0.08 |
| Radiation dermatitis | 1 (0.6%) | 0 (0) | 0.39 |

mutation are seeing a preferable OS outcome in our analysis, respectively consistent with aforementioned studies.

Referring to the optimal initial time point of radiotherapy, about which clear answers are seldom seen, the present study used ROC to firstly statistically calculate the cutoff time point and performed a statistical analysis on this issue. The optimal initial time point of local radiotherapy was within 53 days after diagnosis, which results in a better mPFS outcome. Of note, patients with newly discovered progression may have developed the progression before their routine checkups during the follow-up process. Thus, the PFS discrepancy between the progression patients and the stable ones should have been slightly larger than we could have detected. For patients harboring TKI-sensitive EGFR mutations, Tang et al. found that the median time to maximal tumor shrinkage was 2 months in EGFR-mutated IIIB or IV NSCLC patients treated with EGFR-TKIs. They suggest local therapy to be adopted during this period (29). Ni et al. found that upfront brain radiotherapy before crizotinib for patients with advanced ALK-positive NSCLC postpones disease progression (30). Analogically, Shafie et al. observed a better intracranial progression-free survival in TKI-treated EGFR/ALK mutant NSCLC treated with early local therapy, regardless of the radiotherapy technique (31). A retrospective analysis observed that the mPFS was 36 months in the LCT plus TKI group and 14 months in the TKI-only group in metastatic NSCLC (32). Similar results were obtained from another retrospective analysis conducted by Xu et al. This study found survival benefit not merely in PFS in patients grouped by treatment modality but also in OS outcome (33). This was a result from stage IV patients. For a larger group including IIIb, the benefits still exist (34). Magnuson et al. conducted a retrospective multi-institutional analysis and found that deferral radiotherapy is associated with inferior OS in patients with EGFR-mutant brain-metastatic NSCLC (35). Wang et al. found a better intracranial progression-free survival (iPFS) but similar OS in upfront intracranial radiation for patients with EGFR-mutant, brain-metastatic NSCLC (36). Similarly, a prolonged time to treatment failure (TTF) and central nervous system progression-free survival (CNS-PFS) for EGFR-mutant NSCLC patients with CNS metastases with upfront brain radiotherapy was found by Saida et al. (37). In our analysis in the EGFR-mutant patient cohort, the PFS of the EAR group is superior to that of the DEF group, but no statistical significance was found in PFS nor in OS between the EAR and DEF groups, possibly because patients with EGFR mutations had better disease control and prognosis than those mutant-free (38), so the initial time point of local intervention had little impact on the overall disease progression. Additionally, and surprisingly, for patients with bone metastasis, early initiation of local radiotherapy is responsible for a preferable OS outcome in our analysis. The principle behind this phenomenon remains to be further explored.

In addition to survival benefits, consideration of toxicities is also a vital aspect when making treatment decisions. Severe adverse events can be a major obstacle to prevent patients from accomplishing a full-course treatment. Previous studies showed the potential increasing risk of toxicities for the combination of radiotherapy with other treatment alternative. Jia et al. reported an increasing risk of radiation pneumonitis in patients with a longer overlap time treated with TKIs and radiotherapy (39). Yet no evident higher occurrence of radiation pneumonitis was observed in the EAR group of our cohort. Quite the reverse, the occurrence of pneumonitis in deferred radiotherapy was higher than that in early-to-initiate radiotherapy in our analysis. The inner relations remain unexplained.

Our analysis has several limitations. Although our robust and detailed datum collection and collation about timing of diagnosis, various treatments, and relapse allowed us to thoroughly evaluate the outcomes of patients in the cohort, the types and extent of treatment patients received varied, and posterior treatment after relapse differed, which could produce unmeasured confounding factors into the subsequent assessment of long-term outcomes. Due to limited conditions, no external dataset was available for any kind of external validation. This results in a high risk of deviation from the cutoff values. Therefore, the conclusion has to be considered carefully and interpreted with caution when guiding doctor conduct. Furthermore, although our cohort represented the largest statistical analysis of optimal initial timing of radiotherapy, it was a selected group of patients with appropriate performance status and comorbidities, the majority of whom underwent first-line radiotherapy, presumably indicating their bipolar conditions

of either unbearable local symptoms or physically permitted addition of local therapy. Imbalances in baseline characteristics among sex, M stage, and metastasis sites existed. However, due to the limited number of cases and efforts to avoid loss of available survival data, Cox proportional-hazard analysis was performed, and hazard ratios were calculated to adjust baseline characteristics of the two groups instead of the propensity score matching (PSM) method. In addition, the follow-up time of some patients in our cohort was not long enough for survival data; luckily, the proportion of these patients did not interfere with statistical analysis. Finally, the lack of comparator groups of patients who did not receive any radiation therapy may impede us from distinguishing the true benefit from early radiotherapy.

## CONCLUSIONS

In this retrospective single-institution study of 265 patients with stage IIIb–IV unresectable lung adenocarcinoma who underwent front-line local radiotherapy, mOS was 38.6 months and mPFS was 12.7 months. Age >60, bone and brain metastases, multisite metastases, and EGFR 19 mutation were independent predictors associated with OS. The early initiation of local radiotherapy within 53 days after diagnosis resulted in better PFS but no OS outcome. A better OS was observed in patients with bone metastasis who underwent local radiotherapy initiated within 53 days.

## DATA AVAILABILITY STATEMENT

The original contributions presented in the study are included in the article/supplementary material. Further inquiries can be directed to the corresponding authors.

## ETHICS STATEMENT

Written informed consent was obtained from the individual(s) for the publication of any potentially identifiable images or data included in this article.

## AUTHOR CONTRIBUTIONS

XL and XM made substantial contributions to the conception and design of the study. JW and XC helped with data collection and initial phase improvement. XL, ZG, and FT conducted the data. All authors contributed to the article and approved the submitted version.

## FUNDING

The study received the funding support from the National Natural Science Foundation of China (81627901, 81972863, 81972864, and 82030082) and Natural Science of Shandong Province ZR2020QH177.

## REFERENCES

1. Jones CM, Brunelli A, Callister ME, Franks KN. Multimodality Treatment of Advanced Non-Small Cell Lung Cancer: Where are We With the Evidence? *Curr Surg Rep* (2018) 6(2):5. doi: 10.1007/s40137-018-0202-0
2. Collaud S, Stahel R, Inci I, Hillinger S, Schneiter D, Kestenholz P, et al. Survival of Patients Treated Surgically for Synchronous Single-Organ Metastatic NSCLC and Advanced Pathologic TN Stage. *Lung Cancer* (2012) 78(3):234–8. doi: 10.1016/j.lungcan.2012.09.011
3. Agarwala AK, Hanna NH. Long-Term Survival in a Patient With Stage IV Non-Small-Cell Lung Carcinoma After Bone Metastasectomy. *Clin Lung Cancer* (2005) 6(6):367–8. doi: 10.3816/CLC.2005.n.017
4. Albain KS, Crowley JJ, LeBlanc M, Livingston RB. Survival Determinants in Extensive-Stage Non-Small-Cell Lung Cancer: The Southwest Oncology Group Experience. *J Clin Oncol* (1991) 9(9):1618–26. doi: 10.1200/JCO.1991.9.9.1618
5. Cheruvu P, Metcalfe SK, Metcalfe J, Chen Y, Okunieff P, Milano MT. Comparison of Outcomes in Patients With Stage III Versus Limited Stage IV Non-Small Cell Lung Cancer. *Radiat Oncol* (2011) 6:80. doi: 10.1186/1748-717X-6-80
6. Hotta K, Saeki S, Yamaguchi M, Harada D, Bessho A, Tanaka K, et al. Gefitinib Induction Followed by Chemoradiotherapy in EGFR-Mutant, Locally Advanced Non-Small-Cell Lung Cancer: LOGIK0902/OLCSG0905 Phase II Study. *ESMO Open* (2021) 6(4):100191. doi: 10.1016/j.esmoop.2021.100191
7. Akamatsu H, Murakami H, Harada H, Shimizu J, Hayashi H, Daga H, et al. Gefitinib With Concurrent Thoracic Radiotherapy in Unresectable Locally Advanced NSCLC With EGFR Mutation; West Japan Oncology Group 6911L. *J Thorac Oncol* (2021) 16(10):1745–52. doi: 10.1016/j.jtho.2021.05.019
8. Liang H, Song X, Zhang Y, Zhang S, Li F, Fang J, et al. Real-World Data on EGFR/ALK Gene Status and First-Line Targeted Therapy Rate in Newly Diagnosed Advanced Non-Small Cell Lung Cancer Patients in Northern China: A Prospective Observational Study. *Thorac Cancer* (2019) 10(7):1521–32. doi: 10.1111/1759-7714.13090
9. Greenhalgh J, Boland A, Bates V, Vecchio F, Dundar Y, Chaplin M, et al. *First-Line Treatment of Advanced Epidermal Growth Factor Receptor (EGFR) Mutation Positive Non-Squamous Non-Small Cell Lung Cancer. Cochrane Database Syst Rev* (2021) 3:CD010383. doi: 10.1002/14651858.CD010383.pub3
10. Fairchild A, Harris K, Barnes B, Wong R, Lutz S, Bezjak A, et al. Palliative Thoracic Radiotherapy for Lung Cancer: A Systematic Review. *J Clin Oncol* (2008) 26(24):4001–11. doi: 10.1200/JCO.2007.15.3312
11. Jumeau R, Vilotte F, Durham AD, Ozsahin EM. *Current Landscape of Palliative Radiotherapy for Non-Small-Cell Lung Cancer. Transl Lung Cancer Res* (2019) 8(Suppl 2):S192–201. doi: 10.21037/tlcr.2019.08.10
12. Bergsma DP, Salama JK, Singh DP, Chmura SJ, Milano MT. The Evolving Role of Radiotherapy in Treatment of Oligometastatic NSCLC. *Expert Rev Anticancer Ther* (2015) 15(12):1459–71. doi: 10.1586/14737140.2015.1105745
13. De Rose F, Cozzi L, Navarria P, Ascolese AM, Clerici E, Infante M, et al. Clinical Outcome of Stereotactic Ablative Body Radiotherapy for Lung Metastatic Lesions in Non-Small Cell Lung Cancer Oligometastatic Patients. *Clin Oncol (R Coll Radiol)* (2016) 28(1):13–20. doi: 10.1016/j.clon.2015.08.011
14. Blumenthaler AN, Antonoff MB. Classifying Oligometastatic Non-Small Cell Lung Cancer. *Cancers (Basel)* (2021) 13(19):4822–32. doi: 10.3390/cancers13194822
15. Gomez DR, Blumenschein GR Jr, Lee JJ, Hernandez M, Ye R, Camidge DR, et al. Local Consolidative Therapy Versus Maintenance Therapy or Observation for Patients With Oligometastatic Non-Small-Cell Lung Cancer Without Progression After First-Line Systemic Therapy: A Multicentre, Randomised, Controlled, Phase 2 Study. *Lancet Oncol* (2016) 17(12):1672–82. doi: 10.1016/S1470-2045(16)30532-0
16. Gomez DR, Tang C, Zhang J, Blumenschein GRJr., Hernandez M, Lee JJ, et al. Local Consolidative Therapy vs. Maintenance Therapy or Observation for Patients With Oligometastatic Non-Small-Cell Lung Cancer: Long-Term

Results of a Multi-Institutional, Phase II, Randomized Study. *J Clin Oncol* (2019) 37(18):1558–65. doi: 10.1200/jco.19.00201
17. Iyengar P, Wardak Z, Gerber DE, Tumati V, Ahn C, Hughes RS, et al. Consolidative Radiotherapy for Limited Metastatic Non-Small-Cell Lung Cancer: A Phase 2 Randomized Clinical Trial. *JAMA Oncol* (2018) 4(1): e173501. doi: 10.1001/jamaoncol.2017.3501
18. Palma DA, Olson R, Harrow S, Gaede S, Louie AV, Haasbeek C, et al. Stereotactic Ablative Radiotherapy for the Comprehensive Treatment of Oligometastatic Cancers: Long-Term Results of the SABR-COMET Phase II Randomized Trial. *J Clin Oncol* (2020) 38(25):2830–8. doi: 10.1200/JCO.20.00818
19. Zhou C, Wu YL, Chen G, Feng J, Liu XQ, Wang C, et al. Erlotinib Versus Chemotherapy as First-Line Treatment for Patients With Advanced EGFR Mutation-Positive Non-Small-Cell Lung Cancer (OPTIMAL, CTONG-0802): A Multicentre, Open-Label, Randomised, Phase 3 Study. *Lancet Oncol* (2011) 12(8):735–42. doi: 10.1016/s1470-2045(11)70184-x
20. Rosell R, Carcereny E, Gervais R, Vergnenegre A, Massuti B, Felip E, et al. Erlotinib Versus Standard Chemotherapy as First-Line Treatment for European Patients With Advanced EGFR Mutation-Positive Non-Small-Cell Lung Cancer (EURTAC): A Multicentre, Open-Label, Randomised Phase 3 Trial. *Lancet Oncol* (2012) 13(3):239–46. doi: 10.1016/s1470-2045(11)70393-x
21. Wu YL, Zhou C, Liam CK, Wu G, Liu X, Zhong Z, et al. First-Line Erlotinib Versus Gemcitabine/Cisplatin in Patients With Advanced EGFR Mutation-Positive Non-Small-Cell Lung Cancer: Analyses FromRandomized, Open-Label, ENSURE Study. *Ann Oncol* (2015) 26(9):1883–9. doi: 10.1093/annonc/mdv270
22. De Ruysscher D, Wanders R, van Baardwijk A, Dingemans AM, Reymen B, Houben R, et al. Radical Treatment of Non-Small-Cell Lung Cancer Patients With Synchronous Oligometastases: Long-Term Results of a Prospective Phase II Trial (Nct01282450). *J Thorac Oncol* (2012) 7(10):1547–55. doi: 10.1097/JTO.0b013e318262caf6
23. De Ruysscher D, Wanders R, Hendriks LE, van Baardwijk A, Reymen B, Houben R, et al. Progression-Free Survival and Overall Survival Beyond 5 Years of NSCLC Patients With Synchronous Oligometastases Treated in a Prospective Phase II Trial (NCT 01282450). *J Thorac Oncol* (2018) 13 (12):1958–61. doi: 10.1016/j.jtho.2018.07.098
24. Kwint M, Walraven I, Burgers S, Hartemink K, Klomp H, Knegjens J, et al. Outcome of Radical Local Treatment of Non-Small Cell Lung Cancer Patients With Synchronous Oligometastases. *Lung Cancer* (2017) 112:134–9. doi: 10.1016/j.lungcan.2017.08.006
25. Blake-Cerda M, Lozano-Ruíz F, Maldonado-Magos F, de la Mata-Moya D, Díaz-García D, Lara-Mejía L, et al. Consolidative Stereotactic Ablative Radiotherapy (SABR) to Intrapulmonary Lesions is Associated With Prolonged Progression-Free Survival and Overall Survival in Oligometastatic NSCLC Patients: A Prospective Phase 2 Study. *Lung Cancer* (2021) 152:119–26. doi: 10.1016/j.lungcan.2020.12.029
26. Zhou Y, Yu F, Zhao Y, Zeng Y, Yang X, Chu L, et al. A Narrative Review of Evolving Roles of Radiotherapy in Advanced Non-Small Cell Lung Cancer: From Palliative Care to Active Player. *Transl Lung Cancer Res* (2020) 9 (6):2479–93. doi: 10.21037/tlcr-20-1145
27. Niho S, Ohe Y, Ishikura S, Atagi S, Yokoyama A, Ichinose Y, et al. Induction Chemotherapy Followed by Gefitinib and Concurrent Thoracic Radiotherapy for Unresectable Locally Advanced Adenocarcinoma of the Lung: A Multicenter Feasibility Study (JCOG 0402). *Ann Oncol* (2012) 23(9):2253–8. doi: 10.1093/annonc/mds012
28. Xu K, Liang J, Zhang T, Zhou Z, Chen D, Feng Q, et al. Clinical Outcomes and Radiation Pneumonitis After Concurrent EGFR-Tyrosine Kinase Inhibitors and Radiotherapy for Unresectable Stage III Non-Small Cell Lung Cancer. *Thorac Cancer* (2021) 12(6):814–23. doi: 10.1111/1759-7714.13816
29. Tang Y, Xia B, Xie R, Xu X, Zhang M, Wu K, et al. Timing in Combination With Radiotherapy and Patterns of Disease Progression in Non-Small Cell Lung Cancer Treated With EGFR-TKI. *Lung Cancer* (2020) 140:65–70. doi: 10.1016/j.lungcan.2019.12.009
30. Ni J, Li G, Yang X, Chu L, Wang J, Li Y, et al. Optimal Timing and Clinical Value of Radiotherapy in Advanced ALK-Rearranged Non-Small Cell Lung Cancer With or Without Baseline Brain Metastases: Implications From Pattern of Failure Analyses. *Radiat Oncol* (2019) 14(1):44. doi: 10.1186/s13014-019-1240-1
31. El Shafie RA, Seidensaal K, Bozorgmehr F, Kazdal D, Eichkorn T, Elshiaty M, et al. Effect of Timing, Technique and Molecular Features on Brain Control With Local Therapies in Oncogene-Driven Lung Cancer. *ESMO Open* (2021) 6(3):100161. doi: 10.1016/j.esmoop.2021.100161
32. Elamin YY, Gomez DR, Antonoff MB, Robichaux JP, Tran H, Shorter MK, et al. Local Consolidation Therapy (LCT) After First Line Tyrosine Kinase Inhibitor (TKI) for Patients With EGFR Mutant Metastatic Non-Small-Cell Lung Cancer (NSCLC). *Clin Lung Cancer* (2019) 20(1):43–7. doi: 10.1016/j.cllc.2018.09.015
33. Xu Q, Zhou F, Liu H, Jiang T, Li X, Xu Y, et al. Consolidative Local Ablative Therapy Improves the Survival of Patients With Synchronous Oligometastatic NSCLC Harboring EGFR Activating Mutation Treated With First-Line EGFR-Tkis. *J Thorac Oncol* (2018) 13(9):1383–92. doi: 10.1016/j.jtho.2018.05.019
34. Xu Q, Liu H, Meng S, Jiang T, Li X, Liang S, et al. First-Line Continual EGFR-TKI Plus Local Ablative Therapy Demonstrated Survival Benefit in EGFR-Mutant NSCLC Patients With Oligoprogressive Disease. *J Cancer* (2019) 10 (2):522–9. doi: 10.7150/jca.26494
35. Magnuson WJ, Lester-Coll NH, Wu AJ, Yang TJ, Lockney NA, Gerber NK, et al. Management of Brain Metastases in Tyrosine Kinase Inhibitor-Naïve Epidermal Growth Factor Receptor-Mutant Non-Small-Cell Lung Cancer: A Retrospective Multi-Institutional Analysis. *J Clin Oncol* (2017) 35(10):1070–7. doi: 10.1200/jco.2016.69.7144
36. Wang C, Lu X, Zhou Z, Wang J, Hui Z, Liang J, et al. The Efficacy of Upfront Intracranial Radiation With TKI Compared to TKI Alone in the NSCLC Patients Harboring EGFR Mutation and Brain Metastases. *J Cancer* (2019) 10 (9):1985–90. doi: 10.7150/jca.30131
37. Saida Y, Watanabe S, Abe T, Shoji S, Nozaki K, Ichikawa K, et al. Efficacy of EGFR-Tkis With or Without Upfront Brain Radiotherapy for EGFR-Mutant NSCLC Patients With Central Nervous System Metastases. *Thorac Cancer* (2019) 10(11):2106–16. doi: 10.1111/1759-7714.13189
38. Mok TS, Wu YL, Thongprasert S, Yang CH, Chu DT, Saijo N, et al. Gefitinib or Carboplatin-Paclitaxel in Pulmonary Adenocarcinoma. *N Engl J Med* (2009) 361(10):947–57. doi: 10.1056/NEJMoa0810699
39. Jia W, Gao Q, Wang M, Li J, Jing W, Yu J, et al. Overlap Time is an Independent Risk Factor of Radiation Pneumonitis for Patients Treated With Simultaneous EGFR-TKI and Thoracic Radiotherapy. *Radiat Oncol* (2021) 16 (1):41. doi: 10.1186/s13014-021-01765-x

**Conflict of Interest:** The authors declare that the research was conducted in the absence of any commercial or financial relationships that could be construed as a potential conflict of interest.

frontiers in Oncology

ORIGINAL RESEARCH
published: 18 February 2022
doi: 10.3389/fonc.2022.830470

# Treatment Modality for Stage IB Peripheral Non-Small Cell Lung Cancer With Visceral Pleural Invasion and ≤3 cm in Size

*Weijia Huang[1†], Han-Yu Deng[1*†], Ming-Ying Lin[2], Kai Xu[1,2], Yu-Xiao Zhang[2], Chi Yuan[2] and Qinghua Zhou[1*]*

[1] Lung Cancer Center, West China Hospital, Sichuan University, Chengdu, China, [2] West China School of Medicine, Sichuan University, Chengdu, China

OPEN ACCESS

**Edited by:**
Kristin Higgins,
Emory University, United States

**Reviewed by:**
Nicholas Bucknell,
Peter MacCallum Cancer Centre, Australia
Ben Dunne,
Royal Melbourne Hospital, Australia

***Correspondence:**
Han-Yu Deng
hanyudeng@scu.edu.cn
Qinghua Zhou
zhouqh135@163.com

[†]These authors have contributed equally to this work

**Specialty section:**
This article was submitted to Thoracic Oncology, a section of the journal Frontiers in Oncology

**Received:** 07 December 2021
**Accepted:** 25 January 2022
**Published:** 18 February 2022

**Citation:**
Huang W, Deng H-Y, Lin M-Y, Xu K, Zhang Y-X, Yuan C and Zhou Q (2022) Treatment Modality for Stage IB Peripheral Non-Small Cell Lung Cancer With Visceral Pleural Invasion and ≤3 cm in Size. Front. Oncol. 12:830470. doi: 10.3389/fonc.2022.830470

**Purpose:** To compare the survival difference among lobectomy, segmentectomy, and wedge resection and investigate the role of adjuvant chemotherapy for early-stage small-sized non-small cell lung cancer (NSCLC) with visceral pleural invasion (VPI).

**Methods:** Patients diagnosed with stage IB peripheral NSCLC with VPI and ≤3 cm in size in the Surveillance, Epidemiology, and End Results database between 2004 and 2015 were included, and the pleural layer (PL) invasion status was identified to recognize the tumors with VPI, including PL1 and PL2. We conducted Cox proportional hazards model in multivariable analysis and subgroup analysis *via* propensity score matching (PSM) method and Cox regression method to figure out the optimal therapy for these patients.

**Results:** A total of 1,993 patients were included, all of whom received surgery, and the median follow-up was 33 months (range, 1–83 months). In multivariable analysis, age, gender, histology, pathological grade, lymph node examination, surgical approaches, and radiotherapy were independent prognostic factors for overall survival (OS). Lobectomy was superior to sublobar resection [hazard ratio (HR) = 1.41; 95% CI, 1.08–1.83], and wedge resection was associated with impaired survival compared to lobectomy (HR = 1.64; 95% CI, 1.22–2.20) in PSM analyses. In subgroup analysis, lobectomy was superior to sublobar resection among those aged <70 years (HR = 1.81; 95% CI, 1.13–2.90), female (HR = 1.75; 95% CI, 1.21–2.53), and 1–20 mm in size (HR = 1.61; 95% CI, 1.11–2.33). No survival benefit was observed for adjuvant chemotherapy.

**Conclusions:** Lobectomy was superior to wedge resection and comparable with segmentectomy for stage IB NSCLC (≤3 cm) with VPI, and adjuvant chemotherapy could not benefit these patients, even in those with sublobar resection. The preferred surgical procedure remains to be studied in prospective controlled trials.

**Keywords: non-small cell lung cancer, visceral pleural invasion, surgery, adjuvant chemotherapy, small-sized**

**Abbreviations:** CI, confidence interval; CSS, cancer-specific survival; DFS, disease-free survival; HR, hazard ratio; LVI, lymphovascular invasion; NSCLC, non-small cell lung cancer; OS, overall survival; PL, pleural layer; PSM, propensity score matching; SEER, Surveillance, Epidemiology, and End Results; VPI, visceral pleural invasion.

## INTRODUCTION

Visceral pleural invasion (VPI) was announced as the poor prognostic factor for early-stage non-small cell lung cancer (NSCLC), and previous research indicated that the T category of TNM classification would be further evaluated by VPI extent (1–4). A tumor ≤3 cm in size with VPI and lymph node negative would be upstaged to T2, even though a tumor 3–5 cm in size without other clinicopathological characteristics specified was still T2 disease in the eighth edition of TNM classification (4). VPI could be identified on conventional CT images by pleural tags preoperatively that might increase the accuracy of early diagnosis of VPI (5). A population-based study carried out between 1989 and 2003 by the California Cancer Registry, including 10,545 patients with stage IB NSCLC, announced that around 20% of patients were classified as stage IB resulting from VPI, hilar atelectasis, or obstructive pneumonitis, even though they were ≤3 cm in size (6). Modified Hammar Classification suggested that a tumor invading beneath the elastic layer was referred to as pleural layer 0 (PL0), PL1 as invading beyond the elastic layer, PL2 as invading the pleural surface, and PL3 as invading the parietal pleura, among which PL1 and PL2 were T2 descriptors (7, 8). While prior research indicated that the adverse effect of VPI might be mainly distributed in NSCLC with N0 disease and 1–3 cm in size, the additional effect of invasiveness on VPI was found weakened with N stage upstaging and tumor size increasing (9). Furthermore, a multicenter retrospective study investigated 639 patients with completely resected NSCLC and found that the survival difference in N0 disease was only observed between PL0 and PL1 ($P = 0.003$) but not between PL1 and PL2 ($P = 0.97$) (10). Therefore, the role of VPI in small-sized early-stage NSCLC needs to be established further.

Surgical resection with lymph node dissection was the recommended standard treatment for early-stage NSCLC, and adjuvant chemotherapy might be considered for operable stage IB NSCLC postoperatively, especially when patients were identified with several high-risk clinicopathologic characteristics, including large tumor size (>4 cm), VPI, lymphovascular invasion (LVI), and high-grade histology (4, 11–13). Current randomized controlled trials seldom evaluated the surgical approaches for node-negative NSCLC with VPI, and the preference between lobectomy and sublobar resection has not been determined (14, 15). In the subgroup analysis of the newly published systematic review, including 8,447 patients from 34 trials, an improved 5-year OS from 55% to 60% was noticed resulting from adjuvant chemotherapy in stage IB NSCLC (16). However, there was no significant survival benefit for adjuvant chemotherapy observed among stage IB patients in a large pooled analysis (HR = 0.93; 95% CI, 0.78–1.10) and majority of the randomized controlled trials but effective in stage II and IIIA patients or those with lymph node positive or a larger tumor size (17–20). Moreover, the stage IB patients might be impaired in survival when receiving adjuvant chemotherapy compared with postoperative observation ($P = 0.021$) (21). Nevertheless, Strauss et al. (22) suggested that adjuvant chemotherapy was potentially effective in stage IB malignancy among those with large tumor size (>4 cm).

Although the aggressiveness of VPI has been widely studied, the favorable treatment modality for small-sized node-negative NSCLC with VPI has not been described. The purpose of this study was to compare the survival difference among lobectomy, segmentectomy, and wedge resection and investigate the role of adjuvant chemotherapy for stage IB peripheral NSCLC with VPI and ≤3 cm in size *via* propensity score matching (PSM) method in the Surveillance, Epidemiology, and End Results (SEER) database, which has been operated since 1973 by the National Cancer Institute.

## METHODS

### Patient Selection and Data Extraction

We identified the patients from the SEER database *via* SEER Stat (version 8.3.8; www.seer.cancer.gov) in February 2021 with the identifier 11151-Nov2019. This research was accorded with the amended Declaration of Helsinki, and consent from patients and research ethics approval were not required due to the data anonymization in the SEER database and elimination of patient identification. Patients diagnosed with stage IB peripheral NSCLC with VPI and ≤3 cm in size between 2004 and 2015 were included, and the inclusion and exclusion criteria were shown in a flowchart (**Figure 1**).

### Data Curation and Study Variables

Demographics, baseline characteristics, and treatment modalities were extracted, including age, gender, race, marital status,

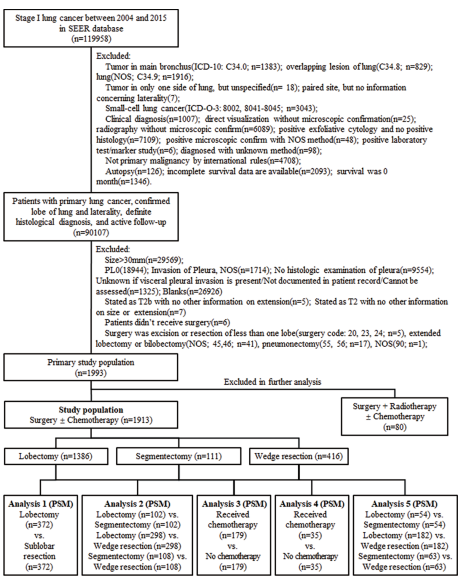


**FIGURE 1** | The process of data extraction from the Surveillance, Epidemiology, and End Results (SEER) database and the following propensity score matching (PSM) analyses. ICD-10, International Classification of Diseases, Tenth Revision; ICD-O-3, International Classification of Disease for Oncology, Third Edition; NOS, not otherwise specified; vs., versus.

primary site, laterality, the total number of *in situ* tumors, tumor size, histology, pathological grade, the status of lymph nodes examined, chemotherapy, and radiotherapy. Cancer staging was in terms of the seventh edition of the American Joint Committee on Cancer Staging Manual, and the histological classification was in accord with the third edition of the International Classification of Disease for Oncology. We excluded centrally located tumors and diligently identified peripheral malignancies. We identified the pleural layer (PL) invasion status (site-specific factor 2; code: PL1/2) in the SEER database to identify the tumors with VPI. Age was divided into two cohorts determined by the median value of the study population. Those who were still alive at the end of the follow-up were considered censored when conducting survival analysis.

## Statistical Analysis

Demographics and baseline characteristics were compared *via* $\chi^2$ or ANOVA test. Considering the potential prognostic heterogeneity of those with radiotherapy compared to those without, we eliminated the patients with radiotherapy in further survival analyses. We first conducted Kaplan–Meier analyses to determine the prognostic factors in the study cohort, and the variables with P-value <0.2 were admitted to the multivariable analysis. We identified independent prognostic factors *via* Cox proportional hazards model in multivariable analysis, which accorded with the assumption of proportional hazards. Then, we conducted five PSM analyses (**Figure 1**), which referred to lower potential bias for nonrandomized patient selection. We conducted the nearest-neighbor matching method and logistic regression in PSM analysis (one unit matched to one unit), and the caliper was set to 0.2. After matching, all these covariables were balanced in each subgroup analysis, including age, race, gender, marital status, the total number of tumors, tumor size, histology, pathological grade, the status of lymph nodes examined, and surgical procedures, which were also assessed by standardized mean difference. In subgroup analysis, sublobar resection was first investigated instead of segmentectomy and wedge resection. The relative hazard ratio (HR) in subgroup analysis was determined by univariable analysis. A P-value <0.05 was identified as statistical significance, and all statistical analyses were performed using R 3.6.1 (R Foundation for Statistical Computing, Vienna, Austria) and R packages (tableone, MatchIt, Hmisc, rms, survival, survminer).

# RESULTS

A total of 1,993 patients were included in the primary study cohort with a median age of 70 years (range, 35–96 years), 80 (4.0%) of whom received radiotherapy. All patients received surgery, in which 1,420 (71.2%) received lobectomy, 116 (5.8%) received segmentectomy, and 457 (22.9%) received wedge resection (**e-Table 1**). In the primary study cohort, the median follow-up was 33 months (range, 1–83 months). The 1-, 3-, and 5-year overall survival (OS) rate was 92.8%, 73.9%, and 60.8%. As divided by surgical approaches, the 5-year OS rate of those with lobectomy, segmentectomy, and wedge resection was 66.0%, 51.8%, and 46.7%, respectively. Then, we eliminated the patients with radiotherapy from the preliminary study cohort, contributing to the exact study population, and conducted survival analyses.

In multivariable analysis, age, gender, histology, pathological grade, lymph node examination, and surgical approaches were independent prognostic factors with regard to OS (**Table 1**). Age over 70 years (HR = 1.75; 95% CI, 1.47–2.10; P < 0.001), male (HR = 1.29; 95% CI, 1.09–1.52; P = 0.003), 21–30 mm (HR = 1.19; 95% CI, 1.00–1.41; P = 0.048), squamous cell carcinoma or other histology types (HR = 1.31; 95% CI, 1.10–1.56; P = 0.002), and receiving wedge resection (HR = 1.31; 95% CI, 1.05–1.63; P = 0.017) were associated with poor OS.

We first compared the OS concerning surgical approaches between lobectomy and sublobar resection *via* PSM method, and lobectomy performed better (HR = 1.41; 95% CI, 1.08–1.83; P = 0.011; **Figure 2A**). In the comparisons of survival difference among these three surgical procedures (**e-Table 3**), only wedge resection was significantly inferior to lobectomy (HR = 1.64; 95% CI, 1.22–2.20; **Figure 2B**), and there was no statistical difference in the remaining (segmentectomy vs. lobectomy, P = 0.735; wedge resection vs. segmentectomy, P = 0.746; **Figures 2C, D**). No positive findings could be concluded in further subgroup analyses with regard to the three surgical procedures (**e-Table 4**).

The OS of the patients treated with lobectomy was significantly superior to those treated with sublobar resection among those aged less than 70 years (HR = 1.81; 95% CI, 1.13–2.90), female (HR = 1.75; 95% CI, 1.21–2.53), and 1–20 mm in size (HR = 1.61; 95% CI, 1.11–2.33; **Table 2**, **Figure 3**). We also compared the three surgical approaches among those over 70 years in the subgroup analysis (**e-Table 5**), and even adjusting for propensity scores, we could not identify the favorable surgical approach that was superior in long-term survival (**e-Table 6**; all P-values >0.05).

To investigate the efficacy of adjuvant chemotherapy, we conducted PSM analysis in the exact study population and patients with sublobar resection in sequence, and the clinical characteristics were shown (**e-Tables 7, 8**). There was no survival benefit observed (**e-Figure 1**) and so as in subgroup analysis (**Table 2**). When stratified by tumor size, no statistical difference was observed (1–20 mm, P = 0.105; 21–30 mm, P = 0.168; **Figure 4**).

# DISCUSSION

Lobectomy with mediastinal systematic lymph node dissection was the standard treatment for early-stage NSCLC, while sublobar resection was likely to be recommended in the small-sized malignancy considering the postoperative cardiopulmonary reserve. However, it remained confused as how to take the tumor size and VPI into account when making clinical decisions because VPI was considered as a poor prognostic factor in the small-sized NSCLC (≤3 cm) (2). We could identify the patients with possible VPI *via* conventional CT images by pleural tags (5),

**TABLE 1** | Univariable analysis and multivariable analysis of the study population regarding overall survival and cancer-specific survival.

| Characteristics | Overall survival | | | Cancer-specific survival | | |
|---|---|---|---|---|---|---|
| | P-Value | HR (95% CI) | P-Value | P-Value | HR (95% CI) | P-Value |
| **Age** | <0.001 | | | 0.002 | | |
| ≤70 years | | Ref. | | | Ref. | |
| >70 years | | 1.75 (1.47–2.10) | <0.001 | | 1.33 (1.01–1.75) | 0.039 |
| **Gender** | 0.001 | | | 0.348 | | |
| Female | | Ref. | | | | |
| Male | | 1.29 (1.09–1.52) | 0.003 | | | |
| **Tumor size** | 0.110 | | | 0.043 | | |
| 1–20 mm | | Ref. | | | Ref. | |
| 21–30 mm | | 1.19 (1.00–1.41) | 0.048 | | 1.36 (1.04–1.78) | 0.023 |
| **Histology** | <0.001 | | | 0.001 | | |
| AC | | Ref. | | | Ref. | |
| SCC/Others | | 1.31 (1.10–1.56) | 0.002 | | 1.34 (1.02–1.76) | 0.034 |
| **Grade** | 0.004 | | | 0.005 | | |
| I/II | | Ref. | | | Ref. | |
| III/IV/UK | | 1.18 (0.99–1.40) | 0.070 | | 1.33 (1.01–1.74) | 0.040 |
| **LN examined** | <0.001 | | | 0.004 | | |
| No/UK | | Ref. | | | Ref. | |
| Yes | | 0.63 (0.49–0.81) | <0.001 | | 0.76 (0.50–1.14) | 0.182 |
| **Surgery** | <0.001 | | | <0.001 | | |
| Lobectomy | | Ref. | | | Ref. | |
| Segmentectomy | | 1.21 (0.85–1.73) | 0.292 | | 1.44 (0.85–2.45) | 0.178 |
| Wedge resection | | 1.31 (1.05–1.63) | 0.016 | | 1.41 (1.00–1.99) | 0.049 |
| **Chemotherapy** | 0.027 | | | 0.085 | | |
| No/UK | | Ref. | | | Ref. | |
| Yes | | 0.88 (0.64–1.22) | 0.452 | | 0.74 (0.43–1.26) | 0.262 |

*HR, hazard ratio; CI, confidence interval; Ref., reference; AC, adenocarcinoma; SCC, squamous cell carcinoma; UK, unknown; LN, lymph node.*

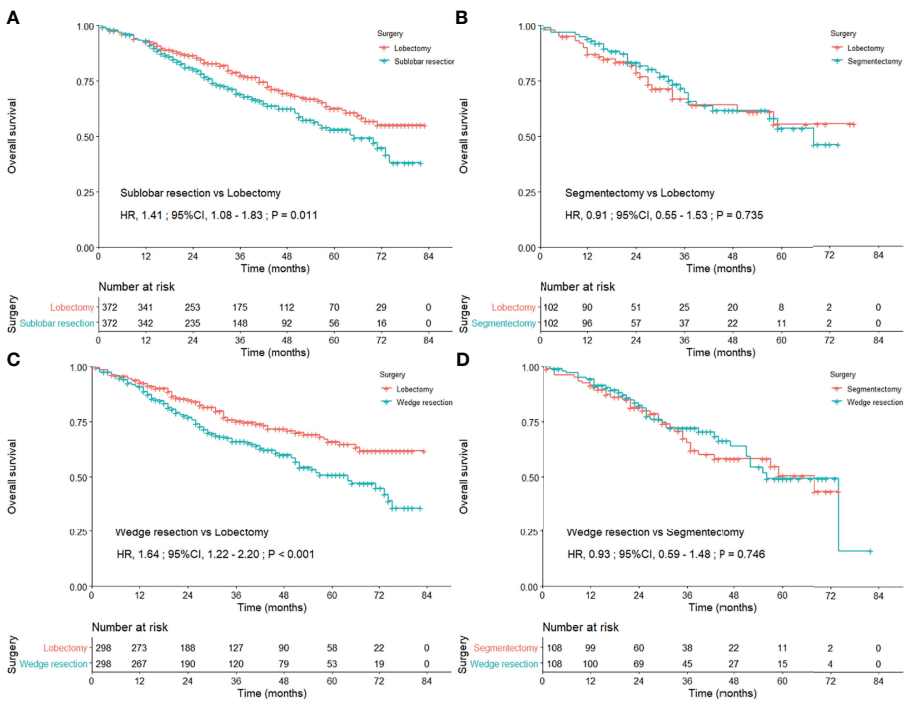


**FIGURE 2** | Kaplan–Meier curves comparing the overall survival after lobectomy and sublobar resection **(A)** lobectomy and segmentectomy **(B)** lobectomy and wedge resection **(C)** and segmentectomy and wedge resection **(D)** among the entire study population after propensity score matching.

**TABLE 2 |** Subgroup analysis of surgical approaches and adjuvant chemotherapy in overall survival *via* Cox regression analysis after propensity score matching.

| Characteristics | Sublobar resection vs. lobectomy | | Chemotherapy, Yes vs. No/UK | |
|---|---|---|---|---|
| | HR (95% CI) | P-Value | HR (95% CI) | P-Value |
| **Age** | | | | |
| ≤70 years | 1.81 (1.13–2.90) | 0.014 | 0.92 (0.52–1.64) | 0.784 |
| >70 years | 1.20 (0.87–1.65) | 0.259 | 1.17 (0.58–2.34) | 0.662 |
| **Gender** | | | | |
| Male | 1.10 (0.76–1.61) | 0.608 | 1.21 (0.57–2.57) | 0.615 |
| Female | 1.75 (1.21–2.53) | 0.003 | 0.91 (0.52–1.61) | 0.755 |
| **Tumor size** | | | | |
| 1–20 mm | 1.61 (1.11–2.33) | 0.012 | 1.78 (0.88–3.59) | 0.110 |
| 21–30 mm | 1.24 (0.85–1.80) | 0.269 | 0.65 (0.36–1.20) | 0.171 |
| **Histology** | | | | |
| AC | 1.54 (1.09–2.19) | 0.016 | 1.04 (0.60–1.80) | 0.885 |
| SCC/Other | 1.24 (0.83–1.84) | 0.292 | 0.91 (0.43–1.94) | 0.807 |
| **Grade** | | | | |
| I/II | 1.64 (1.14–2.35) | 0.007 | 1.14 (0.62–2.09) | 0.676 |
| III/IV/UK | 1.16 (0.79–1.71) | 0.457 | 0.87 (0.45–1.68) | 0.685 |
| **Surgery** | | | | |
| Lobectomy | | | 0.99 (0.59–1.69) | 0.982 |
| Sublobar resection | | | 1.09 (0.48–2.48) | 0.830 |

*vs., versus; HR, hazard ratio; CI, confidence interval; AC, adenocarcinoma; SCC, squamous cell carcinoma; UK, unknown.*

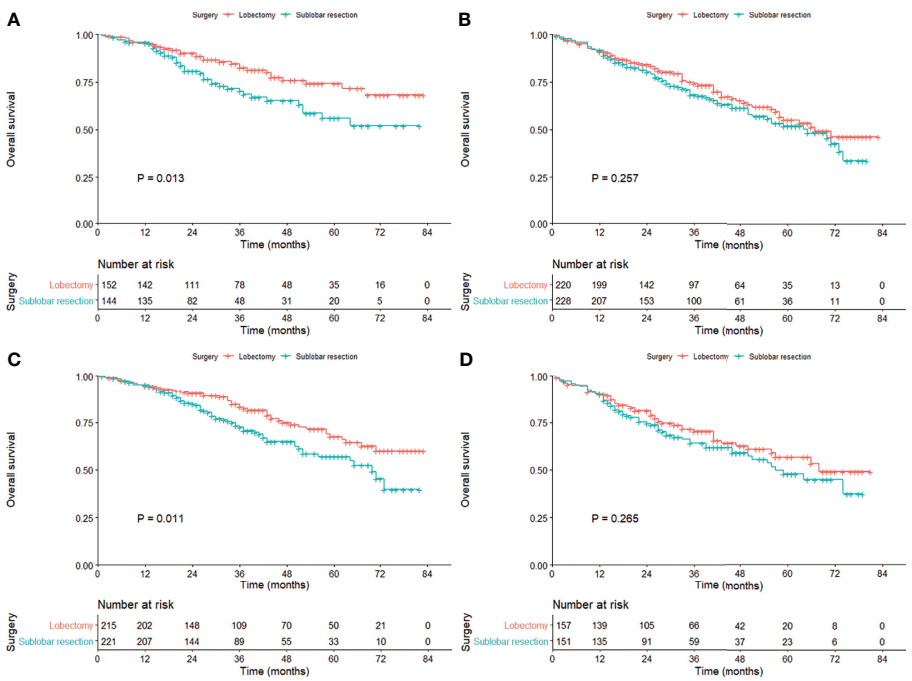


**FIGURE 3** | Kaplan–Meier curves comparing the overall survival between lobectomy and sublobar resection in the cohort subgrouped by age [**(A)** ≤70 years; **(B)**] >70 years) and tumor size [**(C)** 1–20 mm; **(D)**] 21–30 mm) after propensity score matching.

and thus, the result of preoperative VPI detection might be taken into consideration in preoperative conference on surgical procedures. Thus, we investigated the survival benefit from three surgical procedures and role of adjuvant chemotherapy for small-sized NSCLC with VPI. Lobectomy was likely to be superior to wedge resection and comparable to segmentectomy for stage IB NSCLC (≤3 cm) with VPI, and wedge resection was associated with impaired survival. Adjuvant chemotherapy might not improve the prognosis even in those who received sublobar resection.

Our results revealed that lobectomy might be associated with improved survival compared to sublobar resection, especially in tumors ≤20 mm, while lobectomy was comparable to segmentectomy, which was partly in line with

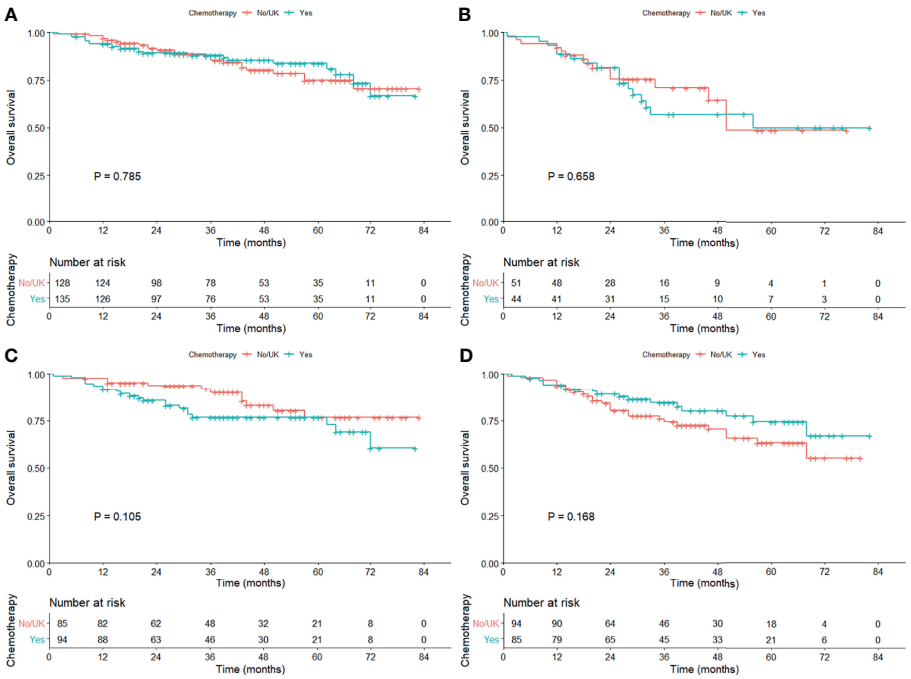


**FIGURE 4** | Kaplan–Meier curves comparing the overall survival among those with or without adjuvant chemotherapy in the cohort subgrouped by age [**(A)** ≤70 years; **(B)**] >70 years) and tumor size [**(C)** 1–20 mm; **(D)**] 21–30 mm) after propensity score matching.

the study by Schuchert et al. (14). Schuchert et al. (14) retrospectively reviewed 899 patients with stage I NSCLC with segmentectomy or lobectomy, in which the data were collected prospectively, and they found that lobectomy was superior to segmentectomy among stage IB patients with VPI (median OS, 29.6 vs. 22.7 months; P = 0.048). However, our findings were supposed to be interpreted with caution. Most of the sublobar resections were wedge resections that would skew the results of the cohort toward a poorer outcome. Besides, we could only identify the impaired survival from wedge resection when investigating these three surgical procedures in the subgroup analyses, with no other positive findings concluded. Moon et al. (15) found that survival was comparable between lobectomy and sublobar resection for stage I NSCLC ≤2 cm with VPI or LVI, and the dissected lymph node count might be responsible for the recurrence (HR = 0.914; 95% CI, 0.845–0.988). Hsu et al. (23) further indicated that more than 14 lymph node removement might be associated with survival improvement. We postulated that lobectomy was associated with more lymph node removement during surgery, and thus, survival benefit might result from the extensive intrapulmonary lymph node resection (24, 25). Secondly, lobectomy was favored in tumors no more than 20 mm but had not shown significant efficacy in tumors 20–30 mm. It might be referred to the inherent aggressiveness of the tumor ≤20 mm surpassing those with 20–30 mm in size that tumor could invade the visceral pleural layer when they were in a small size, and lobectomy might demonstrate improved survival for more aggressive malignancy compared with sublobar resection. The superior outcome of the lobectomy cohort in the smaller tumor group could also be explained by a greater proportion of wedge resections being performed for those tumors <2 cm, and more segmentectomies for those tumors >2 cm resulting in oncologic outcomes approximating lobectomy.

Furthermore, we could not conclude the favorable surgical approach in the elderly patients regarding long-term survival, which was in line with prior research (26), and might be attributed to a low malignant behavior of the tumor among the elderly compared with younger patients (27). Several studies claimed that the OS was not associated with the pathological stage in the elderly, and quite a few elderly patients might die of non-cancer-related causes, and thus, complete tumor resection was only a part in improving the prognosis (26, 28). Considering the preoperative comorbidities and postoperative complications of elderly patients, sublobar resection might be recommended among those over 70 years, which was in agreement with previous research (12, 29, 30).

In our research, adjuvant chemotherapy was not associated with improved survival even in those who received sublobar resection. A large population-based study was conducted between 2003 and 2006 *via* the National Cancer Database, which included 34,360 patients with T1-2N0M0 NSCLC, and no survival benefit was found among patients with ≤3 cm in size (31). In the study, they merely identified the efficacy of adjuvant chemotherapy grouped by tumor size, instead of subgrouping the small-sized tumors (≤3 cm) by the high-risk factors

(including VPI), and thus, the potential beneficiary might be neglected. A large retrospective cohort study, including 50,814 patients with node-negative early-stage NSCLC, also indicated that survival benefit was not noticed in those who received chemotherapy with ≤3 cm in size (HR = 1.10; 95% CI, 0.96–1.26), while chemotherapy was associated with improved survival in 3–4 cm (only in those who received sublobar resection), 4–5 cm (VPI, LVI, or high-grade histology), and >5 cm (regardless of VPI, LVI, or high-grade histology) (13). However, a pooled analysis of systematic review, including six studies, found that the survival was comparable between tumor size ≤3 cm with VPI and 3–5 cm without VPI, and they suggested that stage IB NSCLC with 3–5 cm in size and VPI might be the candidate of adjuvant chemotherapy (2). Therefore, as claimed in our research and in agreement with current guideline (32), the role of adjuvant chemotherapy was still undefined in small-sized NSCLC with VPI, and there were several explanations for the negative findings regarding the efficacy of adjuvant chemotherapy, including the offset of survival benefit and adverse effect from chemotherapy, and the limited quantity of stage IB patients receiving chemotherapy. Our study helped to investigate the role of adjuvant chemotherapy in small-sized NSCLC with VPI, and it reminded that the potential beneficiaries of chemotherapy might be further subgrouped by other baseline characteristics that were not studied above, including performance status and pulmonary function.

Now that the statistical difference was limited when we evaluated the survival difference with respect to surgical approaches and adjuvant chemotherapy, some other clinicopathological characteristics might interfere with the survival benefit. Okada et al. (33) reviewed 498 node-negative NSCLC (227 pure-solid and 271 part-solid) with VPI and ≤3 cm in size, and they concluded that VPI was associated with poor survival in pure-solid tumors (HR = 2.129; 95% CI, 1.048–4.132), but not in part-solid tumors (HR = 0.925; 95% CI, 0.050–4.920). Considering VPI had a negative effect on pure-solid tumors, the association between VPI and solid components was likely to be further investigated. Liang et al. (34) conducted a retrospective study, including 1,055 resected NSCLC with elastic layer staining and found that the disease-free survival (DFS) and OS were comparable in tumors with either PL1 or PL0 (DFS, P = 0.468; OS, P = 0.388). They proposed that the tumors with ≤3 cm in size and PL1 were supposed to be defined as stage T1, and adjuvant chemotherapy might not improve the prognosis (34), which was in line with the previous study (35). Nevertheless, Kawase et al. (36) suggested that a significant survival difference was observed between PL0 and PL1, and PL1 and PL2, while Wo et al. (9) concluded that there was no significant difference in survival between PL1 and PL2. Qian classified the stage I lung adenocarcinoma into three risk stratifications, and they claimed that most patients pertained to be the intermediate-risk population proved by a prognostic model, including six clinicopathological characteristics (age, sex, tumor size, pathological subtype, VPI, LVI) (37). It might explain why no significant survival benefit was observed in those with adjuvant chemotherapy, and in this way, the definite clinicopathological characteristics for risk stratifications might be further investigated. However, with current available evidence, adjuvant chemotherapy may not be suggested for small-sized NSCLC with VPI.

There were several limitations in our research. Firstly, several variables were not available in the SEER database, which might lead to some bias in our conclusions, including performance status, pulmonary function, imaging data, and whether surgery was video-assisted thoracoscopic surgery. Secondly, due to the inherent insufficiency of a retrospective study, we could hardly perform a randomized selection of patients, for which we dedicated to balance the baseline characteristics *via* PSM analysis, and thus, we also tried to avoid making any definite recommendations about treatment modality.

## CONCLUSION

Lobectomy was likely to be superior to wedge resection and comparable to segmentectomy for stage IB NSCLC (≤3 cm) with VPI, and wedge resection was associated with impaired survival. Adjuvant chemotherapy might not be associated with improved survival, even in those with sublobar resection. However, our findings might be interpreted with caution and require further validation in prospective controlled trials.

## DATA AVAILABILITY STATEMENT

Publicly available datasets were analyzed in this study. This data can be found via SEER Stat (www.seer.cancer.gov) with the identifier 11151-Nov2019.

## AUTHOR CONTRIBUTIONS

WH and H-YD contributed to the conception of the study and drafting of the article and took full responsibility for the content, including the data and analysis. WH, KX, M-YL, and Y-XZ contributed to the data extraction. WH, H-YD, M-YL, and CY contributed to the statistical analysis. WH, H-YD, and QZ contributed to the revision of the article. WH, H-YD, M-YL, KX, Y-XZ, CY, and QZ contributed to the approval of the final article.

## SUPPLEMENTARY MATERIAL

The Supplementary Material for this article can be found online at: https://www.frontiersin.org/articles/10.3389/fonc.2022.830470/full#supplementary-material

## REFERENCES


1. Maeda R, Yoshida J, Ishii G, Hishida T, Aokage K, Nishimura M, et al. Long-Term Survival and Risk Factors for Recurrence in Stage I Non-Small Cell Lung Cancer Patients With Tumors Up to 3 Cm in Maximum Dimension. *Chest* (2010) 138(2):357–62. doi: 10.1378/chest.09-3046
2. Jiang L, Liang W, Shen J, Chen X, Shi X, He J, et al. The Impact of Visceral Pleural Invasion in Node-Negative Non-Small Cell Lung Cancer: A Systematic Review and Meta-Analysis. *Chest* (2015) 148(4):903–11. doi: 10.1378/chest.14-2765
3. Huang H, Wang T, Hu B, Pan C. Visceral Pleural Invasion Remains a Size-Independent Prognostic Factor in Stage I Non-Small Cell Lung Cancer. *Ann Thorac surg* (2015) 99(4):1130–9. doi: 10.1016/j.athoracsur.2014.11.052
4. Rami-Porta R, Asamura H, Travis WD, Rusch VW. Lung Cancer - Major Changes in the American Joint Committee on Cancer Eighth Edition Cancer Staging Manual. *CA: Cancer J Clin* (2017) 67(2):138–55. doi: 10.3322/caac.21390
5. Hsu JS, Han IT, Tsai TH, Lin SF, Jaw TS, Liu GC, et al. Pleural Tags on CT Scans to Predict Visceral Pleural Invasion of Non-Small Cell Lung Cancer That Does Not Abut the Pleura. *Radiol* (2016) 279(2):590–6. doi: 10.1148/radiol.2015151120
6. Ou SH, Zell JA, Ziogas A, Anton-Culver H. Prognostic Significance of the non-Size-Based AJCC T2 Descriptors: Visceral Pleura Invasion, Hilar Atelectasis, or Obstructive Pneumonitis in Stage IB Non-Small Cell Lung Cancer is Dependent on Tumor Size. *Chest* (2008) 133(3):662–9. doi: 10.1378/chest.07-1306
7. Travis WD, Brambilla E, Rami-Porta R, Vallières E, Tsuboi M, Rusch V, et al. Visceral Pleural Invasion: Pathologic Criteria and Use of Elastic Stains: Proposal for the 7th Edition of the TNM Classification for Lung Cancer. *J Thorac Oncol Off Publ Int Assoc Study Lung Cancer* (2008) 3(12):1384–90. doi: 10.1097/JTO.0b013e31818e0d9f
8. Dail DH. Common Tumors. In: *Pulmonary Pathology*, *2nd ed*. New York, NY: Springer (1994). p. 1123–278. P. HS.
9. Wo Y, Zhao Y, Qiu T, Li S, Wang Y, Lu T, et al. Impact of Visceral Pleural Invasion on the Association of Extent of Lymphadenectomy and Survival in Stage I non-Small Cell Lung Cancer. *Cancer Med* (2019) 8(2):669–78. doi: 10.1002/cam4.1990
10. Adachi H, Tsuboi M, Nishii T, Yamamoto T, Nagashima T, Ando K, et al. Influence of Visceral Pleural Invasion on Survival in Completely Resected non-Small-Cell Lung Cancer. *Eur J Cardio-Thorac Surg Off J Eur Assoc Cardio-Thorac Surg* (2015) 48(5):691–697; discussion 697. doi: 10.1093/ejcts/ezu515
11. Arriagada R, Auperin A, Burdett S, Higgins JP, Johnson DH, Le Chevalier T, et al. Adjuvant Chemotherapy, With or Without Postoperative Radiotherapy, in Operable non-Small-Cell Lung Cancer: Two Meta-Analyses of Individual Patient Data. *Lancet* (2010) 375(9722):1267–77. doi: 10.1016/S0140-6736(10)60059-1
12. Howington JA, Blum MG, Chang AC, Balekian AA, Murthy SC. Treatment of Stage I and II Non-Small Cell Lung Cancer: Diagnosis and Management of Lung Cancer, 3rd Ed: American College of Chest Physicians Evidence-Based Clinical Practice Guidelines. *Chest* (2013) 143(5, Supplement):e278S–313S. doi: 10.1378/chest.12-2359
13. Pathak R, Goldberg SB, Canavan M, Herrin J, Hoag JR, Salazar MC, et al. Association of Survival With Adjuvant Chemotherapy Among Patients With Early-Stage Non-Small Cell Lung Cancer With vs Without High-Risk Clinicopathologic Features. *JAMA Oncol* (2020) 6(11):1–10. doi: 10.1001/jamaoncol.2020.4232
14. Schuchert MJ, Awais O, Abbas G, Horne ZD, Nason KS, Pennathur A, et al. Influence of Age and IB Status After Resection of Node-Negative non-Small Cell Lung Cancer. *Ann Thorac surg* (2012) 93(3):929–935; discussion 935-926. doi: 10.1016/j.athoracsur.2011.09.047
15. Moon Y, Lee KY, Park JK. Prognosis After Sublobar Resection of Small-Sized Non-Small Cell Lung Cancer With Visceral Pleural or Lymphovascular Invasion. *World J Surg* (2017) 41(11):2769–77. doi: 10.1007/s00268-017-4075-7
16. Burdett S, Pignon JP, Tierney J, Tribodet H, Stewart L, Le Pechoux C, et al. Adjuvant Chemotherapy for Resected Early-Stage Non-Small Cell Lung Cancer. *Cochrane Database Syst Rev* (2015) 3:Cd011430. doi: 10.1002/14651858.CD011430
17. Pignon JP, Tribodet H, Scagliotti GV, Douillard JY, Shepherd FA, Stephens RJ, et al. Lung Adjuvant Cisplatin Evaluation: A Pooled Analysis by the LACE Collaborative Group. *J Clin Oncol Off J Am Soc Clin Oncol* (2008) 26(21):3552–9. doi: 10.1200/JCO.2007.13.9030
18. Douillard JY, Rosell R, De Lena M, Carpagnano F, Ramlau R, Gonzáles-Larriba JL, et al. Adjuvant Vinorelbine Plus Cisplatin Versus Observation in Patients With Completely Resected Stage IB-IIIA Non-Small-Cell Lung Cancer (Adjuvant Navelbine International Trialist Association [ANITA]): A Randomised Controlled Trial. *Lancet Oncol* (2006) 7(9):719–27. doi: 10.1016/S1470-2045(06)70804-X
19. Winton T, Livingston R, Johnson D, Rigas J, Johnston M, Butts C, et al. Vinorelbine Plus Cisplatin vs. Observation in Resected Non-Small-Cell Lung Cancer. *N Engl J Med* (2005) 352(25):2589–97. doi: 10.1056/NEJMoa043623
20. Butts CA, Ding K, Seymour L, Twumasi-Ankrah P, Graham B, Gandara D, et al. Randomized Phase III Trial of Vinorelbine Plus Cisplatin Compared With Observation in Completely Resected Stage IB and II Non-Small-Cell Lung Cancer: Updated Survival Analysis of JBR-10. *J Clin Oncol Off J Am Soc Clin Oncol* (2010) 28(1):29–34. doi: 10.1200/JCO.2009.24.0333
21. Wang J, Wu N, Lv C, Yan S, Yang Y. Should Patients With Stage IB non-Small Cell Lung Cancer Receive Adjuvant Chemotherapy? A Comparison of Survival Between the 8th and 7th Editions of the AJCC TNM Staging System for Stage IB Patients. *J Cancer Res Clin Oncol* (2019) 145(2):463–9. doi: 10.1007/s00432-018-2801-7
22. Strauss GM, Herndon JE 2nd, Maddaus MA, Johnstone DW, Johnson EA, Harpole DH, et al. Adjuvant Paclitaxel Plus Carboplatin Compared With Observation in Stage IB Non-Small-Cell Lung Cancer: CALGB 9633 With the Cancer and Leukemia Group B, Radiation Therapy Oncology Group, and North Central Cancer Treatment Group Study Groups. *J Clin Oncol Off J Am Soc Clin Oncol* (2008) 26(31):5043–51. doi: 10.1200/JCO.2008.16.4855
23. Hsu CP, Hsia JY, Chang GC, Chuang CY, Shai SE, Yang SS, et al. Surgical-Pathologic Factors Affect Long-Term Outcomes in Stage IB (Pt2 N0 M0) Non-Small Cell Lung Cancer: A Heterogeneous Disease. *J Thorac Cardiovasc surg* (2009) 138(2):426–33. doi: 10.1016/j.jtcvs.2008.12.035
24. Dai J, Liu M, Yang Y, Li Q, Song N, Rocco G, et al. Optimal Lymph Node Examination and Adjuvant Chemotherapy for Stage I Lung Cancer. *J Thorac Oncol Off Publ Int Assoc Study Lung Cancer* (2019) 14(7):1277–85. doi: 10.1016/j.jtho.2019.03.027
25. Zhang Z, Feng H, Zhao H, sHu J, Liu L, Liu Y, et al. Sublobar Resection is Associated With Better Perioperative Outcomes in Elderly Patients With Clinical Stage I Non-Small Cell Lung Cancer: A Multicenter Retrospective Cohort Study. *J Thorac dis* (2019) 11(5):1838–48. doi: 10.21037/jtd.2019.05.20
26. Okami J, Higashiyama M, Asamura H, Goya T, Koshiishi Y, Sohara Y, et al. Pulmonary Resection in Patients Aged 80 Years or Over With Clinical Stage I Non-Small Cell Lung Cancer: Prognostic Factors for Overall Survival and Risk Factors for Postoperative Complications. *J Thorac Oncol Off Publ Int Assoc Study Lung Cancer* (2009) 4(10):1247–53. doi: 10.1097/JTO.0b013e3181ae285d
27. Deng HY, Zhou J, Wang RL, Jiang R, Qiu XM, Zhu DX, et al. Age-Different Extent of Resection for Clinical IA non-Small Cell Lung Cancer: Analysis of Nodal Metastasis. *Sci Rep* (2020) 10(1):9587. doi: 10.1038/s41598-020-66509-5
28. Hino H, Murakawa T, Ichinose J, Nagayama K, Nitadori J, Anraku M, et al. Results of Lung Cancer Surgery for Octogenarians. *Ann Thorac Cardiovasc Surg Off J Assoc Thorac Cardiovasc Surgeons Asia* (2015) 21(3):209–16. doi: 10.5761/atcs.oa.14-00160
29. Tsutani Y, Tsubokawa N, Ito M, Misumi K, Hanaki H, Miyata Y, et al. Postoperative Complications and Prognosis After Lobar Resection Versus Sublobar Resection in Elderly Patients With Clinical Stage I Non-Small-Cell Lung Cancer. *Eur J cardio-thorac Surg Off J Eur Assoc Cardio-thorac Surg* (2018) 53(2):366–71. doi: 10.1093/ejcts/ezx296
30. Dong S, Roberts SA, Chen S, Zhong X, Yang S, Qu X, et al. Survival After Lobectomy Versus Sub-Lobar Resection in Elderly With Stage I NSCLC: A Meta-Analysis. *BMC surg* (2019) 19(1):38. doi: 10.1186/s12893-019-0500-1
31. Speicher PJ, Gu L, Wang X, Hartwig MG, D'Amico TA, Berry MF. Adjuvant Chemotherapy After Lobectomy for T1-2n0 Non-Small Cell Lung Cancer: Are the Guidelines Supported? *J Natl Compr Cancer Network JNCCN* (2015) 13(6):755–61. doi: 10.6004/jnccn.2015.0090
32. National Comprehensive Cancer Network. *Non-Small Cell Lung Cancer (Version 4.2020)* . Available at: https://www.nccn.org/professionals/physician_gls/pdf/nscl.pdf (Accessed March 30, 2021).

33. Okada S, Hattori A, Matsunaga T, Takamochi K, Oh S, Inoue M, et al. Prognostic Value of Visceral Pleural Invasion in Pure-Solid and Part-Solid Lung Cancer Patients. *Gen Thorac Cardiovasc surg* (2021) 69(2):303–10. doi: 10.1007/s11748-020-01470-8
34. Liang RB, Li P, Li BT, Jin JT, Rusch VW, Jones DR, et al. Modification of Pathological T Classification for Non-Small Cell Lung Cancer With Visceral Pleural Invasion: Data From 1,055 Cases of Cancers ≤3 cm or Less. *Chest* (2021) 160(2):754–64. doi: 10.1016/j.chest.2021.03.022
35. Hung JJ, Jeng WJ, Hsu WH, Chou TY, Lin SF, Wu YC. Prognostic Significance of the Extent of Visceral Pleural Invasion in Completely Resected Node-Negative non-Small Cell Lung Cancer. *Chest* (2012) 142(1):141–50. doi: 10.1378/chest.11-2552
36. Kawase A, Yoshida J, Miyaoka E, Asamura H, Fujii Y, Nakanishi Y, et al. Visceral Pleural Invasion Classification in non-Small-Cell Lung Cancer in the 7th Edition of the Tumor, Node, Metastasis Classification for Lung Cancer: Validation Analysis Based on a Large-Scale Nationwide Database. *J Thorac Oncol Off Publ Int Assoc Study Lung Cancer* (2013) 8(5):606–11. doi: 10.1097/JTO.0b013e31828632b8
37. Qian J, Xu J, Wang S, Qian F, Yang W, Zhang B, et al. Adjuvant Chemotherapy Candidates in Stage I Lung Adenocarcinomas Following Complete Lobectomy. *Ann Surg Oncol* (2019) 26(8):2392–400. doi: 10.1245/s10434-019-07366-z

**Conflict of Interest:** The authors declare that the research was conducted in the absence of any commercial or financial relationships that could be construed as a potential conflict of interest.

**Publisher's Note:** All claims expressed in this article are solely those of the authors and do not necessarily represent those of their affiliated organizations, or those of the publisher, the editors and the reviewers. Any product that may be evaluated in this article, or claim that may be made by its manufacturer, is not guaranteed or endorsed by the publisher.

frontiers in Oncology

ORIGINAL RESEARCH
published: 23 February 2022
doi: 10.3389/fonc.2021.771988

# Establishing a Macrophage Phenotypic Switch-Associated Signature-Based Risk Model for Predicting the Prognoses of Lung Adenocarcinoma

*Jun Chen*[1], *Chao Zhou*[2] *and Ying Liu*[3]*

[1] Department of Oncology, The First Affiliated Hospital of Nanchang University, Nanchang, China, [2] Department of Neurology, Jiangxi Provincial People's Hospital Affiliated to Nanchang University, Nanchang, China, [3] Department of Emergency, The First Affiliated Hospital of Nanchang University, Nanchang, China

OPEN ACCESS

**Edited by:**
Jessy Deshane,
University of Alabama at Birmingham,
United States

**Reviewed by:**
Karolina Henryka Czarnecka-Chrebelska,
Medical University of Lodz, Poland
Zhiqian Zhang,
Southern University of Science and Technology, China

***Correspondence:**
Ying Liu
liuyingemergency@outlook.com

**Specialty section:**
This article was submitted to Thoracic Oncology, a section of the journal Frontiers in Oncology

**Received:** 02 October 2021
**Accepted:** 30 December 2021
**Published:** 23 February 2022

**Citation:**
Chen J, Zhou C and Liu Y (2022) Establishing a Macrophage Phenotypic Switch-Associated Signature-Based Risk Model for Predicting the Prognoses of Lung Adenocarcinoma. Front. Oncol. 11:771988. doi: 10.3389/fonc.2021.771988

**Background:** Tumor-associated macrophages are important components of the tumor microenvironment, and the macrophage phenotypic switch has been shown to correlate with tumor development. However, the use of a macrophage phenotypic switch-related gene (MRG)-based prognosis signature for lung adenocarcinoma (LADC) has not yet been investigated.

**Methods:** In total, 1,114 LADC cases from two different databases were collected. The samples from TCGA were used as the training set (N = 490), whereas two independent datasets (GSE31210 and GSE72094) from the GEO database were used as the validation sets (N = 624). A robust MRG signature that predicted clinical outcomes of LADC patients was identified through multivariate COX and Lasso regression analysis. Gene set enrichment analysis was applied to analyze molecular pathways associated with the MRG signature. Moreover, the fractions of 22 immune cells were estimated using CIBERSORT algorithm.

**Results:** An eight MRG-based signature comprising CTSL, ECT2, HCFC2, HNRNPK, LRIG1, OSBPL5, P4HA1, and TUBA4A was used to estimate the LADC patients' overall survival. The MRG model was capable of distinguishing high-risk patients from low-risk patients and accurately predict survival in both the training and validation cohorts. Subsequently, the eight MRG-based signature and other features were used to construct a nomogram to better predict the survival of LADC patients. Calibration plots and decision curve analysis exhibited good consistency between the nomogram predictions and actual observation. ROC curves displayed that the signature had good robustness to predict LADC patients' prognostic outcome.

**Conclusions:** We identified a phenotypic switch-related signature for predicting the survival of patients with LADC.

**Keywords: lung adenocarcinoma, tumor-associated macrophages, macrophage phenotypic switch, macrophage phenotypic switch-related gene, MRG signature**

## INTRODUCTION

Lung cancer is the most prevalent cancers with the highest mortality worldwide (1). Non-small cell lung cancer (NSCLC) accounts for nearly 90% of lung cancer cases and is divided into three main types, lung adenocarcinoma (LADC), lung squamous cell carcinoma, and large cell carcinoma (2). As the most prevailing histological type of NSCLC, LADC comprises up to 40–50% of all lung cancer cases (3, 4). Despite the tremendous effort aimed at discovering predictors of recurrence risk that allow prompt therapeutic intervention, most patients are diagnosed with advanced-stage diseases and different types of distant organ metastases (5); thus, the overall 5-year survival rate of LADC remains at approximately 15% (6). This might be primarily due to the high heterogeneity of LADC and the advanced disease stage at which the patients are diagnosed (7).

Advancements in high-throughput sequencing technologies present novel therapeutic strategies for lung cancer (8). Thus, mining genes with LADC prognostic value is necessary to better help improve risk-stratification of patients based on the clinical outcome and develop novel therapeutic targets.

The tumor microenvironment (TME) represents the extracellular environment in which tumor cells reside and it comprises tumor cells, immune cells, extracellular matrix, and growth factors (9). TME plays a crucial role in the progression and migration of LADC (10). Macrophages within the TME, termed tumor-associated macrophages (TAMs), are an important component of the TME (11). TAMs can be polarized to M1/M2 phenotypes based on their functional status as induced by the microenvironment (12). M1 macrophages, highly expressed major histocompatibility complex class II, CD68 labeling and CD80/CD86 costimulatory molecules, located within tumors are thought to induce tumor suppression by activating anti-tumor immunity (13). However, most TAMs in the TME manifest an M2-like phenotype (characterized by up-regulated expression of CD200R membrane glycoprotein, Arg-1, YM1, Fizz1 and other receptors) that facilitates immunological tolerance and promotes tumor progression (14). Tumor cells recruit macrophages by releasing various chemokines, cytokines, and growth factors, and they develop them into pro-tumorigenic M2 macrophages. Therefore, the macrophage phenotypic switch is correlated with tumor development, whereas macrophage phenotypic switch-related genes (MRGs) might provide insightful information to estimate LADC patients' prognosis.

Herein, we analyzed the MRG expression alterations obtained from The Cancer Genome Atlas (TCGA) and Gene Expression Omnibus (GEO) databases regarding LADC patients and identified dysregulated MRGs with prognostic value. Furthermore, we developed a novel and robust gene prognostic signature based on the identified dysregulated MRGs. Finally, a prognostic nomogram integrating the signature and multiple clinical parameters meant to estimate the overall survival (OS) of LADC patients was developed. These results might be meaningful for the development of comprehensive therapeutic approaches for LADC patients.

## METHODS

### Data Collection

The transcriptome profiles and corresponding clinical data of LADC patients were downloaded from TCGA (https://portal.gdc.cancer.gov/) and GEO (https://www.ncbi.nlm.nih.gov/geo/) databases. TCGA-LADC comprised a total of 594 (535 tumor sample and 59 normal samples) adenocarcinoma cases. The main characteristics of the analysis included the following: age, sex, and pathologic stage; details of patient clinical information are described in **Table 1**. GSE31210 comprised a total of 226 primary LADC of pathological stage I-II. The median age was 67 years and the range was 30-76 years, and there were 105 male and 121 female patients. GSE72094 comprised a total of 442 LADC cases. The median age was 70 years and the range was 38-89 years, and there were 202 male and 240 female patients. The samples from TCGA database were defined as the training set, the samples from the GSE31210 database were defined as the validation set, whereas LADC cases from GSE72094 were set as testing set. LADC patients with missing survival values or follow-up time < 1 days were excluded. A total of 1,114 samples (490 from TCGA, 226 from GSE31210, and 398 from GSE72094) were used in our study.

The protein expression data of the MRGs of LADC patients were evaluated using the Human Protein Atlas (https://www.proteinatlas.org/), which is derived from antibody-based protein profiling using immunohistochemistry.

### Acquisition of MRGs

MRGs were obtained from two MRG datasets (188 from GSE5099_CLASSICAL_M1_VS_ALTERNATIVE_M2_MACROPHAGE_UP and 194 from GSE5099_CLASSICAL_M1_VS_ALTERNATIVE_M2_MACROPHAGE_DN) (15) from the gene set enrichment analysis (GSEA) website (http://www.gsea-msigdb.org/gsea/msigdb/). Finally, a total of 382 MRGs were utilized in this study (**Supplementary Table 1**).

### Development and Validation of a Prognostic Model

The univariate Cox regression analysis was used to screen out the genes significantly correlated with OS based on the 382 MRGs (for P-values < 0.05). Next, the overlapped prognosis-related MRGs from TCGA and GEO databases were selected for the least absolute shrinkage and selection operator (Lasso) with ten-fold

**TABLE 1** | Prognostic roles of the MRGs signature with different demographic and clinical characteristics in TCGA training set. .

| Characteristics | No. | | % | HR (95% CI) | *P*-value |
|---|---|---|---|---|---|
| | high-risk | low-risk | | | |
| **Age (years)** | | | | | |
| < 65 | 114 | 105 | 44.69% | 0.549 (0.334-0.901) | 0.018 |
| ≥ 65 | 131 | 140 | 55.31% | 0.359 (0.233-0.552) | 0.000 |
| **Sex** | | | | | |
| Male | 127 | 97 | 45.71% | 0252 (0.148-0.429) | 0.000 |
| Female | 118 | 148 | 54.29% | 0.699 (0.455-1.076) | 0.104 |
| **Stage** | | | | | |
| I | 106 | 155 | 53.27% | 0.517 (0.302-0.886) | 0.016 |
| II | 69 | 48 | 23.88% | 0.592 (0.321-1.091) | 0.093 |
| III | 54 | 25 | 16.12% | 0.510 (0.244-1.067) | 0.074 |
| IV | 15 | 10 | 5.10% | 0.323 (0.089-1.163) | 0.084 |
| NA | 1 | 7 | 1.63% | – | – |
| **T stage** | | | | | |
| T1 | 62 | 104 | 33.88% | 0.780 (0.414-1.472) | 0.444 |
| T2 | 144 | 114 | 52.65% | 0.389 (0.247-0.613) | 0.000 |
| T3 | 29 | 16 | 9.18% | 0.077 (0.010-0.590) | 0.014 |
| T4 | 9 | 9 | 3.67% | 0.574 (0.141-2.343) | 0.440 |
| NA | 1 | 2 | 0.61% | – | – |
| **M stage** | | | | | |
| M0 | 171 | 151 | 65.71% | 0.494 (0.331-0.738) | 0.001 |
| M1 | 15 | 9 | 4.90% | 0.233 (0.051-1.056) | 0.059 |
| NA | 59 | 85 | 29.39% | – | – |
| **N stage** | | | | | |
| N0 | 133 | 184 | 64.69% | 0.475 (0.299-0.756) | 0.002 |
| N1 | 59 | 33 | 18.78% | 0.609 (0.328-1.132) | 0.117 |
| N2 | 48 | 20 | 13.88% | 0.542 (0.246-1.193) | 0.128 |
| N3 | 1 | 1 | 0.041% | – | – |
| NA | 4 | 7 | 2.24% | – | – |

*NA, Not available.*

cross-validation which was subsequently applied using "glmnet" and "survival" packages. Afterwards, a multivariate Cox regression was applied out to select candidate OS-related MRGs and determine a prognostic signature. The risk score was calculated as follows: Risk score = $\beta1 \times$ (expression of RNA1) + $\beta2 \times$ (expression of RNA2) + ⋯ + $\beta n \times$ (expression of RNAn). Median MRG risk scores were used to differentiate high-risk subgroups from LADC patients. The regression coefficient (β) was obtained from the multivariate Cox regression analysis. Additionally, Kaplan-Meier survival analysis was conducted to assess the predictive performance of the prognostic signature. The signature was also externally validated with the GEO dataset using the same formula. All analyses were carried out using R language, version 4.0.5 (www.r-project.org).

## GSEA

Gene set enrichment analysis (GSEA) was conducted to investigate various molecular pathways differentially activated between high- and low-risk subgroups. False discovery rate q-values < 0.05 and |NES| > 1 were defined as statistically significant difference.

## Estimating the Proportion of Immune Cells

We utilized CIBERSORT algorithm to estimate the proportion of 22 immune cells between low- and high-risk patients. The sum of ratio of 22 immune cell types in each sample is 1.

## Construction and Evaluation of a Nomogram

To provide a more individualized predictive model, a nomogram combining the MRG signature and other clinical variables was constructed using the training cohort. The discrimination ability of the nomogram was assessed using the calibration curves and receiver operating characteristic (ROC) curves in the training and validation subgroups. Next, decision curve analysis (DCA) was applied to evaluate the clinical usefulness of the nomogram in the training and testing sets.

## Statistical Analysis

Continuous variables were presented as means ± SD, whereas categorical variables were displayed as percentages. The statistical significance of the differences in survival rate was measured using the log-rank test with a threshold of P-value < 0.05. Kaplan-Meier plots were applied to display the differences in survival duration. All statistical analyses were conducted using the software R (version 3.5.2) with corresponding packages.

# RESULTS

## Establishment of an MRG-Based Prognosis Signature

To limit the candidate prognosis-related MRGs, the OS-related MRGs that were overlapping in the data from TCGA and GEO

databases (23 MRGs) were identified (**Figure 1A**). Next, the 23 MRGs were used to the Lasso-Cox proportional hazards regression and ten-fold cross-validation to construct the best gene signature, and 14 candidate MRGs were ultimately identified (**Figures 1B, C**). Further, a multivariate Cox regression was used, and results exhibited that CTSL, ECT2, HCFC2, HNRNPK, LRIG1, OSBPL5, P4HA1, and TUBA4A were the independent prognostic MRGs (**Figure 1D**). We created a risk score according to the expression of the eight MRGs as follows: Risk score = CTSL × 0.001326639 + ECT2 × 0.023009173 - HCFC2 × 0.257179317 + HNRNPK × 0.010298027 - LRIG1 × 0.024832171 + OSBPL5 × 0.071303241 + P4HA1 × 0.007389189 + TUBA4A × 0.008003706.

## MRG Expression

We investigated the protein levels of these genes, detected using immunohistochemistry and obtained from the HPA database. The immumohistochemical staining of MRGs were based on the normal alveolar and tumor tissues. We discovered that the protein levels of HNRNPK, P4HA1, and TUBA4A were significantly upregulated, while CTSL, HNRNPK, and OSBPL5 were significantly downregulated in the tumor tissues compared to those of normal tissues (**Figure 2A**). The quantitative analysis results for each immunohistochemistry were show in **Supplementary Material**. We also investigated the expression level of the identified MRGs for normal and tumor samples using RNA-Seq data from the training set. The results showed roughly the same trend as the one observed for the protein expression (**Figure 2B**).

## Prognostic Value of the 10-MRG Signature

To identify the MRG signature suitable for LADC survival prediction, the LADC patients were separated into low-risk (N = 245) and high-risk groups (N = 245) based on the median risk score. Kaplan-Meier curve analysis depicted that high-risk patients were associated with poorer OS compared to the low-risk patients ($P < 0.001$, **Figure 3A**). Furthermore, the ROC curve analysis demonstrated that the area under the ROC curve (AUC) of the prognostic MRG model at 1, 3, and 5 years were 0.707, 0.707, and 0.65 in the training set, respectively (**Figure 3B**). The distribution survival status and time for each patient from the training set were plotted with a division line indicating the risk score cutoffs (**Figures 3C, D**). Next, we conducted the univariate and multivariate Cox regression analyses to analyze the signature and clinicopathological independent indices predicting survival. The results showed that the MRG-based signature was able to be an independent prognostic indicator (**Figures 3E, F**). Its prediction capacity was also evaluated through calculating C-index in the training set. The results showed that the C-index for the prediction of OS of the identified MRG signature was 0.72 (95% CI = 0.65–0.76).

We verified the prediction performance of this signature using LADC cases from the GSE31210 dataset. The risk score of each

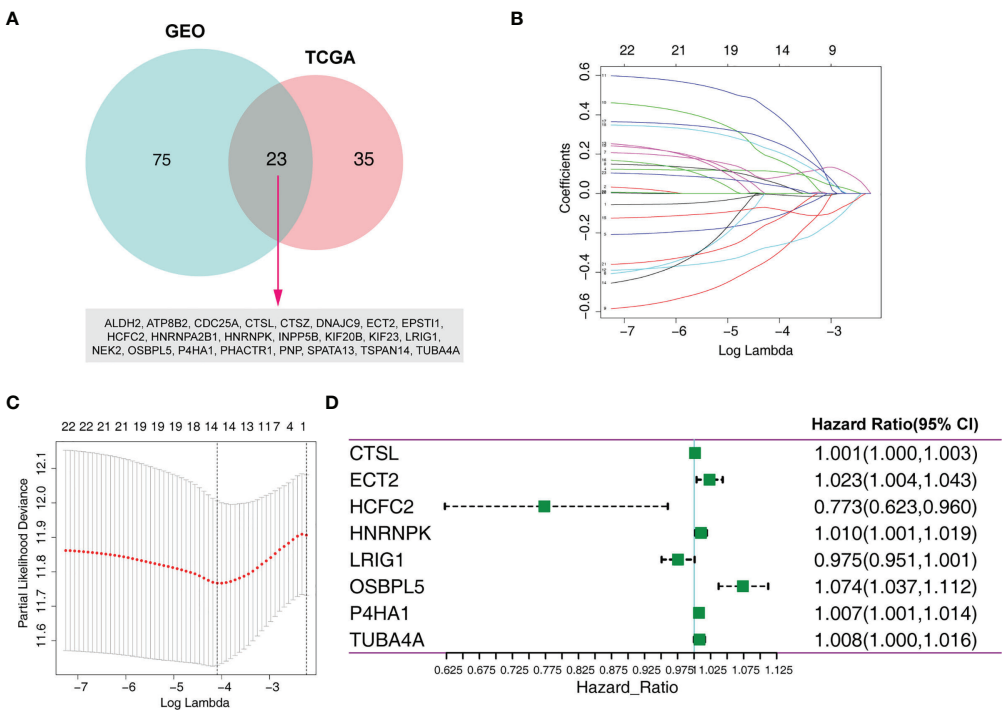


**FIGURE 1** | Identification of an MRG-based prognosis signature. **(A)** Twenty-three overlapping overall survival-related MRGs from TCGA and GEO databases were obtained following univariate Cox regression analysis. **(B)** Lasso coefficient profiles of the 23 prognosis-associated MRGs from the training set. **(C)** Partial likelihood deviance of variables revealed by the Lasso regression model. **(D)** Forest plot of multivariate Cox regression analysis.

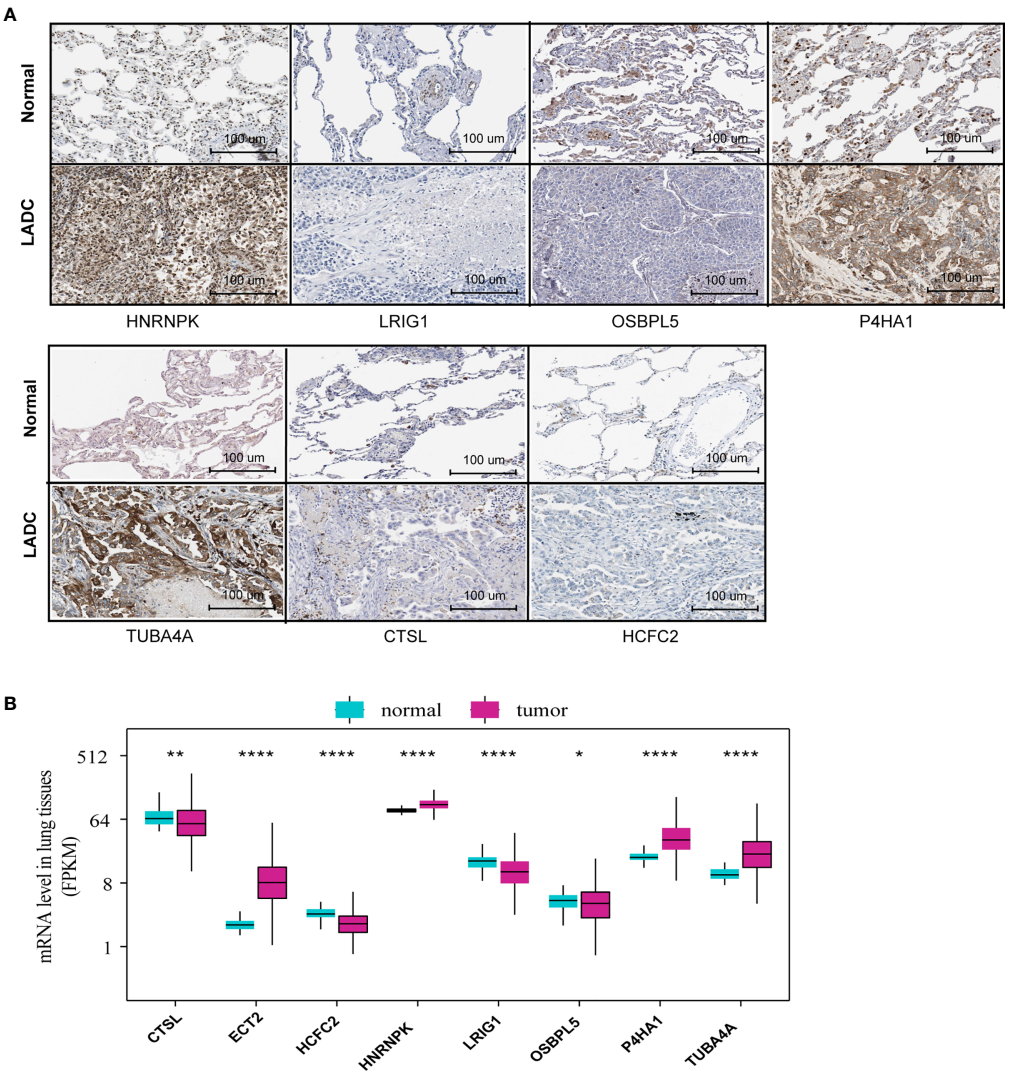


**FIGURE 2** | MRG protein and mRNA level between normal and tumor tissues. **(A)** The MRG protein levels detected *via* immunohistochemistry provided by the HPA database (ETC2 was unavailable in HPA). **(B)** MRG mRNA levels of normal and tumor tissues based on RNA-Seq data from the training set *P<0.05, **P<0.01, ***P<0.001, ****P<0.0001.

patient was calculated based on the indicated formula and separated into low-risk (N = 113) and high-risk groups (N=113) according to the median risk score. Kaplan-Meier analysis demonstrated that high-risk patients were associated with poorer OS and relapse-free survival (RFS) compared to the low-risk patients (**Figures 4A, B**). ROC curve analysis revealed that the AUC of the prognostic MRG model for predicting OS at 1, 3, and 5 years were 0.704, 0.625, and 0.677, respectively (**Figure 4C**). Furthermore, the ROC curve analysis revealed that the AUC of the prognostic MRG model for predicting RFS at 1, 3, and 5 years was 0.661, 0.619, and 0.647, respectively (**Figure 4D**). The survival status and time distribution for each patient from the validation set were plotted with a division line representing risk score cutoffs (**Figures 4E–G**). The expression profiles of the eight prognostic MRGs are illustrated in **Figure 4H**.

In addition, we further tested the prediction performance of this signature using LADC cases from the GSE72094 dataset. the LADC patients were separated into low-risk (N = 199) and high-risk groups (N = 199) based on the median risk score. Kaplan-Meier curve analysis depicted that high-risk patients were associated with poorer OS compared to the low-risk patients (P < 0.001, **Figure 5A**). Furthermore, the ROC curve analysis demonstrated that the area under the ROC curve (AUC) of the prognostic MRG model at 1, 3, and 5 years were 0.621, 0.659, and 0.707 in the test set, respectively (**Figure 5B**). The distribution survival status and time for each patient from the testing set were plotted with a division line indicating the risk score cutoffs (**Figures 5C, D**).

The prognostic significance of the signature was further assessed using subgroups with different demographics and

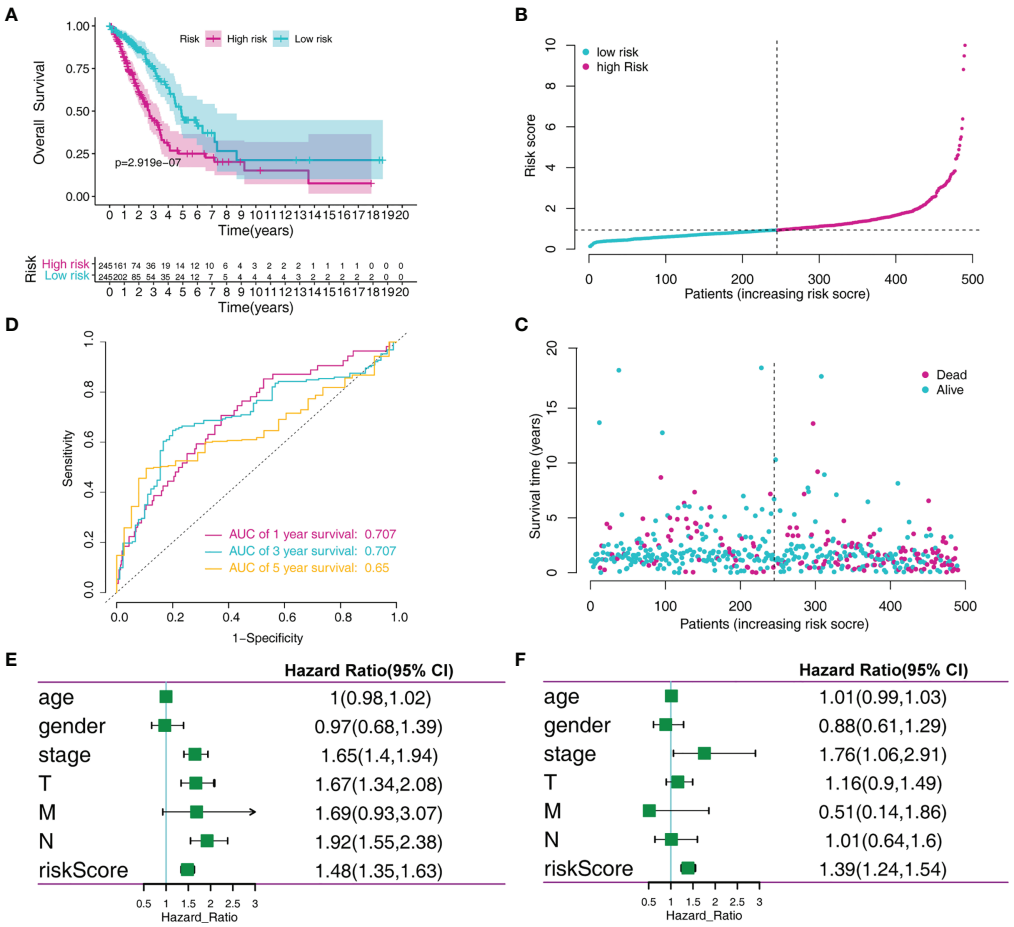


**FIGURE 3** | MRGs-based risk signature evaluation using the training set. **(A)** Kaplan-Meier survival analysis revealed the difference in survival rate between high- and low-risk patients. **(B)** Time-dependent ROC curve analysis for 1-, 3-, and 5-year predictions of overall survival using the MRG-based signature. **(C)** Risk score distribution of patients with the overall survival and signature. **(D)** Overall survival scatter plots for LADC patients. **(E)** Univariate Cox analyses of the MRG signature and clinical variables. **(F)** Multivariate Cox analyses of the MRG signature and clinical variables.

clinical characteristics from the training set, including age, sex, TNM stage, and pathological stage (**Supplementary Figure 2**). We discovered that the MRG signature was useful for most subgroups (**Table 1**). For the validation set, the model can also accurately predict the OS and RFS of low- and high-risk groups in these subgroups (**Supplementary Table 2**).

## Correlation Between the MRGs and Clinicopathological Parameters

We further investigated the association between the MRGs and clinicopathological characteristics such as age, gender, pathological stage, and TNM stage for patients in the training cohort. We observed the differential expression of CTSL, ECT2, HCFC2, HNRNPK, LRIG1, and TUBA4A (**Figures 6A–F**).

## GSEA

Additionally, we explored the differentially signaling pathways between high- and low-risk LADC patient through GSEA. In the high-risk group, the top five enriched GO terms included cadherin binding, cellular response to heat, chromosomal region, chromosome segregation, and mitotic nuclear division (**Figure 7A**). The top five enriched KEGG pathways were basal transcription factors, cell cycle, oocyte meiosis, p53 signaling pathway, and ubiquitin mediated proteolysis (**Figure 7B**).

## Immune Characteristics of Patients in the High- and Low-Risk Groups

We further investigate the tumor-infiltrating immune cells from the high- and low-risk patients using CIBERSORT. The results displayed that the tumors of high-risk patients exhibited a higher proportion of plasma cells, resting CD4 T memory cells, monocytes, resting dendritic cells, resting mast cells, and eosinophils; while activated CD4 T memory cells, M0 macrophages, M1 macrophages, and activated mast cells were higher in low-risk group (**Figures 8A, B**).

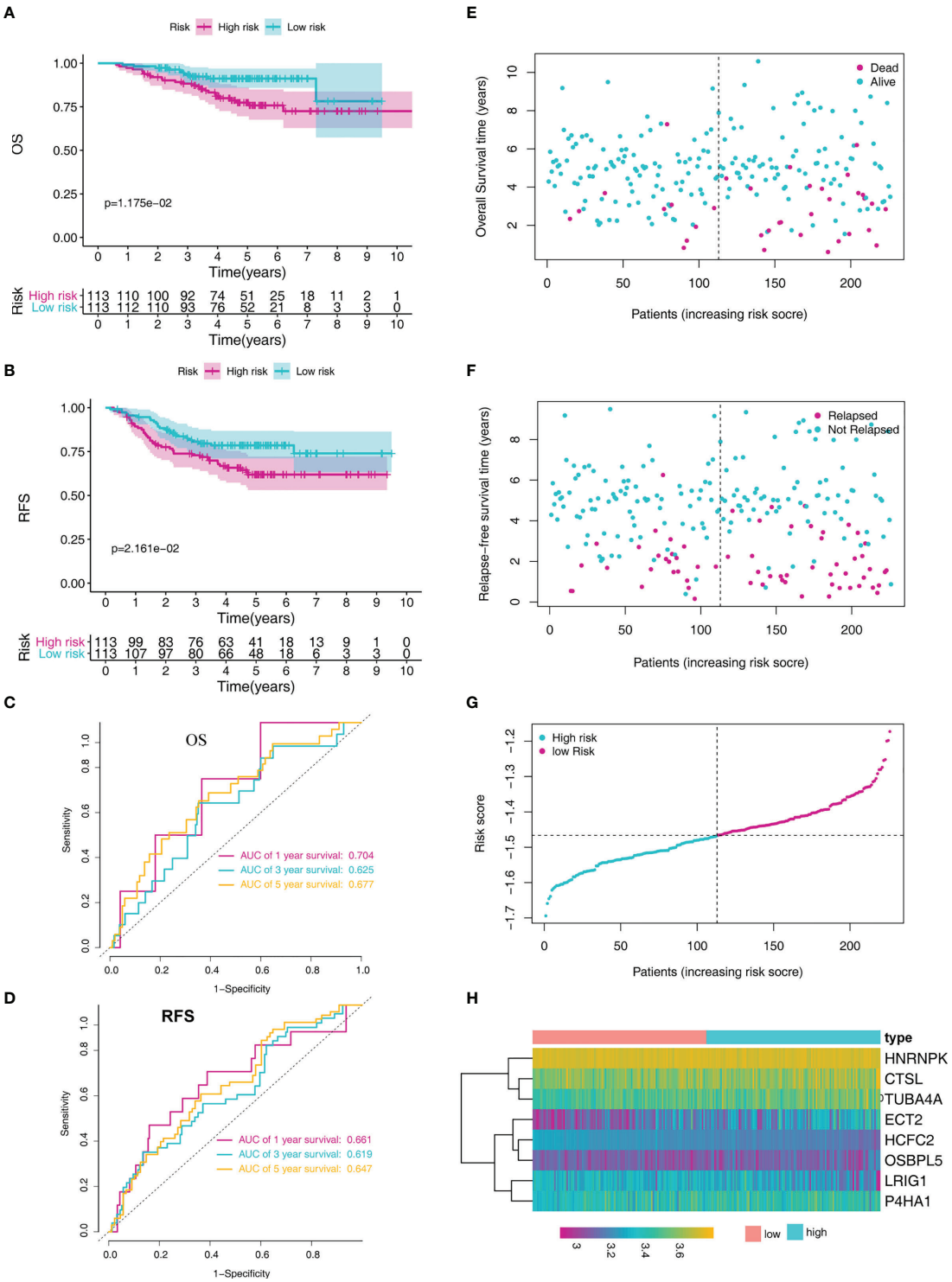


**FIGURE 4** | MRG-based risk signature evaluation using the validation set (GSE31210). **(A)** Kaplan-Meier analysis of the overall survival in LADC patients based on risk stratification. **(B)** Kaplan-Meier analysis for relapse-free survival of LADC patients based on risk stratification. **(C)** Time-dependent ROC curve analysis for 1-, 3-, and 5-year overall survival predictions obtained using the MRG-based signature. **(D)** Time-dependent ROC curve analysis for 1-, 3-, and 5-year relapse-free predictions obtained using the MRG-based signature. **(E)** Overall survival scatter plots for LADC patients. **(F)** Relapse-free survival scatter plots for LADC patients. **(G)** Risk score distribution of the LADC patients. **(H)** The heatmap of the eight MRGs.

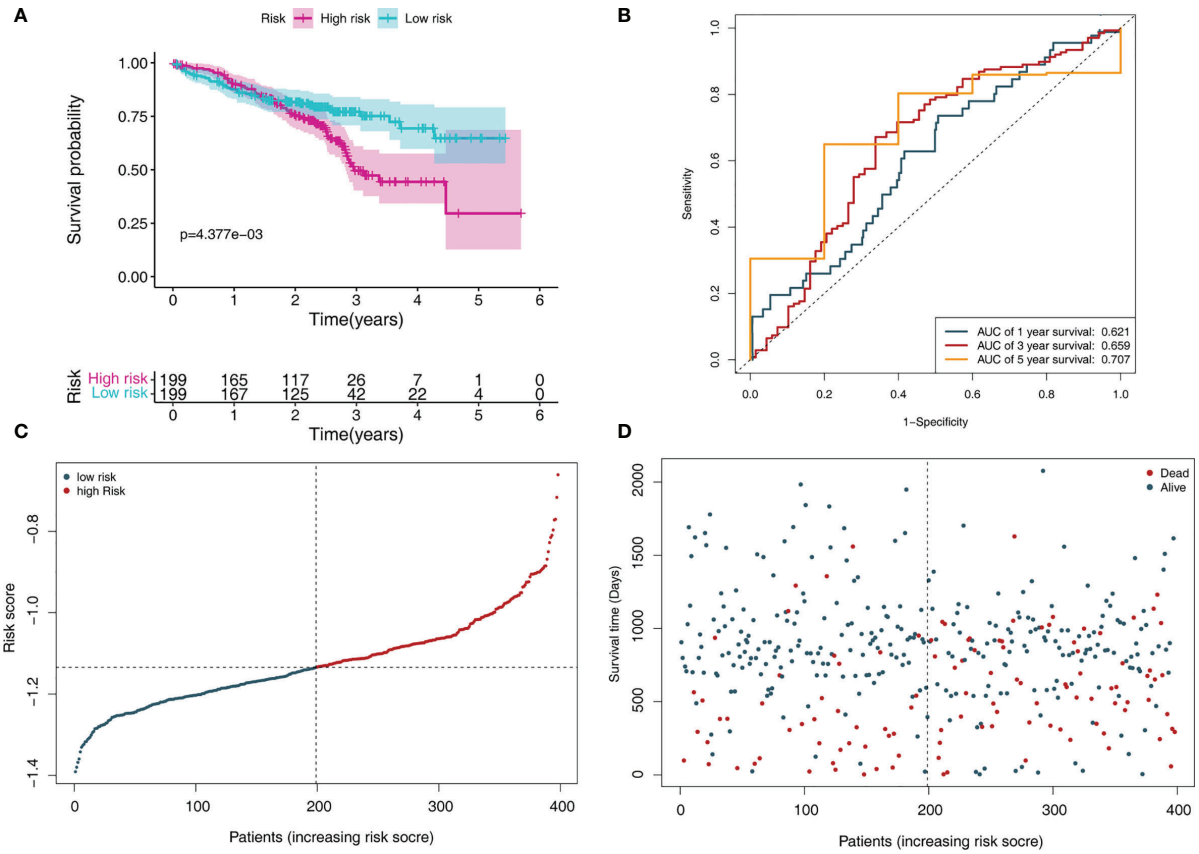


**FIGURE 5** | MRGs-based risk signature evaluation using the testing set (GSE72094). **(A)** Kaplan-Meier survival analysis revealed the difference in survival rate between high- and low-risk patients. **(B)** Time-dependent ROC curve analysis for 1-, 3-, and 5-year predictions of overall survival using the MRG-based signature. **(C)** Risk score distribution of patients with the overall survival and signature. **(D)** Overall survival scatter plots for LADC patients.

## Development and Validation of a Prognostic Nomogram Based on the Signature

To accurately predict a certain clinical outcome, a nomogram was established by integrating stage, age, gender, and the eight MRGs using a Cox model (**Figure 9A**). For the training set, the AUCs of the nomogram at 1-, 3-, and 5-year OS were 0.769, 0.765, and 0.75, respectively (**Figure 9B**). In the validation set, the AUCs of the nomogram at 1-, 3-, and 5- year OS were 0.896, 0.779, and 0.738, respectively (**Figure 9C**). For convenient clinical application and visualization of the prognostic model, we established an easy-to-use web-based calculator (https://emergency.shinyapps.io/LADC/) for predicting the overall survival of LADC (**Figures 9D, E**).

We evaluate the predictive ability and clinical usefulness of the nomogram using calibration curves and DCA. The calibration plots displayed that the nomogram could accurately predict OS (**Supplementary Figures 3A, B**). In addition, we used DCA to assess the clinical usefulness of the nomogram; the results showed good clinical usefulness of this model both in the training and validation sets (**Supplementary Figures 3C, D**).

## DISCUSSION

LADC is one of the most prevalent tumors with low survival rates in advanced stage patients (16). Accurately predicting LADC outcome will be helpful for more aggressive treatment, earlier intervention, and delayed tumor progression (17). The most commonly used tool to predict patient outcome is the AJCC staging system, which only focuses on clinical features; thus, making it difficult to develop individualized risk estimation. In the present study, we collected data on LADC patients and constructed a prognostic MRG-based signature and nomogram to better predict the OS of these patients. We showed that our MRG signature can predict the individual mortality risk of LADC patients and is helpful for devising individualized therapies against LADC.

Immune dysregulation is important in cancer progression. Most studies only focused on the T cell compartment (18, 19). However, macrophage phenotypic polarization represents a key step that accelerates tumor aggressiveness, which further imparts the MRGs satisfactory prognostic value (20). Here, we identified a signature composed of eight MRGs, CTSL, ECT2, HCFC2, HNRNPK, LRIG1, OSBPL5, P4HA1, and TUBA4A. Among

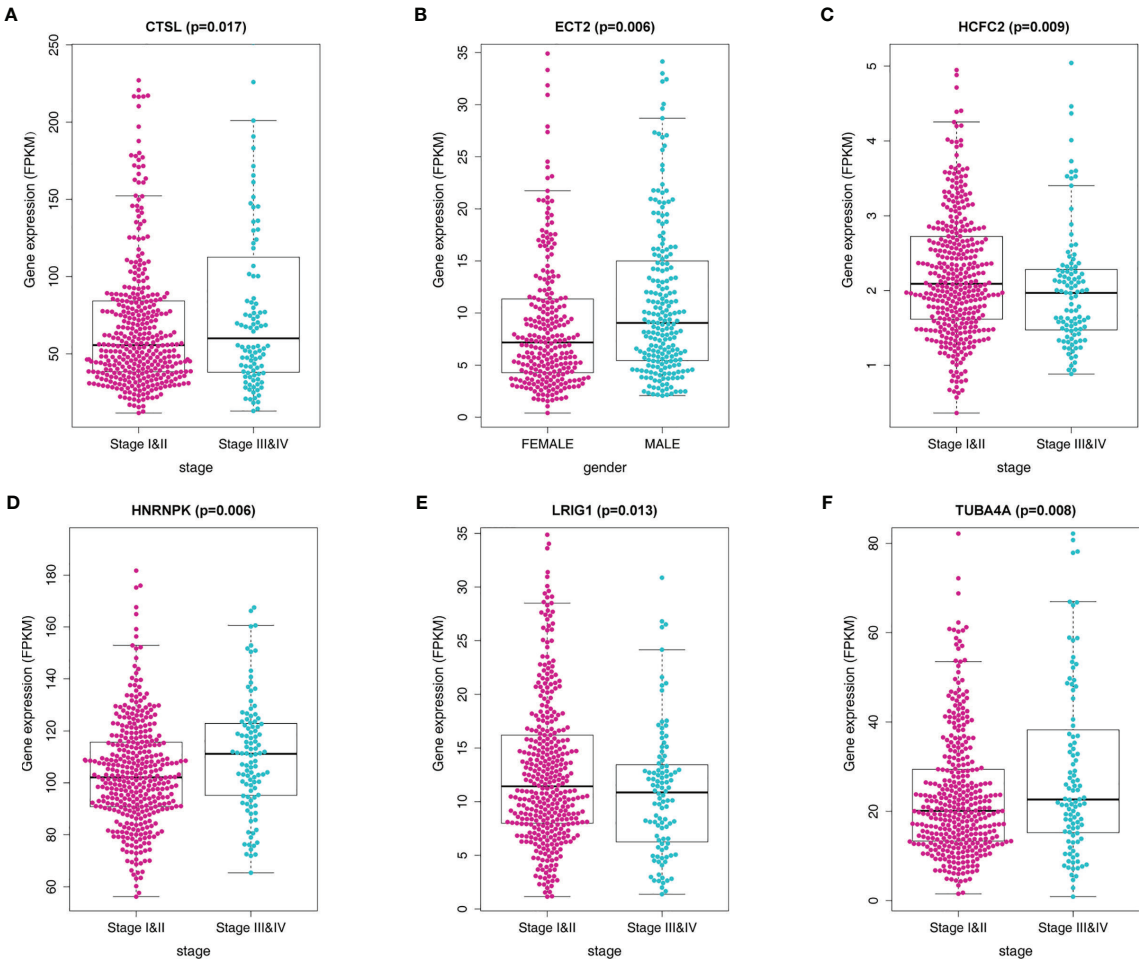


**FIGURE 6** | Correlation of the MRG mRNA expression levels with demographic and clinicopathological characteristics of LADC patients. **(A)** Correlation between CTSL mRNA levels and disease stage. **(B)** Correlation between ECT2 mRNA levels and gender. **(C)** Correlation between HCFC2 mRNA levels and disease stage. **(D)** Correlation between HNRNPK mRNA levels and disease stage. **(E)** Correlation between LRIG1 mRNA levels and disease stage **(F)** Correlation between TUBA4A mRNA levels and disease stage.

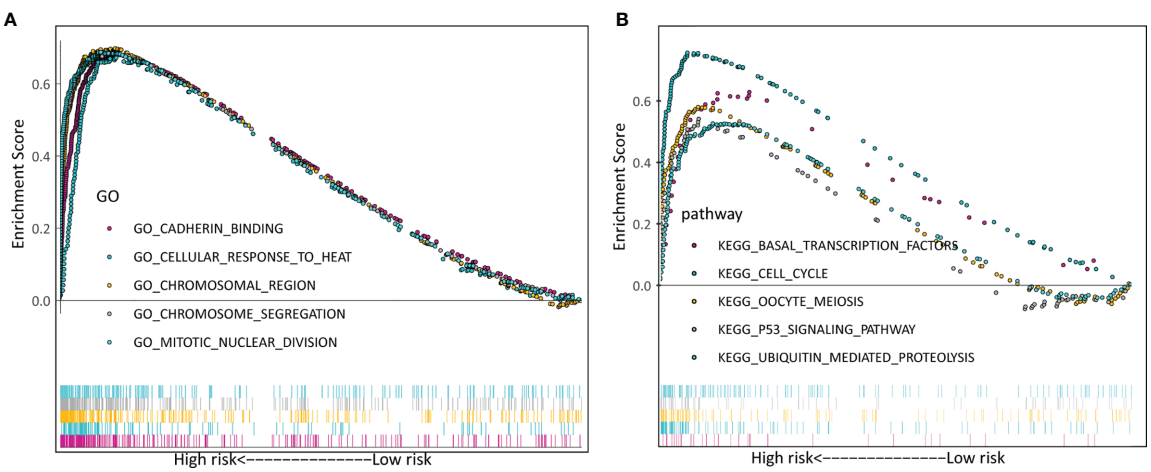


**FIGURE 7** | Verification of the biosignature stratified by different clinical parameters in the training set. **(A)** GO terms. **(B)** KEGG terms.

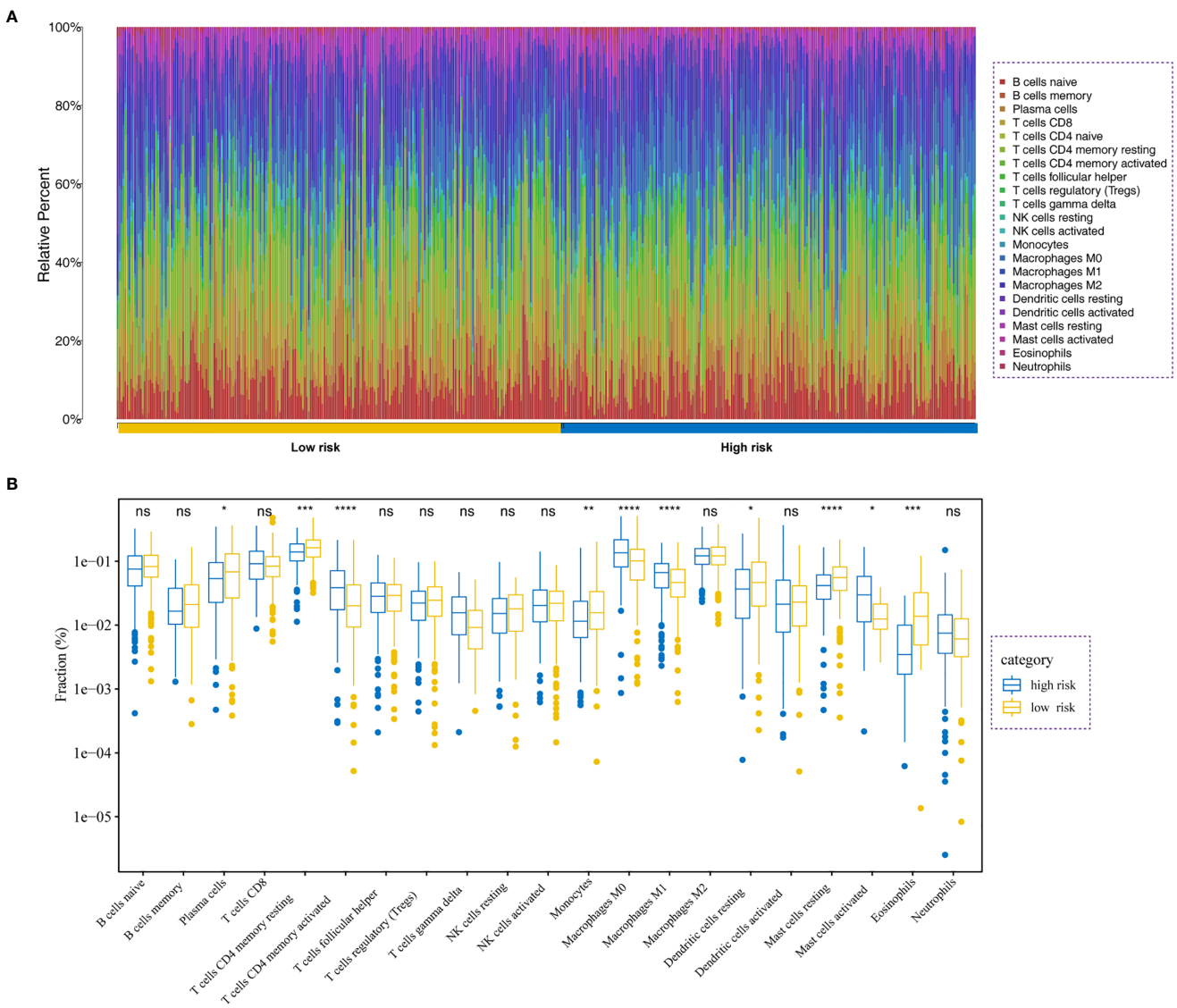


**FIGURE 8** | Immune analysis. **(A)** Relative proportion of immune cell infiltration in high- and low-risk patients. **(B)** Differences in immune cell infiltration between low- and high-risk LADC patients *P<0.05, **P<0.01, ***P<0.001, ****P<0.0001, ns, no significance.

these genes, the mRNA levels of ECT2, HNRNPK, P4HA1, and TUBA4A were significantly upregulated in the tumor tissues, when compared to those in normal tissues. However, the mRNA levels of CTSL, HNRNPK, LRIG1, and OSBPL5 were significantly downregulated in the tumor tissues compared to those observed in normal tissues. Furthermore, GSEA showed that tumor-associated pathways were enriched in samples from high-risk patients.

Cathepsin L (CTSL), one of the human cathepsin proteases, has been shown to be overexpressed in various carcinomas including ovary, cervix, breast, and colon tumors (21, 22). However, the function of CTSL in the complex process of tumorigenesis is not yet fully understood (23). It has been recently observed that CTSL is closely correlated with drug resistance in NSCLC (24). Our analyses showed that the upregulation of CTSL mRNA levels in LADC patients was associated with a higher risk of relapse and worse OS. Epithelial cell transforming sequence 2 (ECT2), a guanine nucleotide exchange factor of the Rho family of GTPases, has been shown to be involved in the oncogenic and malignant phenotypes of LADC (25). Furthermore, ETC2 has been reported to be amplified and its protein overexpressed in early invasive LADC (26). Previous studies indicated that ECT2 may promote the polarization of M2 macrophages by enhancing aerobic glycolysis and inhibiting the functions of immune cells in tumor (27). HNRNPK is a highly conserved RNA- and DNA-binding protein (28) and its dysregulation has been shown to correlate with tumor development, progression, and prognosis (29–31). In line with these results, our analyses indicated an

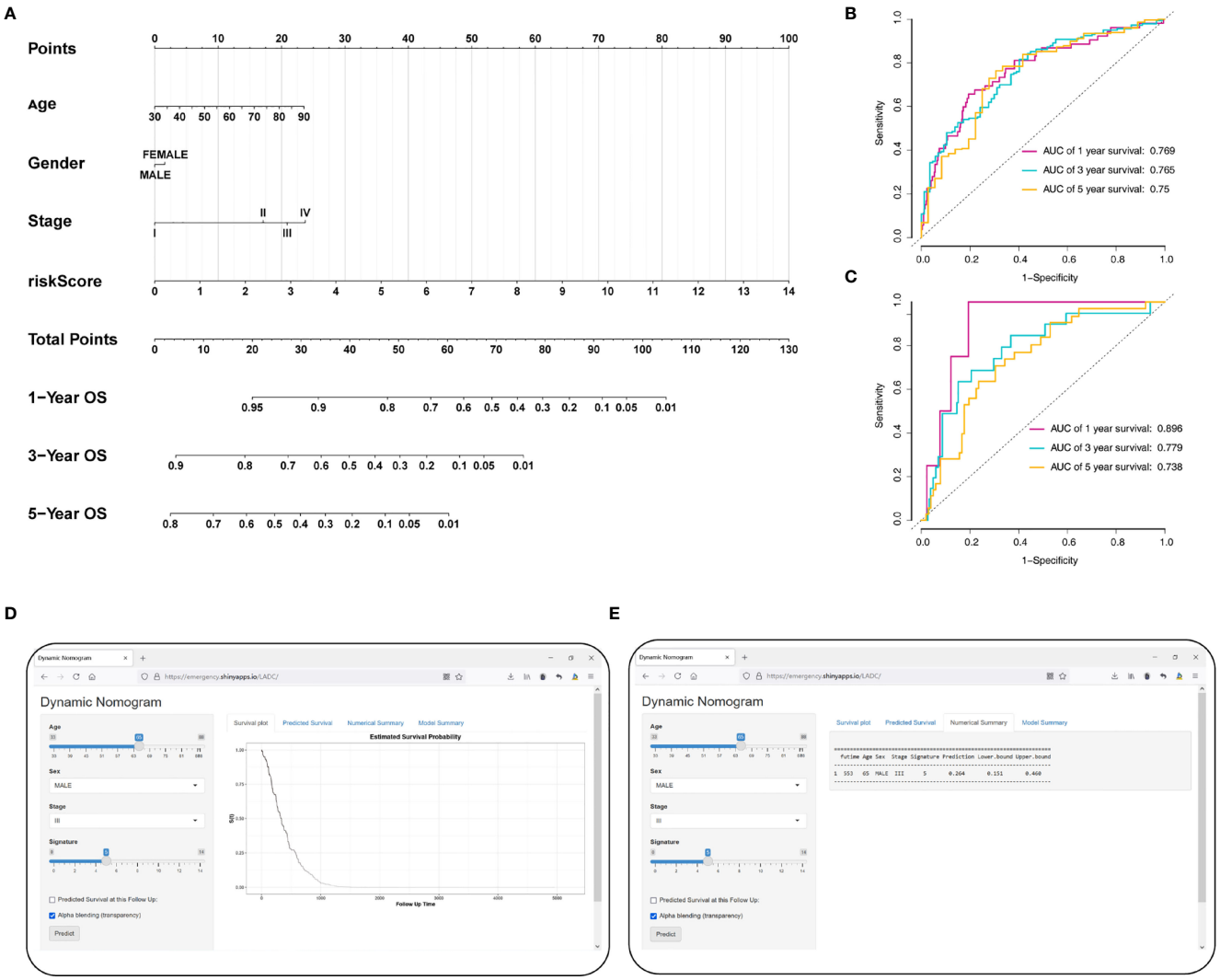


**FIGURE 9** | Construction of the MRG-based nomogram. **(A)** Development of MRG nomogram. **(B)** Time-dependent ROC curve analysis for 1-, 3-, and 5-year overall survival predictions obtained using the nomogram in the training set. **(C)** Time-dependent ROC curve analysis for 1-, 3-, and 5-year overall survival predictions obtained using the nomogram in the validation set. **(D)** Establishing an easy-to-operate web-based calculator for predicting the overall survival of LADC (https://emergency.shinyapps.io/LADC/). **(E)** 95% confidence interval of the web overall survival rate.

association between the HNRNPK mRNA levels and the high-risk score. Leucine-rich repeats and immunoglobulin-like domains 1 (LRIG1) is one of three members of a transmembrane protein family (32). LRIG1 is often regarded as a tumor suppressor in several tumors, including cervical cancer, melanoma, and cutaneous squamous cell carcinoma (33–35). However, we identified an association between the LRIG1 levels and high-risk scores. Oxysterol binding protein-like 5 (OSBPL5), a cytosolic mammalian protein, binds to an oxysterol ligand and interacts with the Golgi membrane; thus, playing a role in vesicle transport, lipid metabolism, and signal transduction (36). Nagano and colleagues reported that OSBPL5 are involved in the metastatic potential of lung cancer (37). P4HA1 was the most common subtype of prolyl 4-hydroxylase which enhanced collagen modification (38). Several studies reported that P4HA1 might serve as a pro-tumorigenic factor (39–41). However, studies investigating the roles of TUBA4A and HCFC2 and their functions in LADC are limited; thus, further studies are necessary to elucidate their associations with LADC.

The immune system can identify and eradicate tumor cells through innate and adaptive immune system. However, the TME could regulate this antitumor response by regulating the immune-infiltrating cells. Notably, TAMs and their progenitors account for the largest proportion of tumor-resident immune cells. M1 macrophages secrete inflammatory cytokines, including tumor necrosis factor-α as well as interleukin-12, and typically suppress tumor development. In the current study, we analyzed the differences in tumor-infiltrating immune cells between the

high- and low-risk groups of patients. Our results showed that the high-risk group exhibited a higher proportion of plasma cells, resting CD4 T memory cells, monocytes, resting dendritic cells, resting mast cells, and eosinophils. Alternatively, the low-risk group showed higher proportions of activated CD4 T memory cells, M0 macrophages, M1 macrophages, and activated mast cells.

As far as we know, this study firstly analyzed the MRGs associated with the prognosis of LADC patients. More importantly, we developed an eight-gene signature to predict LADC patient outcomes with a satisfactory accuracy. However, some limitations of the present study are worth mentioning. First, all cases included in our study were retrospective samples, and the validation of our signature through prospective samples is still needed. Second, this risk score was calculated based on gene expression, without considering the mutations or epigenetic modifications that might represent key MRG drivers. Ultimately, a prognostic nomogram incorporating both the MRG signature and clinicopathological features for individual survival prediction was constructed and validated. The establishment of this model will help in better evaluation of the patients' prognosis in the clinical setting and will aid in guiding follow-up and treatment processes.

## DATA AVAILABILITY STATEMENT

Publicly available datasets were analyzed in this study. This data can be found here: The transcriptome profiles and corresponding clinical data of LADC patients were downloaded from TCGA (https://portal.gdc.cancer.gov/) and GEO (https://www.ncbi.nlm.nih.gov/geo/) databases.

## AUTHOR CONTRIBUTIONS

JC and YL involved in study concept and design. JC and YL involved in acquisition of data. CZ and YL involved in analysis and interpretation of data. JC and CZ drafted the manuscript. YL and JC involved in critical revision of the manuscript for intellectual content. All authors contributed to the article and approved the submitted version.

## FUNDING

This study was supported by The Project of Jiangxi Education Department (No. GJJ200223 and No. GJJ170122).

## SUPPLEMENTARY MATERIAL

The Supplementary Material for this article can be found online at: https://www.frontiersin.org/articles/10.3389/fonc.2021.771988/full#supplementary-material

## REFERENCES


1. Torre LA, Bray F, Siegel RL, Ferlay J, Lortet-Tieulent J, Jemal A. Global Cancer Statistics, 2012. *CA Cancer J Clin* (2015) 65:87–108. doi: 10.3322/caac.21262
2. Wang J, Hu ZG, Li D, Xu JX, Zeng ZG. Gene Expression and Prognosis of Insulin–Like Growth Factor–Binding Protein Family Members in non–Small Cell Lung Cancer. *Oncol Rep* (2019) 42:1981–95. doi: 10.3892/or.2019.7314
3. Zappa C, Mousa SA. Non-Small Cell Lung Cancer: Current Treatment and Future Advances. *Transl Lung Cancer Res* (2016) 5:288–300. doi: 10.21037/tlcr.2016.06.07
4. Rinaldi S, Berardi R. Lung Cancer Prognosis: Can Histological Patterns and Morphological Features Have a Role in the Management of Lung Cancer Patients? *Ann Transl Med* (2017) 5:353. doi: 10.21037/atm.2017.05.18
5. Jones GS, Baldwin DR. Recent Advances in the Management of Lung Cancer. *Clin Med (Lond)* (2018) 18:s41–6. doi: 10.7861/clinmedicine.18-2-s41
6. Parkin DM, Bray F, Ferlay J, Pisani P. Global Cancer Statistics, 2002. *CA Cancer J Clin* (2005) 55:74–108. doi: 10.3322/canjclin.55.2.74
7. Senosain MF, Massion PP. Intratumor Heterogeneity in Early Lung Adenocarcinoma. *Front Oncol* (2020) 10:349. doi: 10.3389/fonc.2020.00349
8. Ben-Aharon I, Elkabets M, Pelossof R, Yu KH, Iacubuzio-Donahue CA, Leach SD, et al. Genomic Landscape of Pancreatic Adenocarcinoma in Younger Versus Older Patients: Does Age Matter? *Clin Cancer Res* (2019) 25:2185–93. doi: 10.1158/1078-0432.CCR-18-3042
9. Gu Y, Wu X, Zhang J, Fang Y, Pan Y, Shu Y, et al. The Evolving Landscape of N(6)-Methyladenosine Modification in the Tumor Microenvironment. *Mol Ther* (2021):1703–15. doi: 10.1016/j.ymthe.2021.04.009
10. Chen Z, Huang Y, Hu Z, Zhao M, Li M, Bi G, et al. Landscape and Dynamics of Single Tumor and Immune Cells in Early and Advanced-Stage Lung Adenocarcinoma. *Clin Transl Med* (2021) 11:e350. doi: 10.1002/ctm2.350
11. Kalogirou EM, Tosios KI, Christopoulos PF. The Role of Macrophages in Oral Squamous Cell Carcinoma. *Front Oncol* (2021) 11:611115. doi: 10.3389/fonc.2021.611115
12. Biswas SK, Mantovani A. Macrophage Plasticity and Interaction With Lymphocyte Subsets: Cancer as a Paradigm. *Nat Immunol* (2010) 11:889–96. doi: 10.1038/ni.1937
13. Noy R, Pollard JW. Tumor-Associated Macrophages: From Mechanisms to Therapy. *Immunity* (2014) 41:49–61. doi: 10.1016/j.immuni.2014.06.010
14. Mantovani A, Allavena P. The Interaction of Anticancer Therapies With Tumor-Associated Macrophages. *J Exp Med* (2015) 212:435–45. doi: 10.1084/jem.20150295
15. Martinez FO, Gordon S, Locati M, Mantovani A. Transcriptional Profiling of the Human Monocyte-to-Macrophage Differentiation and Polarization: New Molecules and Patterns of Gene Expression. *J Immunol* (2006) 177:7303–11. doi: 10.4049/jimmunol.177.10.7303
16. Travis WD, Brambilla E, Noguchi M, Nicholson AG, Geisinger KR, Yatabe Y, et al. International Association for the Study of Lung Cancer/American Thoracic Society/European Respiratory Society International Multidisciplinary Classification of Lung Adenocarcinoma. *J Thorac Oncol* (2011) 6:244–85. doi: 10.1097/JTO.0b013e318206a221
17. Zeng Z, Yang Y, Qing C, Hu Z, Huang Y, Zhou C, et al. Distinct Expression and Prognostic Value of Members of SMAD Family in non-Small Cell Lung Cancer. *Medicine (Baltimore)* (2020) 99:e19451. doi: 10.1097/MD.0000000000019451
18. Bear AS, Vonderheide RH, O'Hara MH. Challenges and Opportunities for Pancreatic Cancer Immunotherapy. *Cancer Cell* (2020) 38:788–802. doi: 10.1016/j.ccell.2020.08.004
19. Zhou Q, Tao X, Xia S, Guo F, Pan C, Xiang H, et al. T Lymphocytes: A Promising Immunotherapeutic Target for Pancreatitis and Pancreatic Cancer? *Front Oncol* (2020) 10:382. doi: 10.3389/fonc.2020.00382
20. Li MX, Wang HY, Yuan CH, Ma ZL, Jiang B, Li L, et al. Establishment of a Macrophage Phenotypic Switch Related Prognostic Signature in Patients With Pancreatic Cancer. *Front Oncol* (2021) 11:619517. doi: 10.3389/fonc.2021.619517
21. Harbeck N, Alt U, Berger U, Krüger A, Thomssen C, Jänicke F, et al. Prognostic Impact of Proteolytic Factors (Urokinase-Type Plasminogen Activator, Plasminogen Activator Inhibitor 1, and Cathepsins B, D, and L)

in Primary Breast Cancer Reflects Effects of Adjuvant Systemic Therapy. *Clin Cancer Res* (2001) 7:2757–64.
22. Skrzypczak M, Springwald A, Lattrich C, Häring J, Schüler S, Ortmann O, et al. Expression of Cysteine Protease Cathepsin L is Increased in Endometrial Cancer and Correlates With Expression of Growth Regulatory Genes. *Cancer Invest* (2012) 30:398–403. doi: 10.3109/07357907.2012.672608
23. Wang Z, Xiang Z, Zhu T, Chen J, Zhong MZ, Huang J, et al. Cathepsin L Interacts With CDK2-AP1 as a Potential Predictor of Prognosis in Patients With Breast Cancer. *Oncol Lett* (2020) 19:167–76. doi: 10.3892/ol.2019.11067
24. Zhao Y, Shen X, Zhu Y, Wang A, Xiong Y, Wang L, et al. Cathepsin L-Mediated Resistance of Paclitaxel and Cisplatin is Mediated by Distinct Regulatory Mechanisms. *J Exp Clin Cancer Res* (2019) 38:333. doi: 10.1186/s13046-019-1299-4
25. Kosibaty Z, Murata Y, Minami Y, Noguchi M, Sakamoto N. ECT2 Promotes Lung Adenocarcinoma Progression Through Extracellular Matrix Dynamics and Focal Adhesion Signaling. *Cancer Sci* (2021) 112:703–14. doi: 10.1111/cas.14743
26. Murata Y, Minami Y, Iwakawa R, Yokota J, Usui S, Tsuta K, et al. ECT2 Amplification and Overexpression as a New Prognostic Biomarker for Early-Stage Lung Adenocarcinoma. *Cancer Sci* (2014) 105:490–7. doi: 10.1111/cas.12363
27. Xu D, Wang Y, Wu J, Zhang Z, Chen J, Xie M, et al. ECT2 Overexpression Promotes the Polarization of Tumor-Associated Macrophages in Hepatocellular Carcinoma *via* the ECT2/PLK1/PTEN Pathway. *Cell Death Dis* (2021) 12:162. doi: 10.1038/s41419-021-03450-z
28. Piñol-Roma S, Choi YD, Matunis MJ, Dreyfuss G. Immunopurification of Heterogeneous Nuclear Ribonucleoprotein Particles Reveals an Assortment of RNA-Binding Proteins. *Genes Dev* (1988) 2:215–27. doi: 10.1101/gad.2.2.215
29. Ostareck-Lederer A, Ostareck DH, Cans C, Neubauer G, Bomsztyk K, Superti-Furga G, et al. C-Src-Mediated Phosphorylation of hnRNP K Drives Translational Activation of Specifically Silenced mRNAs. *Mol Cell Biol* (2002) 22:4535–43. doi: 10.1128/MCB.22.13.4535-4543.2002
30. Takimoto M, Tomonaga T, Matunis M, Avigan M, Krutzsch H, Dreyfuss G, et al. Specific Binding of Heterogeneous Ribonucleoprotein Particle Protein K to the Human C-Myc Promoter, In Vitro. *J Biol Chem* (1993) 268:18249–58. doi: 10.1016/S0021-9258(17)46837-2
31. Chang YI, Hsu SC, Chau GY, Huang CY, Sung JS, Hua WK, et al. Identification of the Methylation Preference Region in Heterogeneous Nuclear Ribonucleoprotein K by Protein Arginine Methyltransferase 1 and its Implication in Regulating Nuclear/Cytoplasmic Distribution. *Biochem Biophys Res Commun* (2011) 404:865–9. doi: 10.1016/j.bbrc.2010.12.076
32. Guo D, Holmlund C, Henriksson R, Hedman H. The LRIG Gene Family has Three Vertebrate Paralogs Widely Expressed in Human and Mouse Tissues and a Homolog in Ascidiacea. *Genomics* (2004) 84:157–65. doi: 10.1016/j.ygeno.2004.01.013
33. Lindström AK, Ekman K, Stendahl U, Tot T, Henriksson R, Hedman H, et al. LRIG1 and Squamous Epithelial Uterine Cervical Cancer: Correlation to Prognosis, Other Tumor Markers, Sex Steroid Hormones, and Smoking. *Int J Gynecol Cancer* (2008) 18:312–7. doi: 10.1111/j.1525-1438.2007.01021.x
34. Rouam S, Moreau T, Broët P. Identifying Common Prognostic Factors in Genomic Cancer Studies: A Novel Index for Censored Outcomes. *BMC Bioinformatics* (2010) 11:150. doi: 10.1186/1471-2105-11-150
35. Tanemura A, Nagasawa T, Inui S, Itami S. LRIG-1 Provides a Novel Prognostic Predictor in Squamous Cell Carcinoma of the Skin: Immunohistochemical Analysis for 38 Cases. *Dermatol Surg* (2005) 31:423–30. doi: 10.1097/00042728-200504000-00008
36. Fairn GD, McMaster CR. Emerging Roles of the Oxysterol-Binding Protein Family in Metabolism, Transport, and Signaling. *Cell Mol Life Sci* (2008) 65:228–36. doi: 10.1007/s00018-007-7325-2
37. Nagano K, Imai S, Zhao X, Yamashita T, Yoshioka Y, Abe Y, et al. Identification and Evaluation of Metastasis-Related Proteins, Oxysterol Binding Protein-Like 5 and Calumenin, in Lung Tumors. *Int J Oncol* (2015) 47:195–203. doi: 10.3892/ijo.2015.3000
38. Chen L, Shen YH, Wang X, Wang J, Gan Y, Chen N, et al. Human Prolyl-4-Hydroxylase Alpha(I) Transcription is Mediated by Upstream Stimulatory Factors. *J Biol Chem* (2006) 281:10849–55. doi: 10.1074/jbc.M511237200
39. Gilkes DM, Bajpai S, Chaturvedi P, Wirtz D, Semenza GL. Hypoxia-Inducible Factor 1 (HIF-1) Promotes Extracellular Matrix Remodeling Under Hypoxic Conditions by Inducing P4HA1, P4HA2, and PLOD2 Expression in Fibroblasts. *J Biol Chem* (2013) 288:10819–29. doi: 10.1074/jbc.M112.442939
40. Balamurugan K. HIF-1 at the Crossroads of Hypoxia, Inflammation, and Cancer. *Int J Cancer* (2016) 138:1058–66. doi: 10.1002/ijc.29519
41. Xiong G, Stewart RL, Chen J, Gao T, Scott TL, Samayoa LM, et al. Collagen Prolyl 4-Hydroxylase 1 is Essential for HIF-1α Stabilization and TNBC Chemoresistance. *Nat Commun* (2018) 9:4456. doi: 10.1038/s41467-018-06893-9

**Conflict of Interest:** The authors declare that the research was conducted in the absence of any commercial or financial relationships that could be construed as a potential conflict of interest.

**Publisher's Note:** All claims expressed in this article are solely those of the authors and do not necessarily represent those of their affiliated organizations, or those of the publisher, the editors and the reviewers. Any product that may be evaluated in this article, or claim that may be made by its manufacturer, is not guaranteed or endorsed by the publisher.

frontiers in Oncology

ORIGINAL RESEARCH
published: 17 March 2022
doi: 10.3389/fonc.2022.840855

# Analgesic Effects of Repetitive Transcranial Magnetic Stimulation in Patients With Advanced Non-Small-Cell Lung Cancer: A Randomized, Sham-Controlled, Pilot Study

*Ying Tang[1], Han Chen[2], Yi Zhou[2], Ming-liang Tan[2], Shuang-long Xiong[1], Yan Li[1], Xiao-hui Ji[1] and Yong-sheng Li[1]**

*[1] Chongqing Key Laboratory of Translational Research for Cancer Metastasis and Individualized Treatment, Chongqing University Cancer Hospital, Chongqing, China, [2] Department of Rehabilitation, Southwest Hospital, Army Medical University, Chongqing, China*

OPEN ACCESS

**Edited by:**
*Fiona Hegi-Johnson, University of Melbourne, Australia*

**Reviewed by:**
*Feng Liu, Central South University, China*
*Ravindra Deshpande, Wake Forest School of Medicine, United States*

***Correspondence:**
*Yong-sheng Li*
*lys@cqu.edu.cn*

**Specialty section:**
*This article was submitted to Thoracic Oncology, a section of the journal Frontiers in Oncology*

**Received:** *21 December 2021*
**Accepted:** *25 February 2022*
**Published:** *17 March 2022*

**Citation:**
*Tang Y, Chen H, Zhou Y, Tan M-l, Xiong S-l, Li Y, Ji X-h and Li Y-s (2022) Analgesic Effects of Repetitive Transcranial Magnetic Stimulation in Patients With Advanced Non-Small-Cell Lung Cancer: A Randomized, Sham-Controlled, Pilot Study. Front. Oncol. 12:840855. doi: 10.3389/fonc.2022.840855*

**Objective:** Current pharmacological intervention for the cancer-related pain is still limited. The aim of this study was to explore whether repetitive transcranial magnetic stimulation (rTMS) could be an effective adjuvant therapy to reduce pain in patients with advanced non-small cell lung cancer (NSCLC).

**Methods:** This was a randomized, sham–controlled study. A total of 41 advanced NSCLC patients with uncontrolled pain (score≥4 on pain intensity assessed with an 11-point numeric rating scale) were randomized to receive active (10 Hz, 2000 stimuli) (n = 20) or sham rTMS (n = 20) for 3 weeks. Pain was the primary outcome and was assessed with the Numeric Rating Scale (NRS). Secondary outcomes were oral morphine equivalent (OME) daily dose, quality of life (WHO Quality of Life-BREF), and psychological distress (the Hospital Depression and Anxiety Scale). All outcomes were measured at baseline, 3 days, 1 week, 2 weeks, and 3 weeks.

**Results:** The pain intensity in both groups decreased gradually from day 3 and decreased to the lowest at the week 3, with a decrease rate of 41.09% in the rTMS group and 23.23% in the sham group. The NRS score of the rTMS group was significantly lower than that of the sham group on the week 2 ($p < 0.001$, Cohen's d =1.135) and week 3 ($p$=0.017, Cohen's d = -0.822). The OME daily dose, physiology and psychology domains of WHOQOL-BREF scores, as well as the HAM-A and HAM-D scores all were significantly improved at week 3 in rTMS group.

**Conclusion:** Advanced NSCL patients with cancer pain treated with rTMS showed better greater pain relief, lower dosage of opioid, and better mood states and quality of life. rTMS is expected to be a new effective adjuvant therapy for cancer pain in advanced NSCLC patients.

**Keywords: cancer pain, non-small-cell lung cancer, repetitive transcranial magnetic stimulation, quality of life, analgesic effects**

# INTRODUCTION

Recently, the incidence of cancer in the world is increasing year by year (1). According to the studies, at least 25-30% of newly diagnosed cancer patients are associated with pain, and the incidence of pain in patients with advanced cancer is as high as 74% (2, 3). Lung cancer is the first cause of cancer death in the world and it is mostly diagnosed at an advanced stage (4). Lung cancer-related pain mainly depends on the location of the primary tumor, local infiltration of the tumor, visceral and lymph node metastasis, compression of nerve and bone metastasis, etc. Pain is a complex symptom that affects many aspects of a cancer patient, including physical function, sleep, ability of daily living, psychological and emotional status, and social relations (5). Therefore, intervention on the pain is of great significance to improve the quality of life and the prognosis of lung cancer patients (6).

The WHO three-step ladder for cancer pain, which is widely used in clinic, follows the rule that the choice of analgesic drugs were based on the pain intensity: step I-nonsteroidal anti-inflammatory drugs (eg, aspirin or ibuprofen) to mild pain, step II- weak opioids (eg, codeine or tramadol) to moderate pain, and step III- strong opioids (morphine or oxycodone) to severe pain (7). Meanwhile, there were also some other treatments for cancer pain, such as radiotherapy, surgery, chemotherapy, radioisotope therapy, bisphosphonate and so on (8). Although those treatments effectively relieve the symptoms of cancer patients to some extent, there were still 50% patients whose pain is undertreated. The serious pain affects the quality of life of cancer patients (9).

In the past two decades, neuromodulation technique has gradually become a new direction of pain treatment. Repetitive transcranial magnetic stimulation (rTMS) is one of the most commonly used non-invasive neuromodulation techniques in clinic (10). rTMS could produce a certain intensity of magnetic field by focusing on the brain with a specific shape coil, which makes cortex neuron depolarization or hyperpolarization, and then regulate the excitability of neuron. Usually, low frequency (< 1Hz) stimulation has an inhibitory effect on the brain, while high frequency (> 5Hz) stimulation excite neurons (11). It has been reported that rTMS relieves various types of pain, such as neuropathic pain after spinal cord injury, stroke or postoperative of trigeminal nerve (12), migraine (13), fibromyalgia (14) and chronic musculoskeletal pain (15). Even less clinical study has been done on the application of rTMS in patients with cancer pain.

In addition, patients with cancer pain are often complicated with depression, which aggravates the complexity and difficulty of cancer pain treatment, and that is also one of the main reasons for poor analgesic effect (16). Many studies have found that high frequency rTMS stimulation of the dorsolateral prefrontal cortex (DLPFC) is an effective method for the treatment of depression (17). At the same time, high-frequency stimulation also relieves neuropathic pain and chronic pain to a certain extent (18). Until now, Food and Drug Administration (FDA) in the United States has officially approved the use of rTMS in the treatment of depression and migraine (19, 20). Based on the above evidence, we hypothesize that high frequency rTMS stimulation in the DLPFC may be a new and effective treatment for cancer pain. Given the efficacy of rTMS on cancer pain remains unclear, we therefore conducted a randomized controlled trial to firstly explore the analgesic effect of rTMS on advanced non-small-cell lung cancer (NSCLC) patients.

# METHODS

## Study Design

This trial was a randomized, double-blind, parallel-group, sham-controlled clinical trial, approved by the Ethics Committee of Chongqing Cancer Hospital and was registered (ChiCTR.org.cn identifier: ChiCTR 2000029130). All patients provided written informed consents before enrolling. After completing consent forms, patients were randomly assigned to either the rTMS group or the sham stimulation group using a block randomization scheme. An independent investigator carried out the randomization. Two independent, trained assessors and enrolled patients were blinded to the group assignments.

## Participants

NSCLC patients with cancer pain were enrolled consecutively from January 2020 to March 2021. The inclusion criteria were: 1) confirmed diagnosis of advanced NSCLC by pathology or cytology, 2) accompanied with pain symptoms, and confirmed as cancer pain by oncologist, 3) experienced worst pain score≥4 (0-to-10 numeric rating scale [NRS]) at the site of pain, 4) age between 18 and 70 years, 5) with clear awareness, and could cooperate to evaluate pain severity, 6) estimated that the survival time is more than 3 months, 7) with completion of signed informed consents, and voluntary participation in this study. The exclusion criteria were: 1) brain tumor patients 2) history of seizure, 3) implanted pacemaker, stent and other metal substances 4) acute pain anywhere in the body due to other diseases, 5) serious psychiatric diagnoses (eg, psychosis)

## Interventions

### Analgesia Treatment

All the participants were treated with medications according to WHO three-step principle. In order to facilitate the statistics of the dosage of opioids in patients with cancer pain, morphine sulfate controlled-release tablets or oxycodone hydrochloride sustained-release tablets were used for analgesia in this study (21).

### rTMS Procedure

rTMS was applied with a magnetic stimulator (CCY-I) with a figure-of-eight coil (B9076; 22 mm inner diameter, 90 mm outer diameter, 76 mm combined long axis length, Wuhan Yiruide Medical Equipment, Wuhan, China). The rTMS protocols used in this study were in accordance with the safety guidelines for rTMS applications (22). The resting motor threshold (RMT) was measured as follows (22): a single TMS pulse stimulated one side of the primary motor cortex, the motor evoked potential (MEP)

was recorded at the first dorsal interosseous (FDI) muscle of the contralateral hand with a surface electrode. The RMT was defined as the lowest stimulation intensity capable of eliciting MEPs ≥ 50μV peak-to-peak amplitude in at least five of ten consecutive stimulations (23). Parameter setting were as follows (23): stimulation target, left side DLPFC; stimulation intensity, 80% RMT; frequency, 10HZ; 15 pulse trains (1.5 s), with intertrain intervals of 3 s (total of 1500pulses). In the control group, the sham stimulation was delivered using a same coil, but with no magnetic stimulation output (only emitting the same sound, with different stimulation angles). Both the two groups (rTMS group and control group) received stimulation once a day, 5 days per week, for a total of 3 weeks.

## Outcome Measurements

The pain intensity was assessed at 1 day before rTMS treatment (T0), 3 days (T1), 1 week (T2), 2 weeks (T3) and 3 weeks (T4) after first rTMS treatment. Mood status and quality of life were evaluated only at T0 and T4 timepoints. **Figure 1** shows the research and evaluation schedule. The primary outcome was:

1. NRS. The NRS consists of 11-point scale, of which 0 represents no pain and 10 represents the strongest pain imaginable, which has been recommended by the Initiative on Methods, Measurement, and Pain Assessment in Clinical Trials (IMMPACT) guidelines (24).

The secondary outcomes were as follows:

1. Oral morphine equivalent (OME). The conversion method of OME refer to the previous literature reports: oral oxycodone hydrochloride is 1:1.5, intravenous morphine is 1:3 converted to oral morphine (25).
2. WHO Quality of Life-BREF (WHOQL-BREF) (26). Quality of life was evaluated by means of the WHOQOL-BREF. The WHOQOL-BREF generates a profile and score for each of the 4 domains, including physiology, psychology, social relationship and environment. Each domain score ranges 0-100, higher scores represent better quality of life.
3. Hamilton Anxiety Scale (HAM-A) (27). HAM-A was used to evaluate the severity of anxiety. HAM-A includes 14 items; each item score ranges 0-4, higher scores represent more severe anxiety.
4. Hamilton Depression Scale (HAM-D) (28). HAM-D was used to evaluate the severity of depression. HAM-D includes 17 items; each item score ranges 0-4, higher scores represent more severe depression.

## Statistical Analysis

Sample size was estimated using the G Power v.3.1 statistical tool. To achieve a statistical power of 85% with statistical significance at $P<0.05$ (two-sided test) and an effect size of $r = 0.45$, a total

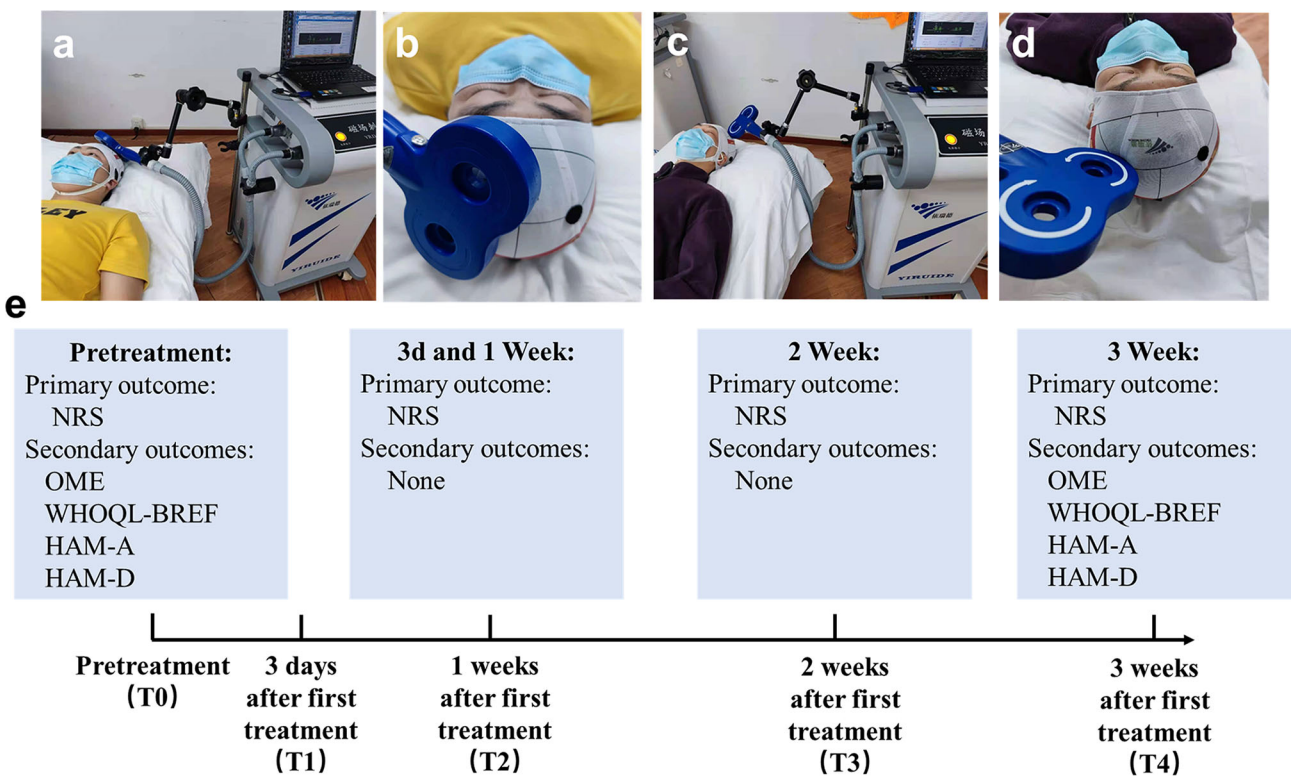


**FIGURE 1** | Schematic diagram of the experimental design. **(A)** Image of the treatment in rTMS group, **(B)** Close-up of the coil in rTMS group. **(C)** Image of the treatment in sham group, **(D)** Close-up of the coil in sham group, **(E)** Primary and secondary outcomes at different time points.

minimum sample size of 38 patients was required. Considering an estimated 10% dropout rate, the sample size was inflated to 21 participants per group (N = 42).

Statistical data analyses were performed using IBM SPSS (version 21; SPSS, Chicago, IL). Baseline group differences were explored with *t* tests or chi-squared tests. A repeated-measures analysis of variance (rmANOVA) was used to analyze the data for the efficacy of rTMS, with time as the within-subjects factor and treatment as the between-subjects factor. *Post hoc* analyses were performed with Bonferroni adjustment for further multiple comparisons. $P<0.05$ were considered statistically significant. The percentage of change within each individual was calculated as follows: [(post-treatment - pre-treatment score)/(pre-treatment score)] *100.

## RESULTS

A total of 63 advanced NSCLC patients with cancer pain were screened and 42 eligible patients were enrolled in the study (**Figure 2**). They were randomly allocated into the rTMS group (n = 21) or the sham group (n = 21). One case in the rTMS group withdrew from the study because of moving to another city in the second week, while two cases in the sham group withdrew from the study because of unwilling to continue to participate in the study in the first week. The remaining 39 patients completed the 3-week trial, with 20 cases in the rTMS group and 19 cases in the sham group. There were no significant differences between the two groups in terms of demographic variables or clinical characteristics (**Table 1**). Of the 39 patients, two patients in the

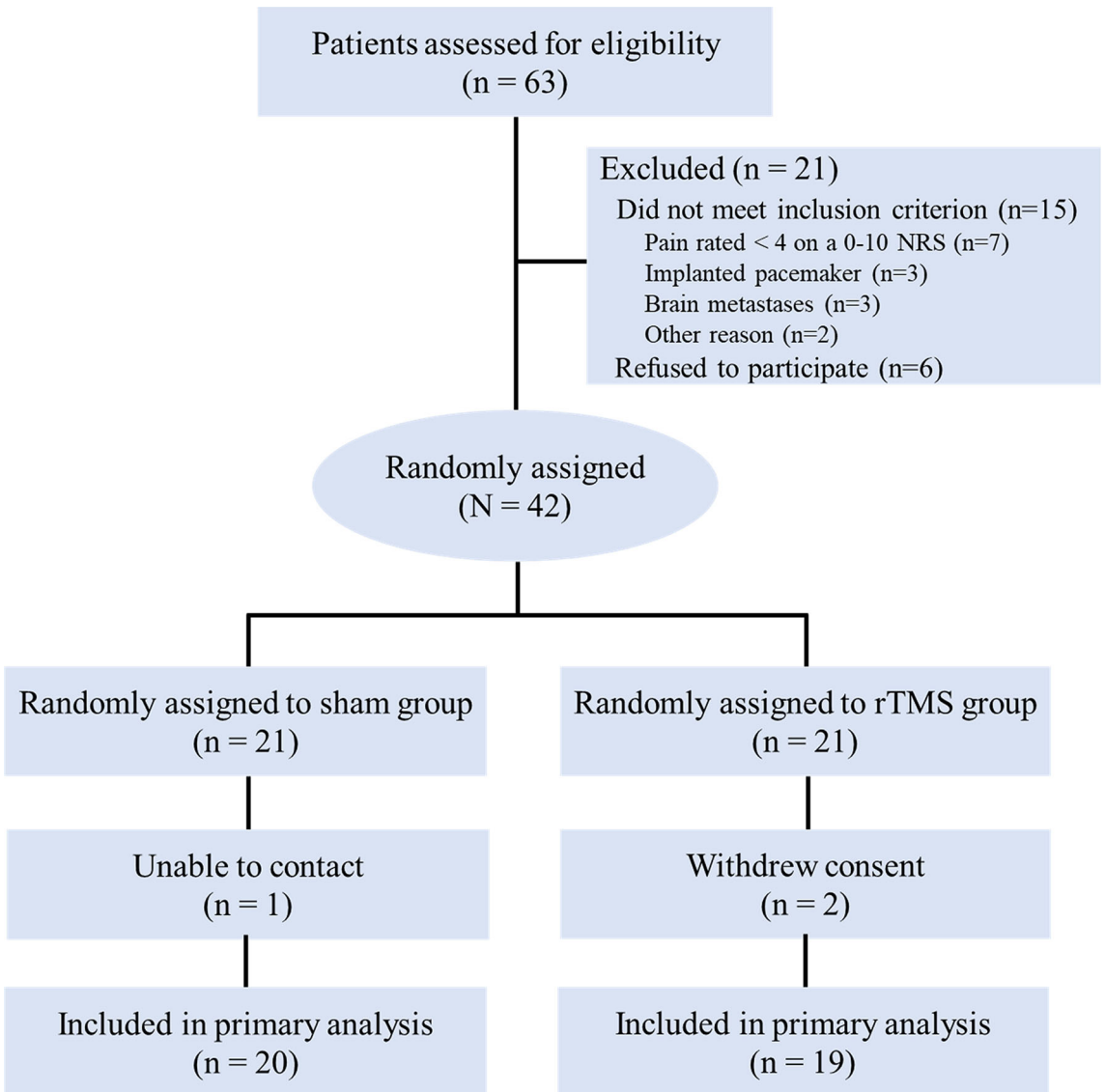


**FIGURE 2** | CONSORT diagram. NRS, numeric rating scale; rTMS, repetitive transcranial magnetic stimulation.

rTMS group reported transient scalp numbness or facial muscle twitching during the rTMS therapy, but no serious adverse effects were observed.

## Primary Outcome

### Pain Scores

The pain intensity before treatment was 6.45 (SD,1.69) in the rTMS group and 6.37 (SD,1.63) in sham group. The pain intensity in both groups decreased gradually from day 3 and decreased to the lowest at the week 3, with a decrease of 41.09% in the rTMS group and 23.23% in the sham group. The NRS score for the rTMS group was significantly lower than that of the sham group on the week 2 ($P$ = 0.04, Cohen's d =-0.735) and week 3 ($P$ = 0.017, Cohen's d =- 0.822) (**Table 2** and **Figure 3**).

## Secondary Outcome

### Oral Morphine Equivalent (OME)

The OME in the rTMS group at baseline and week 3 were 109.5 ± 52.5mg and 111.5 ± 52.4, respectively, and those in the sham group were 115.8 ± 59.6mg and 157.9 ± 84.3 mg, respectively. On week 3, the OME in the rTMS group was similar to that of baseline ($P$ = 0.02, Cohen's $d$ = 0.796), while the sham group both were significantly higher than that of baseline ($P$ = 0.02, Cohen's $d$ = 0.796) (**Table 2** and **Figure 4**).

## Quality of Life

There were significant improvements in all domains of WHOQOL-BREF scores for both the groups when compared with baseline after 3 weeks of treatment. The physiology and psychology domains of WHOQOL-BREF scores showed significant improvements with rTMS group versus sham group ($P$ = 0.02, Cohen's $d$ = 0.796 and $P$ = 0.031, Cohen's $d$ = 0.746, respectively). (**Table 2** and **Figure 4**).

## Mood Changes: HAM-A and HAM-D

The HAM-A and HAMD scores in the rTMS group showed significant improvements after 3 weeks of treatment when compared with baseline ($P$ = 0.005, Cohen's $d$ = -0.949 and $P$ = 0.011, Cohen's $d$ =- 0.869, respectively). However, there were no significant improvements in the sham group (**Table 2** and **Figure 4**).

# DISCUSSION

The findings of this randomized, double-blind, sham-controlled trial showed a significant analgesic benefit by using rTMS in advanced NSCLC patients with cancer pain. Moreover, our study also showed rTMS could reduce the daily dosage of opioids and improve the quality of life and psychological distress of NSCLC patients with cancer pain. To our knowledge, this is the first randomized controlled trial to explore the effective analgesic treatment of rTMS in patients with cancer pain. Accordingly, we expect our findings could have clinical implications.

Recently, there has been increasing evidence that rTMS is a noninvasive and safe treatment option for pain that may benefit

**TABLE 1** | Baseline Demographics and Clinical Characteristics by Group.

| Patient Demographics and Characteristics | rTMS group (n = 20) | sham group (n = 19) | *P* value |
|---|---|---|---|
| Demographics | | | |
| Female/Male | 8/12 | 9/10 | 0.643 |
| Age, mean ± SD, years | 58.5 ± 8.9 | 59.6 ± 7.7 | 0.669 |
| >60 years | 9 (45.0%) | 10 (50.0%) | 0.633 |
| BMI, mean ± SD, kg/m$^2$ | 21.4 ± 1.9 | 21.0 ± 1.5 | 0.505 |
| Clinical characteristics | | | |
| Pathological type | | | 0.72 |
| Adenocarcinoma | 13 (65.0%) | 10 (52.6%) | |
| Squamous cell carcinoma | 5 (25.0%) | 6 (31.6%) | |
| Others | 2 (5%) | 3 (15.8%) | |
| neoplasm stage | | | 0.946 |
| III B | 3 (15.0%) | 3 (15.8%) | |
| IV | 17 (85.0%) | 16 (84.2%) | |
| ECOG performance status | | | 0.839 |
| 0-1 | 12 (60.0%) | 12 (63.2%) | |
| ≥2 | 8 (40.0%) | 7 (36.8%) | |
| Number of organ metastasis | | | 0.557 |
| 0–2 | 13 (65.0%) | 14 (73.7%) | |
| ≥3 | 7 (35.0%) | 5 (26.3%) | |
| Current antitumor treatment | 12 (60%) | 11 (57.9%) | 0.893 |
| Pain site | | | 0.811 |
| Bone pain | 9 (45.0%) | 10 (52.7%) | |
| Chest pain | 9 (45.0%) | 8 (42.1%) | |
| Other | 2 (10%) | 1 (5.2%) | |
| Pain at baseline, mean ± SD | 6.5 ± 1.7 | 6.4 ± 1.6 | 0.882 |
| OME daily dose, mean ± SD, mg | 109.5 ± 52.5 | 115.8 ± 59.6 | 0.735 |

*Data are presented as No. (%) unless indicated otherwise.*

*BMI, body mass index; ECOG, Eastern Cooperative Oncology Group; OME, oral morphine equivalents; SD, standard deviation.*

**TABLE 2** | Primary and Secondary Outcomes.

| Outcome | rTMS group (n = 20) | | | sham group (n = 19) | | | *Cohen's d (rTMS to sham at 3 weeks)* | *P* value |
|---|---|---|---|---|---|---|---|---|
| | Baseline | 3 Weeks | Change From Baseline | Baseline | 3 Weeks | Change From Baseline | | |
| **Primary outcome** | | | | | | | | |
| NRS | 6.5 (1.7) | 3.8 (1.4) | -2.7 (1.2) | 6.4 (1.6) | 4.9 (1.2) | -1.5 (1.3) | -0.822 | 0.017 |
| **Secondary Outcome** | | | | | | | | |
| OME daily dose, mg | 109.5 (52.5) | 111.5 (52.5) | 2.0 (12.5) | 111.8 (59.7) | 157.9 (84.3) | 42.1 (31.7) | -0.603 | 0.05 |
| WHOQOL-BREF domain | | | | | | | | |
| Physiology | 47.9 (15.9) | 66.3 (16.3) | 15.8 (13.9) | 49.4 (15.5) | 55.1 (11.4) | 8.3 (9.5) | 0.796 | 0.02 |
| Psychology | 52.4 (14.3) | 69.7 (14.9) | 12.6 (7.4) | 53.2 (16.1) | 59.7 (11.7) | 8.1 (5.5) | 0.746 | 0.031 |
| Social relationship | 57.1 (15.1) | 72.0 (13.1) | 12.4 (10.2) | 57.8 (15.5) | 70.1 (11.4) | 10.9 (2.0) | 0.155 | 0.638 |
| Environment | 53.9 (14.9) | 66.9 (15.1) | 11.8 (8.9) | 55.5 (14.9) | 64.9 (12.2) | 8.9 (10.6) | 0.146 | 0.654 |
| HAM-A | 13.3 (6.5) | 9.1 (3.9) | -4.2(3.5) | 13.6 (5.7) | 13.2 (4.5) | -0.5 (2.8) | -0.949 | 0.005 |
| HAM-D | 14.1 (5.9) | 9.9 (3.6) | -4.2(2.9) | 14.3 (5.4) | 13.2 (4.2) | -1.1(2.1) | -0.869 | 0.011 |

*Data given as mean (SD) NRS, numeric rating scale; OME, oral morphine equivalent; SD, standard deviation; WHOQOL-BREF, World Health Organization Quality of Life-BREF; HAM-A, Hamilton Anxiety Scale; HAM-D, Hamilton Depression Scale.*

patients who do not respond to conventional pharmacological therapies (29). Functional imaging studies have shown that there was a cognitive regulation circuit of pain in the brain (30). When the pain information is transmitted upward from the spinal cord to the brain, it enters the thalamus, amygdala, anterior cingulate gyrus, primary/secondary somatosensory cortex and other brain areas, and forms the pain sensation or pain emotion through the structural and functional connection with prefrontal cortex. DLPFC directly promotes or inhibits pain through coordination with these brain regions or through modulating the activity of pain descending inhibition pathways (31). Therefore, DLPFC-rTMS was able to reduce pain sensation, as supported by several recent studies, like spinal cord injury (12), migraine (13) and fibromyalgia (14). In this study, we hypothesized that DLPFC-rTMS may also be effective in the treatment of cancer pain and thus conducted this trial. In our trial, the pain intensity in the rTMS group at week 3 was decreased by 2.7 points from baseline, which was significantly higher than the 1.5 points in the sham group. The pain reduction of 2.7 points in the rTMS group exceeded the 2-point reduction by using NRS scale that has been recommended as a clinically significant improvement by the IMMPACT study (24). Meanwhile, we also found that DLPFC-rTMS can reduce the dosage of opioids in NSCLC patients with cancer pain. Reduced pain intensity, together with less opioid dose, revealed the clinical benefit of DLPFC-rTMS in the treatment of cancer pain in NSCLC patients.

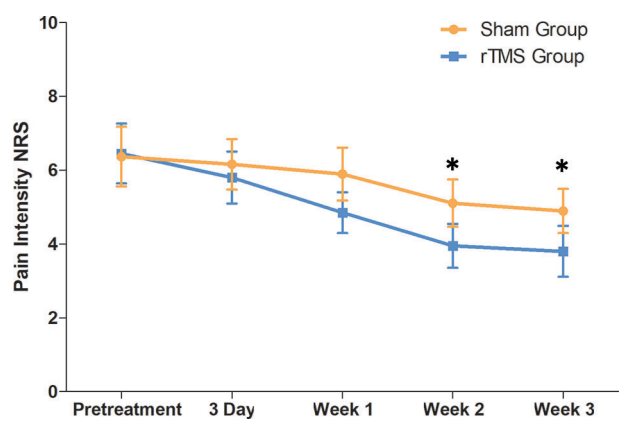


**FIGURE 3** | Raw scores on primary outcome (NRS) from baseline to 3 weeks. The NRS scores were calculated by the average for the preceding 7 days. Error bars indicate 95% confidence intervals, * indicate significant inter-group difference, $P < 0.05$. NRS, numeric rating scale.

In addition to pain, it is evident that mood disorders are also a major problem for NSCLC patients. Undertreatment of cancer pain is often accompanied by physical fitness decline, fatigue and sleep disorders, and even anxiety and depression, which obviously increase the difficulty of analgesic treatment and reduce the quality of life for patients (9). Our data on anxiety and depression, from HAMA and HAMD also demonstrated the existence of poor psychological status among NSCLC patients with cancer pain, which was consistent with the previous studies (32, 33). Therefore, we should pay special attention to the treatment of psychological disorders in patients with cancer pain (16, 34). As shown in this study, improvements in anxiety and depression were significant higher in the rTMS group than that of in the sham group ($P<0.05$). We have also found that DLPFC-rTMS treatment could significantly improve the quality of life versus sham stimulation. This finding is consistent with the role of the DLPFC in modulating brain regions involved in emotions such as the anterior cingulate cortex and insular cortex (35, 36). DLPFC-rTMS has been approved in the US FDA to treat major depressive disorder in adults who have not responded to prior antidepressant medications (19), and this effect might account for the improvement of the mood disorders in patients who were treated with DLPFC-rTMS in this study.

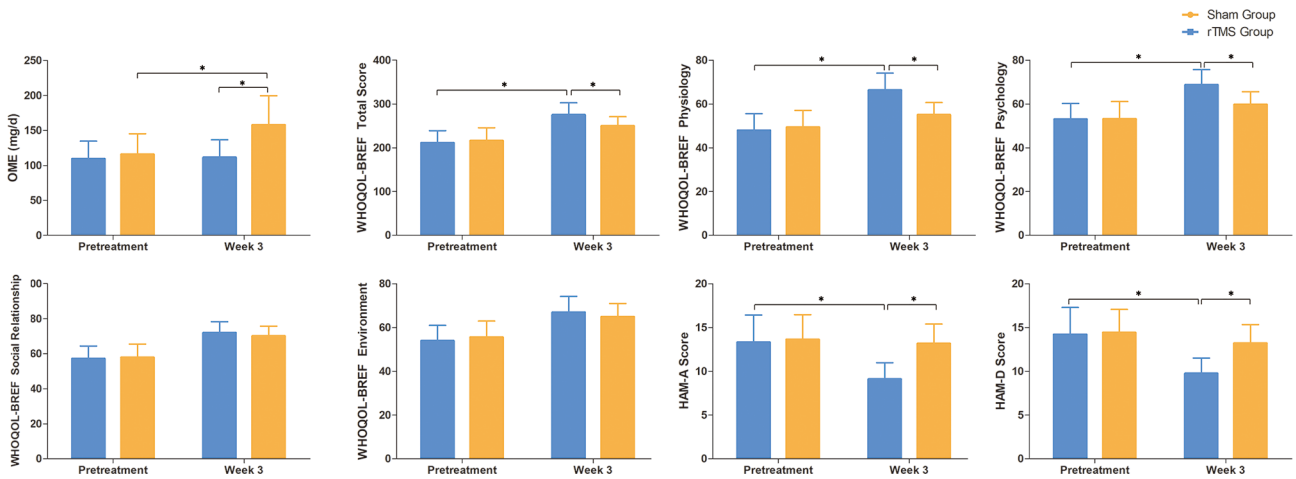


**FIGURE 4** | Raw scores on secondary outcomes at baseline and weeks 3. Error bars indicate 95% confidence intervals, * indicate significant inter-group or pre-post differences, $P < 0.05$. OME, Oral morphine equivalent; WHOQL-BREF, WHO Quality of Life-BREF; HAM-A, Hamilton Anxiety Scale; HAM-D, Hamilton Depression Scale.

There are some strengths in this study. We provided the first clinical RCT study in which high frequency rTMS over the DLPFC is able to decrease cancer pain in advanced NSCLC patients. The undertreatment of cancer pain is still very common in clinic. Clinicians usually gradually increase the dose of analgesic medications. If the findings of this study were further confirmed by multicenter, large sample clinical trials, rTMS could be used clinically as a convenient and effective non-drug adjuvant therapeutic tool. Meanwhile, we also evaluated the outcome comprehensively and appropriately. The outcome measures in our study were consistent with IMMPACT recommendations for chronic pain (24, 37), including measures of dosage of opioids, pain intensity, physical functioning, mood status and quality of life, which ensured a comprehensive evaluation of the treatment. However, there are also some limitations in this study. First, the relatively small number of participants and a single-center trial design is the main limitation of our study, which may increase the risk of type II error. Future large-scale multicenter studies are needed to ameliorate this limitation. Second, due to the small sample size, we didn't conduct further subgroup analysis to explore the differences in the efficacy of rTMS in patients with different stages of metastasis. Third, it is unknown whether the analgesic effects of rTMS on patients with cancer pain are long-lasting, due to lack of long-term follow-up. Fourth, the effects of rTMS on patients' sleep quality and the cost-effective analysis of rTMS on pain treatment are also very interesting questions, future studies could further explore them.

In conclusion, our results support the use of rTMS as a promising adjuvant therapeutic tool for cancer pain, with its dual beneficial effect in decreasing pain intensity and psychological distress in advanced NSCLC patients. If this effect can be confirmed in future larger sample studies, it will undoubtedly have a better clinical application prospect for patients with cancer pain.

## DATA AVAILABILITY STATEMENT

The raw data supporting the conclusions of this article will be made available by the authors, without undue reservation.

## ETHICS STATEMENT

The studies involving human participants were reviewed and approved by Ethics Committee of Chongqing Cancer Hospital. The patients/participants provided their written informed consent to participate in this study. Written informed consent was obtained from the individual(s) for the publication of any potentially identifiable images or data included in this article.

## AUTHOR CONTRIBUTIONS

YT and Y-sL conceived and designed the study. YT and HC analyzed the experimental data and drafted the manuscript. YT, M-lT, and YZ collected the experimental data. Y-sL, S-lX, YL and X-hJ revised the manuscript for important intellectual content. All authors contributed to the article and approved the submitted version.

## FUNDING

This study was supported by the National Nature Science Foundation of China (81902302) and Chongqing Natural Science Foundation (cstc2018jcyjAX0772).

## REFERENCES


1. Mao JJ, Pillai GG, Andrade CJ, Ligibel JA, Basu P, Cohen L, et al. Integrative Oncology: Addressing the Global Challenges of Cancer Prevention and Treatment. *CA Cancer J Clin* (2022) 72(2):144–64. doi: 10.3322/caac.21706
2. Neufeld NJ, Elnahal SM, Alvarez RH. Cancer Pain: A Review of Epidemiology, Clinical Quality and Value Impact. *Future Oncol* (2017) 13 (9):833–41. doi: 10.2217/fon-2016-0423
3. Goudas LC, Bloch R, Gialeli-Goudas M, Lau J, Carr DB. The Epidemiology of Cancer Pain. *Cancer Invest* (2005) 23(2):182–90. doi: 10.1081/CNV-200050482
4. Wu LL, Li CW, Lin WK, Qiu LH, Xie D. Incidence and Survival Analyses for Occult Lung Cancer Between 2004 and 2015: A Population-Based Study. *BMC Cancer* (2021) 21(1):1009. doi: 10.1186/s12885-021-08741-4
5. Mantyh PW. Cancer Pain and its Impact on Diagnosis, Survival and Quality of Life. *Nat Rev Neurosci* (2006) 7(10):797–809. doi: 10.1038/nrn1914
6. Wilton J, Abdia Y, Chong M, Karim ME, Wong S, MacInnes A, et al. Prescription Opioid Treatment for non-Cancer Pain and Initiation of Injection Drug Use: Large Retrospective Cohort Study. *BMJ* (2021) 375: e066965. doi: 10.1136/bmj-2021-066965
7. WHO. *World Health Organization Cancer Pain Relief, With a Guide to Opioid Availability. ed 2*. Geneva, Switzerland: World Health Organization (1996).
8. Fallon M, Giusti R, Aielli F, Hoskin P, Rolke R, Sharma M, et al. Management of Cancer Pain in Adult Patients: ESMO Clinical Practice Guidelines. *Ann Oncol* (2018) 29(Suppl 4):iv166–iv91. doi: 10.1093/annonc/mdy152
9. Deandrea S, Montanari M, Moja L, Apolone G. Prevalence of Undertreatment in Cancer Pain. A Review of Published Literature. *Ann Oncol* (2008) 19 (12):1985–91. doi: 10.1093/annonc/mdn419
10. Jiang X, Yan W, Wan R, Lin Y, Zhu X, Song G, et al. Effects of Repetitive Transcranial Magnetic Stimulation on Neuropathic Pain: A Systematic Review and Meta-Analysis. *Neurosci Biobehav Rev* (2022) 132(1):130–41. doi: 10.1016/j.neubiorev.2021.11.037
11. Edemann-Callesen H, Winter C, Hadar R. Using Cortical non-Invasive Neuromodulation as a Potential Preventive Treatment in Schizophrenia - A Review. *Brain Stimul* (2021) 14(3):643–51. doi: 10.1016/j.brs.2021.03.018
12. Zhang KL, Yuan H, Wu FF, Pu XY, Liu BZ, Li Z, et al. Analgesic Effect of Noninvasive Brain Stimulation for Neuropathic Pain Patients: A Systematic Review. *Pain Ther* (2021) 10(1):315–32. doi: 10.1007/s40122-021-00252-1
13. Ornello R, Caponnetto V, Ratti S, D'Aurizio G, Rosignoli C, Pistoia F, et al. Which is the Best Transcranial Direct Current Stimulation Protocol for Migraine Prevention? A Systematic Review and Critical Appraisal of Randomized Controlled Trials. *J Headache Pain* (2021) 22(1):144. doi: 10.1186/s10194-021-01361-0
14. Su YC, Guo YH, Hsieh PC, Lin YC. Efficacy of Repetitive Transcranial Magnetic Stimulation in Fibromyalgia: A Systematic Review and Meta-Analysis of Randomized Controlled Trials. *J Clin Med* (2021) 10(20):4669. doi: 10.3390/jcm10204669
15. Kandic M, Moliadze V, Andoh J, Flor H, Nees F. Brain Circuits Involved in the Development of Chronic Musculoskeletal Pain: Evidence From Non-Invasive Brain Stimulation. *Front Neurol* (2021) 12:732034. doi: 10.3389/fneur.2021.732034
16. Lyman GH, Greenlee H, Bohlke K, Bao T, DeMichele AM, Deng GE, et al. Integrative Therapies During and After Breast Cancer Treatment: ASCO Endorsement of the SIO Clinical Practice Guideline. *J Clin Oncol* (2018) 36 (25):2647–55. doi: 10.1200/JCO.2018.79.2721
17. Cappon D, den Boer T, Jordan C, Yu W, Metzger E, Pascual-Leone A. Transcranial Magnetic Stimulation (TMS) for Geriatric Depression. *Ageing Res Rev* (2022) 74(2):101531. doi: 10.1016/j.arr.2021.101531
18. Che X, Cash RFH, Luo X, Luo H, Lu X, Xu F, et al. High-Frequency rTMS Over the Dorsolateral Prefrontal Cortex on Chronic and Provoked Pain: A Systematic Review and Meta-Analysis. *Brain Stimul* (2021) 14(5):1135–46. doi: 10.1016/j.brs.2021.07.004
19. Perera T, George MS, Grammer G, Janicak PG, Pascual-Leone A, Wirecki TS. The Clinical TMS Society Consensus Review and Treatment Recommendations for TMS Therapy for Major Depressive Disorder. *Brain Stimul* (2016) 9(3):336–46. doi: 10.1016/j.brs.2016.03.010
20. Clark O, Mahjoub A, Osman N, Surmava AM, Jan S, Lagman-Bartolome AM. Non-Invasive Neuromodulation in the Acute Treatment of Migraine: A Systematic Review and Meta-Analysis of Randomized Controlled Trials. *Neurol Sci* (2022) 43(1):153–65. doi: 10.1007/s10072-021-05664-7
21. Bandieri E, Romero M, Ripamonti CI, Artioli F, Sichetti D, Fanizza C, et al. Randomized Trial of Low-Dose Morphine Versus Weak Opioids in Moderate Cancer Pain. *J Clin Oncol* (2016) 34(5):436–42. doi: 10.1200/JCO.2015.61.0733
22. Rossi S, Hallett M, Rossini PM, Pascual-Leone A. And Safety of TMSCG. Safety, Ethical Considerations, and Application Guidelines for the Use of Transcranial Magnetic Stimulation in Clinical Practice and Research. *Clin Neurophysiol* (2009) 120(12):2008–39. doi: 10.1016/j.clinph.2009.08.016
23. Zhao CG, Sun W, Ju F, Jiang S, Wang H, Sun XL, et al. Analgesic Effects of Navigated Repetitive Transcranial Magnetic Stimulation in Patients With Acute Central Poststroke Pain. *Pain Ther* (2021) 10(2):1085–100. doi: 10.1007/s40122-021-00261-0
24. Dworkin RH, Turk DC, Farrar JT, Haythornthwaite JA, Jensen MP, Katz NP, et al. Core Outcome Measures for Chronic Pain Clinical Trials: IMMPACT Recommendations. *Pain* (2005) 113(1-2):9–19. doi: 10.1016/j.pain.2004.09.012
25. Hale M, Wild J, Reddy J, Yamada T, Arjona Ferreira JC. Naldemedine Versus Placebo for Opioid-Induced Constipation (COMPOSE-1 and COMPOSE-2): Two Multicentre, Phase 3, Double-Blind, Randomised, Parallel-Group Trials. *Lancet Gastroenterol Hepatol* (2017) 2(8):555–64. doi: 10.1016/S2468-1253(17)30105-X
26. Xia P, Li N, Hau KT, Liu C, Lu Y. Quality of Life of Chinese Urban Community Residents: A Psychometric Study of the Mainland Chinese Version of the WHOQOL-BREF. *BMC Med Res Methodol* (2012) 12:37. doi: 10.1186/1471-2288-12-37
27. Hamilton M. The Assessment of Anxiety States by Rating. *Br J Med Psychol* (1959) 32(1):50–5. doi: 10.1111/j.2044-8341.1959.tb00467.x
28. Hamilton M. A Rating Scale for Depression. *J Neurol Neurosurg Psychiatry* (1960) 23:56–62. doi: 10.1136/jnnp.23.1.56
29. Hosomi K, Sugiyama K, Nakamura Y, Shimokawa T, Oshino S, Goto Y, et al. A Randomized Controlled Trial of 5 Daily Sessions and Continuous Trial of 4 Weekly Sessions of Repetitive Transcranial Magnetic Stimulation for Neuropathic Pain. *Pain* (2020) 161(2):351–60. doi: 10.1097/j.pain.0000000000001712
30. Tracey I, Mantyh PW. The Cerebral Signature for Pain Perception and its Modulation. *Neuron* (2007) 55(3):377–91. doi: 10.1016/j.neuron.2007.07.012
31. Martin L, Borckardt JJ, Reeves ST, Frohman H, Beam W, Nahas Z, et al. A Pilot Functional MRI Study of the Effects of Prefrontal rTMS on Pain Perception. *Pain Med* (2013) 14(7):999–1009. doi: 10.1111/pme.12129
32. Johannsen M, O'Connor M, O'Toole MS, Jensen AB, Hojris I, Zachariae R. Efficacy of Mindfulness-Based Cognitive Therapy on Late Post-Treatment Pain in Women Treated for Primary Breast Cancer: A Randomized Controlled Trial. *J Clin Oncol* (2016) 34(28):3390–9. doi: 10.1200/JCO.2015.65.0770
33. Bradt J, Dileo C, Myers-Coffman K, Biondo J. Music Interventions for Improving Psychological and Physical Outcomes in People With Cancer. *Cochrane Database Syst Rev* (2021) 10:CD006911. doi: 10.1002/14651858.CD006911.pub4
34. Greenlee H, DuPont-Reyes MJ, Balneaves LG, Carlson LE, Cohen MR, Deng G, et al. Clinical Practice Guidelines on the Evidence-Based Use of Integrative Therapies During and After Breast Cancer Treatment. *CA Cancer J Clin* (2017) 67(3):194–232. doi: 10.3322/caac.21397
35. Che X, Cash R, Chung SW, Bailey N, Fitzgerald PB, Fitzgibbon BM. The Dorsomedial Prefrontal Cortex as a Flexible Hub Mediating Behavioral as Well as Local and Distributed Neural Effects of Social Support Context on Pain: A Theta Burst Stimulation and TMS-EEG Study. *Neuroimage* (2019) 201:116053. doi: 10.1016/j.neuroimage.2019.116053
36. Ferenczi EA, Zalocusky KA, Liston C, Grosenick L, Warden MR, Amatya D, et al. Prefrontal Cortical Regulation of Brainwide Circuit Dynamics and Reward-Related Behavior. *Science* (2016) 351(6268):aac9698. doi: 10.1126/science.aac9698
37. Jiang J, Li Y, Shen Q, Rong X, Huang X, Li H, et al. Effect of Pregabalin on Radiotherapy-Related Neuropathic Pain in Patients With Head and Neck

Cancer: A Randomized Controlled Trial. *J Clin Oncol* (2019) 37(2):135–43. doi: 10.1200/JCO.18.00896

**Conflict of Interest:** The authors declare that the research was conducted in the absence of any commercial or financial relationships that could be construed as a potential conflict of interest.

**Publisher's Note:** All claims expressed in this article are solely those of the authors and do not necessarily represent those of their affiliated organizations, or those of the publisher, the editors and the reviewers. Any product that may be evaluated in this article, or claim that may be made by its manufacturer, is not guaranteed or endorsed by the publisher.

frontiers | Frontiers in Oncology

REVIEW
published: 20 April 2022
doi: 10.3389/fonc.2022.780186

# A Review of the Correlation Between Epidermal Growth Factor Receptor Mutation Status and $^{18}$F-FDG Metabolic Activity in Non-Small Cell Lung Cancer

*Maoqing Jiang[1,2,3], Xiaohui Zhang[1,2], Yan Chen[4], Ping Chen[5], Xiuyu Guo[1,2], Lijuan Ma[1,2], Qiaoling Gao[1,2], Weiqi Mei[3], Jingfeng Zhang[6] and Jianjun Zheng[1,2]**

*[1] Department of PET/CT Center, Hwa Mei Hospital, University of Chinese Academy of Sciences, Ningbo, China, [2] Ningbo Institute of Life and Health Industry, University of Chinese Academy of Sciences, Ningbo, China, [3] Department of Nuclear Medicine, Hwa Mei Hospital, University of Chinese Academy of Sciences, Ningbo, China, [4] Department of Physical Examination Center, Ningbo First Hospital, Ningbo, China, [5] Department of Nephrology, Hwa Mei Hospital, University of Chinese Academy of Sciences, Ningbo, China, [6] Department of Education, Hwa Mei Hospital, University of Chinese Academy of Sciences, Ningbo, China*

OPEN ACCESS

**Edited by:**
*Luciano Mutti,*
*Temple University, United States*

**Reviewed by:**
*Vassilis Georgoulias,*
*University of Crete, Greece*
*Letizia Gnetti,*
*University Hospital of Parma, Italy*

***Correspondence:**
*Jianjun Zheng*
*zhengjianjun@ucas.ac.cn*

**Specialty section:**
*This article was submitted to Thoracic Oncology, a section of the journal Frontiers in Oncology*

**Received:** *20 September 2021*
**Accepted:** *25 March 2022*
**Published:** *20 April 2022*

**Citation:**
*Jiang M, Zhang X, Chen Y, Chen P, Guo X, Ma L, Gao Q, Mei W, Zhang J and Zheng J (2022) A Review of the Correlation Between Epidermal Growth Factor Receptor Mutation Status and $^{18}$F-FDG Metabolic Activity in Non-Small Cell Lung Cancer. Front. Oncol. 12:780186. doi: 10.3389/fonc.2022.780186*

PET/CT with $^{18}$F-2-fluoro-2-deoxyglucose ($^{18}$F-FDG) has been proposed as a promising modality for diagnosing and monitoring treatment response and evaluating prognosis for patients with non-small cell lung cancer (NSCLC). The status of epidermal growth factor receptor (EGFR) mutation is a critical signal for the treatment strategies of patients with NSCLC. Higher response rates and prolonged progression-free survival could be obtained in patients with NSCLC harboring EGFR mutations treated with tyrosine kinase inhibitors (TKIs) when compared with traditional cytotoxic chemotherapy. However, patients with EGFR mutation treated with TKIs inevitably develop drug resistance, so predicting the duration of resistance is of great importance for selecting individual treatment strategies. Several semiquantitative metabolic parameters, e.g., maximum standard uptake value ($SUV_{max}$), metabolic tumor volume (MTV), and total lesion glycolysis (TLG), measured by PET/CT to reflect $^{18}$F-FDG metabolic activity, have been demonstrated to be powerful in predicting the status of EGFR mutation, monitoring treatment response of TKIs, and assessing the outcome of patients with NSCLC. In this review, we summarize the biological and clinical correlations between EGFR mutation status and $^{18}$F-FDG metabolic activity in NSCLC. The metabolic activity of $^{18}$F-FDG, as an extrinsic manifestation of NSCLC, could reflect the mutation status of intrinsic factor EGFR. Both of them play a critical role in guiding the implementation of treatment modalities and evaluating therapy efficacy and outcome for patients with NSCLC.

**Keywords: non-small cell lung cancer, epidermal growth factor receptor, tyrosine kinase inhibitors, positron emission tomography, $^{18}$F-FDG**

## INTRODUCTION

In 2020, it was estimated that there were approximately 228,820 newly diagnosed lung cancer cases and 135,720 deaths from lung cancer in the United States (1). Non-small cell lung cancer (NSCLC), a major phenotype of lung cancer, accounting for about 80%–85%, is one of the leading causes of cancer-related deaths worldwide despite improvements in diagnostic and therapeutic modalities (1, 2). Epidermal growth factor receptor (EGFR) mutations were found in about 35% of patients with NSCLC in East Asia and 10%–15% in the United States (3, 4). In addition, EGFR mutations were demonstrated to be significantly associated with adenocarcinoma, never smoking, and the female gender (5). Patients with EGFR mutations treated with tyrosine kinase inhibitors (TKIs) were linked to a higher response rate and longer progression-free survival (PFS) than those treated with conventional cytotoxic chemotherapy (6, 7). Eventually, however, resistance to TKIs inevitably occurred with a median PFS of 9 to 13 months (7–9). In this regard, accurate prediction of EGFR mutations and monitoring of TKI response rates and drug resistance will be of great value for clinicians to perform individual treatment strategies.

PET/CT with $^{18}$F-2-fluoro-2-deoxyglucose ($^{18}$F-FDG) has been widely used for pretreatment staging and restaging, monitoring treatment response, and evaluating prognosis for patients with NSCLC (10–14). Several semiquantitative metabolic parameters, e.g., maximal standard uptake value ($SUV_{max}$), total lesion glycolysis (TLG), and metabolic tumor volume (MTV), have been demonstrated to be promising PET/CT indices to reflect the metabolic activity and/or tumor burden (15, 16). $SUV_{max}$, a parameter representing the maximum uptake value of $^{18}$F-FDG in a single-pixel adjusted for lean body mass, has been widely used as a marker for glucose metabolic activity, but it cannot clearly reflect tumor burden. TLG, a quantitative volume-based metabolic PET parameter, has been recognized as a promising index for its advantages to reflect the metabolic activity and tumor burden. Higher $SUV_{max}$, TLG, or MTV on $^{18}$F-FDG PET/CT scan usually revealed a short PFS or overall survival (OS) for patients with NSCLC (17–19). Consequently, a certain cross and overlap may have occurred between the roles of $^{18}$F-FDG PET/CT and EGFR in evaluating the efficacy and outcome of NSCLC patients.

Over the past two decades, a great number of studies have attempted to elucidate the relationship between the status of EGFR mutation and the metabolic activity of $^{18}$F-FDG in NSCLC (20–23). Obviously, EGFR mutation status represents an intrinsic factor of NSCLC, while $^{18}$F-FDG metabolic activity is an extrinsic manifestation of NSCLC. There is a close association between EGFR mutation status and $^{18}$F-FDG metabolic activity in NSCLC, but the relationship between them needs to be further clarified due to contradictory reports (24–26). A large sample study including 849 patients with NSCLC showed that low $SUV_{max}$ of the primary tumor, lymph node, and distant metastasis were associated significantly with EGFR mutations (24), whereas another study presented opposite results that high $SUV_{max}$ (≥6.0) of the primary tumor was more likely to have EGFR mutations in NSCLC (25). In addition, no significant difference in $^{18}$F-FDG uptake between mutant EGFR and wild-type EGFR was also observed in NSCLC patients (26). Accordingly, in this work, we aimed to comprehensively review the biological and clinical correlations between EGFR mutation status and $^{18}$F-FDG metabolic activity in NSCLC.

## BIOLOGICAL CORRELATION BETWEEN EPIDERMAL GROWTH FACTOR RECEPTOR MUTATION STATUS AND $^{18}$F-FDG METABOLIC ACTIVITY IN NON-SMALL CELL LUNG CANCER

Tumor cells utilize a variety of metabolic pathways, especially glucose, to meet the requirements of bioenergy and biosynthesis for growth and proliferation (27, 28). Oncogenic mutations are the driving force of high energetic metabolism that can be maintained persistently in cancer cells (29). In addition, glucose metabolism preferentially tends to aerobic glycolysis rather than mitochondrial oxidative phosphorylation, which is known as the Warburg effect (27). It has been reported that many oncogenic signaling pathways in cancer cells, particularly EGFR aberrant signaling, lead to the metabolic switch from mitochondrial oxidative phosphorylation to aerobic glycolysis (30, 31). Recently, EGFR has been identified as a driver of oncogenes in NSCLC, because the mutation of activating EGFR kinase domain enhances the activity of EGFR tyrosine kinase, leading to continuous activation of the downstream signal pathway, and then drives tumorigenesis and tumor progression (32). Targeted EGFR mutation therapies, such as EGFR-TKIs, including erlotinib and gefitinib, have shown to be highly effective in inhibiting glucose consumption in both *in vitro* and *in vivo* models of NSCLC (**Figure 1**) (33, 34).

$^{18}$F-FDG, a glucose analog, is transported into cells by glucose transporters (GLUTs) and phosphorylated to $^{18}$F-FDG-6-phosphate by hexokinase (HK). It is trapped inside cells and dephosphorylated slowly because $^{18}$F-FDG-6-phosphate is not a substrate of glycolysis or pentose phosphate pathway (PPP) and is unable to diffuse outside cells (**Figure 1**) (35). Now, it has been widely used as a small molecule radiotracer for PET/CT imaging and has been applied extensively as a tracer to reflect glucose metabolic activity in diagnosing and evaluating treatment response of various malignant tumors, including NSCLC (36, 37). The overexpression of GLUT1 and HK-I is highly associated with the increased uptake of $^{18}$F-FDG in NSCLC, showing that the uptake of $^{18}$F-FDG seems to be regulated by glucose metabolism (38–40).

Several mutated oncogenes have been demonstrated to be associated with metabolic signaling pathways that affect tumor cell metabolism (41). In EGFR-mutated adenocarcinoma cells, lactate production, glucose-induced extracellular acidification rate, and glucose consumption were significantly decreased after treatment with TKIs, showing that EGFR signaling played a major role in aerobic glycolysis (33). In gefitinib-sensitive NSCLC cell lines with EGFR mutations, the uptake of $^{18}$F-FDG was also decreased significantly as early as 2 h after treatment,

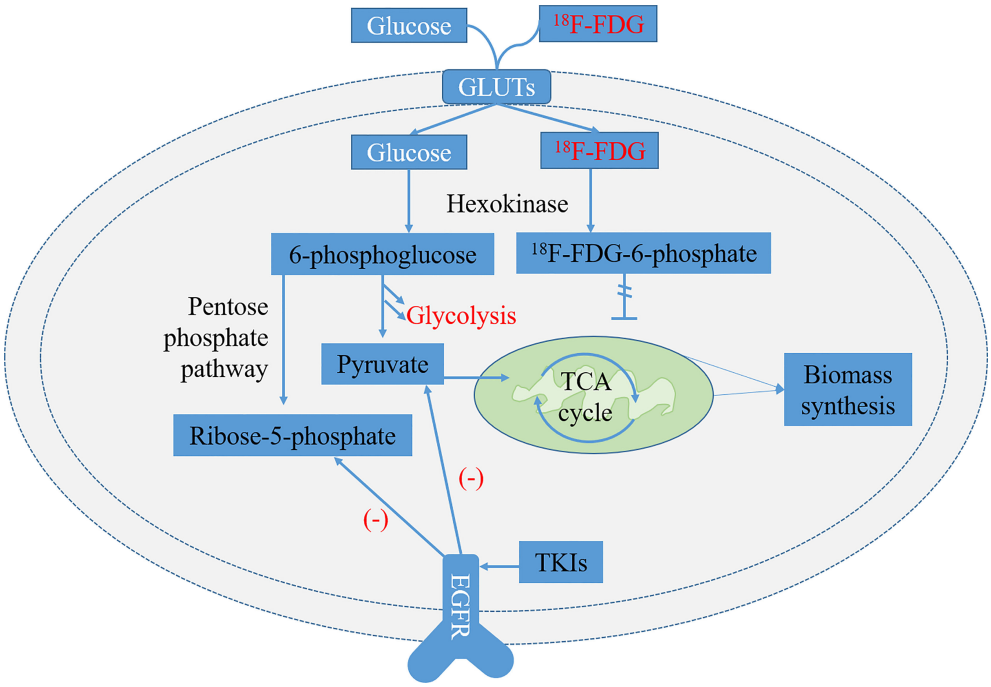


**FIGURE 1** | Glycolysis pathways of $^{18}$F-FDG and normal glucose and related metabolic pathways regulated by epidermal growth factor receptor (EGFR) signaling in EGFR-mutated non-small cell lung cancer (NSCLC). $^{18}$F-FDG is transported into cells by glucose transporters (GLUTs) and phosphorylated to $^{18}$F-FDG-6-phosphate by hexokinase (HK). It is trapped inside cells because $^{18}$F-FDG-6-phosphate is not a substrate of glycolysis or pentose phosphate pathway (PPP) and is unable to diffuse outside cells. The metabolites of pyruvate and ribose-5-phosphate in the glycolysis decreased significantly after treatment of lung adenocarcinoma cells with EGFR tyrosine kinase inhibitors (TKIs) (33).

whereas no measurable changes in $^{18}$F-FDG uptake were observed in gefitinib-resistant cells, representing treatment response of gefitinib that could be closely reflected by glucose metabolic activity (34). Accordingly, to a certain extent, the metabolic activity of $^{18}$F-FDG in NSCLC cell lines is correlated with or may reflect the mutations of EGFR.

## CLINICAL CORRELATION BETWEEN EPIDERMAL GROWTH FACTOR RECEPTOR MUTATION STATUS AND $^{18}$F-FDG METABOLIC ACTIVITY IN NON-SMALL CELL LUNG CANCER

### Predicting Epidermal Growth Factor Receptor Mutation Status With $^{18}$F-FDG PET/CT

A large number of studies reported that compared with traditional cytotoxic chemotherapy, NSCLC patients with EGFR mutation treated with TKIs had a higher response rate and prolonged PFS (6, 7). The presence of EGFR gene mutations in lung adenocarcinoma is a powerful predictor of better prognosis after gefitinib therapy (9). Accordingly, the status of EGFR mutations plays a critical role in selecting suitable treatment modalities for patients with NSCLC. However, in clinical practice, the status of EGFR mutation is usually determined by tissue-based analysis (42), which has a number of limitations, e.g., i) sampling bias due to tumor heterogeneous, ii) associated complications owing to invasive biopsies, iii) not rapid and expensive, and iv) failing to get reliable results due to the low quantity or quality of the tissue samples (43). In addition, the mutation status of EGFR may be changed in the course of chemotherapy or targeted therapy (44). Therefore, a non-invasive method is urgently needed to monitor EGFR mutation status in NSCLC.

PET/CT scan with $^{18}$F-FDG, a non-invasive and functional imaging method, has a powerful ability to predict the mutation status of EGFR in NSCLC (45–47). $SUV_{max}$ is the most widely used index of $^{18}$F-FDG PET/CT in predicting EGFR mutations (24). Patients with NSCLC harboring EGFR mutations usually showed lower $SUV_{max}$ than those with wild-type EGFR (**Table 1**) (21, 24, 48, 49). Normally, $SUV_{max}$ was calculated only from the primary lesions of NSCLC, whereas the distant metastasis and/or metastatic lymph nodes were also monitored in some studies (24, 50). Low $SUV_{max}$ of the distant metastasis was beneficial to the existence of EGFR mutations in advanced lung adenocarcinoma (50). Different cutoff values of $SUV_{max}$ (range, 7.0–9.91) were determined to obtain a relatively high receiver operating characteristic (ROC) curve area (range, 0.557–0.75) (20, 24, 50). In addition to $SUV_{max}$, MTV was also used as a parameter to predict EGFR mutations in NSCLC. Patients with NSCLC

**TABLE 1** | The clinical and pathological features, glucose metabolic activity, and EGFR mutation status in NSCLC of previous studies.

| Studies | No. of patients | | Stage (n) | | Histopathology (n) | | | Lesions measured | | | Metabolic parameters | | | EGFR status (n) | | Metabolic parameters favor EGFR mutation in NSCLC |
|---|---|---|---|---|---|---|---|---|---|---|---|---|---|---|---|---|
| | Male | Female | I–II | III–IV | ADC | SCC | Other | PT | LN | MT | $SUV_{max}$ | MTV | TLG | Mutant | Wild type | |
| Lv et al. (24) | 468 | 340 | 191 | 617 | 731 | 58 | 19 | √ | √ | √ | √ | – | – | 371 | 437 | Low $SUV_{max}$ in PT |
| Mak et al. (21) | 39 | 61 | 40 | 60 | 55 | 2 | 43 | √ | – | √ | √ | – | – | 24 | 76 | Low $SUV_{max}$ in PT |
| Cho et al. (48) | 33 | 28 | 26 | 35 | 57 | 2 | 2 | √ | – | – | √ | – | √ | 30 | 31 | Low $SUV_{max}$ in PT |
| Gao et al. (49) | 87 | 80 | 8 | 159 | 162 | 5 | 0 | √ | √ | – | √ | – | – | 73 | 94 | Low $SUV_{max}$ in PT and LN |
| Lee et al. (50) | 33 | 38 | 0 | 71 | 71 | – | – | √ | √ | √ | √ | – | – | 48 | 23 | Low $SUV_{max}$ in MT |
| Na et al. (20) | 68 | 32 | 57 | 43 | 53 | 40 | 7 | √ | – | – | √ | – | – | 21 | 79 | Low $SUV_{max}$ in PT |
| Gu et al. (51) | 132 | 78 | 58 | 152 | 161 | 34 | 15 | √ | – | – | √ | – | – | 70 | 140 | Low $SUV_{max}$ (<9.0) in PT |
| Ko et al. (25) | 57 | 75 | 49 | 83 | 132 | – | – | √ | – | – | √ | – | – | 69 | 63 | High $SUV_{max}$ (>6.0) in PT |
| Wang et al. (52) | 189 | 122 | 40 | 271 | 233 | 44 | 34 | √ | – | √ | √ | – | – | 128 | 183 | High $SUV_{max}$ (>11.2) in PT |
| Kanmaz et al. (53) | 151 | 67 | 18 | 200 | 218 | – | – | NS | NS | NS | √ | – | – | 63 | 155 | High $SUV_{max}$ |
| Huang et al. (54) | 33 | 44 | 0 | 77 | 77 | – | – | √ | – | – | √ | – | – | 49 | 28 | Higher $SUV_{max}$ in PT |
| Chung et al. (15) | 63 | 43 | 19 | 87 | 106 | – | – | √ | √ | √ | √ | √ | √ | 42 | 64 | No correlation |
| Choi et al. (55) | 99 | 64 | 0 | 163 | 130 | 27 | 6 | √ | – | – | √ | – | – | 57 | 106 | No significant difference of $SUV_{max}$ in PT |
| Caicedo et al. (26) | 62 | 40 | 0 | 102 | 88 | 6 | 8 | NS | NS | NS | √ | – | – | 22 | 80 | No significant difference of $SUV_{max}$ |
| Lee et al. (56) | 148 | 58 | 22 | 184 | 135 | 71 | – | √ | – | – | √ | – | – | 47 | 159 | No significant difference |

*ADC, adenocarcinoma; SCC, squamous cell carcinoma; PT, primary tumor; LN, lymph nodes; MT, metastatic; MTV, metabolic tumor volume; TLG, total lesion glycolysis; EGFR, epidermal growth factor receptor; NSCLC, non-small cell lung cancer; NS, not specified; "-", not done.*

harboring EGFR mutation had lower MTV than those with wild-type EGFR (57). Interestingly, the serum carcinoembryonic antigen (CEA) can increase during all adenocarcinomas not only in those EGFR mutated but also in wild type (58). The combination of serum CEA and $SUV_{max}$ was also performed to predict EGFR mutations in patients with NSCLC, which demonstrated to have a moderate diagnostic accuracy (25, 51).

However, opposite results could be observed that the metabolic activity of $^{18}$F-FDG (e.g., $SUV_{max}$) in NSCLC EGFR-mutant patients was significantly higher than that of wild-type patients (25, 52–54). The expression status of EGFR protein was also evaluated, and higher $SUV_{max}$ was positively correlated with EGFR overexpression (59, 60). Furthermore, no significant difference in $^{18}$F-FDG uptake was observed between EGFR mutant and wild-type NSCLC patients in previous reports (**Table 1**) (26, 55, 56). Several reasons could lead to these conflicting results. First, the number of patients included in the studies varied widely, as low as only 61 patients and as high as up to 808 patients (24, 48, 57). Second, the rate of EGFR mutations varied greatly among NSCLC patients, from 21% to 68% (20, 50). Third, the proportion of histopathological subtypes of NSCLC (adenocarcinoma and squamous cell carcinoma) varied significantly, as EGFR mutations are difficult to detect in squamous cell carcinoma patients who smoke, while EGFR mutations are more common in adenocarcinoma (20, 21, 61). Fourth, the clinical stage (I–II vs. advanced stage) of patients with NSCLC was significantly different (25, 26). More importantly, multiple objective reasons, e.g., different PET/CT scanners, the plasma glucose level before PET/CT scan, fasting time, and region of interest parameters might result in contradictory results. Therefore, many novel techniques of PET/CT are performed to investigate the predictive efficacy of EGFR mutations in NSCLC.

Radiomics, an advanced mathematical model for quantifying the spatial relationships among image voxels, has become a growing research field in which a great number of imaging features are investigated in order to choose the most significantly relevant features with clinical, pathological, molecular, and genetic features, so as to improve the accuracy of diagnosis, prognosis, and curative effect evaluation (62, 63). Accordingly, the role of $^{18}$F-FDG PET/CT radiomics in predicting EGFR mutation status for patients with NSCLC has been evaluated (47, 64–67). The area under the ROC curve (AUC) was usually in the range of 0.57 to 0.86 when based on the radiomics features of PET/CT, whereas the performance would get a significantly higher efficacy when combined with clinical features and/or conventional PET/CT parameters, such as $SUV_{max}$, SUVmean, MTV, and TLG (47, 67, 68). In addition, four exons (18–21) of EGFR mutations have been observed in NSCLC patients (69), in which approximately 90% are exon 21 L858R substitutions and exon 19 deletions (70). Recently, research showed that two sets of prognostic radiomics features of $^{18}$F-FDG PET/CT could distinguish EGFR exon 19 deletions from EGFR exon 21 L858R missense, with an AUC of 0.87 in predicting EGFR mutation status (46).

In short, detection of EGFR mutation status in NSCLC plays a major role in the daily management of individual patients, especially in the selection of TKI targeted therapy. $^{18}$F-FDG PET/CT has been demonstrated to have a powerful efficacy to predict the EGFR mutation status in patients with NSCLC, not only based on conventional PET/CT parameters (e.g., $SUV_{max}$, MTV, and TLG) but also based on radiomics of PET/CT. The combination of clinical features, laboratory results, conventional PET/CT parameters, and PET/CT radiomics would provide higher accuracy in predicting EGFR mutation status. However, there are still many contradictory reports, so $^{18}$F-FDG PET/CT should be used with caution when predicting EGFR mutations in patients with NSCLC. More prospective cohort studies are needed to further verify the role of $^{18}$F-FDG PET/CT in predicting EGFR mutations.

## Evaluating Treatment Response for Patients With Non-Small Cell Lung Cancer

Most patients with NSCLC develop late in the course of the disease, which is inoperable (12, 71). The standard treatment modality for those patients remains systematic chemotherapy (72). However, since not all patients with NSCLC respond well to chemotherapy and the treatment is toxic, it is important to identify those patients who are less or most likely to benefit from chemotherapy. Therefore, early prediction of treatment responses is particularly important, which can avoid the additional costs of unnecessary toxic and ineffective treatment or overtreatment, and possibly increase the chances of receiving other potentially effective therapy. Over the past two decades, EGFR TKIs, e.g., erlotinib and gefitinib, have been proposed to be effective treatment strategies for NSCLC patients with EGFR mutations (9, 73). The mutation status of EGFR is an optimal predictor of treatment response to TKIs for patients with NSCLC (3, 4). Nevertheless, only a small subset of patients with EGFR mutations respond well to TKIs, especially erlotinib, which have prolonged survival (74, 75). The response rate of EGFR mutations to TKIs in patients with NSCLC varied greatly. Accordingly, new approaches are obviously needed to determine which patients will benefit from TKI treatment.

Traditionally, response evaluation for NSCLC patients harboring EGFR mutations treated with TKIs is usually based on anatomic imaging features that mainly present with static, and calculating the change of tumor size on CT and using Response Evaluation Criteria in Solid Tumors (RECIST) for classification (76, 77). However, the differences between atelectasis or fibrosis and residual neoplasm cannot be distinguished significantly by conventional anatomic imaging modalities (78, 79). Accordingly, the detection of early treatment response using these anatomic imaging tools has limited value. $^{18}$F-FDG PET/CT, a molecular and functional imaging method, has emerged as a powerful ability in diagnosing, staging, and evaluating outcomes for patients with NSCLC (80). In addition, $^{18}$F-FDG PET/CT has been proposed to be of great value in predicting the efficacy of radiotherapy, chemoradiotherapy, neoadjuvant chemotherapy, and combined intercalated chemotherapy and erlotinib in patients with advanced NSCLC (81–85).

As for patients with TKI-treated NSCLC, $^{18}$F-FDG PET/CT could be used to monitor response (**Table 2**) as early as 2 days after therapy, and those patients who had a partial metabolic response and stable metabolic disease would have a significantly longer PFS than those with progressive metabolic disease (86). Moreover, patients with partial remission and stable disease showed a decreasing uptake of $^{18}$F-FDG, while patients with progressive disease presented an increasing $^{18}$F-FDG uptake, which was the early response on day 2 and week 4 after treatment with gefitinib (87). In reality, low $SUV_{max}$ of the primary tumor on $^{18}$F-FDG PET/CT scan usually correlated with a higher response rate than high $SUV_{max}$ (88). The subsequent tumor reduction could be predicted by the decreasing uptake of $^{18}$F-FDG on PET/CT scan as an early response to the initiation of TKI treatment for patients harboring EGFR-mutated NSCLC (89). The histopathologic response could also be monitored by $^{18}$F-FDG PET/CT using $SUV_{max}$ changes, and it had an advantage over traditional CT to evaluate histopathologic response for patients with neoadjuvant erlotinib-treated NSCLC (90–92).

The $^{18}$F-FDG metabolic activity of tumor on PET/CT scan can be revealed by several semiquantitative methods, e.g., $SUV_{max}$, $SUV_{2Dpeak}$ (2D peak SUV), $SUV_{3Dpeak}$ (3D peak SUV), $SUV_{A50}$ (3D isocontour at 50% of the maximum pixel value adapted for background), $SUV_{A41}$ (3D isocontour at 41% of the maximum pixel value adapted for background), $SUV_{50}$ (3D isocontour at 50% of the maximum pixel value), MTV, and TLG; these parameters have been demonstrated to be useful in monitoring response for patients with TKI-treated NSCLC (93, 94). However, the best parameters for the early response monitoring might be the $SUV_{max}$, $SUV_{50}$, $SUV_{A50}$, and $SUV_{A41}$ measured with $^{18}$F-FDG on PET/CT scan (94). Recently, tumor heterogeneity on $^{18}$F-FDG PET/CT has been evaluated for monitoring response in patients with erlotinib-treated NSCLC (95). The treatment response to erlotinib was related to the reduced heterogeneity of $^{18}$F-FDG PET. The change of first-order entropy was independently associated with treatment response and outcome (95). This study of NSCLC heterogeneity on $^{18}$F-FDG PET/CT opens a new window for monitoring therapy response.

As stated above, both EGFR and $^{18}$F-FDG PET/CT have potential value in monitoring TKI treatment response for NSCLC patients. Patients with mutant EGFR treated with TKIs benefit more than those with wild-type EGFR. $^{18}$F-FDG PET/CT demonstrates a high advantage in evaluating early treatment response. Several semiquantitative parameters of $^{18}$F-FDG metabolic activity present a significant role in assessing anatomical and histopathological responses for patients with NSCLC treated with TKIs. The heterogeneity of uptake of $^{18}$F-FDG on PET/CT may be a useful method to evaluate treatment response and prognosis for patients with NSCLC.

## Predicting Prognosis for Patients With Non-Small Cell Lung Cancer

The prognosis of patients with NSCLC is heterogeneous and varies greatly. Tumor-node-metastasis (TNM) classification is a measure to specify the disease extent for patients with NSCLC and plays a vital role in choosing a treatment strategy (96). $^{18}$F-FDG PET/CT has been demonstrated to be powerful in staging

**TABLE 2 |** The findings of $^{18}$F-FDG PET/CT in evaluating treatment response and outcome for TKIs treated patients with NSCLC.

| Studies | No. of patients | | Clinical stage | | Treatment strategies | | Response evaluation time | | | Response rate | | | | Prognosis (M) | | Findings |
|---|---|---|---|---|---|---|---|---|---|---|---|---|---|---|---|---|
| | M | F | I–II | III–IV | Erlotinib | Gefitinib | Early | Interim | Late | CR | PR | PD | SD | PFS | OS | |
| Tiseo et al. (86) | 35 | 18 | 0 | 53 | √ | – | D2 | – | – | 0 | 38% | 15% | 47% | 2.1 | 7.6 | Patients with early PMR and SMD have longer PFS and OS than PMD patients |
| Sunaga et al. (87) | 0 | 5 | 0 | 5 | – | √ | D2 | Wk4 | – | 0 | 40% | 20% | 40% | 9.0 | 13.4 | $SUV_{max}$ decreased in patients with PR and SD during treatment |
| Na et al. (88) | 47 | 37 | 0 | 84 | – | √ | – | Every 4 weeks | – | 0 | 50% | 13.1% | 36.9% | 3.0 | 7.5 | Low SUV of the primary tumor shows higher response rate and longer PFS and OS |
| Koizumi et al. (89) | 4 | 6 | – | – | – | √ | D7 | – | – | 0 | 100% | – | – | 15.0 | 70% 1 year | Early reduction of $SUV_{max}$ after therapy can predict subsequent tumor reduction |
| Aukema et al. (90) | 8 | 15 | 21 | 2 | √ | – | D7 | – | – | 0 | 26% | 4% | 70% | – | – | $^{18}$F-FDG PET/CT can predict early response to erlotinib treatment in patients with NSCLC |
| van Gool et al. (91) | 18 | 25 | 37 | 6 | √ | – | D4–7 | Wk3 | – | 0 | 33% | 14% | 53% | – | – | $^{18}$F-FDG PET/CT can monitor early histopathologic response |
| van Gool et al. (92) | 22 | 31 | 47 | 6 | √ | – | – | Wk3 | – | 0 | 15% | 11% | 60% | – | – | $^{18}$F-FDG PET/CT has an advantage over CT to identify histopathologic response |
| Winther et al. (93) | 28 | 22 | 0 | 50 | √ | – | D7 | – | – | 0 | 12% | 14% | 74% | 2.7 | 6.0 | Early increase in TLG correlates with radiological progression and shorter PFS and OS |
| Kahraman et al. (94) | 13 | 17 | 0 | 30 | √ | – | D7 | – | Wk6 | NS | NS | NS | NS | NS | NS | Early $^{18}$F-FDG PET can monitor response and predict PFS |
| Cook et al. (95) | 18 | 29 | 0 | 47 | √ | – | – | – | Wk6 | 34.4% | | 65.6% | | – | 14.1 | Response to erlotinib is associated with reduced heterogeneity at $^{18}$F-FDG PET |

*CR, complete response; PR, partial response; SD, stable disease; PD, progressive disease; M, average months; D, day; Wk, week; PFS, progression-free survival; OS, overall survival; PMR, partial metabolic response; SMD, stable metabolic disease; PMD, progressive metabolic disease; SUV, standard uptake value; NS, not specified; "-", not done.*

procedures and is more accurate than conventional CT in mediastinal staging for patients with NSCLC (97). Patients with advanced stage are usually incurable with a short life expectancy. Accordingly, the choice of treatment methods must be discreetly balanced between the potential benefits and ineffective side, effects and a precise evaluation of the prognosis of patients with NSCLC is of great importance.

In the past two decades, EGFR is a well-known predictive marker of outcome for patients with NSCLC who were treated with TKIs (98). TKIs have become the first-line treatment strategy in standard therapy for advanced-stage NSCLC harboring EGFR mutations, e.g., deletion of exon 19 or exon 21 or the L858R point mutations (7, 8). The mutation in exon 19 of EGFR was a reliable predictor of favorable survival for patients with NSCLC (55). Patients with activated EGFR mutations treated with TKIs had a higher response rate and longer PFS than those treated with standard cytotoxic chemotherapy (6). However, resistance inevitably develops eventually for patients with NSCLC who are treated with EGFR TKIs, and it is difficult for clinicians to predict the time of recurrence or progression owing to the wide range of PFS in individual patients. Some patients progressed several years after starting TKI therapy, while others progressed rapidly and spread widely after just a few months, usually with a median of 9–13 months (7–9). To our knowledge, there is currently no reliable clinical tool to predict the prognosis of EGFR mutant NSCLC patients treated with TKIs. Meanwhile, only two clinical features, TNM staging and performance status, have been considered to be significantly associated with prognosis in patients with NSCLC, but they need to be further validated by prospective studies (99).

The prognosis of patients with NSCLC from early stage to advanced stage has been evaluated by several studies with numerous procedures (100, 101). The role of $^{18}$F-FDG PET and high-resolution CT in predicting the prognosis for patients with clinical stage-IA NSCLC has been assessed, which showed that $SUV_{max}$ of the primary tumor and ground-glass opacity ratios on high-resolution CT images were significant prognosticators of these patients, which should be kept in mind before selecting therapeutic strategies (101). In patients with advanced NSCLC treated with erlotinib, $^{18}$F-FDG PET presented a predictive effect as early as 1 week after initiation of treatment, predicting PFS, OS, and non-progression after 6 weeks of treatment, and was independent of EGFR mutational status (100). Several different semiquantitative parameters, e.g., $SUV_{max}$, $SUV_{2Dpeak}$, $SUV_{3Dpeak}$, $SUV_{50}$, $SUV_{A50}$, and $SUV_{A41}$, have been proved to be useful predictors of short-term prognosis in patients with advanced NSCLC in the early (1 week) and late (6 weeks) $^{18}$F-FDG PET/CT scans after initiation of erlotinib therapy (102). An updated systematic review and meta-analysis by the European lung cancer working party for the international association for the study of lung cancer staging project showed that SUV on $^{18}$F-FDG PET was potentially useful in predicting patient outcomes (13). Low SUVs of the primary tumor could predict favorable survival in NSCLC patients treated with TKIs

(88, 102). Early evaluation of $SUV_{max}$ changes on $^{18}$F-FDG PET at 2 days after initial treatment with gefitinib was of great significance to predict the clinical outcome of patients with lung adenocarcinoma (103). Moreover, early (day 14) partial metabolic response on $^{18}$F-FDG PET was independently associated with prolonged PFS and OS in patients with NSCLC treated with erlotinib (104).

In NSCLC patients with activating EGFR mutation, TLG has the potential role in predicting PFS and gefitinib resistance development on $^{18}$F-FDG PET (105). Measuring the baseline metabolic tumor burden with TLG before first-line TKIs will be very helpful to predict the time of acquired drug resistance (105). Intra-tumoral heterogeneity may be partially explained that not all patients with NSCLC harboring EGFR mutations will benefit from TKI therapy (106). Using an imaging tool may be a potentially simpler approach to assess tumor heterogeneity. Actually, heterogeneous textural parameters derived from baseline $^{18}$F-FDG PET/CT are demonstrated to be high predictors of clinical outcomes for NSCLC patients harboring EGFR mutations treated with TKIs (107). However, even though $^{18}$F-FDG PET/CT plays a vital role in predicting the prognosis for patients with NSCLC, contradictory results are also observed that $SUV_{max}$ of the primary tumor cannot predict survival for patients with NSCLC (108, 109). Accordingly, furthermore, studies are needed to validate these findings to give clinicians an accurate recommendation.

## CONCLUSION

In summary, the $^{18}$F-FDG metabolic activity of NSCLC, as an extrinsic manifestation, plays a critical role in monitoring treatment response and evaluating prognosis. Several semiquantitative parameters (e.g., $SUV_{max}$, MTV, and TLG) on $^{18}$F-FDG PET/CT can be used to reflect metabolic activity and tumor burden. EGFR mutation status, as an intrinsic factor, plays a vital role in guiding the implementation of treatment modalities (e.g., TKIs) and evaluating therapy efficacy and outcome for patients with NSCLC. Significant correlations are observed between $^{18}$F-FDG metabolic activity and EGFR mutation status, not only in biology but also in clinical practice. However, at present, there is still a lack of comprehensive evaluation of the association between $^{18}$F-FDG PET/CT and EGFR mutations in patients with NSCLC, e.g., using $^{18}$F-FDG PET/CT to predict EGFR mutation status and then monitor treatment response and evaluate the outcome, which needs to be carried out simultaneously in a large sample retrospective or prospective study.

## AUTHOR CONTRIBUTIONS

MJ and JJZ were responsible for the conception of this review. All authors contributed to the article and approved the submitted version.

## FUNDING

This work was supported by the Medical Scientific Research Foundation of Zhejiang Province, China (Grant no. 2021KY1014), Research Foundation of Hwa Mei Hospital, University of Chinese Academy of Sciences, China (Grant no. 2022HMKY27), Ningbo Public Service Technology Foundation, China (Grant No. 2021S176), and Medical Science and Technology Project of Ningbo, China (Grant no. 2020Y10), Ningbo Clinical Medical Research Center of Imaging Medicine (Grant No. 2021L003), and Provincial and Municipal Co-construction Key Discipline of Medical Imaging (Grant No. 2022-S02).

## REFERENCES

1. Siegel RL, Miller KD, Jemal A. Cancer Statistics, 2020. *CA Cancer J Clin* (2020) 70:7–30. doi: 10.3322/caac.21590
2. Goldstraw P, Ball D, Jett JR, Le Chevalier T, Lim E, Nicholson AG, et al. Non-Small-Cell Lung Cancer. *Lancet* (2011) 378:1727–40. doi: 10.1016/S0140-6736(10)62101-0
3. Lynch TJ, Bell DW, Sordella R, Gurubhagavatula S, Okimoto RA, Brannigan BW, et al. Activating Mutations in the Epidermal Growth Factor Receptor Underlying Responsiveness of Non-Small-Cell Lung Cancer to Gefitinib. *N Engl J Med* (2004) 350:2129–39. doi: 10.1056/NEJMoa040938
4. Paez JG, Janne PA, Lee JC, Tracy S, Greulich H, Gabriel S, et al. EGFR Mutations in Lung Cancer: Correlation With Clinical Response to Gefitinib Therapy. *Science* (2004) 304:1497–500. doi: 10.1126/science.1099314
5. Tokumo M, Toyooka S, Kiura K, Shigematsu H, Tomii K, Aoe M, et al. The Relationship Between Epidermal Growth Factor Receptor Mutations and Clinicopathologic Features in Non-Small Cell Lung Cancers. *Clin Cancer Res* (2005) 11:1167–73. doi: 10.1016/S0169-5002(05)80493-3
6. Sequist LV, Yang JC, Yamamoto N, O'Byrne K, Hirsh V, Mok T, et al. Phase III Study of Afatinib or Cisplatin Plus Pemetrexed in Patients With Metastatic Lung Adenocarcinoma With EGFR Mutations. *J Clin Oncol* (2013) 31:3327–34. doi: 10.1200/JCO.2012.44.2806
7. Maemondo M, Inoue A, Kobayashi K, Sugawara S, Oizumi S, Isobe H, et al. Gefitinib or Chemotherapy for Non-Small-Cell Lung Cancer With Mutated EGFR. *N Engl J Med* (2010) 362:2380–8. doi: 10.1056/NEJMoa0909530
8. Mitsudomi T, Morita S, Yatabe Y, Negoro S, Okamoto I, Tsurutani J, et al. Gefitinib Versus Cisplatin Plus Docetaxel in Patients With Non-Small-Cell Lung Cancer Harbouring Mutations of the Epidermal Growth Factor Receptor (WJTOG3405): An Open Label, Randomised Phase 3 Trial. *Lancet Oncol* (2010) 11:121–8. doi: 10.1016/S1470-2045(09)70364-X
9. Mok TS, Wu YL, Thongprasert S, Yang CH, Chu DT, Saijo N, et al. Gefitinib or Carboplatin-Paclitaxel in Pulmonary Adenocarcinoma. *N Engl J Med* (2009) 361:947–57. doi: 10.1056/NEJMoa0810699
10. Hicks RJ. Role of 18F-FDG PET in Assessment of Response in Non-Small Cell Lung Cancer. *J Nucl Med* (2009) 50 Suppl 1:31S–42S. doi: 10.2967/jnumed.108.057216
11. Evangelista L, Cuppari L, Menis J, Bonanno L, Reccia P, Frega S, et al. 18f-FDG PET/CT in Non-Small-Cell Lung Cancer Patients: A Potential Predictive Biomarker of Response to Immunotherapy. *Nucl Med Commun* (2019) 40:802–7. doi: 10.1097/MNM.0000000000001025
12. Nahmias C, Hanna WT, Wahl LM, Long MJ, Hubner KF, Townsend DW. Time Course of Early Response to Chemotherapy in Non-Small Cell Lung Cancer Patients With 18F-FDG PET/Ct. *J Nucl Med* (2007) 48:744–51. doi: 10.2967/jnumed.106.038513
13. Berghmans T, Dusart M, Paesmans M, Hossein-Foucher C, Buvat I, Castaigne C, et al. Primary Tumor Standardized Uptake Value (SUVmax) Measured on Fluorodeoxyglucose Positron Emission Tomography (FDG-PET) is of Prognostic Value for Survival in Non-Small Cell Lung Cancer (NSCLC): A Systematic Review and Meta-Analysis (MA) by the European Lung Cancer Working Party for the IASLC Lung Cancer Staging Project. *J Thorac Oncol* (2008) 3:6–12. doi: 10.1097/JTO.0b013e31815e6d6b

14. Kirchner J, Sawicki LM, Nensa F, Schaarschmidt BM, Reis H, Ingenwerth M, et al. Prospective Comparison of (18)F-FDG PET/MRI and (18)F-FDG PET/CT for Thoracic Staging of Non-Small Cell Lung Cancer. *Eur J Nucl Med Mol Imaging* (2019) 46:437–45. doi: 10.1007/s00259-018-4109-x
15. Chung HW, Lee KY, Kim HJ, Kim WS, So Y. FDG PET/CT Metabolic Tumor Volume and Total Lesion Glycolysis Predict Prognosis in Patients With Advanced Lung Adenocarcinoma. *J Cancer Res Clin Oncol* (2014) 140:89–98. doi: 10.1007/s00432-013-1545-7
16. Moon SH, Cho SH, Park LC, Ji JH, Sun JM, Ahn JS, et al. Metabolic Response Evaluated by 18F-FDG PET/CT as a Potential Screening Tool in Identifying a Subgroup of Patients With Advanced Non-Small Cell Lung Cancer for Immediate Maintenance Therapy After First-Line Chemotherapy. *Eur J Nucl Med Mol Imaging* (2013) 40:1005–13. doi: 10.1007/s00259-013-2400-4
17. Nappi A, Gallicchio R, Simeon V, Nardelli A, Pelagalli A, Zupa A, et al. [F-18] FDG-PET/CT Parameters as Predictors of Outcome in Inoperable NSCLC Patients. *Radiol Oncol* (2015) 49:320–6. doi: 10.1515/raon-2015-0043
18. Seban RD, Mezquita L, Berenbaum A, Dercle L, Botticella A, Le Pechoux C, et al. Baseline Metabolic Tumor Burden on FDG PET/CT Scans Predicts Outcome in Advanced NSCLC Patients Treated With Immune Checkpoint Inhibitors. *Eur J Nucl Med Mol Imaging* (2020) 47:1147–57. doi: 10.1007/s00259-019-04615-x
19. Roengvoraphoj O, Kasmann L, Eze C, Taugner J, Gjika A, Tufman A, et al. Maximum Standardized Uptake Value of Primary Tumor (SUVmax_PT) and Horizontal Range Between Two Most Distant PET-Positive Lymph Nodes Predict Patient Outcome in Inoperable Stage III NSCLC Patients After Chemoradiotherapy. *Transl Lung Cancer Res* (2020) 9:541–8. doi: 10.21037/tlcr.2020.04.04
20. Na II, Byun BH, Kim KM, Cheon GJ, Choe du H, Koh JS, et al. 18f-FDG Uptake and EGFR Mutations in Patients With Non-Small Cell Lung Cancer: A Single-Institution Retrospective Analysis. *Lung Cancer* (2010) 67:76–80. doi: 10.1016/j.lungcan.2009.03.010
21. Mak RH, Digumarthy SR, Muzikansky A, Engelman JA, Shepard JA, Choi NC, et al. Role of 18F-Fluorodeoxyglucose Positron Emission Tomography in Predicting Epidermal Growth Factor Receptor Mutations in Non-Small Cell Lung Cancer. *Oncologist* (2011) 16:319–26. doi: 10.1634/theoncologist.2010-0300
22. Guan J, Xiao NJ, Chen M, Zhou WL, Zhang YW, Wang S, et al. 18f-FDG Uptake for Prediction EGFR Mutation Status in Non-Small Cell Lung Cancer. *Med (Baltimore)* (2016) 95:e4421. doi: 10.1097/MD.0000000000004421
23. Yoshida T, Tanaka H, Kuroda H, Shimizu J, Horio Y, Sakao Y, et al. Standardized Uptake Value on (18)F-FDG-PET/CT is a Predictor of EGFR T790M Mutation Status in Patients With Acquired Resistance to EGFR-TKIs. *Lung Cancer* (2016) 100:14–9. doi: 10.1016/j.lungcan.2016.07.022
24. Lv Z, Fan J, Xu J, Wu F, Huang Q, Guo M, et al. Value of (18)F-FDG PET/CT for Predicting EGFR Mutations and Positive ALK Expression in Patients With Non-Small Cell Lung Cancer: A Retrospective Analysis of 849 Chinese Patients. *Eur J Nucl Med Mol Imaging* (2018) 45:735–50. doi: 10.1007/s00259-017-3885-z
25. Ko KH, Hsu HH, Huang TW, Gao HW, Shen DH, Chang WC, et al. Value of (1)(8)F-FDG Uptake on PET/CT and CEA Level to Predict Epidermal Growth Factor Receptor Mutations in Pulmonary Adenocarcinoma. *Eur J Nucl Med Mol Imaging* (2014) 41:1889–97. doi: 10.1007/s00259-014-2802-y
26. Caicedo C, Garcia-Velloso MJ, Lozano MD, Labiano T, Vigil Diaz C, Lopez-Picazo JM, et al. Role of [(1)(8)F]FDG PET in Prediction of KRAS and EGFR Mutation Status in Patients With Advanced Non-Small-Cell Lung Cancer. *Eur J Nucl Med Mol Imaging* (2014) 41:2058–65. doi: 10.1007/s00259-014-2833-4
27. Vander Heiden MG, Cantley LC, Thompson CB. Understanding the Warburg Effect: The Metabolic Requirements of Cell Proliferation. *Science* (2009) 324:1029–33. doi: 10.1126/science.1160809
28. Koppenol WH, Bounds PL, Dang CV. Otto Warburg's Contributions to Current Concepts of Cancer Metabolism. *Nat Rev Cancer* (2011) 11:325–37. doi: 10.1038/nrc3038
29. Cantor JR, Sabatini DM. Cancer Cell Metabolism: One Hallmark, Many Faces. *Cancer Discovery* (2012) 2:881–98. doi: 10.1158/2159-8290.CD-12-0345
30. Levine AJ, Puzio-Kuter AM. The Control of the Metabolic Switch in Cancers by Oncogenes and Tumor Suppressor Genes. *Science* (2010) 330:1340–4. doi: 10.1126/science.1193494
31. Ward PS, Thompson CB. Metabolic Reprogramming: A Cancer Hallmark Even Warburg Did Not Anticipate. *Cancer Cell* (2012) 21:297–308. doi: 10.1016/j.ccr.2012.02.014
32. Pao W, Chmielecki J. Rational, Biologically Based Treatment of EGFR-Mutant Non-Small-Cell Lung Cancer. *Nat Rev Cancer* (2010) 10:760–74. doi: 10.1038/nrc2947
33. Makinoshima H, Takita M, Matsumoto S, Yagishita A, Owada S, Esumi H, et al. Epidermal Growth Factor Receptor (EGFR) Signaling Regulates Global Metabolic Pathways in EGFR-Mutated Lung Adenocarcinoma. *J Biol Chem* (2014) 289:20813–23. doi: 10.1074/jbc.M114.575464
34. Su H, Bodenstein C, Dumont RA, Seimbille Y, Dubinett S, Phelps ME, et al. Monitoring Tumor Glucose Utilization by Positron Emission Tomography for the Prediction of Treatment Response to Epidermal Growth Factor Receptor Kinase Inhibitors. *Clin Cancer Res* (2006) 12:5659–67. doi: 10.1158/1078-0432.CCR-06-0368
35. Kelloff GJ, Hoffman JM, Johnson B, Scher HI, Siegel BA, Cheng EY, et al. Progress and Promise of FDG-PET Imaging for Cancer Patient Management and Oncologic Drug Development. *Clin Cancer Res* (2005) 11:2785–808. doi: 10.1158/1078-0432.CCR-04-2626
36. Humbert O, Cadour N, Paquet M, Schiappa R, Poudenx M, Chardin D, et al. (18)FDG PET/CT in the Early Assessment of Non-Small Cell Lung Cancer Response to Immunotherapy: Frequency and Clinical Significance of Atypical Evolutive Patterns. *Eur J Nucl Med Mol Imaging* (2020) 47:1158–67. doi: 10.1007/s00259-019-04573-4
37. Dissaux G, Visvikis D, Da-Ano R, Pradier O, Chajon E, Barillot I, et al. Pretreatment (18)F-FDG PET/CT Radiomics Predict Local Recurrence in Patients Treated With Stereotactic Body Radiotherapy for Early-Stage Non-Small Cell Lung Cancer: A Multicentric Study. *J Nucl Med* (2020) 61:814–20. doi: 10.2967/jnumed.119.228106
38. Choi WH, Yoo I, O JH, Kim TJ, Lee KY, Kim YK. Is the Glut Expression Related to FDG Uptake in PET/CT of Non-Small Cell Lung Cancer Patients? *Technol Health Care* (2015) 23 Suppl 2:S311–8. doi: 10.3233/THC-150967
39. Higashi K, Ueda Y, Sakurai A, Wang XM, Xu L, Murakami M, et al. Correlation of Glut-1 Glucose Transporter Expression With. *Eur J Nucl Med* (2000) 27:1778–85. doi: 10.1007/s002590000367
40. Suzuki S, Okada M, Takeda H, Kuramoto K, Sanomachi T, Togashi K, et al. Involvement of GLUT1-Mediated Glucose Transport and Metabolism in Gefitinib Resistance of Non-Small-Cell Lung Cancer Cells. *Oncotarget* (2018) 9:32667–79. doi: 10.18632/oncotarget.25994
41. Cairns RA, Harris IS, Mak TW. Regulation of Cancer Cell Metabolism. *Nat Rev Cancer* (2011) 11:85–95. doi: 10.1038/nrc2981
42. Ellison G, Zhu G, Moulis A, Dearden S, Speake G, McCormack R. EGFR Mutation Testing in Lung Cancer: A Review of Available Methods and Their Use for Analysis of Tumour Tissue and Cytology Samples. *J Clin Pathol* (2013) 66:79–89. doi: 10.1136/jclinpath-2012-201194
43. Taniguchi K, Okami J, Kodama K, Higashiyama M, Kato K. Intratumor Heterogeneity of Epidermal Growth Factor Receptor Mutations in Lung Cancer and Its Correlation to the Response to Gefitinib. *Cancer Sci* (2008) 99:929–35. doi: 10.1111/j.1349-7006.2008.00782.x
44. Bai H, Wang Z, Chen K, Zhao J, Lee JJ, Wang S, et al. Influence of Chemotherapy on EGFR Mutation Status Among Patients With Non-Small-Cell Lung Cancer. *J Clin Oncol* (2012) 30:3077–83. doi: 10.1200/JCO.2011.39.3744
45. Yao G, Zhou Y, Gu Y, Wang Z, Yang M, Sun J, et al. Value of Combining PET/CT and Clinicopathological Features in Predicting EGFR Mutation in Lung Adenocarcinoma With Bone Metastasis. *J Cancer* (2020) 11:5511–7. doi: 10.7150/jca.46414
46. Liu Q, Sun D, Li N, Kim J, Feng D, Huang G, et al. Predicting EGFR Mutation Subtypes in Lung Adenocarcinoma Using (18)F-FDG PET/CT Radiomic Features. *Transl Lung Cancer Res* (2020) 9:549–62. doi: 10.21037/tlcr.2020.04.17
47. Zhang J, Zhao X, Zhao Y, Zhang J, Zhang Z, Wang J, et al. Value of Pre-Therapy (18)F-FDG PET/CT Radiomics in Predicting EGFR Mutation Status in Patients With Non-Small Cell Lung Cancer. *Eur J Nucl Med Mol Imaging* (2020) 47:1137–46. doi: 10.1007/s00259-019-04592-1
48. Cho A, Hur J, Moon YW, Hong SR, Suh YJ, Kim YJ, et al. Correlation Between EGFR Gene Mutation, Cytologic Tumor Markers, 18F-FDG

Uptake in Non-Small Cell Lung Cancer. *BMC Cancer* (2016) 16:224. doi: 10.1186/s12885-016-2251-z
49. Gao XC, Wei CH, Zhang RG, Cai Q, He Y, Tong F, et al. (18)F-FDG PET/CT SUVmax and Serum CEA Levels as Predictors for EGFR Mutation State in Chinese Patients With Non-Small Cell Lung Cancer. *Oncol Lett* (2020) 20:61. doi: 10.3892/ol.2020.11922
50. Lee EY, Khong PL, Lee VH, Qian W, Yu X, Wong MP. Metabolic Phenotype of Stage IV Lung Adenocarcinoma: Relationship With Epidermal Growth Factor Receptor Mutation. *Clin Nucl Med* (2015) 40:e190-195. doi: 10.1097/RLU.0000000000000684
51. Gu J, Xu S, Huang L, Li S, Wu J, Xu J, et al. Value of Combining Serum Carcinoembryonic Antigen and PET/CT in Predicting EGFR Mutation in Non-Small Cell Lung Cancer. *J Thorac Dis* (2018) 10:723–31. doi: 10.21037/jtd.2017.12.143
52. Wang Y, Han R, Wang Q, Zheng J, Lin C, Lu C, et al. Biological Significance of (18)F-FDG PET/CT Maximum Standard Uptake Value for Predicting EGFR Mutation Status in Non-Small Cell Lung Cancer Patients. *Int J Gen Med* (2021) 14:347–56. doi: 10.2147/IJGM.S287506
53. Kanmaz ZD, Aras G, Tuncay E, Bahadir A, Kocaturk C, Yasar ZA, et al. Contribution of (1)(8)Fluorodeoxyglucose Positron Emission Tomography Uptake and TTF-1 Expression in the Evaluation of the EGFR Mutation in Patients With Lung Adenocarcinoma. *Cancer biomark* (2016) 16:489–98. doi: 10.3233/CBM-160588
54. Huang CT, Yen RF, Cheng MF, Hsu YC, Wei PF, Tsai YJ, et al. Correlation of F-18 Fluorodeoxyglucose-Positron Emission Tomography Maximal Standardized Uptake Value and EGFR Mutations in Advanced Lung Adenocarcinoma. *Med Oncol* (2010) 27:9–15. doi: 10.1007/s12032-008-9160-1
55. Choi YJ, Cho BC, Jeong YH, Seo HJ, Kim HJ, Cho A, et al. Correlation Between (18)F-Fluorodeoxyglucose Uptake and Epidermal Growth Factor Receptor Mutations in Advanced Lung Cancer. *Nucl Med Mol Imaging* (2012) 46:169–75. doi: 10.1007/s13139-012-0142-z
56. Lee SM, Bae SK, Jung SJ, Kim CK. FDG Uptake in Non-Small Cell Lung Cancer is Not an Independent Predictor of EGFR or KRAS Mutation Status: A Retrospective Analysis of 206 Patients. *Clin Nucl Med* (2015) 40:950–8. doi: 10.1097/RLU.0000000000000975
57. Liu A, Han A, Zhu H, Ma L, Huang Y, Li M, et al. The Role of Metabolic Tumor Volume (MTV) Measured by [18F] FDG PET/CT in Predicting EGFR Gene Mutation Status in Non-Small Cell Lung Cancer. *Oncotarget* (2017) 8:33736–44. doi: 10.18632/oncotarget.16806
58. Gao Y, Song P, Li H, Jia H, Zhang B. Elevated Serum CEA Levels are Associated With the Explosive Progression of Lung Adenocarcinoma Harboring EGFR Mutations. *BMC Cancer* (2017) 17:484. doi: 10.1186/s12885-017-3474-3
59. Lee Y, Lee HJ, Kim YT, Kang CH, Goo JM, Park CM, et al. Imaging Characteristics of Stage I Non-Small Cell Lung Cancer on CT and FDG-PET: Relationship With Epidermal Growth Factor Receptor Protein Expression Status and Survival. *Korean J Radiol* (2013) 14:375–83. doi: 10.3348/kjr.2013.14.2.375
60. Liu X, Zhang H, Yu X, Song T, Huang P, Wang H, et al. The Correlation of Expression of VEGF and EGFR With SUV of (18)FDG-PET-CT in Non-Small Cell Lung Cancer. *Contemp Oncol (Pozn)* (2014) 18:334–9. doi: 10.5114/wo.2014.45308
61. Toh CK, Gao F, Lim WT, Leong SS, Fong KW, Yap SP, et al. Never-Smokers With Lung Cancer: Epidemiologic Evidence of a Distinct Disease Entity. *J Clin Oncol* (2006) 24:2245–51. doi: 10.1200/JCO.2005.04.8033
62. Kuo MD, Jamshidi N. Behind the Numbers: Decoding Molecular Phenotypes With Radiogenomics–Guiding Principles and Technical Considerations. *Radiology* (2014) 270:320–5. doi: 10.1148/radiol.13132195
63. Wu J, Aguilera T, Shultz D, Gudur M, Rubin DL, Loo BWJr., et al. Early-Stage Non-Small Cell Lung Cancer: Quantitative Imaging Characteristics of (18)F Fluorodeoxyglucose PET/CT Allow Prediction of Distant Metastasis. *Radiology* (2016) 281:270–8. doi: 10.1148/radiol.2016151829
64. Zhang M, Bao Y, Rui W, Shangguan C, Liu J, Xu J, et al. Performance of (18) F-FDG PET/CT Radiomics for Predicting EGFR Mutation Status in Patients With Non-Small Cell Lung Cancer. *Front Oncol* (2020) 10:568857. doi: 10.3389/fonc.2020.568857
65. Li X, Yin G, Zhang Y, Dai D, Liu J, Chen P, et al. Predictive Power of a Radiomic Signature Based on (18)F-FDG PET/CT Images for EGFR Mutational Status in NSCLC. *Front Oncol* (2019) 9:1062. doi: 10.3389/fonc.2019.01062
66. Nair JKR, Saeed UA, McDougall CC, Sabri A, Kovacina B, Raidu BVS, et al. Radiogenomic Models Using Machine Learning Techniques to Predict EGFR Mutations in Non-Small Cell Lung Cancer. *Can Assoc Radiol J* (2021) 72:109–19. doi: 10.1177/0846537119899526
67. Koyasu S, Nishio M, Isoda H, Nakamoto Y, Togashi K. Usefulness of Gradient Tree Boosting for Predicting Histological Subtype and EGFR Mutation Status of Non-Small Cell Lung Cancer on (18)F FDG-PET/Ct. *Ann Nucl Med* (2020) 34:49–57. doi: 10.1007/s12149-019-01414-0
68. Mu W, Jiang L, Zhang J, Shi Y, Gray JE, Tunali I, et al. Non-Invasive Decision Support for NSCLC Treatment Using PET/CT Radiomics. *Nat Commun* (2020) 11:5228. doi: 10.1038/s41467-020-19116-x
69. Gazdar AF, Minna JD. Inhibition of EGFR Signaling: All Mutations are Not Created Equal. *PloS Med* (2005) 2:e377. doi: 10.1371/journal.pmed.0020377
70. Shigematsu H, Lin L, Takahashi T, Nomura M, Suzuki M, Wistuba II, et al. Clinical and Biological Features Associated With Epidermal Growth Factor Receptor Gene Mutations in Lung Cancers. *J Natl Cancer Inst* (2005) 97:339–46. doi: 10.1093/jnci/dji055
71. Spiro SG, Silvestri GA. One Hundred Years of Lung Cancer. *Am J Respir Crit Care Med* (2005) 172:523–9. doi: 10.1164/rccm.200504-531OE
72. Pfister DG, Johnson DH, Azzoli CG, Sause W, Smith TJ, Baker SJr., et al. American Society of Clinical Oncology Treatment of Unresectable Non-Small-Cell Lung Cancer Guideline: Update 2003. *J Clin Oncol* (2004) 22:330–53. doi: 10.1200/JCO.2004.09.053
73. Doroshow JH. Targeting EGFR in Non-Small-Cell Lung Cancer. *N Engl J Med* (2005) 353:200–2. doi: 10.1056/NEJMe058113
74. Fukuoka M, Yano S, Giaccone G, Tamura T, Nakagawa K, Douillard JY, et al. Multi-Institutional Randomized Phase II Trial of Gefitinib for Previously Treated Patients With Advanced Non-Small-Cell Lung Cancer (The IDEAL 1 Trial) [Corrected]. *J Clin Oncol* (2003) 21:2237–46. doi: 10.1200/JCO.2003.10.038
75. Tsao MS, Sakurada A, Cutz JC, Zhu CQ, Kamel-Reid S, Squire J, et al. Erlotinib in Lung Cancer - Molecular and Clinical Predictors of Outcome. *N Engl J Med* (2005) 353:133–44. doi: 10.1056/NEJMoa050736
76. Therasse P, Arbuck SG, Eisenhauer EA, Wanders J, Kaplan RS, Rubinstein L, et al. New Guidelines to Evaluate the Response to Treatment in Solid Tumors. European Organization for Research and Treatment of Cancer, National Cancer Institute of the United States, National Cancer Institute of Canada. *J Natl Cancer Inst* (2000) 92:205–16. doi: 10.1093/jnci/92.3.205
77. Eisenhauer EA, Therasse P, Bogaerts J, Schwartz LH, Sargent D, Ford R, et al. New Response Evaluation Criteria in Solid Tumours: Revised RECIST Guideline (Version 1.1). *Eur J Cancer* (2009) 45:228–47. doi: 10.1016/j.ejca.2008.10.026
78. Mac Manus MP, Hicks RJ, Matthews JP, McKenzie A, Rischin D, Salminen EK, et al. Positron Emission Tomography is Superior to Computed Tomography Scanning for Response-Assessment After Radical Radiotherapy or Chemoradiotherapy in Patients With Non-Small-Cell Lung Cancer. *J Clin Oncol* (2003) 21:1285–92. doi: 10.1200/JCO.2003.07.054
79. Wahl RL, Jacene H, Kasamon Y, Lodge MA. From RECIST to PERCIST: Evolving Considerations for PET Response Criteria in Solid Tumors. *J Nucl Med* (2009) 50 Suppl 1:122S–50S. doi: 10.2967/jnumed.108.057307
80. de Geus-Oei LF, van der Heijden HF, Corstens FH, Oyen WJ. Predictive and Prognostic Value of FDG-PET in Nonsmall-Cell Lung Cancer: A Systematic Review. *Cancer* (2007) 110:1654–64. doi: 10.1002/cncr.22979
81. van Baardwijk A, Bosmans G, Dekker A, van Kroonenburgh M, Boersma L, Wanders S, et al. Time Trends in the Maximal Uptake of FDG on PET Scan During Thoracic Radiotherapy. A Prospective Study in Locally Advanced Non-Small Cell Lung Cancer (NSCLC) Patients. *Radiother Oncol* (2007) 82:145–52. doi: 10.1016/j.radonc.2007.01.007
82. de Geus-Oei LF, van der Heijden HF, Visser EP, Hermsen R, van Hoorn BA, Timmer-Bonte JN, et al. Chemotherapy Response Evaluation With 18F-FDG PET in Patients With Non-Small Cell Lung Cancer. *J Nucl Med* (2007) 48:1592–8. doi: 10.2967/jnumed.107.043414
83. Lee DH, Kim SK, Lee HY, Lee SY, Park SH, Kim HY, et al. Early Prediction of Response to First-Line Therapy Using Integrated 18F-FDG PET/CT for Patients With Advanced/Metastatic Non-Small Cell Lung Cancer. *J Thorac Oncol* (2009) 4:816–21. doi: 10.1097/JTO.0b013e3181a99fde

84. Usmanij EA, de Geus-Oei LF, Troost EG, Peters-Bax L, van der Heijden EH, Kaanders JH, et al. 18f-FDG PET Early Response Evaluation of Locally Advanced Non-Small Cell Lung Cancer Treated With Concomitant Chemoradiotherapy. *J Nucl Med* (2013) 54:1528–34. doi: 10.2967/jnumed.112.116921
85. Zwitter M, Rajer M, Stanic K, Vrankar M, Doma A, Cuderman A, et al. Intercalated Chemotherapy and Erlotinib for Non-Small Cell Lung Cancer (NSCLC) With Activating Epidermal Growth Factor Receptor (EGFR) Mutations. *Cancer Biol Ther* (2016) 17:833–9. doi: 10.1080/15384047.2016.1195049
86. Tiseo M, Ippolito M, Scarlattei M, Spadaro P, Cosentino S, Latteri F, et al. Predictive and Prognostic Value of Early Response Assessment Using 18FDG-PET in Advanced Non-Small Cell Lung Cancer Patients Treated With Erlotinib. *Cancer Chemother Pharmacol* (2014) 73:299–307. doi: 10.1007/s00280-013-2356-x
87. Sunaga N, Oriuchi N, Kaira K, Yanagitani N, Tomizawa Y, Hisada T, et al. Usefulness of FDG-PET for Early Prediction of the Response to Gefitinib in Non-Small Cell Lung Cancer. *Lung Cancer* (2008) 59:203–10. doi: 10.1016/j.lungcan.2007.08.012
88. Na II, Byun BH, Kang HJ, Cheon GJ, Koh JS, Kim CH, et al. 18F-Fluoro-2-Deoxy-Glucose Uptake Predicts Clinical Outcome in Patients With Gefitinib-Treated Non-Small Cell Lung Cancer. *Clin Cancer Res* (2008) 14:2036–41. doi: 10.1158/1078-0432.CCR-07-4074
89. Koizumi T, Fukushima T, Gomi D, Kobayashi T, Sekiguchi N, Mamiya K, et al. Correlation of Early PET Findings With Tumor Response to Molecular Targeted Agents in Patients With Advanced Driver-Mutated Non-Small Cell Lung Cancer. *Med Oncol* (2017) 34:169. doi: 10.1007/s12032-017-1032-0
90. Aukema TS, Kappers I, Olmos RA, Codrington HE, van Tinteren H, van Pel R, et al. Is 18f-FDG PET/CT Useful for the Early Prediction of Histopathologic Response to Neoadjuvant Erlotinib in Patients With Non-Small Cell Lung Cancer? *J Nucl Med* (2010) 51:1344–8. doi: 10.2967/jnumed.110.076224
91. van Gool MH, Aukema TS, Schaake EE, Rijna H, Valdes Olmos RA, van Pel R, et al. Timing of Metabolic Response Monitoring During Erlotinib Treatment in Non-Small Cell Lung Cancer. *J Nucl Med* (2014) 55:1081–6. doi: 10.2967/jnumed.113.130674
92. van Gool MH, Aukema TS, Schaake EE, Rijna H, Codrington HE, Valdes Olmos RA, et al. (18)F-Fluorodeoxyglucose Positron Emission Tomography Versus Computed Tomography in Predicting Histopathological Response to Epidermal Growth Factor Receptor-Tyrosine Kinase Inhibitor Treatment in Resectable Non-Small Cell Lung Cancer. *Ann Surg Oncol* (2014) 21:2831–7. doi: 10.1245/s10434-014-3791-6
93. Winther-Larsen A, Fledelius J, Demuth C, Bylov CM, Meldgaard P, Sorensen BS. Early Change in FDG-PET Signal and Plasma Cell-Free DNA Level Predicts Erlotinib Response in EGFR Wild-Type NSCLC Patients. *Transl Oncol* (2016) 9:505–11. doi: 10.1016/j.tranon.2016.09.003
94. Kahraman D, Scheffler M, Zander T, Nogova L, Lammertsma AA, Boellaard R, et al. Quantitative Analysis of Response to Treatment With Erlotinib in Advanced Non-Small Cell Lung Cancer Using 18F-FDG and 3'-Deoxy-3'-18F-Fluorothymidine PET. *J Nucl Med* (2011) 52:1871–7. doi: 10.2967/jnumed.111.094458
95. Cook GJ, O'Brien ME, Siddique M, Chicklore S, Loi HY, Sharma B, et al. Non-Small Cell Lung Cancer Treated With Erlotinib: Heterogeneity of (18) F-FDG Uptake at PET-Association With Treatment Response and Prognosis. *Radiology* (2015) 276:883–93. doi: 10.1148/radiol.2015141309
96. Rami-Porta R, Crowley JJ, Goldstraw P. The Revised TNM Staging System for Lung Cancer. *Ann Thorac Cardiovasc Surg* (2009) 15:4–9.
97. Gould MK, Kuschner WG, Rydzak CE, Maclean CC, Demas AN, Shigemitsu H, et al. Test Performance of Positron Emission Tomography and Computed Tomography for Mediastinal Staging in Patients With Non-Small-Cell Lung Cancer: A Meta-Analysis. *Ann Intern Med* (2003) 139:879–92. doi: 10.7326/0003-4819-139-11-200311180-00013
98. Han SW, Kim TY, Hwang PG, Jeong S, Kim J, Choi IS, et al. Predictive and Prognostic Impact of Epidermal Growth Factor Receptor Mutation in Non-Small-Cell Lung Cancer Patients Treated With Gefitinib. *J Clin Oncol* (2005) 23:2493–501. doi: 10.1200/JCO.2005.01.388
99. Sculier JP, Chansky K, Crowley JJ, Van Meerbeeck J, Goldstraw P, International Staging C, et al. The Impact of Additional Prognostic Factors on Survival and Their Relationship With the Anatomical Extent of Disease Expressed by the 6th Edition of the TNM Classification of Malignant Tumors and the Proposals for the 7th Edition. *J Thorac Oncol* (2008) 3:457–66. doi: 10.1097/JTO.0b013e31816de2b8
100. Zander T, Scheffler M, Nogova L, Kobe C, Engel-Riedel W, Hellmich M, et al. Early Prediction of Nonprogression in Advanced Non-Small-Cell Lung Cancer Treated With Erlotinib by Using [(18)F]fluorodeoxyglucose and [(18)F]fluorothymidine Positron Emission Tomography. *J Clin Oncol* (2011) 29:1701–8. doi: 10.1200/JCO.2010.32.4939
101. Uehara H, Tsutani Y, Okumura S, Nakayama H, Adachi S, Yoshimura M, et al. Prognostic Role of Positron Emission Tomography and High-Resolution Computed Tomography in Clinical Stage IA Lung Adenocarcinoma. *Ann Thorac Surg* (2013) 96:1958–65. doi: 10.1016/j.athoracsur.2013.06.086
102. Kobe C, Scheffler M, Holstein A, Zander T, Nogova L, Lammertsma AA, et al. Predictive Value of Early and Late Residual 18F-Fluorodeoxyglucose and 18F-Fluorothymidine Uptake Using Different SUV Measurements in Patients With Non-Small-Cell Lung Cancer Treated With Erlotinib. *Eur J Nucl Med Mol Imaging* (2012) 39:1117–27. doi: 10.1007/s00259-012-2118-8
103. Takahashi R, Hirata H, Tachibana I, Shimosegawa E, Inoue A, Nagatomo I, et al. Early [18F]Fluorodeoxyglucose Positron Emission Tomography at Two Days of Gefitinib Treatment Predicts Clinical Outcome in Patients With Adenocarcinoma of the Lung. *Clin Cancer Res* (2012) 18:220–8. doi: 10.1158/1078-0432.CCR-11-0868
104. Mileshkin L, Hicks RJ, Hughes BG, Mitchell PL, Charu V, Gitlitz BJ, et al. Changes in 18F-Fluorodeoxyglucose and 18F-Fluorodeoxythymidine Positron Emission Tomography Imaging in Patients With Non-Small Cell Lung Cancer Treated With Erlotinib. *Clin Cancer Res* (2011) 17:3304–15. doi: 10.1158/1078-0432.CCR-10-2763
105. Keam B, Lee SJ, Kim TM, Paeng JC, Lee SH, Kim DW, et al. Total Lesion Glycolysis in Positron Emission Tomography Can Predict Gefitinib Outcomes in Non-Small-Cell Lung Cancer With Activating EGFR Mutation. *J Thorac Oncol* (2015) 10:1189–94. doi: 10.1097/JTO.0000000000000569
106. Gerlinger M, Rowan AJ, Horswell S, Math M, Larkin J, Endesfelder D, et al. Intratumor Heterogeneity and Branched Evolution Revealed by Multiregion Sequencing. *N Engl J Med* (2012) 366:883–92. doi: 10.1056/NEJMoa1113205
107. Park S, Ha S, Lee SH, Paeng JC, Keam B, Kim TM, et al. Intratumoral Heterogeneity Characterized by Pretreatment PET in Non-Small Cell Lung Cancer Patients Predicts Progression-Free Survival on EGFR Tyrosine Kinase Inhibitor. *PloS One* (2018) 13:e0189766. doi: 10.1371/journal.pone.0189766
108. Win T, Miles KA, Janes SM, Ganeshan B, Shastry M, Endozo R, et al. Tumor Heterogeneity and Permeability as Measured on the CT Component of PET/CT Predict Survival in Patients With Non-Small Cell Lung Cancer. *Clin Cancer Res* (2013) 19:3591–9. doi: 10.1158/1078-0432.CCR-12-1307
109. Agarwal M, Brahmanday G, Bajaj SK, Ravikrishnan KP, Wong CY. Revisiting the Prognostic Value of Preoperative (18)F-Fluoro-2-Deoxyglucose ( (18)F-FDG) Positron Emission Tomography (PET) in Early-Stage (I & II) Non-Small Cell Lung Cancers (NSCLC). *Eur J Nucl Med Mol Imaging* (2010) 37:691–8. doi: 10.1007/s00259-009-1291-x


**Conflict of Interest:** The authors declare that the research was conducted in the absence of any commercial or financial relationships that could be construed as a potential conflict of interest.

frontiers | Frontiers in Oncology

ORIGINAL RESEARCH
published: 05 May 2022
doi: 10.3389/fonc.2022.843220

# Survival Benefits for Pulmonary Adenocarcinoma With Malignant Pleural Effusion After Thoracoscopic Surgical Treatment: A Real-World Study

*Xin Li[1†], Mingbiao Li[2†], Jinshuang Lv[1†], Jinghao Liu[1], Ming Dong[1], Chunqiu Xia[1], Honglin Zhao[1], Song Xu[1], Sen Wei[1], Zuoqing Song[1], Gang Chen[1], Hongyu Liu[2*] and Jun Chen[1,2,3*]*

[1] Department of Lung Cancer Surgery, Tianjin Medical University General Hospital, Tianjin, China, [2] Tianjin Key Laboratory of Lung Cancer Metastasis and Tumor Microenvironment, Tianjin Lung Cancer Institute, Tianjin Medical University General Hospital, Tianjin, China, [3] Department of Thoracic Surgery, First Affiliated Hospital, School of Medicine, Shihezi University, Shihezi, China

OPEN ACCESS

**Edited by:**
Marcello Migliore,
University of Catania, Italy

**Reviewed by:**
Michael Ried,
University Hospital Regensburg, Germany
Luca Bertolaccini,
European Institute of Oncology (IEO), Italy

***Correspondence:**
Hongyu Liu
liuhongyu123@hotmail.com
Jun Chen
huntercj2004@qq.com

†These authors have contributed equally to this work

**Specialty section:**
This article was submitted to Thoracic Oncology, a section of the journal Frontiers in Oncology

**Received:** 25 December 2021
**Accepted:** 04 April 2022
**Published:** 05 May 2022

**Citation:**
Li X, Li M, Lv J, Liu J, Dong M, Xia C, Zhao H, Xu S, Wei S, Song Z, Chen G, Liu H and Chen J (2022) Survival Benefits for Pulmonary Adenocarcinoma With Malignant Pleural Effusion After Thoracoscopic Surgical Treatment: A Real-World Study. Front. Oncol. 12:843220. doi: 10.3389/fonc.2022.843220

**Objectives:** Malignant cells in the pleural fluid or pleural metastasis are classified as stage IV non-small cell lung cancer. Radical surgery is generally considered not suitable for such patients. The aim of our study was to discuss the effectiveness of video-assisted thoracoscopic surgery (VATS) in such patients.

**Methods:** A retrospective analysis of the clinical records of 195 patients was performed. These patients were all diagnosed with locally advanced pulmonary adenocarcinomas with malignant pleural effusion (MPE, M1a) but no distant organ metastasis. The 195 patients included 96 patients who underwent VATS plus chemotherapy and 99 patients who received thoracic drainage plus chemotherapy. The baseline characteristics of the patients included age, gender, smoking history, Eastern Cooperative Oncology Group (ECOG) score, and number of chemotherapy cycles (2–4 cycles or >4 cycles); we also analyzed clinical characteristics including the specific surgical options of the VATS group.

**Results:** In multivariate analysis, when compared to the thoracic drainage group, the VATS group remained significantly associated with the overall survival [HR=0.480 (95%CI 0.301-0.765)]; when compared to the lobectomy, the sub-lobectomy and the palliative surgery, remained significantly associated with the overall survival [HR=0.637 (95%CI 0.409-0.993) and HR=0.548 (95%CI 0.435-0.832), respectively]. The median survival time (MST) of patients who underwent VATS (n = 96, 49.2%) was 25 months (95% CI 22.373–27.627) whereas the patients who received thoracic drainage (n = 99, 50.8%) was 11 months (95% CI 9.978–12.022). For patients who underwent VATS, the MST of patients who received a lobectomy (n = 50, 52.1%) was 27 months (95% CI 22.432–31.568), the MST of patients who received a sub-lobectomy plus pleurodesis (n = 26, 27.1%) was 27 months (95% CI 19.157–34.843), and the MST of patients who received only pleurodesis (n = 20, 20.8%) was 12 months (95% CI 7.617–16.383).

**Conclusion:** For pulmonary adenocarcinomas with MPE, receiving a lobectomy or sub-lobectomy plus pleurodesis with VATS was associated with improved survival compared with patients who only received thoracic drainage and chemotherapy. Our results and previously published data may justify the use of VATS for treating pulmonary adenocarcinomas with MPE.

**Keywords: malignant pleural effusion, pulmonary adenocarcinoma, video-assisted thoracoscopic surgery, pleurodesis, chemotherapy**

## INTRODUCTION

Recently, lung cancer has been shown to have the highest death rate of all types of malignant tumors worldwide (1, 2). Non-small cell lung cancer (NSCLC) accounts for 75%–80% of all lung cancers, of which 50% are adenocarcinomas. Parietal pleural metastasis often occurs in advanced-stage adenocarcinoma and often develops into malignant plural effusion (MPE). Although many malignant tumors can cause MPE, adenocarcinoma is the most common pathological type, accounting for 45%–65% of all pathological types (3). Although treatment for NSCLC is constantly improving, the sensitivity of MPE to the current existing treatment methods is poor, which leads to a higher mortality rate. Palliative treatment is often used for treating such patients; however, even with systemic chemotherapy, these patients only have an overall median survival time (MST) of 3–12 months (4, 5). Existing treatment methods for such patients include thoracentesis, pleurodesis, thoracic drainage, chemotherapy, radiotherapy, anti-angiogenesis therapy, targeted therapy, etc. MAY most people consider chemotherapy or targeted therapy after thoracic drainage as appropriate for NSCLC tumors with MPE, but patients with good performance and only local metastasis may have a better quality of life and life expectancy after undergoing more aggressive therapies such as thoracoscopic surgery (6). Several studies have indicated that surgical therapy may provide a survival benefit to specific subsets of NSCLC patients with MPE (7–9). Therefore, in this study, we attempted to explore whether chemotherapy or targeted therapy after video-assisted thoracoscopic surgery (VATS) can improve the prognosis of NSCLC patients with MPE compared with those receiving a traditional treatment method.

## METHODS

### Patients and Groups

After screening, 195 primary lung adenocarcinoma patients with MPE but no distant organ metastasis were admitted to the Tianjin Medical University General Hospital from January 2009 to March 2015. Of these patients, 96 underwent chemotherapy or targeted therapy after VATS (VATS group), and 99 underwent traditional treatment (chemotherapy after thoracic catheterization; thoracic drainage group). Patient demographic information and clinical pathology data were collected. This clinical study was approved by the Ethics Committee of our institute. Preoperatively, the patients received a thorough physical examination and blood examination, respiratory function test, electrocardiogram, bone emission computed tomography (ECT), bronchoscopy, brain magnetic resonance imaging (MRI), and computed tomography (CT) of the chest and abdomen. Preoperative biopsy and intraoperatively biopsy confirmed that all patients had locally advanced stage IV disease.

The OS of the VATS group was defined as the time from the beginning of surgery to death from any cause. The OS of the thoracic drainage group was defined as the time from when the thoracic drainage tube was placed in the patients to death from any cause. For patients who were still alive at the end of data entry, the time of the last follow-up or medical record of the patient was taken as the cut-off time.

The baseline characteristics of the patients included age, gender, smoking history, ECOG score, and number of chemotherapy cycles (2–4 or >4 cycles). The other clinical characteristics we analyzed included the specific surgical options of the VATS group. The different surgical methods of patients in the VATS group were distributed as follows: 50 patients (52.1%) received lobectomy plus pleurodesis and were classified as the "lobectomy subgroup," 26 patients (27.1%) received segment or wedge resection plus pleurodesis and were classified into the "sub-lobectomy subgroup," and 20 patients (20.8%) received only pleurodesis under thoracoscope and were classified into the "palliative surgery subgroup."

All patients (100%) were followed-up in our study. Information was obtained from all patients through outpatient visits or telephone calls. All patients were evaluated every three months by chest and abdominal CT scans and brain MRI, and ECT was performed every six months for the first two years after surgery and annually thereafter. Overall survival (OS) was estimated from the date of lung surgery or thoracic drainage or until the last follow-up.

### Therapy Procedure

All patients were diagnosed with primary lung adenocarcinoma with MPE from tumor cells that were found in the pleural effusion and were then diagnosed with adenocarcinoma by bronchoscopy or percutaneous lung puncture.

In the VATS group, the primary tumors were considered resectable when the patients had a good Eastern Cooperative Oncology Group (ECOG) score and no severe comorbidities. Complete resection and limited resection were defined as lobectomy and sub-lobectomy (wedge or segment resection), respectively. All pleural metastatic lesions were removed or cauterized with a high frequency electric knife as much as possible. After that, pleurodesis was performed with 1% iodine

tincture under thoracoscopy. Those tumors that could not be resected were given only pleurodesis with 1% iodine tincture under thoracoscopy after all pleural metastatic lesions were cauterized with a high frequency electric knife. All the 2mm sizes visible under the microscope are treated. One to two weeks after surgery, the patients were given two cycles of chemotherapy (pemetrexed or paclitaxel plus platinum).

In the thoracic drainage group, a thoracic drainage tube was placed in the patients under the guidance of ultrasonograhy. After the effusion was drained, adhesive, sclerosing agent, or cisplatin were injected into the chest cavity for chemical pleurodesis. The patients were given two cycles of chemotherapy (pemetrexed or paclitaxel plus platinum). The dosage and administration of chemotherapy drugs that all patients received were recommended by the National Comprehensive Cancer Network (10). None of the patients had received neoadjuvant chemotherapy, radiotherapy, or targeted therapy before surgery or thoracic drainage (**Figure 1**).

## Efficacy Evaluation Criteria

The World Health Organization's unified criteria of MPE efficacy defines the responses to MPE treatment as follows: complete response (CR), in which the MPE completely disappeared and symptoms were completely relieved, which was maintained for more than four weeks; partial response (PR), in which the MPE volume was significantly reduced by >50% and the symptoms were obviously relieved for more than four weeks; and no change (NC), in which the above criteria were not met or the MPE was increased a short time after the reduction. The response rate (RR) is defined as CR + PR.

## Statistical Analysis

All data were processed by SPSS 17.0 statistical software. Multivariate Cox regression models were used to assess the association between treatment and OS. The Cochran-Mantel-Haenszel (CMH) $X^2$ test was used to evaluate the treatment effect on MPE between the VATS group and the thoracic drainage group, and the Kaplan–Meier method was used to analyze the OS of the two groups and subgroups. The difference was statistically significant when $p < 0.05$.

# RESULTS

The median age of all patients was 61.6 years old. There were 113 male patients (57.9%) and 82 female patients (42.1%); 104 patients (53.3%) had a smoking history and 91 patients (46.7%) had no smoking history; 79 patients (40.5%) had an ECOG score of 0–1, and 116 patients (59.5%) had an ECOG score of 2 or higher. The baseline characteristics of the two groups are shown in **Table 1**. For the baseline characteristics of age ($p = 0.361$), gender ($p = 0.328$) and smoking history ($p = 0.954$), there were no significant differences between the two groups; however, there was a significant difference in ECOG score ($p < 0.05$). Specifically, 53.1% of patients in the VATS group had an ECOG score of 0–1, which was significantly higher than the 28.3% in the thoracic drainage group. In multivariate analysis, when compared to the thoracic drainage group, the VATS group remained significantly associated with the overall survival [HR=0.480 (95%CI 0.301-0.765)]; when compared to the lobectomy, the sub- lobectomy and the palliative surgery, remained significantly associated with the overall survival [HR=0.637 (95%CI 0.409-0.993) and HR=0.548 (95%CI 0.435-0.832), respectively] (**Tables 2**, **3**).

## Analysis of MPE Therapeutic Effect in the Two Groups

The therapeutic effects of the two groups for MPE were distributed as follows: VATS group: NC (5 cases, 5.2%), CR (71 cases, 74%), and PR (20 cases, 20.8%), with an RR of 94.8%; thoracic drainage group: NC (29 cases, 29.3%), CR (18 cases, 18.2%), and PR (52 cases, 52.5%), with an RR of 70.7%. The CMH $X^2$ test was used to

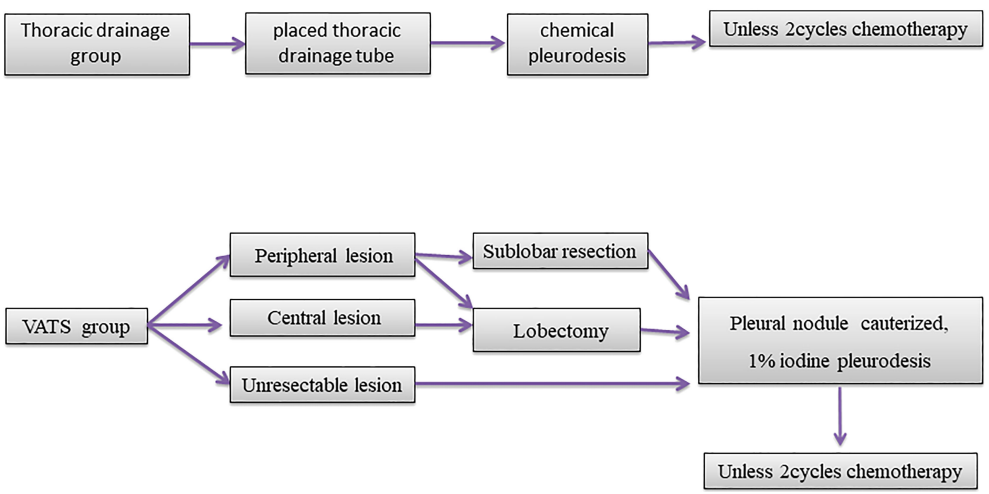


**FIGURE 1** | Outline of two groups of patients with different treatment process.

**TABLE 1** | Baseline characteristics of all patients.

| | | VATS group (n = 96) | Thoracic drainage group (n = 99) | p value |
|---|---|---|---|---|
| | Median age | 61 | 62.3 | |
| Age (years) | ≤60 | 46 (47.9%) | 41 (41.4%) | 0.361 |
| | >60 | 50 (52.1%) | 58 (58.6%) | |
| Gender | Male | 59 (61.5%) | 54 (54.5%) | 0.328 |
| | Female | 37 (38.5%) | 45 (45.5%) | |
| Smoking status | Non smoker | 45 (46.9%) | 46 (46.5%) | 0.954 |
| | smoker | 51 (53.1%) | 53 (53.5%) | |
| ECOG | 0-1 | 51 (53.1%) | 28 (28.3%) | <0.01 |
| | ≥2 | 45 (46.9%) | 71 (71.7%) | |
| Number of chemotherapy cycles | 2-4 | 38 (39.6%) | 38 (38.4%) | 0.864 |
| | >4 | 58 (60.4%) | 61 (61.6%) | |
| Surgical options | Lobectomy | 50 (52.1%) | / | / |
| | Sub-lobectomy | 26 (27.1%) | / | / |
| | palliative surgery | 20 (20.8%) | / | / |

assess whether there was any difference in MPE efficacy between the two groups. The location test results had a p of 0.0037, rejecting the hypothesis of $H_0$; thus, the effect differed between the two groups, and the difference was statistically significant. In conclusion, according to the row average score, the efficacy for treating MPE in the VATS group was better than that in thoracic drainage group (**Figure 2**, **Table 4**).

## Survival Analysis

All 195 patients were followed-up to the last follow-up time (March 2018). The MST from the onset of primary lung adenocarcinoma with MPE to death from any cause was 16 months [95% confidence interval (95% CI) 13.439–18.561]. For the 96 patients in the VATS group (49.2%), the MST was 25 months (95% CI 22.373–27.627), and the one-year and three-year survival rates were 88.6% and 21.6%, respectively. For the 99 patients (50.8%) in the thoracic drainage group, the MST was 11 months (95% CI 9.978–12.022), and the one-year and three-year survival rates were 36.4% and 1%, respectively. The hazard ratio (HR) was 0.480 (95% CI 0.301–0.765, log-rank p = 0.002). The MST in the VATS group was much longer than that in the thoracic drainage group (**Figure 3**). Generally, the Kaplan–Meier method was used to analyze the survival of all subgroups. In all subgroups, the survival benefit of the VATS group was significantly better than that of the thoracic drainage group, as indicated by the statistically significant log-rank test results (log-rank p < 0.01) (**Tables 5**, **6**).

These results indicate that patients in the VATS group have better survival benefits than those in the thoracic drainage group. The question then arises as to which factors can lead to better survival benefits in the VATS group. The Kaplan–Meier method was used to analyze the survival of all subgroups in the VATS group. We found that no smoking history, an ECOG score of 0–1, and undergoing a lobectomy or sub-lobectomy significantly improved OS in the VATS group. When stratified by patients who underwent different surgical options, we found that patients in the lobectomy subgroup had an MST of 27 months (95% CI 22.432–31.568), patients in the sub-lobectomy subgroup had an MST of 27 months (95% CI 19.157–34.843), and patients in the palliative surgery subgroup had an MST of 12 months (95% CI 7.617–16.383). There was no significant difference between the lobectomy subgroup and the sub-lobectomy subgroup (log-rank p = 0.915), but the survival of the lobectomy and sub-lobectomy subgroups was significantly better than that of the palliative surgery subgroup (log-rank p = 0.001 and p < 0.01, respectively). However, age, gender, and number of chemotherapy cycles had no effect on survival, which was evidenced by the lack of statistically significant differences (**Figure 4**, **Table 6**).

# DISCUSSION

According to the 7th edition of the International Lung Cancer TNM staging standard, the M stage of NSCLC with MPE is defined as M1a (11). The prognosis of such patients is generally considered very poor, and some scholars do not recommend surgical treatment (12). The International Association for the Study of Lung Cancer reports that the MST of cancer patients with MPE is approximately five to eight months, and the five-year survival rate is less than 2% (11, 13). Therefore, NSCLC with MPE belongs to stage IV lung cancer in the latest staging system published by the Union for International Cancer Control (14). Some studies have pointed out that MPE is caused by tumor-induced angiogenesis, and some scholars have also pointed out

**TABLE 2** | Multivariate Cox model for overall survival in all patients.

| | | Case (%) | HR (95%CI) | p value |
|---|---|---|---|---|
| Case | | 199 (100%) | | |
| Treatment mode | VATS group | 96 (49.2%) | 0.480 (0.301-0.765) | 0.002 |
| | Thoracic drainage group | 99 (50.8%) | – | – |

**TABLE 3** | Multivariate Cox model for overall survival in the VATS group.

| | | Case (%) | HR (95%CI) | p value |
|---|---|---|---|---|
| Case | | 96 (100%) | | |
| Treatment mode | Lobectomy | 50 (52.1%) | 0.637 (0.409-0.993) | <0.01 |
| | Sub- lobectomy | 26 (27.1%) | 0.548 (0.435-0.832) | 0.001 |
| | Palliative surgery | 20 (20.8%) | – | – |

that vascular endothelial growth factor may be an important cause of MPE by increasing vascular endothelial permeability and exudation (15). Some studies have shown that there are more than 1.5 million new patients with pleural effusion each year in the United States, and MPE caused by cancer accounts for the vast majority of such patients (16, 17). A clinical study involving 1783 patients with MPE found that bronchial lung cancer, particularly lung adenocarcinoma, accounted for disease in 36% of cases (18). There are still no clear guidelines for the treatment of such patients, and there is no confirmed best treatment plan. At present, commonly used clinical treatment methods include continuous therapeutic thoracentesis, chemical pleurodesis, pleural cavity catheter drainage, intrapleural chemotherapy, thoracoscopic pleurodesis and fixation, anti-angiogenesis therapy, molecular targeted therapy, etc. Continuous therapeutic thoracentesis can quickly relieve the clinical symptoms of patients, but the effect is not lasting. It has been reported that 97% of patients with MPE who only undergo continuous thoracentesis will relapse within one month (the average control time is approximately 4.2 days) (19). Spiegler PA et al. reported that the success rate of pleural fixation was approximately 79%, and no recurrence occurred after one month (20). Another study compared the two methods of immediate injection of sclerosing agent after catheter drainage and the injection of sclerosing agent after the drainage volume was less than 150 ml per day. The success rate of both methods of pleural fixation was approximately 79%, which was less than that of the former method only involved the injection of sclerosing agent before hospitalization days (21). With the development of minimally invasive surgical technology, thoracoscopic pleurodesis has been increasingly used by surgeons to control MPE. Several studies have shown that the success rate of thoracoscopic pleurodesis is higher than that after thoracentesis or catheterization, which is approximately 71%–95% (22–24). In our study, thoracoscopic surgery for pleurodesis had an effective rate of 94.8%, which was higher than the 70.7% from thoracic drainage, and according to the CMH $X^2$ test, the difference between the two groups was statistically significant. Thus, the effect of VATS on pleural effusion control was better than that of patients who received thoracic drainage.

For NSCLC patients with MPE, the commonly used therapies were thoracentesis, thoracic catheterization, thoracoscopic or thoracotomy, chemotherapy, radiotherapy, molecular targeted therapy, and other adjuvant treatment. A study from Taiwan included 27 NSCLC patients with MPE from 1998 to 2000. These patients received both intrapleural and systemic chemotherapy with standard gemcitabine plus cisplatin regimen followed by radiotherapy, finally followed by three to six cycles of docetaxel monotherapy. The results showed that the RR was 55%, of whom 7% of patients achieved CR. The median progression-free survival and OS were 8 and 16 months, respectively. The one-year survival rate was 63% (95% CI 45%–80%) (25). In another study from Korea, 40 NSCLC patients with MPE received intrapleural and systemic chemotherapy with cytarabine and cisplatin. The results showed that 86.5% of the patients achieved complete remission and 10.8% achieved partial remission. The overall effective rate was 97.3%. The median remission time was 12

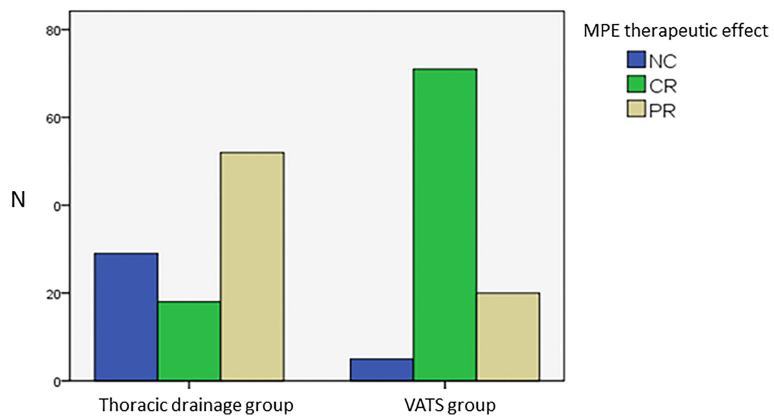


**FIGURE 2** | Analysis of MPE therapeutic effect of two groups.

**TABLE 4** | Comparison of the MPE therapeutic effect between the two groups.

| MPE therapeutic effect | VATS group | Thoracic drainage group | p value |
|---|---|---|---|
| CR | 71 (74%) | 18 (18.2%) | 0.0037 |
| PR | 20 (20.8%) | 52 (52.5%) | |
| NC | 5 (5.2%) | 29 (29.3%) | |

months, and that of two patients was nearly 23 months (26). Tieqin Liu reported in his study that 58 patients with M1a NSCLC with MPE or mural pleural metastasis but without distant organ metastasis underwent primary tumor resection (lobectomy or local resection), mediastinal and intrapulmonary lymph node dissection, intrapleural perfusion chemotherapy, and four to six cycles of platinum-containing chemotherapy after surgery. The results showed that the MST of all patients was 34.3 months, and the five-year survival rate was 12.5%. The five-year survival rate of patients with adenocarcinoma was better than that of patients with other pathological types (32.3% vs 25.4%). The five-year survival rate of patients without a smoking history was significantly higher than that of patients with smoking (40.3% vs 18.6%). The five-year survival rate of patients receiving adjuvant chemotherapy after surgery was better than that of patients without chemotherapy (47% vs 23.1%). Additionally, the five-year survival rate of patients receiving local resection was better than that of patients receiving complete resection (31.4% vs 16.3%) (27). A study conducted by Yasuhiko-ohta et al. included 42 patients with NSCLC with a median age of 63.5 years. All patients were diagnosed with pleural metastasis (M1a). Twenty patients underwent pulmonary wedge resection and pleural resection and pleurodesis, two patients received segmentectomy + pleurotomy and pleurodesis, and nineteen patients received lobectomy + pleurotomy and pleurodesis. The survival analysis showed that the distant metastasis were the only factors affecting the survival of all patients (28).

In our study, 96 patients received surgical treatment, which included either partial or complete resection of the primary tumor and metastasis. All patients received systemic chemotherapy. The 195 patients had an MST of 16 months (95% CI 13.439–18.561), which was similar to the results of previous studies. The MST of patients who underwent surgery was 25 months (95% CI 22.373–27.627), which was better than the MST of patients who received thoracic drainage (11 months, 95% CI 9.978–12.022). The MST of patients who received thoracic drainage was similar to that reported in many previous studies. The one-year and three-year survival rates of the VATS group were 88.6% and 21.6%, respectively, which were better than the respective rates of the thoracic drainage group (36.4% and 1%).

The OS of the patients in the VATS group was statistically analyzed in our study. The survival time of patients receiving lobectomy + pleurodesis ($p < 0.01$) or sub-lobectomy + pleurodesis ($p = 0.001$) was significantly better than that of patients receiving only pleurodesis. However, there was no significant difference in survival between lobectomy and sub-lobectomy ($p = 0.915$). Ohta et al. reported that the three-year survival rate of 42 patients with stage M1a lung cancer who received primary tumor and pleural metastasis was 31.4%, and the MST was 17 months (28). Lida et al. also found that 313 lung cancer patients with only mural pleural metastasis had a five-year survival rate of 29.3% and an MST of 34 months. In that study, 256 patients (81.8%) underwent primary tumor resection, and 152 patients (48.6%) underwent resection of all visible pleural metastases. The five-year survival rates of the two groups were 33.1% and 37.1%,

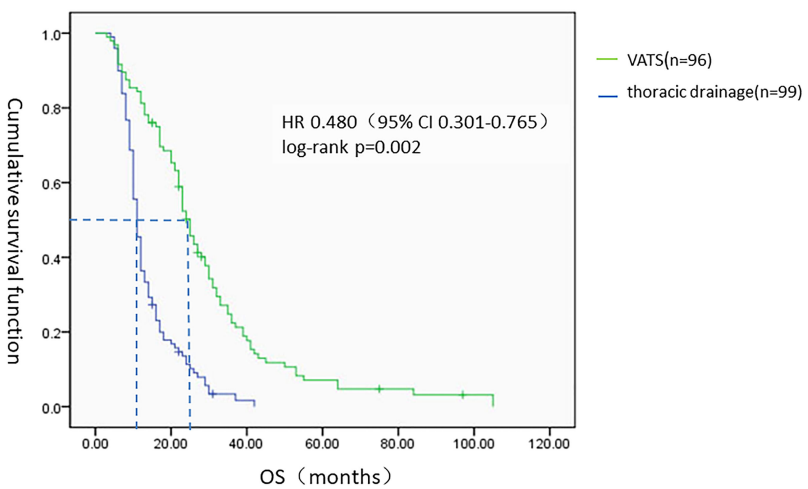


**FIGURE 3** | The Kaplan–Meier survival analysis of two groups. HR, hazard ratio.

**TABLE 5 |** Survival analysis of all subgroups.

| | | VATSMST (months) (95%CI) | Thoracic drainageMST (months) (95%CI) | p |
|---|---|---|---|---|
| Age | ≤60 | 23 (20.610-25.390) | 11 (9.435-12.565) | <0.01 |
| | >60 | 25 (20.541-29.459) | 11 (9.763-12.237) | <0.01 |
| Gender | Male | 23 (19.872-26.128) | 10 (9.042-10.958) | <0.01 |
| | Female | 31 (20.410-41.590) | 12 (9.809-14.191) | <0.01 |
| Smoking history | No | 29 (22.205-35.795) | 15 (10.373-19.627) | <0.01 |
| | Yes | 23 (21.060-24.940) | 10 (9.112-10.888) | <0.01 |
| ECOG | 0-1 | 30 (24.533-35.467) | 20 (14.979-25.021) | <0.01 |
| | ≥2 | 17 (11.920-22.080) | 10 (9.323-10.677) | <0.01 |
| Number of chemotherapy cycles | 2-4 | 23 (13.364-32.636) | 9 (7.792-10.208) | <0.01 |
| | >4 | 26 (21.027-30.973) | 13 (10.915-15.085) | <0.01 |

**TABLE 6 |** Survival analysis of VATS group.

| | | N (%) | MST (months) 95%CI | p value |
|---|---|---|---|---|
| VATS group | | 96 (100%) | 25 (22.373-27.627) | |
| Age(years) | ≤60 | 46 (47.9%) | 23 (20.610-25.390) | 0.292 |
| | >60 | 50 (52.1%) | 25 (20.541-29.459) | |
| Gender | male | 59 (61.5%) | 23 (19.872-26.128) | 0.172 |
| | female | 37 (38.5%) | 31 (20.410-41.590) | |
| Smoking history | No | 45 (46.9%) | 29 (22.205-35.795) | 0.001 |
| | Yes | 51 (53.1%) | 23 (21.060-24.940) | |
| ECOG | 0-1 | 51 (53.1%) | 30 (24.533-35.467) | <0.01 |
| | ≥2 | 45 (46.9%) | 17 (11.920-22.080) | |
| Number of chemotherapy cycles | 2-4 | 38 (39.6%) | 23 (17.449-28.551) | 0.311 |
| | >4 | 58 (60.4%) | 26 (21.027-30.973) | |
| Surgical options | 1.lobectomy | 50 (52.1%) | 27 (22.432-31.568) | 1 vs 2 0.915 |
| | 2.Sub- lobectomy | 26 (27.1%) | 27 (19.157-34.843) | 2 vs 3 0.001 |
| | 3.palliative surgery | 20 (20.8%) | 12 (7.617-16.383) | 1 vs 3 <0.01 |

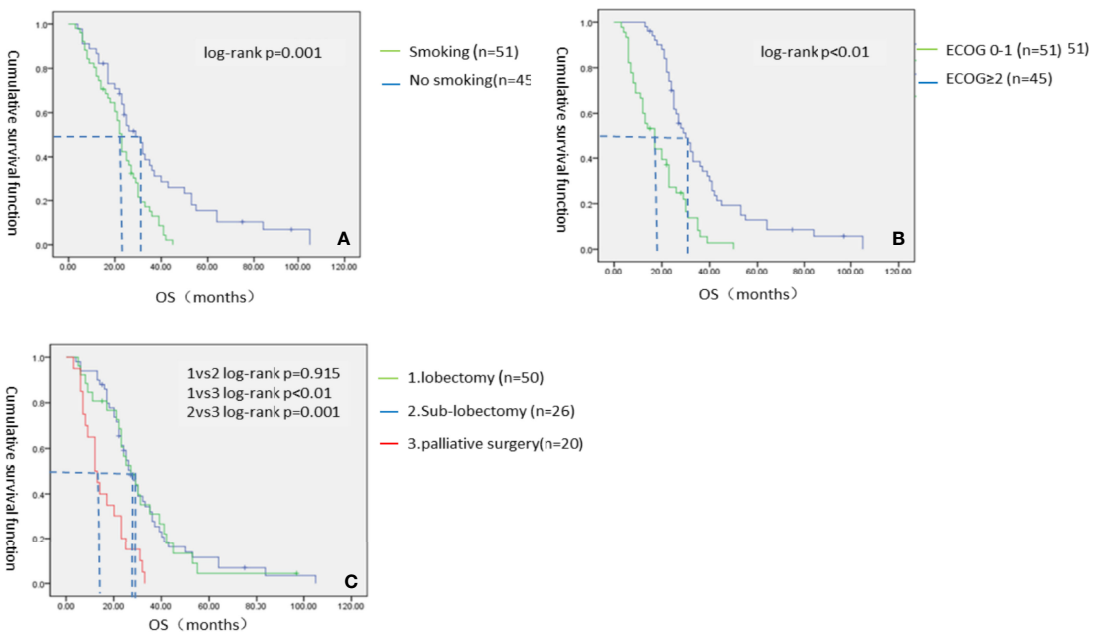


**FIGURE 4** | The Kaplan–Meier survival analysis of VATS groups. **(A)** Smoking status; **(B)** ECOG score; **(C)** Specific surgical options of VATS group.

respectively (29). NSCLC with MPE had a worse prognosis and shorter survival time than that with pleural metastasis but without MPE. A clinical study involving 98 patients showed that the survival time of lung cancer patients with MPE was significantly shorter than that of lung cancer patients with only pleural metastasis but without MPE. The MST was 38 vs 13 months in those two groups (30). Therefore, the resection of as many tumor tissues as possible seems to provide better survival benefits. The other two studies also provide a theoretical basis for surgical intervention of lung cancer with pleural metastasis, which is a special type of advanced lung cancer (31, 32). This is similar to the results in our study. The surgical resection of the primary tumor and visible metastasis simultaneously provided better survival benefits than resection of the primary tumor or resection of the pleural metastasis only (HR 0.637, 95% CI 0.409–0.993, $p < 0.01$). However, there was no significant difference between sub-lobectomy and lobectomy. The underlying reason may be that surgery reduces the tumor burden as much as possible without increasing the risk of death, but additional lobectomy does not provide an OS benefit, similar to early-stage NSCLC. However, it increases the risk of surgery and the potential for a poor pleurodesis effect due to the excessive lung tissue loss. Whether other surgical options, such as lymphadenectomy or total pleural resection, can benefit patient survival remains controversial, and larger sample size trials are necessary to provide theoretical evidence for the optimal surgical model for such patients. As a retrospective clinical study, this study also has some limitations, such as selective bias, which results in not all factors being equal between the two study groups, such as the ECOG score. There was a significantly higher proportion of patients with an ECOG score of 0–1 in the VATS group than in the thoracic drainage group, which may be due to the fact that patients in a good general condition are often selected for surgical operations whereas patients with a poor general condition usually choose a drug treatment with less trauma.

## CONCLUSION

The results of this study showed that VATS was more effective in controlling MPE than thoracic drainage. VATS can significantly improve the OS of patients with advanced lung adenocarcinoma with MPE compared with traditional thoracic drainage methods. Patients who received a lobectomy or sub-lobectomy plus pleurodesis under VATS had a better OS than those who received only pleurodesis under VATS. No smoking history and an ECOG score of 0–1 also improved the OS of these patients.

## DATA AVAILABILITY STATEMENT

The original contributions presented in the study are included in the article/supplementary material. Further inquiries can be directed to the corresponding authors.

## ETHICS STATEMENT

The studies involving human participants were reviewed and approved by Review Board of Tianjin Medical University General Hospital. The patients/participants provided their written informed consent to participate in this study.

## AUTHOR CONTRIBUTIONS

JC, XL, and HL wrote the manuscript. JHL, MD, CX, HZ, SX, SW, ZS, and GC collected the data. ML, JSL, and XL analyzed the data. JC and HL supervised the research. All authors contributed to the article and approved the submitted version.

## FUNDING

This study was supported by grants from the National Natural Science Foundation of China (82072595, 81773207 and 61973232), Natural Science Foundation of Tianjin (17YFZCSY00840, 18PTZWHZ00240, 19YFZCSY00040, and 19JCYBJC27000), Special Support Program for the High Tech Leader and Team of Tianjin (TJTZJH-GCCCXCYTD-2-6) and Tianjin Key Medical Discipline (Specialty) Construction Project. Funding sources had no role in study design, data collection, and analysis; in the decision to publish; or in the preparation of the manuscript.

## REFERENCES

1. Sánchez MJ, Payer T, De Angelis R, Larrañaga N, Capocaccia R, Martinez C. Cancer Incidence and Mortality in Spain: Estimates and Projections for the Period 1981-2012. *Ann Oncol* (2010) 21 Suppl 3:iii30–36. doi: 10.1093/annonc/mdq090
2. Ferlay J, Parkin DM, Steliarova-Foucher E. Estimates of Cancer Incidence and Mortality in Europe in 2008. *Eur J Cancer* (2010) 46(4):765–81. doi: 10.1016/j.ejca.2009.12.014
3. de Andrade FM. The Role of Indwelling Pleural Catheter in Management of Malignant Pleural Effusion: A Creative New Technique for an Old Method. *Lung India* (2015) 32(1):81–2. doi: 10.4103/0970-2113.148461
4. Jemal A, Siegel R, Xu J, Ward E. Cancer Statistics, 2010. *CA Cancer J Clin* (2010) 60(5):277–300. doi: 10.3322/caac.20073
5. Ramalingam S, Belani C. Systemic Chemotherapy for Advanced non-Small Cell Lung Cancer: Recent Advances and Future Directions. *Oncologist* (2008) 13 Suppl 1:5–13. doi: 10.1634/theoncologist.13-S1-5
6. Hellman S, Weichselbaum RR. Importance of Local Control in an Era of Systemic Therapy. *Nat Clin Pract Oncol* (2005) 2(2):60–1. doi: 10.1038/ncponc0075
7. Congedo MT, Cesario A, Lococo F, De Waure C, Apolone G, Meacci E, et al. Surgery for Oligometastatic non-Small Cell Lung Cancer: Long-Term Results From a Single Center Experience. *J Thorac Cardiovasc Surg* (2012) 144(2):444–52. doi: 10.1016/j.jtcvs.2012.05.051
8. Hanagiri T, Takenaka M, Oka S, Shigematsu Y, Nagata Y, Shimokawa H, et al. Results of a Surgical Resection for Patients With Stage IV Non–Small-Cell Lung Cancer. *Clin Lung Cancer* (2012) 13(3):220–4. doi: 10.1016/j.cllc.2011.05.006

9. Parikh RB, Cronin AM, Kozono DE, Oxnard GR, Mak RH, Jackman DM, et al. Definitive Primary Therapy in Patients Presenting With Oligometastatic non-Small Cell Lung Cancer. *Int J Radiat Oncol Biol Phys* (2014) 89(4):880–7. doi: 10.1016/j.ijrobp.2014.04.007
10. Ettinger DS, Akerley W, Borghaei H, Chang AC, Cheney RT, Chirieac LR, et al. Non-Small Cell Lung Cancer, Version 2.2013. *J Natl Compr Canc Netw* (2013) 11(6):645–53; quiz 653. doi: 10.6004/jnccn.2013.0084
11. Goldstraw P, Crowley J, Chansky K, Giroux DJ, Groome PA, Rami-Porta R, et al. The IASLC Lung Cancer Staging Project: Proposals for the Revision of the TNM Stage Groupings in the Forthcoming (Seventh) Edition of the TNM Classification of Malignant Tumours. *J Thorac Oncol* (2007) 2(8):706–14. doi: 10.1097/JTO.0b013e31812f3c1a
12. Ohta Y, Tanaka Y, Hara T, Oda M, Watanabe S, Shimizu J, et al. Clinicopathological and Biological Assessment of Lung Cancers With Pleural Dissemination. *Ann Thorac Surg* (2000) 69(4):1025–9. doi: 10.1016/S0003-4975(99)01579-9
13. Detterbeck FC, Boffa DJ, Tanoue LT, Wilson LD. Details and Difficulties Regarding the New Lung Cancer Staging System. *Chest* (2010) 137(5):1172–80. doi: 10.1378/chest.09-2626
14. Webber C, Gospodarowicz M, Sobin LH, Wittekind C, Greene FL, Mason MD, et al. Improving the TNM Classification: Findings From a 10-Year Continuous Literature Review. *Int J Cancer* (2014) 135(2):371–8. doi: 10.1002/ijc.28683
15. Kraft A, Weindel K, Ochs A, Marth C, Zmija J, Schumacher P, et al. Vascular Endothelial Growth Factor in the Sera and Effusions of Patients With Malignant and Nonmalignant Disease. *Cancer* (1999) 85(1):178–87. doi: 10.1002/(SICI)1097-0142(19990101)85:1<178::AID-CNCR25>3.0.CO;2-7
16. Kruger D. Evaluating the Adult With New-Onset Pleural Effusion. *JAAPA* (2013) 26(7):20–7. doi: 10.1097/01.JAA.0000431507.82701.f7
17. Porcel JM, Esquerda A, Vives M, Bielsa S. Etiology of Pleural Effusions: Analysis of More Than 3,000 Consecutive Thoracenteses. *Arch Bronconeumol* (2014) 50(5):161–5. doi: 10.1016/j.arbr.2014.03.012
18. Li Q, Sun W, Yuan D, Lv T, Yin J, Cao E, et al. Efficacy and Safety of Recombinant Human Tumor Necrosis Factor Application for the Treatment of Malignant Pleural Effusion Caused by Lung Cancer. *Thorac Cancer* (2016) 7 (1):136–9. doi: 10.1111/1759-7714.12296
19. Zahid I, Routledge T, Billè A, Scarci M. What is the Best Treatment for Malignant Pleural Effusions. *Interact Cardiovasc Thorac Surg* (2011) 12 (5):818–23. doi: 10.1510/icvts.2010.254789
20. Spiegler PA, Hurewitz AN, Groth ML. Rapid Pleurodesis for Malignant Pleural Effusions. *Chest* (2003) 123(6):1895–8. doi: 10.1378/chest.123.6.1895
21. Yildirim E, Dural K, Yazkan R, Zengin N, Yildirim D, Gunal N, et al. Rapid Pleurodesis in Symptomatic Malignant Pleural Effusion. *Eur J Cardiothorac Surg* (2005) 27(1):19–22. doi: 10.1016/j.ejcts.2004.08.034
22. Dresler CM, Olak J, Herndon JE 2nd, Richards WG, Scalzetti E, Fleishman SB, et al. Phase III Intergroup Study of Talc Poudrage vs Talc Slurry Sclerosis for Malignant Pleural Effusion. *Chest* (2005) 127(3):909–15. doi: 10.1378/chest.127.3.909
23. Trotter D, Aly A, Siu L, Knight S. Video-Assisted Thoracoscopic (VATS) Pleurodesis for Malignant Effusion: An Australian Teaching Hospital's Experience. *Heart Lung Circ* (2005) 14(2):93–7. doi: 10.1016/j.hlc.2005.02.004
24. Whitworth JM, Schneider KE, Fauci JM, Bryant AS, Cerfolio RJ, Straughn JM. Outcomes of Patients With Gynecologic Malignancies Undergoing Video-Assisted Thoracoscopic Surgery (VATS) and Pleurodesis for Malignant Pleural Effusion. *Gynecol Oncol* (2012) 125(3):646–8. doi: 10.1016/j.ygyno.2012.02.029
25. Su WC, Lai WW, Chen HH, Hsiue TR, Chen CW, Huang WT, et al. Combined Intrapleural and Intravenous Chemotherapy, and Pulmonary Irradiation, for Treatment of Patients With Lung Cancer Presenting With Malignant Pleural Effusion. A Pilot Study. *Oncology* (2003) 64(1):18–24. doi: 10.1159/000066516
26. Kim KW, Park SY, Kim MS, Kim SC, Lee EH, Shin SY, et al. Intrapleural Chemotherapy With Cisplatin and Cytarabine in the Management of Malignant Pleural Effusion. *Cancer Res Treat* (2004) 36(1):68–71. doi: 10.4143/crt.2004.36.1.68
27. Liu T, Liu H, Wang G, Zhang C, Liu B. Survival of M1a Non-Small Cell Lung Cancer Treated Surgically: A Retrospective Single-Center Study. *Thorac Cardiovasc Surg* (2015) 63(7):577–82. doi: 10.1055/s-0034-1396666
28. Ohta Y, Shimizu Y, Matsumoto I, Tamura M, Oda M, Watanabe G. Retrospective Review of Lung Cancer Patients With Pleural Dissemination After Limited Operations Combined With Parietal Pleurectomy. *J Surg Oncol* (2005) 91(4):237–42. doi: 10.1002/jso.20333
29. Iida T, Shiba M, Yoshino I, Miyaoka E, Asamura H, Date H, et al. Surgical Intervention for Non-Small-Cell Lung Cancer Patients With Pleural Carcinomatosis: Results From the Japanese Lung Cancer Registry in 2004. *J Thorac Oncol* (2015) 10(7):1076–82. doi: 10.1097/JTO.0000000000000554
30. Kim YK, Lee HY, Lee KS, Han J, Ahn MJ, Park K, et al. Dry Pleural Dissemination in Non-Small Cell Lung Cancer: Prognostic and Diagnostic Implications. *Radiology* (2011) 260(2):568–74. doi: 10.1148/radiol.11110053
31. Sawabata N, Matsumura A, Motohiro A, Osaka Y, Gennga K, Fukai S, et al. Malignant Minor Pleural Effusion Detected on Thoracotomy for Patients With non-Small Cell Lung Cancer: Is Tumor Resection Beneficial for Prognosis. *Ann Thorac Surg* (2002) 73(2):412–5. doi: 10.1016/S0003-4975(01)03426-9
32. Bernard A, de Dompsure RB, Hagry O, Favre JP. Early and Late Mortality After Pleurodesis for Malignant Pleural Effusion. *Ann Thorac Surg* (2002) 74 (1):213–7. doi: 10.1016/S0003-4975(02)03599-3


**Conflict of Interest:** The authors declare that the research was conducted in the absence of any commercial or financial relationships that could be construed as a potential conflict of interest.

frontiers | Frontiers in Oncology

ORIGINAL RESEARCH
published: 14 June 2022
doi: 10.3389/fonc.2022.816766

# A Prognostic Model of Non-Small Cell Lung Cancer With a Radiomics Nomogram in an Eastern Chinese Population

*Lijie Wang[1†], Ailing Liu[2†], Zhiheng Wang[1,3], Ning Xu[2], Dandan Zhou[2], Tao Qu[2], Guiyuan Liu[4], Jingtao Wang[1,5], Fujun Yang[6], Xiaolei Guo[7], Weiwei Chi[8*] and Fuzhong Xue[1,9*]*

[1] Department of Epidemiology and Health Statistics, School of Public Health, Cheeloo College of Medicine, Shandong University, Jinan, China, [2] Department of Pulmonary and Critical Care Medicine, Weihai Municipal Hospital, Cheeloo College of Medicine, Shandong University, Weihai, China, [3] Shandong Provincial Key Laboratory of Immunohematology, Qilu Hospital, Cheeloo College of Medicine, Shandong University, Jinan, China, [4] Department of Radiology, Weihai Municipal Hospital, Cheeloo College of Medicine, Shandong University, Weihai, China, [5] Department of Hematology, Qilu Hospital, Cheeloo College of Medicine, Shandong University, Jinan, China, [6] Department of Oncology, Weihai Municipal Hospital, Cheeloo College of Medicine, Shandong University, Weihai, China, [7] The Department for Chronic and Non-Communicable Disease Control and Prevention, Shandong Center for Disease Control and Prevention, Jinan, China, [8] National Administration of Health Data, Jinan, China, [9] Institute for Medical Dataology, Shandong University, Jinan, China

OPEN ACCESS

**Edited by:**
*Fiona Hegi-Johnson, University of Melbourne, Australia*

**Reviewed by:**
*John Kipritidis, Northern Sydney Local Health District, Australia*
*Alexis Andrew Miller, Royal North Shore Hospital, Australia*

***Correspondence:**
*Weiwei Chi*
*nahdyw@shandong.cn*
*Fuzhong Xue*
*xuefzh@sdu.edu.cn*

*†These authors have contributed equally to this work*

**Specialty section:**
*This article was submitted to Thoracic Oncology, a section of the journal Frontiers in Oncology*

**Received:** *17 November 2021*
**Accepted:** *11 May 2022*
**Published:** *14 June 2022*

**Citation:**
*Wang L, Liu A, Wang Z, Xu N, Zhou D, Qu T, Liu G, Wang J, Yang F, Guo X, Chi W and Xue F (2022) A Prognostic Model of Non-Small Cell Lung Cancer With a Radiomics Nomogram in an Eastern Chinese Population. Front. Oncol. 12:816766. doi: 10.3389/fonc.2022.816766*

**Background:** The aim of this study was to build and validate a radiomics nomogram by integrating the radiomics features extracted from the CT images and known clinical variables (TNM staging, etc.) to individually predict the overall survival (OS) of patients with non-small cell lung cancer (NSCLC).

**Methods:** A total of 1,480 patients with clinical data and pretreatment CT images during January 2013 and May 2018 were enrolled in this study. We randomly assigned the patients into training ($N$ = 1036) and validation cohorts ($N$ = 444). We extracted 1,288 quantitative features from the CT images of each patient. The Least Absolute Shrinkage and Selection Operator (LASSO) Cox regression model was applied in feature selection and radiomics signature building. The radiomics nomogram used for the prognosis prediction was built by combining the radiomics signature and clinical variables that were derived from clinical data. Calibration ability and discrimination ability were analyzed in both training and validation cohorts.

**Results:** Eleven radiomics features were selected by LASSO Cox regression derived from CT images, and the radiomics signature was built in the training cohort. The radiomics signature was significantly associated with NSCLC patients' OS (HR = 3.913, $p < 0.01$). The radiomics nomogram combining the radiomics signature with six clinical variables (age, sex, chronic obstructive pulmonary disease, T stage, N stage, and M stage) had a better prognostic performance than the clinical nomogram both in the training cohort (C-index, 0.861, 95% CI: 0.843–0.879 vs. C-index, 0.851, 95% CI: 0.832–0.870; $p < 0.001$) and in the validation cohort (C-index, 0.868, 95% CI: 0.841–0.896 vs. C-index, 0.854,

95% CI: 0.824–0.884; $p = 0.002$). The calibration curves demonstrated optimal alignment between the prediction and actual observation.

**Conclusion:** The established radiomics nomogram could act as a noninvasive prediction tool for individualized survival prognosis estimation in patients with NSCLC. The radiomics signature derived from CT images may help clinicians in decision-making and hold promise to be adopted in the patient care setting as well as the clinical trial setting.

**Keywords: non-small cell lung cancer, computed tomography, radiomics, nomogram, survival, TNM staging**

## 1 INTRODUCTION

Lung cancer is one of the most common types of cancer and a major cause of mortality worldwide for both men and women (1). Non-small cell lung cancer (NSCLC) is the most common type, which constitutes 84% of all lung cancer cases (2). Moreover, the 5-year survival rate following the diagnosis for the patients is as low as 17%, even though the prognosis and treatment of lung cancer have already been notably improved (3).

The tumor, node, and metastasis (TNM) staging is the most commonly used and universally accepted staging (clinical and pathological) system for cancer. TNM staging is simple to apply and can be highly discriminatory for survival (4). TNM staging is also beneficial in defining optimal therapeutic strategies in clinical trials. TNM staging gives an indication of prognosis as a probability of survival, but not identifying individual outcomes (5). Current prediction models are based on clinical, imaging, and/or pathological information. We can and should look to improve our classifications by determining additional effective prognostic indicators to achieve individualized management in clinical practice.

Recently, some studies have demonstrated the relations between lung cancer-related genes of tumors and survival prognosis, which can be used to improve the predictions from the traditional TNM staging strategies (6). The direct application of such early genetic information without clinical validation is clinically and ethically concerning (7). Tumors are spatially heterogeneous, making it difficult to apply biopsy data in a meaningful way.

Nowadays, with the help of non-invasive techniques and the ability to extract high-precision information, medical imaging becomes a clinical routine for diagnosis and prognosis (8). As an emerging methodology, radiomics has been used to analyze complicated and confounding information and then quantitatively extract valuable information from medical images by using high-throughput calculations (9). To be more specific, radiomics converted the images into mineable, comprehensive quantitative features following four steps (1): image acquisition and reconstruction, (2) segmentation of ROI, (3) feature extraction and quantification, and (4) model construction (10). The radiomics features can be extracted from not only unmanipulated medical images but also images processed by Gaussian and wavelet filters (8).

In the case of lung cancer, medical images reflecting features of tumors usually rely on radiological data (e.g., chest CT and brain MRI scans). At present, it is a common clinical practice for lung cancer patients to undergo CT examinations in order to identify tumor size and location. Features from CT can be used to predict the malignant potential of a nodule on a chest CT based on the correlations between them (11, 12). In addition, some features of a nodule are identified to be closely related to diagnosis (e.g., lung cancer screening) and tumor genomics (13). In the last decade, many studies have been conducted to figure out which factors measured from CT can be correlated to overall survival (OS) for the tumor patients. Radiomics can also be applied to predict response to some certain treatments (14).

Some previous studies have investigated the correlation between radiomics features and survival (15–20). Hawkins et al. built the classifiers that could predict survival time for adenocarcinoma using CT image features. The highest classification accuracy (AUC) was 77.5% (15). Yang et al. showed that PET/CT imaging data can be potentially used as a biomarker combined with clinical factors (distant metastasis, carcinoembryonic antigen, stage, and targeted therapy) in risk stratification for the OS with NSCLC patients. The performance of the model was 0.789 measured by the Harrell's concordance statistic (C-index) (16). The C-index was the most commonly used performance measure to evaluate the discriminative ability of the developed models for survival data. The calculation of C-index considered the situation of censoring by interpreting for a pair of patients with and without the outcome. It ranged between 0.5 and 1.0; 0.5 indicated the random guesses and 1.0 represented that the predicted probabilities were perfectly the same as the observed survival information. A C-statistic of 0.7 to 0.8 was acceptable, while a C-statistic greater than 0.8 indicated good performance (21, 22). Botta et al. developed the model based on radiomic and clinical features (tumor location and T stage) for OS prediction, and had moderate performance with C-index = 0.57 (17). Xu et al. demonstrated that integrating CT scans at several different time points by the deep learning method could improve clinical prognosis predictions of patients with locally advanced NSCLC (e.g., 2-year OS: AUC = 0.74, $p < 0.05$) (18). Khorrami et al. showed that changes in CT radiographic characteristics correlated with lymphocyte distribution and

**Abbreviations:** NSCLC, non-small cell lung cancer; TNM, tumor-node-metastasis; CT, computed tomography; LASSO, least absolute shrinkage and selection operator; C-index, the Harrell concordance index; HR, hazard ratio; CI, confidence interval.

could predict OS (HR: 1.64, 95% CI: 1.22–2.21, $p$ = 0.001, C-index = 0.72) and response to immunotherapy in NSCLC (19). Yang et al. developed a radiomics nomogram by integrating the radiomics signatures extracted from combined 2D and 3D CT images and clinical factors (age, sex, T stage, and N stage) to evaluate the OS with NSCLC patients (C-index = 0.710) (20). However, these studies used limited mining of imaging data due to relatively small sample sizes or only a small number of extracted radiomics features.

Nomograms are generally accepted as a useful and reliable tool to evaluate risk and predict individualized cancer prognosis (23). Our team had successfully developed a radiomics nomogram to distinguish malignant from benign pulmonary nodules for the early screening and diagnosis of lung cancer clinically (24). In this study, we aimed to further develop a radiomics nomogram incorporating traditional clinical factors, such as TNM, for predicting the OS of patients with NSCLC.

# 2 MATERIALS AND METHODS

## 2.1 Study Cohort

A total of 1,524 patients with clinical data and pretreatment chest CT images at the Weihai Municipal Hospital during January 2013 and May 2018 were identified in this study. The inclusion criteria were defined as follows: (1) patients were histopathologically confirmed with NSCLC either by surgical specimen or by preoperative biopsy, (2) patients who received non-contrast-enhanced CT scans during the diagnosis, (3) patients aged ≥18 years, and (4) patients not diagnosed with lung cancer or other types of malignant tumors in the past 5 years. The exclusion criteria were defined as follows: (1) CT images were too blurry to identify the patient's tumor area, and (2) eligible variables were incomplete. The study protocol was conducted under approval by the Public Health Ethics Committee of Shandong University (Approval No. 20180801). The requirement for informed consent was waived because of the retrospective nature of the study.

## 2.2 Ascertainment of Exposures

The exposure information consisted of two parts: the clinical data and the assessment of CT scans for each patient. In our study, clinical data were collected from electronic medical record and examination data by oncologists (AL, NX, and DZ) and a data manager (ZW). The following variables were collected: the sociodemographics of the patients (age at diagnosis, sex, smoking status, and drinking status), the presence of any comorbidity [chronic obstructive pulmonary disease (COPD), hypertension, diabetes, coronary heart disease (CHD), and cerebrovascular disease], and pathologic data [histopathological diagnosis, tumor location, tumor (T stage), node (N stage), metastasis status (M stage), and staging].

Smoking status was categorized as never, former, and current smoking. Drinking status was categorized as yes and no. Comorbidities were defined according to the International Classification of Diseases, 10th Revision (ICD-10) code: CODP, J40–J44; hypertension, I10–I15; diabetes, E10–E14; CHD, I20–I25; and cerebrovascular disease, I60–I69. The location of the tumor was categorized as the right upper, right middle, right lower, left upper, and left lower. Pathologic staging was defined in accordance with the eighth edition of the American Joint Committee on Cancer TNM staging system (25).

## 2.3 Image Acquisition and Radiomics Feature Extraction

The radiomics workflow is presented in **Supplementary Figure S1**. CT scans were obtained with participants at baseline before percutaneous puncture, bronchoscopic biopsy, or surgery. The included CT images were carried out using a SIEMENS SOMATOM Definition Flash system (Siemens Healthineers, Erlangen, Germany). Detailed CT scan parameters for the reconstructed image were described as follows: the tube voltage, 120 kV; current, 150 effective mAs; beam collimation, 128 × 0.6 mm; pitch, 1.2; slice thickness, 1.0 mm; and gantry rotation time, 0.5 s. These settings were the same for all patients in our study. Both lung window and mediastinum window were included in the CT images of each patient. Here, we used the lung window of the CT images to extract radiomics features.

The segmentation of the tumor region of interest was performed using 3D Slicer (www.slicer.org), a free open-source software (version 4.8.0, National Institutes of Health, Bethesda, MD, USA) (26). Each CT image was semi-automatically segmented for each lesion slice by slice by two doctors in Weihai Municipal Hospital, Weihai, Shandong, China (Dr. Ailing Liu, Department of Respiratory Internal Medicine; Dr. Guiyuan Liu, Department of Radiology) who were blinded to the patient cohort. The guidance of tumor segmentation is listed in Supplementary Material. The interobserver variability of radiomics feature extraction was estimated by the intraclass correlation coefficients (ICC) (27). An ICC value greater than 0.75 was considered to represent good agreement.

The CT scans acquired in the clinical processes, as well as those processed with Gaussian and wavelet filters, had their quantitative radiomics features extracted by using the PyRadiomics library (version 2.1), a free open-source python (version 3.6, https://www.python.org/) package that provides many options to customize extracting the radiomics features from CT images (28). The calculation methods for each radiomics feature were described in the following website: https://pyradiomics.readthedocs.io/en/latest/features.html. Laplacians of Gaussian filtering or wavelet filtering were used in image pre-processing. All radiomics features were defined, adhered to the Imaging Biomarkers Standardization Initiative guidelines, and were assigned into the following three groups: (1) first-order features, (2) shape features, and (3) texture features (29). The features were extracted from the original images and the pre-processed images. In total, 1,288 radiomics features were extracted from CT images per patient (Supplementary Material and Supplementary **Table 1**). More detailed information about the process of image acquisition and reconstruction, region of interest segmentation, and feature extraction and quantification has previously been described by Liu et al. (24).

**TABLE 1** | Baseline demographic and clinical characteristics in the study.

| Variable | Level | Training data (*N* = 1,036) | Validation data (*N* = 444) | Total (*N* = 1,480) | *p*-value |
|---|---|---|---|---|---|
| Age | Mean (SD) median | 60.63 (8.77) 61.00 | 61.08 (8.85) 61.00 | 60.77 (8.79) 61.00 | 0.360 |
| Sex | Female | 517 (49.90) | 216 (48.65) | 733 (49.53) | 0.700 |
| | Male | 519 (50.10) | 228 (51.35) | 747 (50.47) | |
| Tumor location | Right upper | 321 (30.98) | 140 (31.53) | 461 (31.15) | 0.958 |
| | Right lower | 196 (18.92) | 89 (20.05) | 285 (19.26) | |
| | Right middle | 103 (9.94) | 40 (9.01) | 143 (9.66) | |
| | Left upper | 236 (22.78) | 97 (21.85) | 333 (22.50) | |
| | Left lower | 180 (17.37) | 78 (17.57) | 258 (17.43) | |
| Smoking status | Never | 686 (66.22) | 307 (69.14) | 993 (67.09) | 0.455 |
| | Current | 222 (21.43) | 91 (20.50) | 313 (21.15) | |
| | Former | 128 (12.36) | 46 (10.36) | 174 (11.76) | |
| Drinking status | No | 866 (83.59) | 386 (86.94) | 1,252 (84.59) | 0.120 |
| | Yes | 170 (16.41) | 58 (13.06) | 228 (15.41) | |
| T stage | T1 | 517 (49.90) | 242 (54.50) | 759 (51.28) | 0.131 |
| | T2 | 338 (32.63) | 141 (31.76) | 479 (32.36) | |
| | T3 | 77 (7.43) | 32 (7.21) | 109 (7.36) | |
| | T4 | 104 (10.04) | 29 (6.53) | 133 (8.99) | |
| N stage | N0 | 708 (68.34) | 324 (72.97) | 1,032 (69.73) | 0.218 |
| | N1 | 92 (8.88) | 32 (7.21) | 124 (8.38) | |
| | N2 | 159 (15.35) | 65 (14.64) | 224 (15.14) | |
| | N3 | 77 (7.43) | 23 (5.18) | 100 (6.76) | |
| M stage | M0 | 921 (88.90) | 385 (86.71) | 1,306 (88.24) | 0.267 |
| | M1 | 115 (11.10) | 59 (13.29) | 174 (11.76) | |
| COPD | No | 721 (69.59) | 333 (75.00) | 1,054 (71.22) | 0.041 |
| | Yes | 315 (30.41) | 111 (25.00) | 426 (28.78) | |
| Hypertension | No | 755 (72.88) | 306 (68.92) | 1,061 (71.69) | 0.137 |
| | Yes | 281 (27.12) | 138 (31.08) | 419 (28.31) | |
| Diabetes | No | 935 (90.25) | 390 (87.84) | 1,325 (89.53) | 0.195 |
| | Yes | 101 (9.75) | 54 (12.16) | 155 (10.47) | |
| CHD | No | 926 (89.38) | 413 (93.02) | 1,339 (90.47) | 0.037 |
| | Yes | 110 (10.62) | 31 (6.98) | 141 (9.53) | |
| Cerebrovascular disease | No | 1,010 (97.49) | 432 (97.30) | 1,442 (97.43) | 0.971 |
| | Yes | 26 (2.51) | 12 (2.70) | 38 (2.57) | |

*SD, standard deviation; COPD, chronic obstructive pulmonary disease; CHD, coronary heart disease.*

## 2.4 Follow-Up

The study outcome was OS, which was calculated from the date of diagnosis (date of surgery or biopsy) to the date of death, recorded *via* linkages to the database of death registries of Shandong Province by civil ID number, or May 30, 2021, whichever occurred first.

## 2.5 Statistical Analysis

We randomly assigned 70% of the patients to the training cohort, and 30% to the validation cohort. The training cohort was used to develop the model while the validation cohort was used to qualify the performance of the model. **Figure 1** shows the flowchart of the study.

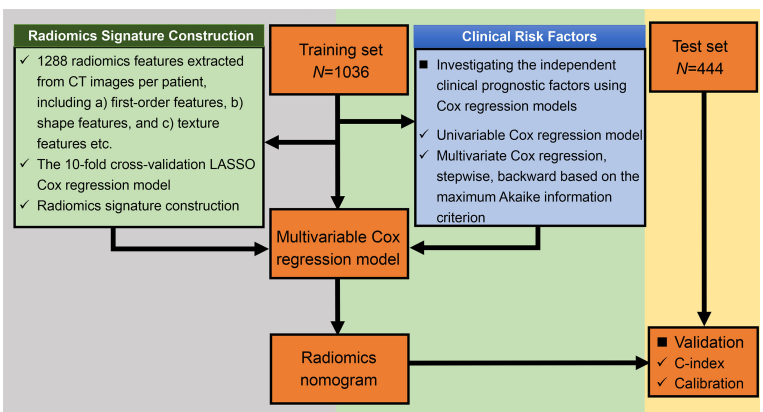


**FIGURE 1** | The flowchart of the study.

### 2.5.1 Descriptive Analyses

Means ± standard deviations (SDs) or medians [interquartile ranges (IQRs)] were reported for quantitative variables. Frequencies and proportions (*N*, %) were reported for categorical variables. Quantitative baseline variables were compared with *t*-tests. Categorical variables were compared by performing the chi-square tests between groups.

### 2.5.2 Construction of the Radiomics Signature

We used the 10-fold cross-validation Least Absolute Shrinkage and Selection Operator (LASSO) Cox regression model, which was an effective attractive method for high-dimensional data in survival analysis, to select the optimal nonzero coefficient features in the training cohort in order to reduce model overfitting (30). The most critical step for the LASSO Cox regression model was to determine the optimized hyperparameter λ, which ensured minimal model deviation. The radiomics signature for each participant was the weighted sum of all the selected radiomics features in terms of the following formula: $Radiomics\ signature = \sum_{i=1}^{N} coef_i X_i$, where $N$ is defined as the total number of selected feature, $coef_i$ is the value of non-zero coefficient of the $i$th selected feature, and $X_i$ is the value of the $i$th selected feature. The C-index was calculated so as to evaluate the predictive performance of the radiomics signature in both the training and validation cohorts (31). In addition, to validate the potential correlation between radiomics signature with OS, we categorized the patients as low-level and high-level risk based on their median radiomics signature. The Kaplan–Meier method was performed to estimate the OS of the two groups, while the difference in the survival curves was tested using the log-rank test.

### 2.5.3 Construction and Validation of the Clinical Model

The correlation between OS and each clinical variable including the TNM stage was first analyzed with the univariable Cox regression model. Significant clinical variables whose *p*-value was less than 0.05 in the univariable analysis were evaluated using the Kaplan–Meier method and then were integrated into a multivariable Cox regression model to identify independent prognostic factors. The final multivariable Cox regression model was constructed using the stepwise backward variable selection process based on the maximum Akaike information criterion (AIC) (32). The corresponding C-index was calculated for evaluating the performance of the predictive probability of OS for each patient in both the training and the validation cohorts.

### 2.5.4 Construction and Evaluation of a Radiomics Nomogram

Finally, the radiomics nomogram for predicting the OS was established based on the multivariable Cox regression model by combining the radiomics signatures and all the independent clinical risk factors derived from the clinical model. To test the robustness of the risk factors in the radiomics nomogram, we also did the stepwise Cox regression with all the risk factors (the clinical risk factors and the radiomics signatures) to see if the same risk factors remained in this time. The C-index and calibration curve were calculated to evaluate the validity of the established radiomics nomogram (33). To further validate the prognostic ability, the survival probabilities of all the patients were classified into four subgroups using the quartile values derived from the radiomics nomogram as thresholds. Survival curves were estimated for four subgroups using the Kaplan–Meier method and compared statistically using the log-rank test.

### 2.5.5 Assessment of the Incremental Value of Radiomics Signature

The incremental value of the radiomics signatures to the clinical factors was evaluated by comparing the performance of the radiomics nomogram derived in this study with the clinical model in respect of discrimination (C-index) and calibration (calibration curves). The calibration curves were constructed to show accordance between nomogram-predicted survival probability with the observed survival probability using 1,000 bootstrap resamples (33). The calibration curve along the diagonal line indicated that the predicted probabilities were exactly the same as the actual outcomes, which is the hypothetical perfect situation.

All statistical analyses were performed using the R software (http://www.r-project.org) and a two-tailed *p*-value less than 0.05 was regarded as statistically significant. The LASSO Cox regression was performed using the R package *glmnet*. Stepwise AIC was implemented using the R function "step", and the nomogram was built using the "rms" package.

## 3 RESULTS

Among 1,524 patients, 44 patients (2.89%) were excluded because they were missing T stage (23 patients) and N stage (37 patients), respectively. Overall, there were 1,480 patients histologically confirmed with NSCLC with complete information in both clinical and CT image data in our study. All the 1,480 patients enrolled had complete follow-up information. Among them, adenocarcinoma ($N$ = 1,218) and squamous cell carcinoma ($N$ = 235) accounted for approximately 98% of patients, while other histology types, such as adenosquamous carcinoma and large cell lung cancer, were present in 2% of patients. Stage distribution of patients was listed as follows: stage IA = 666, stage IB = 220, stage IIA = 42, stage IIB = 125, stage IIIA = 167, stage IIIB = 71, stage IIIC = 15, and stage IV = 174. The observed numbers of deaths were 397 of 1,480 patients. Median follow-up time was 4.06 years (range, 9 days–8.02 years). The median age at diagnosis was 61 years. Approximately one-third of the patients had a history of smoking and COPD. We randomly divided the data into training ($N$ = 1036) and validation cohorts ($N$ = 444). The clinical characteristics are summarized in **Table 1**.

## 3.1 Feature Selection and Radiomics Signature Building

The interobserver ICCs ranged from 0.790 to 0.937, indicating favorable interobserver feature extraction reproducibility. Eleven features with non-zero coefficients were taken as the predictive radiomics features, which were obtained by the LASSO Cox

regression model using 10-fold cross-validation in the training cohort (**Supplementary Materials** and **Supplementary Figure S2**). The optimal $\lambda$ was 0.064 when the model had the minimum deviance. Then, an individual patient's radiomics signature was calculated as a linear combination of the selected features weighted by their respective LASSO coefficients (**Supplementary Table 2**).

## 3.2 Prognostic Validation of the Radiomics Signature

Cox regression analyses showed that radiomics signatures were significantly associated with OS for NSCLC in both the training cohort ($p < 0.001$, HR = 3.913, 95% CI: 3.367–4.547) and the validation cohort ($p < 0.001$, HR = 3.867, 95% CI: 3.100–4.824). Additionally, the performance of radiomics signatures for predicting OS for NSCLC was evaluated using the Cox regression model. The radiomics signature yielded a C-index of 0.808 (95% CI: 0.784–0.831) on the training cohort and 0.820 (95% CI: 0.786–0.853) on the validation set (**Table 2**).

Furthermore, the patients were stratified into low-risk and high-risk groups in terms of the median value of the radiomics signature (−0.716). The Kaplan–Meier method was performed in the training and validation cohorts to analyze the association of the radiomics signature with OS in NSCLC patients (**Supplementary Figure S3**). Apparently, patients from the low-risk group had a notably better OS when compared with those in the high-risk group by the log-rank test in the training set ($p < 0.001$). The consensus result was found in the validation cohort.

## 3.3 Construction of Clinical Model and Radiomics Nomogram

Univariate Cox regression analyses showed that age, sex, smoking status, drinking status, COPD, T stage, N stage, and M stage were significantly associated with an increased risk of death for patients with NSCLC in the training cohort (all $p < 0.01$, **Supplementary Figure S4**). Kaplan–Meier survival analysis showed significant difference in the OS by each clinical factor (**Supplementary Figure S5**). Multivariable Cox analysis included these eight clinical variables and was performed using backward stepwise feature selection based on the maximum AIC. The final clinical Cox regression model included six clinical variables, namely, age, sex, COPD, T stage, N stage, and M stage (all $p < 0.05$, **Supplementary Figure S6).**

We integrated the radiomics signatures with the six clinical variables to apply the stepwise multivariate Cox model, which identified that the radiomics signature remained an independent prognostic factor even after adjusting for clinical variables ($p < 0.001$, HR = 1.829, 95% CI: 1.465–2.283, **Supplementary Figure S7**). On the basis of the final multivariable Cox model, we constructed a radiomics nomogram that visually depicted the multivariate impact of each variable in the Cox regression model (**Figure 2**).

**TABLE 2** | The C-index with 95% confidence intervals calculated for the training and validation cohorts.

| | Training cohort | | Testing cohort | |
|---|---|---|---|---|
| | C-index | 95% CI | C-index | 95% CI |
| Radiomics signature | 0.808 | 0.784–0.831 | 0.820 | 0.786–0.853 |
| Clinical model | 0.851 | 0.832–0.870 | 0.854 | 0.824–0.884 |
| Radiomics nomogram | 0.861 | 0.843–0.879 | 0.868 | 0.841–0.896 |

*CI, confidence interval.*

## 3.4 Performance of the Radiomics Nomogram

The calibration curves for the probability of 1-, 3-, and 5-year OS showed good agreement between the prediction by the radiomics nomogram and the actual observations in the training cohort and in the validation cohort since the predicted survival probability was very close to the actual survival time of patients (**Figure 3**). Furthermore, based on the radiomics nomogram, we subdivided the patients in the training cohort into four subgroups according to quartiles of predicted survival probabilities. The same threshold was applied to the validation cohort. A significant distinction between Kaplan–Meier curves was found ($p < 0.001$ and $p < 0.001$ in the training cohort and validation cohort, respectively) (**Supplementary Figure S8).**

## 3.5 Assessment of the Incremental Value of Radiomics Signature

The C-index and 95% CI for predicting OS using the clinical model were 0.851 (95% CI: 0.832–0.870) and 0.854 (95% CI: 0.824–0.884) in the training cohort and validation cohort, respectively. The C-index from the radiomics nomogram yielded 0.861 (95% CI: 0.843–0.879) in the training cohort and 0.868 (95% CI: 0.841–0.896) in the validation cohort (**Table 2**). The radiomics nomogram that integrated the radiomics

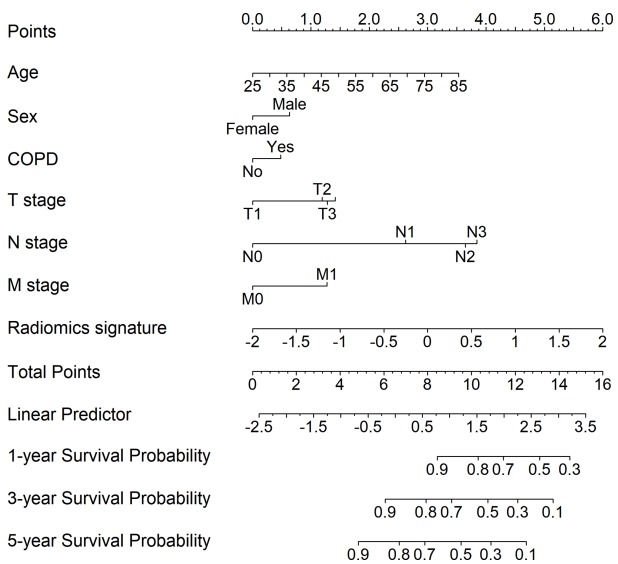


**FIGURE 2** | Development of the radiomics nomogram for patients with non-small cell lung cancer by integrating the radiomics signature with clinical information to predict the probability of overall survival at 1, 3, and 5 years.

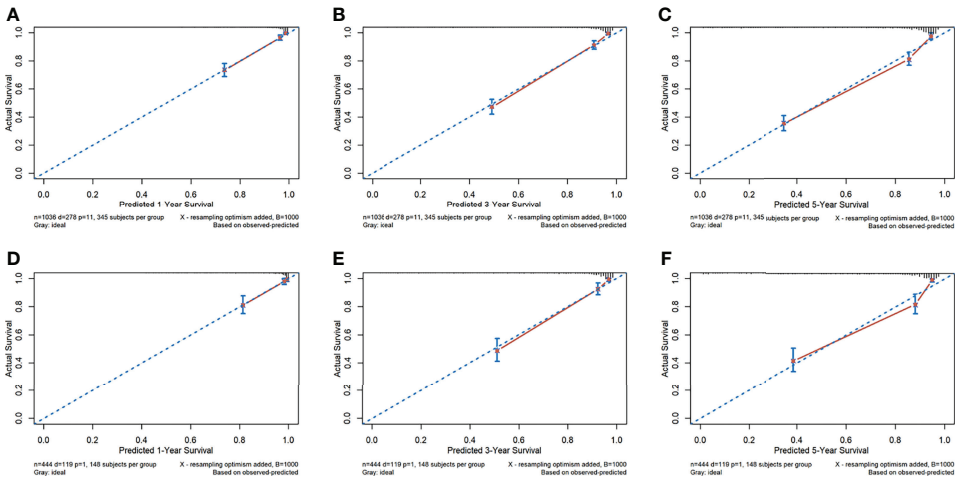


**FIGURE 3** | The calibration curves of the radiomics nomogram. (A–F) Calibration curves for predicting patient survival in the training cohort at 1 year **(A)**, 3 years **(B)**, and 5 years **(C)** and in the validation cohort at 1 year **(D)**, 3 years **(E)**, and 5 years **(F)**. The overall survival predicted by the radiomics nomogram is on the *x*-axis, while the actual overall survival is on the *y*-axis. A graph drawn along the diagonal line represents the perfect prediction in which the predicted probabilities is exactly the same as the actual outcomes.

signature and clinical variables outperformed the clinical model based on clinical variables alone, with a $p$-value < 0.001 in the training cohort and $p = 0.002$ in the validation cohort.

## 4 DISCUSSION

Lung cancer is the world's leading cause of cancer death. Screening for lung cancer by low-dose computed tomography reduces mortality. The NSCLC TNM staging system was developed by the International Association for the Staging of Lung Cancer (IASLC) Lung Cancer Staging Project by a coordinated international effort to develop data-derived TNM classifications with significant survival differences. Based on these TNM groupings, current 5-year survival estimates in NSLCC range from 73% in stage IA disease to 13% in stage IV disease. TNM stage remains the most important prognostic factor in predicting recurrence rates and survival times, followed by tumor histologic grade, and patient sex, age, and performance status (34). However, the wide spectrum of survival times that exists even after complete resection of the same-staged NSCLCs demonstrates the importance of other prognostic factors.

We have developed a radiomics nomogram for predicting the OS of patients with NSCLC in an Eastern Chinese population. The prediction model included the radiomics signatures derived from the CT images using the LASSO Cox regression, and six traditional clinical factors, namely, age, sex, COPD, T stage, N stage, and M stage. The model was developed in the training cohort ($N$ = 1,036) and validated in the test dataset ($N$ = 444). The model showed good discrimination, which was indicated by the C-index over 0.86 in both the training cohort and the validation cohort. The calibration curves for probability of OS demonstrated good agreement between the prediction by the radiomics nomogram and the actual observations. Risk group stratification further guaranteed the prediction power of the established model, and also confirmed the reliability of our results.

Radiological medical images provide patient and tumor-specific information that could provide insights into personalized medicine and be used to improve clinical prognosis assessment. So far, many studies have demonstrated the effectiveness of radiomics for the prognosis of NSCLC (15, 20, 35). Yang et al. developed a radiomics nomogram by combining the radiomics signatures and four clinical predictors (age, sex, T stage, and N stage) to evaluate the OS with NSCLC patients. The performance of the model was 0.710 measured by the C-index (20). This model was similar to our model, except that we included the M stage as the prognosis factor in the radiomics nomogram (HR = 1.670, 95% CI: 1.254–2.223, $p$ < 0.001), and could be applied to a wider range of NSCLC. Moreover, researchers have found that COPD could be a driving factor in lung cancer by increasing oxidative stress and causing DNA damage, inhibiting DNA repair mechanisms, and increasing cell proliferation (36, 37). We have included COPD in our model to make a more precise prediction of OS in NSCLC.

The advantages of our model compared with the other models in predicting NSCLC are listed as follows (1): more comprehensive quantitative features ($N$ = 1,288) were extracted from CT images than the previous study, which led to deeper mining of medical imaging; (2) these studies usually employed methods such as the Kaplan–Meier method to clarify the correlation between radiomics features and prognosis. In this study, we used the tenfold cross-validation LASSO Cox model to select the optimal features from 1,288 radiomics features, which contains first-order statistical features, shape-based features, statistical-based texture features,

and Gaussian and wavelet information that could improve the stability of the radiomics model. Eleven features were used to construct the radiomics signatures. Our team had successfully established the radiomics nomogram as a preoperative prediction tool for malignant pulmonary nodule diagnosis. The validation results showed that the nomogram has good discrimination (C-index = 0.809) and calibration capacities, which indicated its clinical application in the early screening of lung cancer (24). (3) The sample size ($N$ = 1,480) was larger than the previous study; (4) the clinical information was thorough compared with the previous study. We included the sociodemographics of the patients (age at diagnosis, sex, smoking status, and drinking status), the presence of any comorbidity (COPD, hypertension, diabetes, CHD, and cerebrovascular disease), and pathologic data (tumor location, T stage, N stage and M stage) to obtain the optimal prediction clinical variables. Six independent prognostic factors (age, sex, COPD, T stage, N stage, and M stage) were identified by the multivariate Cox model based on the AIC criteria for the best combination to predict the OS and entered into the nomogram; (5) the radiomics signature was an independent prognostic factor and outperformed clinical features in predicting OS of NSCLC patients. Our model yielded a higher C-index of 0.868 (95% CI: 0.841–0.896) in the validation cohort. The performance of our model was measured in a number of ways including calibration and the risk stratification analysis.

In this retrospective study, the data were collected from the Weihai Municipal Hospital located in East China. The characteristics of this Eastern Chinese lung cancer population differ considerably from other, particularly Western, lung cancer populations. On average, people from East China are richer than those in Central and West China, and thanks to widespread screening programs, residents are more willing to undergo routine physical examinations, which is helpful for the early diagnosis of lung cancer. There is a substantial portion of our patients (~60%) who belong to stage I, which inevitably decreases the death rate for the case mix. As shown in **Table 1**, approximately one-third of the patients had a history of smoking and COPD. Female smokers comprise less than 5% of the female patients with lung cancer in our study, which is consistent with a previous study in China and also significantly different from Western lung cancer populations (38). COPD incidence is highly correlated with smoking and female never-smokers comprise a large proportion leading to a lower COPD rate.

In our study, though the radiomics nomogram that integrated the radiomics signature and clinical variables outperformed the clinical model alone (C-index: 0.868 vs. 0.854, $p$-value = 0.002 in validation cohort), the improvement of OS prediction was not very large. Considering that, to some extent, the important prognostic factors (TNM staging, age, etc.) have already been defined. On the other hand, the prediction accuracy of the radiomics signature alone is just slightly lower than the clinical model (C-index: 0.820 vs. 0.854). Therefore, the radiomics signature could also serve as an alternative or auxiliary methodology for the clinical model and confer benefits for the oncologist's decisions.

Our study also has limitations. First, although there are some studies that apply radiomics to PET-CT image data in lung cancer prognosis prediction, we restricted our radiomics study to CT scans, since currently the CT scans were the primary means for monitoring lung cancer in a real-world clinical environment. Other examination methods are required for comprehensive disease assessment. In the future, we could further target other types of images to evaluate the general condition (such as MRI and ultrasound radiography) and obtain a more precise performance of our model. Secondly, we did not include the treatment variables (such as surgery, radiotherapy, chemotherapy, or targeted therapy) in our study. We hope to include these variables to improve the model performance in a future study. Our model performs well in the absence of treatment information (C-index over 0.86), which also proves the importance of radiomics. Third, the follow-up time was not long enough to obtain each patient's end point, indicating the heterogeneity of tumor development. Further efforts on patient follow-up are encouraged to improve our model. Finally, this study collected data from a single center; although we divided the validation set to evaluate the stability of model, it is obvious that data from multicenter cohorts and different populations are better. Therefore, further multicenter studies are encouraged to promote the model generalization and improvement. Future prognostication of outcomes in NSCLC will likely be based on a combination of general condition, radiomics, TNM stage, treatment, and molecular tumor profiling, yielding more precise, individualized survival estimates and treatment algorithms.

In summary, we have developed a radiomics nomogram that combines the optimal radiomics signature from CT images with the TNM staging and other clinical information (age, sex and COPD), showing a significant improvement in predicting OS compared with clinical predictors alone. This nomogram should be validated in other Eastern Chinese populations with NSCLC and in other localities, as this work indicates that the radiomics signature increases the precision of survival prediction.

## DATA AVAILABILITY STATEMENT

The original contributions presented in the study are included in the article/**Supplementary Material.** Further inquiries can be directed to the corresponding authors.

## ETHICS STATEMENT

The study protocol was conducted under approval by the Public Health Ethics Committee of Shandong University (Approval No. 20180801), The requirement for informed consent was waived because of the retrospective nature of the study. Written informed consent for participation was not required for this study in accordance with the national legislation and the institutional requirements.

## AUTHOR CONTRIBUTIONS

LW and AL drafted this manuscript. AL, ZW, NX, DZ, GL, and XG collected the data. LW, ZW, and TQ analyzed the data. WC and FX conceived the study and participated in its design and coordination.

JW and FY contributed to the interpretation. All authors contributed to the article and approved the submitted version.

## FUNDING

This work was supported by Key R & D project of Shandong Province (2018GSF118152), the National Key Research and Development Program of China (2020YFC2003500), the National Natural Science Foundation of China (81773547), and the Natural Science Foundation of Shandong Province (ZR2019ZD02).

## ACKNOWLEDGMENTS

We would like to thank all authors, reviewers, and editors for their critical discussion of this manuscript, and apologize to those not mentioned due to space limitations.

## SUPPLEMENTARY MATERIAL

The Supplementary Material for this article can be found online at: https://www.frontiersin.org/articles/10.3389/fonc.2022.816766/full#supplementary-material

## REFERENCES

1. Global Cancer Statistics 2020. GLOBOCAN Estimates of Incidence and Mortality Worldwide for 36 Cancers in 185 Countries - Sung. *CA: A Cancer J Clin - Wiley Online Library* (2021) 71(3):209–49. doi: 10.3322/caac.21660
2. *Lung Cancer Statistics | How Common is Lung Cancer* . Available at: https://www.cancer.org/cancer/lung-cancer/about/key-statistics.html.
3. Zappa C, Mousa SA. Non-Small Cell Lung Cancer: Current Treatment and Future Advances. *Trans Lung Cancer Res* (2016) 5(3):288. doi: 10.21037/tlcr.2016.06.07
4. Goldstraw P, Chansky K, Crowley J, Rami-Porta R, Asamura H, Eberhardt WEE, et al. The IASLC Lung Cancer Staging Project: Proposals for Revision of the TNM Stage Groupings in the Forthcoming (Eighth) Edition of the TNM Classification for Lung Cancer. *J Thorac Oncol* (2016) 11(1):39–51. doi: 10.1016/j.jtho.2015.09.009
5. Liang W, Zhang L, Jiang G, Wang Q, Liu L, Liu D, et al. Development and Validation of a Nomogram for Predicting Survival in Patients With Resected Non–Small-Cell Lung Cancer. *J Clin Oncol* (2021) 33(8):861–9. doi: 10.1200/JCO.2014.56.6661
6. *Comprehensive Molecular Profiling of Lung Adenocarcinoma* (2021).
7. Horton RH, Lucassen AM. Recent Developments in Genetic/Genomic Medicine. *Clin Sci* (2019) 133(5):697–708. doi: 10.1042/CS20180436
8. *Radiomics: Images Are More Than Pictures, They Are Data | Semantic Scholar* . Available at: https://www.semanticscholar.org/paper/Radiomics:-Images-Are-More-than-Pictures,-They-Are-Gillies-Kinahan/dcd99d49af33bd14e9e0750bcf854e7b306c808a.
9. Lambin P, Rios-Velazquez E, Leijenaar R, Carvalho S, van Stiphout RGPM, Granton P, et al. Radiomics: Extracting More Information From Medical Images Using Advanced Feature Analysis. *Eur J Cancer* (2012) 48(4):441–6. doi: 10.1016/j.ejca.2011.11.036
10. Visvikis D, Cheze Le Rest C, Jaouen V, Hatt M. Artificial Intelligence, Machine (Deep) Learning and Radio(Geno)Mics: Definitions and Nuclear Medicine Imaging Applications. *Eur J Nucl Med Mol Imaging* (2019) 46(13):2630–7. doi: 10.1007/s00259-019-04373-w
11. Wilson R, Devaraj A. Radiomics of Pulmonary Nodules and Lung Cancer. *Trans Lung Cancer Res* (2017) 6(1):86–91. doi: 10.21037/tlcr.2017.01.04
12. *Texture Feature Analysis for Computer-Aided Diagnosis on Pulmonary Nodules* (2021).
13. Thawani R, McLane M, Beig N, Ghose S, Prasanna P, Velcheti V, et al. Radiomics and Radiogenomics in Lung Cancer: A Review for the Clinician. *Lung Cancer* (2018) 115:34–41. doi: 10.1016/j.lungcan.2017.10.015
14. Koo TR, Moon SH, Lim YJ, Kim JY, Kim Y, Kim TH, et al. The Effect of Tumor Volume and its Change on Survival in Stage III non-Small Cell Lung Cancer Treated With Definitive Concurrent Chemoradiotherapy. *Radiat Oncol* (2014) 9:283. doi: 10.1186/s13014-014-0283-6
15. Hawkins SH, Korecki JN, Balagurunathan Y, Gu Y, Kumar V, Basu S, et al. Predicting Outcomes of Nonsmall Cell Lung Cancer Using CT Image Features. *IEEE Access* (2014) 2:1418–26. doi: 10.1109/ACCESS.2014.2373335
16. Yang B, Zhong J, Zhong J, Ma L, Li A, Ji H, et al. Development and Validation of a Radiomics Nomogram Based on 18F-Fluorodeoxyglucose Positron Emission Tomography/Computed Tomography and Clinicopathological Factors to Predict the Survival Outcomes of Patients With Non-Small Cell Lung Cancer. *Front Oncol* (2020) 10:1042. doi: 10.3389/fonc.2020.01042
17. Botta F, Raimondi S, Rinaldi L, Bellerba F, Corso F, Bagnardi V, et al. Association of a CT-Based Clinical and Radiomics Score of Non-Small Cell Lung Cancer (NSCLC) With Lymph Node Status and Overall Survival. *Cancers (Basel)* (2020) 12(6):E1432. doi: 10.3390/cancers12061432
18. Xu Y, Hosny A, Zeleznik R, Parmar C, Coroller T, Franco I, et al. Deep Learning Predicts Lung Cancer Treatment Response From Serial Medical Imaging. *Clin Cancer Res* (2019) 25(11):3266–75. doi: 10.1158/1078-0432.CCR-18-2495
19. Khorrami M, Prasanna P, Gupta A, Patil P, Velu PD, Thawani R, et al. Changes in CT Radiomic Features Associated With Lymphocyte Distribution Predict Overall Survival and Response to Immunotherapy in Non-Small Cell Lung Cancer. *Cancer Immunol Res* (2020) 8(1):108–19. doi: 10.1158/2326-6066.CIR-19-0476
20. *Development of a radiomics nomogram based on the 2D and 3D CT features to predict the survival of non-small cell lung cancer patients* (2021).
21. Steyerberg EW, Vergouwe Y. Towards Better Clinical Prediction Models: Seven Steps for Development and an ABCD for Validation. *Eur Heart J* (2014) 35(29):1925–31. doi: 10.1093/eurheartj/ehu207
22. Kishore AK, Vail A, Bray BD, Chamorro A, Napoli MD, Kalra L, et al. Clinical Risk Scores for Predicting Stroke-Associated Pneumonia: A Systematic Review. *Eur Stroke J* (2016) 1(2):76–84. doi: 10.1177/2396987316651759
23. Iasonos A, Schrag D, Raj GV, Panageas KS. How to Build and Interpret a Nomogram for Cancer Prognosis. *J Clin Oncol* (2008) 26(8):1364–70. doi: 10.1200/JCO.2007.12.9791
24. Liu A, Wang Z, Yang Y, Wang J, Dai X, Wang L, et al. Preoperative Diagnosis of Malignant Pulmonary Nodules in Lung Cancer Screening With a Radiomics Nomogram. *Cancer Commun (Lond)* (2020) 40(1):16–24. doi: 10.1002/cac2.12002
25. Lababede O, Meziane MA. The Eighth Edition of TNM Staging of Lung Cancer: Reference Chart and Diagrams. *Oncologist* (2018) 23(7):844–8. doi: 10.1634/theoncologist.2017-0659
26. Kikinis R, Pieper SD, Vosburgh KG. *3d Slicer: A Platform for Subject-Specific Image Analysis, Visualization, and Clinical Support*. In: Jolesz FA, ed. Intraoperative Imaging and Image-Guided Therapy. Springer (2021) 2014:277–89. doi: 10.1007/978-1-4614-7657-3_19
27. Shrout PE, Fleiss JL. Intraclass Correlations: Uses in Assessing Rater Reliability. *Psychol Bull* (1979) 86(2):420–8. doi: 10.1037/0033-2909.86.2.420
28. van Griethuysen JJM, Fedorov A, Parmar C, Hosny A, Aucoin N, Narayan V, et al. Computational Radiomics System to Decode the Radiographic Phenotype. *Cancer Res* (2017) 77(21):e104–7. doi: 10.1158/0008-5472.CAN-17-0339
29. Zwanenburg A, Leger S, Vallières M, Löck S. Image Biomarker Standardisation Initiative. *Radiology* (2020) 295(2):328–38. doi: 10.1148/radiol.2020191145
30. Meinshausen N, Bühlmann P. High-Dimensional Graphs and Variable Selection With the Lasso. *Ann Statist* (2006) 34(3):1436–62. doi: 10.1214/009053606000000281
31. Uno H, Cai T, Pencina MJ, D'Agostino RB, Wei LJ. On the C-Statistics for Evaluating Overall Adequacy of Risk Prediction Procedures With

Censored Survival Data. *Statist Med* (2011) 30(10):1105–17. doi: 10.1002/sim.4154
32. Akaike H. A New Look at the Statistical Model Identification. In: E Parzen, K Tanabe, G Kitagawa, editor. *Selected Papers of Hirotugu Akaike*. New York, NY: Springer (1998). p. 215–22. doi: 10.1007/978-1-4612-1694-0_16
33. Royston P, Altman DG. External Validation of a Cox Prognostic Model: Principles and Methods. *BMC Med Res Methodol* (2013) 13(1):33. doi: 10.1186/1471-2288-13-33
34. Woodard GA, Jones KD, Jablons DM. Lung Cancer Staging and Prognosis. *Cancer Treat Res* (2016) 170:47–75. doi: 10.1007/978-3-319-40389-2_3
35. Wang X, Duan H, Li X, Ye X, Huang G, Nie S. A Prognostic Analysis Method for non-Small Cell Lung Cancer Based on the Computed Tomography Radiomics. *Phys Med Biol* (2020) 65(4):045006. doi: 10.1088/1361-6560/ab6e51
36. *The Relationship Between COPD and Lung Cancer* (2021).
37. Caramori G, Ruggeri P, Mumby S, Ieni A, Lo Bello F, Chimankar V, et al. Molecular Links Between COPD and Lung Cancer: New Targets for Drug Discovery? *Expert Opin Ther Targets* (2019) 23(6):539–53. doi: 10.1080/14728222.2019.1615884
38. Zhou F, Zhou C. Lung Cancer in Never Smokers—the East Asian Experience. *Trans Lung Cancer Res* (2018) 7(4):450–63. doi: 10.21037/tlcr.2018.05.14

**Conflict of Interest:** The authors declare that the research was conducted in the absence of any commercial or financial relationships that could be construed as a potential conflict of interest.

**Publisher's Note:** All claims expressed in this article are solely those of the authors and do not necessarily represent those of their affiliated organizations, or those of the publisher, the editors and the reviewers. Any product that may be evaluated in this article, or claim that may be made by its manufacturer, is not guaranteed or endorsed by the publisher.

frontiers | Frontiers in Oncology

REVIEW
published: 30 June 2022
doi: 10.3389/fonc.2022.825598

# Based on the Development and Verification of a Risk Stratification Nomogram: Predicting the Risk of Lung Cancer-Specific Mortality in Stage IIIA-N2 Unresectable Large Cell Lung Neuroendocrine Cancer Compared With Lung Squamous Cell Cancer and Lung Adenocarcinoma

*Ying Yang[1†], Cheng Shen[2†], Jingjing Shao[1], Yilang Wang[3], Gaoren Wang[4] and Aiguo Shen[1*]*

[1] Cancer Research Center Nantong, The Affiliated Tumor Hospital of Nantong University, Nantong University, Nantong, China, [2] Department of Computer Science and Engineering, Tandon School of Engineering, New York University, Brooklyn, NY, United States, [3] Department of Oncology, Nantong Tumor Hospital, Nantong University, Nantong, China, [4] Department of Radiology, Nantong Tumor Hospital, Nantong University, Nantong, China

OPEN ACCESS

**Edited by:**
Sri Harsha Tella,
University of South Carolina,
United States

**Reviewed by:**
Michele Avanzo,
Aviano Oncology Reference Center (IRCCS), Italy
Joanna Jane Ludbrook,
Calvary Mater Newcastle Hospital, Australia

***Correspondence:**
Aiguo Shen
aiguoshen_nt@126.com

[†]These authors have contributed equally to this work

**Specialty section:**
This article was submitted to Thoracic Oncology, a section of the journal Frontiers in Oncology

**Received:** 30 November 2021
**Accepted:** 02 May 2022
**Published:** 30 June 2022

**Citation:**
Yang Y, Shen C, Shao J, Wang Y, Wang G and Shen A (2022) Based on the Development and Verification of a Risk Stratification Nomogram: Predicting the Risk of Lung Cancer-Specific Mortality in Stage IIIA-N2 Unresectable Large Cell Lung Neuroendocrine Cancer Compared With Lung Squamous Cell Cancer and Lung Adenocarcinoma. Front. Oncol. 12:825598. doi: 10.3389/fonc.2022.825598

**Background:** The purpose of this study is to predict overall survival (OS) and lung cancer-specific survival (LCSS) in patients with stage IIIA-N2 unresectable lung squamous cell cancer (LUSC), lung adenocarcinoma (LUAD), and large cell neuroendocrine cancer (LCNEC) by constructing nomograms and to compare risk and prognostic factors affecting survival outcomes in different histological subtypes.

**Methods:** We included 11,505 unresectable NSCLC patients at stage IIIA-N2 between 2010 and 2015 from the Surveillance, Epidemiology, and End Results (SEER) database. Moreover, competition models and nomograms were developed to predict prognostic factors for OS and LCSS.

**Results:** Analysis of the SEER database identified 11,505 NSCLC patients, of whom 5,559 (48.3%) have LUAD, 5,842 (50.8%) have LUSC, and 104 (0.9%) have LCNEC. Overall, both OS and LCSS were significantly better in stage IIIA-N2 unresectable LUAD than in LCNEC, while there was no statistically significant difference between LUSC and LCNEC. Age, gender, T stage, chemotherapy, and radiotherapy were significantly associated with OS rates in LUAD and LUSC. However, chemotherapy was the only independent factor for LCNEC ($p < 0.01$).From competitive risk models, we found that older age, larger tumors, non-chemotherapy and non-radiotherapy were associated with a increased risk of death from LUAD and LUSC. Unlike prognostic factors for OS, our

study showed that both chemotherapy and radiotherapy were all LCNEC-specific survival factors for both LCSS and non-LCSS LCNEC.

**Conclusion:** Our study reports that unresectable patients with stage IIIA-N2 LCNEC and LUSC have worse LCSS than LUAD. The study's first prognostic nomogram constructed for patients with unresectable stage IIIA-N2 NSCLC can accurately predict the survival of different histological types, which may provide a practical tool to help clinicians assess prognosis and stratify these prognostic risks to determine which patients should be given an optimized individual treatment strategy based on histology.

**Keywords: nomogram, lung cancer-specific survival, non-small cell lung cancer, histology, unresectable**

## INTRODUCTION

Lung cancer is the leading cause of cancer-related mortality worldwide. According to the latest data from the World Health Organization's (WHO) International Agency for Research on Cancer (IARC), lung cancer has become one of the leading new cases and deaths worldwide in 2020. Non-small cell lung cancer (NSCLC) is the predominant histological type, accounting for approximately 85% of cases, with the majority of patients diagnosed at advanced unresectable stages (1). Of these, about 30% of NSCLC patients with IIIA or IIIB cannot be treated by surgical resection (2). The majority of patients who lose the chance of surgical treatment reportedly receive platinum-based chemotherapy (3). Patients with stage III non-surgical lung cancer achieve improved survival by modulating the dose of radiotherapy (4). These approaches provide partial remission, but patients' 5-year overall survival (OS) remains suboptimal (5).

Chemotherapy or radiotherapy has been reported to exhibit tissue heterogeneity in the treatment of cancer patients. The most recent systematic evaluation analysis concluded that chemotherapy had different effects on OS in triple-negative breast cancer patients with different tissue subtypes (6). Jiang et al. demonstrated that the efficacy of chemotherapy was not statistically significant for signet ring cell cancer (SRCC) and adenocarcinoma (AD) in stage II colon cancer, whereas chemotherapy for stage III SRCC significantly reduced the risk of cancer-specific death (7). Another study found that radiotherapy for urothelial carcinoma improved OS in patients with AD and transitional cell carcinoma, but had no significant effect on squamous cell carcinoma (8). Based on these reports, histological subtype can play an important role in the selection of treatment and in predicting the survival outcomes of cancer patients.

NSCLC is known to include three subtypes: lung adenocarcinoma (LUAD), lung squamous carcinoma (LUSC), and large cell lung cancer (LCLC), with the former two being the most common ones. According to the 2015 Lung Tumor Classification by WHO, large cell neuroendocrine carcinoma (LCNEC) is a rare histologic lung cancer type in LCLC, with an incidence of approximately 3% (9). LCNEC has similar characteristics to small cell lung cancer with high invasiveness and recurrence rates and has a poor impact on patients' survival (10). However, due to its low incidence, it has been rarely studied. The latest Clinical Guidelines for Non-Small Cell Lung Cancer (CSCO) state that LCNEC is a tissue subtype that differs from LUAD and LUSC. Therefore, it is necessary to explore the clinicopathological features, treatment, and prognosis of LCNEC.

Previous studies have found differences in tumor characteristics and prognosis among different tissue types of lung cancer (11). The efficacy of stereotactic body radiation therapy (SBRT) in patients with early-stage NSCLC showed histologically significant differences, and a multicenter study found that LUSC showed a worse OS status compared to LUAD (12). Previous studies have also found that patients with Phase III N2 LUSC treated with surgical resection after neoadjuvant chemotherapy with docetaxel-cisplatin (DP) had significantly better outcomes and survival rate than patients with LUAD (13). Not surprisingly, although clinical decision-making in NSCLC patients is still based on the tumor node metastasis (TNM) stage, the impact of different histologic subtypes on survival remains controversial. Recent literature reported the difference in postoperative survival of N2-III NSCLC patients with different histologic types and found that the OS rate of LUSC patients was worse than that of LUAD patients (14). However, whether different histological types affect the survival of unresectable stage IIIA-N2 patients is poorly defined.

Therefore, the main objective of this study is to assess how survival outcomes in inoperable stage N2-IIIA NSCLC patients vary by histologic subtypes. To assess independent risk factors for OS and lung cancer-specific survival (LCSS) for different histological subtypes, we developed a nomogram and competing risk model for unresectable patients with stage IIIA-N2 based on the SEER database.

## METHOD

### Study Design and Patient Selection

The NSCLC patients included in stage IIIA-N2 were cases from 2010 to 2015 (using the 7th edition of AJCC Cancer Staging Manual 7 classification). Corresponding details were taken from the SEER public access database and the SEER statistics version is 8.3.5.

Inclusion criteria were as follows: (a) NSCLC diagnosed as stage IIIA-N2 from 2010 to 2015; (b) histological subtypes only included LUAD, LUSC, and LCNEC; and (c) patients who could not undergo surgical resection excluding those who received surgical treatment.

Exclusion criteria were as follows: (a) patients with a follow-up period of less than 1 month or the follow-up time was not recorded in the SEER data; and (b) patients with incomplete clinicopathological or follow-up data.

## Statistical Analysis of Overall Survival

First, chi-square and *t*-tests were used to compare statistical differences in the proportions of the variables in the three groups with different tissue types. Survival curves drawn by the Kaplan–Meier method were used to compare the differences in the OS of the variables. Univariate and multivariate analyses were performed by Cox regression models, and independent risk factors were determined by multivariate analysis. Hazard ratios (HRs) and corresponding 95% confidence intervals (CIs) were calculated. Statistical analysis was performed by SPSS 26.0, and a $p$-value < 0.05 was considered statistically significant.

According to the significant independent risk factors, a nomogram model was established with survival and rms R-packages. The nomogram model was built and validated with guided internal verification. Discriminatory ability was determined by applying a Harmony Index (C-index). The 1-, 3-, and 5-year operating systems were calibrated to compare the predicted survival rate with the observed survival rate, and a calibration curve is provided. The above statistical analysis was performed using R version 4.1.0.

## Statistical Analysis of Lung Cancer-Specific Survival Rate

Cumulative incidence curves of lung cancer-related mortality (from the date of diagnosis) were constructed to compare LCSS with non-LCSS and to calculate mortality from other causes. Statistical comparisons of potential harms were performed using the Fine and Gray test (15). Using competing risk regression (Fine and Gray method), we analyzed risk factors for lung cancer-related mortality for three tissue subtypes, LUAD, LUSC, and LCNEC, including age, sex, T stage, histology, chemotherapy, and radiotherapy. We then used rms, cmprsk, and mstate R-packages to create corresponding nomograms for 1 year, 3 years, and 5 years of competitive risk models. $p$-values less than 0.05 were considered statistically significant.

# RESULTS

## Clinical Characteristics of the Patient

As shown in **Figure 1**, 21,690 NSCLC IIIA-N2 patients diagnosed between 2010 and 2015 were finally selected for this study, of which 11,505 met the inclusion criteria for the study. Based on the histological type of NSCLC, we divided unresectable IIIA-N2 patients into the LUAD group (5,559), the LUSC group (5,842), and the LCNEC group (104). In **Table S1**, we divided the included patients into three histological types and compared the basic demographic and clinicopathological characteristics of patients in the three cohorts.

## Independent Risk Factors for Overall Survival

**Tables 1–3** show univariate and multivariate analyses of OS in patients with unresectable IIIA-N2 in LUAD, LUSC, and LCNEC, respectively.

In the LUAD group, univariate analysis showed that age, gender, region (South, Alaska, and Pacific coast), tumor location (middle lobe), T stage (T1b, T2a, and T2b), chemotherapy, and radiotherapy were significantly associated with OS ($p < 0.05$). Multivariate analysis using Cox regression found that age, gender, region (Northern Plains, Alaska, and Pacific Coast), T stage (T1b, T2a, and T2b), chemotherapy, and radiotherapy were independent risk factors for LUAD ($p < 0.05$).

Univariate analysis in the LUSC group showed that age, gender, region (South), tumor location (middle and lower lobe), T stage (T1b, T2a, and T2b), chemotherapy, and radiotherapy were significantly different from OS ($p < 0.05$). Multivariate analysis using Cox regression showed that age, gender, T stage (T1b, T2a, and T2b), chemotherapy, and radiotherapy were independent risk factors for LUSC ($p < 0.05$).

In the LCNEC group, univariate analysis showed that age (60–79 years), chemotherapy, and radiotherapy were significantly different from OS ($p < 0.05$).The multivariate analysis with Cox regression showed that only chemotherapy was an independent risk factor for LCNEC ($p < 0.05$).

## Overall Survival Prognostic Analysis of Patients With Unresectable Stage

OS was better in LUAD than in LUSC and LCNEC, but there was no significant difference between LUSC and LCNEC ($p$ <0.001) (**Figure S1**). According to our multivariate analysis, as shown in **Figure S2**, age ($p < 0.05$), sex ($p$ <0.05), T stage ($p$ <0.001), chemotherapy ($p$ <0.001), and radiotherapy ($p$ <0.001) were significant prognostic factors of OS in the LUAD and LUSC groups. Among patients with LUAD and LUSC, younger age, female, early T stage, and incorporating chemotherapy and radiotherapy had better OS. However age, sex, and T stage were not significantly related to LCNEC. In the LCNEC group, patients who received chemotherapy or radiotherapy had a better OS rate than those who did not receive treatment ($p$ <0.001).

## Creation and Verification of Nomograms

Based on the independent risk factors obtained from Cox regression analysis, the nomogram was constructed to explore the OS rate of 1, 3, and 5 years for patients who were in an unresectable stage in IIIA-N2 (**Figure 2**). The calibration curves for the LUAD, LUSC, and LCNEC groups showed good agreement between the predictions of the nomograms and the actual observations of the OS at 1, 3, and 5 years. We examined the discrimination against nomograms, showing good predictive accuracy and clinical applicability, with C-index values of 0.638, 0.649, and 0.688 for the three groups, respectively.

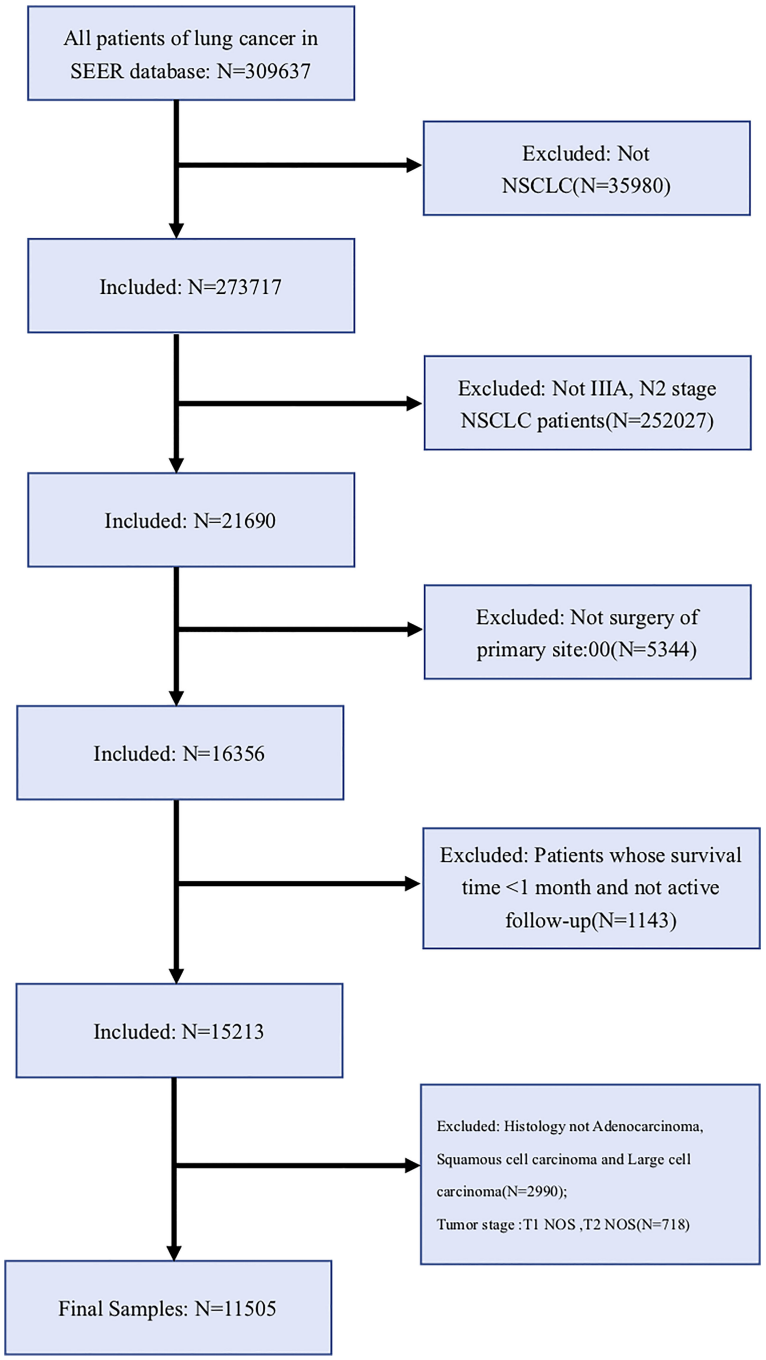


**FIGURE 1** | The flowchart for patient selection.

## Prognostic Factor Analysis of LCSS

In **Figure 3**, we proceeded to divide the patients into three different tissue subtypes to explore the cumulative risk of LCSS in each tissue subtype under different factor stratifications. As shown in **Figure 3A**, there was a statistically significant difference ($p < 0.001$) in the cumulative incidence of LCSS across age groups in LUAD and LUSC after controlling for competing risk events. In particular, the ≥80 years age group was significantly higher than the other groups (60–79, 40–59, and 20–39 years age groups). However, in the LCNEC group, there was no statistical significance ($p = 0.32$). As shown in **Figure 3B**, when patients were grouped by gender, the cumulative incidence of LCSS was significantly higher in male than in female patients in the LUAD group alone ($p < 0.001$), whereas there was no

**TABLE 1** | Univariate and multivariate analyses for OS in patients with unresectable IIIA-N2 LUAD.

| Characteristic Variables | | Univariate | | Multivariate | |
|---|---|---|---|---|---|
| | | HR (95% CI) | *p*-value | HR (95% CI) | *p*-value |
| **Age** | 20–39 | Reference | | Reference | |
| | 40–59 | 0.506 (0.279, 0.918) | 0.025 | 0.594 (0.327, 1.0790) | 0.087 |
| | 60–79 | 0.566 (0.511, 0.626) | <0.001 | 0.693 (0.623, 0.770) | <0.001 |
| | ≥80 | 0.702 (0.65, 0.758) | <0.001 | 0.829 (0.765, 0.898) | <0.001 |
| **Sex** | Female | Reference | | Reference | |
| | Male | 1.215 (1.142, 1.293) | <0.001 | 0.837 (0.786, 0.890) | <0.001 |
| **Race** | White | Reference | | | |
| | Black | 1.12 (0.989, 1.269) | 0.075 | | |
| | Other | 0.989 (0.854, 1.145) | 0.882 | | |
| **Region** | East | Reference | | Reference | |
| | Northern Plains | 0.999 (0.934, 1.068) | 0.968 | 1.078 (1.008, 1.153) | 0.029 |
| | Southern | 0.9 (0.811, 1.000) | 0.049 | 1.008 (0.908, 1.12) | 0.878 |
| | Alaska | 1.353 (1.114, 1.642) | 0.002 | 1.415 (1.164, 1.718) | <0.001 |
| | Pacific Coast | 3.69 (1.382, 9.850) | 0.009 | 4.006 (1.500, 10.700) | 0.006 |
| **Grade** | I | 0.833 (0.573, 1.209) | 0.336 | | |
| | II | 0.8 (0.537, 1.190) | 0.271 | | |
| | III | 0.85 (0.581, 1.242) | 0.4 | | |
| | IV | 0.973 (0.669, 1.415) | 0.886 | | |
| | Unknown | Reference | | | |
| **Tumor Location** | Main bronchus | Reference | | | |
| | Upper lobe | 0.904 (0.7, 1.168) | 0.440 | | |
| | Middle lobe | 0.817 (0.684, 0.975) | 0.025 | | |
| | Lower lobe | 0.803 (0.64, 1.007) | 0.058 | | |
| | Overlapping | 0.904 (0.754, 1.085) | 0.279 | | |
| | NOS | 0.858 (0.503, 1.464) | 0.574 | | |
| **T stage** | T1a | Reference | | Reference | |
| | T1b | 0.641 (0.577, 0.713) | <0.001 | 0.617 (0.555, 0.686) | <0.001 |
| | T2a | 0.86 (0.781, 0.947) | 0.002 | 0.790 (0.717, 0.870) | <0.001 |
| | T2b | 0.874 (0.806, 0.948) | 0.001 | 0.831 (0.766, 0.902) | <0.001 |
| | T3 | 0.991 (0.896, 1.096) | 0.86 | 0.978 (0.884, 1.081) | 0.661 |
| **Chemotherapy** | No/Unknown | Reference | | Reference | |
| | Yes | 1.93 (1.808, 2.061) | <0.001 | 1.567 (1.454, 1.688) | <0.001 |
| **Radiotherapy** | No/Unknown | Reference | | Reference | |
| | Yes | 1.75 (1.642, 1.866) | <0.001 | 1.466 (1.366, 1.573) | <0.001 |

statistically significant difference between the cumulative incidence of LCSS in the LUSC and LCNEC groups ($p = 0.53$ and $p = 0.28$, respectively). Similarly, when stratified by T stage after controlling for competing risk events, the differences in the cumulative incidence of LCSS between the LUAD and LUSC groups were statistically significant for T1a, T1b, T2a, T2b, and T3, with patients in T1a having a lower cumulative incidence of LCSS than in T1b, T2a, T2b, or T3 ($p < 0.001$, **Figure 3C**). However, there was no difference in the LCNEC group ($p = 0.52$). In addition, the cumulative incidence of LCSS was significantly lower in patients receiving chemotherapy and radiotherapy than in those not receiving chemotherapy and radiotherapy in all three subtypes ($p < 0.001$, **Figures 3D, E**).

## Constructing a Prognostic Nomogram for the Competitive Risk Model

The nomogram for predicting LCSS is based on five independent risk factors: age, sex, T stage, chemotherapy, and radiotherapy (**Figure 4**). Each independent risk factor corresponds to a specific score by drawing a line on the dotted axis. The total score reflects the sum of the scores for each factor and is drawn directly down from the total point axis to the LCSS axis at 1, 3, and 5 years, corresponding to the predicted probability of LCSS at 1, 3, and 5 years.

# DISCUSSION

In this study, we analyzed the survival of 11,505 patients with unresectable NSCLC (LUAD, LUSC, and LCNEC) diagnosed between 2010 and 2015 according to histologic subtypes in the SEER database. Based on statistical methods, we evaluated independent predictors of OS in patients with stage IIIA-N2 NSCLC of three histological subtypes. Three nomograms were constructed using the above factors to quantify survival at 1, 3, and 5 years. Calibration analyses were performed to assess the accuracy and validity of these line graphs. Finally, by controlling for competing risk events, we assessed the cumulative incidence of competing risks in the three tissue subtypes and constructed competing risk models and nomograms based on independent predictors. Although several models are available to predict the prognosis of lung cancer, a risk model focusing on different histological subtypes in unresectable IIIA-N2 stage patients has not been developed for patients with NSCLC. Therefore, the aim

**TABLE 2 |** Univariate and multivariate analyses for OS in patients with unresectable IIIA-N2 LUSC.

| Characteristic Variables | | Univariate | | Multivariate | |
|---|---|---|---|---|---|
| | | HR (95% CI) | *p*-value | HR (95% CI) | *p*-value |
| **Age** | 20–39 | Reference | | Reference | |
| | 40–59 | 0.31 (0.116, 0.828) | 0.019 | 0.36 (0.135, 0.962) | 0.042 |
| | 60–79 | 0.618 (0.559, 0.683) | <0.001 | 0.787 (0.710, 0.872) | <0.001 |
| | ≥80 | 0.71 (0.662, 0.763) | <0.001 | 0.861 (0.800, 0.927) | <0.001 |
| **Sex** | Female | Reference | | Reference | |
| | Male | 0.933 (0.879, 0.990) | 0.022 | 0.915 (0.862, 0.972) | 0.004 |
| **Race** | White | Reference | | | |
| | Black | 1.046 (0.913, 1.198) | 0.517 | | |
| | Other | 1.016 (0.87, 1.186) | 0.842 | | |
| **Region** | East | Reference | | | |
| | Northern Plains | 0.973 (0.914, 1.036) | 0.396 | | |
| | Southern | 0.896 (0.810, 0.990) | 0.031 | | |
| | Alaska | 1.106 (0.921, 1.328) | 0.282 | | |
| | Pacific Coast | 1.312 (0.760, 2.264) | 0.330 | | |
| **Grade** | I | 0.823 (0.559, 1.212) | 0.325 | | |
| | II | 0.819 (0.526, 1.276) | 0.378 | | |
| | III | 0.871 (0.59, 1.285) | 0.486 | | |
| | IV | 0.855 (0.58, 1.26) | 0.428 | | |
| | Unknown | Reference | | | |
| **Tumor Location** | Main bronchus | Reference | | | |
| | Upper lobe | 0.809 (0.653, 1.003) | 0.053 | | |
| | Middle lobe | 0.755 (0.63, 0.904) | 0.002 | | |
| | Lower lobe | 0.76 (0.601, 0.959) | 0.021 | | |
| | Overlapping | 0.915 (0.761, 1.101) | 0.347 | | |
| | NOS | 0.9 (0.63, 1.285) | 0.562 | | |
| **T stage** | T1a | Reference | | Reference | |
| | T1b | 0.641 (0.564, 0.728) | <0.001 | 0.543 (0.477, 0.618) | <0.001 |
| | T2a | 0.772 (0.691, 0.863) | <0.001 | 0.720 (0.644, 0.806) | <0.001 |
| | T2b | 0.81 (0.755, 0.870) | <0.001 | 0.750 (0.698, 0.805) | <0.001 |
| | T3 | 0.974 (0.989, 1.057) | 0.526 | 0.943 (0.869, 1.024) | 0.163 |
| **Chemotherapy** | No/Unknown | Reference | | Reference | |
| | Yes | 2.028 (1.910, 2.152) | <0.001 | 1.714 (1.600, 1.836) | <0.001 |
| **Radiotherapy** | No/Unknown | Reference | | Reference | |
| | Yes | 2.006 (1.886, 2.133) | <0.001 | 1.613 (1.507, 1.727) | <0.001 |

of this study was to develop a practical survival prediction model for individualized prediction of survival in patients with unresectable stage IIIA-N2 NSCLC.

Whether histologic subtype affects patient outcomes and survival is controversial. To reduce bias in this study, we included patients with LUSC, LUAD, and LCNEC as defined according to the AJCC 7th edition guidelines to ensure that most patients were treated in a relatively consistent and modern manner. In our study, age, gender, T stage, chemotherapy, and radiotherapy were all independent risk factors for LUAD and LUSC. Our results are consistent with those of recent years exploring the impact of tissue staging on survival and prognosis in NSCLC. The OS was significantly higher in LUAD than in LUSC, and LCSS was significantly lower in LUSC than in LUAD after controlling for competing risks (16, 17). Several studies have shown that LUSC is one of the most aggressive cancers, with a 5-year survival rate of only 10%. Smoking and alcohol consumption are important factors for the low survival rate and accelerated tumor progression in LUSC, which has been confirmed by many studies (18, 19).

To further determine the cause of the survival difference between LUAD and LUSC, a competing risk model was developed. The competing risk model was able to make better clinical predictions than the traditional Kaplan–Meier and Cox regression models. Age, gender, chemotherapy, and radiotherapy were independent risk factors for LCSS in the LUAD and LUSC groups. Compared with the older group, younger non-surgical NSCLC patients had significantly different LCSS, and after controlling for competing risk events, male LUAD patients had significantly lower LCSS than women, but there was no significant difference between the LUSC and LCNEC groups. Age is an important factor influencing lung cancer survival (20). Arnold et al. also found that the OS rate of NSCLC patients and the LCSS rate were significantly better in younger patients than in older patients (21). However, a 2015 retrospective study in Germany found that female lung cancer patients had significantly higher survival rates than men, but they stated that the high survival rates in women were independent of histology (22). This study found that female patients were more likely to develop AD, while male patients tend to suffer from squamous cell carcinoma. Perhaps due to the increased number of women smoking and the sensitivity of women to nicotine, there was no significant difference in the incidence of squamous cell carcinoma similar to the findings of Wheatley et al. (23). It is not difficult to find that age and gender are indeed important factors affecting LUAD and LUSC in this study, but

**TABLE 3 |** Univariate and multivariate analyses for OS in patients with unresectable IIIA-N2 LCNEC.

| Characteristic Variables | | Univariate | | Multivariate | |
|---|---|---|---|---|---|
| | | HR (95% CI) | *p*-value | HR (95% CI) | *p*-value |
| **Age** | 20–39 | / | | | |
| | 40–59 | Reference | | | |
| | 60–79 | 0.494 (0.247, 0.990) | 0.047 | | |
| | ≥80 | 0.629 (0.348,.1.139) | 0.126 | | |
| **Sex** | Female | Reference | | | |
| | Male | 0.717 (0.466, 1.103) | 0.130 | | |
| **Race** | White | Reference | | | |
| | Black | 0.384 (0.052, 2.813) | 0.346 | | |
| | Other | 0.4231 (0.056, 3.329) | 0.420 | | |
| **Region** | East | Reference | | | |
| | Northern Plains | 1.276 (0.810, 2.009) | 0.293 | | |
| | Southern | 0.796 (0.243, 2.613) | 0.707 | | |
| | Alaska | / | | | |
| | Pacific Coast | 1.220 (0.165, 9.006) | 0.845 | | |
| **Grade** | I | 0.738 (0.315, 1.730) | 0.484 | | |
| | II | / | | | |
| | III | 5.948 (0.682, 51.894) | 0.107 | | |
| | IV | 0.830 (0.341, 2.018) | 0.681 | | |
| | Unknown | Reference | | | |
| **Tumor Location** | Main bronchus | Reference | | | |
| | Upper lobe | 2.335 (0.575, 9.479) | 0.236 | | |
| | Middle lobe | 0.779 (0.281, 2.164) | 0.632 | | |
| | Lower lobe | 1.615 (0.450, 5.799) | 0.463 | | |
| | Overlapping | 0.859 (0.293, 2.523) | 0.859 | | |
| | NOS | 1.162 (0.129, 10.486) | 0.894 | | |
| **T stage** | T1a | Reference | | | |
| | T1b | 1.243 (0.663, 2.330) | 0.499 | | |
| | T2a | 1.188 (0.596, 2.369) | 0.625 | | |
| | T2b | 0.870 (0.489, 1.548) | 0.636 | | |
| | T3 | 1.759 (0.838, 3.691) | 0.135 | | |
| **Chemotherapy** | No/Unknown | Reference | | Reference | |
| | Yes | 3.276 (1.969, 5.450) | <0.001 | 3.276 (1.969, 5.450) | <0.001 |
| **Radiotherapy** | No/Unknown | Reference | | | |
| | Yes | 2.102 (1.339, 3.301) | 0.001 | | |

due to the heterogeneity of the survey population, there are many factors that affect the survival of patients, which makes it worthy to provide more targeted and personalized treatment options for lung cancer patients in future clinical treatments and prospective studies.

Previous studies have found that LCNEC, a rare neuroendocrine carcinoma, has a lower survival rate than other NSCLCs (24, 25). In our study, a histological subtype of LCNEC was also available, and we found a significantly lower survival rate than LUAD from the survival curves, but there was no difference in the OS rate with LUSC. This may be due to the fact that only 104 patients with LCNEC met the inclusion criteria for this study, and it is difficult to develop a statistically significant trend due to the small sample size. Although there are fewer studies on unresectable LCNEC, a retrospective study found better survival in patients with stage IA or IB LCNEC who received chemotherapy after surgical resection (26). In an early case report, a combination of irinotecan and fractionated-dose cisplatin chemotherapy was found to be significantly more effective in older LCNEC patients (27). In this study, by controlling for competing risks, we also found that patients with stage IIIA-N2 unresectable LCNEC who received chemotherapy had a higher LCSS rate compared to those who did not receive chemotherapy.

Nomograms for OS and LCSS were constructed based on three tissue subtypes to provide more refined and personalized survival predictions for physicians and patients. In our study, chemotherapy and radiotherapy were independent risk factors associated with LCSS with important histologic subtypes. A retrospective study of the outcomes of unresectable stage III

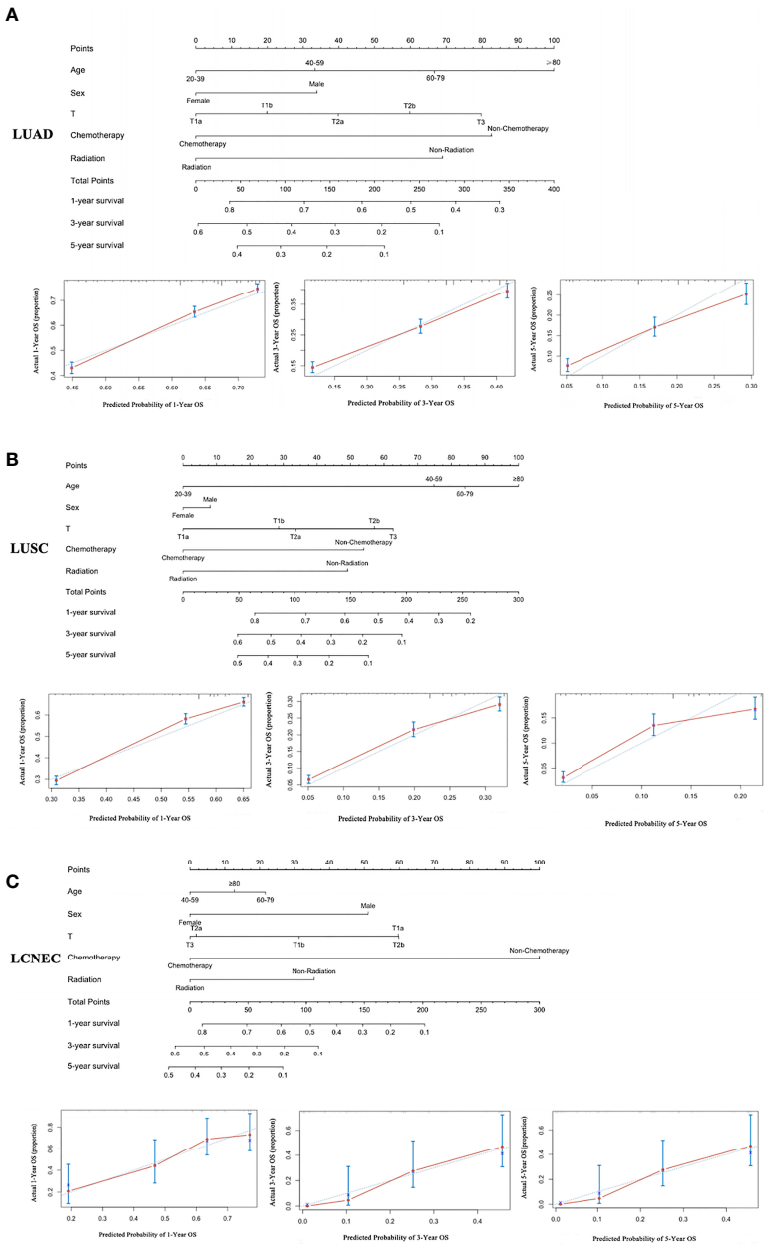


**FIGURE 2** | A nomogram for the prediction of 1-, 3-, and 5-year OS rates and the corresponding calibration curve: **(A)** LUAD, **(B)** LUSC, and **(C)** LCNEC.

NSCLC patients treated with chemotherapy and radiotherapy from 2000 to 2013 also found that chemotherapy and radiotherapy were important in improving survival (5). In addition, with the overall development of lung cancer treatment, an increasing number of therapeutic approaches and predictors have shown great potential in improving patient survival and modeling lung cancer prognosis. The study by Antonia et al. found that the addition of immunotherapy to chemotherapy in patients with stage III unresectable NSCLC significantly improved OS (28). A recent study reported that gefitinib combined with pemetrexed and carboplatin chemotherapy significantly improved both treatment efficacy and survival in EGFR-mutant advanced NSCLC (29). Therefore, in addition to chemotherapy and radiotherapy, targeted therapy, immunotherapy and combination therapy may provide more personalized and specialized options to improve patient survival. Furthermore, a 2021 study by Avanzo et al. found that the application of radiomics is of great value in improving lung stereotactic body radiation therapy (30). In clinical practice, radiomics is an emerging field of research, and it is used as a predictive tool for responses and treatment outcomes. It may be a new strategy to predict the

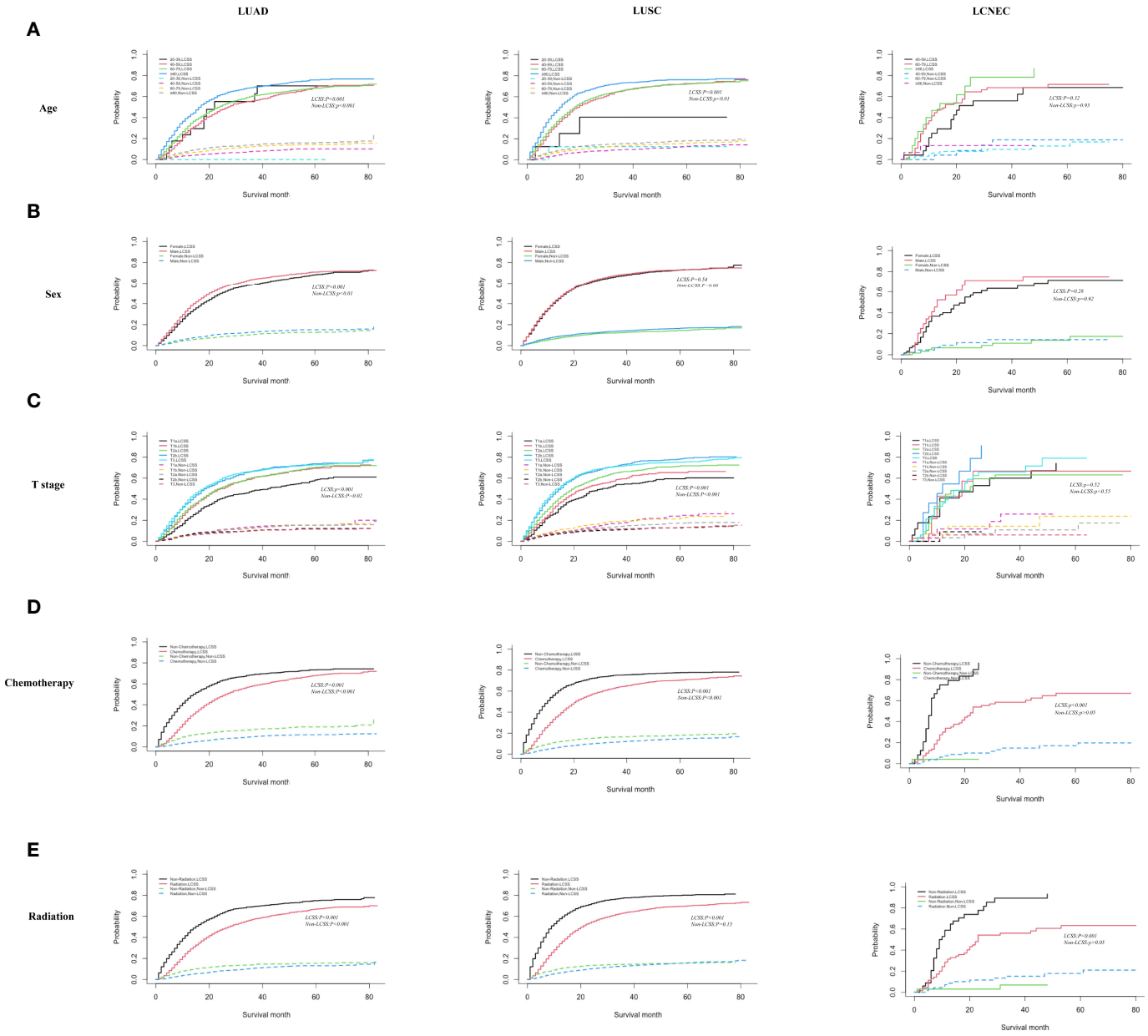


**FIGURE 3** | Competing risk analyses for patients in the LUAD, LUSC, and LCNEC group according to **(A)** age, **(B)** sex, **(C)** T stage, **(D)** chemotherapy, and **(E)** radiation.

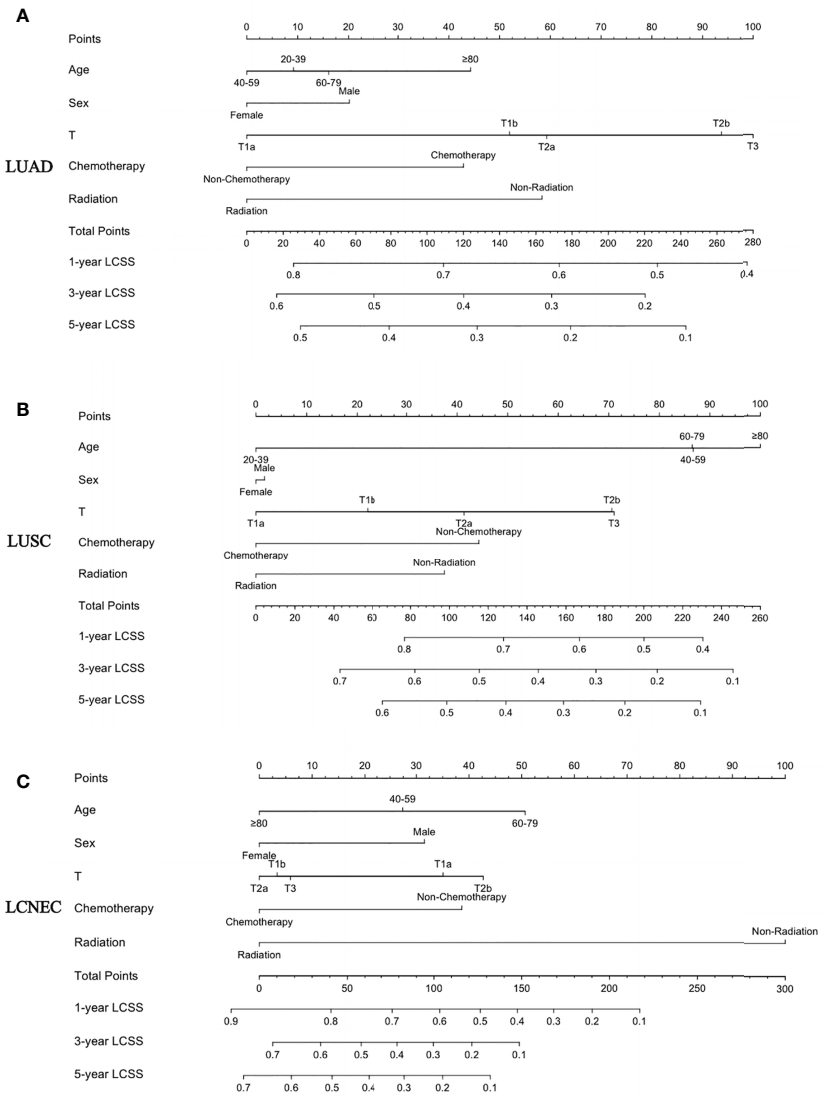


**FIGURE 4** | A nomogram for the prediction of 1-, 3-, and 5-year LCSS rates: **(A)** LUAD, **(B)** LUSC, and **(C)** LCNEC.

efficacy of radiotherapy in lung cancer patients, providing new ideas for patients to choose the best treatment regimen.

In addition, based on nomograms and competing risk models, we can more accurately distinguish and predict the survival of patients with different T stages. Our study found that after controlling for competing risk events, stage T1a patients had lower cumulative morbidity in the LUAD and LUSC groups than patients at stage T1b, T2a, T2b, or T3. Using the nomogram, we could also predict the 1-, 3-, and 5-year survival scores of patients with different T stages based on inoperable stage IIIA-N2 NSCLC patients.

However, our study has several limitations. Firstly, our study was retrospective and included Americans and heterogeneous individuals. Secondly, the treatment records in the SEER database did not contain information on the name of chemotherapy drugs, number of chemotherapy treatments, radiation dose, and number of radiation treatments. Thirdly, the database did not contain important clinical information, such as smoking history, lymphovascular invasion, neural invasion, cancer thrombosis, tumor recurrence, and related treatments. Fourthly, tumor mutation-driver genes such as EGFR, ALK, and ROS1 and the use of targeted therapies were not recorded in the SEER data, and reflecting the time period of this study, neither were tumor PDL-1 status and the use of immunotherapy. Finally, because this study was not validated in multiple centers, we could confirm the findings in our future large-scale multicenter prospective study.

In conclusion, unresectable patients with stage IIIA-N2 LCNEC and LUSC had worse LCSS compared with LUAD. In our study, the prognostic nomogram constructed for patients

with unresectable NSCLC in stage IIIA-N2 could accurately predict survival by histological type, which may be a practical tool for clinicians to assess prognosis and stratify these prognostic risks, thus providing patients with more optimized and personalized treatment strategies based on histology.

## AUTHOR CONTRIBUTIONS

YY and CS: data collection, data analysis, and drafting articles. JS: data collection. YW and GW: research conception, design, and interpretation. AS: manuscript revision and submit manuscript. All authors contributed to the article and approved the submitted version.

## FUNDING

The study was funded by the Scientific Research Project of "333 Project" in Jiangsu Province (BRA2019030), the Nantong Science and Technology Foundation (MS22019008), and the Nantong Municipal Health Commission scientific research project (QA2021028).

## SUPPLEMENTARY MATERIAL

The Supplementary Material for this article can be found online at: https://www.frontiersin.org/articles/10.3389/fonc.2022.825598/full#supplementary-material

## REFERENCES

1. Butkiewicz D, Krześniak MK, Gdowicz-Kłosok A, Giglok M, Marszałek-Zé Nczak M, Suwí Nski R. Polymorphisms in EGFR Gene Predict Clinical Outcome in Unresectable Non-Small Cell Lung Cancer Treated With Radiotherapy and Platinum-Based Chemoradiotherapy. *Int J Mol Sci Artic* (2021) 22(11):5605. doi: 10.3390/ijms22115605
2. Stinchcombe TE, Bogart JA. Novel Approaches of Chemoradiotherapy in Unresectable Stage IIIA and Stage IIIB Non-Small Cell Lung Cancer. *Oncologist* (2012) 17:682. doi: 10.1634/THEONCOLOGIST.2012-0020
3. Xu F, Yang J, Xu B, Li Z, Li X, Wu X, et al. Clinical Research on Systemic Chemotherapy Combined With Bronchoscopic Seed Implantation in the Treatment of Advanced Lung Cancer. *Technol Cancer Res Treat* (2020) 19:1533033820971600. doi: 10.1177/1533033820971600
4. Kong C, Zhu X, Shi M, Wang L, Chen C, Tao H, et al. Survival and Toxicity of Hypofractionated Intensity Modulated Radiation Therapy in 4 Gy Fractions for Unresectable Stage III Non-Small Cell Lung Cancer. *Int J Radiat Oncol Biol Phys* (2020) 107(4):710-9. doi: 10.1016/j.ijrobp.2020.03.038
5. Hansen RN, Zhang Y, Seal B, Ryan K, Yong C, Darilay A, et al. Long-Term Survival Trends in Patients With Unresectable Stage III Non-Small Cell Lung Cancer Receiving Chemotherapy and Radiation Therapy: A SEER Cancer Registry Analysis. *BMC Cancer* (2020) 20(1):276. doi: 10.1186/s12885-020-06734-3
6. Trapani D, Giugliano F, Uliano J, Zia VAA, Marra A, Viale G, et al. Benefit of Adjuvant Chemotherapy in Patients With Special Histology Subtypes of Triple-Negative Breast Cancer: A Systematic Review. *Breast Cancer Res Treat* (2021) 187:323–37. doi: 10.1007/s10549-021-06259-8
7. Jiang H, Shao D, Zhao P, Wu Y. The Predictive and Guidance Value of Signet Ring Cell Histology for Stage II/III Colon Cancer Response to Chemotherapy. *Front Oncol* (2021) 11:631995. doi: 10.3389/fonc.2021.631995
8. Son CH, Liauw SL, Hasan Y, Solanki AA. Optimizing the Role of Surgery and Radiation Therapy in Urethral Cancer Based on Histology and Disease Extent. *Int J Radiat Oncol Biol Phys* (2018) 102(2):304-13. doi: 10.1016/j.ijrobp.2018.06.007
9. Wang J, Ye L, Cai H, Jin M. Comparative Study of Large Cell Neuroendocrine Carcinoma and Small Cell Lung Carcinoma in High-Grade Neuroendocrine Tumors of the Lung: A Large Population-Based Study. *J Cancer* (2019) 10:4226. doi: 10.7150/JCA.33367
10. Sherman S, Rotem O, Shochat T, Zer A, Moore A, Dudnik E. Efficacy of Immune Check-Point Inhibitors (ICPi) in Large Cell Neuroendocrine Tumors of Lung (LCNEC). *Lung Cancer* (2020) 143:40-6. doi: 10.1016/j.lungcan.2020.03.008
11. Wang X, Wang Z, Pan J, Lu Z-Y, Xu D, Zhang H-J, et al. Patterns of Extrathoracic Metastases in Different Histological Types of Lung Cancer. *Front Oncol* (2020) 10:715. doi: 10.3389/FONC.2020.00715
12. Baine MJ, Verma V, Schonewolf CA, Lin C, Ii CBS. Histology Significantly Affects Recurrence and Survival Following SBRT for Early Stage non-Small Cell Lung Cancer. *Lung Cancer* (2018) 118:20–6. doi: 10.1016/j.lungcan.2018.01.021
13. Liao WY, Chen JH, Wu M, Shih JY, Chen KY, Ho CC, et al. Neoadjuvant Chemotherapy With Docetaxel-Cisplatin in Patients With Stage III N2 Non-Small-Cell Lung Cancer. *Clin Lung Cancer* (2013) 14(4):418–24. doi: 10.1016/j.cllc.2012.10.003
14. Jin G, Wang X, Xu C, Sun J, Yuan Z, Wang J, et al. Disparities in Survival Following Surgery Among Patients With Different Histological Types of N2-III Non-Small Cell Lung Cancer: A Surveillance, Epidemiology and End Results (SEER) Database Analysis. *Ann Transl Med* (2020) 8:1288–8. doi: 10.21037/atm-20-4357
15. Fine JP, Gray RJ. A Proportional Hazards Model for the Subdistribution of a Competing Risk. *J Am Stat Assoc* (1999) 94. (446):496–509. doi: 10.2307/2670170
16. Grosu HB, Manzanera A, Shivakumar S, Sun S, Noguras Gonzalez G, Ost DE. Survival Disparities Following Surgery Among Patients With Different Histological Types of Non-Small Cell Lung Cancer. *Lung Cancer* (2020) 140:55–8. doi: 10.1016/j.lungcan.2019.12.007
17. Ost D, Goldberg J, Rolnitzky L, Rom WN. Survival After Surgery in Stage IA and IB Non–Small Cell Lung Cancer. *Am J Respir Crit Care Med* (2008) 177:516. doi: 10.1164/RCCM.200706-815OC
18. Villanueva MT. Squamous Cell Lung Cancer Changes Driver. *Nat Rev Drug Discovery* (2021) 20:177. doi: 10.1038/D41573-021-00028-4
19. Tsai JC, Saad OA, Magesh S, Xu J, Lee AC, Li WT, et al. Tobacco Smoke and Electronic Cigarette Vapor Alter Enhancer RNA Expression That Can Regulate the Pathogenesis of Lung Squamous Cell Carcinoma. *Cancers (Basel)* (2021) 13(16):4225. doi: 10.3390/CANCERS13164225
20. Pilleron S, Maringe C, Charvat H, Atkinson J, Morris E, Sarfati D. Age Disparities in Lung Cancer Survival in New Zealand: The Role of Patient and Clinical Factors. *Lung Cancer* (2021) 157:92-9. doi: 10.1016/j.lungcan.2021.05.015
21. Arnold BN, Thomas DC, Rosen JE, Salazar MC, Blasberg JD, Boffa DJ, et al. Lung Cancer in the Very Young: Treatment and Survival in the National Cancer Data Base. *J Thorac Oncol* (2016) 11(7):1121-31. doi: 10.1016/j.jtho.2016.03.023
22. Eberle A, Jansen L, Castro F, Krilaviciute A, Luttmann S, Emrich K, et al. Lung Cancer Survival in Germany: A Population-Based Analysis of 132,612 Lung Cancer Patients. *Lung Cancer* (2015) 90(3):528-33. doi: 10.1016/j.lungcan.2015.10.007
23. Wheatley-Price P, Blackhall F, Lee SM, Ma C, Ashcroft L, Jitlal M, et al. The Influence of Sex and Histology on Outcomes in Non-Small-Cell Lung Cancer: A Pooled Analysis of Five Randomized Trials. *Ann Oncol* (2010) 21(10):2023-8. doi: 10.1093/annonc/mdq067
24. Ogawa H, Sakai Y, Nishio W, Fujibayashi Y, Nishikubo M, Nishioka Y, et al. DLL3 Expression Is a Predictive Marker of Sensitivity to Adjuvant Chemotherapy for Pulmonary LCNEC. *Thorac Cancer* (2020) 11:2561–9. doi: 10.1111/1759-7714.13574
25. Zou L, Guo T, Ye L, Zhou Y, Chu L, Chu X, et al. Outcomes for Surgery in Stage IA Large Cell Lung Neuroendocrine Compared With Other Types of Non-Small Cell Lung Cancer: A Propensity Score Matching Study Based on

the Surveillance, Epidemiology, and End Results (SEER) Database. *Front Oncol* (2020) 10:572462. doi: 10.3389/FONC.2020.572462
26. Kujtan L, Muthukumar V, Kennedy KF, Davis JR, Masood A, Subramanian J. The Role of Systemic Therapy in the Management of Stage I Large Cell Neuroendocrine Carcinoma of the Lung. *J Thorac Oncol* (2018) 13(5):707–14. doi: 10.1016/j.jtho.2018.01.019
27. Tanno S, Onodera H, Inoue S, Honda R, Nagashima K, Ohsaki Y. An Elderly Patient With Large Cell Neuroendocrine Carcinoma (LCNEC)for Whom Chemotherapy With Irinotecan and Split-Dose Cisplatin(CDDP)proved Very Effective]. *Gan To Kagaku Ryoho* (2013) 40(9):1205–8.
28. Antonia SJ, Villegas A, Daniel D, Vicente D, Murakami S, Hui R, et al. Durvalumab After Chemoradiotherapy in Stage III Non-Small-Cell Lung Cancer. *N Engl J Med* (2017) 377(20):1919–29. doi: 10.1056/NEJMoa1709937
29. Noronha V, Patil VM, Joshi A, Menon N, Chougule A, Mahajan A, et al. Gefitinib Versus Gefitinib Plus Pemetrexed and Carboplatin Chemotherapy in EGFR-Mutated Lung Cancer. *J Clin Oncol* (2020) 38(2):124–36. doi: 10.1200/JCO.19.01154
30. vanzo M, Gagliardi V, Stancanello J, Blanck O, Pirrone G, El Naqa I, et al. Combining Computed Tomography and Biologically Effective Dose in Radiomics and Deep Learning Improves Prediction of Tumor Response to Robotic Lung Stereotactic Body Radiation Therapy. *Med Phys* (2021) 48 (10):6257–69. doi: 10.1002/mp.15178

**Conflict of Interest:** The authors declare that the research was conducted in the absence of any commercial or financial relationships that could be construed as a potential conflict of interest.

**Publisher's Note:** All claims expressed in this article are solely those of the authors and do not necessarily represent those of their affiliated organizations, or those of the publisher, the editors and the reviewers. Any product that may be evaluated in this article, or claim that may be made by its manufacturer, is not guaranteed or endorsed by the publisher.

frontiers | Frontiers in Oncology

TYPE Original Research
PUBLISHED 15 September 2022
DOI 10.3389/fonc.2022.865756



OPEN ACCESS

EDITED BY
Pasquale Pisapia,
University of Naples Federico II, Italy

REVIEWED BY
Hailin Tang,
Sun Yat-sen University Cancer Center (SYSUCC), China
Jingjing Qu,
Zhejiang University, China

*CORRESPONDENCE
Xinglin Gao
xinglingao@hotmail.com

SPECIALTY SECTION
This article was submitted to Thoracic Oncology, a section of the journal Frontiers in Oncology

RECEIVED 30 January 2022
ACCEPTED 29 August 2022
PUBLISHED 15 September 2022

CITATION
Tan J, Chen F, Ouyang B, Li X, Zhang W and Gao X (2022) CDCA4 as a novel molecular biomarker of poor prognosis in patients with lung adenocarcinoma.
*Front. Oncol.* 12:865756.
doi: 10.3389/fonc.2022.865756



# CDCA4 as a novel molecular biomarker of poor prognosis in patients with lung adenocarcinoma

Jianlong Tan[1,2], Fengyu Chen[3], Bin Ouyang[3], Xiuying Li[3], Weidong Zhang[3] and Xinglin Gao[1,2]*

[1]The Second School of Clinical Medicine, Southern Medical University, Guangzhou, China, [2]Department of Geriatric Respiratory Medicine, Guangdong Provincial People's Hospital, Guangdong Academy of Medical Sciences, Guangdong Provincial Geriatrics Institute, Guangzhou, China, [3]Department of Pulmonary and Critical Care Medicine, Hunan Provincial People's Hospital, The First Affiliated Hospital of Hunan Normal University, Changsha, China

**Background:** Because of the high incidence and poor prognoses of lung adenocarcinoma (LUAD), it is essential to identify cost-effective treatment options and accurate and reliable prognostic biomarkers. CDCA4 upregulation has been identified in many cancers. However, the prognostic importance of CDCA4 and its role in LUAD remain unknown.

**Methods:** CDCA4 expression was assessed through IHC, Western blotting (WB) and RT-PCR. The Cancer Genome Atlas (TCGA) provided data from 513 patients to study the expression and prognostic relevance of CDCA4 in LUAD. This study used gene set enrichment analyses (GSEA), gene ontology and KEGG pathway analyses for elucidating potential mechanisms underpinning the function of CDCA4 in LUAD. We also investigated correlations between immune infiltration and CDCA4 expression with single specimen GSEA (ssGSEA).

**Results:** According to database analysis and identification of patient tissue samples, CDCA4 expression in tumour tissues surpassed that in normal tissues ($P< 0.001$). Increased CDCA4 expression was positively correlated with a higher T, N, pathologic stage and poor primary therapy outcome. In addition, the Kaplan–Meier plotter exhibited that an elevated CDCA4 expression was related to worse disease-specific survival(DSS) and overall survival (OS) (DSS HR= 5.145, 95% CI=3.413-7.758, $P<0.001$; OS HR=3.570, 95% CI=2.472-5.155, $P<0.001$). Then multivariate COX regression analyses indicated that the CDCA4 gene was an independent risk consideration for prognoses. GO and KEGG results showed that CDCA4 and its neighbouring genes were enriched in the cell cycle and DNA replication. As determined by GSEA, CDCA4 was related to various immune-related signalling pathways (SPs), Homologous recombination, DNA replication and the cell cycle. SsGSEA analysis showed a significant association between CDCA4 expression and Th2 cells, mast cells, eosinophils and Th17 cells.

**Conclusions:** CDCA4 expression is increased in LUAD and is a potential predictive biomarker and therapeutic target.

KEYWORDS

CDCA4, lung adenocarcinoma, biomarker, prognosis, TCGA

## Introduction

Lung cancer is the most common type of cancer and the primary reason for cancer deaths globally (1). Unfortunately, most lung cancer patients are not detected until the metastatic stage (2). Despite continued advances in treatment strategies (like immunotherapy, targeted therapy, chemotherapy, radiotherapy and surgery), the prognoses remain bleak, with a five-year relative survival rate of only 19.7% in China (3). The five-year relapse-free survival (RFS) after surgical resection is only 70% (4). Based on histological type, non-small cell lung cancer (NSCLC) made up approximately 85% of lung cancer, while lung adenocarcinomas (LUAD) made up nearly 40% (5). LUAD possesses a high burden of tumour mutations such as EGFR, HER2, BRAF, ROS1, ALK, and KRAS (6–9). The discovery of these biomarkers has revolutionized the therapeutic landscape of advanced LUAD. However, the prognosis of LUAD remains unsatisfactory because of its remarkable heterogeneity and aggressiveness. Therefore, developing novel tumour biomarkers with high specificity and sensitivity is crucial for the early detection, treatment and prognosis of LUAD.

The cell division cycle-associated (CDCA) protein family (CDCA1-8) is involved in the cell cycle, which is closely related to carcinogenesis (10, 11). Efforts have been made to identify CDCA genes as biomarkers for the development and prognosis of different malignancies (12, 13). The up-regulation of CDCA gene expression may play a vital role in ovarian cancer oncogenesis through the PLK1 pathway (13). CDCA4, known as HEPP/TRIP-Br3/SEI-3 as well, is associated with the G1/S transition transcription factor. It encodes a protein member of the E2F family of transcription factors involved cell cycle regulation and DNA synthesis (14). According to earlier studies, through the E2F/retinoblastoma protein pathway, CDCA4 controls cell proliferation and E2F-dependent transcriptional activation (15). Various studies have extensively confirmed the close relationship between CDCA4 upregulation and tumorigenesis (12, 13, 16). There is evidence that overexpression of CDCA4 stimulates proliferation and inhibits apoptosis in MCF-7/ADM human breast cancer cells (16). CDCA4 regulates the mRNA expression of the JUN oncogene and acts as a critical determinant of cell fate (17). Notably, overexpression of CDCA4 is directly associated with reduced post-progression survival (PPS) in ovarian cancer (13). CDCA4 has been validated as a prognostic biomarker for various malignancies (12, 18). Wu et al. and colleagues found that increased CDCA4 mRNA expression was strongly related to survival in patients featuring squamous cell carcinoma of the head and neck (12). However, the link between CDCA4 expression and LUAD remains to be fully explored.

The objectives of this study were 1) to understand whether CDCA4 expression correlates with clinical and pathological aspects in patients with LUAD; 2) to investigate the predictive value of CDCA4 in LUAD; 3) to evaluate the expression model of CDCA4 in tumour and peritumor lung tissues, and 4) to understand the underlying mechanisms using bioinformatics analysis. In addition, an online tumour infiltration immune cell tool was employed to assess the association between CDCA4 expression and the clinical characteristics of LUAD.

## Materials and methods

### Clinical samples

From January to December 2020, 39 patients with LUAD underwent surgery in the Department of Thoracic Surgery at Hunan Provincial People's Hospital and paired tumour and normal tissue (>5 cm proximity) specimens adjacent to the tumour were collected for real-time quantitative PCR (RT-qPCR), WB, and immunohistochemical (IHC) experiments. The clinical characteristics of the 39 individuals can be obtained in Supplementary Tables 1, 2. All selected patients received surgery without neoadjuvant therapy, autoimmune diseases or other malignant tumors. The ethics committee of Hunan Provincial People's Hospital authorized this study (No.202049). All patients completed written informed consent, and no additional special treatments were administered preoperatively.

### Immunohistochemistry

LUAD tissues which contained 39 tumours and paired normal tissues were used for immunohistochemical staining of CDCA4. Hematoxylin and eosin staining of the tumour and normal tissues

close to the tumour followed by immunohistochemical staining. The main staining procedure was as follows. Four-millimetre-thick paraffin sections were dewaxed with xylene and washed in an ethanol gradient. After antigen retrieval featuring EDTA buffer (pH=9.0), endogenous peroxidase activity was eliminated by adopting 3% $H_2O_2$ for 10 minutes and incubated with CDCA4 polyclonal antibody (1:300; No. YT0820; ImmunoWay Biotechnology, USA) at 4°C overnight. After rinsing three times with PBS, add the primary antibody and incubate them with the secondary antibody (Goat Anti-Rabbit IgG Antibody-HRP; No.201105S407q; Maixin Biotech Co., Ltd, Fuzhou, China) for 50 min at room temperature(RT). After rising in PBS for three minutes, incubate the sections and stain them with a DAB colour development kit (Fuzhou Maixin Biotech Co., Ltd., China), followed by hematoxylin staining, drying and mounting. CDCA4 expression was quantified in at least five locations under 200x magnification based on staining intensity (0–3) and the proportion of positively stained tumour cells (0-100%). The following are the scoring guidelines. 0 denotes no staining; 1 denotes weak yellow-brown staining; 2 denotes modest yellow-brown staining; and 3 denotes severe yellow-brown staining (strong staining, brown). The latter were classified as follows: 0 (negative); 1 (approximately 25% positive cells); 2 (approximately 25% to 50% positive cells); 3 (approximately 51 to 75% positive cells); and 4 (approximately >75% positive cells). Immunostaining was reviewed separately by two professional pathologists who kept the clinical results of the patients confidential.

## Quantitative real-time PCR analysis

Quantify CDCA4 expression by employing real-time reverse transcription-polymerase chain reaction (RTPCR). Isolate total RNA from tumours, and adjacent normal tissues of 10 patients by applying Trizol reagent (TianGen, Beijing, China) and reverse transcribe them into cDNA using RevertAid reverse transcriptase (Thermo, USA) according to the producer's instructions. Perform qRT-PCR by employing PerfectStart Green qPCR 2x SuperMix (TransGen Biotech, China) and the Q1 Real-Time System (ABI), with GAPDH as an internal reference. Use the primers below in the qRT-PCR. CDCA4: 5'-CACGAGGACTGAAGAGGAAATGT-3' (forward); 5'-TTGGGCTCCACAAGCATGTG-3' (reverse); GAPDH: 5'-CCAGGTGGTCCTGA-3' (forward); 5'- CCAGGTGCTCCTGA-3' (reverse). Calculate all mRNA levels by utilizing the 2Ct approach, and test all samples in triplicate using this method.

## Western blotting

Based on the producer's instructions, isolate total proteins from tissues of 10 patients using the RIPA protein extraction reagent (Beyotime, China). Afterwards, measure protein contents by adopting a BCA kit (Beyotime, China). Proteins were separated and transferred to PVDF membranes using 10% SDS-PAGE (Merck Millipore, Germany). Block the films by employing 5% skimmed dry milk in PBST (1 PBS + 0.1% Tween-20) buffer for 2 h at RT. After rinsing the membranes by utilizing PBST, incubate them by employing anti-CDCA4 (1:5,000, Proteintech, USA) primary antibody at 4°C overnight before incubating them by utilizing horseradish peroxidase-conjugated secondary antibody (1:5,000) for one hour at RT. Wash blots three times with PBST, and quantify protein levels with a ClinxChemiScope 6000 (Clinx Scientific Instruments, China) before visualization using enhanced chemiluminescence. Internal controls were identified as GAPDH, and relative expression was normalized to GAPDH. Perform the experiment in triplicate.

## Data collection

In May 2020, the RNA-seq gene data and associated clinicopathological characteristics were downloaded from the TCGA database (https://portal.gdc.cancer.gov ) as Level 3 gene expression data. The following analysis stage was to convert the level 3 HTSeq-FPKM data into transcripts per million reads (TPM). LUAD patients lacking sufficient survival and/or expression data were excluded. R software (version 3.6.2) was applied for analyzing the data of each RNA-Seq gene expression level 3 and the clinical information of LUAD patients (19). Finally, data from 513 patients, including 57 paired LUAD tissue and para-cancerous tissue samples, were downloaded. Among the enrolled patients, according to the American Joint Committee on Cancer (AJCC) 8th edition staging manual for lung cancer, this study included 274 patients (53.41%) at stage I, 121 patients (23.59%) at stage II, 84 patients (16.37%) at stage III, and 10 patients (1.95%) at stage IV (Table 1).

## CDCA4 correlation genes analysis

After removing the repeated sequences of patients' tumours, we used the Pearson method of cor. test function in R (version: 4.0.2) to detect the TPM expression and CDCA4-related genes in 513 tumours. $P < 0.05$ and $|R| > 0.2$ were statistically, and finally we got 6952 significant correlation genes of CDCA4.

## Gene-set enrichment analyses

Gene Ontology (GO) and Kyoto Encyclopedia of Genes and Genomes (KEGG) pathway enrichment analyses were conducted by employing the R package clusterProfiler (version: v3.18.1) for correlation genes with CDCA4. For identifying over-represented GO terms in three categories (cellular component, molecular function and biological courses), and the KEGG pathway, the R package enrichplot(version: v1.10.2) was adopted to visualize. For these analyses, $p < 0.05$ and $q < 0.2$ were regarded to denote statistical significance.

TABLE 1 The clinicopathological characteristics of LUAD in patients with TCGA.

| Characteristics | N% or median (range) |
|---|---|
| Age | |
| >65 | 262 (51.07%) |
| ≤65 | 241 (46.98%) |
| Data missing | 10 (1.95%) |
| Gender (%) | |
| Female | 276 (53.80%) |
| Male | 237 (46.20%) |
| path T-stage (%) | |
| T1 | 168 (32.75%) |
| T2 | 276 (53.80%) |
| T3 | 47 (9.16%) |
| T4 | 19 (3.70%) |
| Data missing | 3 (0.59%) |
| path N-stage (%) | |
| N0 | 330 (64.33%) |
| N1 | 95 (18.52%) |
| N2 | 74 (14.42%) |
| N3 | 2 (0.39%) |
| Data missing | 12 (2.34%) |
| path M-stage (%) | |
| M0 | 344 (67.06%) |
| M1 | 25 (4.87%) |
| Data missing | 144 (28.07%) |
| Pathologic stage (%) | |
| Stage I | 274 (53.41%) |
| Stage II | 121 (23.59%) |
| Stage III | 84 (16.37%) |
| Stage IV | 10 (1.95%) |
| Data missing | 24 (4.68%) |
| Primary therapy outcome (%) | |
| CR | 315 (61.40%) |
| PD | 68 (13.26%) |
| PR | 6 (1.17%) |
| SD | 37 (7.21%) |
| Data missing | 87 (16.96%) |
| TP53 status (%) | |
| Mut | 241 (46.98%) |
| WT | 267 (52.05%) |
| Data missing | 5 (0.97%) |

## Gene set enrichment analysis

To further determine the function of genes related to CDCA4, we sequenced these genes in LUAD tumours in the TCGA data set according to the relationship between these genes and CDCA4. Then "gseGO" and "gseKEGG" function of the R package clusterProfiler (version: v3.18.1) was used to analyze GO_ BP and KEGG. We set a statistically significant p-value of 0.05 for GO_BP and KEGG enrichment analyses.

## Immune infiltration analysis by single sample gene set enrichment analysis

We assessed the infiltration of 24 immune cell types (ICTs) in tumour tissues by employing the ssGSEA approach of the Gene Set Variation Analysis (GSVA) package (http://www.bioconductor.org/packages/relaease/bioc/html/GSVA.html) of R software (version 3.6.2). The ssGSEA scored the absolute expression of genes in each tumour sample and calculated an enrichment score according to the marker genes of the 24 ICTs found in the literature (20). The Spearman correlation and Wilcoxon rank-sum tests were adopted for assessing the association between the immune cells and CDCA4 and the relationship between CDCA4 low and high expression groups and immune cell infiltration.

## Statistical analysis

R and IBM SPSS 26.0 were applied for evaluating and performing a statistical study of the data. To investigate the association between CDCA4 and clinicopathological characteristics, Pearson $\chi^2$ tests and univariate logistic regression were utilized. The cor.test package in R was used to calculate Pearson correlations, and the ggpubr and corrplot packages in R were used to create correlation graphs. The association between clinical variables and DSS or OS time in patients with TCGA-LUAD was investigated by employing the Kaplan-Meier (KM) technique and COX regression analysis. Multivariate Cox analyses were utilized to determine the effect of CDCA4 expression combined with other clinicopathological variables in survival. The median expression level was used to define the cut-off point of CDCA4 expression. Each hypothesis test was two-sided, and statistical significance was defined as a $P$ of 0.05. In addition, a prognostic nomogram model was created based on multivariate regression results to provide an accurate multivariate clinical prognostic evaluation method for patients. A nomogram was created by applying the rms R package (http://cran.r-project.org/web/packages/rms/index.html). Afterwards, a calibration plot was created to test its predictive power.

# Results

## Elevated expression of CDCA4 in LUAD

First, qRT-PCR and WB analyses were employed for evaluating CDCA4 expression in clinical LUAD samples. In comparison to normal human lung tissue, CDCA4 expression in LUAD was

elevated (Figures 1A, B). Next, immunohistochemical analysis revealed that CDCA4 was mainly located in the cytoplasm and film of tumour cells and exhibited little expression in the normal lung cells. In LUAD, the average scores were 8.85 ± 2.89, whereas the para tumour samples score was 3.28 ± 1.32 (p<0.001; Figures 1C, D). This conclusion was further verified using the TCGA datasets. It was identified that CDCA4 expression levels in 513 tumour tissues substantially surpassed those in normal tissues based on TCGA data (*P*<0.001; Figure 1E). CDCA4 expression was then analyzed using matched plots between LUAD adjacent and tumour samples from the same individuals. CDCA4 expression in 57 tumour tissues surpassed that in 57 matched adjacent tissues (*P*<0.001; Figure 1F). Collectively, the results prove that CDCA4 mRNA and protein contents were significantly upregulated in LUAD tissues.

## CDCA4 upregulation was associated with unfavourable clinicopathological features

We also investigated whether there was an association between CDCA4 expression and clinical and pathological features. According to the Kruskal-Wallis rank-sum test and Wilcoxon rank-sum test, higher CDCA4 levels were associated with younger age (*P*=0.003), more years of smoking (*P*=0.011), T stage, N stage, advanced pathologic stage, poor primary therapy outcome and more P53 mutation (Figures 2A–G, *P*<0.05). As exhibited in Table 2, univariate logistic regression analyses of CDCA4 expression exhibited that high CDCA4 was obviously related to unfavorable characteristics such as younger age [OR=0.61 (0.43-0.87) for >65 vs. <=65, *P*=0.007], more years of smoking [OR=1.53 (1.00-2.33) for >=40 vs. 40<, *P*=0.049], larger primary tumour extent in LUAD [OR=2.21 (1.52-3.25) for T2-4 vs. T1, *P* <0.001], more severe regional lymph node invasion [OR=1.98 (1.36-2.90) for N1-3 vs N0, *P*<0.001], poor primary therapy result [OR=1.89 (1.12-3.25) for PD vs. SD-CR, *P*=0.045], higher incidence of P53 mutations [OR=0.31 (0.21-0.44), *P*< 0. 001], and higher pathologic stage [OR=1.80 (1.26-2.57) for stage II-IV vs. stage I, *P=0*.001]. Together, these results suggest CDCA4 upregulation was related to unfavourable clinicopathological features in LUAD patients.

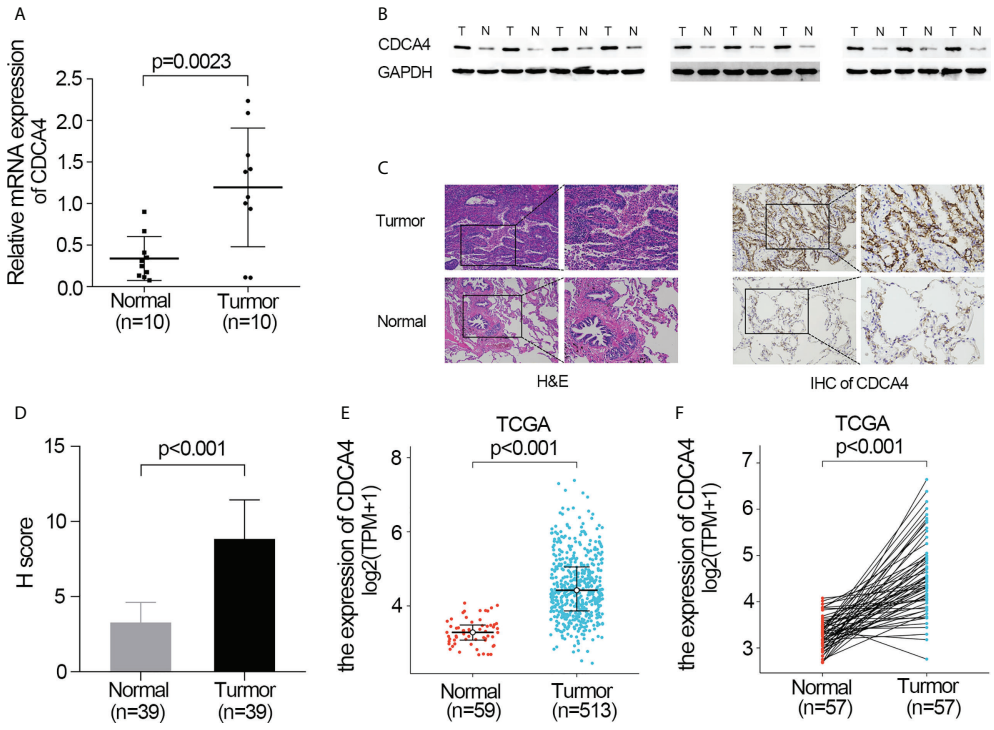


FIGURE 1
Validate the expression of CDCA4 in LUAD. **(A)** qRT-PCR was used to identify the expression of CDCA4 mRNA in tumors and adjacent tissues of 10 LUAD patients. **(B)** Western blotting was used to determine the expression of CDCA4 protein in tumors and adjacent tissues of 10 LUAD patients. **(C)** CDCA4 expression in LUAD tissues and adjacent normal tissues assayed by IHC (×200) and (×400). **(D)** H score of IHC staining of LUAD tissues and adjacent tissues. **(E)** CDCA4 mRNA levels in LUAD tissues from the TCGA database. **(F)** CDCA4 mRNA expression levels in the tumors and adjacent tissues of 57 LUAD patients from the TCGA database. Data are expressed as mean standard deviation (SD). Normal, lung tissue; tumor, lung adenocarcinoma tissue; TCGA, The Cancer Genome Atlas.

## Survival outcomes and multivariate examination

The disease-specific survival (DSS) and OS of the two CDCA4 expression value groups were assessed to determine their predictive relevance. According to Figures 3A, B, KM survival analyses exhibited that patients with high CDCA4 levels had worse prognoses of DSS and OS (DSS HR=1.82,95% CI=1.24-2.67, *P*=0.002; OS HR=1.52; 95% CI=1.13-2.04, *P*=0.006). In addition, univariate and multivariate analyses were conducted by employing the Cox proportional hazards model (CPHM). According to univariate analyses (Table 3A; Supplementary Table 3A), high CDCA4 levels and T stage, N stage, M stage, pathologic stage and primary therapy outcome were related to low DSS and OS. Finally, multivariate analysis showed that high CDCA4 levels (DSS HR=1.674; 95% CI=1.112-2.521, P=0.014; OS HR=1.427, 95% CI=1.017-2.003, P=0.04), advanced pathologic stage (DSS HR=2.885, 95% CI=1.868-4.456, P<0.001; OS HR=2.462, 95% CI=1.731-3.501, P<0.001) and poor primary therapy outcome (DSS HR=5.145, 95% CI=3.413-7.758, P<0.001; OS HR=3.570, 95% CI=2.472-5.155, P<0.001) were independently related to poor prognosis (Table 3B; Supplementary Table 3B). This data implies that CDCA4 may be a useful biomarker for predicting LUAD.

## Risk score model for nomogram

A nomogram consisting of independent prognostic variables was then constructed to quantify the risk assessment and probability of survival for individual LUAD patients. A score was assigned to each variable based on a multivariate Cox proportional hazards model. The multivariate Cox proportional hazards model was adopted for scoring each variable. The weighted scores calculated using all variables were used to estimate the predicted DSS and OS at 1-, 3-, and 5- years. The calculated c-index for predicted DSS and OS was 0.782(95% CI=0.757-0.806), 0.717 (95% CI=0.692-0.742), respectively, indicating that the nomogram was a good predictor for DSS and OS (Figure 3C; Supplementary Figure 1A). In the calibration survey, the 1-, 3-, and 5-year prediction lines for the estimated likelihood of survival showed high agreement with the ideal performance (45-degree dashed line) (Figure 3D; Supplementary Figure 1B).

## Identification of CDCA4 co-expressed differential genes

For further elucidating the biological function of CDCA4 in LUAD, we downloaded the co-DEGs profile of CDCA4 from the

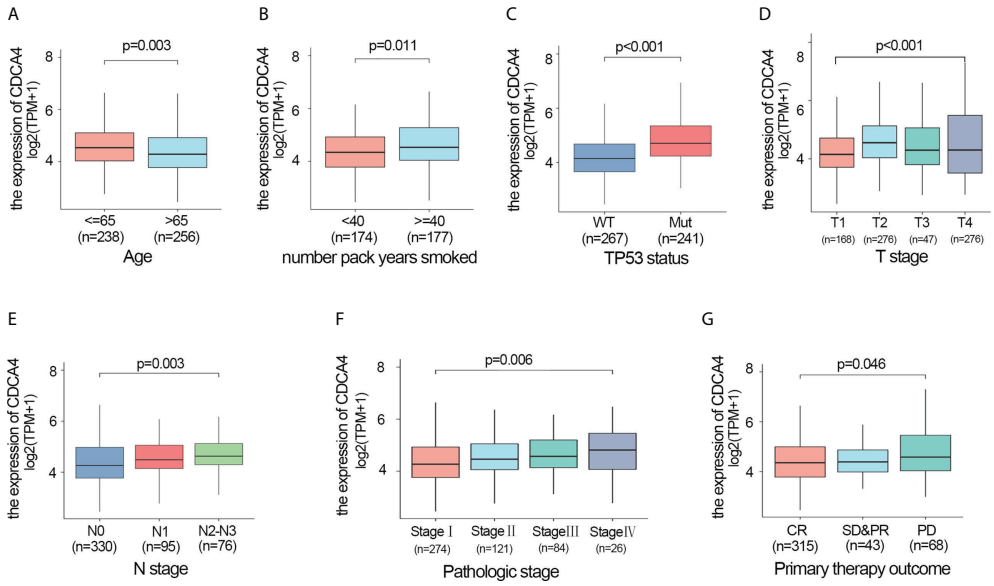


FIGURE 2
Higher CDCA4 expression was associated with unfavourable clinicopathological characteristics in LUAD. **(A–G)** CDCA4 expression was strongly correlated with younger age, more years of smoking, patients' T-stage, N-stage, pathological stage, poor primary therapy outcome and more P53 mutation (*P*<0.05).

TABLE 2 Relationship between CDCA4 expression and clinicopathological characteristics of TCGA database by logistic regression analysis.

| Characteristics | Total number (N) | Odds Ratio (OR) | *P* value |
|---|---|---|---|
| Age (>65 vs. <=65) | 494 | 0.61 (0.43-0.87) | 0.007 |
| Smoker (Yes vs. No) | 499 | 1.46 (0.89-2.42) | 0.137 |
| number pack years smoked (>=40 vs. <40) | 351 | 1.53 (1.00-2.33) | 0.049 |
| T stage (T2-4 vs. T1) | 510 | 2.21 (1.52-3.25) | <0.001 |
| N stage (N1-3 vs. N0) | 501 | 1.98 (1.36-2.90) | <0.001 |
| M stage (M1 vs. M0) | 369 | 2.00 (0.87-5.03) | 0.116 |
| Primary therapy outcome (PD vs. SD-CR) | 426 | 1.89 (1.12-3.25) | 0.019 |
| TP53 status (Mut vs. WT) | 508 | 3.28 (2.28-4.73) | <0.001 |
| Pathologic stage (Stage II- IV vs. Stage I) | 505 | 1.80 (1.26-2.57) | 0.001 |

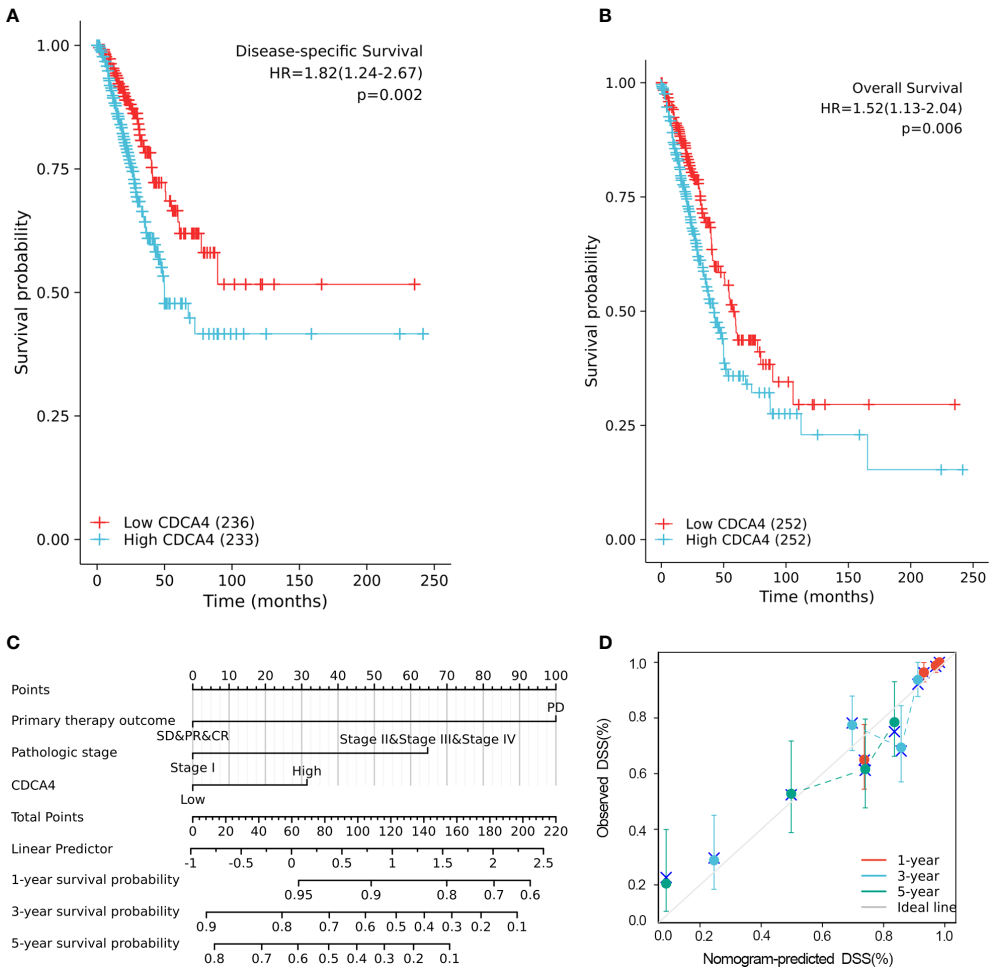


FIGURE 3
Higher CDCA4 expression was associated with poorer prognosis in LUAD. **(A, B)** KM survival analyses exhibited that patients with high CDCA4 levels had worse prognoses of DSS and OS (DSS HR=1.82,95% CI=1.24-2.67, *P*=0.002; OS HR=1.52; 95% CI=1.13-2.04, *P*=0.006). **(C)** Nomogram constructed using DSS related clinical factors and CDCA4. **(D)** Calibration plots showing good agreement with the best performance for DSS. DSS, disease-specific survival.

TABLE 3 Univariate and multivariate analysis of the relationship between disease specific survival and clinicopathologic characteristics in patients with TCGA.

| Characteristics | Total number (N) | HR (95% CI) | *P* value |
|---|---|---|---|
| A | | | |
| Age (>65 vs. <=65) | 459 | 1.039 (0.713-1.513) | 0.842 |
| Gender (Female vs. Male) | 469 | 1.046 (0.720-1.519) | 0.815 |
| Smoker (Yes vs. No) | 455 | 1.013 (0.585-1.755) | 0.962 |
| number pack years smoked (>=40 vs. <40) | 318 | 0.904 (0.569-1.437) | 0.67 |
| T stage (T2-4 vs. T1) | 466 | 1.747 (1.125-2.714) | 0.013 |
| N stage (N1-3 vs. N0) | 457 | 2.795 (1.919-4.071) | <0.001 |
| M stage (M1 vs. M0) | 327 | 2.480 (1.278-4.811) | 0.007 |
| Pathologic stage (Stage II-IV vs. Stage I) | 461 | 3.519 (2.350-5.271) | <0.001 |
| Primary therapy outcome (PD vs. SD-CR) | 408 | 5.929 (3.981-8.830) | <0.001 |
| TP53 status (Mut vs. WT) | 465 | 1.335 (0.920-1.937) | 0.128 |
| CDCA4 (High vs. Low) | 469 | 1.823 (1.243-2.675) | 0.002 |
| B | | | |
| Pathologic stage (Stage II-IV vs. Stage I) | 461 | 2.885(1.868-4.456) | <0.001 |
| Primary therapy outcome (PD vs. SD-CR) | 408 | 5.145(3.413-7.758) | <0.001 |
| CDCA4 (High vs. Low) | 469 | 1.674(1.112-2.521) | 0.014 |

TCGA public database. 256 DEGs, comprising 179 upregulated genes and 77 downregulated ones, were significantly associated with CDCA4 expression according to the criteria of $P<0.05$ and $|logFC|>2$. The overall closely co-expressed genes of CDCA4 in LUAD were shown as a volcano plot map (Figure 4A). Subsequently, these aberrant genes were shown as a heat map (Figure 4B). The PPI network of these 256 common genes was then constructed by STRING based on the correlation coefficients to understand the underlying mechanisms better. The top 20 genes were selected and visualized for analysis (Figure 4C).

## GO and KEGG enrichment analysis identified pathways modulated by CDCA4 in LUAD

To elucidate the potential function of CDCA4 in LUAD progression, we performed GO annotation and KEGG pathway analyses. Various BPs, CCs and MFs. CDCA4 and its adjacent genes were significantly enriched in the biogenesis of ribonucleoprotein complex, the regulation of G2/M phase transition of the cell cycle, G2/M phase transition of mitotic cell cycle, G2/M phase transition of the cell cycle, DNA replication, ncRNA metabolic process and RNA splicing (Figure 4D). The molecular functions of these genes include single-stranded DNA binding, acting on DNA, ATPase activity, acting on RNA and catalytic activity (Figure 4E). The cellular components of these genes comprise kinetochore, condensed chromosome, centromeric region, chromosome, chromosomal region and spliceosomal complex. (Figure 4F). KEGG path analyses exhibited that CDCA4 was related to genes involved in the Base excision repair, Homologous recombination, DNA replication, Proteasome, RNA transport, Cell cycle and Spliceosome. (Figure 4G). Furthermore, GSEA indicated that in the high or low CDCA4 expression group, PD-L1 expression and PD-L1 checkpoint pathway in cancer, Fc gamma R-mediated phagocytosis, intestinal immune network for IgA generation, homologous recombination, proteasome, DNA replication, RNA transport, cell cycle and Spliceosome were enriched (Figures 5A–I). The outcomes imply that CDCA4 upregulation may influence LUAD progression *via* Cell cycle, homologous recombination and DNA replication.

## The relationship between immune cell infiltration and CDCA4 expression in lung adenocarcinoma

For determining the association between CDCA4 expression and immune cell infiltration (ICI) in the LUAD microenvironment, we first used ssGSEA with the Wilcoxon rank-sum test for assessing the difference among 24 different immune cell types of LUAD patients based on CDCA4 expression. It presented an apparent rise in immunological infiltration and heterogeneity. The proportion of follicular helper T cells (Tfh cells), T central memory (TCM), T cells, NK CD56 (bright) NK cells, plasmacytoids (pDCs), NK cells, Mast cells, immature DCs (iDCs), Eosinophils, CD8 T cells and B cells was significantly high in the CDCA4 low-expression group, and the proportion of activated DCs (aDCs), Th2, T gamma delta (Tgd) and CD56 (dim) NK cells was significantly high in the CDCA4 high-expression group (Supplementary Figure 2).

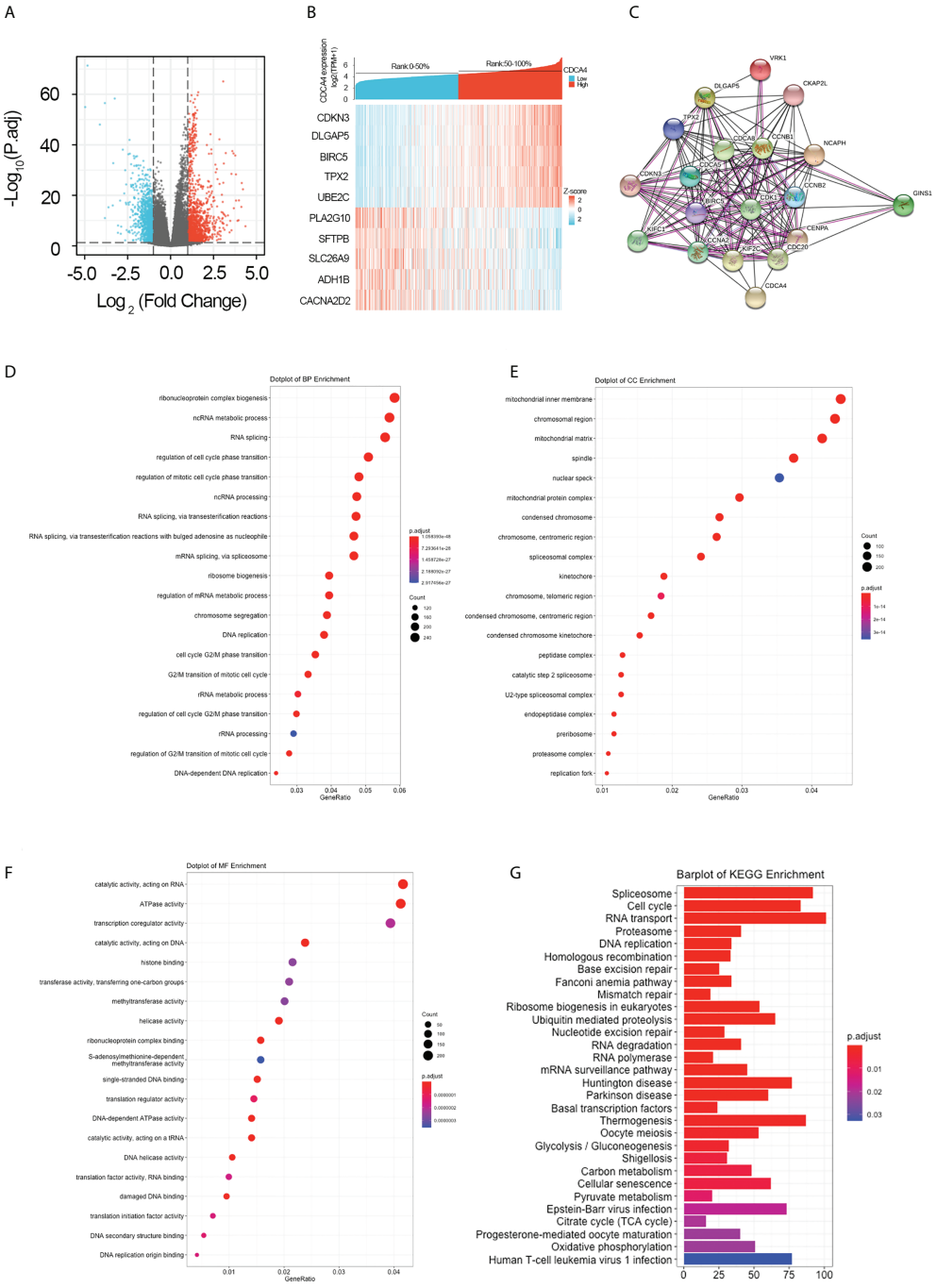


FIGURE 4
Genes co-expressed by CDCA4 and biological functions of CDCA4 associated with LUAD. **(A)** A volcano plot of differential gene profiles between high and low CDCA4 groups shows that 179 genes were up-regulated and 77 were down-regulated (adjusted *P*-value of 0.01 and | log2-fold change [FC]| > 2). **(B)** A heat map illustrating the positive co-expression of ten representative CDCA4 genes in LUAD. Data was normalized using the Z-score normalization method. **(C)** PPI network created and displayed using CDCA4 co-expressed genes from http://string-db.org. **(D)** BP outcomes; **(E)** CC outcomes; **(F)** MF outcomes from Metascape analysis of functionally enriched GO. **(G)**. KEGG results based on the expression levels of CDCA4 in the LUAD and TCGA datasets. PPI, protein-protein interaction; KEGG, Kyoto Encyclopedia of Genes and Genomes; BP, biological process; CC, cellular component; MF, molecular function.

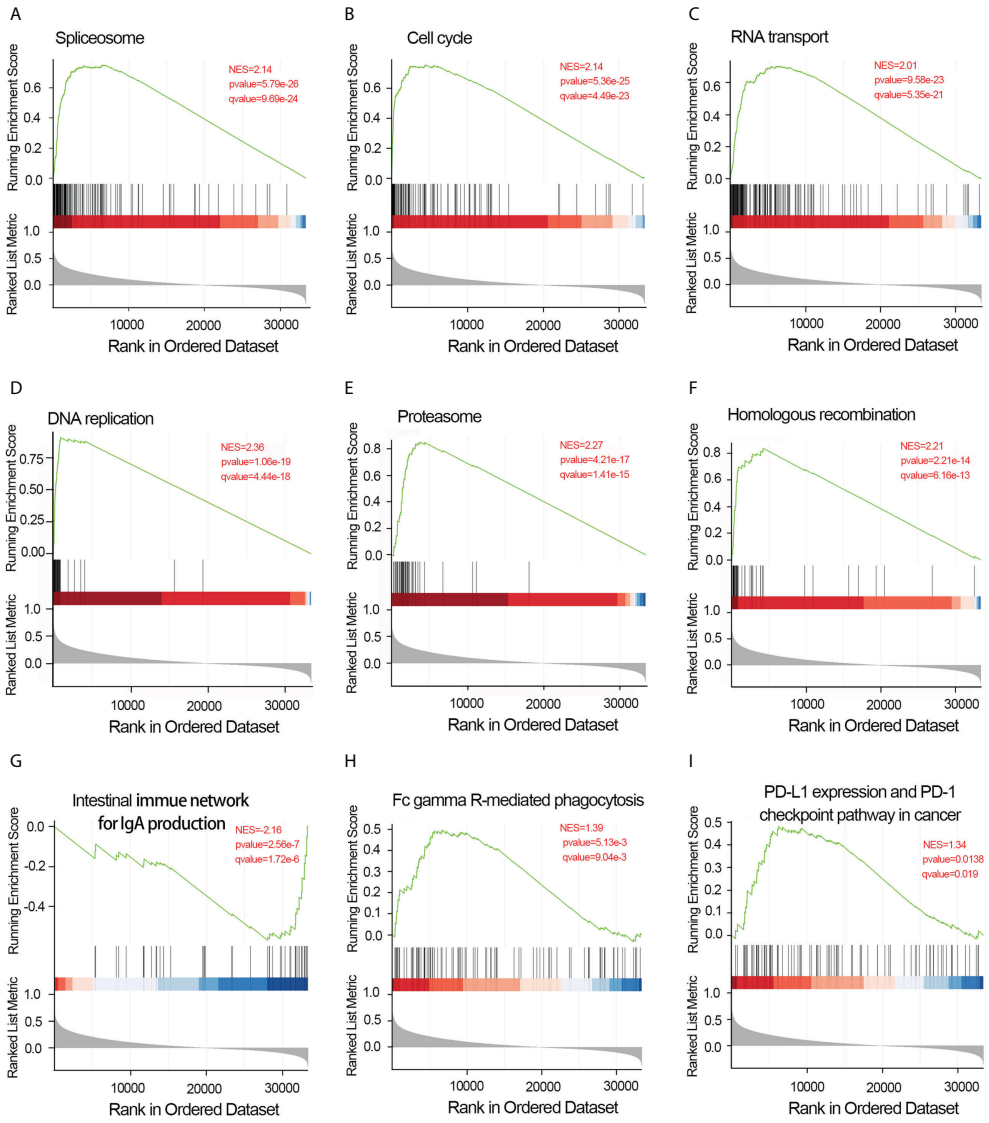


FIGURE 5
Results of gene set enrichment analysis of CDCA4. **(A)** Spliceosome. **(B)** Cell cycle. **(C)** RNA transport. **(D)** DNA replication. **(E)** Proteasome. **(F)** Homologous recombination. **(G)** Intestinal immune network for IgA generation. **(H)** Fc gamma R-mediated phagocytosis. **(I)** PD-L1 expression and PD-L1 checkpoint pathway in cancer. NES, normalized enrichment score; FDR, false discovery rate.

Then we used Spearman correlation analysis for determining the association between CDCA4 expression and ICI in the LUAD microenvironment. Figures 6A–N exhibited that CDCA4 expression had a negatively correlation with the infiltration of Mast cells, Eosinophils, Th17, B cells, T cells, CD8 T cells, T central memory, follicular helper T cells, DCs, immature DCs, pDCs, NK cells, NK CD56 (bright) cells, and Macrophages. Also, a significantly positive correlation was found with T gamma delta, Th2, activated DCs, NK CD56 (dim) cells, T helper cells (Figures 6O–S). As indicated by these findings, CDCA4 could be key to regulating ICI in the tumour microenvironment (TME).

## Discussion

Lung cancer is the most typical fatal disease in China and a severe global public health problem (21). Despite significant advances in recent years, the incidence and mortality of lung cancer continue to rise. Investigation of prognostic factors is a critical component of precision medicine and will value treatment allocation (22). CDCA4, encoding 241 amino acids, is on chromosome 14. *In vitro* studies on breast, cervical and malignant melanoma have investigated the expression and function of CDCA4 in tumorigenesis (16, 17, 23). Multiple signalling pathways,

especially classical signalling pathways involved in carcinogenesis, are closely associated with CDCA4, and several investigations have shown that CDCA4 overexpression is also related to poor prognoses in various malignancies (17, 23, 24). However, the effect of CDCA4 on LUAD remains a mystery to us. Therefore, it is necessary to further understand the role of CDCA4 in LUAD and its prognostic significance, as well as the regulatory mechanism supporting its role.

CDCA4 is aberrantly regulated in various cancers, comprising triple-negative breast cancer (BC), Wilm's tumour, melanoma, and osteosarcoma, and is associated with poor patient outcomes (13, 25–28). Shaul et al. found that CDCA4 is highly expressed in BC tissue in comparison to normal tissues

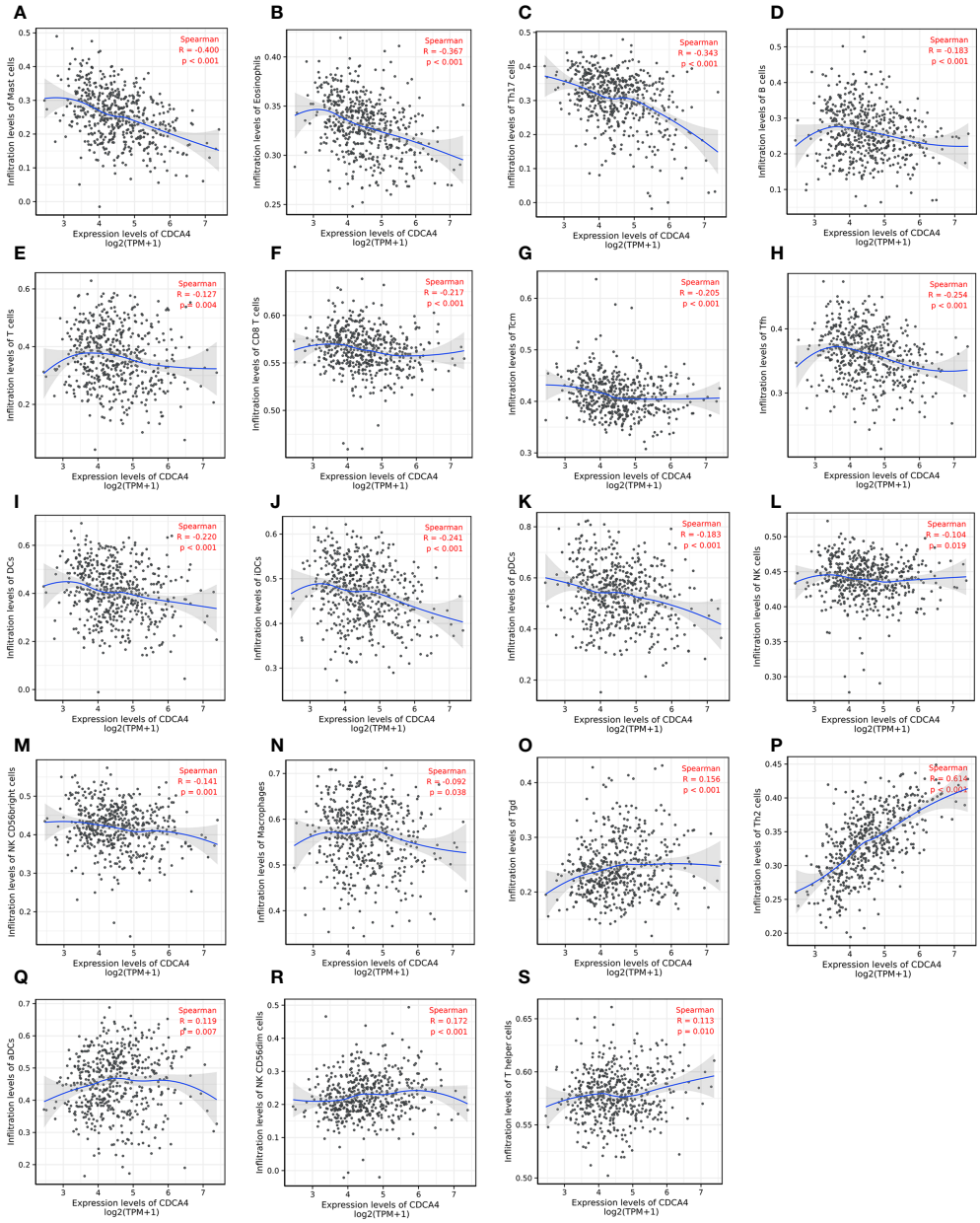


FIGURE 6
Investigation of the correlation between CDCA4 expression and immune cell infiltration in LUAD(P<0.05). **(A-N)** CDCA4 expression was negatively correlated with the infiltration of Mast cells, Eosinophils, Th17, B cells, T cells, CD8 T cells, T central memory, follicular helper T cells, DCs, immature DCs, pDCs, NK cells, NK CD56 (bright) cells, and Macrophages. (O-S) CDCA4 expression was positively correlated with T gamma delta, Th2, activated DCs, NK CD56 (dim) cells, T helper cells.Data were assessed by Spearman correlation analysis.

using the MERAV database (29). Using the ONCOMINE database, Chen et al. compared CDCA4 gene transcriptional data between standard samples and tumour tissues, resulting in a 2.213-fold change in CDCA4 (13). However, there is a little study to explore CDCA4 expression in lung adenocarcinoma. In this investigation, we used qRT-PCR, Western blotting and IHC on paired LUAD and standard lung tissue samples and found increased expression of CDCA4 in LUAD tissues (Figures 1A–D, $P<0.001$). This result was consistent with datasets from TCGA (Figures 1E, F).

Furthermore, ovarian cancer patients with elevated CDCA4 expression levels were related to the lower post-progression survival (13). CDCA4 was also upregulated in neck and head squamous cell carcinoma tissues; nonetheless, the higher expression of CDCA4 was associated with more prolonged relapse-free survival (12). In addition, Ran et al. reported elevated CDCA4 expression in patients with squamous cell carcinoma or lung adenocarcinoma; however, no further studies were performed (30). In the current investigation, increased CDCA4 expression was associated with unfavorable clinicopathological characteristics and worse prognoses (Figures 2, 3). In univariate and multivariate analysis, increased CDCA4 expression was confirmed as an independent adverse prognostic factor (Table 3, Supplementary Table 3). In addition, nomograms combining CDCA4 expression and other independent prognostic variables showed a better prediction of DSS and OS in patients with LUAD (Figure 3, Supplementary Figure 3). These results may help in the development of an effective biomarker.

Aberrancy in cell cycle progression is an essential mechanism underpinning tumorigenesis (31, 32). It is reported that CDCA4 can be transferred to the centrosome during mitosis and then to the intermediate region. Interference with CDCA4 RNA may damage spindle function during chromosome segregation, or lead to abnormal cell division, resulting in multinucleate and multipolar spindles (33). In addition, CDCA4 may act as a "traffic cop", affecting mRNA expression of Jun proto-oncogenes and directing upstream signals to the protective elements to determine cell fate (17). In this study, GO analysis exhibits that CDCA4 is involved in courses highly related to tumorigeneses, like DNA replication, modulation of G2/M transition of mitotic cell cycle, modulation of cell cycle phase transition, modulation of G2/M transition of the cell cycle, modulation of mitotic cell cycle phase transition and DNA-dependent DNA replication (Figures 4D–F). Then, KEGG analyses exhibited genes co-expressed with CDCA4 in the spliceosome, DNA replication, cell cycle, proteasome and RNA transport (Figure 4G). We further validated these results by using GSEA, which indicated that CDCA4 overexpression was collected with Spliceosome, Fc gamma R-mediated phagocytosis, IgA production by the intestinal immune network, homologous recombination, proteasome, DNA replication, RNA transport, cell cycle, PD-L1 expression and PD-1 checkpoint pathway (Figure 5). CDCA4 is associated with the destiny of BC cells, and downregulation of CDCA4 in human BC cells *in vitro* may inhibit proliferation while promoting apoptosis (16). Down-regulation of CDCA4, a miR-15a target, leads to cell cycle arrest in malignant melanoma cells in the G0/G1 phase (23). CDCA4 silencing impeded the transition from S to G2, leading to a reduction in cell growth and proliferation of triple-negative BC cells *in vivo* and *in vitro* (26).

Moreover, interference of CDCA4 significantly increased the fraction of the G0/G1 phase of MCF−7/ADM human BC cells and reduced its proliferation by inducing apoptosis (16). Ran et al. reported that over-expression of miR-15a-5p of A549 cells raised the ratio of the G1 phase, and inhibited cell proliferation, clonal formation, and invasion *in vitro*. Furthermore, they reported that CDCA4 constituted a candidate target for miR-15a-5p. The outcomes indicate that CDCA4 is closely related to tumour progression in LUAD by influencing the cell cycle (30). In lung squamous cell carcinoma (LUSC), CDCA4 overexpression significantly inhibited apoptosis, and enhanced the invasion and migration *in vitro*, leading to a deterioration of LUSC progression (34). However, Xu et al. reported that inhibiting CDCA4 induced Epithelial-Mesenchymal Transition, invasion and migration of NSCLC cells while suppressing autophagy of NSCLC cells (35). The inconsistent results of numerous studies suggest that CDCA4 can be involved in a more complicated regulatory network, and its specific regulatory mechanisms remain unknown.

In addition, CDCA4 is related to immune infiltrates in lung adenocarcinoma. The outcome of the connection between CDCA4 and TIICs indicated CDCA4 might play a role in modulating ICI (Figure 6). CDCA4 showed the closest relationship with Th2 cells (Figure 6P, Supplementary Figure 2C). The group with high CDCA4 expression had more Th2 cells but lower mast cells, eosinophils and Th17 cells (Supplementary Figure 2). Moreover, the GSEA analyses exhibited CDCA4 affects various immune-associated signalling pathways (Figures 5G–I). The quantity, type, and location of immune cells in the tumour microenvironment (TME) influence disease development and progression (36). There are a wide variety of immune cells like macrophages, B and T lymphocytes, and mast cells that can infiltrate tumours, and their composition and organization within the TME are closely linked to cancer patients' clinical outcomes (37, 38). T cells constitute adequate immune cells. Miller et al. first discovered elevated Th2-type responses in basal cell carcinomas, whereas benign tumours showed a predominance of Th1-type responses, implying dominant expression of Th2-type factors in malignant tumours (39). Thereafter, in a range of malignancies, including lung and cervical cancers, a significant predominance of Th2-type cytokines and Th1/Th2 imbalance was found in cancer tissues and immune cells from patients' peripheral blood (40–42). The interaction between T lymphocytes and NSCLC cells within the TME is essential to NSCLC development (43). As the tissue-resident, innate immune cell, Mast cells contribute to the cancer microenvironment by modulating various tumour

biology events. Salamon et al. found that the internalization of tumour-derived microvesicles from NSCLC cell lines can enhance mast cell migratory capability and increase TNF-α and MCP-1 release, thereby affecting tumorigenesis (44). Th17 cells feature complicated biological functions in cancer development. Ye et al. reported that high counts of pleural Th17 cells in malignant pleural effusion are related to promoted survival of NSCLC (45). However, little study focused on the relationship between CDCA4 and tumour-infiltrating immune cells. Only one previous study determined that CDCA4 regulates monocyte adhesion, leukocyte infiltration, and cytotoxicity of tumour cells (46). Therefore, plans for further understanding the CDCA4-medicated crosstalk with TIICs in the TME are necessary, which may help understand tumour progression and develop probable therapeutic modalities.

However, there are certain limitations. Firstly, there are inconsistent treatments and a lack of clinical information in public databases as the experiments were conducted in various laboratories. Secondly, potential molecular mechanisms of CDCA4 in carcinogenesis have not been investigated. We have formulated several plans for further wet lab work soon to explore the relevant signalling pathways of CDCA4 in LUAD.

## Conclusion

The present outcomes exhibit that CDCA4 levels are significantly higher in LUAD samples and are linked with unfavourable clinicopathological characteristics and poor prognoses of LUAD patients. Furthermore, CDCA4 is related to immune infiltrates in LUAD. In addition, CDCA4 may promote the progression of LUAD by regulating spliceosome, Fc gamma R-mediated phagocytosis, intestinal immune network for IgA production, homologous recombination, proteasome, DNA replication, RNA transport, Cell cycle, PD-L1 expression and PD-1 checkpoint pathway, making it an attractive prognostic biomarker for LUAD. Nonetheless, additional experimental investigations are required to determine the underlying processes and therapeutic effects in patients with LUAD.

## Data availability statement

The original contributions presented in the study are included in the article/Supplementary Material. Further inquiries can be directed to the corresponding author.

## Ethics statement

The studies involving human participants were reviewed and approved by Hunan Provincial People's Hospital. The patients/participants provided their written informed consent to participate in this study.

## Author contributions

TJL and GXL designed and analyzed this study. TJL, CFY, LXY, OYB and ZWD collected the data. TJL and GXL wrote and revised the manuscript. All authors contributed to and approved the final version of the manuscript.

## Funding

This study was supported by Hunan Provincial Health Commission (Grant Nos.202203023386), the RENSHU funding of Hunan Provincial People's Hospital (Grant Nos.201911) and the Science and Technology Planning Project of Guangdong Province (2017A070701014).

## Acknowledgments

The authors gratefully acknowledge the contribution of the TCGA database and the Molecular Signatures Database.

## Conflict of interest

The authors declare that the research was conducted in the absence of any commercial or financial relationships that could be construed as a potential conflict of interest.

## Publisher's note

## Supplementary material

The Supplementary Material for this article can be found online at: https://www.frontiersin.org/articles/10.3389/fonc.2022.865756/full#supplementary-material

## References


1. Mattiuzzi C, Lippi G. Current cancer epidemiology. *J Epidemiol Glob Health* (2019) 9(4):217–22. doi: 10.2991/jegh.k.191008.001

2. Siegel RL, Miller KD, Jemal A. Cancer statistics, 2020. *CA Cancer J Clin* (2020) 70(1):7–30. doi: 10.3322/caac.21590

3. Zeng H, Chen W, Zheng R, Zhang S, Ji JS, Zou X, et al. Changing cancer survival in China during 2003-15: a pooled analysis of 17 population-based cancer registries. *Lancet Glob Health* (2018) 6(5):e555–67. doi: 10.1016/S2214-109X(18)30127-X

4. Guerrera F, Errico L, Evangelista A, Filosso PL, Ruffini E, Lisi E, et al. Exploring stage I non-small-cell lung cancer: development of a prognostic model predicting 5-year survival after surgical resection. *Eur J Cardiothorac Surg* (2015) 47(6):1037–43. doi: 10.1093/ejcts/ezu410

5. Barta JA, Powell CA, Wisnivesky JP. Global epidemiology of lung cancer. *Ann Glob Health* (2019) 85(1):8. doi: 10.5334/aogh.2419

6. Dogan S, Shen R, Ang DC, Johnson ML, D'Angelo SP, Paik PK. Molecular epidemiology of EGFR and KRAS mutations in 3,026 lung adenocarcinomas: higher susceptibility of women to smoking-related KRAS-mutant cancers. *Clin Cancer Res* (2012) 18(22):6169–77. doi: 10.1158/1078-0432.CCR-11-3265

7. Vigneswaran J, Tan YH, Murgu SD, Won BM, Patton KA, Villaflor VM, et al. Comprehensive genetic testing identifies targetable genomic alterations in most patients with non-small cell lung cancer, specifically adenocarcinoma, single institute investigation. *Oncotarget* (2016) 7(14):18876–86. doi: 10.18632/oncotarget.7739

8. Devarakonda S, Morgensztern D, Govindan R. Genomic alterations in lung adenocarcinoma. *Lancet Oncol* (2015) 16(7):e342–51. doi: 10.1016/S1470-2045(15)00077-7

9. Zhou J, Sanchez-Vega F, Caso R, Tan KS, Brandt WS, Jones GD, et al. Analysis of tumor genomic pathway alterations using broad-panel next-generation sequencing in surgically resected lung adenocarcinoma. *Clin Cancer Res* (2019) 25(24):7475–84. doi: 10.1158/1078-0432.CCR-19-1651

10. Collins I, Garrett MD. Targeting the cell division cycle in cancer: CDK and cell cycle checkpoint kinase inhibitors. *Curr Opin Pharmacol* (2005) 5:366–73. doi: 10.1016/j.coph.2005.04.009

11. Tokuzen N, Nakashiro K, Tanaka H, Iwamoto K, Hamakawa H. Therapeutic potential of targeting cell division cycle associated 5 for oral squamous cell carcinoma. *Oncotarget* (2016) 7(3):2343–53. doi: 10.18632/oncotarget.6148

12. Wu ZH, Fang M, Zhou Y. Comprehensive analysis of the expression and prognosis for CDCAs in head and neck squamous cell carcinoma. *PloS One* (2020) 15(7):e0236678. doi: 10.1371/journal.pone.0236678

13. Chen C, Chen S, Luo M, Yan H, Pang L, Zhu C, et al. The role of the CDCA gene family in ovarian cancer. *Ann Transl Med* (2020) 8(5):190. doi: 10.21037/atm.2020.01.99

14. Abdullah JM, Jing X, Spassov DS, Nachtman RG, Jurecic R. Cloning and characterization of hepp, a novel gene expressed preferentially in hematopoietic progenitors and mature blood cells. *Blood Cells Mol Dis* (2001) 27(3):667–76. doi: 10.1006/bcmd.2001.0434

15. Hayashi R, Goto Y, Ikeda R, Yokoyama KK, Yoshida K. CDCA4 is an E2F transcription factor family-induced nuclear factor that regulates E2F-dependent transcriptional activation and cell proliferation. *J Biol Chem* (2006) 281(47):35633–48. doi: 10.1074/jbc.M603800200

16. Xu Y, Wu X, Li F, Huang D, Zhu W. CDCA4, a downstream gene of the Nrf2 signaling pathway, regulates cell proliferation and apoptosis in the MCF-7/ADM human breast cancer cell line. *Mol Med Rep* (2018) 17(1):1507–12. doi: 10.3892/mmr.2017.8095

17. Tategu M, Nakagawa H, Hayashi R, Yoshida K. Transcriptional co-factor CDCA4 participates in the regulation of JUN oncogene expression. Biochimie. (2008) 90(10):1515–22. doi: 10.1016/j.biochi.2008.05.014

18. Liu ZL, Bi XW, Liu PP, Lei DX, Wang Y, Li ZM, et al. Expressions and prognostic values of the E2F transcription factors in human breast carcinoma. *Cancer Manag Res* (2018) 10:3521–32. doi: 10.2147/CMAR.S172332

19. Kruppa J, Jung K. Automated multigroup outlier identification in molecular high-throughput data using bagplots and gemplots. *BMC Bioinf* (2017) 18(1):232. doi: 10.1186/s12859-017-1645-5

20. Bindea G, Mlecnik B, Tosolini M, Kirilovsky A, Waldner M, Obenauf AC, et al. Spatiotemporal dynamics of intratumoral immune cells reveal the immune landscape in human cancer. *Immunity* (2013) 39(4):782–95. doi: 10.1016/j.immuni.2013.10.003

21. He H, Liang L, Han D, Xu F, Lyu J. Different trends in the incidence and mortality rates of prostate cancer between China and the USA: A joinpoint and age-Period-Cohort analysis. *Front Med (Lausanne)* (2022) 9:824464. doi: 10.3389/fmed.2022.824464

22. Thai AA, Solomon BJ, Sequist LV, Gainor JF, Heist RS. Lung cancer. *Lancet* (2021) 398(10299):535–54. doi: 10.1016/S0140-6736(21)00312-3

23. Alderman C, Sehlaoui A, Xiao Z, Yang Y. MicroRNA-15a inhibits the growth and invasiveness of malignant melanoma and directly targets on CDCA4 gene. *Tumour Biol* (2016) 37(10):13941–50. doi: 10.1007/s13277-016-5271-z

24. Li C, Jung S, Lee S, Jeong D, Yang Y, Kim KI, et al. Nutrient/serum starvation derived TRIP-Br3 down-regulation accelerates apoptosis by destabilizing XIAP. *Oncotarget* (2015) 6(10):7522–35. doi: 10.18632/oncotarget.3112

25. Li J, Zhang F, Li H, Peng F, Wang Z, Peng H, et al. Circ_0010220-mediated miR-503-5p/CDCA4 axis contributes to osteosarcoma progression tumorigenesis. *Gene* (2020) 763:145068. doi: 10.1016/j.gene.2020.145068

26. Pang S, Xu Y, Chen J, Li G, Huang J, Wu X. Knockdown of cell division cycle-associated protein 4 expression inhibits proliferation of triple negative breast cancer MDA-MB-231 cells *in vitro* and *in vivo*. *Oncol Lett* (2019) 17(5):4393–400. doi: 10.3892/ol.2019.10077

27. Li S, Qin C, Chen Y, Wei D, Tan Z, Meng J. Implications of cell division cycle associated 4 on the wilm's tumor cells viability *via* AKT/mTOR signaling pathway. *Ren Fail* (2021) 43(1):1470–78. doi: 10.1080/0886022X.2021.1994994

28. Alderman C, Yang Y. The anti-melanoma activity and oncogenic targets of hsa-miR-15a-5p. *RNA Dis* (2016) 3(4):e1450.

29. Shaul YD, Yuan B, Thiru P, Nutter-Upham A, McCallum S, Lanzkron C, et al. MERAV: a tool for comparing gene expression across human tissues and cell types. *Nucleic Acids Res* (2016) 44(D1):D560–6. doi: 10.1093/nar/gkv1337

30. Ran J, Li Y, Liu L, Zhu Y, Ni Y, Huang H, et al. Apelin enhances biological functions in lung cancer A549 cells by downregulating exosomal miR-15a-5p. *Carcinogenesis* (2021) 42(2):243–53. doi: 10.1093/carcin/bgaa089

31. Ning Y, Zheng H, Zhan Y, Liu S, Yang Y, Zang H, et al. Overexpression of P4HA1 associates with poor prognosis and promotes cell proliferation and metastasis of lung adenocarcinoma. *J Cancer* (2021) 12(22):6685–94. doi: 10.7150/jca.63147

32. Zhang W, Zhang R, Zeng Y, Li Y, Chen Y, Zhou J, et al. ALCAP2 inhibits lung adenocarcinoma cell proliferation, migration and invasion *via* the ubiquitination of β-catenin by upregulating the E3 ligase NEDD4L. *Cell Death Dis* (2021) 12(8):755. doi: 10.1038/s41419-021-04043-6

33. Wang L, Zhu G, Yang D, Li Q, Li Y, Xu X, et al. The spindle function of CDCA4. *Cell Motil Cytoskeleton* (2008) 65(7):581–93. doi: 10.1002/cm.20286

34. Hu J, Xiang X, Guan W, Lou W, He J, Chen J, et al. MiR-497-5p down-regulates CDCA4 to restrains lung squamous cell carcinoma progression. *J Cardiothorac Surg* (2021) 16(1):330. doi: 10.1186/s13019-021-01698-2

35. Xu C, Cao H, Sui Y, Zhang H, Shi C, Wu J, et al. CDCA4 suppresses epithelial-mesenchymal transtion (EMT) and metastasis in non-small cell lung cancer through modulating autophagy. *Cancer Cell Int* (2021) 21(1):48. doi: 10.1186/s12935-021-01754-w

36. Horne ZD, Jack R, Gray ZT, Siegfried JM, Wilson DO, Yousem SA, et al. Increased levels of tumor-infiltrating lymphocytes are associated with improved recurrence-free survival in stage 1A non-small-cell lung cancer. *J Surg Res* (2011) 171(1):1–5. doi: 10.1016/j.jss.2011.03.068

37. Fridman WH, Pagès F, Sautès-Fridman C, Galon J. The immune contexture in human tumours: impact on clinical outcome. *Nat Rev Cancer* (2012) 12(4):298–306. doi: 10.1038/nrc3245

38. Becht E, Giraldo NA, Germain C, de Reyniès A, Laurent-Puig P, Zucman-Rossi J, et al. Immune contexture, immunoscore, and malignant cell molecular subgroups for prognostic and theranostic classifications of cancers. *Adv Immunol* (2016) 130:95–190. doi: 10.1016/bs.ai.2015.12.002

39. Miller AR, McBride WH, Hunt K, Economou JS. Cytokine-mediated gene therapy for cancer. *Ann Surg Oncol* (1994) 1(5):436–50. doi: 10.1007/BF02303818

40. Okamoto M, Hasegawa Y, Hara T, Hashimoto N, Imaizumi K, Shimokata K, et al. T-Helper type 1/T-helper type 2 balance in malignant pleural effusions compared to tuberculous pleural effusions. *Chest* (2005) 128(6):4030–5. doi: 10.1378/chest.128.6.4030

41. Lin W, Zhang HL, Niu ZY, Wang Z, Kong Y, Yang XS, et al. The disease stage-associated imbalance of Th1/Th2 and Th17/Treg in uterine cervical cancer patients and their recovery with the reduction of tumor burden. *BMC Womens Health* (2020) 20(1):126. doi: 10.1186/s12905-020-00972-0

42. Zhu N, Yang Y, Wang H, Tang P, Zhang H, Sun H, et al. CSF2RB is a unique biomarker and correlated with immune infiltrates in lung adenocarcinoma. *Front Oncol* (2022) 12:822849. doi: 10.3389/fonc.2022.822849

43. Stankovic B, Bjørhovde HAK, Skarshaug R, Aamodt H, Frafjord A, Müller E, et al. Immune cell composition in human non-small cell lung cancer. *Front Immunol* (2019) 9:3101. doi: 10.3389/fimmu.2018.03101

44. Salamon P, Mekori YA, Shefler I. Lung cancer-derived extracellular vesicles: a possible mediator of mast cell activation in the tumor microenvironment. *Cancer Immunol Immunother* (2020) 69(3):373–81. doi: 10.1007/s00262-019-02459-w

45. Ye ZJ, Zhou Q, Gu YY, Qin SM, Ma WL, Xin JB, et al. Generation and differentiation of IL-17-producing CD4+ T cells in malignant pleural effusion. *J Immunol* (2010) 185(10):6348–54. doi: 10.4049/jimmunol.1001728

46. Ren Z, Kang W, Wang L, Sun B, Ma J, Zheng C, et al. E2F1 renders prostate cancer cell resistant to ICAM-1 mediated antitumor immunity by NF-κB modulation. *Mol Cancer* (2014) 13:84. doi: 10.1186/1476-4598-13-84

# Frontiers in Oncology

**Advances knowledge of carcinogenesis and tumor progression for better treatment and management**

The third most-cited oncology journal, which highlights research in carcinogenesis and tumor progression, bridging the gap between basic research and applications to imrpove diagnosis, therapeutics and management strategies.

---

## Discover the latest Research Topics

See more →


**Frontiers**

Avenue du Tribunal-Fédéral 34
1005 Lausanne, Switzerland
frontiersin.org

**Contact us**

+41 (0)21 510 17 00
frontiersin.org/about/contact